

LONDON
SCHOOL of
HYGIENE
& TROPICAL
MEDICINE



Robinson, A (2017) An investigation into the effects of Plasmodium parasite infection on the human odour profile. PhD thesis, London School of Hygiene & Tropical Medicine. DOI: <https://doi.org/10.17037/PUBS.04539377>

Downloaded from: <http://researchonline.lshtm.ac.uk/4539377/>

DOI: [10.17037/PUBS.04539377](https://doi.org/10.17037/PUBS.04539377)

Usage Guidelines

Please refer to usage guidelines at <http://researchonline.lshtm.ac.uk/policies.html> or alternatively contact researchonline@lshtm.ac.uk.

Available under license: <http://creativecommons.org/licenses/by-nc-nd/2.5/>

LONDON
SCHOOL of
HYGIENE
& TROPICAL
MEDICINE



**An investigation into the effects of *Plasmodium*
parasite infection on the human odour profile**

Ailie Robinson

**Thesis submitted for the degree of Doctor of Philosophy of the
University of London**

London School of Hygiene & Tropical Medicine

July 2017

**Funding details: ZonMw
(The Netherlands Organisation for Health Research and Development)**

Declaration of own work

All students are required to complete the following declaration when submitting their thesis. A shortened version of the School's definition of Plagiarism and Cheating is as follows (*the full definition is given in the Research Degrees Handbook*):

"Plagiarism is the act of presenting the ideas or discoveries of another as one's own. To copy sentences, phrases or even striking expressions without acknowledgement in a manner which may deceive the reader as to the source is plagiarism. Where such copying or close paraphrase has occurred the mere mention of the source in a biography will not be deemed sufficient acknowledgement; in each instance, it must be referred specifically to its source. Verbatim quotations must be directly acknowledged, either in inverted commas or by indenting" (University of Kent).

Plagiarism may include collusion with another student, or the unacknowledged use of a fellow student's work with or without their knowledge and consent. Similarly, the direct copying by students of their own original writings qualifies as plagiarism if the fact that the work has been or is to be presented elsewhere is not clearly stated.

Cheating is similar to plagiarism, but more serious. Cheating means submitting another student's work, knowledge or ideas, while pretending that they are your own, for formal assessment or evaluation.

Supervisors should be consulted if there are any doubts about what is permissible.

DECLARATION BY CANDIDATE

I have read and understood the School's definition of plagiarism and cheating given in the Research Degrees Handbook. I declare that this thesis is my own work, and that I have acknowledged all results and quotations from the published or unpublished work of other people.

I have read and understood the School's definition and policy on the use of third parties (either paid or unpaid) who have contributed to the preparation of this thesis by providing copy editing and, or, proof reading services. I declare that no changes to the intellectual content or substance of this thesis were made as a result of this advice, and, that I have fully acknowledged all such contributions.

I have exercised reasonable care to ensure that the work is original and does not to the best of my knowledge break any UK law or infringe any third party's copyright or other intellectual property right.

To be completed by the candidate

NAME IN FULL (*Block Capitals*):

STUDENT ID NO:

SIGNED: DATE:

Abstract

Some studies suggest that *Plasmodium* parasites can change the attractiveness of their vertebrate hosts to *Anopheles* vectors. This is suggestive of parasite manipulation, where the parasite alters a host phenotype to the parasite's own fitness benefit. In this instance, *Plasmodium* parasites may benefit from increased transmission via a greater number of vector-host contacts. Despite evidence that variation in human host attractiveness to biting insects is manifest through differences in the human odour profile (volatile compounds produced by the skin), the association between odour profile and *Plasmodium* infection has never been studied in humans. The skin odour profile of individuals infected with *Plasmodium* in both experimental- and natural-infection settings was investigated using gas chromatography (GC). In the experimentally-infected (EI) cohort, adults were infected with *Plasmodium falciparum* and their odour profile sampled before, during and after infection. In the naturally-infected (NI) cohort, children aged 5-12 years with *Plasmodium* infections of varied parasite density, stage and species were sampled before and after treatment with antimalarials. Odour samples from both cohorts were further screened for infection-associated compounds using coupled GC-electroantennography (GC-EAG). In both EI and NI cohorts, changes in the production of several compounds in skin odour were found to be associated with the presence of *Plasmodium* parasites. Of these, production of the aldehydes heptanal, octanal and nonanal (C7-C9) was both increased in association with the presence of parasites in a density-dependent manner, and found to induce antennal response in *Anopheles coluzzi*. The production of C7-C9 and other infection-associated compounds via malaria-induced oxidative stress is a suggested mechanism. Malaria remains one of the most important diseases worldwide. As the global strategy for malaria control and elimination evolves, to combat both parasite and vector resistance to drugs and insecticides, the need for innovative tools intensifies. If malaria parasites can alter the human odour profile and attractiveness to mosquitoes, the repercussions would be far reaching: this would likely have a profound influence on the way that malaria spreads through populations, and malaria-specific volatile biomarkers could provide a basis for novel diagnostic tools.

Acknowledgements

Over the last few years I have definitely put all of my energy and dedication into this project, but without the support and advice I've received from colleagues, friends and family, I doubt that I would have accomplished this. First, I would like to particularly thank my supervisor, James Logan, for advising and guiding but also for allowing me the academic freedom to develop my own ideas and pathway. I am also grateful for being indulged on most of my whims of attending conferences far and wide, taking time off for public engagement projects, and additionally a six-week sabbatical. I would like to thank all members of my advisory panel: Jetske De Boer, Steve Powers, Colin Sutherland, Teun Bousema, Willem Takken and John Pickett. All have provided me with invaluable help and advice when needed, often at the drop of a hat. Particular thanks goes to Jetske, who has allowed me so much of her time and patience, discussed every detail of the project with me and supported me as well as a friend and mentor.

I am thankful to all past and present members of the Logan group, particularly Christina, Vicki, James Cook, James O, Nando, Victor and Nina, all of whom have given encouragement, support and a few beers when necessary. This project was collaborative, and thanks goes out to all participating institutes for their hard work and effort, but especially the chemistry team at Rothamsted Research (John Caulfield, John Pickett, Mick Birkett and Keith Chamberlain), again, those at Wageningen University (Jetske De Boer and Willem Takken), those at the University Medical Centre, Nijmegen (Teun Bousema and Robert Sauerwein), and those at the International Centre of Insect Physiology and Ecology, Kenya, for their work in the field and for making me so welcome there (particularly Annette O Busula, David John Odoyo and Geoffrey Omondi Olweru).

Several parts of this thesis required a little more help from those with the right expertise. Steve Powers provided me with statistical training and advice throughout, and without this I would not have gotten far. Development of the MALDIquant technique for analysis of GC data would not have been possible without help, encouragement and training from Pete Winskill, and thanks as well to the package author, Sebastian Gibb, for his contributions. Mojca Kristan and Mary Oguike were kind enough to allow me to help myself to their *Anopheles* colony, and special thanks to the Sutherland lab, particularly Khalid Beshir and Colin Sutherland, for their support in the parasitology work. I would also like to thank my academic mentor Hazel Dockrell, whose door has been open to me throughout these years, for help with science, plans, project

management or whatever I came along with. These conversations often had a profound impact on my outlook and really helped me along the way.

I am deeply grateful to those who helped in the final stages by reading various chapter drafts: Mojca Kristan, Jetske De Boer, Geoff Targett, Vicki Austin, Sarah Dewhirst, Dave Baker and Colin Sutherland. The thesis would really be in a much poorer shape without your suggestions, comments and corrections. Also, very special thanks to my brother, Iain Robinson, for his fantastic EAG graphic (the best page in the thesis), and to mum, for her speedy and dedicated proof-reading.

I am very thankful to all the participants in these trials, both from The Netherlands and Kenya, without whom there would be no project, no discovery, and indeed, no inspiration. Especially those in Kenya, who gave so much of their time freely, and with such good humour (even as we put their feet in bags).

Finally, I cannot thank deeply enough my friends, office-mates and family, including Katie, Ghislaine, Claire, Lucy, Pete, Soph, Cheryl, Phill, Freddy, Iain, Janet, and of course mum and dad. You have supported me throughout, and I know that it has been hard on you as well! Thank you all for the times you took away the stress, made me laugh, gave me (another) pep talk (Freddy!) or just listened to my current moan. At times you reminded me of the other things in life, and kept me moving forwards.

Contents

1	Literature review.....	36
1.1	Malaria	36
1.2	Malaria control.....	37
1.3	Olfaction.....	39
1.4	Olfactory apparatus	40
1.5	The attractiveness of human hosts to mosquitoes.....	42
1.6	Olfactory cues used for host location	43
1.7	Infection and body odour	46
1.8	Parasite manipulation	47
1.9	Direct evidence for <i>Plasmodium</i> manipulation of vertebrate host attractiveness	49
1.10	Parasite manipulation of host attractiveness in other vector-borne diseases.....	52
1.11	No increased attractiveness with parasite infection	55
1.12	Indirect evidence for <i>Plasmodium</i> manipulation of vertebrate host attractiveness..	56
1.12.1	Production of compounds by <i>Plasmodium</i> -infected red blood cells.....	56
1.12.2	Unexplained clustering of malaria cases.....	58
1.13	Anticipated outcomes.....	59
1.13.1	Odour-baited traps	59
1.13.2	Transmission	61
1.13.3	Diagnostics	62
1.14	Summary	63
1.15	Aim and objectives.....	64
1.16	Chapter references	65
2	Odour profile analysis of individuals experimentally infected with <i>Plasmodium falciparum</i> 78	
2.1	Introduction	78
2.2	Aim and objectives.....	80
2.3	Methods.....	81

2.3.1	Overview of the study	81
2.3.2	Ethics	81
2.3.3	Participants	81
2.3.4	<i>Plasmodium falciparum</i> parasite strains and infection monitoring	82
2.3.5	TIP5A and TIP5B	82
2.3.6	Bill and Melinda Gates Foundation (BMGF)	82
2.3.7	Air entrainment.....	83
2.3.8	Chemical analysis	84
2.3.9	Data analysis	86
2.4	Results.....	90
2.4.1	Study population.....	90
2.4.2	Hierarchical cluster analysis: exploration of data	92
2.4.3	CVA analysis of association between parasitological status and compound production.....	96
2.4.4	Infection-associated compounds.....	98
2.4.5	CVA analysis of association between other infection parameters and compound production (BMGF)	105
2.5	Discussion.....	106
2.5.1	Summary	106
2.5.2	BMGF cohort	106
2.5.3	TIP5A and TIP5B cohorts.....	108
2.5.4	Hierarchical cluster analysis.....	108
2.5.5	Methodological considerations	109
2.5.6	Other parameters of infection	110
2.6	Conclusion.....	111
2.7	Chapter references	112
2.8	Appendix: SED tables from experimentally-infected odour profile analysis.....	115
2.8.1	Cohort TIP5A	115

2.8.2	Cohort TIP5B	116
2.8.3	Cohort BMGF.....	116
3	Parasitology of Kenyan study population	118
3.1	Introduction	118
3.2	Aim and objectives.....	120
3.3	Methods.....	121
3.3.1	Summary	121
3.3.2	Field measures	121
3.3.3	Molecular diagnostic measures	123
3.3.4	<i>Plasmodium</i> -species specific nested PCR	128
3.3.5	18S ribosomal RNA qPCR and QT-NASBA (conducted by collaborators at Nijmegen).....	129
3.3.6	Comparative analysis of multiple diagnostic assays	129
3.4	Results.....	130
3.4.1	Summary	130
3.4.2	Comparability of diagnostic assays used	131
3.4.3	Categorisation of odour profile samples by parasitology.....	138
3.4.4	<i>Plasmodium</i> parasite densities present in the sampled population	141
3.4.5	Repeat sampling of odour profile individuals.....	142
3.5	Discussion.....	143
3.5.1	Summary	143
3.5.2	uRDT vs. wDBS template for PgMET qPCR.....	143
3.5.3	18S qPCR vs. other quantitative methods	144
3.5.4	Parasitological categorisation of odour samples	145
3.5.5	Methodological considerations	146
3.6	Conclusion.....	147
3.7	Chapter references	148
4	Method development for analysis of GC data.....	151

4.1	Introduction	151
4.1.1	Gas chromatography analysis	151
4.1.2	Rationale for method development	153
4.1.3	MALDIquant: a possible solution?	155
4.2	Aim and objectives.....	157
4.3	Methods.....	158
4.3.1	Pre-processing steps for MALDIquant	158
4.3.2	MALDIquant package parameters	158
4.3.3	Trialling the use of MALDIquant for the Kenyan odour samples.....	159
4.3.4	tRI- vs. MALDIquant-generated compound amounts.....	160
4.4	Results.....	162
4.4.1	Trial 1. Alignment of alkane standards and mini dataset	162
4.4.2	Trial 2. Alignment of samples according to GC machine	163
4.4.3	Trial 3. Verifying tRI alignment with MALDIquant	165
4.4.4	tRI vs. MALDIquant generated compound amounts: infection-associated compounds	166
4.5	Discussion.....	167
4.5.1	Summary	167
4.5.2	Use of the MALDIquant package for analysing GC data	167
4.5.3	Solving methodological issues in this dataset.....	168
4.6	Conclusion.....	169
4.7	Chapter references	170
4.8	Appendix: MALDIquant package parameters	171
4.8.1	Appendix references	178
4.9	Appendix: tRI- vs. MALDIquant-generated peak amounts	179
5	Odour profile analysis of children naturally infected with <i>Plasmodium</i> species.....	188
5.1	Introduction	188
5.2	Aim and objectives.....	191

5.3	Methods.....	192
5.3.1	Study site.....	192
5.3.2	Study protocol.....	192
5.3.3	Ethics.....	193
5.3.4	Infection status: parasitology.....	194
5.3.5	Odour profile sampling	194
5.3.6	Chemical analysis of odour profile: gas chromatography.....	194
5.3.7	Analysis of gas chromatography traces	195
5.3.8	Generating compounds of interest and investigating parasitological grouping 196	
5.3.9	Parasitological categorisation	198
5.3.10	Statistical analysis of compounds of interest	204
5.3.11	Ranked production of compounds and intra-individual changes in infection- associated compound production	204
5.3.12	Compound identification	205
5.4	Results.....	206
5.4.1	Summary	206
5.4.2	Compound identification by peak enhancement	208
5.4.3	Infection-associated compounds (IAC)	209
5.4.4	Summary tables: infection-associated compounds.....	228
5.4.5	Total amount.....	232
5.4.6	Non-significant: compounds not associated with infection	233
5.4.7	Proportion of total odour sample and ranked compound production.....	234
5.4.8	Intra-individual changes in IAC production.....	235
5.5	Discussion.....	239
5.5.1	Summary	239
5.5.2	<i>Plasmodium</i> infection-associated compounds	240
5.5.3	Aldehydes as a product of oxidative stress.....	241

5.5.4	Aldehyde production by human skin and the association with disease	242
5.5.5	Other mechanisms of aldehyde production	244
5.5.6	Aldehydes and entomology	245
5.5.7	Non-aldehyde infection-associated compounds	246
5.5.8	Further observations.....	247
5.5.9	Other covariates and factors that were associated with infection	248
5.5.10	Methodological considerations	250
5.6	Conclusion.....	251
5.7	Chapter references	252
5.8	Appendix: Parasitological categorisation for Kenyan odour samples	258
5.8.1	Level one	258
5.8.2	Level two	259
5.8.3	Level three	260
5.8.4	Level four	260
5.8.5	Level five	263
5.8.6	Levels six - ten	263
5.8.7	Appendix references.....	265
5.9	Appendix: Canonical Variates Analysis loadings.....	266
5.10	Appendix: 'Natural infections' study population.....	269
5.11	Appendix: compound identification by Peak Enhancement.....	271
5.11.1	Negative blend	272
5.11.2	Sub-gametocyte blend	276
5.11.3	Gametocyte blend.....	278
5.11.4	Sample KA078 23MAY14: Hexanal.....	280
5.11.5	Sample KA078 23MAY14: Phenol	281
5.11.6	Sample AL029 13FEB14: Phenol.....	282
5.11.7	Sample AL029 13FEB14: 1-octen-3-one.....	283
5.11.8	Sample PO014 10JUN14: Hexanal.....	284

5.12	Appendix: SED tables from Kenyan odour profile analysis.....	285
6	Electroantennography of human odour samples	290
6.1	Introduction	290
6.2	Aim and objectives.....	295
6.3	Methods.....	296
6.3.1	Blends of odour sample extract for GC-EAG testing.....	296
6.3.2	Mosquitoes	297
6.3.3	Study design.....	298
6.3.4	Gas chromatography-electroantennography	298
6.3.5	Data analysis	301
6.3.6	Compound identification by gas chromatography mass spectrometry	301
6.4	Results.....	302
6.4.1	BMGF dataset (EI cohort).....	302
6.4.2	Kenyan dataset (NI cohort)	302
6.4.3	Commonality in EAG-activity between both datasets	303
6.5	Discussion.....	307
6.5.1	Summary	307
6.5.2	<i>Anopheles</i> response to C7-C9 aldehydes	308
6.5.3	The response of <i>Aedes</i> and <i>Culex</i> to C7-C9 aldehydes	309
6.5.4	Entomological response to 6-methyl-5-hepten-2-one and 1-octen-3-one	310
6.5.5	Other EAG-active compounds.....	311
6.5.6	Methodological considerations	312
6.6	Conclusion.....	313
6.7	Chapter references	319
7	Discussion and conclusions.....	326
7.1	Summary of findings	326
7.2	Natural infection IAC in the experimental infection odour profiles	327
7.3	Experimental infection IAC in the natural infection odour profiles.....	329

7.4	Do these changes in odour profile constitute parasite manipulation?	331
7.5	The behavioural role of infection-associated compounds	332
7.6	Infection-associated compounds are attractive to mosquitoes	334
7.7	Infection-associated compounds are repellent to mosquitoes	335
7.8	Infection-associated compounds as biomarkers for malaria?	336
7.9	Other significant findings of this thesis.....	337
7.10	Methodological limitations of the study.....	337
7.11	Conclusions	339
7.12	Chapter references	340

List of Figures

- Figure 1-1. Countries endemic for malaria in 2000 and 2016. Countries coloured green were endemic in 2000 and not in 2016. Countries must attain zero indigenous cases (acquired in the country) for three consecutive years to be considered to have achieved elimination. Taken from WHO 2016. .36
- Figure 1-2. The mosquito olfactory apparatus. **(A)** A schematic of the mosquito olfactory system. The antenna, maxillary palp, and tip of proboscis (not shown) are covered with sensilla, which house olfactory sensory neurons. OR = olfactory receptor, IR = ionotropic receptor, GR = gustatory receptor, OBP = odour binding protein. Taken from McBride (2016). **(B)** The structural arrangement of olfactory sensillum, the peg-shaped structures that detect odours, showing how dendrites of the olfactory neurons connect to the insect central nervous system (CNS). Taken from Syntech (2004) **(C)** A schematic showing the functioning sensillum. Odorant molecules enter the perforated cuticle, and are thought to bind to soluble proteins in the sensillum lymph including odorant binding proteins (OBP). These transport the odorants to the ORs on the dendritic membrane of the olfactory receptor neuron (ORNs). Taken from Ignell et al. (2011)..... 41
- Figure 2-1. Schematic of air entrainment timeline. Individuals were sampled before sporozoite challenge by infected mosquitoes, during infection, and following treatment PI. All individuals were monitored for infection by microscopy and 18S qPCR, from day five PI until antimalarial treatment. The BMGF participants were sampled twice at the ‘during infection’ moment, on days 6 and 8 PI.83
- Figure 2-2. Overview of participants in EI cohorts TIP5A, TIP5B and BMGF. Sex, immunization status, strain of *P. falciparum*, and the number of infectious bites used for parasite challenge is indicated per individual. Antimalarial treatment was given after two positive qPCR results. On day zero, individuals were challenged by the strain indicated, via the number of bites from infectious mosquitoes also indicated. Replicated with permission from De Boer (2017) (in prep)..... 91
- Figure 2-3. Dendrogram (A) and minimum spanning trees (B) for hierarchical cluster analysis of **TIP5A** dataset, created using an Ecological similarity matrix with the ‘group average’ clustering technique. Samples are labelled by: day PI (i.e. pre-challenge [day -2 PI] and during infection [day 7 PI]), identifier, and parasitological status (positive, POS; negative, NEG). 93
- Figure 2-4. Dendrogram (A) and minimum spanning trees (B) for hierarchical cluster analysis of **TIP5B** dataset, created using an Ecological similarity matrix. Samples are coded by: unique identifier, status (positive, POS; negative, NEG; and control), time point (**1**: day -2 PI, **2**: day 8 PI, **3**: day 34 PI). 94
- Figure 2-5. Dendrogram (A) and minimum spanning tree (B) for hierarchical cluster analysis of **BMGF** dataset using a Euclidean similarity matrix and ‘group average’ clustering method. Samples are coded by: unique identifier (11 individuals designated A-K, see Figure 2-2), time point (**1**: day -2 PI, **2**: day 6 PI, **3**: day 8 PI, **4**: day 34 PI), and status (negative, N; positive, P; control, C)..... 95

Figure 2-6. Canonical variates plot of the TIP5A (A) and TIP5B (B) data, grouped by parasitological status, irrespective of sampling moment. Samples are positioned by scores on canonical variates axes, relative to the presence and quantity of compounds contributing to these axes. The percentage of possible discrimination accounted for is included in the axes labels, circles represent 95 % confidence intervals. **A:** Negative group, circles and intact line, observations=14, n=10; Positive group, plus signs and dashed line, n=6; controls not shown, n=3. **B:** Negative group, circles and intact line, observations=15, n=6; Positive group, plus signs and dashed line, n=3; controls not shown, n=6. Control groups not shown, to enhance clarity..... 96

Figure 2-7. Canonical variates plot of the BMGF data, grouped by parasitological status, irrespective of sampling moment. Circles represent 95 % confidence intervals. Negative group, circles and intact line, observations=29, n=11; Positive group, plus signs and dashed line, observations=9, n=8; Bag control, not shown, n=6; Ether control, not shown, n=3. Control groups not shown, to enhance clarity..... 97

Figure 2-8 **(A)** Predicted mean total amount produced in 100-minute entrainment, log transformation, for three compounds found to be produced in significantly (RI 1598) or approaching significantly (RI 792 and RI 1167) different amounts between groups. For RI 792, $P=0.09$ (DF=14) and average standard error of the difference=0.737. For RI 1167, $P=0.148$ (DF=11) and average standard error of the difference=0.979. For RI 1598, $P<0.001$ (DF=11) and average standard error of the difference=0.339. **(B)** Predicted means back transformed, same data. Sample sizes were: before, n=10; during [-], n=4; during [+], n=6; control, n=2..... 98

Figure 2-9. **(A)** Predicted mean total amount produced in 100-minute entrainment, log transformation, for RI 1095, found in significantly greater amounts in the ‘during [-]’ and ‘[+]’ groups, relative to ‘after’ and controls ($P=0.028$, 13 DF). Error bars=predicted standard error. **(B)** Predicted means back transformed. Average standard error of the difference=0.734. Sample sizes were: before, n=6; during [-], n=3; during [+], n=3; after, n=6; control, n=2. 99

Figure 2-10. Flow chart showing the number of COI in the BMGF dataset at each stage in the analytical process, through to significance of final candidate compounds. Bold typeface indicates important pairwise differences in the production of compound between parasitological categories, CE = co-eluting, CNLs = empty bag controls and solvent controls (distinct groups). 101

Figure 2-11. Effect of *P. falciparum* infection on levels of specific human volatile compounds. Predicted mean **(A)** (log transformation), and back transformation **(B)**, of the total amount of each compound in ng, collected over 100 minutes. MHO=6-methyl-5-hepten-2-one. C-E indicates peak contained a co-eluting compound, error bars are predicted standard error. Predictions derived from linear mixed models, which were fitted using the method of residual maximum likelihood (REML), and testing the combined effect of parasitological status and sampling moment. Before (prior to malaria challenge) n=8; during (day 6 or 8 PI, with [-] and [+] referring to parasitological status) [-] observations = 5 (n = 5); during [+] observations = 9 (n = 8); after (day 34, after parasite clearance) n=9, control (sample collected from empty control bags), n=6. 103

Figure 2-12. Canonical variates plot for BMGF cohort, grouped by **(A)** *P. falciparum* strain and **(B)** number of infectious bites received. Samples restricted to PI time points (days 6, 8 and 34), and only individuals who became positive (i.e. excluding BMGF_006 and BMGF_028). Samples are positioned by scores on canonical variates axes; relative to the presence and quantity of compounds contributing to these axes. The percentage of possible discrimination accounted for is included in the axes labels. Circles represent 95 % confidence intervals. **(A)** NF 135, grey, observations=13, n=5; NF 166, black, observations=10, n=4. Control groups not shown, to enhance clarity. **(B)** 1 bite (plus signs, grey): observations=8, n=3; 2 bites (crosses, dashed line): observations=12, n=4; 5 bites (circles, black): observations=9, n=4). Control groups not shown, to enhance clarity. 105

Figure 3-1. Parasite densities (p/μL) calculated from microscopy, by field reader (reader 1) and re-reader (reader 2). Twenty samples read by both readers were available, and the correlation was good (r=0.76, n=20 P<0.001). 123

Figure 3-2. Used rapid diagnostic tests from the field were opened, and a central section of the nitrocellulose strip inside was cut out. This was cut into several pieces to optimise DNA extraction efficacy. The DNA extract was then used as a template for qPCR. Taken from Cnops et al. (2011). 124

Figure 3-3. Parasite density (p/μL) measured by PgMET qPCR based on uRDT and wDBS. There was a good correlation between these two measures (r=0.78, n=141, P<0.001), here all samples with both template types available are shown. 131

Figure 3-4. Parasite density (p/μL) measured by PgMET qPCR based on uRDT or wDBS. **(A)** Ordered by uRDT value, **(B)** by wDBS value, both omitting samples for which both results were zero. Multiple values at 0.29 (log (0.93+1)) p/μL represent ‘inconsistent’ samples (test result for that sample was one positive and one negative repeat, see methods, ‘PgMET: analysis’). 132

Figure 3-5. The relationship between parasite density (p/μL) as determined by 18S qPCR result vs **(A)** PgMET qPCR (uRDT template), **(B)** PgMET qPCR (wDBS template), and **(C)** microscopy results. The horizontal band of data points in A and B are those PgMET qPCR results that had a positive and negative repeat (‘inconsistent’ samples), as all were assigned the value of 0.93 p/μL (see methods: PgMET analysis). 136

Figure 3-6. For samples that were negative by 18S qPCR, positivity by the other diagnostic assays was compared. Sample sizes were 18S qPCR negative and microscopy, 51; RDT, 53; PgMET (uRDT), 47; PgMET (wDBS), 32; SNN *P. falciparum* (P.f.) (uRDT), 53; SNN *P. falciparum* (P.f.) (wDBS), 32..... 137

Figure 3-7. Number of odour samples that were available in each parasitological category. **(A-C)** the same 117 odour samples were categorised in three different ways, **(A)** separating out higher and lower total parasite density, **(B)** separating out high and low gametocyte (‘sub-gametocyte’) density, and **(C)** separating simply by *Plasmodium*-positive vs. parasite-free. **(D)** ‘Higher density’ and ‘lower density’ samples from **(A)** were sub-divided into quartiles, with 116 odour samples

included (one 'lower density' individual was excluded as no quantitative measure available). Here all <i>Plasmodium</i> species are considered together.	140
Figure 3-8. <i>Plasmodium</i> parasite densities (circles) were measured for 362 samples, including those corresponding to an odour sample. Squares represent gametocyte densities. Five quantitative methods were used: diagnostic method (1)=microscopy, n=82; (2)=18S qPCR, n=130; (3)=PgMET qPCR wDBS template, n=110; (4)=PgMET qPCR uRDT template, n=730; (5)=QT-NASBA for gametocytes, n=89. Colours represent samples from the four schools (study locations, given in legend). Threshold at 50 p/μL blood indicates cut-off between 'high' and 'low' parasite densities used in 'total density' categorisation, described above.	141
Figure 4-1. Schematic of GC analysis. Samples are injected by syringe at the inlet directly into the end of the column, where they are vaporised, and carried through the column by the carrier gas (here hydrogen). During passage through the (50 m) HP1 column, different constituents of the sample are separated primarily by the oven temperature ramp but also according to their respective affinities for the stationary and mobile phases of the column (i.e. the inner surface of the column and the carrier gas). At the flame ionisation detector (FID), hydrocarbons in the sample produce ions when burnt, and these are detected as a current that is proportional to the amount of hydrocarbons. The signal generated is represented by a peak on the trace, according to its strength. The trace is defined by a series of x and y co-ordinates, describing the time taken to move through the column and the FID signal for each component of the sample.	152
Figure 4-2. This sample was run after extensive GC use and column deterioration (purple trace). After the column was cut to improve chromatography, the sample was re-run (pink trace).....	154
Figure 4-3. Variation in baseline level, caused by differing GC machine detector sensitivity, renders visual comparison of peak size between traces difficult with the Chemstation package.	156
Figure 4-4. For the IAC (chapter 5), the amount present in each sample was calculated using both the tRI method (based on peak area) and the MALDIquant method (based on peak height). For samples where the values were discrepant, traces were examined by overlaying in MALDIquant. This indicated issues such as seen here, where poor chromatography had not separated the small peak of interest from a neighbouring peak in several samples. Here, red traces are those that were excluded from the final analysis for this reason, with the black trace showing expected peak position and shape.	161
Figure 4-5. C7 to C18 of the alkane series (A) prior to MALDIquant analysis, and (B) after successful alignment in MALDIquant. All 21 alkane peaks, run across three GC machines, were successfully binned using the following functions: smoothing (method="SavitzkyGolay", halfWindowSize=5), baseline removal (method="SNIP", iterations=25), peak detection (SNR=3, halfWindowSize=8) and peak binning (tolerance=2). In (B), the reference trace peaks are represented with lines and all other traces annotated with crosses.	162

Figure 4-6. Here samples are visualised as (A) raw traces and (B) the product of MALDIquant peak detection and binning. The MALDIquant steps used were: baseline removal (method="SNIP", iterations=25), peak detection (SNR=2, halfWindowSize=10) and peak binning (tolerance=2).	163
Figure 4-7. For traces 1-42 there was a good correlation between the amounts of compound present in the peak as determined using either method. However, traces 43 – 56 were not correctly aligned by MALDIquant as the chromatography was too different (Figure 4-8). Therefore, the package binned these peaks separately, and no values were generated at this position.	164
Figure 4-8. Samples run on GC[1] formed distinct groups according to GC issues. Traces 1-42 aligned well. Traces 43-52, run after a method change, aligned together, as did traces 53-56. Here, the MALDIquant package could successfully align samples and bin peaks of the same colour, while samples of different colour (those analysed at a different time) were too discrepant to be aligned.	164
Figure 4-9. MALDIquant was used to overlay samples that had been used to link disparate subsets of traces. Here it is easy to determine that these peaks are equivalent between these traces, which are different samples from Kamsama and Powo schools.	165
Figure 4-10. By colour-coding the larger sets of well-aligned traces in MALDIquant according to parasitology, compounds possibly associated with infection were immediately apparent. Peaks seen to be consistently increased in infected individuals are indicated with arrows.	166
Figure 4-11. An example spectrum in its raw form and following square root transformation.	172
Figure 4-12. An example spectrum in its raw form and smoothed according to different half window sizes.	173
Figure 4-13. A trace is plotted with baselines of varying iterations, to determine the appropriate number for baseline removal.	174
Figure 4-14. An example trace with three levels of increasing SNR (code above).	175
Figure 4-15. As in Figure 4-14, with the peaks detected using the variable SNR as visualised above.	176
Figure 4-16. Here three traces are overlaid, each with peaks marked by dots of the appropriate colour. The stars show binned peaks, with the middle peaks demonstrating that MALDIquant recognised that traces have the same peak here, and therefore the stars are aligned.	177
Figure 4-17. Comparing the amount of hexanal per sample, as calculated by either MALDIquant or by the traditional retention index method (tRI). MALDIquant calculates amount based on peak height, and the tRI method based on peak area.	180
Figure 4-18. Comparing the amount of heptanal per sample, as calculated by either MALDIquant or by the traditional retention index method (tRI). MALDIquant calculates amount based on peak height, and the tRI method based on peak area.	181
Figure 4-19. Comparing the amount of RI 965 per sample, as calculated by either MALDIquant or by the traditional retention index method (tRI). MALDIquant calculates amount based on peak height, and the tRI method based on peak area.	182

Figure 4-20. Comparing the amount of 2-octanone per sample, as calculated by either MALDIquant or by the traditional retention index method (tRI). MALDIquant calculates amount based on peak height, and the tRI method based on peak area.	183
Figure 4-21. Comparing the amount of octanal per sample, as calculated by either MALDIquant or by the traditional retention index method (tRI). MALDIquant calculates amount based on peak height, and the tRI method based on peak area.	184
Figure 4-22. Comparing the amount of (<i>E</i>)-2-octenal per sample, as calculated by either MALDIquant or by the traditional retention index method (tRI). MALDIquant calculates amount based on peak height, and the tRI method based on peak area.	185
Figure 4-23. Comparing the amount of nonanal per sample, as calculated by either MALDIquant or by the traditional retention index method (tRI). MALDIquant calculates amount based on peak height, and the tRI method based on peak area.	186
Figure 4-24. Comparing the amount of (<i>E</i>)-2-decenal per sample, as calculated by either MALDIquant or by the traditional retention index method (tRI). MALDIquant calculates amount based on peak height, and the tRI method based on peak area.	187
Figure 5-1. Protocol for air entrainment (odour profile sampling) in the Kenya population. Children were recruited for odour sampling in groups of three to represent uninfected, infected with asexual parasites, and gametocyte carriers, if parasite prevalence allowed. Following malaria diagnosis and sampling, individuals with malaria parasites were treated, and the same cohort re-sampled on days 8 and 22.	193
Figure 5-2. Hexanal peak in raw GC output. Individual lines represent odour profile samples, here coloured according to the parasitological status of the individual from whom the odour sample was taken. Note that slight misalignment of peaks does not prevent patterns from being observed, and the true identify of misaligned peaks (e.g. the left-aligned red trace in this image) could be confirmed by the peak retention index.	197
Figure 5-3. 'Total density' parasitological categorisation, showing actual parasite densities p/μL per group. (A) Plasmodium parasite densities: LOWER, total <50 p/μL blood; HIGHER, total >50 p/μL blood; GAM, gametocyte carriers by microscopy, here total parasites (all stages) shown. Note, of GAM category samples, 65 % harboured total parasite densities of > 50 p/μL (HIGHER category). Colours represent the diagnostic technique used to inform categorisation. (B) Gametocyte densities per μL blood, in 'total density' categories (measured by QT-NASBA or microscopy).	201
Figure 5-4. 'Quartile' parasitological categorisation, showing actual parasite densities (p/μL) per group. Here all 'higher density' and 'lower density' samples from the 'total density' categories were re-classified: L=low, mean/median parasite density 0.38/0.3, n=21; M-L=medium-low, mean/median parasite density 16.77/8.3, n=17; M-H=medium-high, mean/median parasite density 296.60/214.18, n=19; H=high, mean/median parasite density 102669.46/13304.54, n=23. Colours represent the diagnostic technique used to inform categorisation.	202

- Figure 5-5 ‘Gametocyte’ parasitological categorisation, showing actual parasite densities (/μL blood) per group. **(A)**: Gametocyte densities (per μL blood), SUB-GAM, gametocytes <50/μL blood; GAM, gametocytes >50/μL blood or microscopic gametocytes. ‘Asexuals’ category not shown as there were no gametocytes. Colours represent the diagnostic technique used to inform categorisation. **(B)** *Plasmodium* densities (p/μL) in the ‘gametocyte’ categories..... 203
- Figure 5-6. The output from gas chromatography is a trace, where compounds are represented by peaks according to the amount present. Here, representative traces from an individual with a ‘high density’ infection (>50 *Plasmodium* p/μL blood) and ‘low density’ infection (<50 *Plasmodium* p/μL blood) are shown. Compounds found to be significant in the ‘total density’ analysis are annotated. 207
- Figure 5-7. Peak enhancement was conducted to formally identify all compounds found to be associated with infection in the statistical analysis (hexanal, heptanal, octanal, nonanal, (*E*)-2-octenal, (*E*)-2-decenal, 2-octanone, 6-methyl-5-hepten-2-one, 1-octen-3-ol and 1-octen-3-one). Here octanal and nonanal are shown, full details for all compounds are given in appendix 5.11. 208
- Figure 5-8. Heptanal production (relative to all compounds in odour sample) per group. Predicted means (+SE) given by linear mixed modelling (REML). Sample size in bar ends, significant pairwise differences are indicated by different letters above bars, tested by Least Significant Differences ($P < 0.05$). **(A)** ‘total density’ categorisation; ‘NEG’=negative, ‘lower’ and ‘higher’ refer approximately to parasite densities of lesser or greater than 50 p/μL, ‘GAM’=microscopic gametocytes **(B)** ‘quartile’ categorisation; ‘NEG’ and ‘GAM’ as before, L=low, M-L=medium-low, M-H=medium-high and H=high **(C)** ‘positive vs. negative’ categorisation; ‘positive’=harbouring parasite densities greater than the test lower limit of detection, ‘negative’=parasite free. For all CNL(A)=solvent control, CNL(B)=empty bag control. 210
- Figure 5-9. Heptanal peak in raw gas chromatography output. Individual lines represent odour profile samples, here coloured according to the parasitological status of the individual from whom the odour sample was taken. ‘Higher density’, samples from individuals with >50 p/μL; ‘lower density’, samples from individuals with <50 p/μL; ‘negative’, samples from parasite-free individuals. Gametocyte carriers are excluded for clarity, as compound production spanned higher and lower parasite density groups. 210
- Figure 5-10. Octanal production (relative to all compounds in odour sample) per group. Predicted means (+SE) given by linear mixed modelling (REML). Sample size in bar ends, significant pairwise differences indicated by different letters above bars, tested by Least Significant Differences ($P < 0.05$) **(A)** ‘total density’ categorisation; ‘NEG’=negative, ‘lower’ and ‘higher’ refer approximately to parasite densities of lesser or greater than 50 p/μL, ‘GAM’=microscopic gametocytes **(B)** ‘quartile’ categorisation; ‘NEG’ and ‘GAM’ as before, L=low, M-L=medium-low, M-H=medium-high and H=high **(C)** ‘gametocyte’ categorisation; ‘NEG’ as before, ‘SUB-GAM’ and ‘GAM’ refer approximately to gametocyte densities of lesser or greater than 50/μL, ‘ASEX’=parasites but no gametocytes. For all CNL(A)=solvent control, CNL(B)=empty bag control. 212

- Figure 5-11. Octanal peak in raw gas chromatography output. Individual lines represent odour profile samples, here coloured according to the parasitological status of the individual from whom the odour sample was taken. ‘Higher density’, samples from individuals with >50 p/μL; ‘lower density’, samples from individuals with <50 p/μL; ‘negative’, samples from parasite-free individuals. Gametocyte carriers are excluded for clarity, as compound production spanned higher and lower parasite density groups. 212
- Figure 5-12. There is an inverse parabolic relationship between age and octanal production (REML, predicted means + SE), with a peak at eight years. Octanal production presented as a percentage of all compounds in the odour sample. Samples further split by (A) parasitology (‘total density’ categories, control groups modelled but omitted as not biologically appropriate), or (B) sex of individual. Predictions for REML covariates have no sample size, population parameters given in Table 5-3 and appendix 5.10. 213
- Figure 5-13. Nonanal production (relative to all compounds in odour sample) per group. Predicted means (+SE) given by linear mixed modelling (REML). Sample size in bar ends, significant pairwise differences indicated by different letters above bars, tested by Least Significant Differences ($P<0.05$) (A) ‘total density’ categorisation; ‘NEG’=negative, ‘lower’ and ‘higher’ refer approximately to parasite densities of lesser or greater than 50 p/μL, ‘GAM’=microscopic gametocytes (B) ‘quartile’ categorisation; ‘NEG’ and ‘GAM’ as before, L=low, M-L=medium-low, M-H=medium-high and H=high. For both, CNL(A)=solvent control, CNL(B)=empty bag control. 214
- Figure 5-14. Nonanal peak in raw gas chromatography output. Individual lines represent odour profile samples, here coloured according to the parasitological status of the individual from whom the odour sample was taken. ‘Higher density’, samples from individuals with >50 p/μL; ‘lower density’, samples from individuals with <50 p/μL; ‘negative’, samples from parasite-free individuals. Gametocyte carriers are excluded for clarity, as compound production spanned higher and lower parasite density groups. 215
- Figure 5-15. There is an inverse parabolic relationship between haemoglobin level and nonanal production (REML, predicted means + SE), with a peak at 6.12 g/dL (averaged across parasitological groups). Nonanal production presented as a percentage of all compounds in the odour sample. Samples split by parasitology (‘total density’ categories, control groups modelled but omitted as not biologically appropriate). Predictions for REML covariates have no sample size, population parameters given in Table 5-3 and appendix 5.10. 215
- Figure 5-16. (E)-2-Octenal production (relative to all compounds in odour sample) per group. Predicted means (+SE) given by linear mixed modelling (REML). Sample size in bar ends, significant pairwise differences indicated by different letters above bars, tested by Least Significant Differences ($P<0.05$) (A) ‘total density’ categorisation; ‘NEG’=negative, ‘lower’ and ‘higher’ refer approximately to parasite densities of lesser or greater than 50 p/μL, ‘GAM’=microscopic gametocytes, (B) ‘gametocyte’ categorisation; ‘NEG’ as before, ‘SUB-GAM’ and ‘GAM’ refer approximately to gametocyte densities of lesser or greater than 50 p/μL, ‘ASEX’=parasites but no gametocytes, (C)

‘positive vs. negative’ categorisation; ‘positive’ = harbouring parasite densities greater than the test lower limit of detection, ‘negative’=parasite-free. For all CNL(A)=solvent control, CNL(B)=empty bag control.	217
Figure 5-17. (E)-2-Octenal peak in raw gas chromatography output. Individual lines represent odour profile samples, here coloured according to the parasitological status of the individual from whom the odour sample was taken (‘positive vs. negative’ categories, Table 5-1).....	217
Figure 5-18. (E)-2-Octenal production decreased with increasing haemoglobin level (REML, predicted means + SE), shown as a percentage of all compounds in the odour sample. Samples split by parasitology (‘total density’ categories, control groups modelled but omitted as not biologically appropriate). Predictions for REML covariates have no sample size, population parameters given in Table 5-3 and appendix 5.10.	218
Figure 5-19. (E)-2-Decenal production (relative to all compounds in odour sample) per group. Predicted means (+SE) given by linear mixed modelling (REML). Sample size in bar ends, significant pairwise differences indicated by different letters above bars, tested by Least Significant Differences ($P<0.05$) (A) ‘total density’ categorisation; ‘NEG’=negative, ‘lower’ and ‘higher’ refer approximately to parasite densities of lesser or greater than 50 p/μL, ‘GAM’=microscopic gametocytes, (B) ‘gametocyte’ categorisation; ‘NEG’ as before, ‘SUB-GAM’ and ‘GAM’ refer approximately to gametocyte densities of lesser or greater than 50 p/μL, ‘ASEX’=parasites but no gametocytes, (C) ‘positive vs. negative’ categorisation; ‘positive’ = harbouring parasite densities greater than the test lower limit of detection, ‘negative’=parasite-free. For all CNL(A)=solvent control, CNL(B)=empty bag control.	219
Figure 5-20. (E)-2-Decenal peak (annotated by arrow) in raw gas chromatography output. Individual lines represent odour profile samples, here coloured according to the parasitological status of the individual from whom the odour sample was taken (‘positive vs. negative’ categories, Table 5-1).	219
Figure 5-21. (E)-2-Decenal production decreased with increasing age (REML, predicted means + SE), shown as a percentage of all compounds in the odour sample. Samples split by parasitology (‘total density’ categories, control groups modelled but omitted as not biologically appropriate). Predictions for REML covariates have no sample size, population parameters given in Table 5-3 and appendix 5.10.	220
Figure 5-22. RI 965 production (relative to all compounds in odour sample) per group. Predicted means (+SE) given by linear mixed modelling (REML). Sample size in bar ends, significant pairwise differences indicated by different letters above bars, tested by Least Significant Differences ($P<0.05$) (A) ‘total density’ categorisation; ‘NEG’=negative, ‘lower’ and ‘higher’ refer approximately to parasite densities of lesser or greater than 50 p/μL, ‘GAM’=microscopic gametocytes (B) ‘quartile’ categorisation; ‘NEG’ and ‘GAM’ as before, L=low, M-L=medium-low, M-H=medium-high and H=high (C) ‘gametocyte’ categorisation; ‘NEG’ as before, ‘SUB-GAM’ and ‘GAM’ refer	

- approximately to gametocyte densities of lesser or greater than 50 p/μL, 'ASEX'=parasites but no gametocytes. For all CNL(A)=solvent control, CNL(B)=empty bag control..... 221
- Figure 5-23. 2-Octanone production (relative to all compounds in odour sample) per group. Predicted means (+SE) given by linear mixed modelling (REML). Sample size in bar ends, significant pairwise differences indicated by different letters above bars, tested by Least Significant Differences ($P<0.05$) (A) 'total density' categorisation; 'NEG'=negative, 'lower' and 'higher' refer approximately to parasite densities of lesser or greater than 50 p/μL, 'GAM'=microscopic gametocytes, (B) 'gametocyte' categorisation; 'NEG' as before, 'SUB-GAM' and 'GAM' refer approximately to gametocyte densities of lesser or greater than 50 p/μL, 'ASEX'=parasites but no gametocytes. For both CNL(A)=solvent control, CNL(B)=empty bag control..... 222
- Figure 5-24. 2-Octanone peak (indicated by arrow) in raw gas chromatography output. Individual lines represent odour profile samples, here coloured according to the parasitological status of the individual from whom the odour sample was taken. 'Gametocytes', samples from individuals with >50 gametocytes/μL blood or gametocyte stages by microscopy; 'sub-gametocyte', samples from individuals with <50 gametocytes/μL blood; 'negative', samples from parasite-free individuals. Asexual-stage-only carriers are excluded for clarity, as compound production was not significantly increased. 223
- Figure 5-25. Hexanal production (relative to all compounds in odour sample) per group. Predicted means (+SE) given by linear mixed modelling (REML). (A) 'Gametocyte' categorisation; 'NEG'=negative, 'SUB-GAM' and 'GAM' refer approximately to gametocyte densities of lesser or greater than 50/μL, 'ASEX'=parasites but no gametocytes, CNL(A)=solvent control, CNL(B)=empty bag control. Sample size in bar ends, significant pairwise differences indicated by different letters above bars, tested by Least Significant Differences ($P<0.05$). (B) Hexanal production increased and then decreased with increasing weight. Samples split by parasitology ('gametocyte' categories, control groups modelled but omitted as not biologically appropriate). Predictions for REML covariates have no sample size, population parameters given in Table 5-3 and appendix 5.10. ... 224
- Figure 5-26. Hexanal peak in raw gas chromatography output. Individual lines represent odour profile samples, here coloured according to the parasitological status of the individual from whom the odour sample was taken. 'Gametocytes', samples from individuals with >50 gametocytes/μL or gametocyte stages by microscopy; 'sub-gametocyte', samples from individuals with <50 gametocytes/μL; 'negative', samples from parasite-free individuals. Asexual-stage-only carriers are excluded for clarity, as compound production was not significantly increased..... 225
- Figure 5-27. 1-Octen-3-one peak in raw gas chromatography output. Individual lines represent odour profile samples, here coloured according to the parasitological status of the individual from whom the odour sample was taken. 'Gametocytes', samples from individuals with >50 gametocytes/μL blood or gametocyte stages by microscopy; 'sub-gametocyte', samples from individuals with <50 gametocytes/μL blood; 'negative', samples from parasite-free individuals. Asexual-stage-only carriers are excluded for clarity, as compound production was not significantly increased. 226

Figure 5-28. 1-Octen-3-one production (relative to all compounds in odour sample) per group. Predicted means (+SE) given by linear mixed modelling (REML). **(A)** ‘Gametocyte’ categorisation; ‘NEG’=negative, ‘SUB-GAM’ and ‘GAM’ refer approximately to gametocyte densities of lesser or greater than 50/μL, ‘ASEX’=parasites but no gametocytes, CNL(A)=solvent control, CNL(B)=empty bag control. Sample size in bar ends, significant pairwise differences indicated by different letters above bars, tested by Least Significant Differences ($P<0.05$). **(B)** 1-Octen-3-one production decreased with increasing Hb. Samples split by parasitology (‘gametocyte’ categories, control groups modelled but omitted as not biologically appropriate). Model predictions have no sample size. **(C)** Age and age² significantly influenced 1-octen-3-one production, however both terms interacted with the main treatment effect (‘gametocyte’ categories). Samples split by parasitology (‘gametocyte’ categories, control groups modelled but omitted as not biologically appropriate). Predictions for REML covariates have no sample size, population parameters given in Table 5-3 and appendix 5.10. 227

Figure 5-29 **(A)** Total amount of all compounds collected (100-minute odour profile sampling). Predicted means (+SE) given by linear mixed modelling (REML). Sample size in bar ends, significant pairwise differences indicated by different letters above bars, tested by Least Significant Differences ($P<0.05$). ‘Total density’ categorisation; ‘NEG’=negative, ‘lower’ and ‘higher’ refer approximately to parasite densities of lesser or greater than 50 p/μL, ‘GAM’=microscopic gametocytes, CNL(A) is solvent control, CNL(B) is empty bag control. **(B)** Total amount of sample decreased over the sampling period, with a subsequent late slight increase in CNL(B) (closed bag control). No values for the analytical control (A; solvent) as not relevant to sampling period. 232

Figure 5-30. The proportion (%) that IAC contributed towards the entire odour profile, grouped by parasitological category (‘total density’ categories used, but compounds from the gametocyte-specific analysis hexanal and 1-octen-3-one are included, to demonstrate their relative contribution to the odour profile). The average number of non-IAC per group (i.e. ‘all other volatile compounds’), annotated in grey bar. RI 965 = co-eluting 6-methyl-5-hepten-2-one and 1-octen-3-ol. Sample sizes are: negative, $n=16$; lower, $n=32$; higher, $n=49$; gametocyte, $n=20$ 234

Figure 5-31. Production of IAC within individuals whose parasitological status changed between significant groups (or remained the same) in the ‘total density’ categorisation. Mean (+/- SEM) compound production (relative to all compounds in odour sample, %) displayed. ‘Higher’ = ‘higher density’ category, ‘lower’ = ‘lower density’ category. Per compound, ‘same’ = production by individuals staying within either (A) category. Heptanal, no individuals moved from ‘negative’ to ‘higher’. Significance indicated by P value (T test), sample sizes in bar base. 236

Figure 5-32. Production of IAC within individuals whose parasitological status changed between significant groups (or remained the same). Mean (+/- SEM) compound production (relative to all compounds in odour sample, %) displayed. (*E*)-2-octenal and (*E*)-2-decenal, samples presented in ‘positive vs. negative’ categorisation (Table 5-1), only one individual moved from ‘negative’ to ‘positive’ and one from ‘negative’ to ‘negative’ (data not shown). 2-Octanone, samples presented

in 'total density' categorisation (Table 5-1). 'Gam' = 'gametocyte' category, 'Other' = 'Lower density'/'Higher density'/'Negative'. Only two individuals moved from 'other' to 'gametocyte' (data not shown). Significance indicated by *P* value (T test), sample sizes in bar base. 237

Figure 5-33. Production of IAC within individuals whose parasitological status changed between significant groups (or remained the same) in the 'gametocyte' categorisation. Mean (+/- SEM) compound production (relative to all compounds in odour sample, %) displayed. Hexanal, 'lower' = 'asexual' or 'negative' categories, 'higher' = 'gametocyte' or 'sub-gametocyte'. 1-Octen-3-one, 'Gam' = 'gametocyte' category, 'lower' = 'negative' or 'asexual', only one individual moved from 'lower' to 'gametocyte' (data not shown). Hexanal and 1-octen-3-one, 'same' to 'same' = moving within lower or higher groups. Significance indicated by *P* value (T test), sample sizes in bar base. 238

Figure 5-34. The best separation of parasitological groups by CVA was achieved using 'level four' categorisation, designed to mimic microscopic levels of detection..... 262

Figure 5-35. Co-injections for standards of heptanal, (*E*)-2-octenal and (*E*)-2-decenal with the 'negative' blend, comprising mixed extracts of 15 parasite-free samples. (A) co-injections on HP1 column, (B) co-injections on DB wax column. Note 'sample' was run on HP1 pre column-cut, hence poor resolution, and could not be repeated due to lack of sample. 272

Figure 5-36. Co-injections for standards of octanal and nonanal with the 'negative' blend, comprising mixed extracts of 15 parasite-free samples. (A) co-injections on HP1 column, (B) co-injections on DB wax column. Note 'sample' was run on HP1 pre column-cut, hence poor resolution, and could not be repeated due to lack of sample. 273

Figure 5-37. Co-injections for standards of 6-methyl-5-hepten-2-one, 1-octen-3-ol and 2-octanone on HP1 column (A). Note, here 6-methyl-5-hepten-2-one and 1-octen-3-ol co-elute. (B) Co-injections of 6-methyl-5-hepten-2-one and 1-octen-3-ol on DB wax column. Note 'sample' was run on HP1 pre column-cut, hence poor resolution, and could not be repeated due to lack of sample. 274

Figure 5-38. Co-injections on a DB wax column for standards of 2-octanone with the 'negative' blend, comprising mixed extracts of 15 parasite-free samples. 275

Figure 5-39. Co-injections for standards of heptanal, octanal and nonanal with the 'sub-gametocyte' blend, comprising mixed extracts of 14 samples from lower-density gametocyte infections. (A) co-injections on HP1 column, (B) co-injections on DB wax column. 276

Figure 5-40. Co-injections for standards of 6-methyl-5-hepten-2-one, 1-octen-3-ol and (*E*)-2-octenal with the 'sub-gametocyte' blend, comprising mixed extracts of 14 samples from lower-density gametocyte infections. (A) co-injections on HP1 column, (B) co-injections on DB wax column. Note virtual absence of (*E*)-2-octenal in the DB wax blend. 277

Figure 5-41. Co-injections for standards of heptanal, 6-methyl-5-hepten-2-one, 1-octen-3-ol, 2-octanone, octanal and (*E*)-2-octenal with the 'gametocyte' blend, comprising mixed extracts of 13 samples from high-density gametocyte infections. (A) co-injections on HP1 column, (B) co-injections on DB wax column. 278

Figure 5-42. Co-injections for standards of nonanal and (<i>E</i>)-2-decenal with the ‘gametocyte’ blend, comprising mixed extracts of 13 samples from high-density gametocyte infections. (A) co-injections on HP1 column, (B) co-injections on DB wax column.	279
Figure 5-43. Co-injections for hexanal standard with sample KA078 23MAY14 (A) co-injections on HP1 column, (B) co-injections on DB wax column.	280
Figure 5-44. Co-injections for phenol standard with sample KA078 23MAY14 (A) co-injections on HP1 column, (B) co-injections on DB wax column. Note this co-injection indicated that the compound of interest, RI 958, was (in the case of the GC analysis) not phenol, as the wrong peak enhanced (A). However, for the GC-EAG analysis, EAG-active RI 958 was co-eluting phenol and 1-octen-3-one, therefore formal identification of phenol was required irrespectively.	281
Figure 5-45. Co-injections for phenol standard with sample AL029 13FEB14 (A) co-injections on HP1 column, (B) co-injections on DB wax column. Note this co-injection indicated that the compound of interest, RI 958, was (in the case of the GC analysis) not phenol, as the wrong peak enhanced (A). However, for the GC-EAG analysis, EAG-active RI 958 was co-eluting phenol and 1-octen-3-one, therefore formal identification of phenol was required irrespectively.	282
Figure 5-46. Co-injections for 1-octen-3-one standard with sample AL029 13FEB14 (A) co-injections on HP1 column, (B) co-injections on DB wax column. This peak enhancement revealed the correct identity of RI 958 in the GC analysis.	283
Figure 5-47. Co-injections for hexanal standard with sample PO014 10JUN14 (A) co-injections on HP1 column, (B) co-injections on DB wax column.	284
Figure 6-1. GC-EAG circuit. Sample is injected into the gas chromatograph (GC) (1); passes through the column of the GC and separates into its constituent parts (2); at the GC splitter the analytes are split 50:50 to the flame ionisation detector (FID) and the insect (3); the latter proportion passes through a heated transfer line and is added to a stream of filtered, humidified air (4); before this passes over the dissected mosquito head at the same time that the other portion of the sample is detected at the FID (5). Two traces are generated, here the top trace is the GC trace and the bottom the EAD (antennal response). Upwards EAD deflections are noise, while downwards deflections indicate a true response of nerve cell depolarisation. Example responses are marked with arrows. Image courtesy of Iain Robinson, copyright 2017 (www.iain-robinson.com).	300
Figure 6-2. The percentage of antennae responding in the BMGF dataset increased with peak amount (ng, log scale, mean of amount in all blends), but was a non-significant correlation ($r=0.3$, $n=25$ $P=0.17$). Dots (one per peak) represent the correlation between the peak amount and proportion of all antennae that responded. Geranylacetone (pink) and RI 951 (blue, co-eluting phenol and 1-octen-3-one) elicited the greatest number of responses. Peak RI 791+ was excluded as the amount was not measureable (immediately adjacent/under another peak).	304
Figure 6-3. The percentage of antennae responding in the Kenyan dataset increased with peak amount (ng, log scale, mean of amount in all blends), but was a non-significant correlation ($r=0.187$, $n=22$ $P=0.42$). Dots (one per peak) represent the correlation between the peak amount and proportion	

of all antennae that responded. Benzaldehyde (pink) and nonanal (green) elicited the greatest number of responses..... 306

List of tables

Table 1-1. A simplified overview of odour and visual cues, and their resultant behavioural output, used by female mosquitoes during host location. Mechanosensory input is also important to maintain upwind movement. Table from Cardé and Gibson (2010).	40
Table 2-1. Number of individuals (n) and total number of odour samples (OS) collected from EI population. Note, samples from the final time point are missing for TIP5A, and an extra sampling moment in BMGF.	81
Table 2-2. Integration parameters used during GC analysis	85
Table 2-3. Summary of CVA groupings used to investigate the influence of parasitological status per dataset, with sample size per group. Positive and During [+] indicate samples from individuals who tested Plasmodium parasite positive by qPCR on the same day. Negative and During [-] refer to samples from individuals who were parasite free by qPCR on the same day. *In BMGF, repeat 'during' sampling occurred due to two 'during' sampling efforts. **TIP5A 'after' samples were not considered adequate for analysis.....	87
Table 2-4. CVA groupings used in BMGF dataset to investigate associations between compound production and <i>P. falciparum</i> strain, and number of infectious bites received, with sample size per group. For these analyses, samples from day -2 PI were excluded (prior to challenge), as were samples from the two individuals who remained negative throughout (BMGF2_006 and BMGF2_028).....	88
Table 2-5. Parasitological categories to which odour profile samples were assigned, for predicting the effect of infection status on compound production (REML mixed models).	89
Table 2-6. COI derived from BMGF cohort, with the most interesting significant pairwise differences (LSD, 5%) between parasitological groups. RI = retention index, Av SED= Average standard error of the difference, <i>P</i> -value and degrees of freedom (DF) derived from linear mixed models, which were fitted using the method of residual maximum likelihood. Before (prior to malaria challenge) n=8; during (day 6 or 8 PI, with [-] and [+] referring to parasitological status) [-] observations = 5 (n = 5); during [+] observations = 9 (n = 8); after (day 34, after parasite clearance) n=9; control (sample collected from empty control bags), n=6. Full matrices of SEDs and all pairwise comparisons are given in Appendix 2.8.	104
Table 2-7 Summary of significant pairwise differences between groups of samples for compounds of interest from BMGF. MHO=6-methyl-5-hepten-2-one, full matrices of SEDs and all pairwise comparisons are given in Appendix 2.8.....	104
Table 3-1. Amplification primers and double-labelled hydrolysis probes for PgMET and HumTuBB, reproduced with permission from Beshir et al. (2010).	125
Table 3-2. Primer sequences for the <i>P. falciparum</i> , <i>P. malariae</i> and <i>P. ovale</i> species-specific nested PCR.	128

Table 3-3. Characteristics of parasitology study population (362 repeat samples were taken over 1-4 time points on 118 individuals). Schools constitute the four study sites. Seven individuals from Kamsama had no accompanying descriptive data.	130
Table 3-4. Parasite density (p/μL) measured by PgMET qPCR based on uRDT and wDBS templates. Considering only results >5 p/μL, both templates indicate positivity at times that the alternative template indicates negativity. Top half of table: uRDT template negative, wDBS template positive; bottom half of table: wDBS template negative, uRDT template positive. Other columns are results of other diagnostic assays. GAM = gametocytes by QT-NASBA; 18S= 18S qPCR; SNN= nested end-point PCR for <i>P. falciparum</i> (P.f.); <i>P. ovale</i> tested by SNN or PoTRA. 1/0 = binary outcome of positive and negative, POS = positive, NEG = negative, * not available.	133
Table 3-5. Correlation in species-specific PCR results based on uRDT and wDBS template, for three <i>Plasmodium</i> species tested. R[+] = positive uRDT result, R[-] = negative uRDT result, D[+] = positive wDBS result, D[-] = negative wDBS result. Values are agreement between templates in %, with number of samples given in parentheses. Note, some <i>P. ovale</i> results from PoTRA assay.	134
Table 4-1. GC machines used during analysis of Kenyan odour samples, analysis period per dataset (school), and issues that led to changes in peak elution times. GC[1] = machine 7890A at LSHTM; GC[2] = machine 6890N at Rothamsted Research; GC[3] = machine HP6890 at Rothamsted Research. Start and end refer to the time-period during which those samples were run, n = number of samples.	154
Table 5-1. Parasitological categories used for statistical analysis of compounds of interest. Asexuals=non-gametocyte stage parasites. RDT=rapid diagnostic test., p/μL=parasites per μL blood. Samples with parasite densities beneath test limit of detection thresholds were excluded from all analyses, as were any samples that were negative by microscopy but which had no verification by a molecular test.	200
Table 5-2. Covariates and factors tested with treatment term (parasitology) for significance by forward selection in REML models.	204
Table 5-3. Characteristics of Kenyan odour profile study population (repeat samples were taken at 1-4 time points on these 56 individuals). Schools constitute the four study sites. N = number of individuals. CNL = controls (odour samples from empty bags).	206
Table 5-4. Mean amount of compound produced per group ('total density' categories), expressed as a percentage of all compounds in odour samples. Predicted means derived from linear mixed modelling (REML). CNL(A) is solvent control, CNL(B) is empty bag control. MHO=6-methyl-5-hepten-2-one, *designates co-elution.	228
Table 5-5. Mean amount of compound produced per group ('quartile' categories), expressed as a percentage of all compounds in odour samples. Predicted means derived from linear mixed modelling (REML). Quartile analysis was conducted for those compounds where production appeared to be correlated with parasite density in the 'total density' categorisation. Densities are (1), low; (2), medium-low; (3), medium-high and (4), high. CNL(A) is solvent control, CNL(B) is	

empty bag control, Gam=gametocyte category, Neg=negative category, MHO=6-methyl-5-hepten-2-one, *designates co-elution.	228
Table 5-6. Mean amount of compound produced per group ('gametocyte' categories), expressed as a percentage of all compounds in odour samples. Predicted means derived from linear mixed modelling (REML). Sub-gam = sub-gametocyte, CNL(A) is solvent control, CNL(B) is empty bag control. MHO=6-methyl-5-hepten-2-one, *designates co-elution.	228
Table 5-7. Mean amount of compound produced per group ('positive vs. negative' categories), expressed as a percentage of all compounds in odour samples. Predicted means derived from linear mixed modelling (REML). CNL(A) is solvent control, CNL(B) is empty bag control.	229
Table 5-8. Significance of covariates and factors from linear mixed modelling (REML) for infection-associated compounds. Here parasitology predicted by 'total density' categories. Sample type refers to human odour profile sample or control (solvent or empty bag). Round is sequential sampling round. P/C=parasitological category. MHO=6-methyl-5-hepten-2-one, *designates co-elution.	229
Table 5-9. Significance of covariates and factors from linear mixed modelling (REML) for infection-associated compounds. Here parasitology predicted by 'gametocyte' categories. Sample type refers to human odour profile sample or control (solvent or empty bag). Round is sequential sampling round, Hb=haemoglobin, P/C=parasitological category. MHO=6-methyl-5-hepten-2-one, *designates co-elution.	230
Table 5-10. Significance of covariates and factors from linear mixed modelling (REML) for infection-associated compounds. Here parasitology predicted by 'positive vs. negative' categories. Sample type refers to human odour profile sample or control (solvent or empty bag). Round is sequential sampling round, Hb=haemoglobin, P/C=parasitological category.	231
Table 5-11. Significance of covariates and factors from linear mixed modelling (REML) for infection-associated compounds. Here parasitology predicted by 'quartile' categories. Sample type refers to human odour profile sample or control (solvent or empty bag), round is sequential sampling round, P/C=parasitological category, *designates co-elution.	231
Table 5-12. Significance of covariates and factors from linear mixed modelling (REML) for total amount of sample. All three parasitological categories were attempted. Sample type refers to human odour profile sample or control (solvent or empty bag). P/C=parasitological category.	233
Table 5-13. Level one parasitological categories attempted in CVA of odour profile datasets. PARA= <i>Plasmodium</i> parasites (all stages), gametocytes/GAM= <i>P. falciparum</i> gametocyte stages. RDT=rapid diagnostic test. P/ μ L = parasites per microlitre of blood.	259
Table 5-14. Level two parasitological categories attempted in CVA of odour profile datasets. PARA= <i>Plasmodium</i> parasites (all stages), gametocytes/GAM= <i>P. falciparum</i> gametocyte stages. RDT=rapid diagnostic test. P/ μ L = parasites per microlitre of blood.	260

Table 5-15. Level three parasitological categories attempted in CVA of odour profile datasets. PARA= <i>Plasmodium</i> parasites (all stages), gametocytes/GAM= <i>P. falciparum</i> gametocyte stages. RDT=rapid diagnostic test. P/ μ L = parasites per microlitre of blood.	260
Table 5-16. Level four parasitological categories attempted in CVA of odour profile datasets. PARA= <i>Plasmodium</i> parasites (all stages), gametocytes/GAM= <i>P. falciparum</i> gametocyte stages. RDT=rapid diagnostic test. P/ μ L = parasites per microlitre of blood.	261
Table 5-17. Level five parasitological categories attempted for separation of group mean COI production. PARA= <i>Plasmodium</i> parasites (all stages), gametocytes/GAM= <i>P. falciparum</i> gametocyte stages. RDT=rapid diagnostic test. P/ μ L = parasites per microlitre of blood.	263
Table 5-18. Level 6-10 parasitological categories attempted for separation of group mean COI production. PARA= <i>Plasmodium</i> parasites (all stages), gametocytes/GAM= <i>P. falciparum</i> gametocyte stages. RDT=rapid diagnostic test. P/ μ L = parasites per microlitre of blood.	264
Table 5-19. All compounds contributing to group separation (at least 50% of that of the compound with the greatest loading) for the 'level four' parasitological categorisation CVA. Those in bold font did appear infection-associated across all samples and were investigated in final REML analyses. Greatest and smallest loadings are given in shaded boxes.	266
Table 5-20. Age, sex and number of odour samples taken, per individual in the Kenyan ('natural infections') study. The number of empty bag control samples taken is also shown.	269
Table 5-21. The compounds that were definitively identified by peak enhancement, which samples were used for the process and their location in the appendix. MHO = 6-methyl-5-hepten-2-one, note RI here on HP1 column.	271
Table 6-1. Overview of compounds that elicited an electrophysiological (E+) or behavioural (B+, attraction, B-, repellency) response in <i>Anopheles gambiae</i> . Concentrations are omitted, as are constituents of complex attractive or repellent blends, as are oviposition behavioural studies. Table adapted from Takken & Knols (2010).	292
Table 6-2. Parasitological information GC-EAG blends, Kenya cohort. LOD = test limit of detection. For further information on parasitological diagnosis and interpretation, see chapter 3. P/ μ L = parasites/ μ L blood, n = number of odour samples. *When species-specific information available ** Highest value was 304 gametocytes / μ L ***RDT positivity was allowed on the basis that these tests can remain positive for some time following curative treatment, due to circulating HRP-2 protein	297
Table 6-3. Proportion of all antennae tested that responded to each peak of interest, per treatment group, in the BMGF dataset. Peaks (identified by retention index, RI) were selected as those that elicited >2 responses in one of the treatment groups, and then fewer responses in other groups were added. Table colour scale according to number of responses. Number of antennal preps per treatment group: Before, 5; During [-], 5; During [+], 3; After, 4; Control, 5. Infection-associated compounds from chapter 5 highlighted yellow.	303

Table 6-4. Proportion of all antennae tested that responded to each peak of interest, per treatment group, in the Kenya dataset. Peaks (identified by retention index, RI) were selected as those that elicited >3 responses in one of the treatment groups, and then fewer responses in other groups were added. Table colour scale according to number of responses. Number of antennal preps per treatment group: Negative (NEG), 7; No gametocyte (NO GAM), 6; Sub-gametocyte (SUB-GAM), 7; Control (CNL), 7. IAC (chapter 5) highlighted yellow.	305
Table 6-5. Antennal responses to compounds revealed to be infection-associated by quantitative analysis of (Kenyan) samples by gas chromatography (chapter 5). Table colour scale according to number of responses.	305
Table 6-6. Type and likely provenance of compounds eliciting electroantennal response in BMGF dataset. Entomological responses of mosquitoes only. RI = retention index, N/A=not applicable. *Indicates compounds found to be EAG-active in both datasets. Entomological responses in the literature, both electrophysiological (E+) or behavioural (B+, attraction, B-, repellency).	314
Table 6-7. Type and likely provenance of compounds eliciting electroantennal response in Kenyan dataset. Entomological responses of mosquitoes only. RI = retention index, NS=not significant, N/A=not applicable. *Indicates compounds found to be EAG-active in both datasets. Entomological responses in the literature, both electrophysiological (E+) or behavioural (B+, attraction, B-, repellency).	317

List of contributions

The work presented in this thesis was a component of a larger, collaborative project. As such, there are parts included herein that were not conducted by the author, but by colleagues. These are acknowledged within, but a concise list of contributions is presented below.

Chapter 2.

1. The controlled human malaria infections ('experimental infections') were conducted by medical colleagues at the department of Medical Microbiology, Radboud University Medical Centre, Geert Grooteplein 26-28, 6525 GA Nijmegen, The Netherlands.
2. Air entrainment sampling of human odour profile in The Netherlands was conducted by Dr Jetske de Boer, although the author assisted at one of the sampling rounds.
3. Gas-chromatography mass-spectrometry here, and additionally in chapter five, was conducted by Dr John Caulfield (Rothamsted Research). The author worked alongside during this process, directing peak identification and assisting.
4. Statistical analysis by REML models was, in this chapter, run by Stephen Powers (Rothamsted Research). The author provided the dataset, discussed the most appropriate model parameters and interpreted the output. Further REML analysis in the thesis (e.g. chapter 5) was conducted by the author, with support from Stephen Powers.
5. Figure 2-2 (experimental infection timeline) was designed by Dr Jetske de Boer.

Chapter 3.

1. All parasitological sample collection conducted in the field (W. Kenya) was done by colleagues at the International Centre of Insect Physiology and Ecology, Mbita, Kenya (specifically Annette O Busula, David John Odoyo and Geoffrey Omondi Olweru). The author assisted with this for a five-week period at the start of the project (January – February 2014), and instigated the collection of rapid diagnostic test (RDT) and Whatman dried blood spot samples.
2. The RDT results, and malaria blood films, were read by David John Odoyo and Geoffrey Omondi Olweru, from the International Centre of Insect Physiology and Ecology, Mbita, Kenya. Re-reading of malaria films was conducted by Angela Hunt-Cooke, at the malaria reference laboratory, LSHTM.
3. The 18S qPCR and QT-NASBA assays were conducted and interpreted by colleagues at the department of Medical Microbiology, Radboud University Medical Centre, Geert Grooteplein 26-28, 6525 GA Nijmegen, The Netherlands. They were interpreted in the context of the other parasitological diagnostic assays, as described here, by the author.
4. Mary Oguike conducted the *Plasmodium ovale* spp. tryptophan-rich antigen (PoTRA) assays to confirm species-specific PCR where necessary.
5. Julian Mwanguzi (LSHTM) conducted the uRDT and wDBS DNA extractions using the QIAasymphony automated system, after the author had prepared the samples for extraction.

Chapter 4.

1. Dr Peter Winskill (Imperial College London, London) assisted with the initial MALDIquant script.

Chapter 5.

1. Air entrainment sampling of human odour profile in Kenya was conducted by colleagues at the International Centre of Insect Physiology and Ecology, Mbita, Kenya (specifically Annette O Busula, David John Odoyo and Geoffrey Omondi Olweru). The author assisted with this for a five-week period at the start of the project (January – February 2014).
2. As described for chapter 3, the 18S qPCR and QT-NASBA assays were conducted and interpreted by colleagues at the department of Medical Microbiology, Radboud University Medical Centre, Geert Grooteplein 26-28, 6525 GA Nijmegen, The Netherlands. They were interpreted in the context of the other parasitological diagnostic assays, as described here, by the author.
3. As described for chapter 2, gas-chromatography mass-spectrometry here, and additionally in chapter five, was conducted by Dr John Caulfield (Rothamsted Research). The author worked alongside during this process, directing peak identification and assisting.

Abbreviations

BMGF: Bill and Melinda Gates Foundation, cohort of individuals in the experimental infections work

COI: Compounds of interest – those thought to have a possible association with *Plasmodium* infection

EAG: Electroantennography

EI-IAC: Experimental-infections infection-associated compounds

GC: Gas chromatography

GC-MS: Gas chromatography-mass spectrometry

GC-EAG: Gas chromatography-electroantennography

IAC: Infection-associated compounds - these found to be statistically associated with infection

LSHTM: London School of Hygiene & Tropical Medicine

NI-IAC: Natural-infections infection-associated compounds

RR: Rothamsted Research

SNR: Signal-to-noise ratio

TIP5A: Cohort of individuals in the experimental infections work

TIP5B: Cohort of individuals in the experimental infections work

tRI: traditional retention index method

UI: Uncertainty interval

WU: Wageningen University

attributable to the improvement of housing and nutrition, due to overall economic development and increased urbanisation (WHO, 2016). Malaria is a disease that is associated with low socioeconomic status, although the direction of causality is unclear (Tusting et al., 2013). Between the years 2005 and 2010, funding for malaria control increased year on year, although it has subsequently fluctuated. This is probably reflective of another threat to malaria control, so-called donor fatigue, brought about by the recent economic crisis (Tusting et al., 2013).

Despite recent gains, in 2015 there were an approximated 212 million cases of malaria (uncertainty interval (UI) 148 – 304 million) which led to approximately 429 000 deaths (UI: 235 000–639 000) globally (WHO, 2016). Of these, 92 % occurred in the WHO African region, 99 % were due to *P. falciparum*, and an estimated 70 % were of children under five years of age (WHO, 2016). This equates to a child dying of malaria every two minutes. Further, although reductions in malaria mortality have been reported in many countries (Chizema-Kawesha et al., 2010; Mmbando et al., 2010; O’Meara et al., 2010; Okiro et al., 2006), for others there is a dearth of data (e.g. countries in Central Africa), or that which exists indicates little change in the malaria burden (Assele et al., 2015). In Central Africa, the absence of data is attributable to a lack of research and poor infrastructure (O’Meara et al., 2010). Malaria is a disease that is treatable and preventable, and disproportionately affects the world’s poor. Apart from the burden on human life, the economic costs of malaria control and elimination are substantial. In 2015, it is estimated that US\$ 2.9 billion was spent to this end.

1.2 Malaria control

Because malaria is a vector-borne disease, for much of the world’s population, mosquito control is the primary preventative measure. Currently, the two most successful control interventions, indoor residual spraying (IRS) and insecticide-treated bed nets (ITNs) (Pluess et al., 2010), are insecticide-based. Expanded coverage of these interventions contributed significantly to the recent declines in malaria; in sub-Saharan Africa the proportion of the at-risk population sleeping under an ITN, or protected by IRS, increased from 37 % (UI 25-48 %) to 57 % (UI 44-70 %) between 2010 and 2015 (WHO, 2016). While the use of IRS declined in 2015, probably due to reduced use of pyrethroids in this context in an attempt to preserve the utility on nets, 53 % of the population at risk in sub-Saharan Africa slept under an ITN in 2015 (95% confidence interval 50–57 %) (WHO, 2016). Other insecticides can be used for IRS, however, costs are greater for insecticides other than pyrethroids or DDT (Macdonald, 2016). The contribution of

vector control to malaria declines is undisputed, yet the prevalence of insecticide resistance across multiple anopheline species is now critical (Seyoum et al., 2014). For both *Anopheles gambiae* and *Anopheles funestus*, susceptible populations are becoming the exception rather than the norm (Ranson and Lissenden, 2016). Populations of *An. gambiae s.l.* that are resistant to all four classes of insecticide available for malaria control have been reported (Cisse et al., 2015; Edi et al., 2012), and 60 of 73 malaria-endemic countries have reported resistance to at least one insecticide since 2010 (WHO, 2016). Furthermore, even under full implementation of the core interventions of ITNs or IRS, effectiveness is dependent on factors other than susceptibility. Under these circumstances, there is now considerable evidence that residual malaria parasite transmission still occurs, due to both human and vector behaviours (WHO, 2014). These include people sleeping outside, or changes in vector behaviour including outdoor biting and resting (Braumah et al., 2005; Oyewole and Awolola, 2006; Russell et al., 2011; Thomsen et al., 2016). Imposing extreme selection pressure on mosquito populations by the continued use of insecticides can be viewed as a zero-sum game.

Universal access to quality-assured vector control rightly remains one of the core interventions advocated by the WHO global technical strategy (GTS) for malaria 2016-2030 (WHO, 2015). Yet, the tools currently available are widely considered to be inadequate for continued use. Five years ago, a Global Plan for Insecticide Resistance Management (GPIRM) was released (WHO, 2012). Then, as well as advocating resistance management strategies and enabling mechanisms, the development of new and innovative vector control tools was advocated (WHO, 2012). The GTS repeats this appeal, and additionally encourages basic parasite and vector research. An even more ambitious Global Vector Control Response strategy has recently been published by the WHO, with an overarching aim of reducing the burden and threat of vector-borne disease worldwide by 2030 (WHO, 2017). Both the percentage of the estimated global burden of communicable diseases that are accountable to vector-borne disease (17 %), and recent major outbreaks including Zika and Yellow Fever, are part of the rationale for this document. Here, all action points are built upon two foundational elements, one of which is to increase basic and applied research that will underpin optimised vector control, and innovate new tools and technologies (WHO, 2017).

1.3 Olfaction

At specific time points in the female mosquitoes' lifecycle, bloodmeals are required to derive sufficient protein to produce eggs. It is during this process, if the mosquito bites a *Plasmodium*-infected individual, that it can become infected with the gametocyte (transmission) stages of the parasite. Mosquitoes primarily use their sense of smell (olfaction) to locate hosts for a bloodmeal. They use a number of cues to locate their hosts, most of which interact with one another (Shen, 2017). Olfaction is the process whereby volatile stimuli are sensed in the olfactory apparatus. The binding of volatile stimuli to olfactory receptors is translated into neural code, and provides the principle sensory interface to the mosquitoes' environment. Olfaction is therefore crucial to life-cycle behaviours, including the location of mates, hosts, oviposition sites, and nectar-feeding sites. Host seeking and blood-feeding behaviours are initiated when the female reaches a certain age, and afterwards, host location is not necessary for another 48 to 72 hours while the eggs mature (Qiu and van Loon, 2010). Regulation of the expression of genes and corresponding abundance of proteins involved in the olfactory pathway, and parallel changes in olfactory sensitivity, have been documented (Davis, 1984a, 1984b; Fox et al., 2001; Gadenne et al., 2016; Qiu et al., 2013; Qiu et al., 2006; Rund et al., 2013; Siju et al., 2010). These studies suggest that mosquito behavioural events, e.g. nocturnal blood-feeding in *Anopheles*, are regulated by genetically-driven changes in the responsiveness of the olfactory system.

A series of behaviours are completed as a blood-feeding insect moves towards a host: activation, orientation and landing (Dekker et al., 2005; Lacey and Cardé, 2011). When initiated at long range from the host (i.e. more than five metres (Dekker et al., 2005)), it is thought that the mosquito responds to a series of olfactory stimuli while moving upwind within an odour plume (Ansell et al., 2002; Cardé and Gibson, 2010) (Table 1-1). The odour plume forms downwind of the host, which is a point source (Gillies, 1980), and mosquitoes orient by flying upwind using optomotor anemotaxis (using visual feedback to regulate manoeuvres, while maintaining a set angle to air flow). It is speculated that mosquitoes will use alternative mechanisms of orientation in still air or at close range, including klinokinesis (turning in response to changes in odour concentration), or following temperature gradients (Cardé and Gibson, 2010). In close proximity, visual and odour cues (Hawkes and Gibson, 2016), body heat (Gillett and Connor, 1976), body humidity (Wright and Kellogg, 1962), fluctuating carbon dioxide (CO₂) (Gillies, 1980) and other kairomones may contribute to host location. The ecology of the mosquito species influences the

extent to which visual cues contribute to host location (i.e. having a greater role in diurnal species (Kennedy, 1940; van Breugel et al., 2015)).

Table 1-1. A simplified overview of odour and visual cues, and their resultant behavioural output, used by female mosquitoes during host location. Mechanosensory input is also important to maintain upwind movement. Table from Cardé and Gibson (2010).

Sensory input and behavioural output	Distance from host			
	> 10 m	~10 – 1 m	~1 m	Host contact
Odour cues	Fluctuating CO ₂	Fluctuating CO ₂ + other kairomones	Fluctuating CO ₂ + other kairomones, heat? Humidity?	Fluctuating CO ₂ + other kairomones inducing landing? heat? Humidity?
Visual cues	Visual surround	Host body	Host body	Host body
Behavioural output	Upwind anemotaxis	Upwind anemotaxis	Hovering near host	Landing on host

1.4 Olfactory apparatus

The olfactory organs of mosquitoes comprise the antennae, proboscis and maxillary palps (Figure 1-2). Air-borne chemical signals (i.e. volatile compounds) are detected by small, porous structures called sensilla, which are present over the surface of these organs (Steinbrecht, 1996). Volatile compounds enter the perforated cuticle of the sensilla, and initiate a signal transduction cascade that ultimately activates olfactory receptor neurons (ORNs) (insect olfaction is reviewed in greater detail in Guidobaldi et al. (2014)). Typically, one sensillum will contain two or more bipolar ORNs and the supporting tissue (auxiliary cells, glia, epidermis and cuticle) (Qiu and van Loon, 2010). During the transduction process within the sensilla, the quality (molecular structure), quantity (concentration), and temporal changes in odorant molecules are converted into neural code in the form of action potentials (Qiu et al., 2006; Qiu and van Loon, 2010). This information is then processed in the olfactory lobe of the insect's brain, subsequently either generating or suppressing a behavioural response (Qiu and van Loon, 2010).

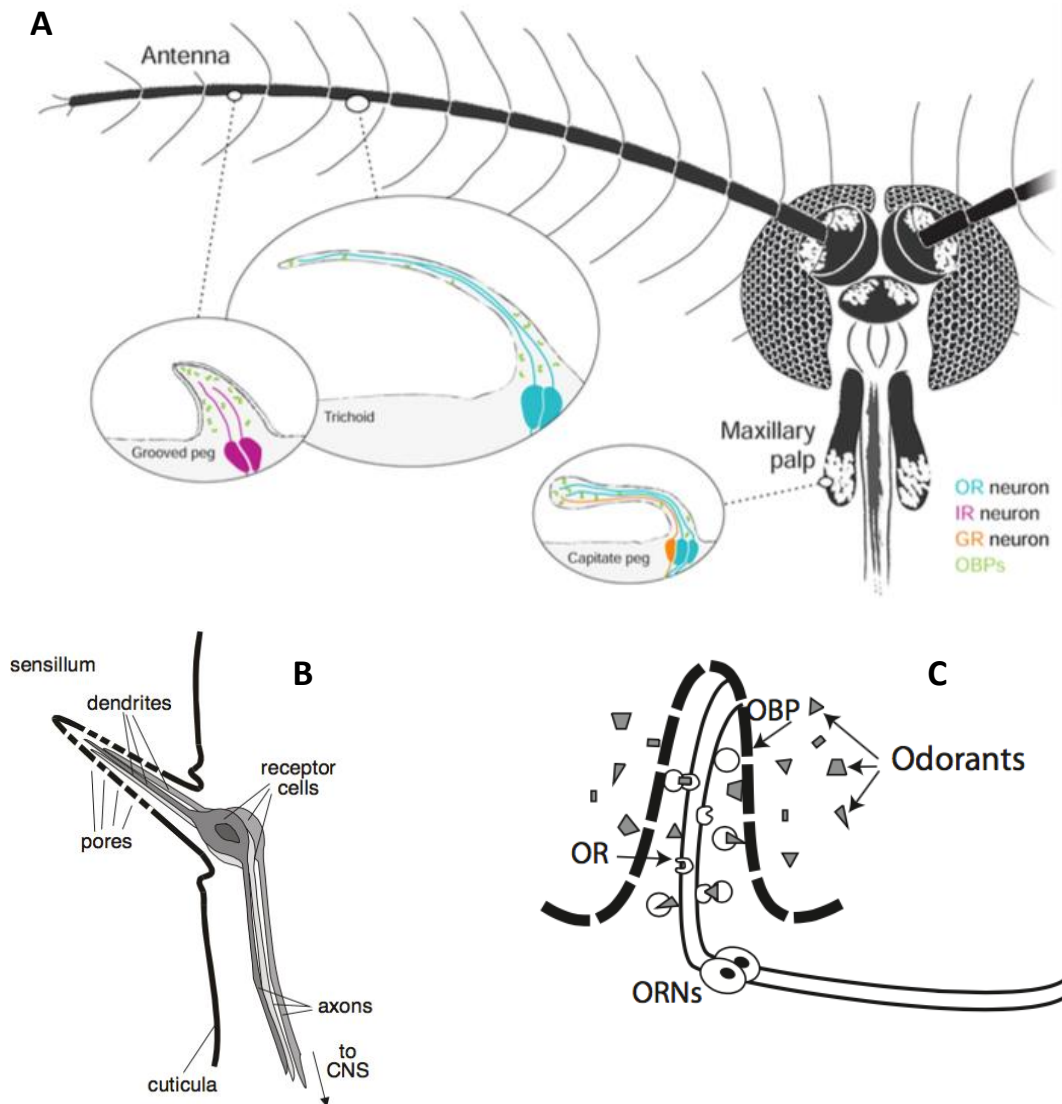


Figure 1-2. The mosquito olfactory apparatus. (A) A schematic of the mosquito olfactory system. The antenna, maxillary palp, and tip of proboscis (not shown) are covered with sensilla, which house olfactory sensory neurons. OR = olfactory receptor, IR = ionotropic receptor, GR = gustatory receptor, OBP = odour binding protein. Taken from McBride (2016). (B) The structural arrangement of olfactory sensillum, the peg-shaped structures that detect odours, showing how dendrites of the olfactory neurons connect to the insect central nervous system (CNS). Taken from Syntech (2004) (C) A schematic showing the functioning sensillum. Odorant molecules enter the perforated cuticle, and are thought to bind to soluble proteins in the sensillum lymph including odour binding proteins (OBP). These transport the odorants to the ORs on the dendritic membrane of the olfactory receptor neuron (ORNs). Taken from Ignell et al. (2011).

Typical olfactory sensilla have a hydrophobic cuticular surface that repels water, yet odour molecules can penetrate it and initiate signal transduction. There are three major morphological types of sensilla: trichoid and grooved peg sensilla, found on the antennae, and capitate peg sensilla, found on the maxillary palps (McBride, 2016) (Figure 1-2). Three types of trichoid sensilla (T1–T3) are found on the labellar lobe of the proboscis of mosquitoes (Qiu and van Loon, 2010). Within the sensilla, receptors on the maxillary palps play an important role in the

detection of CO₂ (Grant et al., 1995), while those on the labellum are predominantly gustatory (Kwon et al., 2006).

When an odour molecule passes through a sensillar pore, it enters an aqueous environment known as the sensillum lymph. Odour molecules are thought to be transported through the lymph to olfactory receptors by binding to soluble proteins, including odorant-binding proteins (OBPs) and possibly the similar, binding, chemosensory proteins (CSPs) (Iovinella et al., 2013). It is thought that the transmembrane sensory neuron membrane proteins (SNMPs) associate odour ligands with olfactory receptor proteins (ORs) (Bohbot et al., 2010), a spectrum of which are found on the dendrite membrane of ORNs (Suh et al., 2014). The specificity profile of 54 ORs of *An. gambiae* has been characterised, revealing both broadly and narrow-tuned ORs (Qiu et al., 2013). Relative to other components of the olfactory signal transduction pathway, the role of ORs is well characterised, and to date 79 candidate *Or* genes have been identified in the genome of *An. gambiae* (Carey et al., 2010; Hill et al., 2002). The functional OR in insects is a heteromeric complex, which acts as a ligand-dependent ion channel (Ray et al., 2014). It is composed of a conventional yet divergent OR that dictates the odorant binding specificity of that ORN (ORx), and a highly conserved, non-conventional co-receptor which appears to be functionally orthologous across all insects, known as Orco. This receptor functions as a co-receptor chaperone for the specific ORN (Vosshall and Hansson, 2011), and is thought to be expressed in the majority of olfactory neurons of *An. gambiae* (Riabinina et al., 2016). *Aedes aegypti* defective in Orco have been shown to be impaired in their ability to discriminate between hosts, indicating a role of the OR/Orco pathway in host specificity (DeGennaro et al., 2013). In addition to ORs, gustatory receptors (GRs) (reviewed in Suh et al. (2014)) and ionotropic receptors (IRs) (Liu et al., 2010) have been described for *An. gambiae*. To ensure appropriate signalling in space and time, the transduction cascade must subsequently be terminated, and receptors deactivated. Arrestin proteins function by competing for binding sites within the activated, phosphorylated form of the receptor, preventing further signal transduction (Walker 2008).

1.5 The attractiveness of human hosts to mosquitoes

Inter-individual differences in attractiveness to mosquitoes and other haematophagous insects is commonly recognised, and this is supported by a large body of evidence (Bernier et al. 2002; Brady 1997; Knols et al. 1995; Lindsay et al. 1993; Qiu et al. 2006; Verhulst et al. 2011; Khan et

al. 1969). Although an individual's 'innate' attractiveness is thought to fluctuate temporally (i.e. in time) to some degree (Bernier et al., 2002), it remains constant enough to permit ranking of 'attractiveness' relative to others, that holds over time (Knols et al. 1995; Logan et al. 2008; Bernier et al. 2002; Qiu et al. 2006). Many factors have been implicated in this variation in attractiveness, including sweating (Healy and Copland, 2000; Khan et al., 1969), age (Muirhead-Thomson, 1951; Spencer, 1967; Thomas, 1951), age-related attractiveness ascribed to differences in body weight and surface area (Port and Boreham, 1980), sex or hormones (Gilbert et al., 1966; Muirhead-Thomson, 1951), hereditary factors (Fernández-Grandon et al., 2015; Logan et al., 2010a) and pregnancy (Ansell et al., 2002; Himeidan et al., 2004; Lindsay et al., 2000). The potential for confounding between these factors should be acknowledged. Several studies have eliminated factors other than olfactory cues, and determined that the variability in attractiveness, irrespective of the proximate cause, can be entirely accounted for by body odour (Qiu et al. 2006; Schreck et al. 1990; Logan et al. 2008).

1.6 Olfactory cues used for host location

Carbon dioxide, emitted in large amounts on the breath and also in small amounts by the microflora present on human skin, is an important activator to haematophagous insects during host location (Dekker et al., 2005; Healy and Copland, 1995; Smallegange et al., 2011). However, it is thought that CO₂ only accounts for approximately 50 % of the attraction of the anthropophilic *An. gambiae* s.s. to humans (Costantini et al., 2001). One reason for this is that CO₂ is not a species-specific cue (Braks et al., 1999; Knols and De Jong, 1996); however, it has been reasoned that vertebrates do release CO₂ at rates according to both body size and metabolic rate (Smallegange et al., 2011). CO₂ naturally occurs in the atmosphere, at a concentration of 0.03 to 0.04 %, which means that over certain distances dilution of host-derived CO₂ will make detection against atmospheric CO₂ impossible (Knols, 1996). The most important host location cues are other host-specific chemicals, odours that originate from the body and breath, which act synergistically with CO₂ (Ray, 2015). Body odour can be detected at distances of up to 20 metres (Knols, 1996), and importantly, is highly host-specific.

Of the hundreds of compounds that have been associated with the human odour profile, many have been shown to elicit nervous signalling in the antennae and subsequent behavioural responses in *An. gambiae*. Determining which volatile compounds are most important in the location of a human host is a rapidly expanding field in entomology and chemical ecology. Human odour is mainly a result of chemicals emanating from the skin. These constitute human-

derived compounds originating from sweat glands or skin cells, by-products of the microbiome (commensal microorganisms that inhabit the skin and function to protect the body from invasive organisms) and other processes, and environmental contaminants (Rebollar-Téllez, 2005). Three types of secretory gland are found on the human skin: the eccrine, sebaceous and apocrine glands. These are differentially distributed over the body, each concentrated in regions appropriate to their function. Eccrine glands produce odourless sweat and are distributed across the skin surface, but with increased density on the hands and feet. Sebaceous glands are also found all over the body but particularly on the head, and these secrete sebum and lipids. Apocrine glands are found primarily in the axillae and genital regions, and these secrete proteins, lipids and steroids (Dormont et al., 2013). The secretions of these glands are modified and metabolised by the microbiome, giving odourless sweat a smell (Shelley et al., 1953). Many of the components of body odour that are known to be involved in haematophagous insect attraction are products of these microorganisms rather than the glands themselves. Early studies of mosquito attractants hypothesised a possible role for the microbiome, observing the decreased attractiveness of freshly washed hands relative to those unwashed for several hours (Schreck and James, 1968), and the increased attractiveness of houses of unwashed, relative to washed, individuals (Haddow, 1942). The role of the skin microbiome in mosquito attraction is now established (De Jong and Knols, 1995; Verhulst et al., 2011, 2010b), indeed, bacterial cultures have been demonstrated to elicit equivalent attractiveness to skin volatile samples (Verhulst et al., 2010a, 2009). Further to this, fresh, non-incubated sweat has been shown to be unattractive to mosquitoes, while sweat allowed to incubate with skin flora attracted mosquitoes (Braks and Takken, 1999). An individual's microbiome composition (and the resultant odour profile, as different bacteria species' metabolism will produce unique by-products) is known both to be unique (Fierer et al., 2010), and remain relatively constant over time (Costello et al., 2009). Significant associations between higher bacterial abundance, lowered bacterial diversity and increased attractiveness to mosquitoes have been shown (Verhulst et al., 2011), and it is thought that this unique microbiota 'profile' could be genetically influenced, e.g. by HLA genes (Penn and Potts, 1998; Verhulst et al., 2013). In all, this could provide, or contribute to, a basis for heritability of attractiveness, as demonstrated by Fernández-Grandon et al. (2015).

Dormont et al. (2013) published a table of the 25 most frequently isolated compounds from human skin, based on the results of 31 studies. Relatively few chemical families were represented, including: carboxylic acids of various chain lengths and derivative esters,

aldehydes, alkanes, short chain alcohols, and some ketones. Four compounds were often found to dominate the volatile profile; 6-methyl-5-hepten-2-one, nonanal, decanal, and (*E*)-6,10-dimethyl-5,9-undecadien-2-one (geranylacetone). As many as 350 compounds have been demonstrated to occur in the human volatile odour profile (Dormont et al., 2013). Although the odour responsible for attracting mosquitoes constitutes a blend of compounds, not all contribute (Zwiebel and Takken, 2004). Some volatile compounds in skin odour have been empirically demonstrated to be mosquito attractants, including carboxylic acids (Cork and Park, 1996; Costantini et al., 2001; Meijerink and van Loon, 1999; Smallegange and Takken, 2010), aliphatic fatty acids (van den Broek & den Otter 1999; Bosch et al. 2000; Verhulst et al. 2010), lactic acid (Carlson 1973; Acree et al. 1968), ammonia (Braks et al. 2001; Smallegange & Takken 2009), 1-octen-3-ol (Takken et al. 1997; Lu et al. 2007; Kemme et al. 1993; Kline et al. 1990) and acetone (Takken and Knols, 1999). It has been suggested that the relatively greater amounts of carboxylic acids and lactic acid found on human skin may enable anthropophilic mosquito species to differentiate humans from other vertebrates (Smallegange et al., 2011). Because of the heightened attraction of some mosquitoes to foot odour (De Jong and Knols, 1995), foot-specific bacterial profiles and their metabolic products have been investigated. Fatty acids can be produced via breakdown of triglycerides to free glycerol by skin bacteria including *Corynebacterium* and *Malessezia* (Takken and Knols, 1999). Lower fatty acids, e.g. isovaleric acid (3-methylbutanoic acid), are thought to be produced by the foot microflora (including *Staphylococcus* species and aerobic coryneform bacteria) during the metabolism of products of the eccrine and sebaceous glands (Ara et al., 2006).

Generally, research in this field has focussed on the identification of compounds in the human odour profile that are attractive to mosquitoes, because of their possible exploitation as lures, as well as the necessity to understand mechanisms of attraction. However, while characterising differences in skin odour profile between highly- and poorly-attractive people, increased production of compounds found to interfere with attractiveness by the latter group was shown (Logan et al., 2010b, 2008). So-called 'maskers', that block attraction (Ray, 2015), have been documented in other vertebrate species, e.g. unattractive cattle producing more 6-methyl-5-hepten-2-one were protected from the horn fly (*Haematobia irritans*) (Birkett et al., 2004), and the reticulated giraffe (*Giraffa camelopardalis*) has been shown to produce compounds that repel ectoparasites (Wood and Weldon, 2002).

1.7 Infection and body odour

It is known that some pathological processes, including metabolic disease, genetic disorders and other infections, can influence human odour (Shirasu and Touhara, 2011). Smell has been used as a diagnostic tool for centuries; Hippocrates noted, around 400 BC, the association of particular odours in urine and sputum with disease (Lloyd, 1983). One of the originators of ancient Hindu medicine, Susruta Samhita, is reputed to have said almost 2000 years ago 'by the sense of smell we can recognize the peculiar perspiration of many diseases, which has an important bearing on their identification' (Liddell, 1976). Only some decades ago, the odour that a patient emitted was cited as one of the first major clues for diagnosis (Liddell, 1976), with particular odours described from conditions including diabetic ketosis (ketones on the patient's breath giving a fruity aroma like decomposing apples), typhoid (freshly baked brown bread smell), or Yellow Fever (the smell of a butcher's shop). In recent years, and with the advent of highly sensitive analytical equipment that can be used to decipher odour signals, the smell of disease is receiving renewed attention as a diagnostic tool. Disease-associated volatile compounds, if sufficiently specific, can be thought of as biomarkers. Several studies have investigated the diagnosis of *Mycobacterium tuberculosis* (TB) by detection of emitted volatile compounds. These include studies of cultures of the bacterium itself (Syhre et al., 2008), or the breath of affected patients (Phillips et al., 2007; Syhre et al., 2009). A recent paper even investigated the possibility of training honeybees (*Apis mellifera*) to detect the volatiles associated with TB in culture (Suckling and Sagar, 2011). The possibility of detecting TB-specific volatiles in the breath is enhanced by the pulmonary location of the disease, and traditional laboratory diagnosis is hindered by the slow growth rate of this organism (myco, i.e. 'fungal'), thus novel techniques are desirable. Similarly, the detection of lung cancer by breath volatiles has received some attention, with correlations being found between the volatile compounds detected from lung cancer culture medium and the breath of patients (Chen et al., 2007). Sniffer dogs have successfully distinguished the breath of both lung and breast cancer patients from healthy controls with high degrees of sensitivity and specificity (McCulloch, 2006), and 'diabetic alert dogs' are trained to indicate hypoglycaemic episodes to their diabetic owners (Chen et al., 2000). While in practice the physiological basis for detection may include behavioural, in addition to olfactory, cues, dog recognition of hypoglycaemia from perspiration samples alone has been experimentally demonstrated (Hardin et al., 2015).

The importance of these studies in the context of mosquito olfaction is as follows. The 'scent of disease' principle is now widely accepted and increasingly discussed in the literature, and this is

supportive of the possibility that malarious individuals may smell differently. Further, there is an increasingly large body of evidence that suggests malaria parasites may manipulate vertebrate host attractiveness to mosquitoes, to influence their onwards transmission. Given the crucial importance of body odour to mosquito host location, and the proposition that body odour can be altered during disease, here we hypothesise that the host odour profile is a likely target for *Plasmodium* parasite manipulation.

1.8 Parasite manipulation

That parasites may manipulate the attractiveness of hosts in order to maximise transmission is a logical prediction according to evolutionary theory, as any infection effect that increases mosquito-vertebrate contact rates would result in preferential spread of the infecting parasites. It is advantageous for pathogens to exert influence over their transmission to the next host, particularly when considering the population bottleneck that transmission manifests (Poulin, 2010). This is relevant both when parasites are transmitted to the mosquito and to the vertebrate. The benefits to *Plasmodium* parasites within their vertebrate hosts of attracting mosquitoes, thus increasing mosquito-vector contacts, are therefore apparent. However, what is less clear are the repercussions for the mosquito.

The female mosquito's fitness entirely depends on taking a bloodmeal to produce eggs. However, the impact of becoming infected with *Plasmodium* parasites during this process is still debated. Some studies have shown that infected bloodmeals are associated with large fitness costs, including reductions in fecundity (i.e. reduced egg production) (Ferguson et al., 2003b; Freier and Friedman, 1976; Hacker, 1971; Hogg and Hurd, 1997, 1995a, 1995b; Hurd et al., 2005; Vézilier et al., 2012) and shorter lifespan of infected mosquitoes (Anderson et al., 1999; Dawes et al., 2009; Ferguson et al., 2003a; Ferguson and Read, 2002), possibly due to the costly immune defence or stress (Aboagye-Antwi et al., 2010). One study argued that reductions in fecundity are countered by an increase in longevity (Vézilier et al., 2012). In other studies, the reduction in fecundity was only observed under specific conditions, e.g. infection with multiple parasite genotypes (Ferguson et al., 2003b), or a reduction in vector survivorship was not observed (Chege and Beier, 1990; Robert et al., 1990). Further, reductions in fecundity have been associated with a decrease in bloodmeal size, thought to be caused by high density parasite infections, rather than the presence of oocysts *per se* (Ferguson et al., 2003b).

Chapter 1: Literature review

However, mosquitoes may experience advantages from feeding on infected hosts, including reduced defensiveness (Day et al., 1983), faster engorgement due to reduced host platelets (thrombocytopenia) (Rossignol et al., 1985), or reduced haematocrit (Daniel and Kingsolver, 1983). Thrombocytopenia is a common sequelae in vector-borne infections (Rossignol et al., 1985), and is well known in clinical malaria (Lacerda et al., 2011). Contrary to the findings of Ferguson et al. (2003), where mixed (parasite) genotype infections and high parasite density correlated with reduced bloodmeal size, *Anopheles* feeding from *Plasmodium*-infected mice were found to benefit from an increased bloodmeal size (Taylor and Hurd, 2001). It is likely that the fecundity of infected mosquitoes is determined by several (interlinked) factors, including blood meal quantity and quality (Hurd, 2003), parasite factors including load and genotype, and environmental conditions (Sangare et al., 2013). This makes it difficult to speculate if the evolution of infected-host avoidance would be advantageous to the mosquito. Further, it could be that the 'infected individual' signal is cryptic, an exaggerated normal host cue: a 'supernormal stimulus' (Dawkins and Krebs, 1979). In this instance, if *Plasmodium* parasites in the vertebrate host manipulate odour cues used by blood-seeking mosquitoes, evolution for avoidance by mosquitoes would result in avoidance of bloodmeals, and the resultant zero-offspring fitness cost.

Host manipulation can be defined as any alteration in host phenotype, induced by a parasite, that confers fitness benefits to the parasite (Poulin, 2010). It has been stated that this should be distinguished from differences in pathology between infected and uninfected individuals, that are coincidentally beneficial to the parasite (Poulin, 2010). However, a co-incidental effect of pathology that is beneficial to a parasite still derives from the infection, thus the parasites responsible for that effect would probably be selected for. It has been stated that "it seems clear that natural selection will rarely be indifferent to pathological effects of infection that significantly influence parasite transmission" (Mauck et al., 2010, p. 3600). Although the distinction of these two scenarios is therefore questionable, four criteria have been proposed to help differentiate them (Poulin, 1995), explained simply as (1) changes should conform to expectations for increased transmission, (2) complex changes are to be regarded as suspect, as they are less likely to arise spontaneously, (3) evolutionary convergence of these changes between unrelated lineages is supportive, and (4) the trait must confer fitness benefits to the parasite.

In the specific case of *Plasmodium* manipulation of vertebrate attractiveness, the first, third and fourth criteria are likely met. The second relies upon the underlying mechanism, which is suspected but thus far unproven. We hypothesise that *Plasmodium* parasites manipulate the vertebrate host odour profile, to influence host attractiveness to mosquitoes and therefore increase their own transmission probability. The complexity of a mechanism that governs change in odour profile may become apparent upon experimental demonstration of this phenomenon, as the identity of chemical compounds may allude to their provenance. To date, there is some 'direct' evidence of an influence of *Plasmodium* infection on vertebrate host attractiveness, as assayed by variables including mosquito host choice, engorgement success or the number of successful bloodmeals. Additionally, there is some 'indirect' evidence, including detection of compounds produced by *Plasmodium*-infected red blood cells that are attractive to mosquitoes, and the clustering of malaria cases that is not fully explained by other variables.

1.9 Direct evidence for *Plasmodium* manipulation of vertebrate host attractiveness

Recently, evidence from the current project indicated that 5-12 year old children in Kenya who were infected with gametocytes at microscopic densities were almost two times more attractive to *An. gambiae* than comparative groups: parasite-free individuals, those with asexual parasites or those with sub-microscopic gametocyte densities (Busula et al., 2017). This study essentially repeated work conducted by Lacroix et al. (2005), where attractiveness was seen to be approximately double in children harbouring gametocytes, relative to those with asexual stages or no parasites. This effect was nullified on treatment with the antimalarial Fansidar (sulfadoxine/pyrimethamine). The results of the Lacroix study were weakened by several methodological shortcomings, however, including low numbers of responding mosquitoes, a lack of controlling for positional bias in the experimental design (each individual was not tested in each location), and inappropriate antimalarial treatment. Fansidar is known to increase gametocyte prevalence and density (Putu and Manyando, 1997), and poor parasite clearance upon treatment with Fansidar had recently been reported in the area (Bousema et al., 2003). Because the investigators detected *Plasmodium* infections by microscopy, the results instead represented a comparison of the attractiveness of individuals with intense infection relative to low-level infection. These issues were addressed by Busula et al. (2017) with a rigorous experimental design, molecular diagnostic methods, and appropriate drug treatment (artemether-lumefantrine) that was confirmed to be curative. Following treatment, the

Chapter 1: Literature review

attractiveness of children returned to levels similar to that of children harbouring low-density gametocytes, asexual stages or no parasites.

Very few studies of this phenomenon in the human malaria system have been conducted. One examined short-range attraction of *An. darlingi* to patients infected with *Plasmodium vivax* in Brazil (Batista et al., 2014). Again, individuals harbouring gametocytes were found to be significantly more attractive than non-gametocyte carriers. Further, febrile patients bearing gametocytes were found to be significantly more attractive than febrile patients without gametocytes, indicating a synergistic effect of elevated body temperature and the presence of gametocytes on attractiveness. In follow-up experiments, post-treatment, no significant differences in attractiveness between the individuals were observed. While these are intriguing results, again, aspects of the methodology are questionable. Participants were not tested for *P. vivax* infection in follow-up experiments and post-treatment. Given the nature of the research question, an assumption of treatment efficacy is surprising, and the possibility of treatment failure should be acknowledged. The authors do not explicitly state which antimalarials were used. If primaquine and chloroquine were used, as is likely in this setting (Prof. G. Targett, pers.comm., 12/2014), treatment regimens can span two weeks. If so, only the final experiment was conducted after treatment was complete. Although 11 participants were recruited to this study, only six (three with and three without gametocytes) were followed up for all three time points. Further details concerning the participants, which might have influenced the findings, are lacking. Attractiveness to mosquitoes is affected by a number of characteristics, possibly including gender and age (Gilbert et al., 1966; Muirhead-Thomson, 1951). Participants in this study were aged 20 to 50 years and of both sexes, raising questions regarding appropriate matching between study groups. Taken together, these issues preclude any firm conclusions being drawn regarding an association between host attractiveness to mosquitoes and *P. vivax* infection status.

A larger body of evidence for increased attractiveness of *Plasmodium*-infected individuals is available in model malaria systems, particularly murine and avian. Some of the first studies conducted in this field remain convincing today (Day et al., 1983; Day and Edman, 1983), although consideration should be given to the use of non-anopheline mosquito species. These studies were designed to examine the possibility that a reduction in 'anti-mosquito' behaviour by individuals infected with *Plasmodium chabaudi*, *P. berghei* or *P. yoelii* was responsible for increased mosquito engorgement success, which was observed on specific days post-infection

only. Decreased activity of the (unrestrained) mice indeed correlated with periods of increased *Ae. aegypti* and *Culex quinquefasciatus* engorgement success, as did, however, peaks in bloodstream parasite density and gametocytaemia (Day and Edman, 1983). Therefore, an alternative explanation for the observed effects might be that the bloodstream parasites present influenced the feeding preferences or behaviours of the mosquitoes. A subsequent publication repeated these results, although motor activity was not recorded (Day et al., 1983), and additionally the engorgement success of *Ae. aegypti* fed on mice infected with *Leishmania major amazonensis*, alone or in mixed infections with *Plasmodium*, was compared (Coleman et al., 1988). Here, engorgement success on mice infected with both pathogens was greatest, relative to the increased engorgement on *Plasmodium*-infected mice as was previously observed. Again, the entomological effects could be explained by either activity patterns or parasite density. No increased engorgement was observed on the *L. amazonensis*-infected mice, and the mixed infection group experienced the highest *Plasmodium* parasitaemias (35 %). Mice infected with *Plasmodium* alone demonstrated a maximal parasitaemia of 15 %.

The hypothesis that increased feeding on infected hosts is a result of decreased defensive behaviour was challenged by the finding that *An. stephensi* mosquitoes retained the preference in immobilised mice for *P. chaboudi*-infected, relative to uninfected, hosts (Ferguson et al. 2003). Here, among the infected hosts, feeding propensity rose with both asexual- and gametocyte-stage density, which were themselves correlated. By combining the effects of asexual parasite density, gametocyte density and red blood cell density in a single model to predict the proportion of mosquitoes feeding, only the significance of asexual parasite density remained.

Thus far, only one study concerning the increased attractiveness of *Plasmodium*-infected individuals has included an investigation of the underlying mechanism (De Moraes et al., 2014). Attraction of *An. stephensi* to *P. chaboudi*-infected mice, relative to healthy mice, was found to be significantly greater in the later stages of infection and when gametocyte levels are typically high. Further, among those infected mice, mosquito preference was greater for those harbouring detectable gametocytes. The investigators incriminated odour cues alone for the described alterations in attractiveness, by sampling whole-body odour and testing those samples for attractiveness to mosquitoes. While in early-stage infection there was a significant preference for 'healthy' volatiles, later on and when gametocytes were more prevalent, there was a significant preference for 'infected' volatiles. Following odour profile analysis, the

characteristic components of 'infected' odour were identified and subsequently confirmed to increase mosquito attraction individually, when added to the odour of healthy mice. This is noteworthy, given that odour detection is highly contextual (Mcbride, 2016). As the other infection-associated compounds were omitted during the testing of each compound, the artificial 'infected' odour would not have represented the natural 'infected' odour blend. Overall, clear differences in the volatile profile of infected versus healthy individuals were revealed, and statistical techniques could reliably predict infection status in the latter stages of infection. This study, therefore, strongly indicates that infection-associated changes in host attractiveness manifest from changes in the odour profile.

Studies of an avian malaria system have provided some of the most compelling evidence of *Plasmodium*-induced changes in attractiveness to date. Cornet et al. (2012) presented *Culex pipiens* mosquitoes with the choice of pairs of birds, one parasite-free and one infected with *Plasmodium relictum*. Host choice, assayed by blood feeding, was measured pre-infection, during acute infection and in the chronic phase (later stages of infection). During the chronic phase of the infection only, there was a clear preference for the infected birds, however, in this malaria system gametocytes are strongly present in both acute and chronic phases. Preference could not be attributed to reduced defensiveness, as the birds were immobilised. Interestingly, there was a consistent preference for birds with higher haematocrits at all three time points, an effect that appeared to be overridden by strong attraction to the infected bird at the chronic time point. One explanation proposed for the temporal differences in response to infected individuals was that the observed behaviour resulted from the strength of two opposing effects: parasite-induced attraction vs. poor quality bloodmeal-associated repellency. Preferential attraction to chronically infected birds was corroborated in a further study (Cornet et al., 2013). By offering both the parasite-infected and the parasite-free individuals simultaneously, these dual-choice assays provide compelling evidence of host preference.

1.10 Parasite manipulation of host attractiveness in other vector-borne diseases

As discussed, evolutionary convergence of possible parasite manipulation phenomena between unrelated lineages is supportive of true manipulation (Poulin, 2010). Increased attractiveness of vertebrate hosts in vector-borne disease systems has also been documented in leishmaniasis, Rift Valley fever and trypanosomiasis.

O'Shea et al. (2002) tested the attractiveness of hamsters infected with *Leishmania infantum* to *Lutzomyia longipalpis*, relative to age- and sex- matched controls. Odour alone was assayed, by use of a wind tunnel. In two experiments, each comprising two pairs, the infected hamsters were found to be more attractive. However, testing only two individuals per experiment leaves no margin for individual variation in attractiveness. It is likely that this phenomenon, well-known in humans (Logan et al. 2008; Qiu et al. 2006; Verhulst et al. 2013), is also observed in other vertebrate species. Although volatile compounds specific to the odour of infected animals were detected by analytical chemistry, these were not identified. Again, with such a small sample size, the detection of compounds truly associated with infection, and not with inter-individual variation, seems unlikely. An older but similar study examined the feeding behaviour of *Lu. longipalpis* on mice infected with *L. mexicana amazonensis*, but here sandflies were allowed access to the anaesthetised mice (Coleman and Edman, 1988). Significantly more insects probed on infected relative to uninfected mice, and those probing events occurred on the infected foot at the site of the leishmaniasis lesion. The authors propose that the infection induced blood vessel dilation, which possibly aided blood meal availability through the epidermis of the lesion. Here, insect feeding times did not vary between infected and uninfected hosts. It is possible that the skin lesion area was warmer, which may cause increased feeding (Gillett and Connor, 1976), but a further hypothesis is the localised emission of infection-specific, attractive, volatiles. Again, this study presents altered vector feeding parameters in response to infected vertebrate hosts, results which are compatible with increased attractiveness (mediated by odour profile) of the infected individual.

In a different disease system, *Cx. pipiens* feeding was observed on twin lamb pairs, one infected with Rift Valley Fever (RVF) and the other uninfected (Turell et al., 1984). Increased feeding on the viraemic lamb was reported, and attributed to increased host temperature and reduced defensiveness, in accordance with the paradigm at that time (Day et al., 1983; Day and Edman, 1983). It is also possible that infection increased the attractiveness of the infected individual. However, data were interpreted in a slightly misleading manner. Mosquitoes were allowed to feed on either lamb for three hours, and feeding on the viraemic lamb was assayed by detection of virus in the mosquitoes. Across all feeding events, 65 % of engorged mosquitoes were found to contain virus, leading the authors to conclude that even accounting for mixed feedings, 65 % is a deviation from the null hypothesis of 50 % feeding on either lamb. It is possible that mixed feeding (mosquitoes feeding on both lambs) was minimal, and these data do indicate mosquito preference for the infected lamb. Evidence from another study indicated that mixed feeding

Chapter 1: Literature review

could, and might, have caused mechanical transmission (Hoch et al., 1985). In that case, that the control lambs remained virus negative throughout the study is supportive of minimal mixed feeding. However, if mixed feeding did occur (not causing mechanical transmission), the data are synonymous with 65% mosquitoes feeding on the viraemic lamb and, for example, 100 % on the control lamb, as feeding on the control lamb was not assayed. In this scenario, the 65 % simply indicates the proportion of mixed feeding. Further, this study concerned only five pairs of lambs, therefore it is possible that the viraemic lamb was innately more attractive. Although the study stated the use of twin lambs, sheep twins are often not identical, therefore with differing genetic make-up.

In the trypanosoma-tsetse system, significantly increased engorgement success (75 % greater) was observed in *Glossina pallidipes* feeding on *Trypanosoma congolense*-infected cattle, relative to uninfected cattle (Baylis and Nambiro, 1993). Here, cattle were individually assayed for attractiveness by the number of tsetse flies approaching or leaving ('relative catch'), and the engorgement success of those flies was recorded. Although no difference in attractiveness between infected and uninfected individuals was observed, engorgement success on infected cattle was greater. That this difference was noted in the absence of increased attractiveness is indicative of variation in parameters that affect blood feeding. Cattle with very low packed cell volume (PCV<20) were excluded, but overall, infected individuals still had a significantly lower PCV. Although this may have increased ease of fly feeding, independently, there was no correlation between PCV and feeding success in either infected or uninfected cattle. Additionally, having corrected for PCV, there was no effect of infection on bloodmeal size. Although this study presents intriguing evidence of an influence of parasite infection of the vertebrate host on vector feeding parameters, the results are difficult to explain and not synonymous with increased attraction via host odour profile, as this would likely have been manifested as variation in relative catch.

In another similar experiment, parameters of *G. pallidipes* feeding on cattle were again measured, but cattle infections were either *T. vivax* or *T. congolense* (Baylis and Mbwabi, 1995). Feeding success (engorgement) was again greater on *T. congolense*-infected cattle, by approximately 60 % (a result that approached, but was not, significant). However, feeding success on *T. vivax*-infected cattle was equivalent to that on 'uninfected' cattle (in reality, these cattle may have harboured sub-microscopic parasites). Unlike the previous study however, *T. congolense*-infected cattle were found to attract more flies, with 70 % greater trap catches than

uninfected cattle or those infected with *T. vivax*. There was no relationship between infection status and anti-fly movement or body temperature, and between the two infected groups there was no variation in platelet concentration or packed cell volume. Here, the increase in *T. congolense*-infected host attractiveness could be explained by variation in odour profile; however, the lack of influence by *T. vivax* is curious.

1.11 No increased attractiveness with parasite infection

Other studies have found either no influence of parasite infection on host attractiveness, or a negative influence of infection. Freier & Friedman (1976) investigated several parameters of mosquito blood-feeding on *Plasmodium*-infected chickens, using the non-malaria vector species *Ae. aegypti*. In a series of experiments, smaller bloodmeals, reduced feeding on immobilised birds, and then reduced probing towards birds that were beyond reach were observed towards infected birds. In a more recent wind tunnel experiment, examining olfactory cues alone, *Plasmodium*-infected *Parus major* (Great Tits) were significantly less attractive to the natural avian malaria vector *Cx. pipiens* than their uninfected counterparts (Lalubin et al., 2012). As stated by the authors, it may be that the observed effects, which are counter to most literature on the subject, are the result of divergent evolution in these different malaria systems. In humans, the influence of both *Plasmodium* parasites and *Wuchereria bancrofti* bloodstream parasites on *Anopheles* host preference was measured in villages in Papua New Guinea (Burkot et al., 1989). Engorgement rates were non-random, with preference for both infected and uninfected persons, with either parasite species, documented in different houses. Finally, in a dual-choice experiment with two *Plasmodium*-infected humans only, each individual in turn became relatively less attractive to *An. gambiae* for the duration of symptoms (noted as fever and profuse sweating) (Mukabana et al., 2007). This study, however, included only two individuals who naturally differed in attractiveness, and as such the conclusions that can be drawn are limited.

1.12 Indirect evidence for *Plasmodium* manipulation of vertebrate host attractiveness

1.12.1 Production of compounds by *Plasmodium*-infected red blood cells

Some studies have investigated the possible production of volatile compounds from *Plasmodium*-infected red blood cells, hypothesising release of the compounds from the bloodstream into the general odour profile and a subsequent influence on host attractiveness. In one study, several compounds were found specifically and consistently in the headspace (air sampled directly above) of parasite-infected red blood cells (iRBC), of which two were terpenes (Kelly et al., 2015). In samples collected above all five *P. falciparum*-infected cultures tested, at least one 10-carbon monoterpene was detected. The apparent significance of this finding was that apicomplexan parasites, including *Plasmodium* species, contain an apicoplast (an organelle with a similar endosymbiotic evolutionary origin to plant chloroplasts) that synthesises isoprenoids via a specific metabolic route, not found in animals (the methylerythritol phosphate (MEP) pathway). Isoprenoids are a large group of some 30,000 compounds that serve multiple biochemical functions, including roles in electron transport chains, as membrane components, and as hormones (Lange et al., 2000). Terpenes belong to the isoprenoid class, and could be produced by the MEP pathway. By blocking this (here, parasite-specific) MEP pathway, and observing a dramatic decrease in isoprenoid production, the authors further demonstrated likely parasite-specific production of these terpenes. Finally, to demonstrate a possible role in mosquito attraction, the electrophysiological response of *An. gambiae* receptor neurons to these compounds was assayed (via a *Drosophila* expression system). While responses were generated, it is noted that these compounds are known attractants for *An. gambiae* (Nyasembe et al., 2012), involved in nectar-seeking behaviours, and so neuronal response is expected. Although a compelling story is presented, only the production of isoprenoids by *Plasmodium*-iRBC cultures and the response of *An. gambiae* neurons to (known attractant) terpenoid volatiles is supported by empirical evidence. However, the study certainly suggests that further investigation of the proposed pathway is merited.

In a similar, more recent, study, Emami et al. (2017) investigated another aspect of the MEP pathway, involving (*E*)-4-hydroxy-3-methyl-but-2-enyl pyrophosphate (HMBPP), which is a precursor in the synthesis of isoprenoids. They found HMBPP-supplemented RBCs (hmbRBCs) to be relatively more attractive to female *An. gambiae* mosquitoes than control RBCs, and in cage assays, observed increased feeding on hmbRBCs, trophozoite-infected, or gametocyte-infected RBCs relative to control RBCs. Headspace analysis of the volatiles released by hmbRBC

cultures indicated that not only did hmbRBCs produce more CO₂ than RBC, but other volatiles were increased, including C8 to C10 aldehydes and monoterpenes (α - and β -pinene, limonene). It is notable that the headspace components of gametocyte-infected RBC (giRBC) are not presented, as the hmbRBC cultures are proposed to functionally mimic parasitized RBCs, and this comparison should be ascertained. A further omission is an explanation of the proposed source of monoterpenes in the hmbRBC cultures: RBC have no mitochondria, and as such no organelle would be present that synthesises isoprenoids using the MEP route. This brings contamination into question, as terpenes are ubiquitous compounds, and widely found in cosmetics (Cabaleiro et al., 2012). Details of the compound amounts are omitted, although referred to as 'minute'. Following mosquito feeding assays, HMBPP was found to have further influence on mosquito infection parameters including bloodmeal size and oocyst/sporozoite intensity. The overall hypothesis is that parasite-derived HMBPP enhances the emission of volatile compounds from host RBCs, which then are released, attracting mosquitoes and increasing the likelihood of transmission, with further influence on downstream vector-specific aspects of the parasite lifecycle. It is notable that both studies document the release of monoterpenes by *Plasmodium*-iRBCs, and incriminate the parasite MEP pathway. Interestingly, it has been proposed that for such mechanisms, i.e. iRBC-mediated release of volatile compounds, cytoadherence of these cells in the pulmonary microvasculature could enhance their release in the breath (Wong et al., 2012). A recent paper proposed that the origin of parasite-specific volatiles may be the extracellular vesicles (EVs) released from *Plasmodium*-iRBC (Correa et al., 2017). Investigators captured and compared the headspace of EVs and culture supernatant (SNU) from uninfected RBC culture and iRBC cultures at both low and high parasitaemia. Insufficient replication (biological replicates of only three *Plasmodium* cultures were examined) and poor consistency of volatile composition, collected in the EV headspace of infected cultures, precluded identification of infection-specific volatiles. However, the SNU headspace was found to contain greater numbers of volatiles, including several that were seemingly infection-specific. Importantly, and in concordance with Emami et al. (2017), the aldehyde hexanal was detected in the headspace of all SNU iRBC, but was absent from that of uninfected RBC. It is thought that the production of extracellular vesicles by iRBC can modulate the host immune response and disease development, in addition to stimulating differentiation of *P. falciparum* asexual stages into gametocytes (Szempruch et al., 2016). A possible role of EV in the production of attractant volatiles represents an exciting development.

Other studies have examined the volatile headspace of *Plasmodium*-iRBC and have not detected any association between particular volatile compounds and infection. In one study, several methods were used to sample the headspace above high density (>20 % parasitaemia) iRDC cultures, but no specific volatiles were detected relative to the control cultures (Wong et al., 2012). In another study, where breath samples from individuals with controlled human malaria infection were analysed before, during and after infection, the production of several volatile compounds was found to correlate with infection (Berna et al., 2016). Other than the murine odour study (De Moraes et al., 2014), this is the only other study (to my knowledge) that has tested for volatile biomarkers of malaria *in vivo*. In addition to varying in concentration with infection, four thioethers were found to cycle in production with parasitaemia (albeit with a phase shift of 24 hours), and also decline in production following antimalarial drug treatment. However, on examination of the headspace of *Plasmodium*-iRBC (parasitaemia 0.5 % - 39 %), neither thioethers nor any other volatile compounds were detected that distinguished infected from control cultures. The authors do not suggest a mechanistic pathway for the presence of thioethers on *Plasmodium*-infected individuals' breath.

1.12.2 Unexplained clustering of malaria cases

In a study of the transmission dynamics of *P. vivax* and *P. falciparum* malaria in Brazil, investigators noticed that at both sites and over the study duration, malaria incidence was not randomly distributed between houses (Katsuragawa et al., 2010). At two sites, malaria was only observed in a proportion of the houses, and those houses remained constant for the respective study durations. This clustering was observed after other risk factors were accounted for, including proximity to *Anopheles* breeding sites, use of personal protection against bites, and number of residents per house. Although clustering could be explained by *P. vivax* relapses in the shorter term, clustering over two years and of both *P. falciparum* and *P. vivax* cases was indicative of mosquito attraction to (parasite) 'positive' houses (Katsuragawa et al., 2010). The authors suggest that malarial fevers may have caused this increase in mosquito attraction; however, the data are consistent with infection-induced changes in odour profile. A similar finding was observed in another malaria risk factor analysis conducted in Chennai, India (Srinivas et al., 2005). Here, after accounting for open windows and doors, window netting, proximity to stagnant water, construction activity and repellent usage, an independent risk (OR 1.64; 95% CL 1.12–2.42) of history of malaria in family members was detected. Further studies detailing analogous clustering are available (Rulisa et al., 2013; Stresman et al., 2010). As with all such analyses, it is important to recognise possible correlation with other, unmeasured, risk factors.

Although controlled for in some studies, important factors would include housing, as some housing designs are associated with a greater risk of malaria infection (Tusting et al., 2017, 2015; Wanzirah et al., 2015), and the possible influence of behaviours. For example, it is possible that disturbed feeding of an infected mosquito within a household would lead to clustering around an index malaria case.

1.13 Anticipated outcomes

The identification of malaria-specific volatiles emanating from human skin could have several profound repercussions. These include: further improvement of already highly effective odour 'lures' for entomological monitoring and control, empirical evidence to inform epidemiological models of non-heterogeneous mosquito biting rates, and a possible basis for a non-invasive diagnostic tool for malaria, with potential stage-specificity.

1.13.1 Odour-baited traps

A large body of literature exists concerning the use of volatile compounds to lure and trap disease vectors. In 2016, the results were published for the 'SolarMal' project: a four-year, stepped-wedge cluster-randomised trial, investigating the impact of mass deployment of odour-baited mosquito traps for malaria control (Homan et al., 2016). Trapping systems were deployed to augment the existing malaria control strategies of LLINs and anti-malarial treatment, and outcome measures included the incidence of clinical malaria and prevalence of malaria parasites. Throughout the trial, the prevalence of malaria parasites was found to be lower in the intervention clusters, until at the final time point when universal coverage was achieved. The bait used was a synthetic organic attractant known as MB5 (containing ammonia, (S)-lactic acid, tetradecanoic acid, 3-methyl-1-butanol and butan-1-amine), with 2-butanone additionally added (Homan et al., 2016). While olfactory cues have been exploited for monitoring and control of vector populations for many years, this was the first demonstration that odour-baited traps can contribute to a reduction in the prevalence of malaria.

Volatile chemicals that have been identified as species-specific olfactory cues have long been used in traps for surveillance. The majority of research has focussed on mosquitoes; functional odour-baited traps are now available that target both host-seeking (Costantini et al., 1993; Jawara et al., 2011; Krockel et al., 2006; Njiru et al., 2006; Nyasembe et al., 2014; Okumu et al., 2010) and ovipositing (Englbrecht et al., 2015; Leal et al., 2008; Nyasembe et al., 2012; Perich et

al., 2003; Wondwosen et al., 2017) insects. The study of cues that could be exploited in this way in other insect species has been less intense (Takken and Knols, 2010). However, there have been recent developments in this field for some disease vectors, including midges (reviewed by Carpenter et al. 2008), kissing bugs (Guidobaldi et al., 2016; Guidobaldi and Guerenstein, 2013; Rojas de Arias et al., 2012) and sandflies (Bray et al. (2010), discussed below).

One of the most long-standing and effective examples of the use of odour-baited traps is for the control of tsetse flies in East Africa, to reduce the transmission of human African trypanosomiasis. These diurnal insects respond well to traps with visual lures alone, and in a recent field trial, 'tiny traps' consisting of blue polyester cloth (25 cm²) attached to black deltamethrin-impregnated mosquito netting (25 cm²) were deployed. The 90 % reduction in tsetse population density was compared to a previously published transmission model (Gouteux and Artzrouni, 1996), which indicated that a 72 % reduction in tsetse population would halt transmission in that setting (Tirados et al., 2015). Tsetse flies have a uniquely slow reproductive cycle, which enhances the utility of vector control. In sandflies, a synthetic version of the sex pheromone of *Lutzomyia longipalpis* is available, and has been used effectively in trap-and-kill strategies. Sand flies, which breed in lekks over host animals, are attracted and aggregate on these lekking sites. Both males and females are attracted to a combination of sex pheromone and host odour. Lekking sites have traditionally been treated with insecticide, but by killing the pheromone-producing males, flies will move to alternative lekking sites (Bray et al., 2010). By dispensing synthetic pheromone simultaneously to insecticidal treatment, lekking sites were converted into large-scale killing zones (Bray et al., 2010).

These examples demonstrate how through studying the cues used by host-seeking vectors, and expanding our basic knowledge of their biology, novel control mechanisms can materialise. Further optimisation of the MB5 blend that was deployed in the 'SolarMal' trial is likely to allow larger gains in effectiveness, with more powerful lures increasing the speed of population reduction (Takken and Knols, 2010). The MB5 blend was designed to mimic the odour of a 'healthy' human. Should infection-mediated differences in attractiveness be caused by changes to host odour, novel attractants may be identified by studying 'infected' human odour. As outlined above, current insecticide-based methods are failing, and similar alternatives will fail in turn. Odour-based control methods, relying on the cues used by insects for fundamental life history behaviours, are less likely to be selected against because the same cues continue to signify survival and reproduction. Also, lures usually comprise blends of compounds, which are

less easily selected against. Further advantages concern the environmental impact: sustained use of insecticide can be and historically has been damaging to the environment, though exceptions were made for the use of toxic chemicals to control vectors of disease, due to the benefit to human life. In some countries, expired stock of insecticides has become a disposal issue, with significant amounts of dichlorodiphenyltrichloroethane (DDT) now being shipped overseas (e.g. from Ethiopia to Poland (<http://www.africairs.net/2017/03/pmi-helps-ethiopia-clean-hazardous-waste/>, accessed 3rd April 2017)) for incineration where safe disposal facilities exist. Because lures are designed to target one species, non-target species are less affected by odour-based methods than by insecticidal methods, thus there is an environmental benefit (Carlson et al., 2011).

1.13.2 Transmission

The possibility of parasite manipulation of vertebrate host attractiveness in vector-borne diseases should be considered in terms of disease transmission dynamics. The aspects of a mosquito's life history that contribute most importantly to transmission are included in the classical formula for 'vectorial capacity' (VC, Brady et al. 2016; MacDonald 1952). VC is an expression of the number of infections that will arise in a non-immune population, arising per case per day at a given place and time, by a given vector (Garrett-Jones, 1964). Here, important mosquito life history elements are daily survival and human biting rates. In this model, the human biting rate is multiplied by the ratio of mosquitoes to humans, to parameterise the number of new bites (transmission events) possible in the population. While the basic premise of the model remains accurate, the complexities of malaria transmission become more apparent. Even basic (and observed) variation in human attractiveness to mosquitoes would lead to heterogeneity in biting frequency, which would have a profound impact on VC. Smith et al. (2007) altered the VC parameter to account for this heterogeneity, by the addition of a squared coefficient for biting rate, alpha, as follows:

$$VC (1+ \alpha)$$

With α = the index of biting disparity (σ^2/μ)

Without the addition of α , VC assumes that there is zero variance in biting in the population. However, here it is easy to see how even a slightly skewed distribution of biting in the population, giving a variance that is greater than the mean, quickly amplifies estimates of VC.

Further, models have been proposed that describe an increased attractiveness of infected individuals, but both an increase in further host infections (because more mosquitoes will more rapidly become infected) or a decrease in further infections (as biting is restricted to the infected individuals) could result, depending on other population parameters (Kingsolver, 1987).

1.13.3 Diagnostics

Should this study reveal and characterise specific *Plasmodium* infection-associated compounds, these could serve as biomarkers for use in diagnostics. The benefits of developing such a system for malaria would be considerable, in the first instance because improved sensitivity diagnostics are increasingly necessary. As the incidence of malaria falls in sub-Saharan Africa (Bhatt et al., 2015), it is increasingly important to find and treat those remaining individuals harbouring parasites, to prevent them from transmitting further. Often, infected individuals are asymptomatic, with low-density infections, and are therefore invisible to the health system (WHO, 2015). These people represent a large (and unwitting) parasite reservoir (WHO, 2015). A tool that could be used to actively, yet non-invasively, detect these individuals would represent a considerable advantage on the current status quo, where rapid diagnostic tests or microscopy (both requiring a blood sample) may not have sufficient sensitivity. In most settings, RDTs and microscopy will miss 30-50 % of PCR-detectable infections (Chen et al., 2016). Further, should a *Plasmodium*-infection volatile signal be gametocyte-associated, i.e. for the attraction of mosquitoes towards a gametocytaemic vertebrate host, specific detection of this signal could underpin a transmission-blocking strategy. By targeting for treatment those individuals who contribute most to transmission, greater control of transmission at the population level could be achieved.

1.14 Summary

In summary, several strands of evidence suggest *Plasmodium* manipulation of the vertebrate host odour profile, with repercussions on attractiveness to anophelines. These are:

1. The emission of disease-specific volatiles across a range of other pathologies in humans
2. Empirical evidence of the phenomenon of increased attractiveness in this, and other vector-borne, disease systems
3. The apparent direct release of volatiles from *Plasmodium*-infected red blood cells *in vitro*
4. The possibility of unaccounted for clustering of malaria in households

This thesis therefore seeks to address the question of whether individuals who are infected with *Plasmodium* species emit disease-specific volatile compounds from their skin, and whether the mosquito vectors detect and respond to these in a specific way.

1.15 Aim and objectives

The aim of this PhD was to determine whether infection of the human host by *Plasmodium* species alters the skin volatile odour profile in a manner that is detected by the mosquito vector *Anopheles*.

The objectives of the PhD are as follows:

1. To investigate qualitative and quantitative differences in the volatile odour profile of individuals infected with *Plasmodium* parasites and uninfected persons
 - a. In a controlled human malaria infection (experimental infections) population
 - b. In a population with endemic malaria (natural infections)
2. To describe the parasitological infection status of the endemic malaria population that was odour sampled, to inform the investigation into disease-specific volatiles
3. To examine the response of mosquitoes to these odour samples by coupled gas chromatography-electroantennography, to further identify entomologically significant, infection-associated compounds
4. To definitively identify any *Plasmodium* infection-associated compounds by gas chromatography-mass spectrometry and peak enhancement

1.16 Chapter references

- Aboagye-Antwi, F., Guindo, A., Traor?, A.S., Hurd, H., Coulibaly, M., Traor?, S., Tripet, F., 2010. Hydric stress-dependent effects of *Plasmodium falciparum* infection on the survival of wild-caught *Anopheles gambiae* female mosquitoes. *Malar. J.* 9, 243. doi:10.1186/1475-2875-9-243
- Acree, F., Turner, R.B., Gouck, H.K., Beroza, M., Smith, N., 1968. L-Lactic acid: a mosquito attractant isolated from humans. *Science* 161, 1346–7.
- Anderson, R.A., Koella, J.C., Hurd, H., 1999. The effect of *Plasmodium yoelii nigeriensis* infection on the feeding persistence of *Anopheles stephensi* Liston throughout the sporogonic cycle. *Proc. Biol. Sci.* 266, 1729–33. doi:10.1098/rspb.1999.0839
- Ansell, J., Hamilton, K.A.A., Pinder, M., Walraven, G.E.L.E.L., Lindsay, S.W., Pindeti, M., 2002. Short-range mosquitoes attractiveness of pregnant women to *Anopheles gambiae*. *Trans. R. Soc. Trop. Med. Hyg.* 96, 113–116.
- Ara, K., Hama, M., Akiba, S., Koike, K., Okisaka, K., Hagura, T., Kamiya, T., Tomita, F., 2006. Foot odor due to microbial metabolism and its control. *Can. J. Microbiol.* 52, 357–64. doi:10.1139/w05-130
- Assele, V., Ndoh, G.E., Nkoghe, D., Fandeur, T., 2015. No evidence of decline in malaria burden from 2006 to 2013 in a rural Province of Gabon: implications for public health policy. *BMC Public Health* 15, 81. doi:10.1186/s12889-015-1456-4
- Batista, E.P., Costa, E.F., Silva, A. a, 2014. *Anopheles darlingi* (Diptera: Culicidae) displays increased attractiveness to infected individuals with *Plasmodium vivax* gametocytes. *Parasit. Vectors* 7, 251. doi:10.1186/1756-3305-7-251
- Baylis, M., Mbwabi, A.L., 1995. Feeding behaviour of tsetse flies (*Glossina pallidipes* Austen) on *Trypanosoma*-infected oxen in Kenya 297–305.
- Baylis, M., Nambiro, C.O., 1993. The effect of cattle infection by *Trypanosoma congolense* on the attraction, and feeding success, of the tsetse fly *Glossina pallidipes*. *Parasitology* 106 (Pt 4, 357–61.
- Berna, A.Z., McCarthy, J.S., Trowell, S.C., 2016. Malaria detection using breath biomarkers. *Med. J. Aust.* 204, 50.
- Bernier, U.R., Kline, D.L., Schreck, C.E., Yost, R.A., Barnard, D.R., 2002. Chemical analysis of human skin emanations: comparison of volatiles from humans that differ in attraction of *Aedes aegypti* (Diptera: Culicidae). *J. Am. Mosq. Control Assoc.* 18, 186–95.
- Bhatt, S., Weiss, D.J., Cameron, E., Bisanzio, D., Mappin, B., Dalrymple, U., Battle, K.E., Moyes, C.L., Henry, A., Eckhoff, P.A., Wenger, E.A., Briët, O., Penny, M.A., Smith, T.A., Bennett, A., Yukich, J., Eisele, T.P., Griffin, J.T., Fergus, C.A., Lynch, M., Lindgren, F., Cohen, J.M., Murray, C.L.J., Smith, D.L., Hay, S.I., Cibulskis, R.E., Gething, P.W., 2015. The effect of malaria control on *Plasmodium falciparum* in Africa between 2000 and 2015. *Nature* 526, 207–211. doi:10.1038/nature15535
- Birkett, M.A., Agelopoulos, N., Jensen, K.M. V, Jespersen, J.B., Pickett, J.A., Prijs, H.J., Thomas, G., Trapman, J.J., Wadhams, L.J., Woodcock, C.M., 2004. The role of volatile semiochemicals in mediating host location and selection by nuisance and disease-transmitting cattle flies. *Med. Vet. Entomol.* 18, 313–322. doi:10.1111/j.0269-283X.2004.00528.x
- Bohbot, J.D., Lu, T., Zwiebel, L.J., 2010. Molecular regulation of olfaction in mosquitoes, in: Takken, W., Knols, B.G. (Eds.), *Olfaction in Vector-Host Interactions*. Wageningen Academic Publishers, pp. 17–38.
- Bosch, O.J., Geier, M., Boeckh, J., 2000. Contribution of Fatty Acids to Olfactory Host Finding of Female *Aedes aegypti*. *Chem. Senses* 25, 323–330. doi:10.1093/oxfordjournals.chemse.a014042
- Bousema, J.T., Gouagna, L.C., Meutstege, A.M., Okech, B.E., Akim, N.I.J., Githure, J.I., Beier, J.C.,

- Sauerwein, R.W., 2003. Treatment failure of pyrimethamine-sulphadoxine and induction of *Plasmodium falciparum* gametocytaemia in children in western Kenya. *Trop. Med. Int. Health* 8, 427–30.
- Brady, J., 1997. The role of body odours in the relative attractiveness of different men to malarial vectors in Burkina Faso. *Ann. Trop. Med. Parasitol.* 91, 121–122. doi:10.1080/00034989761436
- Brady, O.J., Godfray, H.C.J., Tatem, A.J., Gething, P.W., Cohen, J.M., Ellis McKenzie, F., Alex Perkins, T., Reiner, R.C., Tusting, L.S., Sinka, M.E., Moyes, C.L., Eckhoff, P.A., Scott, T.W., Lindsay, S.W., Hay, S.I., Smith, D.L., 2016. Vectorial capacity and vector control: Reconsidering sensitivity to parameters for malaria elimination. *Trans. R. Soc. Trop. Med. Hyg.* 110, 107–117. doi:10.1093/trstmh/trv113
- Braimah, N., Drakeley, C., Kweka, E., Mosha, F., Helinski, M., Pates, H., Maxwell, C., Massawe, T., Kenward, M.G., Curtis, C., 2005. Tests of bednet traps (Mbita traps) for monitoring mosquito populations and time of biting in Tanzania and possible impact of prolonged insecticide treated net use. *Int. J. Trop. Insect Sci.* 25, 208–213. doi:10.1079/IJT200576
- Braks, M.A.H., Anderson, R.A., Knols, B.G.J., 1999. Infochemicals in Mosquito Host Selection: Human Skin Microflora and *Plasmodium* Parasites. *Parasitol. Today* 15, 409–413.
- Braks, M.A.H., Meijerink, J., Takken, W., 2001. The response of the malaria mosquito, *Anopheles gambiae*, to two components of human sweat, ammonia and l-lactic acid, in an olfactometer. *Physiol. Entomol.* 26, 142–148. doi:10.1046/j.1365-3032.2001.00227.x
- Braks, M.A.H., Takken, W., 1999. Incubated Human Sweat but not Fresh Sweat Attracts the Malaria Mosquito *Anopheles gambiae sensu stricto*. *J. Chem. Ecol.* 25, 663–672. doi:10.1023/A:1020970307748
- Bray, D.P., Alves, G.B., Dorval, M.E., Brazil, R.P., Hamilton, J.G., Grimaldi, G., Tesh, R., McMahon-Pratt, D., Davies, C., Kaye, P., Croft, S., Sundar, S., Noazin, S., Khamesipour, A., Moulton, L., Tanner, M., Nasser, K., Modabber, F., Sharifi, I., Khalil, E., Bernal, I., Antunes, C., Smith, P., Maia-Elkhoury, A., Alves, W., et al., 2010. Synthetic sex pheromone attracts the leishmaniasis vector *Lutzomyia longipalpis* to experimental chicken sheds treated with insecticide. *Parasit. Vectors* 3, 16. doi:10.1186/1756-3305-3-16
- Burkot, T.R., Narara, A., Paru, R., Graves, P.M., Garner, P., 1989. Human host selection by anophelines: no evidence for preferential selection of malaria or microfilariae-infected individuals in a hyperendemic area. *Parasitology* 98 Pt 3, 337–42.
- Busula, A.O., Bousema, T., Mweresa, C.K., Masiga, D., Logan, J.G., Sauerwein, R.W., Verhulst, N.O., Takken, W., de Boer, J.G., 2017. Gametocytaemia increases attractiveness of *Plasmodium falciparum*-infected Kenyan children to *Anopheles gambiae* mosquitoes. *J. Infect. Dis.* 1–5. doi:10.1093/infdis/jix214
- Cabaleiro, N., de la Calle, I., Bendicho, C., Lavilla, I., 2012. Fast screening of terpenes in fragrance-free cosmetics by fluorescence quenching on a fluorescein–bovine serum albumin probe confined in a drop. *Anal. Chim. Acta* 719, 61–67. doi:10.1016/j.aca.2011.12.061
- Cardé, R.T., Gibson, G., 2010. Host finding by female mosquitoes: mechanisms of orientation to host odours and other cues., in: Takken, W., Knols, B.G.J.J. (Eds.), *Olfaction in Vector-Host Interactions*. Wageningen Academic Publishers, pp. 115–141.
- Carey, A.F., Wang, G., Su, C.-Y., Zwiebel, L.J., Carlson, J.R., 2010. Odorant reception in the malaria mosquito *Anopheles gambiae*. *Nature* 464, 66–71. doi:10.1038/nature08834
- Carlson, D.A., Smith, N., Gouck, H.K., Godwin, D.R., 1973. Yellowfever Mosquitoes: Compounds Related to Lactic Acid that Attract Females. *J. Econ. Entomol.* 66, 329–331. doi:10.1093/jee/66.2.329
- Carlson, J.R., Carey, A.F., Carlson, B.J.R., 2011. Scent of a human. Decoding how a mosquito sniffs out human targets could lead to better traps and repellents that cut malaria's spread. *Sci. Am.* 305, 76–9.
- Carpenter, S., Mellor, P.S., Torr, S.J., 2008. Control techniques for *Culicoides* biting midges and

- their application in the U.K. and northwestern Palaearctic. *Med. Vet. Entomol.* 22, 175–187. doi:10.1111/j.1365-2915.2008.00743.x
- Chege, G.M., Beier, J.C., 1990. Effect of *Plasmodium falciparum* on the survival of naturally infected afrotropical *Anopheles* (Diptera: Culicidae). *J. Med. Entomol.* 27, 454–8.
- Chen, I., Clarke, S.S.E., Gosling, R., Hamainza, B., Killeen, G., Magill, A., O'Meara, W.W., Price, R.N.R., Riley, E.E.M., O'Meara, W., Price, R.N.R., Riley, E.E.M., Doolan, D., Dobano, C., Baird, J., Lindblade, K., Steinhardt, L., Samuels, A., Kachur, S., Slutsker, L., Greenwood, B., Bousema, T., Okell, L., Felger, I., et al., 2016. "Asymptomatic" Malaria: A Chronic and Debilitating Infection That Should Be Treated. *PLOS Med.* 13, e1001942. doi:10.1371/journal.pmed.1001942
- Chen, M., Daly, M., Williams, N., Williams, S., Williams, C., Williams, G., 2000. Non-invasive detection of hypoglycaemia using a novel, fully biocompatible and patient friendly alarm system. *BMJ* 321, 1565–6.
- Chen, X., Xu, F., Wang, Y., Pan, Y., Lu, D., Wang, P., Ying, K., Chen, E., Zhang, W., 2007. A study of the volatile organic compounds exhaled by lung cancer cells in vitro for breath diagnosis. *Cancer* 110, 835–844. doi:10.1002/cncr.22844
- Chizema-Kawesha, E., Mukonka, V.M., Mukuka, C., Miti, S.K., Miller, J.M., Campbell, C.C., Steketee, R.W., Mohamed, A.D., 2010. Scaling Up Malaria Control in Zambia: Progress and Impact 2005-2008. *Am. J. Trop. Med. Hyg.* 83, 480–488. doi:10.4269/ajtmh.2010.10-0035
- Cisse, M.B.M., Keita, C., Dicko, A., Dengela, D., Coleman, J., Lucas, B., Mihigo, J., Sadou, A., Belemvire, A., George, K., Fornadel, C., Beach, R., 2015. Characterizing the insecticide resistance of *Anopheles gambiae* in Mali. *Malar. J.* 14, 327. doi:10.1186/s12936-015-0847-4
- Coleman, R.E., Edman, J.D., 1988. Feeding-site selection of *Lutzomyia longipalpis* (Diptera: Psychodidae) on mice infected with *Leishmania mexicana amazonensis*. *J. Med. Entomol.* 25, 229–33.
- Coleman, R.E., Edman, J.D., Semprevivo, L.H., 1988. Interactions between malaria (*Plasmodium yoelii*) and leishmaniasis (*Leishmania mexicana amazonensis*): effect of concomitant infection on host activity, host body temperature, and vector engorgement success. *J. Med. Entomol.* 25, 467–71.
- Cork, A., Park, K.C., 1996. Identification of electrophysiologically-active compounds for the malaria mosquito, *Anopheles gambiae*, in human sweat extracts. *Med. Vet. Entomol.* 10, 269–76.
- Cornet, S., Nicot, A., Rivero, A., Gandon, S., 2013. Both infected and uninfected mosquitoes are attracted toward malaria infected birds. *Malar. J.* 12, 179. doi:10.1186/1475-2875-12-179
- Cornet, S., Nicot, A., Rivero, A., Gandon, S., 2012. Malaria infection increases bird attractiveness to uninfected mosquitoes. *Ecol. Lett.* 16, 323–9. doi:10.1111/ele.12041
- Correa, R., Coronado, L.M., Garrido, A.C., Durant-Archibold, A.A., Spadafora, C., 2017. Volatile organic compounds associated with *Plasmodium falciparum* infection in vitro. *Parasit. Vectors* 10, 215. doi:10.1186/s13071-017-2157-x
- Costantini, C., Birkett, M. a, Gibson, G., Ziesmann, J., Sagnon, N.F., Mohammed, H. a, Coluzzi, M., Pickett, J.A., 2001. Electroantennogram and behavioural responses of the malaria vector *Anopheles gambiae* to human-specific sweat components. *Med. Vet. Entomol.* 15, 259–266.
- Costantini, C., Gibson, G., Brady, J., Merzagora, L., Coluzzi, M., 1993. A new odour-baited trap to collect host-seeking mosquitoes. *Parassitologia* 35, 5–9.
- Costello, E.E.K., Lauber, C.C.L., Hamady, M., Fierer, N., Gordon, J.I., Knight, R., 2009. Bacterial community variation in human body habitats across space and time. *Science (80-.)*. 326, 1694–7. doi:10.1126/science.1177486.Bacterial
- Daniel, T.L., Kingsolver, J.G., 1983. Feeding strategy and the mechanics of blood sucking in insects. *J. Theor. Biol.* 105, 661–677. doi:10.1016/0022-5193(83)90226-6

- Davis, E.E., 1984a. Development of lactic acid-receptor sensitivity and host-seeking behaviour in newly emerged female *Aedes aegypti* mosquitoes. *J. Insect Physiol.* 30, 211–215. doi:10.1016/0022-1910(84)90005-2
- Davis, E.E., 1984b. Regulation of sensitivity in the peripheral chemoreceptor systems for host-seeking behaviour by a haemolymph-borne factor in *Aedes aegypti*. *J. Insect Physiol.* 30, 179–183. doi:10.1016/0022-1910(84)90124-0
- Dawes, E.J., Churcher, T.S., Zhuang, S., Sinden, R.E., Bas??ez, M.-G., 2009. Anopheles mortality is both age- and Plasmodium-density dependent: implications for malaria transmission. *Malar. J.* 8, 228. doi:10.1186/1475-2875-8-228
- Dawkins, R., Krebs, J.R., 1979. Arms Races between and within Species. *Proc. R. Soc. B Biol. Sci.* 205, 489–511.
- Day, J.F., Ebert, K.M., Edman, J.D., 1983. Feeding patterns of mosquitoes (Diptera: culicidae) simultaneously exposed to malarious and health mice, including a method for separating blood meals from conspecific hosts. *J. Med. Entomol.* 20, 120–7.
- Day, J.F., Edman, J.D., 1983. Malaria renders mice susceptible to mosquito feeding when gametocytes are most infective. *J. Parasitol.* 69, 163–70.
- De Jong, R., Knols, B.G.J., 1995. Selection of biting sites on man by two malaria mosquito species. *Experientia* 51, 80–84. doi:10.1007/BF01964925
- De Moraes, C.M., Stanczyk, N.M., Betz, H.S., Pulido, H., Sim, D.G., Read, A.F., Mescher, M.C., Science, E.S., Meinwald, J., 2014. Malaria-induced changes in host odors enhance mosquito attraction. *Proc. Natl. Acad. Sci. U. S. A.* doi:10.1073/pnas.1405617111
- DeGennaro, M., McBride, C.S., Seeholzer, L., Nakagawa, T., Dennis, E.J., Goldman, C., Jasinskiene, N., James, A.A., Vosshall, L.B., 2013. orco mutant mosquitoes lose strong preference for humans and are not repelled by volatile DEET. *Nature* 498, 487–491.
- Dekker, T., Geier, M., Cardé, R.T., 2005. Carbon dioxide instantly sensitizes female yellow fever mosquitoes to human skin odours. *J. Exp. Biol.* 208, 2963–72. doi:10.1242/jeb.01736
- Dormont, L., Bessière, J.-M., Cohuet, A., 2013. Human skin volatiles: a review. *J. Chem. Ecol.* 39, 569–78. doi:10.1007/s10886-013-0286-z
- Drakeley, C., Lines, J., 2014. In for the long haul: 20 years of malaria surveillance. *Lancet Infect. Dis.* 14, 445–446. doi:10.1016/S1473-3099(14)70742-X
- Edi, C.V.A., Koudou, B.G., Jones, C.M., Weetman, D., Ranson, H., 2012. Multiple-insecticide resistance in *Anopheles gambiae* mosquitoes, Southern Côte d’Ivoire. *Emerg. Infect. Dis.* 18, 1508–11. doi:10.3201/eid1809.120262
- Emami, S.N., Emami, S.N., Lindberg, B.G., Hua, S., Hill, S., Mozuraitis, R., Birgersson, G., Ignell, R., Faye, I., 2017. A key malaria metabolite modulates vector blood seeking , feeding , and susceptibility to infection. *Science* (80-.). 4563, 1–9.
- Engbrecht, C., Gordon, S., Venturelli, C., Rose, A., Geier, M., 2015. Evaluation of BG-Sentinel Trap as a management tool to reduce *Aedes albopictus* nuisance in an urban environment in Italy. *J. Am. Mosq. Control Assoc.* 31, 16–25. doi:10.2987/14-6444.1
- Ferguson, H.M., Mackinnon, M.J., Chan, B.H., Read, A.F., 2003a. Mosquito mortality and the evolution of malaria virulence. *Evolution* 57, 2792–804.
- Ferguson, H.M., Read, A.F., 2002. Genetic and environmental determinants of malaria parasite virulence in mosquitoes. *Proceedings Biol. Sci.* 269, 1217–24. doi:10.1098/rspb.2002.2023
- Ferguson, H.M., Rivero, A., Read, A.F., 2003b. The influence of malaria parasite genetic diversity and anaemia on mosquito feeding and fecundity. *Parasitology* 127, 9–19.
- Fernández-Grandon, G.M., Gezan, S. a., Armour, J. a. L., Pickett, J. a., Logan, J.G., 2015. Heritability of Attractiveness to Mosquitoes. *PLoS One* 10, e0122716. doi:10.1371/journal.pone.0122716
- Fierer, N., Lauber, C.C.L., Zhou, N., McDonald, D., Costello, E.K., Knight, R., 2010. Forensic identification using skin bacterial communities. *Proc. Natl. Acad. Sci. U. S. A.* 107, 6477–81. doi:10.1073/pnas.1000162107

Chapter 1: Literature review

- Fox, a N., Pitts, R.J., Robertson, H.M., Carlson, J.R., Zwiebel, L.J., 2001. Candidate odorant receptors from the malaria vector mosquito *Anopheles gambiae* and evidence of down-regulation in response to blood feeding. *Proc. Natl. Acad. Sci. U. S. A.* 98, 14693–7. doi:10.1073/pnas.261432998
- Freier, J.E., Friedman, S., 1976. Effect of host infection with *Plasmodium gallinaceum* on the reproductive capacity of *Aedes aegypti*. *J. Invertebr. Pathol.* 28, 161–6.
- Gadenne, C., Barrozo, R.B., Anton, S., 2016. Plasticity in Insect Olfaction: To Smell or Not to Smell? *Annu. Rev. Entomol.* 61, 317–333. doi:10.1146/annurev-ento-010715-023523
- Garrett-Jones, C., 1964. The human blood index of malarial vectors in relationship to epidemiological assessment. *Bull. World Heal. Organ. Hlth. Org.* 30, 241–261.
- Gilbert, I.H., Gouck, H.K., Smith, N., 1966. Attractiveness of Men and Women to *Aedes aegypti* and Relative Protection Time Obtained with Deet. *Florida Entomol.* 49, 53. doi:10.2307/3493317
- Gillett, J.D., Connor, J., 1976. Host Temperature and the Transmission of Arboviruses by Mosquitoes. *Mosq. News.*
- Gillies, M.T., 1980. The role of carbon dioxide in host-finding by mosquitoes (Diptera: Culicidae): a review. *Bull. Entomol. Res.* 70, 525. doi:10.1017/S0007485300007811
- Gouteux, P.J., Artzrouni, M., 1996. [Is vector control needed in the fight against sleeping sickness? A biomathematical approach]. *Bull. Soc. Pathol. Exot.* 89, 299–305.
- Grant, A.J., Wigton, B.E., Aghajanian, J.G., O’Connell, R.J., 1995. Electrophysiological responses of receptor neurons in mosquito maxillary palp sensilla to carbon dioxide. *J. Comp. Physiol. A.* 177, 389–96.
- Guidobaldi, F., Guerenstein, P.G., 2013. Evaluation of a CO₂-free commercial mosquito attractant to capture triatomines in the laboratory. *J. Vector Ecol.* 38, 245–250. doi:10.1111/j.1948-7134.2013.12037.x
- Guidobaldi, F., Guerenstein, P.G., J., P.R., A., V.G., E., G.R., E., Z., G., T., H., M., J., C.-P.C., I., S., 2016. A CO₂-Free Synthetic Host-Odor Mixture That Attracts and Captures Triatomines: Effect of Emitted Odorant Ratios. *J. Med. Entomol.* 53, 770–775. doi:10.1093/jme/tjw057
- Guidobaldi, F., May-Concha, I.J., Guerenstein, P.G., 2014. Morphology and physiology of the olfactory system of blood-feeding insects. *J. Physiol.* 108, 96–111. doi:10.1016/j.jphysparis.2014.04.006
- Hacker, C., 1971. The differential effect of *Plasmodium gallinacium* on the fecundity of several strains of *Aedes aegypti*. *J. Invertebr. Pathol.* 18, 373–377.
- Haddow, A.J., 1942. The Mosquito Fauna and Climate of native Huts at Kisumu, Kenya. *Bull. Entomol. Res.* 33, 91–142.
- Hardin, D.S., Anderson, W., Cattet, J., 2015. Dogs Can Be Successfully Trained to Alert to Hypoglycemia Samples from Patients with Type 1 Diabetes. *Diabetes Ther.* 6, 509–517. doi:10.1007/s13300-015-0135-x
- Hawkes, F., Gibson, G., 2016. Seeing is believing: the nocturnal malarial mosquito *Anopheles coluzzii* responds to visual host-cues when odour indicates a host is nearby. *Parasit. Vectors* 9, 320. doi:10.1186/s13071-016-1609-z
- Healy, T.P., Copland, M.J.W., 2000. Human sweat and 2-oxopentanoic acid elicit a landing response from *Anopheles gambiae*. *Med. Vet. Entomol.* 14, 195–200. doi:10.1046/j.1365-2915.2000.00238.x
- Healy, T.P., Copland, M.J.W., 1995. Activation of *Anopheles gambiae* mosquitoes by carbon dioxide and human breath. *Med. Vet. Entomol.* 9, 331–336. doi:10.1111/j.1365-2915.1995.tb00143.x
- Hill, C.A., Fox, A.N., Pitts, R.J., Kent, L.B., Tan, P.L., Chrystal, M.A., Cravchik, A., Collins, F.H., Robertson, H.M., Zwiebel, L.J., 2002. G protein-coupled receptors in *Anopheles gambiae*. *Science* 298, 176–8. doi:10.1126/science.1076196
- Himeidan, Y.E., Elbashir, M.I., Adam, I., 2004. Attractiveness of pregnant women to the malaria

- vector, *Anopheles arabiensis*, in Sudan. *Ann. Trop. Med. Parasitol.* 98, 631–3. doi:10.1179/000349804225021307
- Hoch, A.L., Gargan, T.P., Bailey, C.L., 1985. Mechanical transmission of Rift Valley fever virus by hematophagous Diptera. *Am. J. Trop. Med. Hyg.* 34, 188–93.
- Hogg, J.C., Hurd, H., 1997. The effects of natural *Plasmodium falciparum* infection on the fecundity and mortality of *Anopheles gambiae* s. l. in north east Tanzania. *Parasitology* 114 (Pt 4), 325–31.
- Hogg, J.C., Hurd, H., 1995a. Malaria-induced reduction of fecundity during the first gonotrophic cycle of *Anopheles stephensi* mosquitoes. *Med. Vet. Entomol.* 9, 176–80.
- Hogg, J.C., Hurd, H., 1995b. *Plasmodium yoelii nigeriensis*: the effect of high and low intensity of infection upon the egg production and bloodmeal size of *Anopheles stephensi* during three gonotrophic cycles. *Parasitology* 111 (Pt 5), 555–62.
- Homan, T., Hiscox, A., Mweresa, C.K., Masiga, D., Mukabana, W.R., Oria, P., Maire, N., Pasquale, A. Di, Silkey, M., Alaii, J., Bousema, T., Leeuwis, C., Smith, T.A., Takken, W., Bhatt, S., Weiss, D., Cameron, E., Al., E., Durnez, L., Coosemans, M., Killeen, G., Ranson, H., N’Guessan, R., Lines, J., Moiroux, N., et al., 2016. The effect of mass mosquito trapping on malaria transmission and disease burden (SolarMal): a stepped-wedge cluster-randomised trial. *Lancet* 388, 207–211. doi:10.1016/S0140-6736(16)30445-7
- Hurd, H., 2003. Manipulation of medically important insect vectors by their parasites. *Annu. Rev. Entomol.* 48, 141–161. doi:10.1146/annurev.ento.48.091801.112722
- Hurd, H., Taylor, P.J., Adams, D., Underhill, A., Eggleston, P., 2005. Evaluating the costs of mosquito resistance to malaria parasites. *Evolution* 59, 2560–72. doi:10.1554/05-211.1
- Ignell, R., Sengul, M.S., Hill, S.R., Hansson, B.S., 2011. Odour coding and neural connections, in: Takken, W., Knols, B.G.J. (Eds.), *Olfaction in Vector–Host Interactions, Ecology and Control of Vector-Borne Diseases*. Wageningen Academic Publishers, The Netherlands, pp. 63–90. doi:10.3920/978-90-8686-698-4
- Iovinella, I., Bozza, F., Caputo, B., della Torre, A., Pelosi, P., 2013. Ligand-Binding Study of *Anopheles gambiae* Chemosensory Proteins. *Chem. Senses* 38, 409–419. doi:10.1093/chemse/bjt012
- Jawara, M., Awolola, T.S., Pinder, M., Jeffries, D., Smallegange, R.C., Takken, W., Conway, D.J., 2011. Field testing of different chemical combinations as odour baits for trapping wild mosquitoes in The Gambia. *PLoS ONE [Electronic Resour.]* 6, e19676.
- Katsuragawa, T.H., Gil, L.H.S., Tada, M.S., de Almeida e Silva, A., Costa, J.D.N., Araújo, M.D.S., Escobar, A.L., da Silva, L.H.P., 2010. The dynamics of transmission and spatial distribution of malaria in riverside areas of Porto Velho, Rondônia, in the Amazon region of Brazil. *PLoS One* 5, e9245. doi:10.1371/journal.pone.0009245
- Kelly, M., Su, C.-Y., Schaber, C., Crowley, J.R., Hsu, F.-F., Carlson, J.R., Odom, A.R., 2015. Malaria parasites produce volatile mosquito attractants. *MBio* 6, e00235-15-. doi:10.1128/mBio.00235-15
- Kemme, J.A., Van Essen, P.H., Ritchie, S.A., Kay, B.H., 1993. Response of mosquitoes to carbon dioxide and 1-octen-3-ol in southeast Queensland, Australia. *J. Am. Mosq. Control Assoc.* 9, 431–5.
- Kennedy, J.S., 1940. The Visual Responses of Flying Mosquitoes. *Proc. Zool. Soc. London* A109, 221–242. doi:10.1111/j.1096-3642.1940.tb00831.x
- Khan, A.A., Maibach, H.I., Strauss, W.G., Fisher, J.L., 1969. Increased Attractiveness of Man to Mosquitoes with Induced Eccrine Sweating. *Nature* 223, 859–860. doi:10.1038/223859a0
- Kingsolver, J.G., 1987. Mosquito host choice and the epidemiology of malaria [WWW Document]. URL <http://www.jstor.org/discover/10.2307/2461780?uid=2446975375&uid=3738032&uid=2129&uid=2134&uid=2&uid=70&uid=3&uid=67&uid=62&uid=2446974975&sid=21103231276811>

- Kline, D.L., Takken, W., Wood, J.R., Carlson, D.A., 1990. Field studies on the potential of butanone, carbon dioxide, honey extract, 1-octen-3-ol, L-lactic acid and phenols as attractants for mosquitoes. *Med. Vet. Entomol.* 4, 383–91.
- Knols, B.G., 1996. On human odour, malaria mosquitoes, and Limburger cheese. *Lancet*.
- Knols, B.G., De Jong, R., 1996. Limburger cheese as an attractant for the malaria mosquito *Anopheles gambiae* s.s. *Parasitol. Today* 12, 159–61.
- Knols, B.G.J.J., de Jong, R., Takken, W., Jong, R. De, Agricultural, W., 1995. Differential attractiveness of isolated humans to mosquitoes in Tanzania. *Trans. R. Soc. Trop. Med. Hyg.* 89, 604–606.
- Krockel, U., Rose, A., Lvaro, E., Geier, M., 2006. New tools for surveillance of adult yellow fever mosquitoes: comparison of trap catches with human landing rates in an urban environment. *J. Am. Mosq. Control Assoc.* 22, 229–238.
- Kwiatkowski, D.P., 2005. How malaria has affected the human genome and what human genetics can teach us about malaria. *Am. J. Hum. Genet.* 77, 171–92. doi:10.1086/432519
- Kwon, H.-W., Lu, T., Rützler, M., Zwiebel, L.J., 2006. Olfactory responses in a gustatory organ of the malaria vector mosquito *Anopheles gambiae*. *Proc. Natl. Acad. Sci. U. S. A.* 103, 13526–31. doi:10.1073/pnas.0601107103
- Lacerda, M.V.G., Mourão, M.P.G., Coelho, H.C.C., Santos, J.B., 2011. Thrombocytopenia in malaria: who cares? *Mem. Inst. Oswaldo Cruz* 52–63.
- Lacey, E.S., Cardé, R.T., 2011. Activation, orientation and landing of female *Culex quinquefasciatus* in response to carbon dioxide and odour from human feet: 3-D flight analysis in a wind tunnel. *Med. Vet. Entomol.* 25, 94–103. doi:10.1111/j.1365-2915.2010.00921.x
- Lacroix, R., Mukabana, W.R., Gouagna, L.C., Koella, J.C., 2005. Malaria infection increases attractiveness of humans to mosquitoes. *PLoS Biol.* 3, e298. doi:10.1371/journal.pbio.0030298
- Lalubin, F., Bize, P., van Rooyen, J., Christe, P., Glaizot, O., 2012. Potential evidence of parasite avoidance in an avian malarial vector. *Anim. Behav.* 84, 539–545. doi:10.1016/j.anbehav.2012.06.004
- Lange, B.M., Rujan, T., Martin, W., Croteau, R., 2000. Isoprenoid biosynthesis: the evolution of two ancient and distinct pathways across genomes. *Proc. Natl. Acad. Sci. U. S. A.* 97, 13172–7. doi:10.1073/pnas.240454797
- Leal, W.S., Barbosa, R.M.R., Xu, W., Ishida, Y., Syed, Z., Latte, N., Chen, A.M., Morgan, T.I., Cornel, A.J., Furtado, A., 2008. Reverse and conventional chemical ecology approaches for the development of oviposition attractants for *Culex* mosquitoes. *PLoS One* 3, e3045. doi:10.1371/journal.pone.0003045
- Liddell, K., 1976. Smell as a diagnostic marker. *Postgrad. Med. J.* 52, 136–8.
- Lindsay, S., Ansell, J., Selman, C., Cox, V., Hamilton, K., Walraven, G., 2000. Effect of pregnancy on exposure to malaria mosquitoes. *Lancet* 355, 1972.
- Lindsay, S.W., Adiamah, J.H., Miller, J.E., Pleass, R.J., Armstrong, J.R., 1993. Variation in attractiveness of human subjects to malaria mosquitoes (Diptera: Culicidae) in The Gambia. *J. Med. Entomol.* 30, 368–73.
- Liu, C., Pitts, R.J., Bohbot, J.D., Jones, P.L., Wang, G., Zwiebel, L.J., Gibson, T.J., Benton, R., 2010. Distinct olfactory signaling mechanisms in the malaria vector mosquito *Anopheles gambiae*. *PLoS Biol.* 8, e1000467. doi:10.1371/journal.pbio.1000467
- Lloyd, G.E.R. (Ed.), 1983. *Hippocratic Writings*. Penguin Classics.
- Logan, J.G., Birkett, M.A., Clark, S.J., Powers, S., Seal, N.J., Wadhams, L.J., Mordue Luntz, A.J., Pickett, J.A., 2008. Identification of human-derived volatile chemicals that interfere with attraction of *Aedes aegypti* mosquitoes. *J Chem Ecol* 34, 308–322. doi:10.1007/s10886-008-9436-0
- Logan, J.G., Cook, J.I., Stanczyk, N.M., Weeks, E.N., Welham, S.J., Mordue(Luntz), A.J., 2010a. To

- bite or not to bite! A questionnaire-based survey assessing why some people are bitten more than others by midges. *BMC Public Health* 10, 275. doi:10.1186/1471-2458-10-275
- Logan, J.G., Stanczyk, N.M., Hassanali, A., Kemei, J., Santana, A.E.G., Ribeiro, K. a L., Pickett, J. a, Mordue Luntz, a J., 2010b. Arm-in-cage testing of natural human-derived mosquito repellents. *Malar. J.* 9, 239. doi:10.1186/1475-2875-9-239
- Lu, T., Qiu, Y.T., Wang, G., Kwon, J.Y., Rutzler, M., Kwon, H.-W., Pitts, R.J., van Loon, J.J.A., Takken, W., Carlson, J.R., Zwiebel, L.J., 2007. Odor Coding in the Maxillary Palp of the Malaria Vector Mosquito *Anopheles gambiae*. *Curr. Biol.* 17, 1533–1544.
- MacDonald, G., 1952. The analysis of equilibrium in malaria. *Trop. Dis. Bull.* 49, 813–29.
- Macdonald, M., 2016. New Ways of Approaching Indoor Residual Spraying for Malaria. *Glob. Heal. Sci. Pract.* 4, 511–513. doi:10.9745/GHSP-D-16-00354
- Mauck, K.E., De Moraes, C.M., Mescher, M.C., 2010. Deceptive chemical signals induced by a plant virus attract insect vectors to inferior hosts. *Proc. Natl. Acad. Sci. U. S. A.* 107, 3600–5. doi:10.1073/pnas.0907191107
- Mcbride, C.S., 2016. Genes and odors underlying the recent evolution of mosquito preference for humans. *Curr. Biol.* 26, 1–12. doi:10.1016/j.cub.2015.11.032.Genes
- McCulloch, M., 2006. Diagnostic Accuracy of Canine Scent Detection in Early- and Late-Stage Lung and Breast Cancers. *Integr. Cancer Ther.* 5, 30–39. doi:10.1177/1534735405285096
- Meijerink, J., van Loon, J.J., 1999. Sensitivities of antennal olfactory neurons of the malaria mosquito, *Anopheles gambiae*, to carboxylic acids. *J. Insect Physiol.* 45, 365–373.
- Mmbando, B.P., Vestergaard, L.S., Kitua, A.Y., Lemnge, M.M., Theander, T.G., Lusingu, J.P., 2010. A progressive declining in the burden of malaria in north-eastern Tanzania. *Malar. J.* 9, 216. doi:10.1186/1475-2875-9-216
- Muirhead-Thomson, R.C., 1951. The distribution of anopheline mosquito bites among different age groups; a new factor in malaria epidemiology. *Br. Med. J.* 1, 1114–7.
- Mukabana, W.R., Takken, W., Coe, R., Knols, B.G.J., 2002. Host-specific cues cause differential attractiveness of Kenyan men to the African malaria vector *Anopheles gambiae*. *Malar. J.* 1, 17.
- Mukabana, W.R., Takken, W., Killeen, G.F., Bart, G.J., 2007. Clinical malaria reduces human attractiveness to mosquitoes. *Proc. Netherlands Entomol. Soc. Meet.* 18, 125–129.
- Njiru, B.N., Mukabana, W.R., Takken, W., Knols, B.G.J., 2006. Trapping of the malaria vector *Anopheles gambiae* with odour-baited MM-X traps in semi-field conditions in western Kenya. *Malar. J.* 5, 39. doi:10.1186/1475-2875-5-39
- Nyasembe, V.O., Tchouassi, D.P., Kirwa, H.K., Foster, W.A., Teal, P.E.A., Borgemeister, C., Torto, B., 2014. Development and assessment of plant-based synthetic odor baits for surveillance and control of malaria vectors. *PLoS One* 9, e89818. doi:10.1371/journal.pone.0089818
- Nyasembe, V.O., Teal, P.E.A., Mukabana, W.R., Tumlinson, J.H., Torto, B., 2012. Behavioural response of the malaria vector *Anopheles gambiae* to host plant volatiles and synthetic blends. *Parasit Vectors* 5, 234.
- O’Meara, W.P., Mangeni, J.N., Steketee, R., Greenwood, B., Ghani, A., Lien, J., 2010. Changes in the burden of malaria in sub-Saharan Africa. *Lancet. Infect. Dis.* 10, 545–55. doi:10.1016/S1473-3099(10)70096-7
- O’Shea, B., Rebollar-Tellez, E., Ward, R.D., Hamilton, J.G.C., el Naiem, D., Polwart, A., 2002. Enhanced sandfly attraction to *Leishmania*-infected hosts. *Trans. R. Soc. Trop. Med. Hyg.* 96, 117–8.
- Okiro, E., Hay, S., Gikandi, P., Sharif, S., Noor, A., Peshu, N., Marsh, K., Snow, R., 2006. The decline in paediatric malaria admissions on the coast of Kenya. *Malar. J.* 5, 5. doi:10.1186/1475-2875-5-5
- Okumu, F.O., Madumla, E.P., John, A.N., Lwetoijera, D.W., Sumaye, R.D., 2010. Attracting, trapping and killing disease-transmitting mosquitoes using odor-baited stations - The Ifakara Odor-Baited Stations. *Parasit. Vectors* 3, 12. doi:10.1186/1756-3305-3-12

- Oyewole, I.O., Awolola, T.S., 2006. Impact of urbanisation on bionomics and distribution of malaria vectors in Lagos, southwestern Nigeria. *J. Vector Borne Dis.* 43, 173–178.
- Penn, D., Potts, W., 1998. How Do Major Histocompatibility Complex Genes Influence Odor and Mating Preferences?, in: *Advances in Immunology*. pp. 411–436. doi:10.1016/S0065-2776(08)60612-4
- Perich, M.J., Kardec, A., Braga, I.A., Portal, I.F., Burge, R., Zeichner, B.C., Brogdon, W.A., Wirtz, R.A., 2003. Field evaluation of a lethal ovitrap against dengue vectors in Brazil. *Med. Vet. Entomol.* 17, 205–10.
- Phillips, M., Cataneo, R.N., Condos, R., Ring Erickson, G.A., Greenberg, J., La Bombardi, V., Munawar, M.I., Tietje, O., 2007. Volatile biomarkers of pulmonary tuberculosis in the breath. *Tuberculosis* 87, 44–52. doi:10.1016/j.tube.2006.03.004
- Pluess, B., Tanser, F.C., Lengeler, C., Sharp, B.L., 2010. Indoor residual spraying for preventing malaria. *Cochrane database Syst. Rev.* CD006657. doi:10.1002/14651858.CD006657.pub2
- Port, G.R., Boreham, P.F.L., 1980. The relationship of host size to feeding by mosquitoes of the *Anopheles gambiae* Giles complex (Diptera : Culicidae) 133–144.
- Poulin, R., 2010. Chapter 5 – Parasite Manipulation of Host Behavior: An Update and Frequently Asked Questions, in: *Advances in the Study of Behavior*. pp. 151–186. doi:10.1016/S0065-3454(10)41005-0
- Poulin, R., 1995. “Adaptive” changes in the behaviour of parasitized animals: A critical review. *Int. J. Parasitol.* 25, 1371–1383. doi:10.1016/0020-7519(95)00100-X
- Puta, C., Manyando, C., 1997. Enhanced gametocyte production in Fansidar-treated *Plasmodium falciparum* malaria patients: implications for malaria transmission control programmes. *Trop. Med. Int. Health* 2, 227–9.
- Qiu, Y.-T., Gort, G., Torricelli, R., Takken, W., van Loon, J.J.A., 2013. Effects of blood-feeding on olfactory sensitivity of the malaria mosquito *Anopheles gambiae*: application of mixed linear models to account for repeated measurements. *J. Insect Physiol.* 59, 1111–8. doi:10.1016/j.jinsphys.2013.09.001
- Qiu, Y.-T., van Loon, J.J., 2010. Olfactory physiology of blood-feeding vector mosquitoes., in: Takken, W., Knols, B.G.J. (Eds.), *Olfaction in Vector-Host Interactions*. Wageningen Academic Publishers, Wageningen, pp. 39–61.
- Qiu, Y.-T., van Loon, J.J.A., Takken, W., Meijerink, J., Smid, H.M., 2006. Olfactory Coding in Antennal Neurons of the Malaria Mosquito, *Anopheles gambiae*. *Chem. Senses* 31, 845–63. doi:10.1093/chemse/bjl027
- Qiu, Y.T., Smallegange, R.C., Van Loon, J.J.A., Ter Braak, C.J.F., Takken, W., 2006. Interindividual variation in the attractiveness of human odours to the malaria mosquito *Anopheles gambiae* s. s. *Med. Vet. Entomol.* 20, 280–7. doi:10.1111/j.1365-2915.2006.00627.x
- Ranson, H., Lissenden, N., 2016. Insecticide Resistance in African *Anopheles* Mosquitoes: A Worsening Situation that Needs Urgent Action to Maintain Malaria Control. *Trends Parasitol.* 32, 187–196. doi:10.1016/j.pt.2015.11.010
- Ranson, H., N’guessan, R., Lines, J., Moiroux, N., Nkuni, Z., Corbel, V., 2011. Pyrethroid resistance in African anopheline mosquitoes: what are the implications for malaria control? *Trends Parasitol.* 27, 91–8. doi:10.1016/j.pt.2010.08.004
- Ray, A., 2015. Reception of odors and repellents in mosquitoes. *Curr. Opin. Neurobiol.* 34, 158–164. doi:10.1016/j.conb.2015.06.014
- Ray, A., van Naters, W.G., Carlson, J.R., 2014. Molecular determinants of odorant receptor function in insects. *J. Biosci.* 39, 555–63.
- Rebollar-Télez, E.A., 2005. Human body odour, mosquito bites and the risk of disease transmission. *Mex. Folia Entomol.* 44, 247–265.
- Riabinina, O., Task, D., Marr, E., Lin, C., Alford, R., Brochta, D.A.O., Potter, C.J., 2016. Organization of olfactory centres in the malaria mosquito *Anopheles gambiae*. doi:10.1038/ncomms13010

- Robert, V., Verhave, J.P., Carnevale, P., 1990. Plasmodium falciparum infection does not increase the precocious mortality rate of Anopheles gambiae. *Trans. R. Soc. Trop. Med. Hyg.* 84, 346–347. doi:10.1016/0035-9203(90)90309-3
- Rojas de Arias, A., Abad-Franch, F., Acosta, N., López, E., González, N., Zerba, E., Tarelli, G., Masuh, H., 2012. Post-Control Surveillance of Triatoma infestans and Triatoma sordida with Chemically-Baited Sticky Traps. *PLoS Negl. Trop. Dis.* 6, e1822. doi:10.1371/journal.pntd.0001822
- Rossignol, P.A., Ribeiro, J.M.C., Jungery, M., Spielman, A., 1985. Enhanced mosquito blood-finding success on parasitemic hosts : Evidence for vector-parasite mutualism. *Proc. Natl. Acad. Sci. U. S. A.* 82, 7725–7727.
- Rulisa, S., Kateera, F., Bizimana, J.P., Agaba, S., Dukuzumuremyi, J., Baas, L., de Dieu Harelimana, J., Mens, P.F., Boer, K.R., de Vries, P.J., 2013. Malaria prevalence, spatial clustering and risk factors in a low endemic area of Eastern Rwanda: a cross sectional study. *PLoS One* 8, e69443. doi:10.1371/journal.pone.0069443
- Rund, S.S.C., Bonar, N.A., Champion, M.M., Ghazi, J.P., Houk, C.M., Leming, M.T., Syed, Z., Duffield, G.E., 2013. Daily rhythms in antennal protein and olfactory sensitivity in the malaria mosquito Anopheles gambiae. *Sci. Rep.* 3, 2494. doi:10.1038/srep02494
- Russell, T.L., Govella, N.J., Azizi, S., Drakeley, C.J., Kachur, S.P., Killeen, G.F., 2011. Increased proportions of outdoor feeding among residual malaria vector populations following increased use of insecticide-treated nets in rural Tanzania. *Malar. J.* 10, 80. doi:10.1186/1475-2875-10-80
- Sangare, I., Michalakakis, Y., Yameogo, B., Dabire, R., Morlais, I., Cohuet, A., 2013. Studying fitness cost of Plasmodium falciparum infection in malaria vectors: validation of an appropriate negative control. *Malar. J.* 12, 2. doi:10.1186/1475-2875-12-2
- Schreck, C.E., James, J., 1968. Broth cultures of bacteria that attract female mosquitoes. *Mosq. News* 28, 33–38.
- Schreck, C.E., Kline, D.L., Carlson, D. a, 1990. Mosquito attraction to substances from the skin of different humans. *J. Am. Mosq. Control Assoc.* 6, 406–410.
- Seyoum, A., Dengela, D., Lucas, B., Belemvire, A., George, K., Fornadel, C., 2014. Multi-country profile of insecticide resistance on malaria vectors in the president's malaria initiative (PMI) Africa Indoor residual spraying (AIRS) Project Countries [WWW Document]. URL <http://www.africairs.net/wp-content/uploads/2014/11/Multi-Country-Profile-of-Insecticide-Resistance-on-Malaria-Vectors.pdf>
- Shelley, W.B., Hurley, H.J., Nichols, A.C., 1953. Axillary odor; experimental study of the role of bacteria, apocrine sweat, and deodorants. *AMA. Arch. Derm. Syphilol.* 68, 430–46.
- Shen, H.H., 2017. Inner Workings: How do mosquitoes smell us? The answers could help eradicate disease. *Proc. Natl. Acad. Sci.* 114, 2096–2098. doi:10.1073/pnas.1701738114
- Shirasu, M., Touhara, K., 2011. The scent of disease: volatile organic compounds of the human body related to disease and disorder. *J. Biochem.* 150, 257–66. doi:10.1093/jb/mvr090
- Siju, K.P.P., Hill, S.R., Hansson, B.S., Ignell, R., 2010. Influence of blood meal on the responsiveness of olfactory receptor neurons in antennal sensilla trichodea of the yellow fever mosquito, Aedes aegypti. *J. Insect Physiol.* 56, 659–65. doi:10.1016/j.jinsphys.2010.02.002
- Smallegange, R.C., Takken, W., 2010. Host-seeking behaviour of mosquitoes: responses to olfactory stimuli in the laboratory, in: Takken, W., Knols, B.G.J. (Eds.), *Olfaction in Vector–Host Interactions*. Wageningen Academic Publishers.
- Smallegange, R.C., Takken, W., 2009. 7 . Host-seeking behaviour of mosquitoes : responses to olfactory stimuli in the laboratory 143–180.
- Smallegange, R.C., Verhulst, N.O., Takken, W., 2011. Sweaty skin: an invitation to bite? *Trends Parasitol.* 27, 143–148. doi:10.1016/j.pt.2010.12.009
- Smith, D.L., McKenzie, F.E., Snow, R.W., Hay, S.I., 2007. Revisiting the basic reproductive number

- for malaria and its implications for malaria control. *PLoS Biol.* 5, 0531–0542. doi:10.1371/journal.pbio.0050042
- Spencer, M., 1967. Anopheline attack on mother and infant pairs, Fergusson Island. *Papua New Guin. Med.* 10.
- Srinivas, G., Edwin Amalraj, R., Dhanraj, B., 2005. The use of personal protection measures against malaria in an urban population. *Public Health* 119, 415–7. doi:10.1016/j.puhe.2004.05.017
- Steinbrecht, R.A., 1996. Structure and function of insect olfactory sensilla. *Ciba Found. Symp.* 200, 158–74–7.
- Stresman, G.H., Kamanga, A., Moono, P., Hamapumbu, H., Mharakurwa, S., Kobayashi, T., Moss, W.J., Shiff, C., 2010. A method of active case detection to target reservoirs of asymptomatic malaria and gametocyte carriers in a rural area in Southern Province, Zambia. *Malar. J.* 9, 265. doi:10.1186/1475-2875-9-265
- Suckling, D.M., Sagar, R.L., 2011. Honeybees *Apis mellifera* can detect the scent of *Mycobacterium tuberculosis*. *Tuberculosis* 91, 327–328. doi:10.1016/j.tube.2011.04.008
- Suh, E., Bohbot, J.D., Zwiebel, L.J., 2014. Peripheral olfactory signaling in insects. *Curr. Opin. Insect Sci.* 6, 86–92. doi:10.1016/j.cois.2014.10.006
- Syhre, M., Chambers, S.T., Perkins, M.D., Cunningham, J., Ernst, J.D., Trevejo-Nunez, G., Banaiee, N., Phillips, M., Cataneo, R.N., Condos, R., Erickson, G.A.R., Greenberg, J., Bombardi, V.L., Al., E., Pavlou, A.K., Magan, N., Jones, J.M., Brown, J., Klatser, P.R., Turner, A.P.F., Fend, R., Kolk, A.H.J., Bessant, C., Buijtel, P., Klatser, P.R., Woodman, A.C., Okada, H., Nomura, N., Nakahra, T., Maruhashi, K., Xu, P., Yu, B., Li, F.I., Cai, X.F., Ma, C.Q., Edens, C.O., Creighton, M.M., Anderson, R.J., Ratledge, C., 2008. The scent of *Mycobacterium tuberculosis*. *Tuberculosis* 88, 317–323. doi:10.1016/j.tube.2008.01.002
- Syhre, M., Manning, L., Phuanukoonnon, S., Harino, P., Chambers, S.T., 2009. The scent of *Mycobacterium tuberculosis* - Part II breath. *Tuberculosis* 89, 263–266. doi:10.1016/j.tube.2009.04.003
- Syntech, 2004. EAG: a Practical Introduction. Syntech 29.
- Szempruch, A.J., Dennison, L., Kieft, R., Harrington, J.M., Hajduk, S.L., 2016. Sending a message: extracellular vesicles of pathogenic protozoan parasites. *Nat. Rev. Microbiol.* 14, 669–675. doi:10.1038/nrmicro.2016.110
- Takken, W., Dekker, T., Wijnholds, Y.G., 1997. Odor-mediated flight behavior of *Anopheles gambiae* *sensu stricto* and *An. stephensi* liston in response to CO₂, acetone, and 1-octen-3-ol (Diptera: Culicidae). *J. Insect Behav.* 10, 395–407. doi:10.1007/BF02765606
- Takken, W., Knols, B.G., 1999. Odor-mediated behavior of Afrotropical malaria mosquitoes. *Annu. Rev. Entomol.* 44, 131–57. doi:10.1146/annurev.ento.44.1.131
- Takken, W., Knols, B.G.J.J., 2010. Exploitation of olfactory-mediated behaviour, in: Takken, W., Knols, B.G.J.J. (Eds.), *Olfaction in Vector-Host Interactions*. Wageningen Academic Publishers, pp. 399–407.
- Taylor, P.J., Hurd, H., 2001. The influence of host haematocrit on the blood feeding success of *Anopheles stephensi*: implications for enhanced malaria transmission. *Parasitology* 122, 491–496. doi:10.1017/S0031182001007776
- Thomas, T.C., 1951. Biting activity of *Anopheles gambiae*. *Br. Med. J.* 2, 1402.
- Thomsen, E.K., Koimbu, G., Pulford, J., Jamea-Maiasa, S., Ura, Y., Keven, J.B., Siba, P.M., Mueller, I., Hetzel, M.W., Reimer, L.J., 2016. Mosquito behaviour change after distribution of bednets results in decreased protection against malaria exposure. *J. Infect. Dis.* 13, jiw615. doi:10.1093/infdis/jiw615
- Tirados, I., Esterhuizen, J., Kovacic, V., Mangwiro, T.N.C., Vale, G.A., Hastings, I., Solano, P., Lehane, M.J., Torr, S.J., 2015. Tsetse Control and Gambian Sleeping Sickness; Implications for Control Strategy. *PLoS Negl. Trop. Dis.* 9, e0003822. doi:10.1371/journal.pntd.0003822
- Turell, M.J., Bailey, C.L., Rossi, A.A., 1984. Increased mosquito feeding on rift valley fever virus-

- infected lambs 33, 1232–1238.
- Tusting, L.S., Bottomley, C., Gibson, H., Kleinschmidt, I., Tatem, A.J., Lindsay, S.W., Gething, P.W., 2017. Housing Improvements and Malaria Risk in Sub-Saharan Africa: A Multi-Country Analysis of Survey Data. *PLOS Med.* 14, e1002234. doi:10.1371/journal.pmed.1002234
- Tusting, L.S., Ippolito, M.M., Willey, B.A., Kleinschmidt, I., Dorsey, G., Gosling, R.D., Lindsay, S.W., 2015. The evidence for improving housing to reduce malaria: a systematic review and meta-analysis. *Malar. J.* 14, 209. doi:10.1186/s12936-015-0724-1
- Tusting, L.S., Willey, B., Lucas, H., Thompson, J., Kafy, H.T., Smith, R., Lindsay, S.W., 2013. Socioeconomic development as an intervention against malaria: a systematic review and meta-analysis. *Lancet* 382, 963–972. doi:10.1016/S0140-6736(13)60851-X
- van Breugel, F., Riffell, J., Fairhall, A., Dickinson, M., 2015. Mosquitoes Use Vision to Associate Odor Plumes with Thermal Targets. *Curr. Biol.* 25, 2123–2129. doi:10.1016/j.cub.2015.06.046
- van den Broek, I.V.F., den Otter, C.J., 1999. Olfactory sensitivities of mosquitoes with different host preferences (*Anopheles gambiae* s.s., *An. arabiensis*, *An. quadriannulatus*, *An. m. atroparvus*) to synthetic host odours. *J. Insect Physiol.* 45, 1001–1010.
- Verhulst, N.O., Andriessen, R., Groenhagen, U., Bukovinszky Kiss, G., Schulz, S., Takken, W., van Loon, J.J.A., Schraa, G., Smallegange, R.C., 2010a. Differential attraction of malaria mosquitoes to volatile blends produced by human skin bacteria. *PLoS ONE [Electronic Resour.* 5, e15829.
- Verhulst, N.O., Beijleveld, H., Knols, B.G., Takken, W., Schraa, G., Bouwmeester, H.J., Smallegange, R.C., 2009. Cultured skin microbiota attracts malaria mosquitoes. *Malar. J.* 8, 302.
- Verhulst, N.O., Beijleveld, H., Qiu, Y.T., Maliepaard, C., Verduyn, W., Haasnoot, G.W., Claas, F.H.J., Mumm, R., Bouwmeester, H.J., Takken, W., van Loon, J.J. a, Smallegange, R.C., Tong, Y., Loon, J.J.A. Van, 2013. Relation between HLA genes, human skin volatiles and attractiveness of humans to malaria mosquitoes. *Infect. Genet. Evol.* 18, 87–93. doi:10.1016/j.meegid.2013.05.009
- Verhulst, N.O., Qiu, Y.T., Beijleveld, H., Maliepaard, C., Knights, D., Schulz, S., Berg-Lyons, D., Lauber, C.L., Verduijn, W., Haasnoot, G.W., Mumm, R., Bouwmeester, H.J., Claas, F.H.J., Dicke, M., van Loon, J.J.A., Takken, W., Knight, R., Smallegange, R.C., 2011. Composition of human skin microbiota affects attractiveness to malaria mosquitoes. *PLoS ONE [Electronic Resour.* 6, e28991.
- Verhulst, N.O., Takken, W., Dicke, M., Schraa, G., Smallegange, R.C., 2010b. Chemical ecology of interactions between human skin microbiota and mosquitoes. *FEMS Microbiol. Ecol.* 74, 1–9. doi:10.1111/j.1574-6941.2010.00908.x
- Vézilier, J., Nicot, A., Gandon, S., Rivero, A., 2012. Plasmodium infection decreases fecundity and increases survival of mosquitoes. *Proc. R. Soc. London B Biol. Sci.*
- Vosshall, L.B., Hansson, B.S., 2011. A unified nomenclature system for the insect olfactory coreceptor. *Chem. Senses* 36, 497–8. doi:10.1093/chemse/bjr022
- Wanzirah, H., Tusting, L.S., Arinaitwe, E., Katureebe, A., Maxwell, K., Rek, J., Bottomley, C., Staedke, S.G., Kanya, M., Dorsey, G., Lindsay, S.W., 2015. Mind the Gap: House Structure and the Risk of Malaria in Uganda. *PLoS One* 10, e0117396. doi:10.1371/journal.pone.0117396
- WHO, 2017. Global Vector Control Response [WWW Document]. World Heal. Organ. URL http://www.who.int/malaria/areas/vector_control/Draft-WHO-GVCR-2017-2030.pdf?ua=1&ua=1
- WHO, 2016. World Malaria Report, World Health Organization. doi:10.4135/9781452276151.n221
- WHO, 2015. Global technical strategy for malaria 2016-2030. WHO Geneva 1–35.
- WHO, 2014. Control of residual malaria parasite transmission [WWW Document]. URL

Chapter 1: Literature review

<http://www.who.int/malaria/publications/atoz/technical-note-control-of-residual-malaria-parasite-transmission-sep14.pdf> (accessed 6.17.17).

- WHO, 2012. Global plan for insecticide resistance management in malaria vectors, World Health Organization press.
- Wondwosen, B., Hill, S.R., Birgersson, G., Seyoum, E., Tekie, H., Ignell, R., 2017. A(maize)ing attraction: gravid *Anopheles arabiensis* are attracted and oviposit in response to maize pollen odours. *Malar. J.* 16, 39. doi:10.1186/s12936-016-1656-0
- Wong, R.P.M., Flematti, G.R., Davis, T.M.E., 2012. Investigation of volatile organic biomarkers derived from *Plasmodium falciparum* in vitro. *Malar. J.* 11, 314. doi:10.1186/1475-2875-11-314
- Wood, W.F., Weldon, P.J., 2002. The scent of the reticulated giraffe (*Giraffa camelopardalis reticulata*). *Biochem. Syst. Ecol.* 30, 913–917. doi:10.1016/S0305-1978(02)00037-6
- Wright, R.H., Kellogg, F.E., 1962. Response of *Aedes aegypti* to moist convection currents. *Nature* 194, 402.
- Zwiebel, L., Takken, W., 2004. Olfactory regulation of mosquito–host interactions. *Insect Biochem. Mol. Biol.* 34, 645–652.

2 Odour profile analysis of individuals experimentally infected with *Plasmodium falciparum*

2.1 Introduction

Skin volatiles are the most important cues to haematophagous insects for locating bloodmeal hosts (Keystone, 1996; Price et al., 1979; Schreck et al., 1982; Smallegange et al., 2011; Verhulst et al., 2011). Further to this, differences in skin volatile profile are thought to mediate differences in host attractiveness to mosquitoes. Natural variation in attractiveness in humans to mosquitoes is thought to be innate, and the level of attractiveness remains approximately constant over time (De Jong and Knols, 1995; Logan et al., 2008; Qiu et al., 2006), with possible influences of factors including age, body weight, sex and pregnancy (Ansell et al., 2002; Lindsay et al., 2000; Port and Boreham, 1980). Influences on attractiveness appear to be mediated through body odour, as this variability is observed in the absence of all but olfactory cues (Logan et al., 2008; Schreck et al., 1990). It was hypothesised that the odour profile of malarious individuals, those infected with *Plasmodium* parasites, would differ from that of parasite-free individuals.

Skin odour can be sampled directly using either solvent or another adsorbent material (e.g. cotton pad). This method can be sub-optimal as highly volatile compounds may be insufficiently sampled, plus non-volatile compounds are collected, which may be less relevant to blood-feeding insects. Dynamic headspace adsorption (or 'air entrainment') circumvents this problem by collecting only emanating volatile compounds. While this can involve an intermediary medium, e.g. entraining clothing worn by an individual, analytical cleanliness is improved by sampling directly over the subject/item.

Air entrainment reduces the number of exogenous compounds inadvertently collected during sampling. Afterwards, volatiles are eluted from the filter with a solvent. This sample (the 'extract') is then concentrated prior to analysis, with the risk of losing some very low molecular weight volatile compounds during the concentration process (Dormont et al., 2013b). Due to the advantages of analytical cleanliness, and because collection favours the volatile compounds important to host-seeking mosquitoes, air entrainment was chosen for sampling in the current study.

In the case of skin volatiles, an accessible part of the body can be enclosed in a bag and an airflow used to direct volatiles from the skin over a filter. This has even been accomplished with an entire person in the bag, with only the head unenclosed (Logan et al., 2008). The feet are a preferred biting site for some insects including *Anopheles gambiae*, further, washing the feet with non-perfumed anti-bacterial soap reduces the volatile emissions and dramatically diverts *An. gambiae* to bite other body regions (De Jong and Knols, 1995). This, and other studies that demonstrate the response of *An. gambiae* to foot odour (Jawara et al., 2009; Njiru et al., 2006; Olanga et al., 2010; Omolo et al., 2013), informed our decision to sample the skin odour of the feet. In addition to the biological rationale, sampling the feet minimises discomfort to volunteers.

Access to *Plasmodium*-infected individuals was made possible by collaboration with the Radboud University Nijmegen Medical Centre (Department of Medical Microbiology, Nijmegen, The Netherlands), where controlled human malaria infections (CHMI, further referred to as 'experimental infections' (EI)) were being conducted (Roestenberg et al., 2013). EI are frequently used in the drug and vaccine development pipeline, where the parasite development, immunology, and pathology of infection can be closely monitored. We collaborated for three EI cohorts, of which some were designed to assess the utility of inactivated *Plasmodium falciparum* sporozoites in combination with chloroquine prophylaxis for protection against infection by *P. falciparum* (Bijker et al., 2013). In others, EI procedures were being optimised using two distinct *P. falciparum* strains, to mimic natural malaria infections that would comprise high genetic diversity (Vellefaux, 2012).

2.2 Aim and objectives

The aim of this chapter was to compare the odour profile of parasitologically positive, and parasite-free, individuals who were experimentally-infected with *Plasmodium falciparum* by bites from infected mosquitoes.

This aim was achieved through the following objectives:

1. To collect and analyse odour samples from the feet of individuals experimentally-infected with *P. falciparum*
2. To examine for quantitative or qualitative differences in the odour profiles of parasitologically positive and parasite-free individuals
3. To examine the influence of other infection parameters on the odour profiles where possible, including *P. falciparum* strain

2.3 Methods

2.3.1 Overview of the study

Individuals were experimentally-infected with *P. falciparum* parasites via the bites of infected mosquitoes (*Anopheles stephensi*), either following the intervention (drug treatment and vaccination) or not (control cohort). Participants from three of the trials (Table 2-1) were given the choice of whether to additionally participate in this ‘odour study’. Infections were performed by Radboud University, sampling was done in collaboration with Wageningen University (WU) and analysis took place at the London School of Hygiene & Tropical Medicine (LSHTM).

Table 2-1. Number of individuals (n) and total number of odour samples (OS) collected from EI population. Note, samples from the final time point are missing for TIP5A, and an extra sampling moment in BMGF.

Dataset	Sampling date (day PI)				n	OS (controls)
TIP5A	03/02/2013 (-2)		12/02/2013 (7)		10	24 (4)
TIP5B	06/10/2013 (-2)		16/10/2013 (8)	11/11/2013 (34)	6	24 (6)
BMGF	05/10/2014 (-2)	13/10/2014 (6)	15/10/2014 (8)	10/11/2014 (34)	11	45 (5)

2.3.2 Ethics

Full ethical approval was gained for each component of the study from the Dutch Committee on Research Involving Human Subjects (CCMO protocols NL39541.091.12 and NL48704.000.14, and the Research Ethics Committee at LSHTM (LSHTM ethics ref: 8510).

2.3.3 Participants

Exclusion criteria were regular smoking and regular use of medicines. For 24 hours prior to odour collection, and 12 hours after commencement of measurements, participants were asked to abstain from the consumption of alcohol, garlic, onion, potent herbs and spices. They were also asked not to shower or use perfumed cosmetics during this time period, or use perfumed soap during the last shower before this period. These measures were put in place to minimise the contamination of odour profile samples with exogenous compounds. A total of 27 participants participated in the odour sub-study across the three trials, and all were between 18 and 35 years old and in good health.

2.3.4 *Plasmodium falciparum* parasite strains and infection monitoring

Participants were infected with one of three strains; NF54, NF135 and NF166. The NF54 strain was derived from a patient isolate near Schiphol Airport (The Netherlands), thought to be of West African origin (the patient having never left the Netherlands; <https://www.beiresources.org/Catalog/BEIParasiticProtozoa/MRA-1000.aspx>, accessed 24/05/2017, (Delemarre and van der Kaay, 1979)). NF135.C10 (NF135) originates from Cambodia, and shows a reduced growth rate *in vitro* as compared to NF54. NF166.C8 (NF166) is from Equatorial Guinea (Vellefaux, 2012). Both NF135 and NF166 give rise to higher liver parasite loads than NF54, and it is thought that these strains are characterised by more infective sporozoites (Vellefaux, 2012). Infections were monitored from day five (TIP5A), seven (TIP5B) and six (BMGF) post-challenge (from here on referred to as post-infection, PI) until antimalarial treatment, using both thick smear microscopy and 18S qPCR (Hermsen et al., 2001). Antimalarial treatment (Malarone®; 250 mg atovaquone and 100 mg proguanil) was administered following two consecutive positive qPCR results, or at day 21 (TIP5A and TIP5B) or day 13 PI (BMGF).

2.3.5 TIP5A and TIP5B

In these cohorts all participants were exposed to the bites of five mosquitoes infected with NF54 *P. falciparum* sporozoites (Bastiaens et al., 2016). Previously, half of each cohort was inoculated with the test vaccine and half with saline solution, while all received chloroquine prophylaxis simultaneously for 14 weeks. Parasite challenge took place 33 days after the last dose of chloroquine. Odour profiles were collected before (day -2 PI), during (day 8 PI) and after (day 34 PI, after antimalarial treatment) infection for each trial (Table 2-1, Figure 2-1); however, samples from day 34 PI for TIP 5A were not preserved adequately for further analysis.

2.3.6 Bill and Melinda Gates Foundation (BMGF)

In this study participants were exposed to the bites of one, two or five mosquitoes infected with *P. falciparum* sporozoites of either NF135 or NF166 strain, as the investigators (Radboud University) were optimising CHMI protocols. No individuals were vaccinated or treated with antimalarials prior to challenge. Odour profiles were collected via air entrainment before (day -2 PI), twice during (days 6 and 8 PI) and after (day 34 PI, after antimalarial treatment) infection (Table 2-1, Figure 2-1). Participants who had already started antimalarial treatment on day seven PI were excluded from odour sampling on day eight PI.

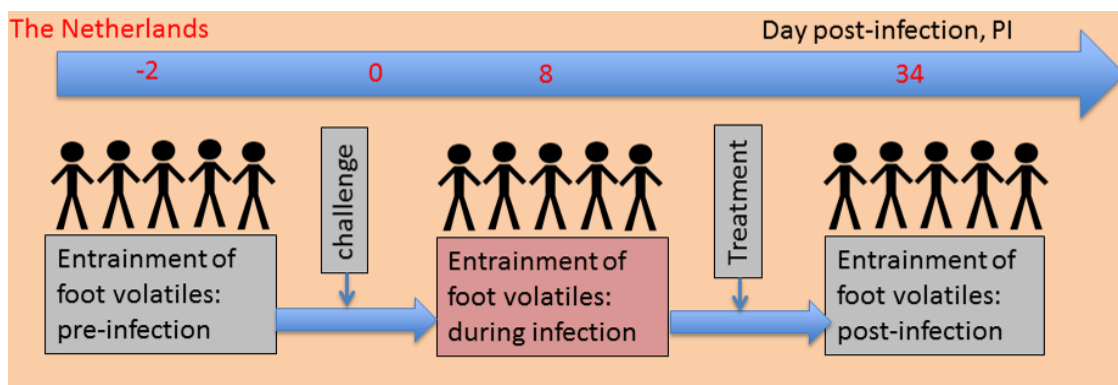


Figure 2-1. Schematic of air entrainment timeline. Individuals were sampled before sporozoite challenge by infected mosquitoes, during infection, and following treatment PI. All individuals were monitored for infection by microscopy and 18S qPCR, from day five PI until antimalarial treatment. The BMGF participants were sampled twice at the 'during infection' moment, on days 6 and 8 PI.

2.3.7 Air entrainment

Having ensured the volunteer was sitting comfortably, one foot was placed into a clean oven bag which was sealed tightly, while ensuring comfort, around the calf using bulldog clips. Charcoal-filtered air was directed (1400 mL/min) into the top of the bag via polytetrafluoroethylene (PTFE) tubing and Swagelok fittings. The air in the bag was allowed to purge by drawing air (700 mL/min) out of the bottom. After 30 minutes, a clean Tenax filter (Tenax TA, 60/80, Supelco Analytical, Bellefonte, PA, USA) was inserted into the bottom Swagelok fitting, and the vacuum pump (450 mL/min) connected. After 20 minutes the Tenax filter was replaced with a Porapak filter (Porapak Q, mesh size 50/80, Supelco Analytical, Bellefonte, PA, USA) which sampled for 100 minutes (650 mL/min). Controls were conducted in the same manner but with empty (sealed) bags. Following entrainment, all filters were placed into clean glass tubes and a cool box. Prior to use, all PTFE tubing was cleaned by running 70 % ethanol through and baking in an oven at 150°C for two hours. Bags were cleaned with the same baking protocol, and all Swagelok fittings were both baked and sprayed with ethanol prior to use. Charcoal filters were cleaned (minimum once per week) by baking the charcoal contents at 150°C for two hours. Glassware was cleaned with 70 % ethanol, acetone, and baked. Clean cotton gloves were worn by the investigators, and the comfort and wellness of the volunteers checked regularly. Filters were sealed in clean glass ampoules under a flow of purified nitrogen the following morning (TIP5B), or immediately (BMGF), while those from cohort TIP5A were not sealed under nitrogen.

2.3.8 Chemical analysis

The chemical analyses of Porapak filters were conducted jointly by LSHTM and Rothamsted Research (RR). Tenax analyses and interpretation were conducted jointly by RR and WU (data not shown).

Gas chromatography analysis

Porapak filters were removed from glass ampoules and immediately eluted with redistilled diethyl ether (750 μ L). These extracts were then concentrated by a stream of filtered nitrogen (to 50 μ L). Three gas chromatographs were used for analysis, one located in London (Agilent Technologies 7890A, "GC[1]") and two located at RR (Agilent Technologies 6890N and HP6890, termed "GC[2]" and "GC[3]" respectively). All samples in TIP5A were analysed using GC[2], those in TIP5B with GC[1], and those in BMGF with both GC[2] and GC[3]. All GC machines were fitted with a cool-on-column injector, flame ionization detector, used hydrogen carrier gas, and 1 μ L of sample was injected. All were fitted with a HP1 column, 50 m x 0.32 mm, film thickness 0.52 μ m, and the following programme was used: temperature maintained at 40 °C for 0.5 minutes, increased by 5 °C per minute to 150 °C, held for 0.1 minute, raised by 10 °C per minute to 230 °C, held for 30 minutes. Latterly, for samples run at RR, the final holding time was extended by 10 minutes to ensure exit of all volatiles. The remaining amount of extract was measured, then extracts were diluted to 1 mL with re-distilled diethyl ether and stored in ampoules at -20 °C.

Integration of GC traces

GC traces were analysed using Agilent ChemStation (C.01.04). Integration parameters were set by excluding peaks of less than a designated amount (the 'area reject'). Here, the area reject was set to 0.05 ng, which was sensitive enough to capture even very small analytes (peaks), though not so sensitive that noise was inadvertently detected. Other integration parameters were fixed (Table 2-2).

Table 2-2. Integration parameters used during GC analysis

Integration parameter	Value
Slope sensitivity	1
Peak width	0.04
Height reject	0
Area reject	X (equivalent to 0.05 ng)
Integration on/off	Integration was set to come on after the solvent peak

Calculating Retention Indices and compound amount

Peak retention time was used to calculate the retention index (RI), a system-independent constant that approximately identifies a compound relative to a set of alkane standards. Retention Indices were calculated for all peaks eluting between the first (heptane, C₇H₁₆), and last (pentacosane, C₂₅H₅₂), alkane (Equation 2-1). Peak amounts were adjusted to represent the total amount of compound collected during the 100-minute entrainment.

Equation 2-1. Retention index (RI) calculation

$$RI = 100 (\log_{10}Rt_x - \log_{10}Rt_n / \log_{10}Rt_{n+1} - \log_{10}Rt_n) + 100n$$

Rt_x = Retention time for compound of interest

Rt_n = Retention time for alkane before compound of interest

Rt_{n+1} = Retention time for alkane after compound of interest

n = number of carbons in alkane before compound of interest

Gas chromatography-mass spectrometry

Compounds determined to be of importance, following the below analysis, were tentatively identified by gas chromatography-mass spectrometry (GC-MS). For BMGF (samples analysed on GC[2] and GC[3]), peaks were identified in samples run on both GC machines. This verified the alignment of peaks between different instruments.

GC-MS was performed on a Micromass Autospec Ultima, a magnetic sector mass spectrometer, equipped with a PTV unit (ATAS GL) and Agilent 6890N GC (fitted with a non-polar HP1 column 50 m length x 0.32 mm and 0.52 µm film thickness, J & W Scientific). Ionization was by electron impact (70 eV, 220 °C). The GC-oven temperature was maintained at 30 °C for 5 minutes and then programmed at 5 °C/minute to 250 °C. Samples were analysed by thermal desorption (PTV unit programmed to start at 30 °C then rise to 250 °C at 160 °C/second). The software package was Masslynx V4.1, which uses the commercial NIST database. When necessary, authentic

standards were run to ensure matching of mass spectra and elution time. Synthetic standards were run for 2-ethylhexanoic acid, 1-dodecene, dodecanal, and methyl dodecanoate. This was not considered necessary for 6-methyl-5-hepten-2-one, as tentative identification based on mass spectra was considered conclusive.

2.3.9 Data analysis

Data cleaning

BMGF samples were analysed using two GCs, and on manual inspection of the traces (GC output) it was apparent that peak RI values generated by the two machines were slightly different, in a non-uniform manner across the trace. Characteristic peaks were used to align as far as possible, and a stringent approach was adopted by only retaining peaks that could be aligned with certainty. The number of peaks analysed in the BMGF dataset was therefore reduced relative to the other datasets, but this was not a reflection of the quantity of material in the samples.

Hierarchical Cluster Analysis

Data were initially explored using a hierarchical cluster analysis. Cluster analysis is an exploratory technique that groups units of data (here, odour samples) according to their similarities across all variables (peaks). Grouping is based entirely on information within the data: the analysis assigns an index of similarity between every combination of units (samples) and across all variables. Clustering is therefore independent of any underlying theory or biological context (i.e. it does not tell you in what way samples are different). Here, similarity matrices were created using Euclidean, Manhattan and Ecological methods. The Manhattan method uses absolute rather than squared (i.e. Euclidean) distances, and the Ecological method excludes the contribution to similarity by matches of zeros between profiles of subjects. Manhattan and Ecological matrices were more appropriate for the TIP5B and TIP5A datasets as respectively all, and most, variables (peaks) were retained including many with primarily zero values, whereas Euclidean was more appropriate to the restricted BMGF dataset (see Data cleaning). The clustering technique used was 'group average', which forms new group clusters by joining the most similar pairs of current clusters. Minimum spanning trees were also constructed. These give a two-dimensional representation of the overall distances between the (chemical) profiles of samples, demonstrating how the samples cluster together via lines joining them in the plot, and therefore any outliers are joined by relatively long lines.

Multivariate analyses

Several multivariate methods were attempted, including principle component analysis (PCA), principle co-ordinate analysis (PCO) and canonical variate analysis (CVA), a form of linear discriminant analysis (LDA). LDA identifies combinations of variables that can be used to discriminate between groups and generates rules that will allocate new observations to the groups. Here, LDA was used to attempt to discriminate between parasitologically positive, negative and control samples according to their chemical profile. CVA was the most appropriate technique for these datasets as there were known groups in the data (parasitological status), while PCO and PCA seek groupings as a statistical solution. Parasitological status was the CVA grouping factor, defined as a binary ‘positive vs. negative’, or additionally incorporating temporal differences (i.e. before, during and after challenge) (Table 2-3). In the BMGF dataset, *P. falciparum* strain and number of infectious bites received varied, so these groupings were also examined (Table 2-4). Here, pre-exposure samples were excluded (day -2 PI) but post-clearance samples (day 34 PI) were retained, as in other analyses (i.e. parasitological status) the continued upregulation of some infection-associated compounds (IAC) at day 34 had been observed.

Table 2-3. Summary of CVA groupings used to investigate the influence of parasitological status per dataset, with sample size per group. Positive and During [+] indicate samples from individuals who tested Plasmodium parasite positive by qPCR on the same day. Negative and During [-] refer to samples from individuals who were parasite free by qPCR on the same day. *In BMGF, repeat ‘during’ sampling occurred due to two ‘during’ sampling efforts. **TIP5A ‘after’ samples were not considered adequate for analysis.

Canonical Variate Analysis	Group	Observations (Individuals)		
		TIP5A	TIP5B	BMGF
Parasitological status	Positive	6 (6)	3 (3)	9 (8)
	Negative	14 (10)	15 (6)	29 (11)
	Control (empty bag)	2	6	6
	Ether control	1	Not included	3
Parasitological status with sampling time point	Before	10 (10)	6 (6)	9 (9)
	During [-]	4 (4)	3 (3)	9 (7)*
	During [+]	6 (6)	3 (3)	9 (8)*
	After	None **	6 (6)	11 (11)
	Control (empty bag)	2	6	6
	Ether control	1	Not included	3
Total (human samples)		20 (10)	18 (6)	38 (11)
Total (control samples)		3	6	9

Chapter 2: Odour profile analysis of individuals experimentally infected with *P. falciparum*

Table 2-4. CVA groupings used in BMGF dataset to investigate associations between compound production and *P. falciparum* strain, and number of infectious bites received, with sample size per group. For these analyses, samples from day -2 PI were excluded (prior to challenge), as were samples from the two individuals who remained negative throughout (BMGF2_006 and BMGF2_028).

Canonical Variate Analysis	Group	Observations (Individuals)
<i>P. falciparum</i> strain	NF135	13 (5)
	NF166	10 (4)
	Control (empty bag)	6
	Control (ether)	3
Number of infectious mosquito bites received	1	8 (3)
	2	12 (4)
	5	9 (4)
	0 (controls)	9 (as above)

For each compound, the magnitude of the loading it exerted on the canonical variate (CV) was inspected, to determine which compounds contributed most to the differences between group means. Those contributing to separation on the CV important in separating groups, by at least 50 % of the influence of the most important compound, were examined by comparing group means (and error bars). The amount produced per sample was also considered. ‘Compounds of interest’ (COI) were chosen on the premise that some differences in compound production were observed according to parasitological categorisation. All COI were re-examined manually on a trace-by-trace basis, to ensure that the peak had been appropriately aligned. In addition to multivariate analysis, summary statistics (median and interquartile range) were examined according to parasitological category (positive or negative), as a final visual check for compounds that characterised parasitological status.

Univariate analysis (linear mixed models)

All COI from the above analyses (multivariate and boxplot) were tested for significant differences between parasitological groups using linear mixed models. The models were fitted using the method of residual maximum likelihood (REML), which tested (F tests) for the overall effect of parasitological infection while allowing for repeated observations on the same individuals, and unequal sample sizes. The influence of individual and individual by time point was incorporated into the random model. The main effect of parasitological infection was tested using the categories given in Table 2-5, replicating the categories used for CVA when positivity and negativity ‘during’ infection was split (Table 2-3, ‘Parasitological status with sampling time point’). It was preferable to investigate differences in odour profile over the course of infection, rather than oversimplifying by grouping ‘Before’, ‘During [-]’ and ‘After’ as ‘Negative’. Additionally, it was considered possible that some effects of infection could linger, thus it was

important to take into account the temporal nature of these samples. In the final REML analysis for the BMGF dataset, individuals BMGF2_006 and BMGF2_028 were excluded as they did not become positive for *P. falciparum* parasites at any time point. In this way, innate variation in compound production leading to differences in infection outcome could be excluded, as all individuals in the final analysis became parasite positive. Thus, the ‘During [-]’ individuals represent odour profile prior to bloodstream parasitaemia, in individuals who subsequently became positive. No exclusions were necessary for TIP5A and TIP5B as all individuals became positive. A natural logarithmic transformation, with unit adjustment (1 or 0.01) to allow for zero observations, was applied to the data to account for heterogeneity of variance. Predicted group means from the model were compared between groups of interest by examining the least significant difference (LSD) at the 5 % level of significance. Data analysis was conducted using GenStat (16th edition, VSNi).

Table 2-5. Parasitological categories to which odour profile samples were assigned, for predicting the effect of infection status on compound production (REML mixed models).

Category	Description	Notes
Before	Odour profile samples taken before infection. Always sampled two days prior to challenge (day -2 PI)	All individuals parasite-free
During [-]	Odour profiles sampled after challenge, but before the detection of blood stage parasites by qPCR	Individuals parasite-free, but to become parasite positive
During [+]	Odour profiles sampled after challenge, and following detection of blood stage parasites by qPCR	Individuals parasite-positive at that time point, with exceptions made in TIP5B (see results)
After	Odour profile samples taken after parasite clearance. Always sampled 34 days PI	All individuals had received antimalarial treatment
Control	Empty bag samples taken at any of the above sampling moments	

2.4 Results

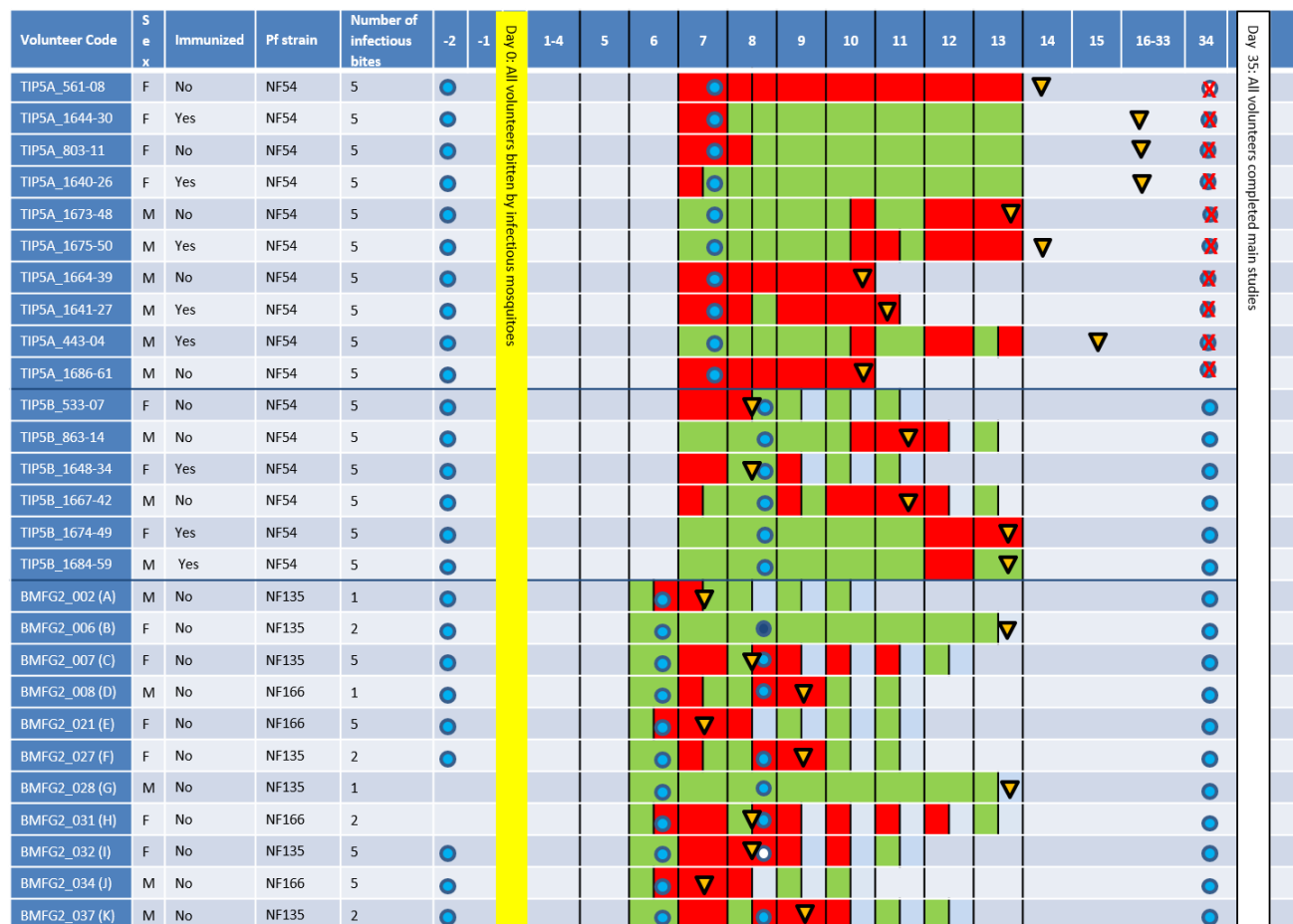
2.4.1 Study population

The TIP5A study cohort comprised six males and four females. At the second time point, on day seven PI, seven of ten individuals were positive for *P. falciparum* and the remaining three were negative. All negative individuals did become positive by day ten.

The TIP5B study cohort comprised three males and three females. By day eight PI, three individuals had tested positive for malaria parasites, although it should be noted that on the evening of odour sampling all three tested negative. Two of these individuals (TIP5B_533-07 and TIP5B_1648-34, Figure 2-2), were considered positive as they had tested positive just previously in two consecutive moments (i.e. twice in 24 hours), and had received antimalarial treatment immediately prior to odour profile sampling. Because of atovaquone proguanil parasite clearance times (approximately 100 % of baseline parasite count remains at 12 hours, 0 % at 48 hours (Bustos et al., 1999)), these individuals would have still harboured bloodstream parasites. The third (1667-42, Figure 2-2) was considered positive because he/she had tested positive both the day before sampling and on the morning after, therefore, must have harboured parasites in-between. Here, parasite densities were not allowed to progress above a very low level for ethical reasons, and that level fluctuated around the qPCR test limit of detection. By day 34 PI, all individuals had become positive, been treated, and were clear of parasites.

The BMGF study cohort contained 11 individuals, five male and six female. Of these 11, nine became parasitologically positive. As this was complicated by the two 'during' odour sampling moments (days six and eight), for analysis, all parasitologically positive samples from both of these days were grouped. Therefore, there were nine 'during positive [+]' and nine 'during negative [-]' samples, with only one individual represented at both time points in the positive group (BMGF2_031, Figure 2-2). Two positive individuals received treatment during odour sample collection (BMGF2_007 and BMGF2_031), but were considered positive for analyses. The negative group contained two individuals with repeated measures, as these two remained negative throughout (BMGF2_006 and BMGF2_028, Figure 2-2). These two individuals were excluded from the final univariate analysis. By day 34, all individuals had been treated and were clear of parasites.

Chapter 2: Odour profile analysis of individuals experimentally infected with *P. falciparum*



● Odour samples collected ○ Porapak missing ✖ Sample lost ● Tenax missing ■ PCR-negative ■ PCR-positive ▼ Antimalarial treatment

Figure 2-2. Overview of participants in EI cohorts TIP5A, TIP5B and BMGF. Sex, immunization status, strain of *P. falciparum*, and the number of infectious bites used for parasite challenge is indicated per individual. Antimalarial treatment was given after two positive qPCR results. On day zero, individuals were challenged by the strain indicated, via the number of bites from infectious mosquitoes also indicated. Replicated with permission from De Boer (2017) (in prep).

2.4.2 Hierarchical cluster analysis: exploration of data

Overall, there was a lack of clustering according to parasitological status, indicating that a more complex statistical analysis was necessary.

TIP5A and TIP5B hierarchical cluster analysis

Hierarchical cluster analysis of odour profile samples from the TIP5A and TIP5B datasets did not indicate clustering by parasitological parameters (e.g. parasitological status or sampling day) by any method tested. Additionally, repeat odour profile samples from the same individual did not cluster together (Ecological method shown in Figure 2-3, Figure 2-4).

BMGF hierarchical cluster analysis

In the BMGF dataset there was clear grouping of controls and individuals (e.g. control cluster at the top of the dendrogram, Figure 2-5A), some grouping by individuals at different time points (e.g. individual 'F', Figure 2-5), and some grouping of different individuals from the same time point (e.g. time point 4, Figure 2-5, Figure 2-2). Two positive individuals, BMGF_031 and BMGF_034 (also termed individuals 'H' and 'J', Figure 2-5), at time point two (day 6 PI) were quite distinct from other samples, as seen in the minimum spanning tree (Figure 2-5B). This pattern was seen irrespective of which cluster analysis method was used (data not shown).

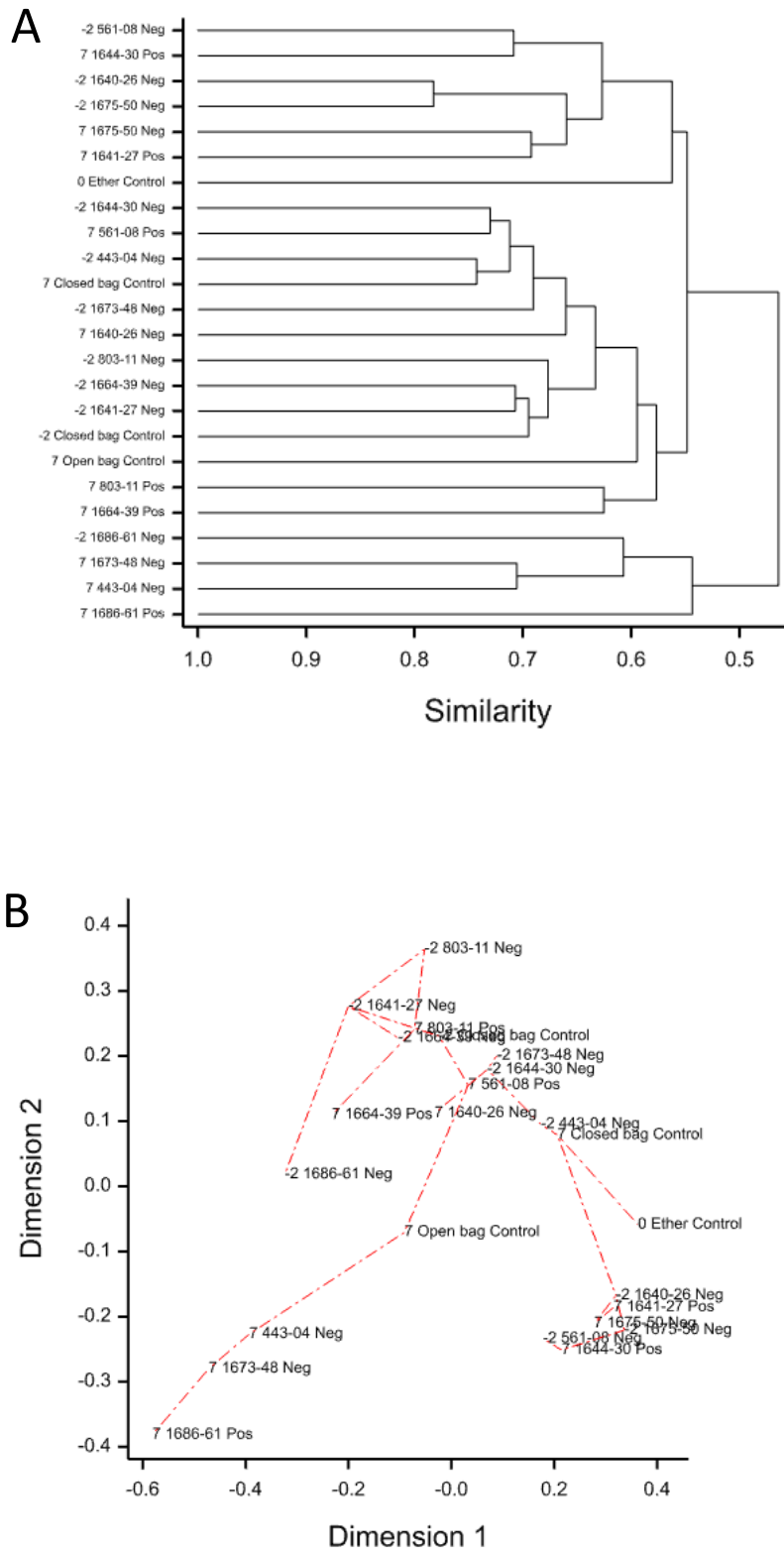


Figure 2-3. Dendrogram (A) and minimum spanning trees (B) for hierarchical cluster analysis of **TIP5A** dataset, created using an Ecological similarity matrix with the 'group average' clustering technique. Samples are labelled by: day PI (i.e. pre-challenge [day -2 PI] and during infection [day 7 PI]), identifier, and parasitological status (positive, POS; negative, NEG).

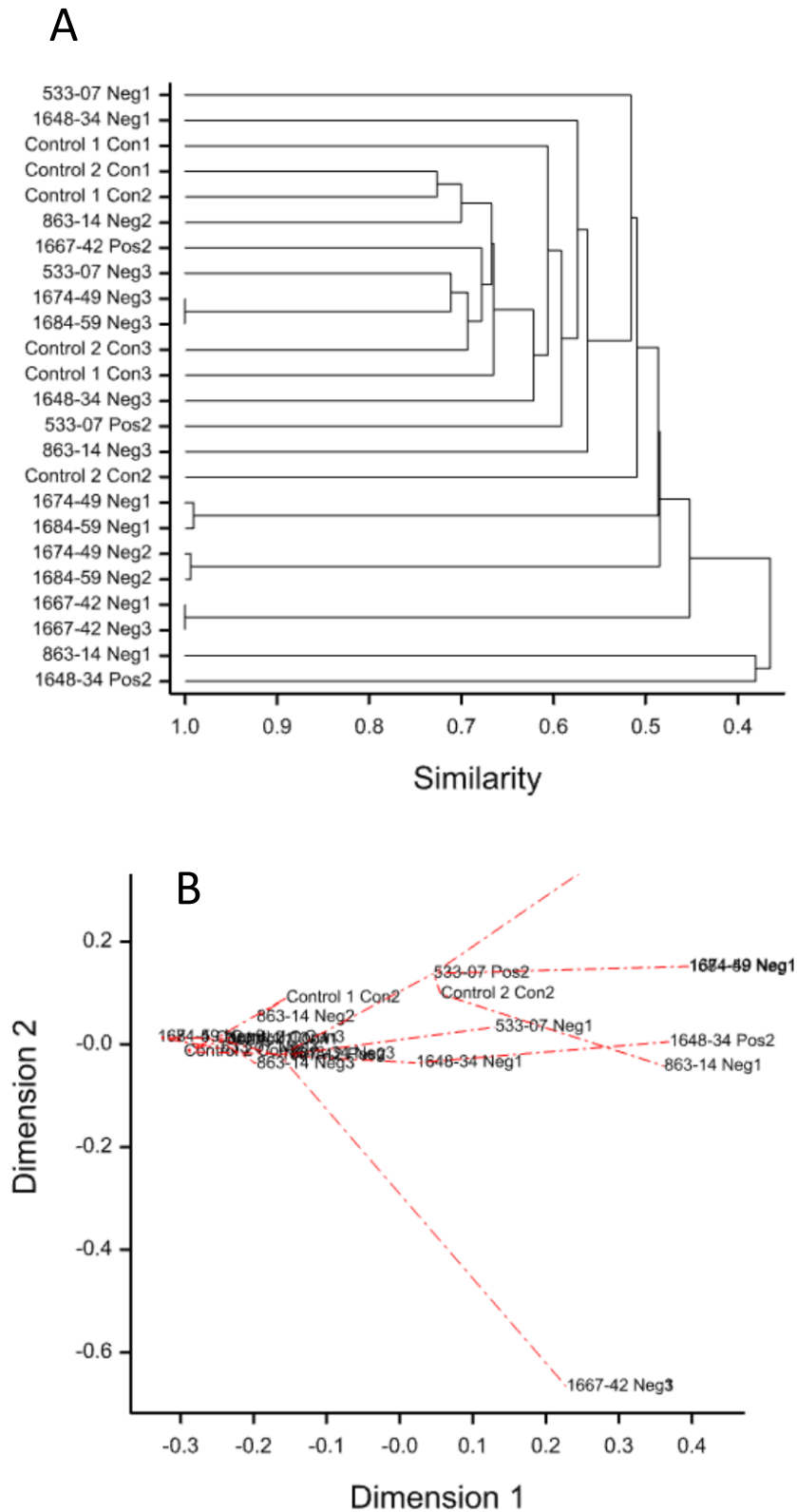


Figure 2-4. Dendrogram (A) and minimum spanning trees (B) for hierarchical cluster analysis of **TIP5B** dataset, created using an Ecological similarity matrix. Samples are coded by: unique identifier, status (positive, POS; negative, NEG; and control), time point (**1**: day -2 PI, **2**: day 8 PI, **3**: day 34 PI).

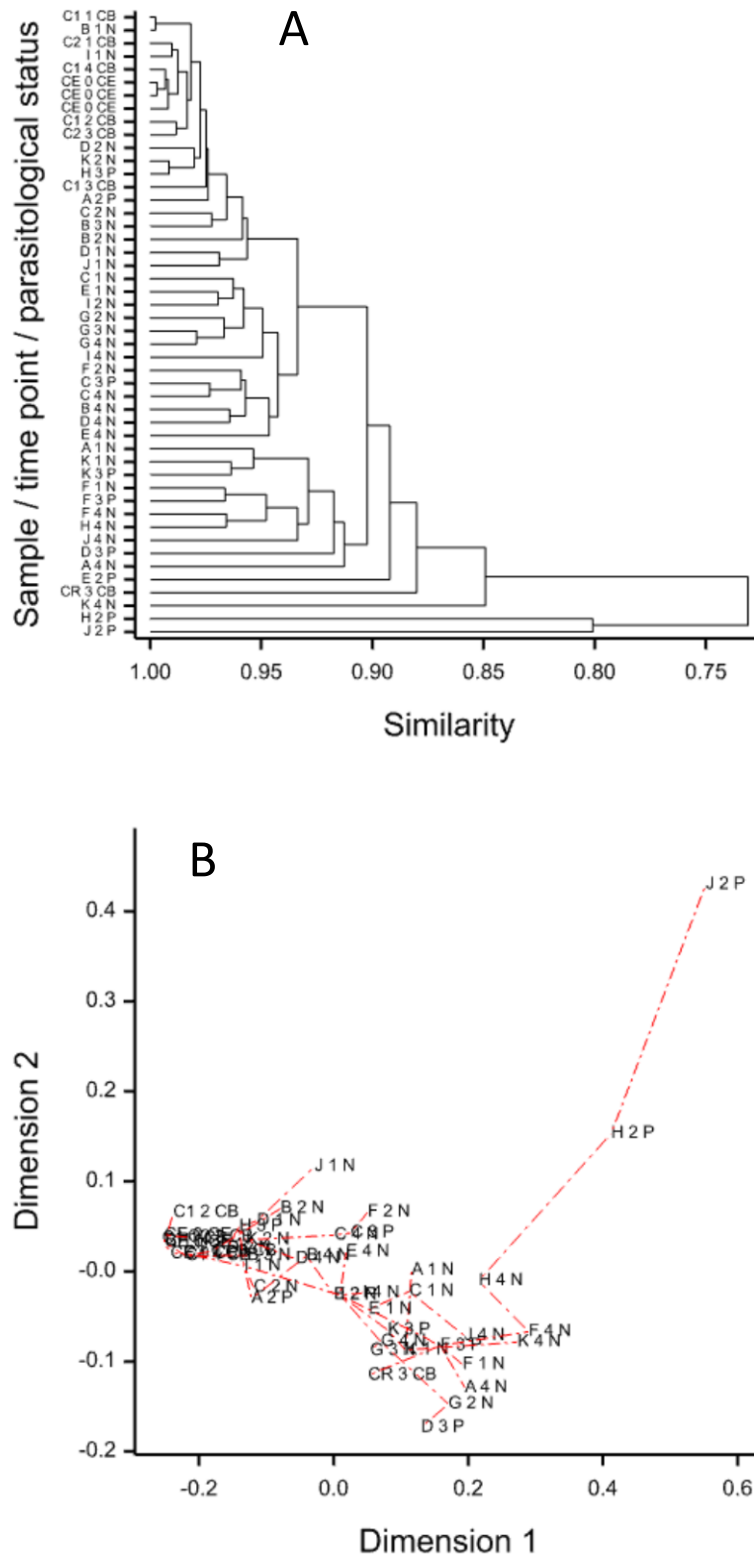


Figure 2-5. Dendrogram (A) and minimum spanning tree (B) for hierarchical cluster analysis of **BMGF** dataset using a Euclidean similarity matrix and ‘group average’ clustering method. Samples are coded by: unique identifier (11 individuals designated A-K, see Figure 2-2), time point (1: day -2 PI, 2: day 6 PI, 3: day 8 PI, 4: day 34 PI), and status (negative, N; positive, P; control, C).

2.4.3 CVA analysis of association between parasitological status and compound production

Canonical variates analysis, grouped by parasitological status as a binary of 'Positive' or 'Negative' (Table 2-3), allowed relatively good separation between the groups for BMGF, but limited separation in TIP5A and B. Positive and negative groups in TIP5A and TIP5B were slightly separated by both CV1 and CV2, revealing some main effect of status (Figure 2-6). The large 95 % confidence interval for the TIP5B positive group is a consequence of the low sample size (n=3, Figure 2-6B). In the BMGF cohort, samples were quite well separated by CV1 and CV2, albeit with overlapping 95 % confidence intervals (Figure 2-7). CVA analysis using the temporal parasitological status ('Before', 'During [-]', 'During [+]' and 'After') showed less distinct separation of groups (data not shown).

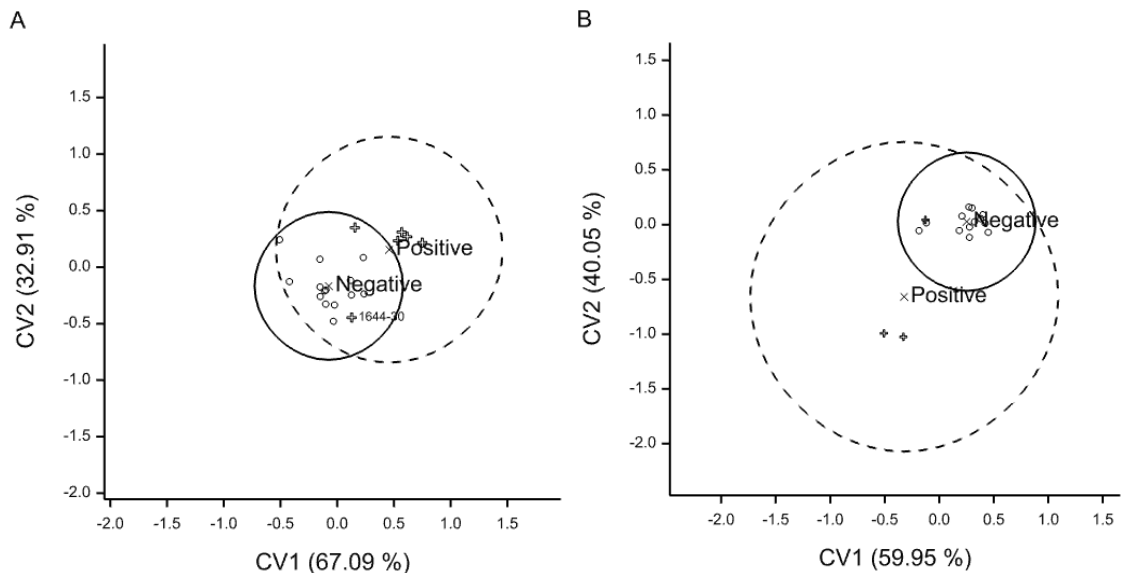


Figure 2-6. Canonical variates plot of the TIP5A (A) and TIP5B (B) data, grouped by parasitological status, irrespective of sampling moment. Samples are positioned by scores on canonical variates axes, relative to the presence and quantity of compounds contributing to these axes. The percentage of possible discrimination accounted for is included in the axes labels, circles represent 95 % confidence intervals. **A:** Negative group, circles and intact line, observations=14, n=10; Positive group, plus signs and dashed line, n=6; controls not shown, n=3. **B:** Negative group, circles and intact line, observations=15, n=6; Positive group, plus signs and dashed line, n=3; controls not shown, n=6. Control groups not shown, to enhance clarity.

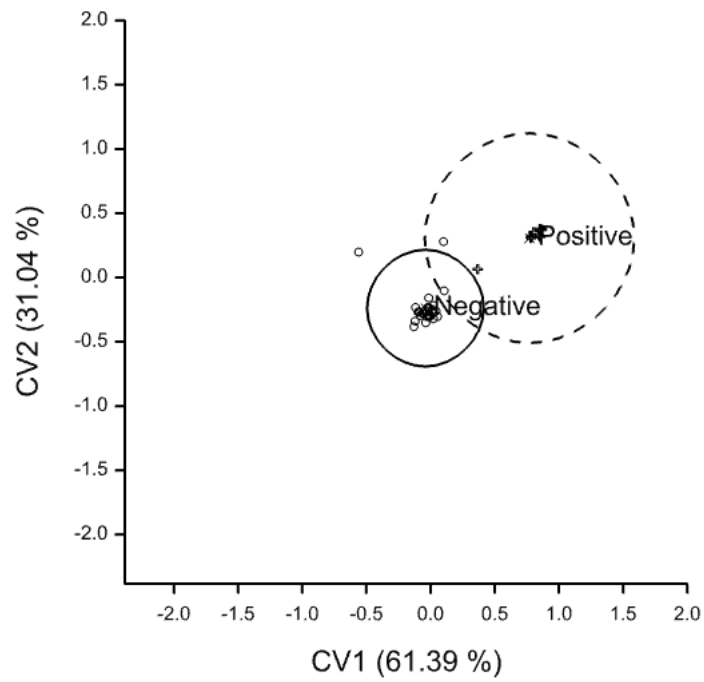


Figure 2-7. Canonical variates plot of the BMGF data, grouped by parasitological status, irrespective of sampling moment. Circles represent 95 % confidence intervals. Negative group, circles and intact line, observations=29, n=11; Positive group, plus signs and dashed line, observations=9, n=8; Bag control, not shown, n=6; Ether control, not shown, n=3. Control groups not shown, to enhance clarity.

2.4.4 Infection-associated compounds

TIP5A

Of the 661 peaks examined, nine were considered to be COI. Of those nine, compound RI 1598 was present in significantly different amounts between groups ($P<0.001$), while compounds RI 792 and RI 1167 were approaching significance (Figure 2-8) ($P=0.09$, 14 DF; $P=0.148$, 11 DF respectively). There was no association between compound production and parasitological status for the remaining six compounds ($P>0.05$). Production of RI 1598 by 'During [-]' samples was significantly greater than by 'Before' samples (difference greater than the least significant difference at the 5 % level, LSD 5 %) (Significant pairwise differences given in Appendix 2.8). While intriguing, this variation cannot be attributed to the presence of parasites. RI 792 was found in significantly greater amount in 'During [+]' samples relative to 'Before [-]' and 'During [-]', and the amount of RI 1167 dropped significantly in 'During [-]' samples relative to 'Before [-]' and 'During [+]' . However, for both RI 792 and RI 1167, human entrainments did not differ significantly from the system controls, which were found to contain high amounts of both compounds.

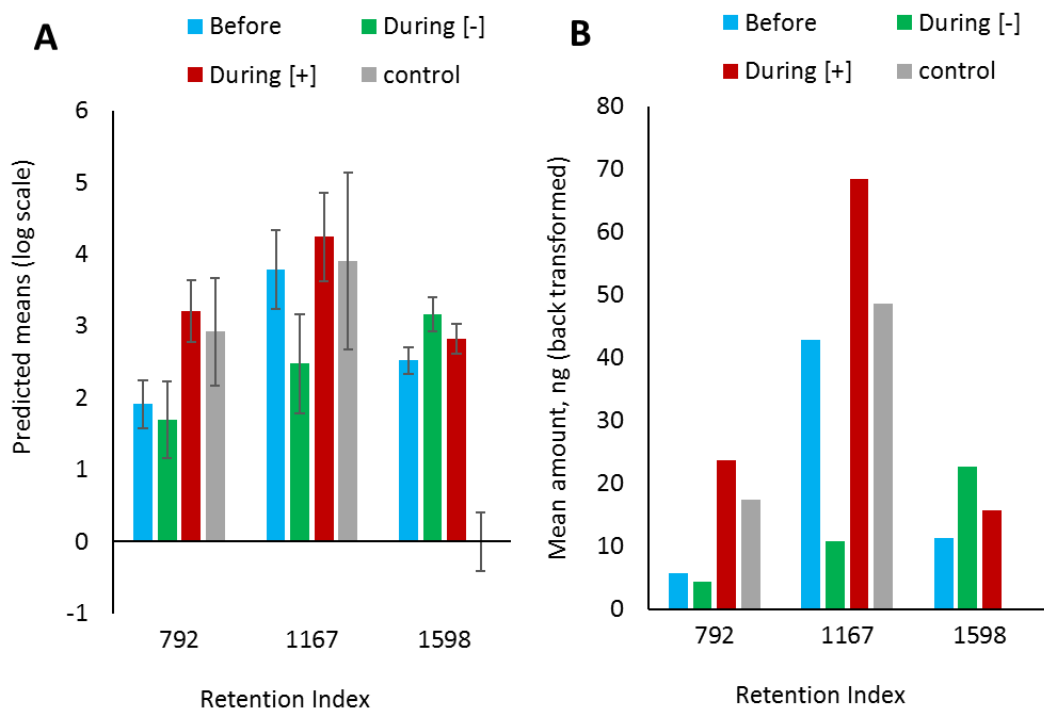


Figure 2-8 (A) Predicted mean total amount produced in 100-minute entrainment, log transformation, for three compounds found to be produced in significantly (RI 1598) or approaching significantly (RI 792 and RI 1167) different amounts between groups. For RI 792, $P=0.09$ (DF=14) and average standard error of the difference=0.737. For RI 1167, $P=0.148$ (DF=11) and average standard error of the difference=0.979. For RI 1598, $P<0.001$ (DF=11) and average standard error of the difference=0.339. (B) Predicted means back transformed, same data. Sample sizes were: before, $n=10$; during [-], $n=4$; during [+], $n=6$; control, $n=2$.

TIP5B

Of 434 peaks in the TIP5B dataset, loadings of more than 50 % on those CV that accounted for the separation of groups (Figure 2-6B) were accountable to three analytes, RI 973, RI 1092 and RI 1095. When modelled by REML using parasitological groupings split at 'During' ('Before', 'During [-]/[+]' and 'After'), RI 1095 was significantly predicted by the main effect ($P=0.028$, Figure 2-9A,B). 'During' [-]/[+] groups were found to produce more of RI 1095 than both 'After' and controls. Additionally, samples in the 'After' group produced significantly less than 'Before' (LSD, 5 %). Inspection of GC-MS data for RI 1095 showed two compounds co-eluting, (*R*)- or (*S*)-2-ethylhexanoic acid, a likely human volatile product, and another compound of exogenous origin. Peaks RI 973 and RI 1092 were not significantly predicted by parasitological status ($P=0.331$ and $P=0.405$ respectively) (data not shown).

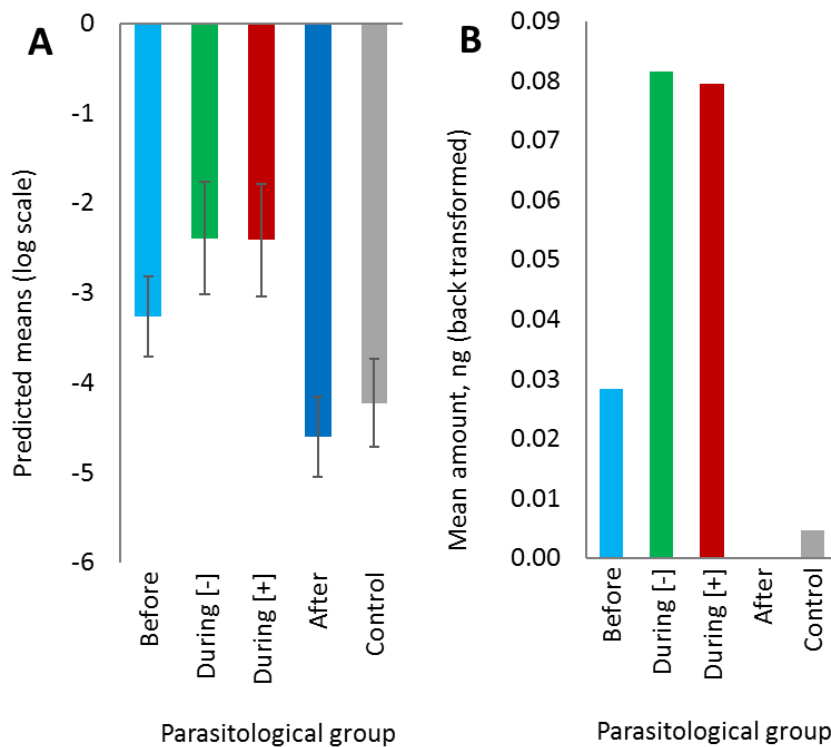


Figure 2-9. (A) Predicted mean total amount produced in 100-minute entrainment, log transformation, for RI 1095, found in significantly greater amounts in the 'during [-]' and '[+]' groups, relative to 'after' and controls ($P=0.028$, 13 DF). Error bars=predicted standard error. (B) Predicted means back transformed. Average standard error of the difference=0.734. Sample sizes were: before, $n=6$; during [-], $n=3$; during [+], $n=3$; after, $n=6$; control, $n=2$.

BMGF

Of 132 peaks examined, 25 were subject to more detailed statistical analysis as COI (Figure 2-10). At this stage, GC-MS identification led to the exclusion of eight compounds, which were determined to be clearly of exogenous origin. A further eight were excluded on the basis that variation between parasitological groups lay solely between human odour samples and the system controls (i.e. empty bags and ether). In the final analysis, excluding those individuals who remained negative throughout, the production of two compounds, dodecanal and biphenyl, was significantly predicted by parasitological status at the 1 % level (REML, both $P < 0.001$). Two further peaks, significant at the 5 % level, were identified as 6-methyl-5-hepten-2-one ($P = 0.002$) and a co-eluting phthalate and sesquiterpene (RI 1416, $P = 0.031$). The production of 1-dodecene and methyl dodecanoate was of borderline significance ($P = 0.05$ and $P = 0.076$ respectively), while the production of tridecane and an unidentified ring-structured compound (RI 1222) were not found to be significantly predicted by infection status ($P = 0.184$ and 0.328 respectively) (Figure 2-11).

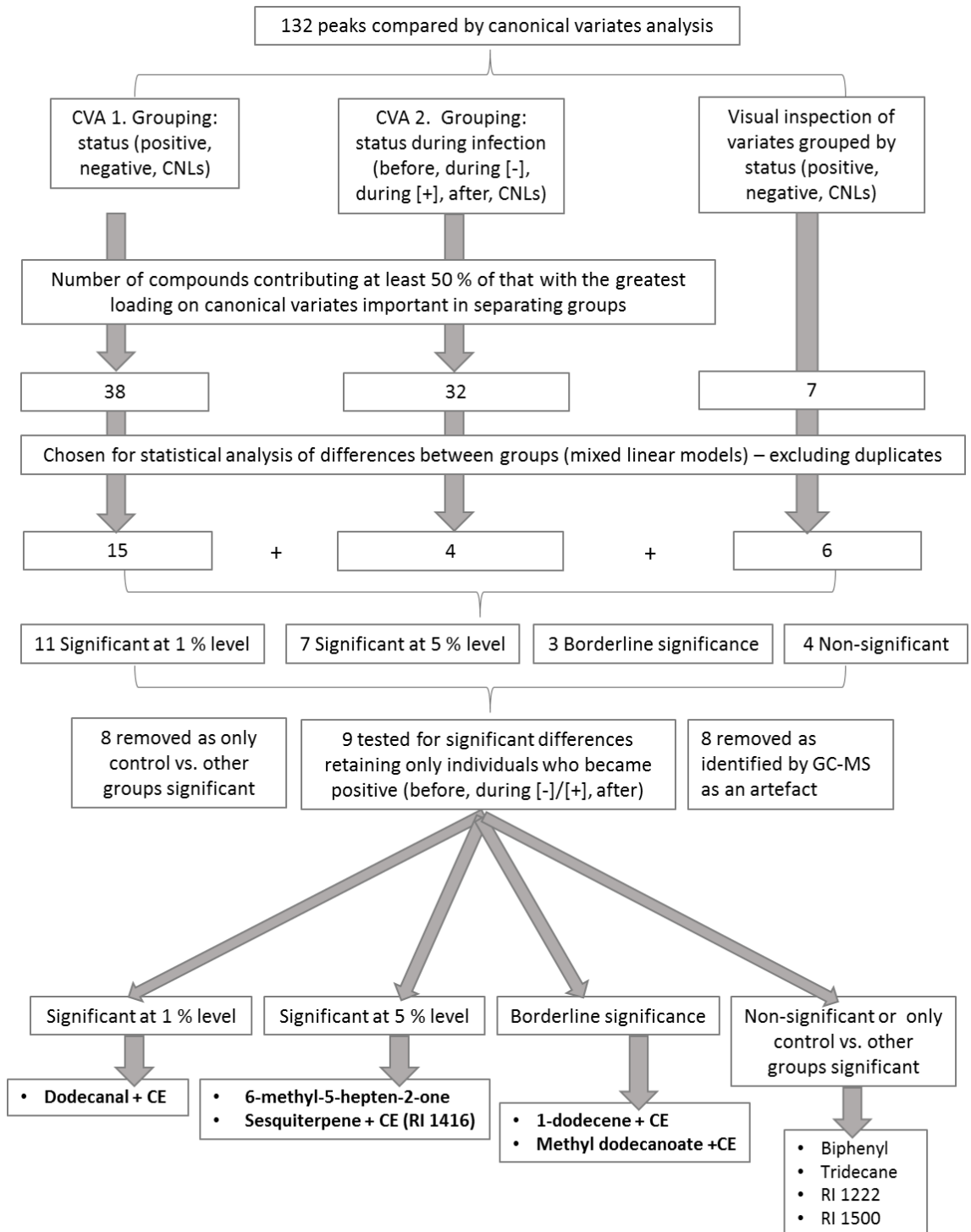


Figure 2-10. Flow chart showing the number of COI in the BMGF dataset at each stage in the analytical process, through to significance of final candidate compounds. Bold typeface indicates important pairwise differences in the production of compound between parasitological categories, CE = co-eluting, CNLs = empty bag controls and solvent controls (distinct groups).

The production of 6-methyl-5-hepten-2-one (RI 972, Figure 2-11) was seen to decrease in both 'During' groups (irrespective of positivity), with the greatest decrease in 'During [-]', where production was significantly less than that by both 'Before' and 'After' groups (LSD, 5 %). Production of 6-methyl-5-hepten-2-one by 'During [+]' individuals was non-significantly reduced relative to that by 'Before' or 'After' groups. Therefore, during infection, 6-methyl-5-hepten-2-one production decreased initially but as parasites became detectable in the blood (individuals moved from 'During [-]' to 'During [+]' status), production started to increase again. Significant pairwise differences between important group means are summarised for all compounds in Table 2-6 and Table 2-7. In the final analysis, two individuals were removed as they remained parasitologically negative throughout. The level of 6-methyl-5-hepten-2-one was unaffected in these two participants, considered to be non-immune challenged, supporting the association of infection and emission of 6-methyl-5-hepten-2-one (data not shown).

The production of 1-dodecene (RI 1193) was increased in the 'During [+]' group relative to the 'Before' group (LSD, 5 %; Figure 2-11). This effect was not seen in the 'During [-]' group, strengthening the association with the presence of parasites. Production decreased again in the 'After' group. Similarly, dodecanal (RI 1392) was present in greater amount in 'During [+]' samples relative to 'Before', again with no significant increase in the 'During [-]' group (LSD, 5 %, Figure 2-11). However, production of dodecanal remained increased in the 'After' group. Co-eluting compounds were, however, detected in both peaks, and so it is possible that the described trends may not directly reflect patterns in the production of 1-dodecene or dodecanal.

Analyte RI 1416, identified as a co-eluting sesquiterpene and phthalate, was found in greater amounts in samples from the 'During [+]' group relative to 'Before' and controls. Further, this analyte was increased in the 'After' group relative to controls (LSD, 5 %; Figure 2-11). Although parasitological status was marginally insignificant in predicting the amount of methyl dodecanoate (RI 1509) in different groups, when examining pairwise differences, significantly more of this compound was found in the 'During [+]' group relative to controls (LSD, 5 %, Figure 2-11). Production then decreased significantly between 'During [+]' and 'After', supporting an association between compound production and the presence of parasites. Again, a co-eluting compound was observed in the methyl dodecanoate peaks. Full matrices of standard error of the difference (SED) tables, with all pairwise comparisons, are given in Appendix 2.8. No overall

significance of parasitology (tridecane, RI 1222), or no significant pairwise differences between parasitological groups (biphenyl, RI 1500) was observed for the remaining four compounds.

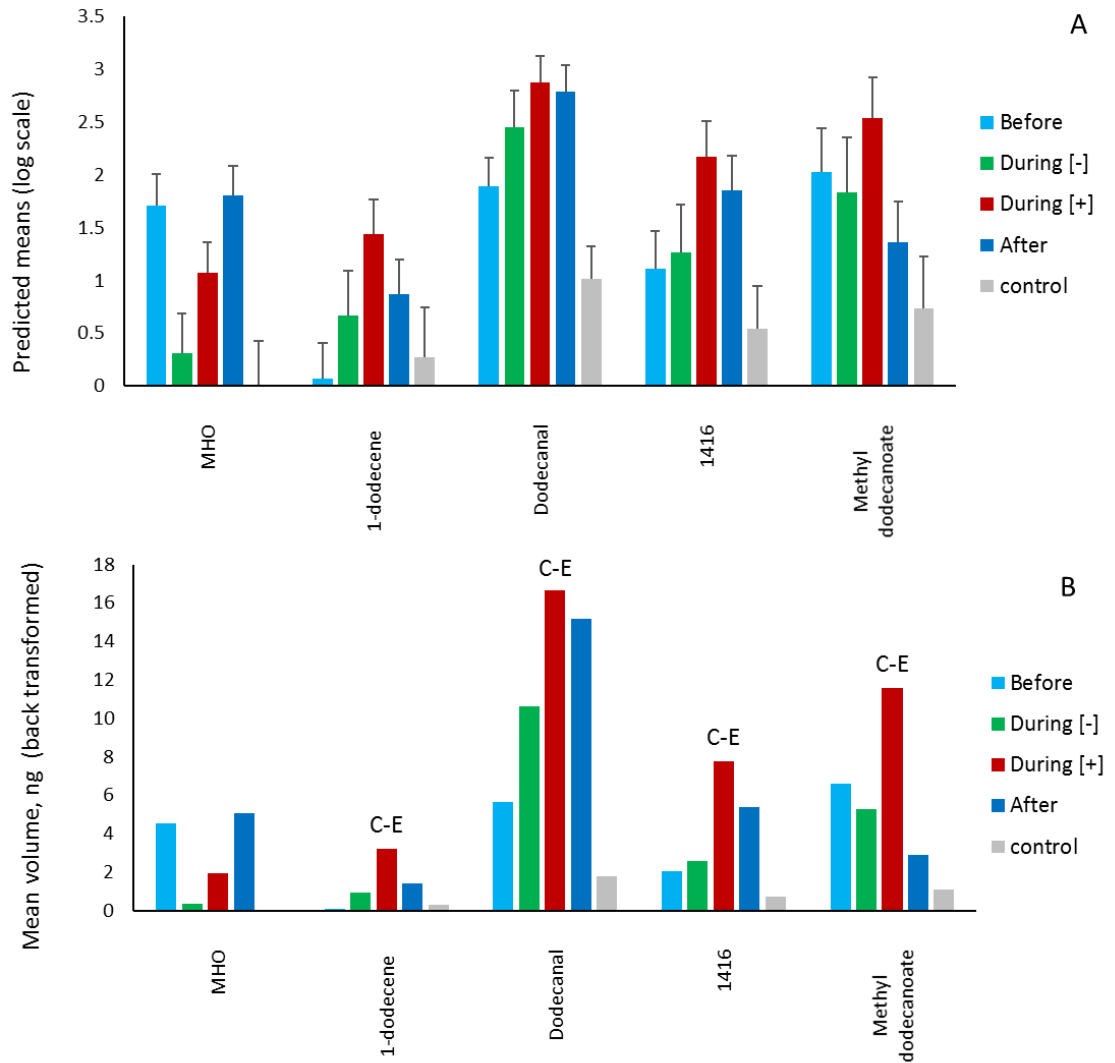


Figure 2-11. Effect of *P. falciparum* infection on levels of specific human volatile compounds. Predicted mean **(A)** (log transformation), and back transformation **(B)**, of the total amount of each compound in ng, collected over 100 minutes. MHO=6-methyl-5-hepten-2-one. C-E indicates peak contained a co-eluting compound, error bars are predicted standard error. Predictions derived from linear mixed models, which were fitted using the method of residual maximum likelihood (REML), and testing the combined effect of parasitological status and sampling moment. Before (prior to malaria challenge) n=8; during (day 6 or 8 PI, with [-] and [+] referring to parasitological status) [-] observations = 5 (n = 5); during [+] observations = 9 (n = 8); after (day 34, after parasite clearance) n=9, control (sample collected from empty control bags), n=6.

Chapter 2: Odour profile analysis of individuals experimentally infected with *P. falciparum*

Table 2-6. COI derived from BMGF cohort, with the most interesting significant pairwise differences (LSD, 5%) between parasitological groups. RI = retention index, Av SED= Average standard error of the difference, *P*-value and degrees of freedom (DF) derived from linear mixed models, which were fitted using the method of residual maximum likelihood. Before (prior to malaria challenge) n=8; during (day 6 or 8 PI, with [-] and [+] referring to parasitological status) [-] observations = 5 (n = 5); during [+] observations = 9 (n = 8); after (day 34, after parasite clearance) n=9; control (sample collected from empty control bags), n=6. Full matrices of SEDs and all pairwise comparisons are given in Appendix 2.8.

RI	GC-MS ID	CAS number	Av SED	<i>P</i> , DF
972	6-Methyl-5-hepten-2-one	110-93-0	0.452	<i>P</i> = 0.002, 24
1193	1-Dodecene ^a	112-41-4	0.512	<i>P</i> = 0.050, 24
1392	Dodecanal ^a	112-54-9	0.404	<i>P</i> < 0.001, 32
1416	Sesquiterpene ^b	n/a	0.532	<i>P</i> = 0.031, 32
1509	Methyl dodecanoate ^a	111-82-0	0.621	<i>P</i> = 0.076, 24

^(a) A co-eluting compound was detected at the same retention time, ^(b) A co-eluting phthalate was detected at the same retention time, more specific identification not possible.

Table 2-7 Summary of significant pairwise differences between groups of samples for compounds of interest from BMGF. MHO=6-methyl-5-hepten-2-one, full matrices of SEDs and all pairwise comparisons are given in Appendix 2.8.

Category (parasitology)	Compounds with significant difference				
Before					
During [-]	MHO				
During [+]	1-dodecene dodecanal 1416	None			
After	dodecanal	MHO	methyl dodecanoate		
Control	dodecanal MHO	dodecanal	dodecanal methyl dodecanoate MHO 1416	dodecanal MHO 1416	
	Before	During [-]	During [+]	After	Control

2.4.5 CVA analysis of association between other infection parameters and compound production (BMGF)

Grouping the BMGF individuals according to infection by *P. falciparum* strain (NF166 or NF135) allowed quite good separation of odour profile (Figure 2-12A). Additionally, grouping according to the number of infectious bites received per individual (1, 2 or 5) allowed some separation of odour profiles (Figure 2-12B). A more detailed analysis of the compounds contributing to the separation seen in this preliminary analysis was not conducted, due to small sample sizes and time restraint considerations of deviating too far from the hypothesis under investigation.

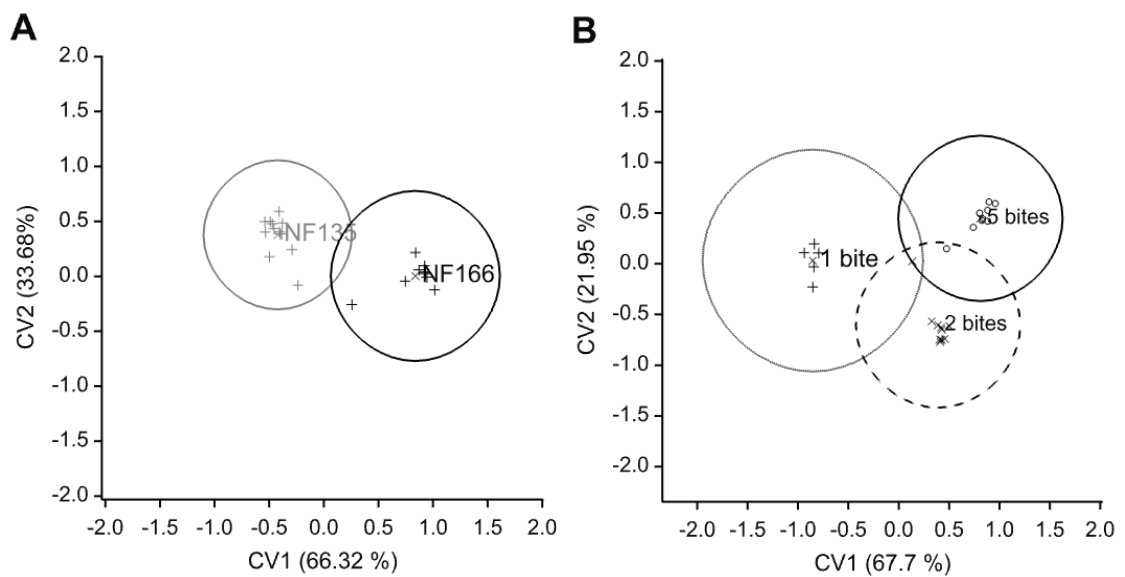


Figure 2-12. Canonical variates plot for BMGF cohort, grouped by (A) *P. falciparum* strain and (B) number of infectious bites received. Samples restricted to PI time points (days 6, 8 and 34), and only individuals who became positive (i.e. excluding BMGF_006 and BMGF_028). Samples are positioned by scores on canonical variates axes; relative to the presence and quantity of compounds contributing to these axes. The percentage of possible discrimination accounted for is included in the axes labels. Circles represent 95 % confidence intervals. (A) NF 135, grey, observations=13, n=5; NF 166, black, observations=10, n=4. Control groups not shown, to enhance clarity. (B) 1 bite (plus signs, grey): observations=8, n=3; 2 bites (crosses, dashed line): observations=12, n=4; 5 bites (circles, black): observations=9, n=4). Control groups not shown, to enhance clarity.

2.5 Discussion

2.5.1 Summary

In this chapter, the odour profile of individuals who had been infected with *P. falciparum* in three cohorts of clinical studies was investigated. Several compounds in the skin odour of the BMGF cohort, which benefitted from nine of 11 individuals becoming parasitologically positive and no prior influence of vaccination or drug treatment, were found to be significantly associated with the presence of parasites. These were 6-methyl-5-hepten-2-one, 1-dodecene, dodecanal, methyl dodecanoate and sesquiterpene with co-eluting phthalate (RI 1416). No compounds were found to be produced only by infected persons, indicating that here, infection did not qualitatively influence the odour profile.

2.5.2 BMGF cohort

The production of 6-methyl-5-hepten-2-one significantly decreased in the 'During [-]' time point, but increased again in the 'During [+]' time point. As all individuals in this analysis did become parasitologically positive, these data suggest that in very early stage infection the production of 6-methyl-5-hepten-2-one is inhibited (i.e. just prior to bloodstage parasites, 'During [-]' time point), but increases with the appearance of bloodstage parasites ('During [+]' time point). The production of 1-dodecene, dodecanal and RI 1416 was seen to significantly increase in 'During [+]' individuals relative to 'Before', indicating a possible association between the production of these compounds and the presence of bloodstream *Plasmodium* parasites. Interestingly, dodecanal production was increased in the 'During [-]' group, although insignificantly, possibly indicating that already in very early stage infection and prior to bloodstage parasites, compound production had begun to increase. The production of dodecanal remained significantly increased in the 'After' group, and RI 1416 remained raised, but not significantly. Finally, the production of methyl dodecanoate did increase in the 'During [+]' group, although not significantly in relation to 'Before'. There was a subsequent, significant, decrease in the 'After' group. The decrease in production of methyl dodecanoate and 1-dodecene, between the parasitologically positive time point and after treatment with antimalarials, may be indicative of an association between compound production and the presence of parasites themselves. This is because the compounds ceased to be produced in greater amounts after the parasites were cleared. Compounds that increased on infection (i.e. dodecanal and RI 1416), but which continued to be produced in greater amount following curative treatment, may be correlated with some (ongoing) immunological mechanism, rather than parasites *per se*. Co-eluting

compounds were detected for four of the five IAC in the BMGF dataset. While often present at a low level, these co-eluting compounds do preclude firm conclusions regarding associations between parasite challenge and these intriguing changes in compound production.

Compounds identified in this study as possibly being associated with infection, and previously reported to be produced by the human skin, include dodecanal and 6-methyl-5-hepten-2-one (Dormont et al. 2013b; Bernier et al. 2000; Meijerink et al. 2000; Harraca et al. 2012). Dodecanal is known to stimulate an electrophysiological response in *Aedes aegypti* (Ghaninia et al., 2008; Logan et al., 2008) and *Culex quinquefasciatus* (Cooperband et al., 2008). If *Anopheles* mosquitoes also respond to dodecanal, altered production by *Plasmodium*-infected persons could indeed influence transmission. 6-Methyl-5-hepten-2-one, seen here to decrease in its production on infection, is also known to affect mosquito behaviour. However, the role of this compound is unclear: it has been found to be attractive to *Ae. aegypti* (Bernier et al., 2002), repellent at a range of concentrations to *Ae. aegypti* (Logan et al., 2010; Menger et al., 2014), and repellent at high concentrations to *An. gambiae* s.s. and *Cx. quinquefasciatus*. In another study, 6-methyl-5-hepten-2-one was found to be both significantly attractive and significantly repellent to cattle flies, when tested in two different contexts (Birkett et al., 2004). It is thus difficult to predict the role of this compound on the host-seeking behaviour of *Anopheles*, but should it be repellent in this context, a decrease in production by parasitologically positive individuals may serve to increase attractiveness and therefore biting rate. In this instance, our findings are counterintuitive, as the greatest decrease in 6-methyl-5-hepten-2-one production occurred prior to the presence of bloodstage parasites and it was latterly confirmed that transmissible stages were not present (Dr J. de Boer, pers.comm., 4th June 2017). 1-Dodecene is not specifically reported as a skin-derived compound, although both methyl dodecene and 3-dodecene have been identified as such (Bernier et al., 2000; Zhang et al., 2005). Another study found 1-dodecene to be produced by *Pseudomonas aeruginosa* (Filipiak et al., 2012), which is a known skin commensal, indicating a possible pathway for production in our study cohort. Analyte RI 1416 was identified as containing a sesquiterpene (a terpene). Terpenes and their derivatives have been associated with *Plasmodium*-infected red blood cells in a previous study (Kelly et al., 2015), and it is possible that direct production by infected red blood cells contributes to the possible association described here. While methyl dodecanoate has previously been identified as a component of human skin odour (Dormont et al. 2013b), it has not been cited as an entomologically active compound.

2.5.3 TIP5A and TIP5B cohorts

In cohort TIP5A, compound RI 1598 was found to be produced in significantly different amounts between different parasitological groups. However, since the increase in production was seen in 'During [-]' individuals, relative to the 'Before' group, there was no association with the presence of parasites in peripheral blood. The COI RI 792 and RI 1167 were present at high concentrations in the control samples, and as such were disregarded.

In cohort TIP5B, only one analyte was found to be statistically associated with parasitological status: production of RI 1095 increased in both 'During [+] and [-]' groups. Again, in this cohort, 'During [-]' individuals all became positive, here by day 12 (four days after the 'During' odour sampling moment). It is therefore possible that the production of RI 1095 is upregulated very early in parasite infection. (*R*)- or (*S*)-2-ethylhexanoic acid was identified in this peak. Although this is thought to be of human origin, and possibly eliciting an electrophysiological response in *An. gambiae* (Knols, 1996), co-elution with an unidentified compound prevents the association from being stated with certainty.

Of all datasets investigated in this thesis, odour profiles from cohorts TIP5A and TIP5B were the first to be sampled and analysed, and here sample sizes were smallest. Methodologies for volatile collection were still being optimised. Filters from TIP5A were not sealed under nitrogen, which may have led to the oxidation or decomposition of some compounds on the filters. Additionally, samples from the 'After' time point were lost, thus preventing confirmation that production of IAC is reduced following parasite clearance. It is possible that the presence of two TIP5A IAC in the control samples is indicative that they were contaminants. It is important to note that whichever odour sampling technique is applied, it is probable that compounds of non-human origin will be detected (Dormont et al., 2013a), these often being derived from industrial products, the use of skin cosmetics, or contamination of the sampling materials themselves.

2.5.4 Hierarchical cluster analysis

No clustering was observed between repeat samples from the same individuals in cohorts TIP5A and 5B, unlike in BMGF. Intra-individual clustering of odour profile samples would be expected, as although an individual's odour profile can fluctuate, it remains relatively constant over time (Knols et al., 1995; Logan et al., 2008; Qiu et al., 2006). Similarly, in these two datasets, human odour profiles did not cluster separately from control odour profiles, indicating that the

constituent volatiles were similar. Some contamination of samples in TIP5A and 5B would have increased the difficulty of identifying IAC. However, this would not affect the validity of those that were detected, as exogenous compounds are relatively easily identified during analysis.

The lack of clustering (by HCA) according to parasitological status across all three cohorts should not be interpreted as a lack of compounds associated with infection. The production of one or two compounds in greater amount, a discreet odour change, would likely not lead to association by this statistical technique. The clustering technique gives a similarity measure per pair of samples, across all chemicals. This is an oversimplified representation of differences in odour profile, and few IAC would be outnumbered by many other compounds that were produced in similar amount.

2.5.5 Methodological considerations

The TIP5B cohort comprised six individuals, of which a 'During [+]' odour sample was available from only three. Small sample sizes increase the possibility that sampling bias occurred, i.e. those individuals, by chance, were an anomaly in the population, or within the tail of the distribution for compound production. In addition, for this cohort, all three individuals considered to be positive in the analysis did not test positive on the evening of odour profile sampling. The categorisation of these samples as positive is supported in two cases by the time delay of parasite clearance following treatment (Bustos et al., 1999) and in the third by the presence of parasites at both the previous and subsequent time points. However, the latter sample does reinforce the point that the parasitological positivity defined in these experimental cohorts is of extremely low density, and borders the (highly sensitive) qPCR test limit of detection. That fewer compounds were found to be associated with infection in the TIP5A and 5B datasets relative to the BMGF dataset might, therefore, be explained by lower sample sizes, possible masking of trends by contamination, or, for TIP5B, insufficient *Plasmodium* parasitaemia.

Associations between *Plasmodium* infection status and the production of some volatile compounds were observed. All three experimental cohorts included both male and female volunteers, and it is thought that the female hormonal cycle influences body odour profile (Singh and Bronstad, 2001). However, in the BMGF cohort, any influence of sex would have been mitigated, as the balance of male and female volunteers was well divided between positive and negative status at each time point, and one male and one female volunteer remained negative

throughout. Should drug or vaccination treatment have an influence on odour profile, this was not relevant to the BMGF cohort as no participants had been vaccinated or prophylactically drug treated. Further, work conducted by project collaborators confirmed an absence of influence of antimalarial treatment on host attractiveness to *Anopheles coluzzii* (Dr J. de Boer, pers.comm., 4th June 2017), although chemical analysis of the associated odour profile was not undertaken.

Samples classified as 'parasitologically positive' in the EI datasets were determined as such on the basis of (a maximum) of two positive results by 18S qPCR. This is a highly sensitive diagnostic tool, detecting as few as 0.02 parasites per μL of blood (Hermsen et al., 2001). Hence, the positive samples in the current dataset represent a very low infection density and early stage infection, where parasites were essentially detected as they began the bloodstream (erythrocytic) lifecycle stage. It is perhaps surprising that changes in the production of volatile compounds from the skin could be detected this early in the infection cycle. Any hypothesised mechanism, e.g. modification of skin commensal populations, direct release of volatiles from the infected red blood cells across cell membranes, will encompass a minimum time delay over which that odour change can manifest. However, it is conceivable that the underlying mechanism could occur over a short timescale: skin bacteria populations, known to be responsible in part for odour, can change over several hours (Costello et al., 2009; Meadow et al., 2013).

With regards to future studies of the odour profile of infected persons, an advantage of studying experimental infections over natural infections involves the 'forced' infection of pre-determined individuals. One possible explanation for an increased attractiveness of malarious individuals is that those who naturally produce more or less of certain compounds attract greater or fewer mosquitoes (and subsequently have a greater or lesser risk of infection). Therefore, changes in odour profile observed in EI individuals more probably reflect the direct influence of *Plasmodium* infection. This conclusion is reinforced here by measuring 'innate' compound levels, both before and after infection.

2.5.6 Other parameters of infection

These data indicated a possibility of distinction in odour profile according to the *P. falciparum* strain that individuals were infected with, or the number of infectious bites that they were exposed to. It should be noted that here, grouping may have been enhanced by the lack of full independence between observations. Because repeated measures on the same individuals did

not place individuals into different groups (as they did with the 'parasitological status' analysis), each group comprised odour profile samples more likely to be more similar (i.e. from the same people), regardless of other parasitological factors. With this caveat, it is still notable that the two *P. falciparum* strains are allopatric, with strain NF166 originating from Equatorial Guinea, and NF135 from Cambodia. The difference in odour profile of infected hosts may therefore result from divergence due to geographical isolation, either by parasite-, host-, or vector-specific factors (or some combination thereof). The BMGF cohort was the only group in which individuals were experimentally-infected with different *P. falciparum* strains, thus limiting the sample size. Some separation was also observed when individuals were grouped by the number of infectious bites that they received. It is likely that the number of infectious bites does indeed correlate with the sporozoite load that each individual received, as all mosquitoes used for infections were from populations that demonstrated greater than or equal to 90 % sporozoite positivity (Vellefaux 2012). It is thus possible that a larger challenge of sporozoites induced infections of greater parasitaemia. However, this preliminary finding should be investigated further in an appropriately designed, and powered, experiment.

2.6 Conclusion

By comparing the changing odour profiles of individuals who were experimentally-infected with *P. falciparum*, associations between the production of certain volatile compounds and the infected or uninfected state were observed. Some of these compounds, including dodecanal and 6-methyl-5-hepten-2-one, are known to be involved in the attraction of mosquitoes to humans. Conducting odour profile analyses of individuals in a naturally malaria-endemic setting would provide further evidence, as sample sizes could be larger and natural infection parameters observed, including parasite genetic diversity and high density *Plasmodium* infections.

2.7 Chapter references

- Ansell, J., Hamilton, K.A.A., Pinder, M., Walraven, G.E.L.E.L., Lindsay, S.W., Pindeti, M., 2002. Short-range mosquitoes attractiveness of pregnant women to *Anopheles gambiae*. *Trans. R. Soc. Trop. Med. Hyg.* 96, 113–116.
- Bastiaens, G.J.H., Van Meer, M.P.A., Scholzen, A., Obiero, J.M., Vatanshenassan, M., Van Grinsven, T., Lee Sim, B.K., Billingsley, P.F., James, E.R., Gunasekera, A., Bijker, E.M., Van Gemert, G.J., Van De Vegte-Bolmer, M., Graumans, W., Hermsen, C.C., De Mast, Q., Van Der Ven, A.J.A.M., Hoffman, S.L., Sauerwein, R.W., 2016. Safety, immunogenicity, and protective efficacy of intradermal immunization with aseptic, purified, cryopreserved plasmodium falciparum sporozoites in volunteers under chloroquine prophylaxis: A randomized controlled trial. *Am. J. Trop. Med. Hyg.* 94, 663–673. doi:10.4269/ajtmh.15-0621
- Bernier, U.R., Kline, D.L., Barnard, D.R., Schreck, C.E., Yost, R.A., 2000. Analysis of human skin emanations by gas chromatography/mass spectrometry. 2. Identification of volatile compounds that are candidate attractants for the yellow fever mosquito (*Aedes aegypti*). *Anal. Chem.* 72, 747–56.
- Bernier, U.R., Kline, D.L., Schreck, C.E., Yost, R.A., Barnard, D.R., 2002. Chemical analysis of human skin emanations: comparison of volatiles from humans that differ in attraction of *Aedes aegypti* (Diptera: Culicidae). *J. Am. Mosq. Control Assoc.* 18, 186–95.
- Bijker, E.M., Bastiaens, G.J.H., Teirlinck, A.C., van Gemert, G.-J., Graumans, W., van de Vegte-Bolmer, M., Siebelink-Stoter, R., Arens, T., Teelen, K., Nahrendorf, W., Remarque, E.J., Roeffen, W., Jansens, A., Zimmerman, D., Vos, M., van Schaijk, B.C.L., Wiersma, J., van der Ven, A.J.A.M., de Mast, Q., van Lieshout, L., Verweij, J.J., Hermsen, C.C., Scholzen, A., Sauerwein, R.W., 2013. Protection against malaria after immunization by chloroquine prophylaxis and sporozoites is mediated by preerythrocytic immunity. *Proc. Natl. Acad. Sci. U. S. A.* 110, 7862–7. doi:10.1073/pnas.1220360110
- Birkett, M.A., Agelopoulos, N., Jensen, K.M. V, Jespersen, J.B., Pickett, J.A., Prijs, H.J., Thomas, G., Trapman, J.J., Wadhams, L.J., Woodcock, C.M., 2004. The role of volatile semiochemicals in mediating host location and selection by nuisance and disease-transmitting cattle flies. *Med. Vet. Entomol.* 18, 313–322. doi:10.1111/j.0269-283X.2004.00528.x
- Bustos, D.G., Canfield, C.J., Canete-Miguel, E., Hutchinson, D.B.A., 1999. Atovaquone-Proguanil Compared with Chloroquine and Chloroquine-Sulfadoxine-Pyrimethamine for Treatment of Acute Plasmodium falciparum Malaria in the Philippines. *J. Infect. Dis.* 179, 1587–1590. doi:10.2307/30117441
- Cooperband, M.F., McElfresh, J.S., Millar, J.G., Cardé, R.T., 2008. Attraction of female *Culex quinquefasciatus* Say (Diptera: Culicidae) to odors from chicken feces. *J. Insect Physiol.* 54, 1184–1192. doi:10.1016/j.jinsphys.2008.05.003
- Costello, E.E.K., Lauber, C.C.L., Hamady, M., Fierer, N., Gordon, J.I., Knight, R., 2009. Bacterial community variation in human body habitats across space and time. *Science (80-.)*. 326, 1694–7. doi:10.1126/science.1177486.Bacterial
- De Jong, R., Knols, B.G.J., 1995. Selection of biting sites on man by two malaria mosquito species. *Experientia* 51, 80–84. doi:10.1007/BF01964925
- Delemarre, B.J., van der Kaay, H.J., 1979. [Tropical malaria contracted the natural way in the Netherlands]. *Ned. Tijdschr. Geneeskd.* 123, 1981–2.
- Dormont, L., Bessièrè, J.-M., Cohuet, A., 2013a. Human skin volatiles: a review. *J. Chem. Ecol.* 39, 569–78. doi:10.1007/s10886-013-0286-z
- Dormont, L., Bessièrè, J.-M., McKey, D., Cohuet, A., 2013b. New methods for field collection of human skin volatiles and perspectives for their application in the chemical ecology of human-pathogen-vector interactions. *J. Exp. Biol.* 216, 2783–8. doi:10.1242/jeb.085936

- Emami, S.N., Emami, S.N., Lindberg, B.G., Hua, S., Hill, S., Mozuraitis, R., Birgersson, G., Ignell, R., Faye, I., 2017. A key malaria metabolite modulates vector blood seeking, feeding, and susceptibility to infection. *Science* (80-.). 4563, 1–9.
- Filipiak, W., Sponring, A., Baur, M., Filipiak, A., Ager, C., Wiesenhofer, H., Nagl, M., Troppmair, J., Amann, A., 2012. Molecular analysis of volatile metabolites released specifically by *Staphylococcus aureus* and *Pseudomonas aeruginosa*. *BMC Microbiol.* 12, 113. doi:10.1186/1471-2180-12-113
- Ghaninia, M., Larsson, M., Hansson, B.S., Ignell, R., 2008. Natural odor ligands for olfactory receptor neurons of the female mosquito *Aedes aegypti*: use of gas chromatography-linked single sensillum recordings. *J. Exp. Biol.* 211, 3020–3027. doi:10.1242/jeb.016360
- Harraca, V., Ryne, C., Birgersson, G., Ignell, R., 2012. Smelling your way to food: can bed bugs use our odour? *J Exp Biol* 215, 623–629. doi:10.1242/jeb.065748
- Hermesen, C.C., Telgt, D.S., Linders, E.H., van de Locht, L. a, Eling, W.M., Mensink, E.J., Sauerwein, R.W., 2001. Detection of *Plasmodium falciparum* malaria parasites in vivo by real-time quantitative PCR. *Mol. Biochem. Parasitol.* 118, 247–251. doi:S0166685101003796 [pii]
- Jawara, M., Smallegange, R.C., Jeffries, D., Nwakanma, D.C., Awolola, T.S., Knols, B.G.J., Takken, W., Conway, D.J., 2009. Optimizing odor-baited trap methods for collecting mosquitoes during the malaria season in The Gambia. *PLoS One* 4, e8167. doi:10.1371/journal.pone.0008167
- Kelly, M., Su, C.-Y., Schaber, C., Crowley, J.R., Hsu, F.-F., Carlson, J.R., Odom, A.R., 2015. Malaria parasites produce volatile mosquito attractants. *MBio* 6, e00235-15-. doi:10.1128/mBio.00235-15
- Keystone, J.S., 1996. Of bites and body odour. *Lancet* 347, 1423.
- Knols, B.G.J.J., de Jong, R., Takken, W., Jong, R. De, Agricultural, W., 1995. Differential attractiveness of isolated humans to mosquitoes in Tanzania. *Trans. R. Soc. Trop. Med. Hyg.* 89, 604–606.
- Lindsay, S., Ansell, J., Selman, C., Cox, V., Hamilton, K., Walraven, G., 2000. Effect of pregnancy on exposure to malaria mosquitoes. *Lancet* 355, 1972.
- Logan, J.G., Birkett, M.A., Clark, S.J., Powers, S., Seal, N.J., Wadhams, L.J., Mordue Luntz, A.J., Pickett, J.A., 2008. Identification of human-derived volatile chemicals that interfere with attraction of *Aedes aegypti* mosquitoes. *J Chem Ecol* 34, 308–322. doi:10.1007/s10886-008-9436-0
- Logan, J.G., Stanczyk, N.M., Hassanali, A., Kemei, J., Santana, A.E.G., Ribeiro, K. a L., Pickett, J. a, Mordue Luntz, a J., 2010. Arm-in-cage testing of natural human-derived mosquito repellents. *Malar. J.* 9, 239. doi:10.1186/1475-2875-9-239
- Meadow, J.F., Bateman, A.C., Herkert, K.M., O'Connor, T.K., Green, J.L., 2013. Significant changes in the skin microbiome mediated by the sport of roller derby. *PeerJ* 1, e53. doi:10.7717/peerj.53
- Meijerink, J., Braks, M.A.H., Brack, A.A., Adam, W., Dekker, T., Posthumus, M.A., Beek, T.A.V.A.N., Loon, J.J.A. Van, 2000. Identification of Olfactory Stimulants for *Anopheles gambiae* from Human Sweat Samples. *J. Chem. Ecol.* 26, 1367–1382. doi:10.1023/A:1005475422978
- Menger, D.J., Van Loon, J.J.A., Takken, W., 2014. Assessing the efficacy of candidate mosquito repellents against the background of an attractive source that mimics a human host. *Med. Vet. Entomol.* 28, 407–13. doi:10.1111/mve.12061
- Njiru, B.N., Mukabana, W.R., Takken, W., Knols, B.G.J., 2006. Trapping of the malaria vector *Anopheles gambiae* with odour-baited MM-X traps in semi-field conditions in western Kenya. *Malar. J.* 5, 39. doi:10.1186/1475-2875-5-39
- Olanga, E.A., Okal, M.N., Mbadi, P. a, Kokwaro, E.D., Mukabana, W.R., 2010. Attraction of *Anopheles gambiae* to odour baits augmented with heat and moisture. *Malar. J.* 9, 6. doi:10.1186/1475-2875-9-6

- Omolo, M.O., Njiru, B., Ndiege, I.O., Musau, R.M., Hassanali, A., 2013. Differential attractiveness of human foot odours to *Anopheles gambiae* Giles sensu stricto (Diptera: Culicidae) and variation in their chemical composition. *Acta Trop.* 128, 144–148. doi:10.1016/j.actatropica.2013.07.012
- Port, G.R., Boreham, P.F.L., 1980. The relationship of host size to feeding by mosquitoes of the *Anopheles gambiae* Giles complex (Diptera : Culicidae) 133–144.
- Price, G.D., Smith, N., Carlson, D.A., 1979. The attraction of female mosquitoes (*Anopheles quadrimaculatus* Say) to stored human emanations in conjunction with adjusted levels of relative humidity, temperature, and carbon dioxide. *J. Chem. Ecol.* 5, 383–395. doi:10.1007/BF00987924
- Qiu, Y.T., Smallegange, R.C., Van Loon, J.J.A., Ter Braak, C.J.F., Takken, W., 2006. Interindividual variation in the attractiveness of human odours to the malaria mosquito *Anopheles gambiae* s. s. *Med. Vet. Entomol.* 20, 280–7. doi:10.1111/j.1365-2915.2006.00627.x
- Roestenberg, M., Bijker, E.M., Sim, B.K.L., Billingsley, P.F., James, E.R., Bastiaens, G.J.H., Teirlinck, A.C., Scholzen, A., Teelen, K., Arens, T., van der Ven, A.J.A.M., Gunasekera, A., Chakravarty, S., Velmurugan, S., Hermsen, C.C., Sauerwein, R.W., Hoffman, S.L., 2013. Controlled human malaria infections by intradermal injection of cryopreserved *Plasmodium falciparum* sporozoites. *Am. J. Trop. Med. Hyg.* 88, 5–13. doi:10.4269/ajtmh.2012.12-0613
- Schreck, C.E., Kline, D.L., Carlson, D. a, 1990. Mosquito attraction to substances from the skin of different humans. *J. Am. Mosq. Control Assoc.* 6, 406–410.
- Schreck, C.E., Smith, N., Carlson, D.A., Price, G.D., Haile, D., Godwin, D.R., 1982. A material isolated from human hands that attracts female mosquitoes. *J. Chem. Ecol.* 8, 429–438. doi:10.1007/BF00987791
- Singh, D., Bronstad, P.M., 2001. Female body odour is a potential cue to ovulation. *Proc. Biol. Sci.* 268, 797–801. doi:10.1098/rspb.2001.1589
- Smallegange, R.C., Verhulst, N.O., Takken, W., 2011. Sweaty skin: an invitation to bite? *Trends Parasitol.* 27, 143–148. doi:10.1016/j.pt.2010.12.009
- Vellefaux, C., 2012. Clinical Trial Protocol - BMGF.
- Verhulst, N.O., Qiu, Y.T., Beijleveld, H., Maliepaard, C., Knights, D., Schulz, S., Berg-Lyons, D., Lauber, C.L., Verduijn, W., Haasnoot, G.W., Mumm, R., Bouwmeester, H.J., Claas, F.H.J., Dicke, M., van Loon, J.J.A., Takken, W., Knight, R., Smallegange, R.C., 2011. Composition of human skin microbiota affects attractiveness to malaria mosquitoes. *PLoS ONE* [Electronic Resour. 6, e28991.
- Zhang, Z.M., Cai, J.J., Ruan, G.H., Li, G.K., 2005. The study of fingerprint characteristics of the emanations from human arm skin using the original sampling system by SPME-GC/MS. *J. Chromatogr. B Anal. Technol. Biomed. Life Sci.* 822, 244–252. doi:10.1016/j.jchromb.2005.06.026

2.8 Appendix: SED tables from experimentally-infected odour profile analysis

Matrices of pairwise comparisons between groups, modelled by parasitological infection status for the compounds of interest identified in all experimentally-infected cohorts. Standard errors of differences between groups are shown, as derived from linear mixed models (REML), and compound names or retention indices given. Significance ($P < 0.05$) for comparisons made using the least significant difference (LSD, 5 %) values (= SED multiplied by the 2.5 % t-value) is indicated by a '+' symbol, DF = degrees of freedom, Av SED = average standard error of the difference.

2.8.1 Cohort TIP5A

RI 792

Category (parasitology)	Standard error of differences			
Before	*			
During [-]	0.6043	*		
During [+]	0.5217 +	0.6820 +	*	
control	0.8252	0.9211	0.8692	*
DF = 14, Av SED = 0.737	Before	During [-]	During [+]	control

RI 1167

Category (parasitology)	Standard error of differences			
Before	*			
During [-]	0.5616 +	*		
During [+]	0.4640	0.7075 +	*	
control	1.3483	1.4135	1.3776	*
DF = 11, Av SED = 0.979	Before	During [-]	During [+]	control

RI 1598

Category (parasitology)	Standard error of differences			
Before	*			
During [-]	0.2132 +	*		
During [+]	0.1769	0.2659	*	
control	0.4450 +	0.4727 +	0.4575 +	*
DF = 11, Av SED = 0.339	Before	During [-]	During [+]	control

2.8.2 Cohort TIP5B

RI 1095 (includes (R)- or (S)-2-ethylhexanoic acid)

Category (parasitology)	Standard error of differences				
Before	*				
During [-]	0.7390	*			
During [+]	0.7390	0.8797	*		
After	0.5938 +	0.7390 +	0.7390 +	*	
Control	0.6617	0.7946 +	0.7946 +	0.6617	*
DF = 13, Av SED = 0.734	Before	During [-]	During [+]	After	Control

2.8.3 Cohort BMGF

6-Methyl-5-hepten-2-one (RI 972)

Category (parasitology)	Standard error of differences				
Before	*				
During [-]	0.434 +	*			
During [+]	0.372	0.435	*		
After	0.365	0.427 +	0.356	*	
Control	0.525 +	0.569	0.518 +	0.516 +	*
DF = 24, Av SED = 0.452	Before	During [-]	During [+]	After	Control

1-Dodecene (RI 1193)

Category (parasitology)	Standard error of differences				
Before	*				
During [-]	0.500	*			
During [+]	0.428 +	0.499	*		
After	0.421	0.491	0.410	*	
Control	0.584	0.636	0.576	0.574	*
DF = 24, Av SED = 0.512	Before	During [-]	During [+]	After	Control

Dodecanal (RI 1392)

Category (parasitology)	Standard error of differences				
Before	*				
During [-]	0.433	*			
During [+]	0.369 +	0.423	*		
After	0.369 +	0.423	0.358	*	
Control	0.410 +	0.459 +	0.400 +	0.400 +	*
DF = 32, Av SED = 0.404	Before	During [-]	During [+]	After	Control

Unidentified sesquiterpene (RI 1416)

Category (parasitology)	Standard error of differences				
Before	*				
During [-]	0.570	*			
During [+]	0.486 +	0.557	*		
After	0.486	0.557	0.471	*	
Control	0.540	0.605	0.527 +	0.527 +	*
DF = 39, Av SED = 0.516	Before	During [-]	During [+]	After	Control

Chapter 2: Odour profile analysis of individuals experimentally infected with *P. falciparum*

Methyl dodecanoate (RI 1509)

Category (parasitology)	Standard error of differences				
Before	*				
During [-]	0.655	*			
During [+]	0.559	0.644	*		
After	0.557	0.642	0.541 +	*	
Control	0.641	0.716	0.627 +	0.626	*
DF = 24, Av SED = 0.621	Before	During [-]	During [+]	After	Control

3 Parasitology of Kenyan study population

3.1 Introduction

We hypothesised that *Plasmodium*-parasite associated changes in human host attractiveness were governed by changes in the human volatile odour profile. To enable investigation of the Kenyan odour samples (chapter 5), it was essential to fully characterise the *Plasmodium* infection status of the odour-sampled individuals. To enable odour sampling of individuals harbouring varied *Plasmodium* stages (e.g. gametocytes) and parasite densities, more individuals were blood sampled for parasitology than were ultimately odour sampled. A large subset of these blood samples were investigated for parasitology, including samples from odour-profile individuals and samples from those who were not odour-tested. This allowed an overview of *Plasmodium* infection parameters in the population, and constituted the following 'parasitological' analysis of the Kenyan study cohort.

Thick and thin film microscopy remains the gold standard for point-of-care malaria diagnosis (Wu et al., 2015). When conducted proficiently, this technique can have high levels of specificity and sensitivity, for example, by thick film 10 parasites per μL blood (p/ μL) were detected by a lead microscopist in a reference laboratory in the UK (Bejon et al., 2006). In a resource-limited setting, as generally applies in malaria-endemic regions, the sensitivity of microscopy can be hindered by lower quality reagents and reduced access to high quality training (Wongsrichanalai, 2001). In this context, a sensitivity of between 50 and 100 p/ μL is good, with lower sensitivity likely (Bousema et al., 2014). In the last twenty years, the use of rapid diagnostic tests (RDT) that detect a specific parasite protein, primarily histidine-rich protein-2 (HRP-2) and/or lactate dehydrogenase (LDH), has become increasingly prevalent (Humar et al., 1997; Mishra et al., 1999; WHO, 1996). These small, handheld immunochromatographic tests require minimal technical training and are easy to procure and store. RDTs operate at about an equivalent range of sensitivity to thin film microscopy, approximately 100 – 200 p/ μL (Moody, 2002; Ochola et al., 2006; Wu et al., 2015). HRP-2 is specific to *P. falciparum*, and LDH is produced by all *Plasmodium* species. Usually, symptomatic malaria infections are detectable by microscopy or RDT; however, in an endemic region the majority of people are asymptomatic, often with parasite densities that are not detectable by these methods. The most sensitive diagnostic measures for malaria are nucleic acid amplification tests. Quantitative polymerase chain reaction (qPCR) can accurately measure one parasite per μL of blood (Andrews et al., 2005;

Wu et al., 2015), or less (Hermsen et al., 2001). These tests amplify parasite DNA from patient blood samples.

Measuring gametocyte density in the blood, or gametocytaemia, was traditionally only possible by observing the distinctive late gametocyte stages in blood films by microscopy. However, gametocytes can be missed by microscopy as they often circulate at densities close to the threshold for microscopic detection (Bousema and Drakeley, 2011). Further, non-*Plasmodium falciparum* gametocytes may go unobserved even more frequently, as they lack the characteristic crescent morphology of the *P. falciparum* gametocytes (Bousema and Drakeley, 2011). Recently, qPCR methods have been established that can specifically detect this lifecycle stage in *P. falciparum*, by amplifying gametocyte-specific RNA. Mature gametocytes rapidly synthesise a large number of proteins upon gametogenesis (i.e. on ingestion by a mosquito) that are specific to this activated stage, and subsequent zygote and ookinete stages (Babiker et al., 1999). Because any asexual stages also present in a sample carry only the DNA that encodes RNA transcripts, amplification of the RNA by reverse transcriptase PCR can form the basis of a gametocyte-specific diagnostic assay, e.g. those based on zygote and ookinete surface protein Pfs25, including QT-NASBA (Babiker et al., 1999; Bousema and Drakeley, 2011; Schneider et al., 2006). One disadvantage of RNA-based qPCR methods such as QT-NASBA is the requirement for whole blood to be stored at -80°C, which can be difficult in the field-based setting, both in terms of availability in the laboratory, and the cold chain required to ship such samples.

Fieldwork for the 'natural infection' study population, described here, was conducted in rural Western Kenya, near Mbita Point Township. Further details of the study site are given in 'study site', chapter 5. The study was conducted at four schools between January and July 2014, encompassing the long rainy season from March to August. Some children were odour profile sampled by air entrainment (analysed in this thesis, chapter 5) and others by wearing socks (these were tested by collaborators, data not shown). *Plasmodium* infection status for all participants was assessed, and multiple diagnostic assays were used: point-of-care tests informed odour profile collection because of their rapidity and ease of use in the field, while molecular assays were used retrospectively to describe parasite species, stage and density. Further, protocols were altered during the fieldwork, with additional dried blood spot samples collected in the latter stages. The use of multiple diagnostic tools both permitted collection of as much data as possible, and maximised the probability that parasitological information was available for all odour samples, in the event of sample loss.

3.2 Aim and objectives

The aim of this chapter was to explore and describe the *Plasmodium* infections of the children tested for malaria in the Kenyan study cohort, to allow appropriate parasitological categorisation for those who were odour sampled.

This aim was achieved through the following objectives:

1. To assess the comparability of the multiple diagnostic assays used, in terms of correlation in outcome measures
 - a. To ensure that use of multiple diagnostic assays to inform odour profile categorisation is valid, due to missing assay data for some odour samples
2. Based on the diagnostic assays, to allocate odour profile samples into parasitological categories, and determine sample size in each category for the odour profile analysis
3. To investigate *Plasmodium* parasite densities present in the sampled population

3.3 Methods

3.3.1 Summary

At the sampling sites, point-of-care tests including RDT and microscopy were used to inform collection of odour profile samples from *Plasmodium*-infected and parasite-free individuals. Additionally, peripheral whole blood (50 μ L) was collected from a finger prick into RNA protect (Qiagen, Cat No: 76526), and stored at -80 °C for QT-NASBA testing for the presence of *P. falciparum* gametocytes, and by 18S qPCR to obtain an estimate of *P. falciparum* parasitaemia.

Due to the fragile nature of whole blood samples stored at -80 °C, and to maximise the parasitological information available per odour profile individual, these procedures were supplemented as follows. Starting at the end of January, used rapid diagnostic tests (uRDT) were stored as blood template for retrospective analysis by qPCR (Figure 3-2). From May until July (two of the four schools), dried blood spots were additionally stored on Whatman filter paper (wDBS) as a comparator template to the uRDT.

Retrospective analyses, therefore, included the whole-blood-template based assays for *P. falciparum* DNA (18S qPCR) and *P. falciparum* gametocyte RNA (QT-NASBA), while filter-paper-template (uRDT and wDBS) based assays were examined for *Plasmodium* DNA (PgMET qPCR), and *Plasmodium* species by nested PCR. The species-specific nested PCR was used to examine for the presence of *P. falciparum*, as well as *P. malariae* and *P. ovale*, due the known presence of these species (Gouagna et al., 2003; Mutero et al., 1998; Olanga et al., 2015), but absence of *P. vivax*, in the locality.

3.3.2 Field measures

Malaria films

Peripheral blood was sampled in the field and placed directly onto the slide. The finger was first cleaned with an alcohol wipe and allowed to air dry, then pricked using the RDT kit lancet (see below for test specifics). Two drops of blood were spotted onto either end of a glass slide (VWR international) using the inverted cup, and one was smeared to make a thin film and the other (3-5 μ L blood) spread to achieve a spot (10-15 mm diameter) for the thick film. Films were air dried horizontally before being transported back to the laboratory for Geimsa staining. The thin smear end of the slide was dipped in methanol then allowed to air dry. Smears were then stained with 10 % Geimsa (in buffered water, pH 7.2) for ten minutes, rinsed briefly in tap water, and

Chapter 3: Parasitology of Kenyan study population

stood on end to dry. The thick film end was stained by dipping in buffered water, allowing the red blood cells (RBC) to lyse and then staining with 10 % Geimsa as per the thin film. To read the slide, the thick smear was initially examined for parasites until 200 white blood cells (WBC) had been counted. If gametocytes were seen, counting was continued to 500 WBC. The thin film was read if non-*P. falciparum* species were seen, and 2000 RBC (ten fields of 200 RBC) were counted, noting infected cells. The number of parasites present per μL blood was obtained using Equation 3-1, assuming a standard WBC count of $8000/\mu\text{L}$ (with the caveat that the presence of HIV in the population may bias this result). All slides were read at the International Centre of Insect Physiology and Ecology (*icipe*), Kenya, on the same day as collection, and then stored until shipment back to The London School of Hygiene & Tropical Medicine (LSHTM).

Equation 3-1. Calculation to determine parasites per μL blood from thick blood film.

$\text{Parasites}/\mu\text{L} = (\text{number of parasites} \times 8000)/\text{number of WBC counted}$
WBC= white blood cells (200 were counted)

Due to time and cost restraints not all films could be re-read, therefore, approximately 10 % were re-read. While ideally this would have been a random subset, missing data points across other diagnostic measures meant that parasitological categorisation of some odour profile samples relied heavily upon microscopy. This is because, either, storage of uRDT had not yet been implemented, whole blood samples had been inappropriately stored, or samples had been insufficiently labelled for certainty of identification. Therefore, 31 films (10 % of the 301 retained) were chosen for re-reading, and of these, 11 had no comparator due to the above reasons. For the remaining films, correlation between the two readers was good ($r=0.76$, $n=20$, $P<0.001$) (Figure 3-1). Prior to re-reading, all were submersed in acetone for ten minutes to ensure sterility. The re-reading protocol was as above, and films were read blind by an accredited person not involved in the project.

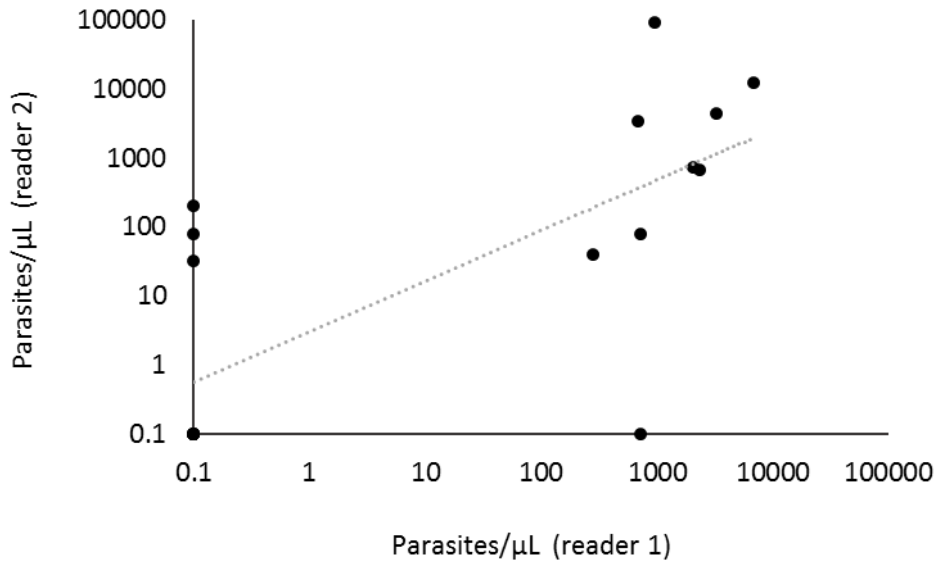


Figure 3-1. Parasite densities (p/μL) calculated from microscopy, by field reader (reader 1) and re-reader (reader 2). Twenty samples read by both readers were available, and the correlation was good ($r=0.76$, $n=20$ $P<0.001$).

Rapid diagnostic tests

Peripheral blood from a finger prick was used as for malaria films, and RDTs were performed as per guidelines, but in brief: One Step malaria HRP-2 (*P. falciparum*) and pLDH (pan *Plasmodium*) antigen rapid tests were used (SD BIOLINE, Cat no 05FK60, referred to below as 05FK60). Blood (5 μL) was collected from the finger prick using the inverted cup, and dispensed into the sample well. Four drops of assay diluent were added, and the result was read between 15 and 30 minutes later. 05FK60 detects histidine-rich protein-2 (HRP-2) of *P. falciparum*, and lactate dehydrogenase (pLDH) of all *Plasmodium* species.

3.3.3 Molecular diagnostic measures

qPCR: PgMET

To maximise information gained concerning the participant's *Plasmodium* infection status, RDTs collected from the field were used as templates for a post-hoc, real time, qPCR. Used RDTs (uRDT, 05FK60, as described above) were stored from the last week of sampling at Obambo (the first school sampled, in late January 2014) until the end of field sampling (July 2014). RDTs were air dried on the benchtop prior to storage in sealed plastic bags with silica gel (silicon dioxide). To enable assessment of the performance of uRDT as DNA templates for qPCR, approximately 3

mm diameter dried blood spots were taken on Whatman No. 3 filter paper (Whatman, Maidstone, United Kingdom) from participants in the two final schools, Kamsama and Powo. In this qPCR, adapted from Beshir et al. (2010), part of the *Plasmodium* tRNA methionine (PgMET) gene is amplified simultaneously to a human gene (part of the human beta tubulin exon 4 gene, HumTuBB), allowing *Plasmodium* species DNA to be quantified relative to human DNA, with a sensitivity in the range of five to 20 p/μL.

DNA extraction

Used RDT (uRDT) cassettes were opened laterally and the nitrocellulose strip was removed from inside. A central section of the nitrocellulose strip (Figure 3-2) was cut out using a sterile scalpel blade (treated with 70 % EtOH and flame between each sample) and then into 1-3 small pieces (Cnops et al., 2011). For Whatman filter paper dried blood spots (wDBS), a 3 mm diameter circle was punched from the blood spot, again, treating with 70 % EtOH and flamed between samples. All uRDT nitrocellulose pieces, per sample, were extracted together. DNA extraction was performed in a deep well plate using an automated extraction system (QIAAsymphony), with the QIAAsymphony DSP DNA mini kit (QIAGEN, Germany) and according to the manufacturer's instructions. In brief, buffer ATL (180 μL) and proteinase K (20 μL) were added to each well and mixed by thermomixer at 900 rpm at 56°C for 15 minutes. The deep-well plate was then placed directly into the sample compartment of the QIAAsymphony for DNA extraction (Beshir et al., in preparation).

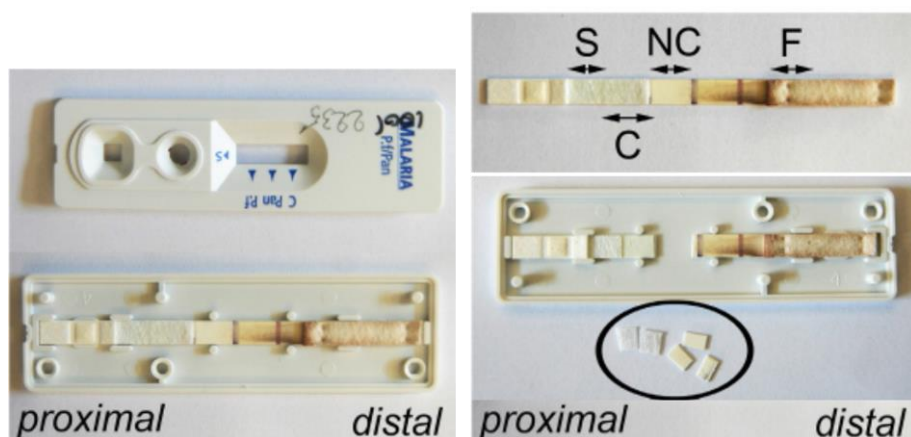


Figure 3-2. Used rapid diagnostic tests from the field were opened, and a central section of the nitrocellulose strip inside was cut out. This was cut into several pieces to optimise DNA extraction efficacy. The DNA extract was then used as a template for qPCR. Taken from Cnops et al. (2011).

Assay methodology: PgMET

Methodology was taken from Beshir et al. (2010). PCR master mix was prepared (per run) with the following component concentrations per 20 µL reaction: 5.5 mM MgCl₂ buffer (Bioline), 10x NH₄ buffer (160mM (NH₄)₂SO₄, 670mM Tris-HCl (pH 8.8 at 25 °C) and stabiliser, Bioline), 0.3 mM dNTPs (Bioline), 0.3 µM PgMET primers (F & R)(MWG-Biotech), 0.3 µM HumTuBB primers (F & R)(MWG-Biotech), 0.2 µM PgMET probe (MWG-Biotech), 0.2 µM HumTuBB probe (MWG-Biotech) (Table 3-1), 1 unit of BIOTAQ™ DNA polymerase (Bioline) and molecular grade water (Sigma-Aldrich). After vortexing, master mix (20 µL) was dispensed into individual Rotorgene PCR tubes and subsequently template (uRDT or wDBS DNA extraction) added (5 µL), and lids fitted. No-template and positive control reactions were set up per PCR plate in duplicate, the latter being International Standard (INT) for *P. falciparum* DNA (Padley et al., 2008). Real-time amplification assays were performed using probe-based quantitative PCR on RG3000 and RG6000 thermo-cyclers (Beshir et al., 2010). Cycling conditions were: 95 °C for 15 minutes; 45 cycles of 94 °C for 15 seconds and 60 °C for 1 minute. All preparation was conducted in a laminar airflow cabinet (TWO 30, Mason Technology) and all samples were amplified in duplicate, so per sample, the average parasite density was obtained.

Table 3-1. Amplification primers and double-labelled hydrolysis probes for PgMET and HumTuBB, reproduced with permission from Beshir et al. (2010).

Primer/Probe	5' Fluorophore	Sequence	3' Quencher
PgMET_F1		5'-TGAAAGCAGCGTAGCTCAGA	
PgMET_R2		5'-CGCGTGGTTTCGATCCACG	
PgMET_pB	FAM	5'-GGGGCTCATAACCCCAAGGA	BHQ2
HumTuBB_F2		5'-AAGGAGGTCGATGAGCAGAT	
HumTuBB_R2		5'-GCTGTCTTGACATTGTTGGG	
HumTuBB_Joe	JOE	5'-TTAACGTGCAGAACAAGAACAGCAGCT	BHQ2

PgMET: analysis

The cycle number at which the amplification curve of each sample crossed the pre-determined threshold (0.025) was taken as the cycle threshold (Ct), which represented the point at which the fluorescent signal started to increase. Positive samples were defined as those that crossed this fluorescence threshold, using the dynamic tube setting (this determines the average background of each sample before amplification commences, as an average from cycle 1 to the

Chapter 3: Parasitology of Kenyan study population

amplification 'take-off' cycle number), and ensuring that both no-template-control reactions (NTC) per run did not cross the threshold. If both NTCs crossed, the mean Ct value of both NTCs, less three cycles, was taken to signify positivity. If one NTC crossed, the same procedure was followed using the mean of the NTC Ct and 45 (total number of cycles). If an NTC crossed the Ct but there were other blank reactions in the run that did not, the amplified NTC was taken as an anomaly and the non-amplified blanks were used as NTCs (and the usual criteria for positivity retained). Ct values of the sample and INT parasite gene (PgMET) were normalised to their respective reference gene (HumTuBB), and then $\Delta\Delta\text{Ct}$ calculated by comparing ΔCt (sample) with ΔCt (INT)). Parasite density was then calculated using $2^{-\Delta\Delta\text{Ct}}$, and normalising to the INT (Beshir et al., 2010) (Equation 3-2).

Equation 3-2. Delta delta Ct calculation for normalising sample and calibrator (International Standard, INT) to reference gene amplification, and to each other.

$$\text{Parasite density} = [2^{(\Delta\text{Ct}_{\text{sample}} - \Delta\text{Ct}_{\text{reference}})}] * \text{Dint}$$

$\Delta\text{Ct}_{\text{sample}} = \Delta\text{Ct}_{\text{PgMET}} - \Delta\text{Ct}_{\text{HumTuBB}}$ (Ct value of sample normalised to reference gene)

$\Delta\text{Ct}_{\text{reference}} = \Delta\text{Ct}_{\text{PgMET}} - \Delta\text{Ct}_{\text{HumTuBB}}$ (Ct value of calibrator normalised to reference gene)

Dint = number of parasites (p/ μL) in international standard

All samples for which the two repeats were a positive and a negative were assigned the same overall parasite density, 0.93 p/ μL , and referred to as 'inconsistent' samples. This value was the median parasite density of all the positive samples in this group (n=71), excluding any that had been flagged for poor human gene amplification as the normalisation process would have artificially raised parasite density. The analytical parameters (i.e. Ct 0.025) were set to detect parasite DNA with high sensitivity, favouring false positives over false negatives. This was because the overall research question required identification of truly parasite-free individuals as a comparator group to *Plasmodium*-infected individuals. By designating low levels of fluorescence as positivity, the possibility of classifying a parasite-free individual as positive was reduced. Comparisons between parasite densities obtained using the uRDT or wDBS template were analysed using the Wilcoxon matched-pairs test. Data analysis was conducted using Rotor-Gene Q (version 2.3.1, Qiagen) and GenStat (16th edition, VSNi).

Pgmet: quality control

To maximise accuracy in calculating parasite density with the PgMET assay, the following quality control steps were taken: examination of both human and parasite gene Ct values to check the normalisation process, a sensitivity analysis for the PgMET calculation, and statistically examining the difference between parasite density as calculated per sample using uRDT vs. wDBS template. Because parasite DNA amplification was normalised to human DNA amplification, poor human gene amplification could lead to an artificially raised parasite density. In the case of poor amplification of both DNA types, samples may have been falsely designated parasite-free. For each PCR assay, one standard deviation more than the mean human Ct value was calculated, excluding samples with poor amplification (to ensure a stricter pass criterion). Any sample with a human Ct value outside this range was examined: all were highlighted for comparison against the other diagnostic measures, and some re-classified as fails. For those samples with poor human amplification, the possibility of inaccurate PgMET quantification was taken into consideration when categorising for the odour profile study (Appendix 5.8). Additionally, mean human and parasite gene Ct values were calculated per PCR plate and compared between runs for outliers. Mean Ct values were found to be relatively constant between runs, with outliers explicable by small sample size (i.e. fewer reactions per PCR plate).

A sensitivity analysis was conducted by raising the level at which the cycle threshold was set (from 0.025 to 0.03) and monitoring which samples changed in parasitological status (no repeat PCR plates were included in this analysis). All other rules for determining positivity were kept constant. In raising the threshold from 0.025 to 0.03, 17.22 % (36/209) uRDT template samples changed in positivity, while 9.10 % (18/198) wDBS template samples changed in positivity. Taken together, 13.25 % of all samples changed (54/407). Comparing those samples with data from other diagnostic assays did not resolve these discrepant results, as both positive and negative results were recorded. Correlation in parasite density, measured by PgMET qPCR based on either uRDT or wDBS template, was compared at each threshold. As correlation was very similar (0.025 threshold, $r=0.88$, $n=112$ $P<0.001$; 0.03 threshold, $r=0.89$, $n=112$ $P<0.001$), and increased sensitivity was favoured over specificity (we preferred to classify any parasite amplification as positivity to favour the identification of truly parasite-free individuals), the 0.025 threshold was retained and used for analysis.

3.3.4 *Plasmodium*-species specific nested PCR

A nested PCR (Snounou et al. 1993) was used to differentiate *Plasmodium* species, using the same filter paper extracts as the PgMET qPCR (see above, DNA extraction), thus testing both uRDT and wDBS templates where available. Methodology was taken from Snounou et al. (1993). For nest one, a master mix was prepared per run with the following component concentrations per reaction: 1X NH₄ Buffer (Bioline, as before), 2 mM MgCl₂ (Bioline), 200 μM dNTPs (Bioline), 250 nM Primer mix (rPLU5+rPLU6, Table 3-2) (Eurofins), 0.025 U BioTaq and molecular grade water (Sigma-Aldrich). After vortexing, master mix (15 μL) was dispensed into each well of a PCR plate and template (DNA extract, 5 μL) was added. Positive controls were included in each plate (from the Malaria Reference Laboratory, LSHTM), as were no-template controls. Amplification assays were performed using a Dyad® DNA Engine (Peltier Thermal Cycler), cycling conditions were: 95 °C for 5 minutes, (58 °C for 2 minutes; 72 °C for 2 minutes; 94 °C for 1 minute) x 25 cycles; 58°C for 2 minutes, 72 °C for 5 minutes, 4 °C forever. Nest two required master mix components and concentrations as for nest one, other than 0.5 U BioTaq, *P. falciparum*, *P. ovale* or *P. malariae* primers (Table 3-2), and nest one product (1 μL) was used as template. Cycle conditions were the same as for nest one, other than an extended duration, with 30 rather than 25 cycles. All preparation was conducted in a laminar airflow cabinet (TWO 30, Mason Technology), electrophoresis of the product was performed in a 2 % agarose gel.

Table 3-2. Primer sequences for the *P. falciparum*, *P. malariae* and *P. ovale* species-specific nested PCR.

Reaction	Identification	Primer	Sequence	Product (bp)
Nest 1	<i>Plasmodium</i>	rPLU 6	TTAAAATTGTTGCAGTTAAAACG	1200
		rPLU 5	CCTGTTGTGCCTTAACTTC	
Nest 2	<i>P. falciparum</i>	rFAL1	5'-TTAAACTGGTTTGGGAAAACCAAATATATT-3'	205
		rFAL2	5'-ACACAATGAACTCAATCATGACTACCCGTC-3'	
	<i>P. malariae</i>	rMAL1	5'-ATAACATAGTTGTACGTTAAGAATAACCGC-3'	144
		rMAL2	5'-AAAATCCCATGCATAAAAAATTATACAAA-3'	
	<i>P. ovale</i>	Pova FWD	CTGTTCTTTGCATTCCTTATGC	375
		RVS common	GTATCTGATCGTCTTCACTCCC	

Due to some uncertainty over the *P. ovale* nested PCR results, testing was repeated by another person, using the *P. ovale* tryptophan-rich antigen (PoTRA) assay (Oguike et al., 2011).

3.3.5 18S ribosomal RNA qPCR and QT-NASBA (conducted by collaborators at Nijmegen)

DNA was extracted from the whole blood sample (50 µL) stored in RNA protect, using automated extraction of total nucleic acids by MagNAPure LC automatic extractor (Total Nucleic Acid Isolation Kit–High Performance; Roche Applied Science, Indianapolis, IN, USA). A real-time qPCR based on the multicopy 18S (small subunit) ribosomal RNA gene (here referred to as 18S qPCR) was used to quantify *P. falciparum* parasites (5 µL template used) in the whole blood samples (Hermsen et al., 2001; Tadesse et al., 2017). Additionally, a real-time Pfs25 mRNA quantitative Nucleic Acid Sequence-based Amplification (QT-NASBA) assay was used to detect mature stage V *P. falciparum* gametocytes in the same samples (Pett et al., 2016; Schneider et al., 2006) (2.5 µL template). These assays were conducted by collaborators at the University Medical Centre, Nijmegen (The Netherlands).

3.3.6 Comparative analysis of multiple diagnostic assays

A 5 µL whole blood template was used in the 18S qPCR. Relative to the filter paper templates (wDBS and uRDT), this was considered to be better quality, and storage at -80 °C was highly stable. Because of this, when available, the 18S qPCR result was taken as the reference test for comparison of parasite density. Although 18S qPCR quantifies *P. falciparum* only, not all *Plasmodium* species, the majority of infections in this population were *P. falciparum*. Additionally, those individuals with *P. ovale* or *P. malariae* often harboured mixed-species infections with *P. falciparum* (7 of 8 were mixed infections). Comparisons between parasite densities obtained by different assays were made using the Wilcoxon matched-pairs test. Data analysis was conducted in GenStat (16th edition, VSNi).

3.4 Results

3.4.1 Summary

At four study sites (Obambo, Alero, Kamsama and Powo schools) between January and July 2014, 212 children were tested for their *Plasmodium* infection status by point-of-care measures, including RDT and microscopy. All children were asymptomatic (tympanic temperature <37.5 °C). Based on RDT and microscopy results, some children were selected for odour sampling, with the intention to sample these children three times, once 'during' infection (round one, R1), and twice following treatment with antimalarials (artemether lumefantrine) (round two, R2, at day seven and round three, R3, at day 21). Considering all malaria-tested individuals at R1 only, prior to antimalarial treatment, *Plasmodium* prevalence was 37.07 % (76 of 205) as tested by microscopy and 68.12 % (141 of 207) as tested by RDT.

362 samples were analysed by multiple diagnostic assays to characterise *Plasmodium* infection in the study population. Of these, 149 corresponded to an odour sample (although only 117 odour profile samples were used in the final analysis, chapter 5). 213 samples corresponded to other odour samples (worn cotton pads), which were analysed by collaborators (University of Wageningen, data not reported here). The 362-sample subset comprised repeat measures on 118 individuals, as occasionally children were tested multiply at the same round, or over four rounds. Among these children, the age range was 5-12 years, with a median of eight years, and relatively even distribution of ages between schools (Table 3-3). The sex ratio of this cohort was 53 % male and 47 % female.

Table 3-3. Characteristics of parasitology study population (362 repeat samples were taken over 1-4 time points on 118 individuals). Schools constitute the four study sites. Seven individuals from Kamsama had no accompanying descriptive data.

School	Individuals	Male	Female	% male	% female	Age range (years)
Obambo	12	6	6	50	50	6 - 11
Alero	22	13	9	59.09	40.91	6 - 12
Kamsama	34 (41)	17	17	50	50	5 - 10
Powo	43	23	20	53.49	46.51	5 - 9
all sites	118	59	52	53.15	46.85	5 - 12

3.4.2 Comparability of diagnostic assays used

The same diagnostic assays were not available for all 362 samples, due to sample loss and changing methodology (i.e. additionally collecting wDBS for Kamsama and Powo). It was therefore imperative to examine correlation between the results of different diagnostic tests.

PgMET qPCR parasite density assessed from two templates

Both template types (uRDT, and wDBS) were available for 141 samples. There was a strong correlation in parasite density measured by these templates ($r=0.78$, $n=141$, $P<0.001$) (Figure 3-3). No significant difference was found between parasite density as measured by either (Wilcoxon Matched-Pairs test $Z = 2686$, $n=104$ $P=0.636$) (Figure 3-4). On excluding densities of less than 5 p/μL (a published sensitivity for this assay, referred to here as the PgMET test limit of detection (LOD) (Beshir et al., 2010)) the correlation further improved ($r=0.83$, $n=81$, $P<0.001$). The PgMET qPCR assay, using uRDT template, allowed the molecular measurement of parasite density for 19 odour profile samples that would otherwise have had only point-of-care measures.

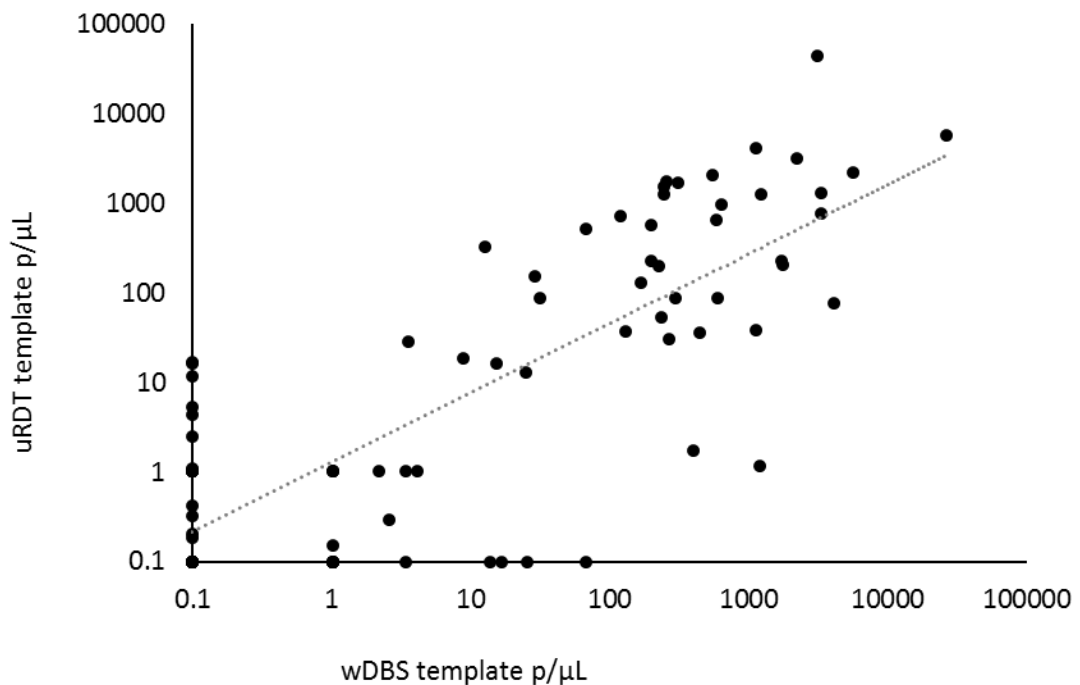


Figure 3-3. Parasite density (p/μL) measured by PgMET qPCR based on uRDT and wDBS. There was a good correlation between these two measures ($r=0.78$, $n=141$, $P<0.001$), here all samples with both template types available are shown.

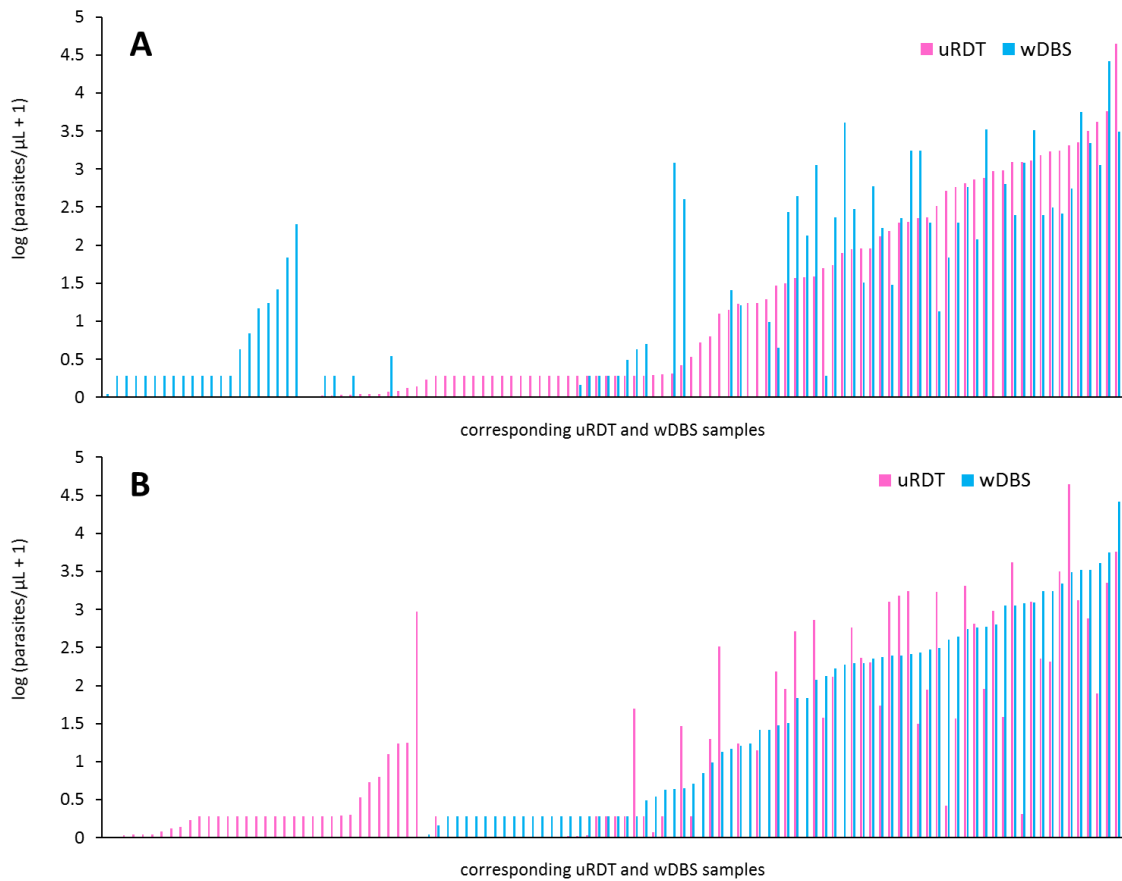


Figure 3-4. Parasite density ($p/\mu\text{L}$) measured by PgMET qPCR based on uRDT or wDBS. **(A)** Ordered by uRDT value, **(B)** by wDBS value, both omitting samples for which both results were zero. Multiple values at 0.29 ($\log(0.93+1)$) $p/\mu\text{L}$ represent 'inconsistent' samples (test result for that sample was one positive and one negative repeat, see methods, 'PgMET: analysis').

For both wDBS and uRDT template PgMET qPCR reactions, there were numerous samples with detectable parasite DNA that were found to be negative by the corresponding template (wDBS positive uRDT negative, 21; uRDT positive wDBS negative, 34). A relatively high proportion of test results were positive by uRDT template but negative by wDBS template.

If samples with less than 5 $p/\mu\text{L}$ (LOD) were excluded, discrepancies were reduced (wDBS positive uRDT negative, 6 (Table 3-4); uRDT positive wDBS negative, 5 (Table 3-4)). For six samples found to be negative by uRDT but positive and greater than the LOD by wDBS, four were supported (as positive) by at least one other diagnostic measure (Table 3-4). For five samples found to be negative by wDBS but positive and greater than the LOD by uRDT, four were supported (as positive) by at least one other diagnostic measure (Table 3-4).

Chapter 3: Parasitology of Kenyan study population

Table 3-4. Parasite density (p/μL) measured by PgMET qPCR based on uRDT and wDBS templates. Considering only results >5 p/μL, both templates indicate positivity at times that the alternative template indicates negativity. Top half of table: uRDT template negative, wDBS template positive; bottom half of table: wDBS template negative, uRDT template positive. Other columns are results of other diagnostic assays. GAM = gametocytes by QT-NASBA; 18S= 18S qPCR; SNN= nested end-point PCR for *P. falciparum* (P.f.); *P. ovale* tested by SNN or PoTRA. 1/0 = binary outcome of positive and negative, POS = positive, NEG = negative, * not available.

Sample	uRDT PgMET	wDBS PgMET	GAM	18S	SNN uRDT	SNN wDBS	<i>P. ovale</i>	Microscopy	RDT
KA085 05-Jun-2014	0	13.65	*	*	0	1	0	0	POS P.f.
PO046 18-Jun-2014	0	16.48	0.54	169.82	1	1	0	P.f. 520	POS P.f.
PO047 11-Jun-2014	0	187.50	*	*	0	0	0	0	NEG
PO048 11-Jun-2014	0	67.69	*	*	0	1	1	0	POS P.f.
PO048 18-Jun-2014	0	25.33	*	*	1	1	0	0	NEG
PO052 11-Jun-2014	0	6.00	*	*	0	0	0	0	NEG
Sample	uRDT PgMET	wDBS PgMET	GAML	18S	SNN uRDT	SNN wDBS	<i>P. ovale</i>	Microscopy	RDT
KA069 21-May-2014	5.29	0	*	*	0	0	0	0	NEG
KA089 22-May-2014	11.49	0	*	*	0	1	0	0	NEG
KA089 05-Jun-2014	16.54	0	*	*	1	1	1	0	NEG
PO025 02-Jul-2014	16.42	0	60.39	116.14	1	0	0	P.f. 240	POS P.f.
PO032 03-Jul-2014	940.78	0	0	0.09	0	0	0	0	POS P.f.

Chapter 3: Parasitology of Kenyan study population

Plasmodium parasite species presence assessed from two templates

The correlation in species-specific PCR results, based on uRDT vs. wDBS template, is given in Table 3-5. For each *Plasmodium* species, positives were detected using uRDT template that were negative by wDBS template (pale yellow). However, more uRDT negatives were found to be positive by wDBS (pale orange).

Table 3-5. Correlation in species-specific PCR results based on uRDT and wDBS template, for three *Plasmodium* species tested. R[+] = positive uRDT result, R[-] = negative uRDT result, D[+] = positive wDBS result, D[-] = negative wDBS result. Values are agreement between templates in %, with number of samples given in parentheses. Note, some *P. ovale* results from PoTRA assay.

<i>P. falciparum</i> (180)	R[+]	R[-]
D[+]	25.56 (46)	23.89 (43)
D[-]	3.89 (7)	46.67 (84)
<i>P. malariae</i> (170)	R[+]	R[-]
D[+]	0	2.35 (4)
D[-]	0.59 (1)	97.06 (65)
<i>P. ovale</i> (170)	R[+]	R[-]
D[+]	0.59 (1)	3.53 (6)
D[-]	1.18 (2)	94.71 (161)

Examining *Plasmodium* species present at the first sampling moment only (R1), prior to any antimalarial treatment and including no repeat measures, allowed estimation of the population prevalence. At R1, by uRDT template, *P. malariae* prevalence was 2.29 % (2/87) and by wDBS 4 % (3/75). *Plasmodium ovale* prevalence at R1 was zero by uRDT and 5.3 % (4/75) by wDBS. For all these positive samples, the corresponding template result was negative (although in one case, missing). Assuming both measures to be correct, the overall prevalence at R1 by either template was 5.05 % *P. malariae* (5 of 99 samples) and 3.96 % *P. ovale* (4 of 101 samples). The prevalence of mixed infections at R1, again with the assumption that positivity by either DNA template is correct, was 7.92 % (8/101). These were: four *P. falciparum* and *P. malariae*, three *P. falciparum* and *P. ovale*, and one *P. malariae* and *P. ovale*.

Chapter 3: Parasitology of Kenyan study population

Comparability of 18S qPCR vs. other quantitative assays

Parasite densities as measured by 18S qPCR were significantly different to densities measured by PgMET qPCR or microscopy. However, in general there was good correlation between these measures, which was considered adequate for direct comparison of parasite density as measured by the various assays.

i. 18S qPCR vs uRDT PgMET qPCR

Despite a good correlation between (log) parasite density measured by uRDT PgMET qPCR and 18S qPCR ($r=0.71$, $n=147$, $P<0.001$) (Figure 3-5A), there was a statistically significant difference between these values (Wilcoxon Matched-Pairs test $Z = 2100$, $n=120$, $P<0.001$). This difference remained significant (Wilcoxon Matched-Pairs test $Z = 637$, $n=74$, $P<0.001$) when samples with parasite densities that were beneath the published test LOD were excluded.

ii. 18S qPCR vs wDBS PgMET qPCR

Similarly, there was a statistically significant difference between parasite density as measured by wDBS PgMET and 18S qPCR (Wilcoxon Matched-Pairs test $Z = 779$, $n=93$, $P<0.001$), despite good correlation between parasite densities ($r=0.83$, $n=117$, $P<0.001$) (Figure 3-5B). Again, this difference remained significant (Wilcoxon Matched-Pairs test $Z = 327$, $n=68$, $P<0.001$) following exclusion of samples with parasite densities lower than the published LOD.

iii. Microscopy vs 18S qPCR

To validate field microscopy, 20 malaria blood films were re-read by a second microscopist (Figure 3-1), and correlation in parasite density between the two readers was good ($r=0.76$, $n=20$, $P<0.001$). There was a statistically significant difference between parasite density as measured by microscopy and 18S qPCR (Wilcoxon Matched-Pairs test $Z = 2230$, $n=121$, $P<0.001$), despite a reasonable correlation between (logged) data points ($r=0.67$, $n=168$, $P<0.001$) (Figure 3-5C). As only one 18S qPCR result (with corresponding microscopy) was less than the test LOD (0.02 p/μL), analysis of correlation excluding samples with densities lower than the LOD was not conducted.

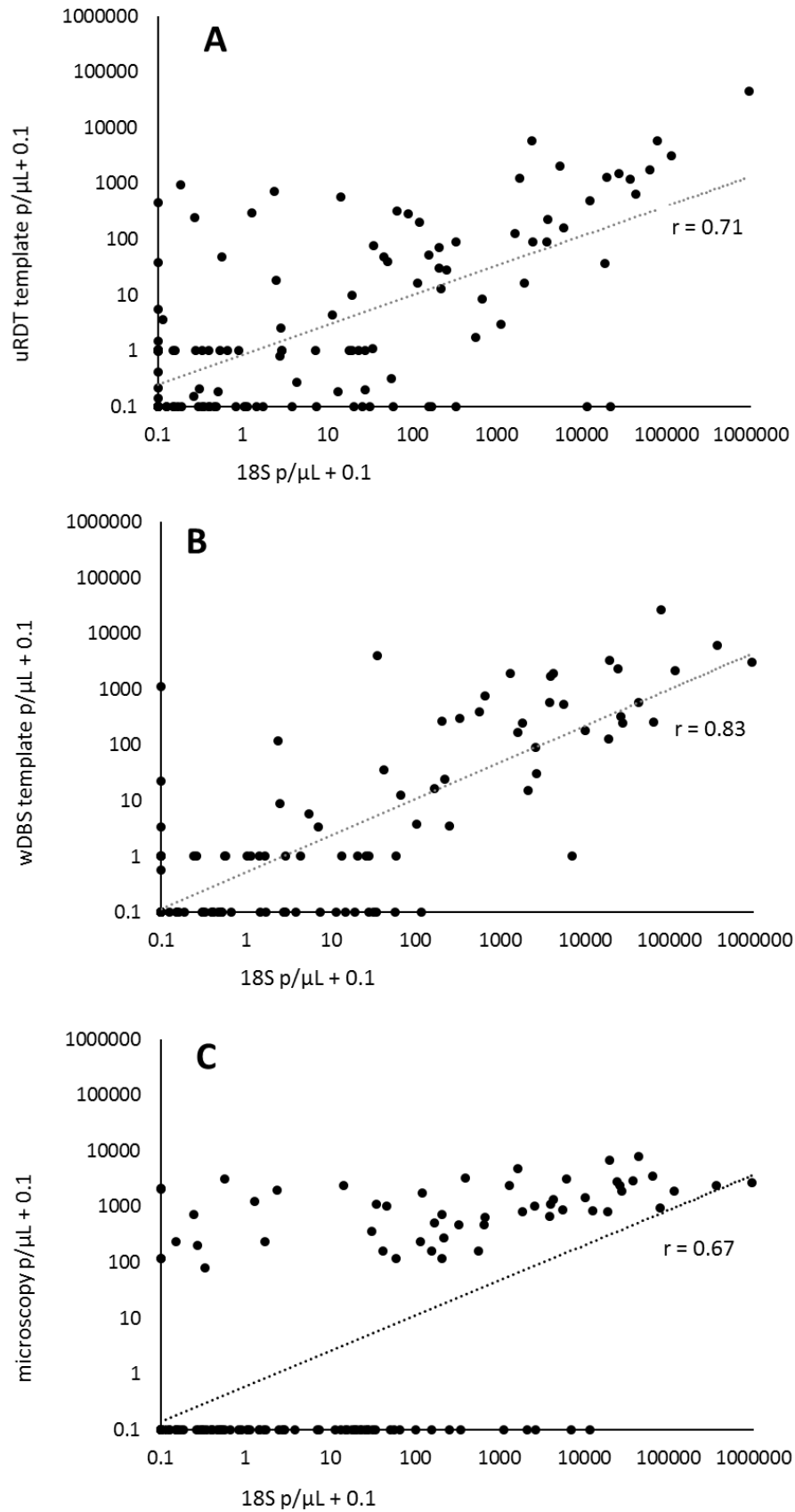


Figure 3-5. The relationship between parasite density (p/μL) as determined by 18S qPCR result vs (A) PgMET qPCR (uRDT template), (B) PgMET qPCR (wDBS template), and (C) microscopy results. The horizontal band of data points in A and B are those PgMET qPCR results that had a positive and negative repeat ('inconsistent' samples), as all were assigned the value of 0.93 p/μL (see methods: PgMET analysis).

Comparison of negative assay results

A high proportion of samples were 18S qPCR negative, but positive by uRDT PgMET qPCR (34.81 %, Figure 3-6). This was additionally seen in the RDT results, where the RDT signal was probably circulating parasite proteins, derived from dead, rather than viable, parasites.

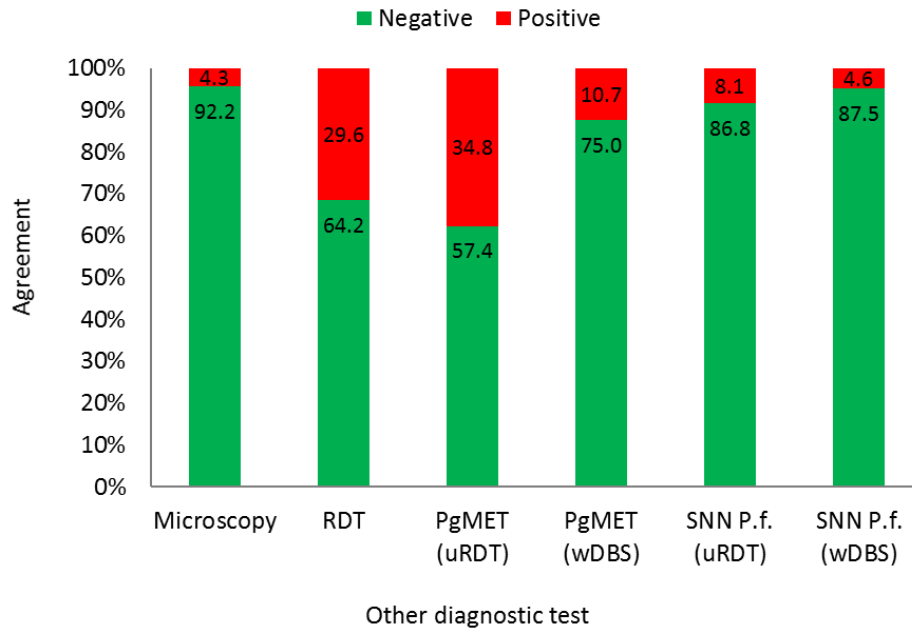


Figure 3-6. For samples that were negative by 18S qPCR, positivity by the other diagnostic assays was compared. Sample sizes were 18S qPCR negative and microscopy, 51; RDT, 53; PgMET (uRDT), 47; PgMET (wDBS), 32; SNN *P. falciparum* (P.f.) (uRDT), 53; SNN *P. falciparum* (P.f.) (wDBS), 32.

3.4.3 Categorisation of odour profile samples by parasitology

Relating parasitology to odour samples

By describing the parasitology of samples from individuals for whom odour profile had been measured, odour samples could be allocated to parasitological categories for analysis (chapter 5). Numerous iterations of parasitological categories were attempted, to determine which distinguished the production of volatile compounds, and these were based on parameters of *Plasmodium* parasite density and stage. Ultimately, *Plasmodium* species were not considered to be distinct in this analysis. Cut-offs (bins) were biologically informed, using parasitological data from individuals found to vary in attractiveness in the field, and published data, e.g. concerning the infectiousness of individuals to mosquitoes. Details of this process, and full descriptions of category parameters, are given in Appendix 5.8.

Parasitology samples were required for 149 odour samples (58 individuals, repeat sampling). Of these, six were excluded due to conflicting or unusual parasitological measurements, nine were excluded as all parasitological test results fell between zero p/μL and the test LOD (0-0.02 p/μL for 18S qPCR and 0-5 p/μL for PgMET, with the caveat that these limits may not be strictly applicable to the current samples, due to differences in DNA extraction procedures), 14 were excluded because they were determined to be parasite-free by microscopy alone (not considered sensitive enough for this analysis), and three were excluded as there was no parasitological data available. Final analyses of odour profile therefore included 117 samples from 56 individuals (chapter 5). Individuals were only considered to be truly parasite-free if all assay results were negative (no detection of parasite DNA), and these included at least one molecular test. Further, in negative samples, a positive RDT result was allowed. In those cases, the individual had previously harboured parasites, been treated, and this positivity could be attributed to circulating protein from dead parasites.

Number of odour samples in each parasitological category

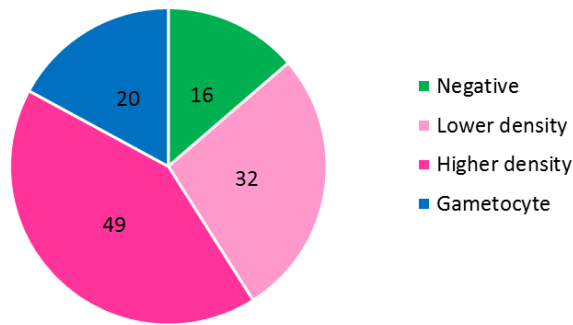
The 117 samples were analysed in three ways. 'Total density' categories focussed on the separation of samples according to two bins, of higher and lower *Plasmodium* parasite density (negative, 16; lower density, 32; higher density, 49; gametocyte, 20, Figure 3-7A). 'Gametocyte' categorisation focussed on separation according to two bins of higher and lower *P. falciparum* gametocyte density, plus those with only asexual stage parasites (negative, 16; sub-gametocyte,

Chapter 3: Parasitology of Kenyan study population

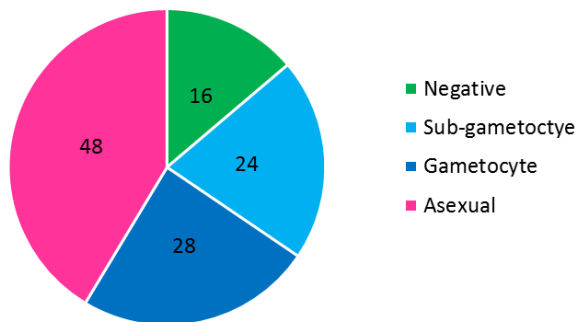
24; gametocyte, 28; asexual, 48, Figure 3-7B), and a simpler categorisation of 'positive vs. negative' was also included (negative, 16; positive, 101, Figure 3-7C).

Due to an observed effect of total parasite density on the production of certain compounds, a final set of categories was designed in which samples in 'higher' and 'lower' density categories ('total density' categorisation) were subdivided into quartiles according to parasite density (details in chapter 5 and appendix 5.8). Here, one 'lower density' sample was excluded as only an end-point PCR result was available, disallowing accurate quantification, giving a total of 116 odour samples (negative, 16; low, 21; medium-low, 17; medium-high, 19; high, 23; gametocyte, 20, Figure 3-7D).

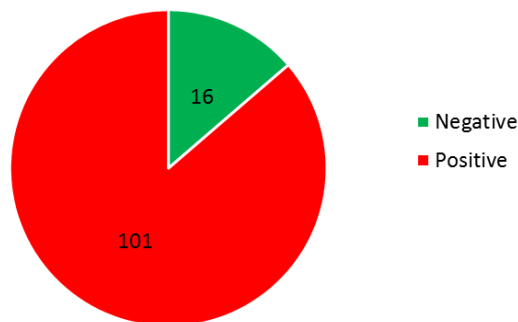
(A) 'Total density' categorisation



(B) 'Gametocyte' categorisation



(C) 'Positive vs. negative' categorisation



(D) 'Quartile' categorisation

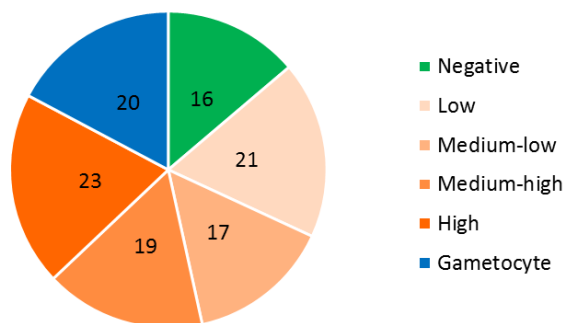


Figure 3-7. Number of odour samples that were available in each parasitological category. (A-C) the same 117 odour samples were categorised in three different ways, (A) separating out higher and lower total parasite density, (B) separating out high and low gametocyte ('sub-gametocyte') density, and (C) separating simply by *Plasmodium*-positive vs. parasite-free. (D) 'Higher density' and 'lower density' samples from (A) were sub-divided into quartiles, with 116 odour samples included (one 'lower density' individual was excluded as no quantitative measure available). Here all *Plasmodium* species are considered together.

3.4.4 *Plasmodium* parasite densities present in the sampled population

Parasite densities measured by microscopy clustered considerably, relative to densities measured by the molecular assays (Figure 3-8). The lowest parasite density recorded by microscopy was 80 p/μL, i.e. detection of two parasites on a thick film counting 200 white blood cells, and the highest density recorded was 7840 p/μL (196 on the film). Of the three qPCR methods (18S / PgMET uRDT / PgMET wDBS) used to assess parasite density, 18S qPCR appeared to detect more very low density infections (<5 p/μL); however, the grouping of samples seen at 1.93 p/μL for PgMET assays (uRDT / wDBS template) encompasses many low density measures. These samples returned one positive and one negative result ('inconsistent samples'), and were all consequently allocated the same value. The PgMET qPCR assay with uRDT template detected more very low density infections than the equivalent with wDBS template (Figure 3-8).

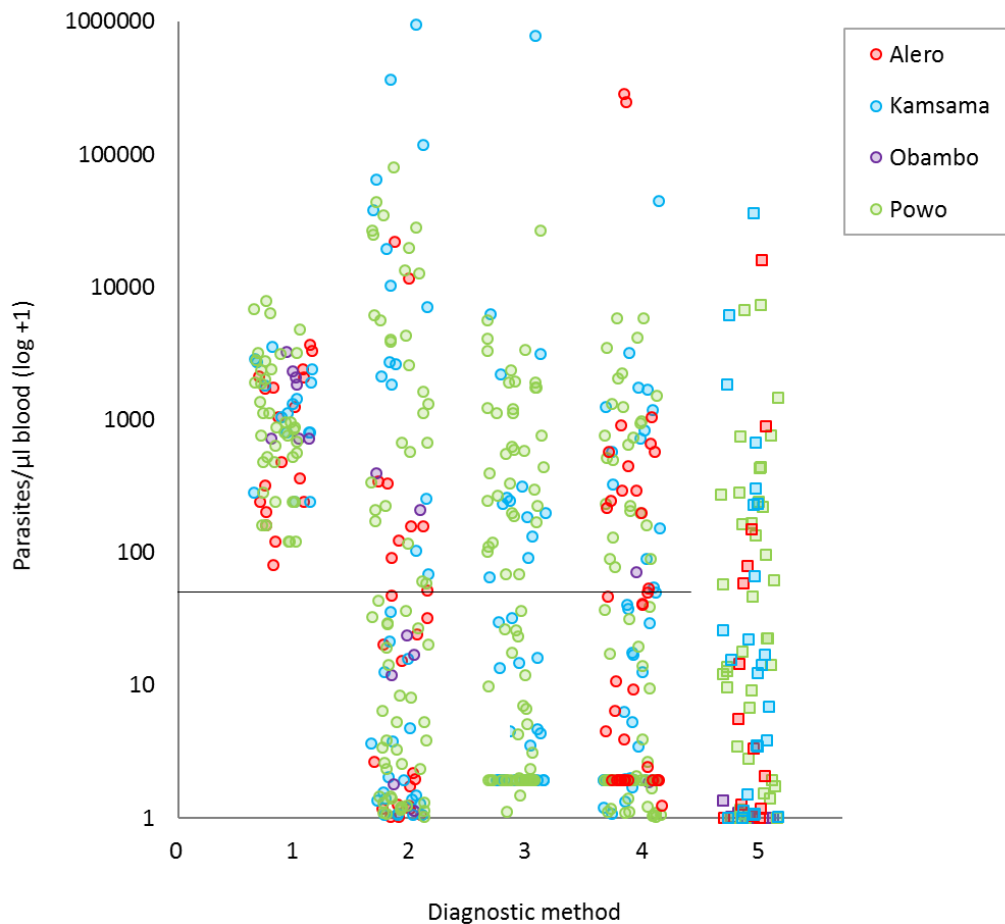


Figure 3-8. *Plasmodium* parasite densities (circles) were measured for 362 samples, including those corresponding to an odour sample. Squares represent gametocyte densities. Five quantitative methods were used: diagnostic method (1)=microscopy, n=82; (2)=18S qPCR, n=130; (3)=PgMET qPCR wDBS template, n=110; (4)=PgMET qPCR uRDT template, n=730; (5)=QT-NASBA for gametocytes, n=89. Colours represent samples from the four schools (study locations, given in legend). Threshold at 50 p/μL blood indicates cut-off between 'high' and 'low' parasite densities used in 'total density' categorisation, described above.

3.4.5 Repeat sampling of odour profile individuals

Despite intended antimalarial treatment of *Plasmodium*-positive individuals at R1 (first sampling time point), many individuals remained positive at R2 (approximately seven days later). In some cases the QT-NASBA value was negative, indicating these were not gametocytes. Although these data suggest treatment failure, the weight-dosed artemether-lumefantrine (20 mg artemether/120 mg lumefantrine per tablet, Coartem-D™; Novartis, Basel, Switzerland) used here for treatment requires repeat dosing over three days. While the first dose was administered by the investigators, the following five doses were given to the individual to take over the next two days without supervision. As such, the treatment regime may have been incomplete, therefore positivity following treatment cannot be attributed to treatment failure.

3.5 Discussion

3.5.1 Summary

In this chapter, *Plasmodium* infection parameters, determined by different diagnostic assays, were estimated for the population from whom odour samples (chapter 5) were taken. The remit of this thesis was to investigate an association between *Plasmodium* infection and the production of volatile compounds by the skin, which may play a role in mosquito attraction. To achieve this goal, it was crucial to measure parameters of parasite infection, including parasite species, stage and density. By using multiple field- and laboratory-based diagnostic assays, a large body of data was generated, which allowed parasitological categorisation in the odour profile investigation (chapter 5). Several different assays were used, to both describe infection parameters thoroughly, and to increase the amount of parasitological information in case of sample loss.

3.5.2 uRDT vs. wDBS template for PgMET qPCR

All odour samples required categorisation by parasitology, yet all diagnostic assays were not available for all samples. The comparability of different assays was therefore investigated. The PgMET qPCR was found to give consistent parasite densities, irrespective of DNA template (uRDT or wDBS). Our odour profile study was not designed to test the utility of RDTs as a DNA template for qPCR, and as such this is an important coincidental finding. RDTs are one of the most frequently used malaria diagnostic tools (Boyce and O'Meara, 2017), as the WHO recommends that every suspected case of malaria should be confirmed by either microscopy or an RDT before treatment (WHO, 2016). Used RDTs as a source of parasite DNA for further work has been demonstrated previously, for the detection, quantification and speciation of parasites by PCR (Cnops et al., 2011; Ishengoma et al., 2011; Nabet et al., 2016; Papa Mze et al., 2016; Veron and Carme, 2006) and also for genetic studies including screening for resistance mutations (Papa Mze et al., 2015). The advantages are multiple: the used tests are widely available across most malaria endemic settings where treatment is often governed by RDT testing, the volume of blood used is generally small (e.g. 5 µL), minimising discomfort and inconvenience to the patient, there are minimal storage requirements and such methodologies can significantly contribute to clinical or research studies where whole blood samples are not available. Further, as RDTs are passively collected during patient care and would normally be discarded, patient consent is not required (Nabet et al., 2016).

There was a greater frequency of very low parasite density infections detected by the uRDT PgMET qPCR relative to the wDBS PgMET qPCR. Some of these results may originate from poor DNA storage by the uRDT, leading to poor DNA amplification, also indicated by a corresponding higher parasite density determined by wDBS. However, for several samples, the corresponding wDBS assay was negative. The same effect was seen when examining samples negative by 18S qPCR; 34.8 % (n=20/47) of these were positive by uRDT PgMET qPCR. It is possible that false positives were being detected by uRDT PgMET qPCR. For both assays conducted on the two filter paper templates (uRDT and wDBS), PgMET qPCR and species-specific nested PCR, the converse was frequently detected, with wDBS samples positive and uRDT negative. This is more easily explicable, probably being due to poor DNA storage by the uRDT leading to DNA degradation and failure to amplify, as previously mentioned. The first nest product of the species-specific PCR is large (> 1kb), and larger DNA fragments are more fragile. Therefore, degradation of this fragment on the uRDT template would contribute to false negatives. For the lowest density infections identified by PgMET qPCR, results of the other diagnostic assays were mixed, i.e. either positive or negative. This could be due to the different test limits of detection, or the stochasticity of parasite presence at these densities. At very low parasite densities, a degree of randomness will exist both in the likelihood of parasite presence in that particular blood aliquot, or in the location of the parasites on the dried blood spot and whether that area was tested.

3.5.3 18S qPCR vs. other quantitative methods

Good correlations existed between parasite density measured by the 18S qPCR assay and PgMET qPCR assay, although the results were significantly different. This difference is unlikely due to the difference between amplifying all *Plasmodium* parasites (PgMET) versus only *P. falciparum* (18S) because the great majority of infections were *P. falciparum*. Despite significant differences, the correlations were considered adequate to allow cross-test comparison of parasite densities in the odour sample categorisation. The significant deviations in parasite density most likely arose at the lower densities, where comparison of assays with different sensitivities is difficult, and the stochasticity previously mentioned becomes more apparent. There was a weaker correlation between 18S qPCR and microscopic parasite density. In addition to the much higher microscopy LOD, lower density infections were consistently over-estimated by microscopy and higher density infections consistently under-estimated. This is a standard outcome for this type of work, as readers do not want to miss a low-density infection and high density infections are more difficult to accurately quantify. Ideally, all films would have been re-read in the field; however, this was not possible due to logistical constraints.

3.5.4 Parasitological categorisation of odour samples

Because odour samples were analysed categorically (chapter 5), with bins of parasite density, slight deviation in different assay results could be tolerated. The 'total density' categories centred on a cut-off of 50 p/ μ L, defining 'higher' and 'lower' parasite densities. The possibility of inappropriate categorisation of samples bordering this value should be considered. However, in light of the clear and often significant differences in compound production between individuals in these two groups (found in chapter 5), it seems likely that categorisation was conducted appropriately. This conclusion is reinforced by clear trends of increasing compound production by increasing parasite density, when individuals are sub-divided into quartiles according to parasite density (chapter 5). One further consideration regarding the categorisation of odour samples by parasitology is the time delay of approximately one day between blood sampling (for parasitology) and odour sampling. Parasite numbers can fluctuate considerably, over short periods, and the parasite density in peripheral blood on one day will probably be different the next day. However, although exact densities would change, the general trends of higher or lower density infections should remain broadly comparable, as indeed should the relative differences in parasite density between samples.

Detection of any parasite DNA was taken to indicate a positive sample. Samples with a quantitative result of less than a set value (a published limit of detection), and no positive result from another assay, were excluded. Therefore, PgMET qPCR 'inconsistent' results (one positive and one negative repeat), in the absence of further assay results, were excluded as the parasite density assigned to all such samples was less than the LOD. It was crucial to the research question that samples designated parasite-free were indeed thus, hence, analytical parameters were set to favour sensitivity. It is important to note that for the purpose of categorisation, some negative samples (9 of 16) had a positive RDT result. This was allowed, on the condition of a negative molecular test result from the same sample, as RDT positivity was taken to indicate circulating parasite protein due to delayed clearance. It is possible to detect HRP-2 parasite protein in the blood for up to 28 days following antimalarial therapy, and for this reason such RDTs are not recommended to test for parasite clearance (Abba et al., 2011). Although some samples were found to harbour *P. malariae* and *P. ovale*, for the purpose of categorisation for odour profile analysis, infection at the genus level only was considered. This was because of time constraints, and as mixed infections were too few to comprise a distinct comparator group.

Plasmodium parasite densities as measured by the two qPCR assays (PgMET and 18S) were broadly comparable. Although more low-density infections were recorded from the 18S assay, this is due in part to acceptance of such values following validation of this assay for rigorous detection of low-density parasitaemia (Hermsen et al., 2001). The good quality, large volume whole-blood template may have additionally contributed to the detection of very low parasite numbers. As stated above, if the only parasitological information available was a PgMET qPCR density of less than 5 p/μL, the odour sample was excluded on the basis of uncertain positivity. This cut-off was taken from a published study (Beshir et al., 2010), but was a conservative estimate, due to differences in the extraction procedures between that and the current study.

3.5.5 Methodological considerations

In attempting to rigorously characterise the parasitological status of individuals tested for odour profile, multiple diagnostic assays were used. While visiting the field site, and on discussion with colleagues, storage of used RDTs for further molecular testing by PgMET qPCR was implemented. Latterly, we decided that a comparator template would be necessary, and so instigated dried blood spot storage on Whatman filter paper. The use of multiple diagnostic assays, each with differing sensitivity and specificity, complicated parasitological categorisation of odour samples. In future studies, where comparison of parasite parameters between individuals of a population is paramount, it would be optimal to use one assay and strive to ensure test availability for each individual. However, of all odour samples collected and included in the final analysis, only three were omitted because of missing parasitological information. Whole blood samples taken for 18S qPCR and QT-NASBA were stored at -80°C in RNA protect, necessary for the latter test. However, storage and transport under these conditions can be difficult. Several whole blood samples were lost, but the corresponding filter paper template(s) could be used to measure parasite density by PgMET qPCR. Thus, the complication of reconciling different assay outcome measures was more than compensated for by availability of parasitological information for almost all samples.

Our study protocol intended to test all individuals at three time points, once during infection and twice following treatment. Many individuals remained parasite positive, with asexuals by microscopy, at the second time point (approximately seven days after treatment was initiated). Treatment with ACT should clear more than 98 % of ring stage parasites within three days, although there can be some persistence of parasites at very low concentrations (Chang et al.,

2016). The presence of these residual asexual parasites may be indicative of treatment failure. However, the treatment regime employed required repeat dosing over three days, and only the first dose was administered by project investigators. Because we cannot guarantee that these children were correctly treated, it is not possible to ascribe residual parasitaemia to treatment failure. Here, the most likely cause is failure of young, asymptomatic children to comply with the treatment programme.

3.6 Conclusion

To enable the investigation of a malaria-specific skin odour profile, a thorough investigation of the *Plasmodium* parasite status of all individuals who were odour sampled was necessary. In this study cohort, odour samples were taken by air entrainment (as analysed in this thesis) and by testing worn socks (conducted by collaborators, data not shown). The parasitology of all these participants was described in this chapter. By examining parasitology in this large cohort, the comparability of multiple diagnostic assays, used to increase the parasitological information available, could be more rigorously assessed. For odour profile analysis (chapter 5), samples were categorised according to the results of these diagnostic assays. While quantitative measures of parasite density often significantly differed between assays, correlations were considered sufficient to allow cross-assay comparisons for categorisation. Considerable thought was given to the categorisation of the many individuals with very low-density parasitaemias. Rigorous exclusion criteria were employed to ensure that those individuals considered to be negative were truly parasite-free, and those with conflicting or unusual parasitological measurements were excluded.

3.7 Chapter references

- Abba, K., Deeks, J.J., Olliaro, P., Naing, C.-M., Jackson, S.M., Takwoingi, Y., Donegan, S., Garner, P., 2011. Rapid diagnostic tests for diagnosing uncomplicated *P. falciparum* malaria in endemic countries. *Cochrane database Syst. Rev.* CD008122. doi:10.1002/14651858.CD008122.pub2
- Andrews, L., Andersen, R.F., Webster, D., Dunachie, S., Walther, R.M., Bejon, P., Hunt-Cooke, A., Bergson, G., Sanderson, F., Hill, A.V.S., Gilbert, S.C., 2005. Quantitative Real-Time Polymerase Chain Reaction for Malaria Diagnosis and Its Use in Malaria Vaccine Clinical Trials. *Am. J. Trop. Med. Hyg.* 73, 191–198.
- Babiker, H. a, Abdel-Wahab, A., Ahmed, S., Suleiman, S., Ranford-Cartwright, L., Carter, R., Walliker, D., 1999. Detection of low level *Plasmodium falciparum* gametocytes using reverse transcriptase polymerase chain reaction. *Mol. Biochem. Parasitol.* 99, 143–148. doi:10.1016/S0166-6851(98)00175-3
- Bejon, P., Andrews, L., Hunt-Cooke, A., Sanderson, F., Gilbert, S.C., Hill, A.V.S., 2006. Thick blood film examination for *Plasmodium falciparum* malaria has reduced sensitivity and underestimates parasite density. *Malar. J.* 5, 104. doi:10.1186/1475-2875-5-104
- Beshir, K.B., Hallett, R.L., Eziefula, A.C., Bailey, R., Watson, J., Wright, S.G., Chiodini, P.L., Polley, S.D., Sutherland, C.J., 2010. Measuring the efficacy of anti-malarial drugs in vivo: quantitative PCR measurement of parasite clearance. *Malar. J.* 9, 312. doi:10.1186/1475-2875-9-312
- Bousema, T., Drakeley, C., 2011. Epidemiology and infectivity of *Plasmodium falciparum* and *Plasmodium vivax* gametocytes in relation to malaria control and elimination. *Clin. Microbiol. Rev.* 24, 377–410. doi:10.1128/CMR.00051-10
- Bousema, T., Okell, L., Felger, I., Drakeley, C., 2014. Asymptomatic malaria infections: detectability, transmissibility and public health relevance. *Nat. Rev. Microbiol.* 12, 833–840. doi:10.1038/nrmicro3364
- Boyce, M.R., O’Meara, W.P., 2017. Use of malaria RDTs in various health contexts across sub-Saharan Africa: a systematic review. *BMC Public Health* 17, 470. doi:10.1186/s12889-017-4398-1
- Chang, H.-H., Meibalan, E., Zelin, J., Daniels, R., Eziefula, A.C., Meyer, E.C., Tadesse, F., Grignard, L., Joice, R.C., Drakeley, C., Wirth, D.F., Volkman, S.K., Buckee, C., Bousema, T., Marti, M., 2016. Persistence of *Plasmodium falciparum* parasitemia after artemisinin combination therapy: evidence from a randomized trial in Uganda. *Sci. Rep.* 6, 26330. doi:10.1038/srep26330
- Cnops, L., Boderie, M., Gillet, P., Van Esbroeck, M., Jacobs, J., 2011. Rapid diagnostic tests as a source of DNA for *Plasmodium* species-specific real-time PCR. *Malar. J.* 10, 67. doi:10.1186/1475-2875-10-67
- Gouagna, L.C., Okech, B.A., Kabiru, E.W., Killeen, G.F., Obare, P., Ombonya, S., Bier, J.C., Knols, B.G.J., Githure, J.I., Yan, G., 2003. Infectivity of *Plasmodium falciparum* gametocytes in patients attending rural health centres in western Kenya. *East Afr. Med. J.* 80, 627–34.
- Hermesen, C.C., Telgt, D.S., Linders, E.H., van de Locht, L. a, Eling, W.M., Mensink, E.J., Sauerwein, R.W., 2001. Detection of *Plasmodium falciparum* malaria parasites in vivo by real-time quantitative PCR. *Mol. Biochem. Parasitol.* 118, 247–251. doi:S0166685101003796 [pii]
- Humar, A., Ohrt, C., Harrington, M.A., Pillai, D., Kain, K.C., 1997. Parasight F test compared with the polymerase chain reaction and microscopy for the diagnosis of *Plasmodium falciparum* malaria in travelers. *Am. J. Trop. Med. Hyg.* 56, 44–8.
- Ishengoma, D.S., Lwitiho, S., Madebe, R.A., Nyagonde, N., Persson, O., Vestergaard, L.S., Bygbjerg, I.C., Lemnge, M.M., Alifrangis, M., 2011. Using rapid diagnostic tests as source of malaria parasite DNA for molecular analyses in the era of declining malaria prevalence. *Malar. J.* 10, 6. doi:10.1186/1475-2875-10-6

- Mishra, B., Samantaray, J.C., Mirdha, B.R., 1999. Evaluation of a rapid antigen capture assay for the diagnosis of falciparum malaria. *Indian J. Med. Res.* 109, 16–9.
- Moody, A., 2002. Rapid diagnostic tests for malaria parasites. *Clin. Microbiol. Rev.* 15, 66–78. doi:10.1128/CMR.15.1.66-78.2002
- Mutero, C.M., Ouma, J.H., Agak, B.K., Wanderi, J.A., Copeland, R.S., 1998. Malaria prevalence and use of self-protection measures against mosquitoes in Suba District, Kenya. *East Afr. Med. J.* 75, 11–5.
- Nabet, C., Doumbo, S., Jeddi, F., Sagara, I., Manciuilli, T., Tapily, Amadou, L'Ollivier, C., Djimde, A., Doumbo, O.K., Piarroux, R., 2016. Analyzing Deoxyribose Nucleic Acid from Malaria Rapid Diagnostic Tests to Study Plasmodium falciparum Genetic Diversity in Mali. *Am. J. Trop. Med. Hyg.* 94, 1259–1265. doi:10.4269/ajtmh.15-0832
- Ochola, L.B., Vounatsou, P., Smith, T., Mabaso, M.L.H., Newton, C.R.J.C., 2006. The reliability of diagnostic techniques in the diagnosis and management of malaria in the absence of a gold standard. *Lancet Infect. Dis.* 6, 582–8. doi:10.1016/S1473-3099(06)70579-5
- Oguike, M.C., Betson, M., Burke, M., Nolder, D., Stothard, J.R., Kleinschmidt, I., Proietti, C., Bousema, T., Ndounga, M., Tanabe, K., Ntege, E., Culleton, R., Sutherland, C.J., 2011. Plasmodium ovale curtisi and Plasmodium ovale wallikeri circulate simultaneously in African communities. *Int. J. Parasitol.* 41, 677–683. doi:10.1016/j.ijpara.2011.01.004
- Olanga, E.A., Okombo, L., Irungu, L.W., Mukabana, W.R., 2015. Parasites and vectors of malaria on Rusinga Island, Western Kenya. *Parasit. Vectors* 8, 250. doi:10.1186/s13071-015-0860-z
- Padley, D.J., Heath, A.B., Sutherland, C., Chiodini, P.L., Baylis, S. a, 2008. Establishment of the 1st World Health Organization International Standard for Plasmodium falciparum DNA for nucleic acid amplification technique (NAT)-based assays. *Malar. J.* 7, 139. doi:10.1186/1475-2875-7-139
- Papa Mze, N., Ahouidi, A.D., Diedhiou, C.K., Silai, R., Diallo, M., Ndiaye, D., Sembene, M., Mboup, S., 2016. Distribution of Plasmodium species on the island of Grande Comore on the basis of DNA extracted from rapid diagnostic tests. *Parasite* 23, 34. doi:10.1051/parasite/2016034
- Papa Mze, N., Ndiaye, Y.D., Diedhiou, C.K., Rahamatou, S., Dieye, B., Daniels, R.F., Hamilton, E.J., Diallo, M., Bei, A.K., Wirth, D.F., Mboup, S., Volkman, S.K., Ahouidi, A.D., Ndiaye, D., 2015. RDTs as a source of DNA to study Plasmodium falciparum drug resistance in isolates from Senegal and the Comoros Islands. *Malar. J.* 14, 373. doi:10.1186/s12936-015-0861-6
- Pett, H., Gonçalves, B.P., Dicko, A., Nébié, I., Tiono, A.B., Lanke, K., Bradley, J., Chen, I., Diawara, H., Mahamar, A., Soumare, H.M., Traore, S.F., Baber, I., Sirima, S.B., Sauerwein, R., Brown, J., Gosling, R., Felger, I., Drakeley, C., Bousema, T., 2016. Comparison of molecular quantification of Plasmodium falciparum gametocytes by Pfs25 qRT-PCR and QT-NASBA in relation to mosquito infectivity. *Malar. J.* 15, 539. doi:10.1186/s12936-016-1584-z
- Schneider, P., Bousema, T., Omar, S., Gouagna, L., Sawa, P., Schallig, H., Sauerwein, R., 2006. (Sub)microscopic Plasmodium falciparum gametocytaemia in Kenyan children after treatment with sulphadoxine-pyrimethamine monotherapy or in combination with artesunate. *Int. J. Parasitol.* 36, 403–8. doi:10.1016/j.ijpara.2006.01.002
- Snounou, G., Viriyakosol, S., Xin Ping Zhu, Jarra, W., Pinheiro, L., do Rosario, V.E., Thaithong, S., Brown, K.N., 1993. High sensitivity of detection of human malaria parasites by the use of nested polymerase chain reaction. *Mol. Biochem. Parasitol.* 61, 315–320. doi:10.1016/0166-6851(93)90077-B
- Tadesse, F.G., van den Hoogen, L., Lanke, K., Schildkraut, J., Tetteh, K., Aseffa, A., Mamo, H., Sauerwein, R., Felger, I., Drakeley, C., Gadissa, E., Bousema, T., 2017. The shape of the iceberg: quantification of submicroscopic Plasmodium falciparum and Plasmodium vivax parasitaemia and gametocytaemia in five low endemic settings in Ethiopia. *Malar. J.* 16, 99. doi:10.1186/s12936-017-1749-4

Chapter 3: Parasitology of Kenyan study population

- Veron, V., Carne, B., 2006. Recovery and use of Plasmodium DNA from malaria rapid diagnostic tests. *Am. J. Trop. Med. Hyg.* 74, 941–3.
- WHO, 2016. World Malaria Report, World Health Organization. doi:10.4135/9781452276151.n221
- WHO, 1996. A rapid dipstick antigen capture assay for the diagnosis of falciparum malaria. WHO Informal Consultation on Recent Advances in Diagnostic Techniques and Vaccines for Malaria. *Bull. World Health Organ.* 74, 47–54.
- Wongsrichanalai, C., 2001. Rapid diagnostic techniques for malaria control. *Trends Parasitol.* 17, 307–9.
- Wu, L., van den Hoogen, L.L., Slater, H., Walker, P.G.T., Ghani, A.C., Drakeley, C.J., Okell, L.C., 2015. Comparison of diagnostics for the detection of asymptomatic Plasmodium falciparum infections to inform control and elimination strategies. *Nature* 528, S86–S93. doi:10.1038/nature16039

4 Method development for analysis of GC data

4.1 Introduction

The first aim of this thesis was to investigate qualitative and quantitative differences in the odour profile of individuals of differing malaria infection status. The scale of this study was ambitious, with 193 human and 77 control odour samples in the final analyses of the two study cohorts, experimentally- and naturally-*Plasmodium*-infected adults and children. While gas chromatography (GC) analysis of the experimental infections (EI) cohort was complicated by the use of three GC machines, the study was sufficiently small-scale to allow successful analysis. However, the number and complexity of odour samples from the natural infections (NI) cohort required further method development.

4.1.1 Gas chromatography analysis

This analytical technique separates a complex mixture of compounds into its constituent parts, while quantifying them and providing a basis for identification (Figure 4-1). The GC output is a chromatogram (also known as a trace), whereby analytes, the separated compounds that elute from the GC, are represented by peaks. The signal generated by the detector on the GC machine is proportional to the amount of each analyte. The retention time (RT) of each peak (the time taken for the compound to transition through the GC column) depends upon its vapour pressure and affinity for the stationary phase of the column (McNair and Miller, 2009), and the oven temperature ramp used.

Chapter 4: Method development for analysis of GC data

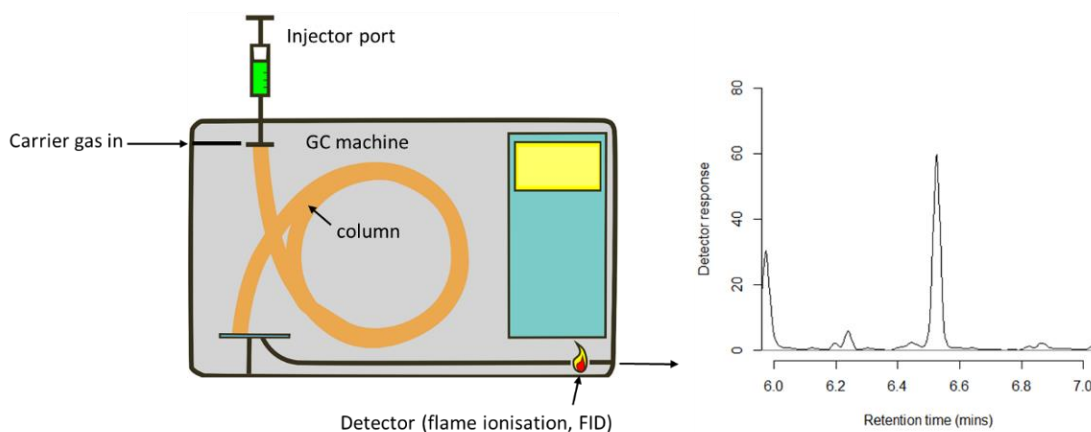


Figure 4-1. Schematic of GC analysis. Samples are injected by syringe at the inlet directly into the end of the column, where they are vaporised, and carried through the column by the carrier gas (here hydrogen). During passage through the (50 m) HP1 column, different constituents of the sample are separated primarily by the oven temperature ramp but also according to their respective affinities for the stationary and mobile phases of the column (i.e. the inner surface of the column and the carrier gas). At the flame ionisation detector (FID), hydrocarbons in the sample produce ions when burnt, and these are detected as a current that is proportional to the amount of hydrocarbons. The signal generated is represented by a peak on the trace, according to its strength. The trace is defined by a series of x and y co-ordinates, describing the time taken to move through the column and the FID signal for each component of the sample.

It is standard practice to separately run a series of *n*-alkanes, injected in known amounts (e.g. 100 ng/ μ L) which elute at a regular frequency (i.e. along the series each differs by one carbon atom, therefore they elute with an according increase in RT). By comparing to the alkanes, the retention index (RI) and amount of compound in a peak can be calculated (see chapter 2). RIs are a system-independent measurement, derived by allocating set values to the alkane standards (e.g. 800 for octane, 900 for nonane), and then determining the hypothetical position of peaks relative to those alkanes. The use of RI aids identification of an analyte, because irrespective of machine-specific differences, if the same oven temperature programme and column type are used, then the analyte should elute in the same relative position. In some circumstances, however, the same analyte can elute on different occasions with an RI that varies by as much as 10 integers (Dr S. Dewhirst, pers.comm., 02/2017) due to those system-specific differences and/or the amount of compound present in the peak. Because of this, it is necessary to visually check traces and ensure that between samples, the same peaks have been allocated the same RI value.

For the analysis of a large number of samples by GC, to minimise discrepancies in peak retention times and variation in the volume of sample injected, it is standard practice to use an autosampler. This device automatically injects samples in sequence, minimising the human error associated with the lag time between sample injection and starting the programme. It

additionally ensures that precisely the same volume of each sample is injected, and allows high throughput. Another common practice is the addition of an internal standard to samples (a known amount of a known compound), which can help to ensure correct calibration and peak alignment.

4.1.2 Rationale for method development

For the Kenyan odour sample cohort, a total of 224 samples were analysed by gas chromatography (although only 176 were in the final analysis). All samples were run under the same conditions (using the same column type, temperature programme and gas flow rates). An autosampler could not be used here, as sample volumes were very small (i.e. 1 μ L injection of 50 μ L sample) and evaporation would have occurred after the vial lid was punctured for injection. This would have affected further analysis, including electroantennography (EAG) and identification by gas chromatography-mass spectrometry. Internal standards were not introduced in case of co-elution with important compounds, and because the samples were required in their original state for EAG. Therefore, three GC machines were used to expedite analysis. However, the following problems were encountered: differing retention times and slight variation in chromatography (retrospectively thought to be caused by minor variation in GC conditions including machine fittings, plus a probable influence of human error), differing sensitivities of the GC detectors, and column deterioration (probably due to the prevalence of fatty acids in skin odour samples (Smallegange et al., 2011)) necessitating column maintenance (including column cuts, where a section of column is removed to improve analysis quality) that further disrupted retention times (Table 4-1).

Chapter 4: Method development for analysis of GC data

Table 4-1. GC machines used during analysis of Kenyan odour samples, analysis period per dataset (school), and issues that led to changes in peak elution times. GC[1] = machine 7890A at LSHTM; GC[2] = machine 6890N at Rothamsted Research; GC[3] = machine HP6890 at Rothamsted Research. Start and end refer to the time-period during which those samples were run, n = number of samples.

Dataset	GC machine	Start	End	n	Issues
Obambo	GC[1]	03/04/14	30/04/14	34	01/04/14 column cut
	GC[2]	18/08/14	18/08/14	1	None
Alero	GC[1]	29/04/14	31/07/14	23	14/05/14 new column installed 29/05/14 old column re-installed 10/06/14 method adjusted for correct column dimensions (previous samples run with wrong dimensions)
	GC[2]	21/07/14	26/08/14	63	21/08/14 column cut
	GC[3]	21/08/14	26/08/14	7	None
Kamsama	GC[2]	25/09/14	27/10/14	14	Unaccounted for discrepancy in chromatography between samples run in September and October*
	GC[3]	26/09/14	10/10/14	13	
Powo	GC[2]	10/10/14	27/10/14	36	
	GC[3]	13/10/14	27/10/14	31	

* Shifts in retention time and peak appearance made alignment between sample sets difficult, with no obvious cause

Such problems are typical of GC analysis. Usually, by calculating peak RI, and converting the detector signal into amount, between-machine variation can be accounted for, allowing rigorous comparison of samples. However, it is unusual to process this number of samples manually, over such an extended time-period. Making changes to the GC machine (e.g. column cuts) during analysis of a dataset should be avoided. The extent to which these human samples degraded the column was also unprecedented (Figure 4-2).

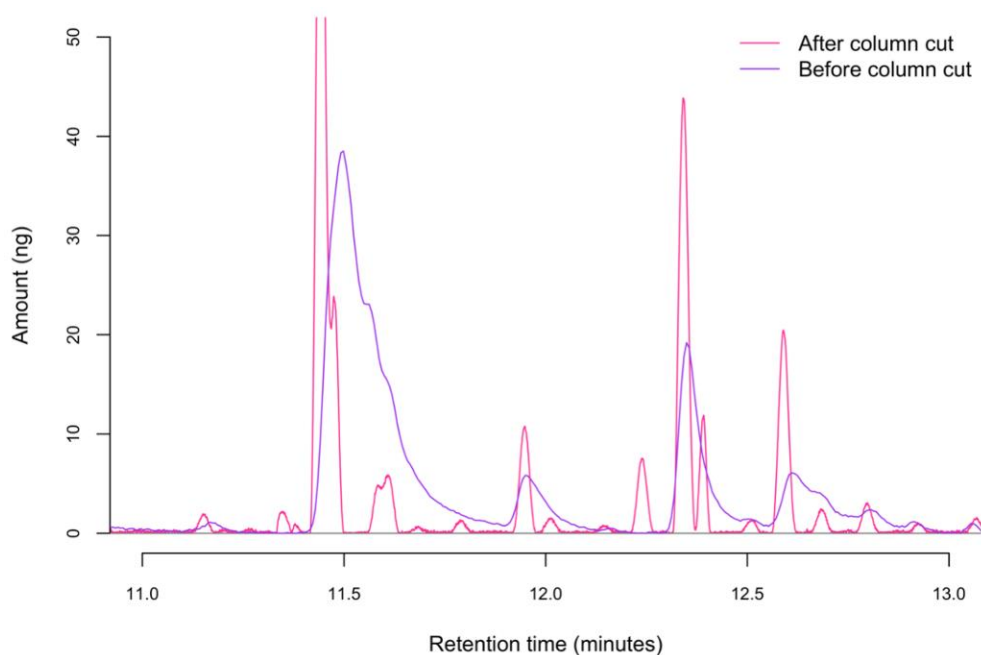


Figure 4-2. This sample was run after extensive GC use and column deterioration (purple trace). After the column was cut to improve chromatography, the sample was re-run (pink trace).

Because of these problems, attempting to satisfactorily align peaks to ensure appropriate and consistent RI allocation across the entire dataset became extremely laborious and appeared at times to be subjective. This prevented the amalgamation of all samples into one dataset by this 'traditional' retention index (tRI) method of analysis.

4.1.3 MALDIquant: a possible solution?

The R package 'MALDIquant' was developed in 2012, primarily for the analysis of clinical proteomics Matrix-Assisted Laser Desorption/Ionization (MALDI) data (Gibb, 2014). The algorithms used, however, are generic and designed to be applicable to any two-dimensional spectrometry data (i.e. similar to those generated by GC). The possibility of using MALDIquant for GC analysis was explored for the following reasons. Most importantly, MALDIquant offers a series of data processing steps that includes flexibly controlled steps for peak detection, alignment and binning (i.e. designating peaks to be the same across samples, in a controlled way). The alignment and binning functions can provide an automated and standardised way of aligning peaks between samples, while allowing quick and easy manual checking by multiple trace overlay. The latter is optimised by a baseline removal step that allows alignment of all traces on the y dimension. In itself, this represents a considerable advantage when comparing samples run on different GC machines, with their respective detectors (Figure 4-3). As an R package, MALDIquant software is freely available. Agilent (manufacturers of GC machines and software) charge for additional copies of Chemstation (C.01.04, analysis software referred to here as Chemstation), and as such, with multiple users, analysis can become difficult and may be restricted to the location of the machine.

Chapter 4: Method development for analysis of GC data

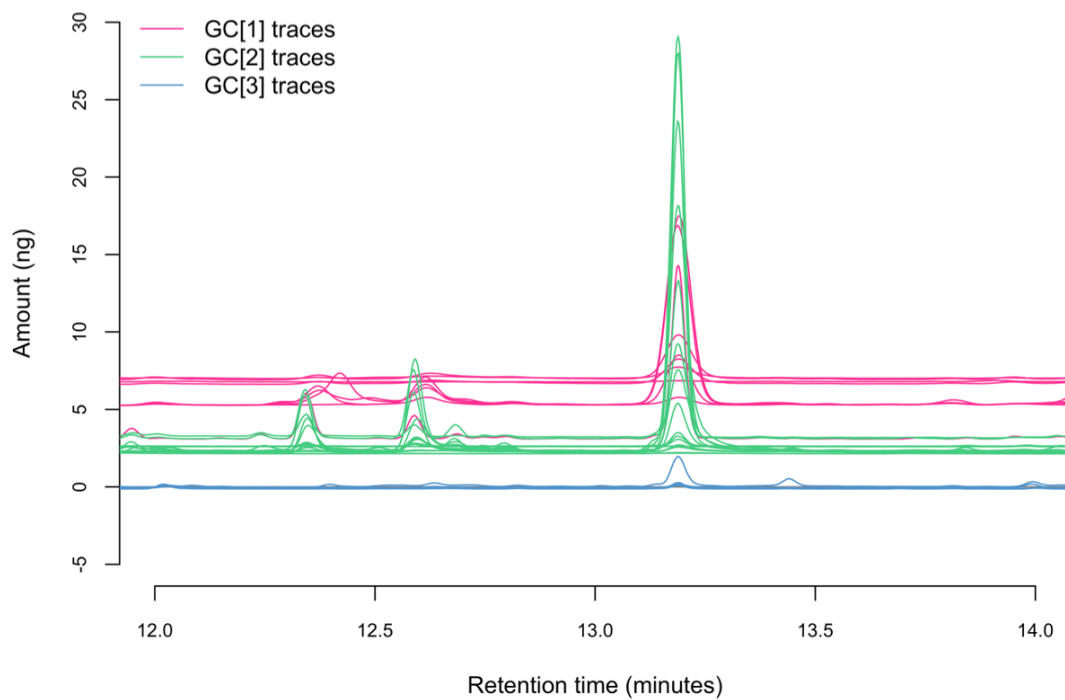


Figure 4-3. Variation in baseline level, caused by differing GC machine detector sensitivity, renders visual comparison of peak size between traces difficult with the Chemstation package.

4.2 Aim and objectives

The aim of this chapter was to test the R package MALDIquant for visualising and aligning GC traces, to allow investigation of the Kenyan odour samples.

This aim was achieved through the following objectives:

1. To trial and implement use of the MALDIquant package for analysing gas chromatography data
2. To attempt automatic alignment of peaks in the Kenyan odour profile samples, or in subsets of these samples, using MALDIquant
3. To verify that MALDIquant correctly aligns the peaks by comparison with the retention index method
4. To generate a dataset of Kenyan odour profile samples (or several smaller datasets) which can be examined for the presence of infection-associated compounds

4.3 Methods

4.3.1 Pre-processing steps for MALDIquant

Data was initially exported from Chemstation as raw x,y coordinates. For import to MALDIquant, these were stacked in a CSV file, alongside a numerical identifier per sample. To apply MALDIquant to GC data, calibration between GC machines both in terms of x axis (retention time) and y axis (peak height) was necessary, in an equivalent manner to using alkanes in the tRI method.

Calibration on the x axis in MALDIquant was only possible by manually shifting peak retention time, by deleting an appropriate section of x axis co-ordinates. Deleting a section of the ether peak (the solvent containing the sample is always the first component to elute from the GC) manually alters the retention time of the whole trace by an appropriate number of minutes. Alternatively, Chemstation offers a time-alignment function, where two peaks of known identity can be aligned to the same in other samples, prior to exportation of raw data. This method can lead to warping of traces. However, this was a possible solution to large shifts in retention time when using the MALDIquant method, which would then function to resolve the slight inter-sample variation in peak alignment that normally requires visual checking.

Relatively good calibration on the y axis was possible. As described above, while equivalent relative amounts of compound are detected by different GC machines, the absolute value may vary according to the detector. MALDIquant does not offer a function to determine peak area. Determining the amount of analyte in a peak using peak area is preferable, because certain circumstances (e.g. column deterioration) lead to peaks becoming shorter and wider (see Figure 4-2). While the area would remain the same, decreased height would indicate a lesser amount of compound. As the only option, here, the amount of compound present in each peak ($\text{ng}/\mu\text{L}$) was instead approximated by calibrating to peak height of the alkane standards. This was then adjusted to represent the amount present in the entire sample. The validity of calibrating by peak height, rather than peak area, was later tested.

4.3.2 MALDIquant package parameters

The vignette was followed according to Gibb (2014) and Gibb & Strimmer (2012). The following steps were performed: installing MALDIquant package, creating MALDIquant objects (here referred to as spectra, but equivalent to traces), transformation and smoothing, baseline

removal, intensity calibration (intensity is equivalent to y value), spectra alignment, peak detection, peak binning, and exporting a data matrix. The steps appropriate to the dataset were determined using a subset of samples, and then the same steps/parameters applied to all samples (traces) to allow comparability. Each is described in appendix 4.8, with the accompanying code. For full details and information concerning the package, see <https://www.rdocumentation.org/packages/MALDIquant/versions/1.16.1>.

4.3.3 Trialling the use of MALDIquant for the Kenyan odour samples

Three trials were conducted to determine whether alignment of the entire Kenyan odour profile dataset (i.e. all four schools, Table 4-1) was possible in MALDIquant.

Trial 1. Alignment of alkane standards and mini dataset

The first trial was an attempt to align the alkane standards that had been run throughout the analytical period. Because aliquots of the same sample were always used, shifts in peak position seen in the alkanes (due to the described analytical problems) reflected the shifts in peak position occurring in the samples. It was reasoned that if alignment by MALDIquant could be optimised for the alkanes, the same parameters could then be applied to the sample datasets. Next, a small-scale test in aligning samples across the whole dataset, applying the same steps that were successfully used to align the alkane series, was conducted. A mini set of samples were specifically chosen from the most discrepant analytical periods.

Trial 2. Alignment of samples according to GC machine

To minimise chromatography and retention time discrepancy, while maximising within-dataset sample size, alignment of all samples run on each GC machine was then attempted. Following optimisation of parameters, to check that MALDIquant had binned peaks appropriately, easily recognisable peaks were examined. These were matched between the tRI and MALDIquant methods using retention time, and the amount of compound calculated by both peak area (tRI) and height (MALDIquant) in these peaks compared. If the amounts differed significantly, MALDIquant had not appropriately aligned those peaks.

Trial 3. Verifying tRI alignment with MALDIquant

In attempting to analyse using the tRI method (see introduction; Rationale for method development), four smaller datasets had been generated: (A) Obambo, all run on GC[1], (B) Alero, run on GC[1]/[2]/[3], (C) Kamsama and Powo, samples run on GC [2], and (D), Kamsama and Powo, samples run on GC[3]. Correct alignment within each dataset had been verified as far as possible using several samples that had been run on different GC machines to 'link' between discrepant areas. However, this linking process could be considered subjective, and lacked a method of verification. Here, MALDIquant was used as a visual aid for validating these links. Where peaks had been aligned and allocated the same RI, this could be checked by overlaying those samples in MALDIquant. Further, greater assurance could be achieved by further overlay with more samples.

4.3.4 tRI- vs. MALDIquant-generated compound amounts

The amount of compound determined to be present per peak, per sample, was calculated by both the MALDIquant (peak height) and the tRI (peak area) method, and the two outcome measures were plotted against each other. This method was used in trial 2, to assess MALDIquant functionality in aligning and binning peaks.

After the datasets for analysis were finalised (ultimately using the method described in trial 3), parasitological status allocated, and infection-associated compounds (IAC) determined by statistical analysis (i.e. the IAC from chapter 5), amounts per compound by each method were again compared. This post-hoc analysis was conducted to formally assess the comparability of peak amount as calculated by area (tRI method) or height (MALDIquant method), and to highlight any inconsistencies that may have arisen. Values were compared by T tests. Amounts (ng) that differed between the two methods by greater than the mean amount of that IAC (an arbitrary value, calculated across all samples using the tRI amounts) were inspected (Figure 4-4). Data analysis was conducted using GenStat (16th edition, VSNi).

Chapter 4: Method development for analysis of GC data

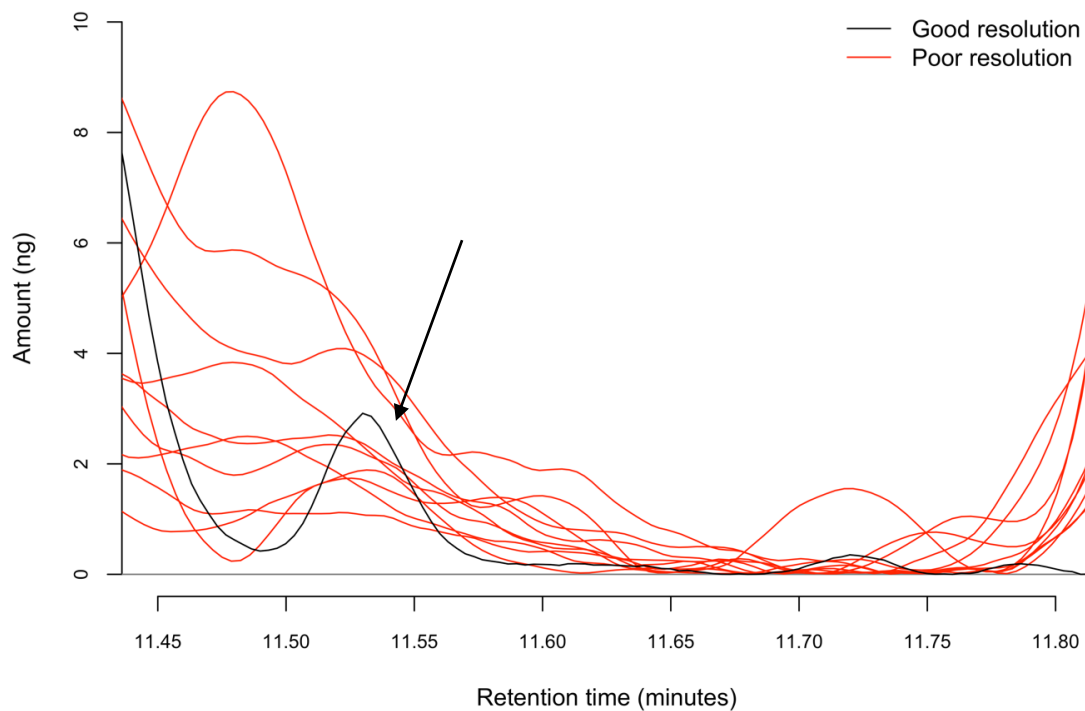


Figure 4-4. For the IAC (chapter 5), the amount present in each sample was calculated using both the tRI method (based on peak area) and the MALDIquant method (based on peak height). For samples where the values were discrepant, traces were examined by overlaying in MALDIquant. This indicated issues such as seen here, where poor chromatography had not separated the small peak of interest from a neighbouring peak in several samples. Here, red traces are those that were excluded from the final analysis for this reason, with the black trace showing expected peak position and shape.

4.4 Results

4.4.1 Trial 1. Alignment of alkane standards and mini dataset

It was possible to optimise MALDIquant parameters such that the weekly alkane standards were aligned across all samples and the peaks binned (Figure 4-5), but it was not possible to align and bin all peaks in the mini dataset (data not shown). Those that had been run on different GC machines, or before and after a column cut, were misaligned to an extent that could not be resolved by MALDIquant functions. Alignment of all samples as one dataset (i.e. across all four schools) in MALDIquant was therefore abandoned. A revised aim was adopted: to align three datasets of samples according to the GC machine used for analysis.

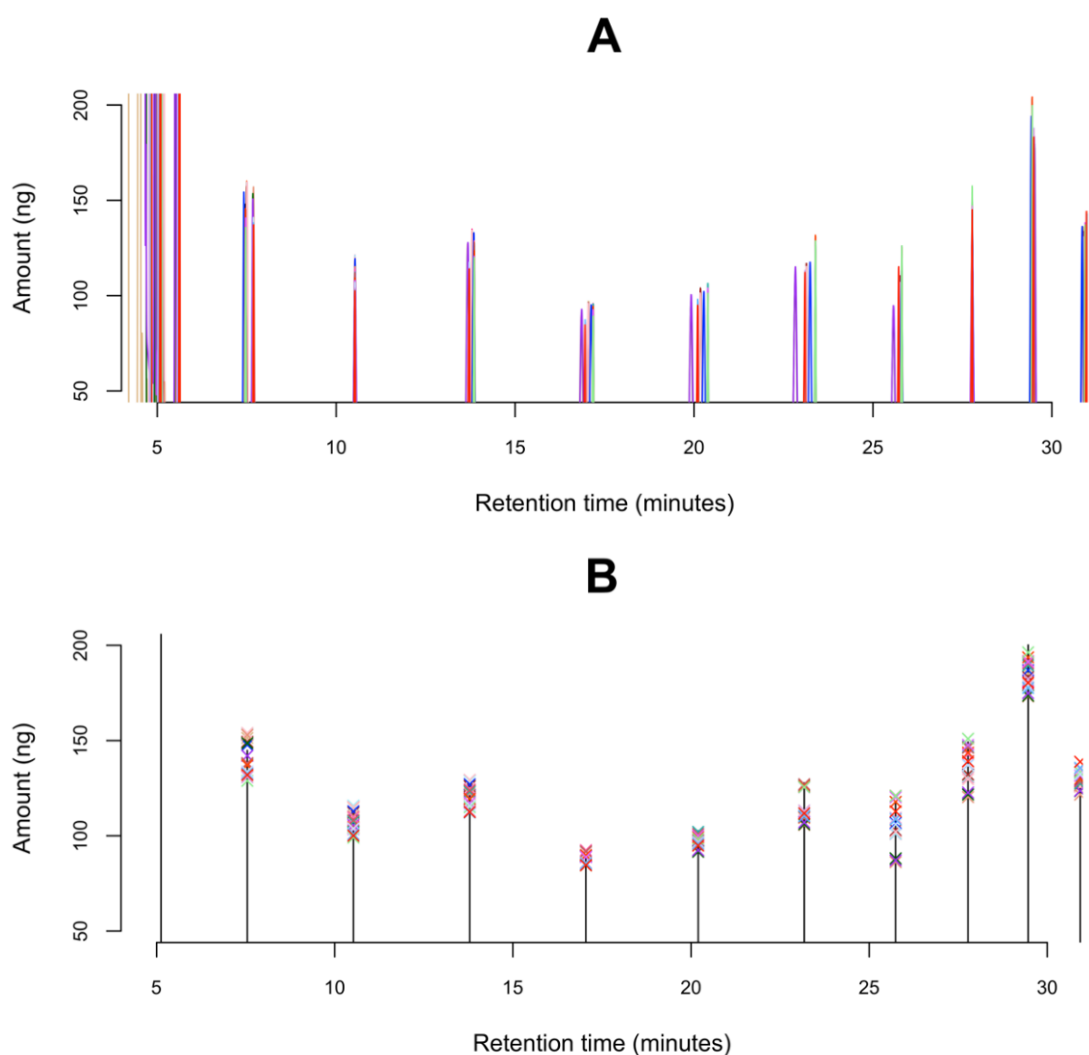


Figure 4-5. C7 to C18 of the alkane series (A) prior to MALDIquant analysis, and (B) after successful alignment in MALDIquant. All 21 alkane peaks, run across three GC machines, were successfully binned using the following functions: smoothing (method="SavitzkyGolay", halfWindowSize=5), baseline removal (method="SNIP", iterations=25), peak detection (SNR=3, halfWindowSize=8) and peak binning (tolerance=2). In (B), the reference trace peaks are represented with lines and all other traces annotated with crosses.

4.4.2 Trial 2. Alignment of samples according to GC machine

Within subsets of samples that were analysed without disruption to the GC machine (e.g. column cut), MALDIquant could be successfully used to automatically align and bin peaks correctly (Figure 4-6). Here, because the amount of compound present in peaks (as measured by MALDIquant) directly reflected the amount calculated for those peaks using the tRI method, the MALDIquant method was validated (see Figure 4-7, traces 1-42).

However, this was not possible between samples subject to these more profound disruptions, where it was clear that the discrepancy could not be resolved by binning or alignment functions (Figure 4-8, MALDIquant could not align traces of different colour). This was confirmed by comparison of tRI- and MALDIquant-generated peak amounts (Figure 4-7, samples 43-56). Because of these issues, creating a dataset of aligned traces per GC machine was not possible.

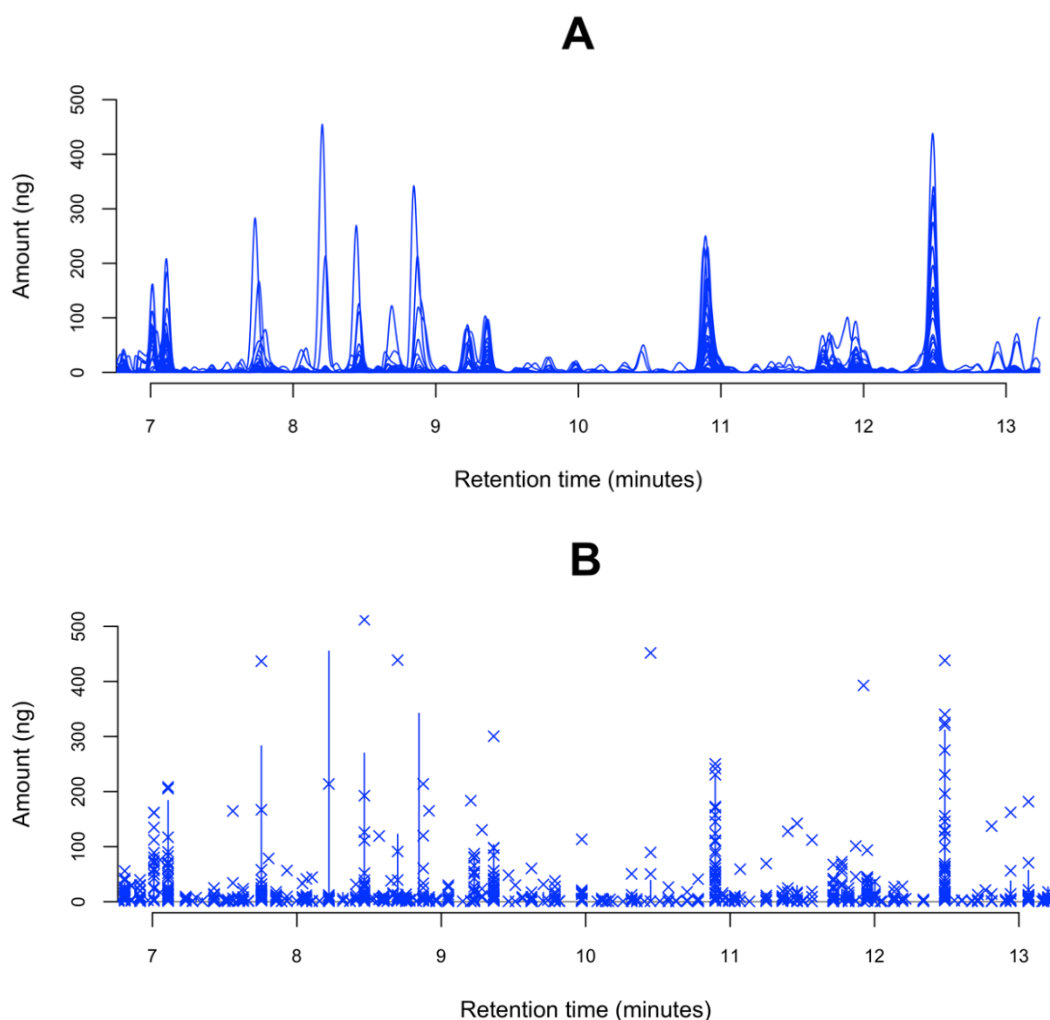


Figure 4-6. Here samples are visualised as (A) raw traces and (B) the product of MALDIquant peak detection and binning. The MALDIquant steps used were: baseline removal (method="SNIP", iterations=25), peak detection (SNR=2, halfWindowSize=10) and peak binning (tolerance=2).

Chapter 4: Method development for analysis of GC data

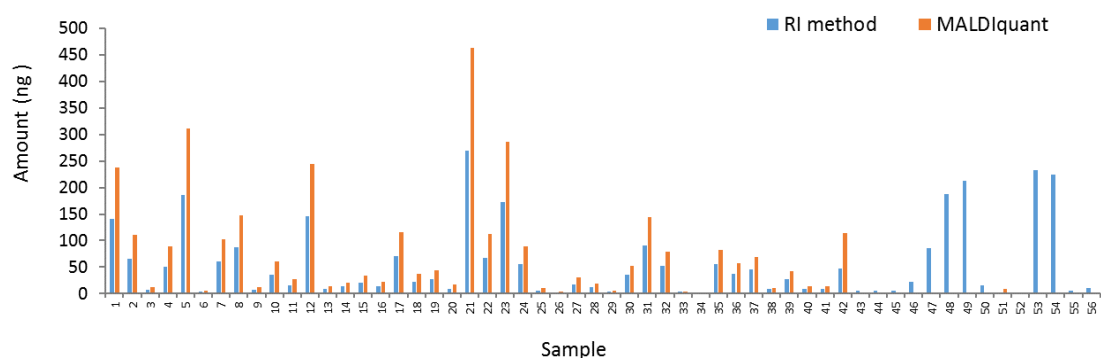


Figure 4-7. For traces 1-42 there was a good correlation between the amounts of compound present in the peak as determined using either method. However, traces 43 – 56 were not correctly aligned by MALDIquant as the chromatography was too different (Figure 4-8). Therefore, the package binned these peaks separately, and no values were generated at this position.

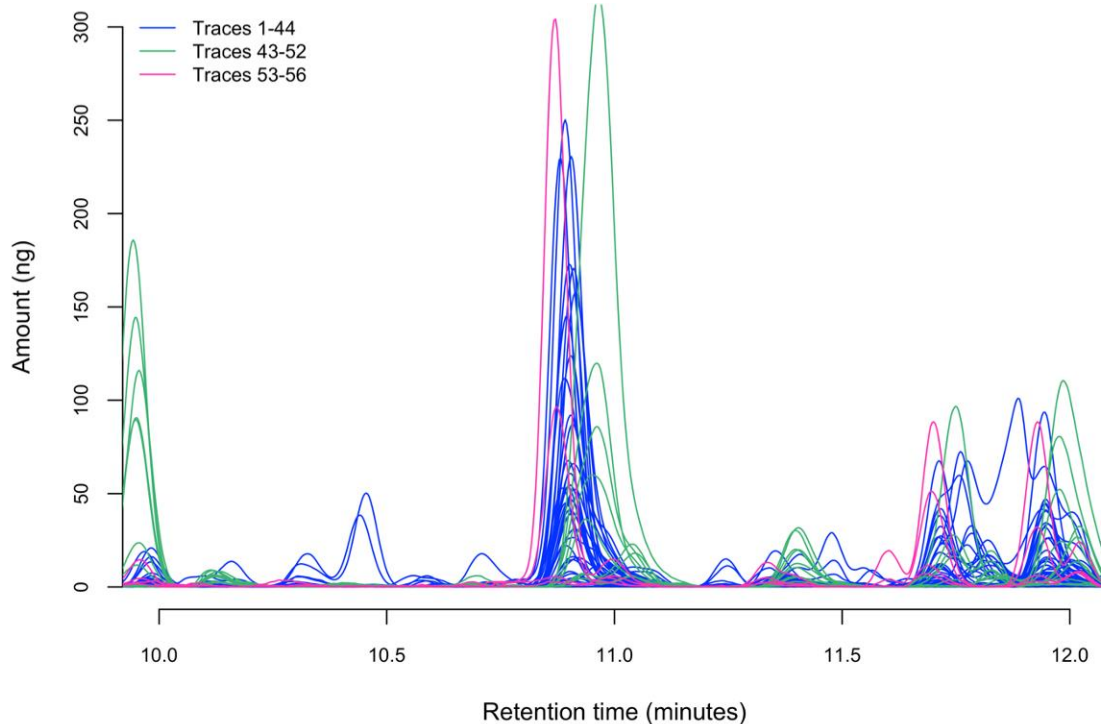


Figure 4-8. Samples run on GC[1] formed distinct groups according to GC issues. Traces 1-42 aligned well. Traces 43-52, run after a method change, aligned together, as did traces 53-56. Here, the MALDIquant package could successfully align samples and bin peaks of the same colour, while samples of different colour (those analysed at a different time) were too discrepant to be aligned.

4.4.3 Trial 3. Verifying tRI alignment with MALDIquant

The issues affecting GC analysis of the Kenyan dataset were profound, hence it was not possible to align all samples as one dataset using MALDIquant. However, robust dataset alignment was achieved by combining the tRI and MALDIquant methods. The package allowed flexible visual assessment of the 'links' between samples, by overlaying traces (Figure 4-9).

While examining subsets of traces during this process, it became clear that IAC could be identified by colour-coding the traces in MALDIquant, according to parasitological status. Candidate peaks were immediately and consistently apparent (Figure 4-10). Crucially, the same IAC emerged across all datasets.

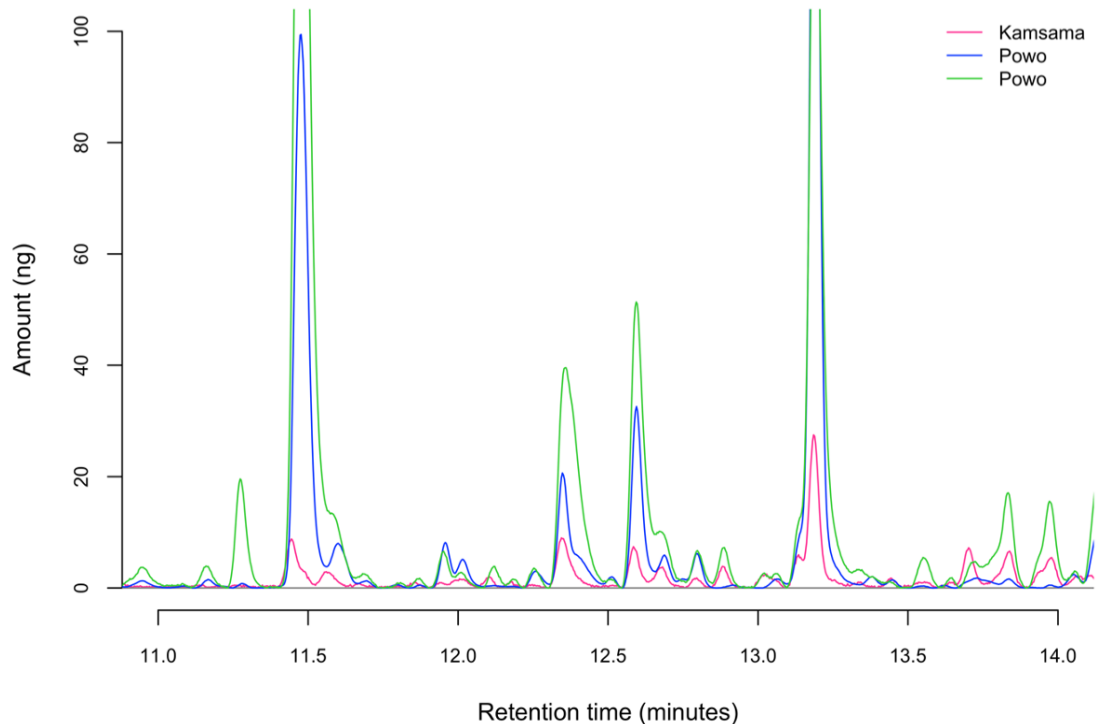


Figure 4-9. MALDIquant was used to overlay samples that had been used to link disparate subsets of traces. Here it is easy to determine that these peaks are equivalent between these traces, which are different samples from Kamsama and Powo schools.

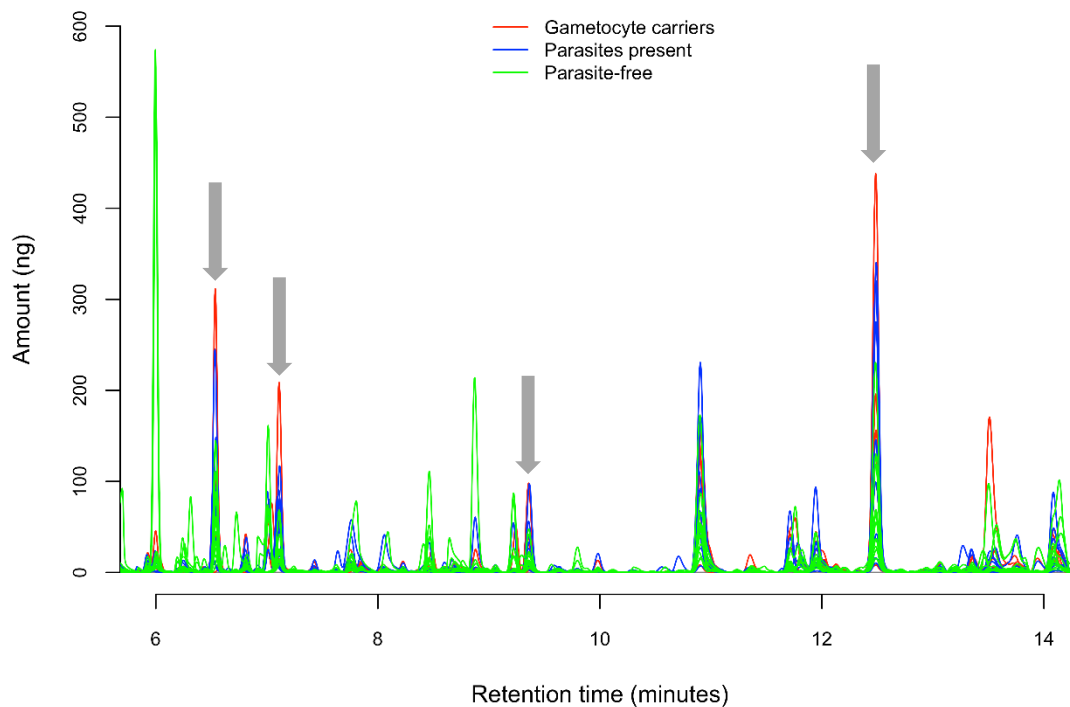


Figure 4-10. By colour-coding the larger sets of well-aligned traces in MALDIquant according to parasitology, compounds possibly associated with infection were immediately apparent. Peaks seen to be consistently increased in infected individuals are indicated with arrows.

4.4.4 tRI vs. MALDIquant generated compound amounts: infection-associated compounds

Ten samples were retrospectively excluded from the analysis of one compound, as chromatography was considered to be too poor to allow peak resolution and calculation of the amount present (Figure 4-4).

Of the eight infection-associated compounds assessed in this way, the amount present as determined by the two methods (tRI vs. MALDIquant) was significantly different for three ($P < 0.05$, T test). Full information for each compound is given in appendix 4.9 (note, the IAC from the Kenyan dataset are named).

4.5 Discussion

4.5.1 Summary

It has been demonstrated that the MALDIquant package is a useful tool that can be applied to GC data, to visualise traces, bin peaks and generate data matrices for analysis of compounds. To my knowledge, this is the first time that the MALDIquant package has been established as a highly functional tool for the analysis of GC data. In using the traditional retention index method, the issues causing unexpected variation in chromatography made robust visual assessment of RI alignment extremely challenging. Although the influence of these issues was too great to align all samples in MALDIquant, the package provided a method of overlaying and comparing traces, in turn allowing larger datasets of samples to be manually aligned with certainty. In this way, four rigorously verified datasets were generated for analysis.

4.5.2 Use of the MALDIquant package for analysing GC data

The MALDIquant package is a freely available and flexible tool that can significantly reduce the subjectivity of visual checking of RI allocation in the traditional method. Here, traces were initially time-aligned using the GC software prior to exporting to MALDIquant, to overcome large shifts in retention time. However, this neither worked, nor would be necessary in the context in which the use of MALDIquant should be advocated for analysis of GC data. MALDIquant operates best in the circumstances that the tRI method also operates best, in the absence of fundamental changes to GC operating parameters. In this context, the MALDIquant package is a powerful analytical method. Using a personal laptop, traces can be overlaid and compared in fine detail and with great flexibility. Peaks can be binned with variable tolerance, and examining the exported data matrix allows fast assessment of peaks that need to be reviewed for appropriate binning. Each step in the package should be optimised per dataset, although in the current datasets, surprisingly few functions were necessary. Because the baseline is removed in MALDIquant, all traces are calibrated on the y axis, and the threshold for peak detection is decided by optimising the signal-to-noise ratio (SNR), as opposed to the 'area reject' tRI method. Any further investigation into the detection of a peak, e.g. with greater sensitivity (lower SNR), is easily conducted. Further, the automatic integration algorithm used in Chemstation is imperfect, and requires to be checked, and in some cases manual integration of peaks is necessary. This subjectivity is circumvented in MALDIquant, where all processing steps are applied uniformly to all peaks/samples.

One caveat of applying MALDIquant is the slight discrepancy between peak amounts calculated via peak height, relative to the tRI method, via peak area. Here, the variation in amount as calculated by either method was compared statistically, per sample, for IAC (from chapter 5). While the amounts were not found to be significantly different for five compounds, for three there was a significant difference. Two compounds in the latter group were present in substantially lower amounts than the other IAC tested. It is possible that in some cases, the discrepancy is explained by the area reject threshold used in the tRI method, leading to omission of samples that did not cross that threshold yet were still detected by MALDIquant. Thus, for very small peaks, discrepancy originated from peak detection by the MALDIquant method, but not by the tRI method (see appendix 4.9, 2-octanone, traces 106-130). The smaller the peak, the greater the influence that baseline removal, detection thresholds and peak integration will exert on the resultant peak area or height. Here, such differences are of little importance, given that the difference between greater or lesser production of such a compound would be indicated by either method. Discrepancies were seen in a larger peak however (hexanal, appendix 4.9), with the biggest differences in the biggest peaks. Here, it is possible that good quality chromatography led to high, sharp peaks that artificially increased the amount as determined by MALDIquant (peak height). Amounts as per the tRI method should be taken as absolute, as peak area accurately represents the amount of compound present. Therefore, in quantitative analyses, the tRI-generated amounts would be optimal. As this was the case for the current dataset, statistical tests (chapter 5) were conducted using amounts as determined by the tRI method.

Another caveat to the MALDIquant method is the continued necessity for a series of standards by which to calibrate sample data. This is, however, only necessary to estimate specific amounts or for comparison between different GC machines. Irrespectively, optimal GC practice would include regular standard runs. In this way, either the tRI or MALDIquant method could be employed for trace analysis.

4.5.3 Solving methodological issues in this dataset

Although not in the expected way, MALDIquant did assist in generating odour profile datasets suitable for analysis. Additionally, many of the IAC from the Kenyan dataset were identified by visually examining samples in MALDIquant, although it is possible that analysing in this way was not highly sensitive. This is because differences in the amount of smaller peaks would be more difficult to detect.

The problems that arose during GC analysis were perhaps foreseeable. Both the sample sizes entailed in this ambitious study, and the fatty and acidic nature of these human-derived samples, led to several issues affecting chromatography. A further complication was that parasitological status of the individuals from whom the samples were taken was not confirmed until after GC analysis. This meant that prioritising samples for analysis, and running accordingly (i.e. on the same GC/at the same time), was difficult. With hindsight, the need for column maintenance could have been predicted and samples that already naturally grouped (e.g. by school) could have all been run on the same GC machine. This would have generated several smaller datasets, as were ultimately produced here. If all were run on the same machine these might then be aligned over the column cut to generate one large dataset. However, despite difficulties encountered due to the analytical schedule, datasets suitable for statistical analysis were successfully generated and found to contain clear and significant results. In the process, a novel method of exploring and analysing GC traces was piloted.

4.6 Conclusion

This body of work attempted to generate datasets for statistical analysis by both the traditionally used retention index method, and an R package for aligning spectral traces, MALDIquant. Ultimately, robust datasets were generated by combining these methods, allowing alignment of samples and amount of compound per peak to be conclusively validated. This chapter demonstrates proof-of-concept that MALDIquant is an extremely useful tool for analysis of gas chromatography traces. By visualising the traces in this way, compounds associated with infection were identified.

4.7 Chapter references

Gibb, S., 2014. MALDIquant : Quantitative Analysis of Mass Spectrometry Data.

Gibb, S., Strimmer, K., 2012. Maldiquant: A versatile R package for the analysis of mass spectrometry data. *Bioinformatics* 28, 2270–2271. doi:10.1093/bioinformatics/bts447

McNair, H.M., Miller, J.M., 2009. *Basic gas chromatography*, second. ed. Wiley.

Smallegange, R.C., Verhulst, N.O., Takken, W., 2011. Sweaty skin: an invitation to bite? *Trends Parasitol.* 27, 143–148. doi:10.1016/j.pt.2010.12.009

4.8 Appendix: MALDIquant package parameters

The data processing steps available in MALDIquant for peak detection, alignment and binning are described below.

- i. Install MALDIquant package and read in data

```
> library(MALDIquant)
x<-read.csv("I am your stacked data.csv")
```

After loading the MALDIquant package, stacked data are uploaded from the CSV file. All three columns require appropriate headers, here denoted as C1-C3, with C1 here representing the sample identifier, and C2/C3 the data matrix (x, y co-ordinates).

```
> head(x)
```

C1	C2	C3
1	4.699859	2.027614
1	4.703193	1.978171
1	4.706526	1.916798
1	4.709859	1.871666
1	4.713193	1.801957
1	4.716526	1.711550

- ii. Create MALDIquant objects

```
x<- split(x , f = x$C1 )
spectra <- lapply(x, function(y){
  createMassSpectrum(y[, 'C2'], y[, 'C3'])
})
```

This function turns the matrix X into a series of spectra (i.e. sample traces), each distinguished according to C1.

- iii. Transformation and smoothing

Spectra can be transformed (e.g. square root transformation) to stabilise variance between different samples (Figure 4-11). Additionally, the spectra can be smoothed (Figure 4-12), using

Chapter 4: Method development for analysis of GC data

either "savitzkyGolay" or "MovingAverage" (Bromba and Ziegler, 1981; Savitzky and Golay, 1964). The period over which smoothing is applied is determined by the half window size.

```
transformedspectra<- transformIntensity(spectra, method="sqrt")
smoothedspectra<- smoothIntensity(spectra,
method="savitzkyGolay", halfwindowSize=8)
```

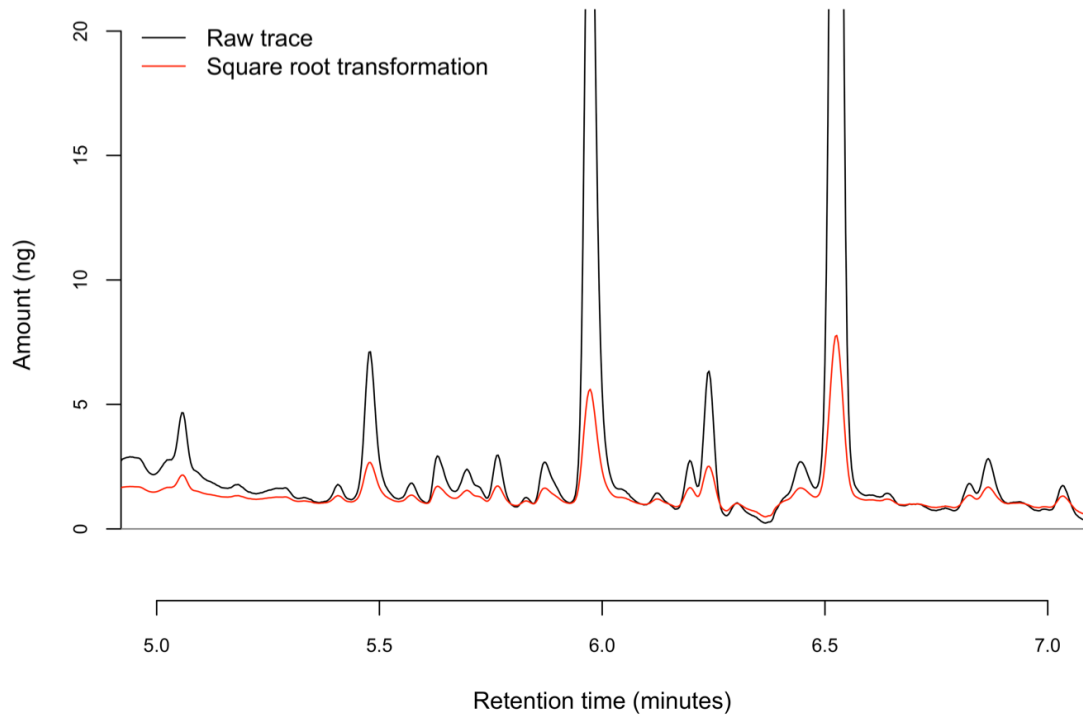


Figure 4-11. An example spectrum in its raw form and following square root transformation.

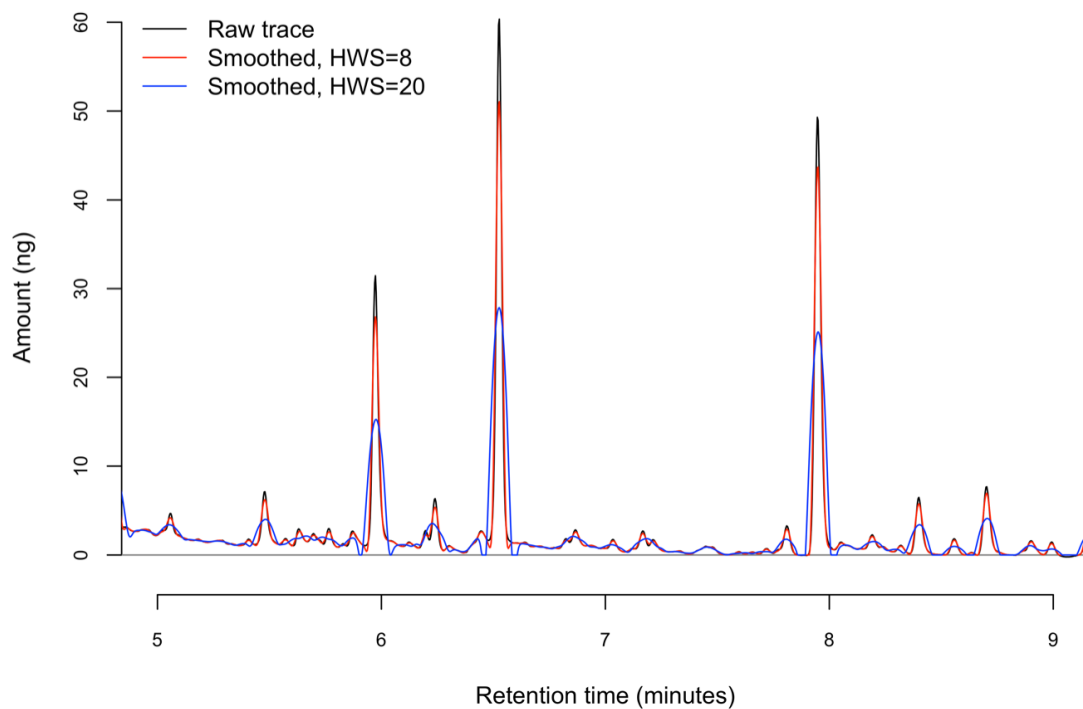


Figure 4-12. An example spectrum in its raw form and smoothed according to different half window sizes.

- iv. Visualise and remove baseline

This was one of the most useful steps in the MALDIquant package, allowing alignment of spectra on the y axis, therefore overlay and comparison. The baseline at various iterations is first visualised on the spectra, and then removed at the most appropriate level (Figure 4-13).

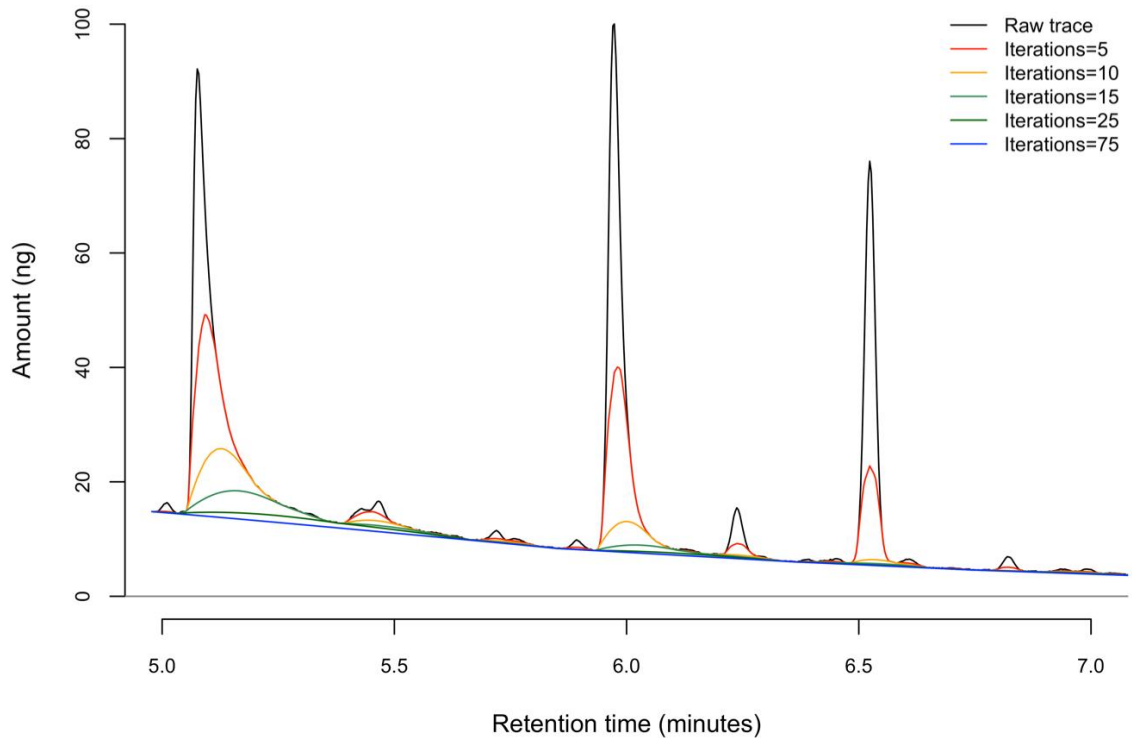


Figure 4-13. A trace is plotted with baselines of varying iterations, to determine the appropriate number for baseline removal.

```
spectraBaseline25<- removeBaseline(spectra, method="SNIP", iterations=25)
```

v. Calibrate intensity

This step can be employed to calibrate (normalise) intensities (the y value) of the spectra.

```
calibratespectrabaseline <- calibrateIntensity(spectraBaseline25, method="TIC")
```

vi. Alignment

Here alignment of the spectra (peaks) can be attempted using several parameters, each of which can be optimised. In the current dataset, the following parameters were tested: varying the half window size (the frame over which alignment would be attempted), tolerance (maximal relative deviation of a peak position to be considered as identical) (Gibb, 2014) and the warping method (warping is spectra alignment: can employ various warping functions).

```
Alignedspectrabaseline <- alignSpectra(spectra, halfWindowSize=20,
noiseMethod="MAD", SNR=2,reference, tolerance=0.002, warpingMethod="lowess",
...)
```

vii. Noise

To estimate the signal-to-noise ratio (SNR) required to appropriately identify the peaks, the SNR of different levels can be plotted on the spectra (Figure 4-14). This step was repeated on several spectra within the dataset, and one optimal SNR value used to detect peaks across the whole dataset.

```
noise <- estimateNoise(aIspectraBaseline_1[[9]])
```

Plotting with various levels:

```
lines(noise, col="red") # SNR == 1  
lines(noise[, 1], 2*noise[, 2], col="blue") # SNR == 2  
lines(noise[, 1], 3*noise[, 2], col="purple") # SNR == 3
```

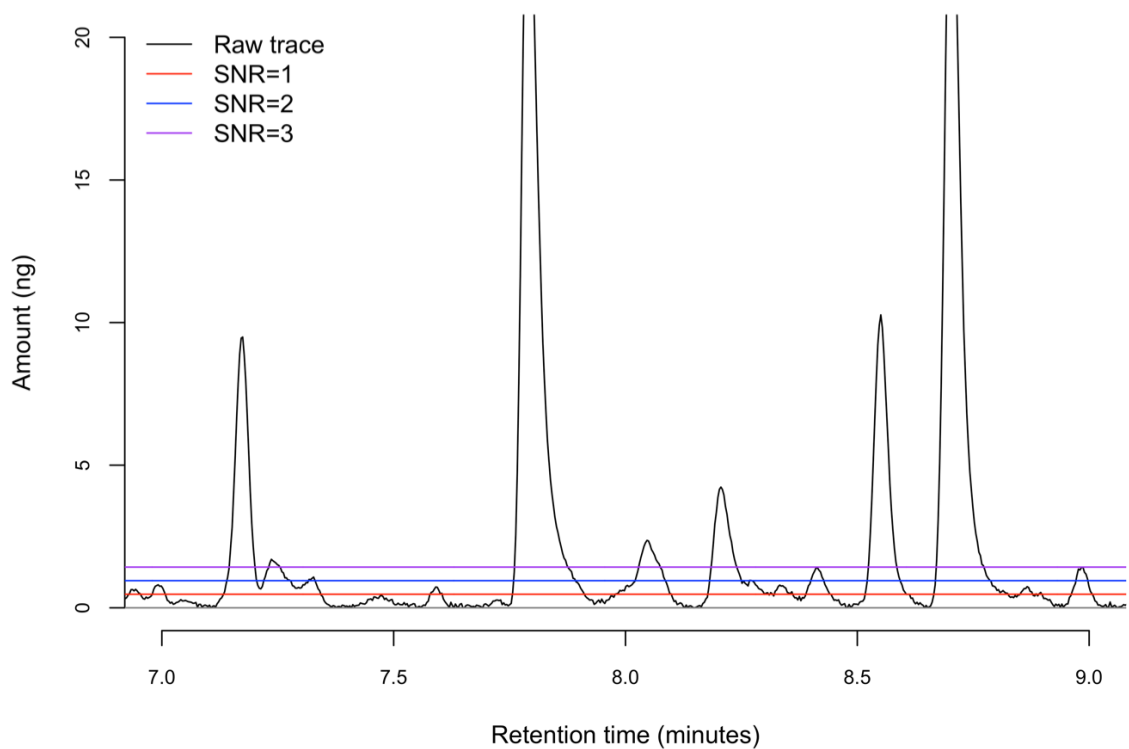


Figure 4-14. An example trace with three levels of increasing SNR (code above).

viii. Detect peaks

Peaks are then detected using the pre-determined SNR. In Figure 4-15 peaks are detected with the same SNR visualised in Figure 4-14.

```

peaks_HWS_1_SNR_10 <- detectPeaks(alSpectraBaseline_1, SNR=1,
halfWindowSize=10)
peaks_HWS_2_SNR_10 <- detectPeaks(alSpectraBaseline_1, SNR=2,
halfWindowSize=10)
peaks_HWS_3_SNR_10 <- detectPeaks(alSpectraBaseline_1, SNR=3,
halfWindowSize=10)
    
```

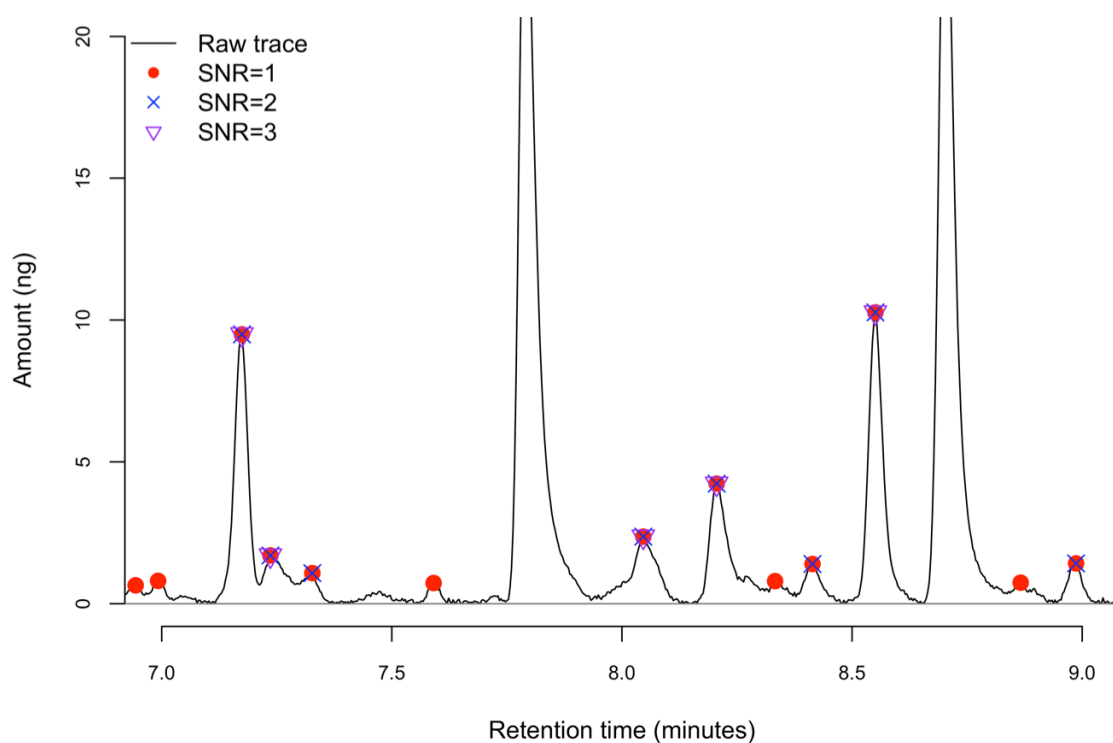


Figure 4-15. As in Figure 4-14, with the peaks detected using the variable SNR as visualised above.

Chapter 4: Method development for analysis of GC data

ix. Bin peaks

The peaks of the different spectra are binned. When the 'strict' method is used, bins never contain more than one peak from the same sample, while the 'relaxed' method can bin multiple peaks from the same sample. Some flexibility in the binning process is governed by the tolerance with which they are binned (the maximal relative deviation of a peak position to be considered as identical). An example of peak binning is given in Figure 4-16.

```
binnedpeaks <- binPeaks(peaks_HWS_2_SNR_10, method=c("strict"), tolerance=0.002)
```

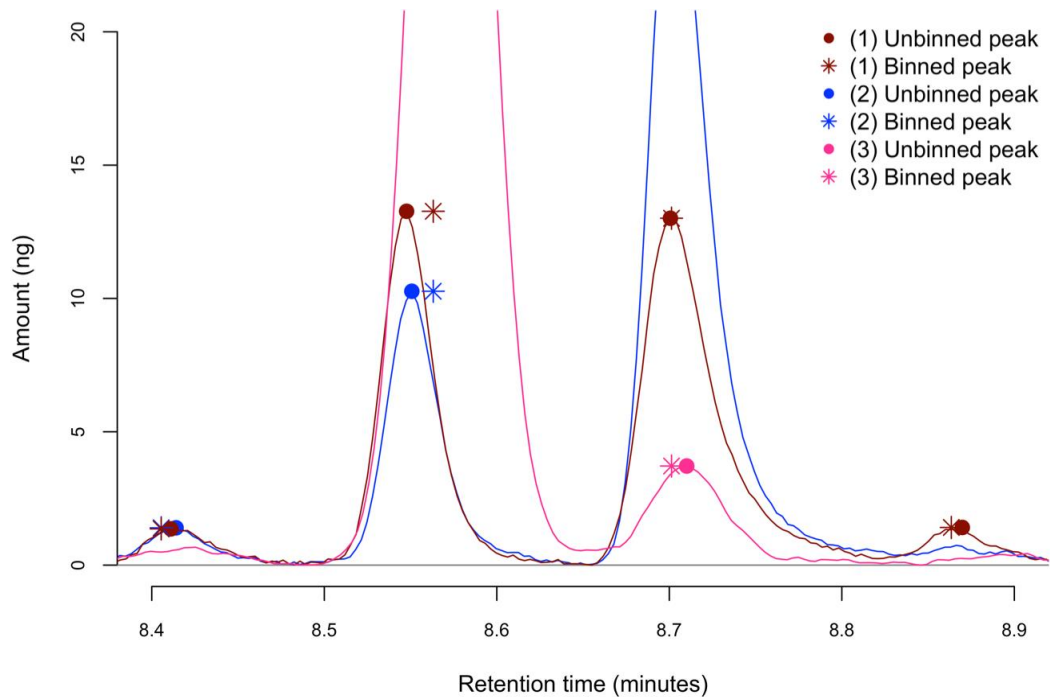


Figure 4-16. Here three traces are overlaid, each with peaks marked by dots of the appropriate colour. The stars show binned peaks, with the middle peaks demonstrating that MALDIquant recognised that traces have the same peak here, and therefore the stars are aligned.

Chapter 4: Method development for analysis of GC data

- x. Export matrix of peaks

The matrix of peak data is composed of retention time, peak height and peak number:

```
IM<-intensityMatrix(binnedpeaks)
output<-data.frame(x=attr(IM, 'mass'), y=t(IM))
output[is.na(output)]<-0

write.csv(output, 'H:/ZonMW/"location"/peaks_MALDIcommands.csv',
row.names=FALSE)
```

4.8.1 Appendix references

- Bromba, M.U.A., Ziegler, H., 1981. Application hints for Savitzky-Golay digital smoothing filters. *Anal. Chem.* 53, 1583–1586. doi:10.1021/ac00234a011
- Gibb, S., 2014. MALDIquant : Quantitative Analysis of Mass Spectrometry Data.
- Savitzky, A., Golay, M.J.E., 1964. Smoothing and Differentiation of Data by Simplified Least Squares Procedures. *Anal. Chem.* 36, 1627–1639. doi:10.1021/ac60214a047

4.9 Appendix: tRI- vs. MALDIquant-generated peak amounts

The amount of eight infection-associated compounds present, according to the 'traditional' retention index (tRI) and MALDIquant calculation methods, was compared for each sample. The tRI method estimates amount from peak area, while the MALDIquant method estimates amount from peak height. While area is the preferred method, this is not possible in MALDIquant and so peak height was used as a proxy.

There was no significant difference between the amounts calculated by either method for five of the eight compounds: heptanal, ($T = -1.10$, 334 DF, $P = 0.270$); RI 965 ($T = 0.23$, 353 DF, $P=0.821$); octanal, ($T = -0.11$, 354 DF, $P=0.912$); nonanal ($T = 0.54$, 354 DF, $P=0.591$); (*E*)-2-decenal, ($T = 1.02$, 354 DF, $P=0.310$). However, there was a significant difference in the amounts calculated by the two methods for: hexanal, ($T = -2.60$, 305 DF, $P=0.010$); 2-octanone ($T = -2.78$, 309 DF, $P=0.006$); and (*E*)-2-octenal ($T = 2.19$, 352 DF, $P=0.029$). Amounts are given in the figures below.

Hexanal (RI 774)

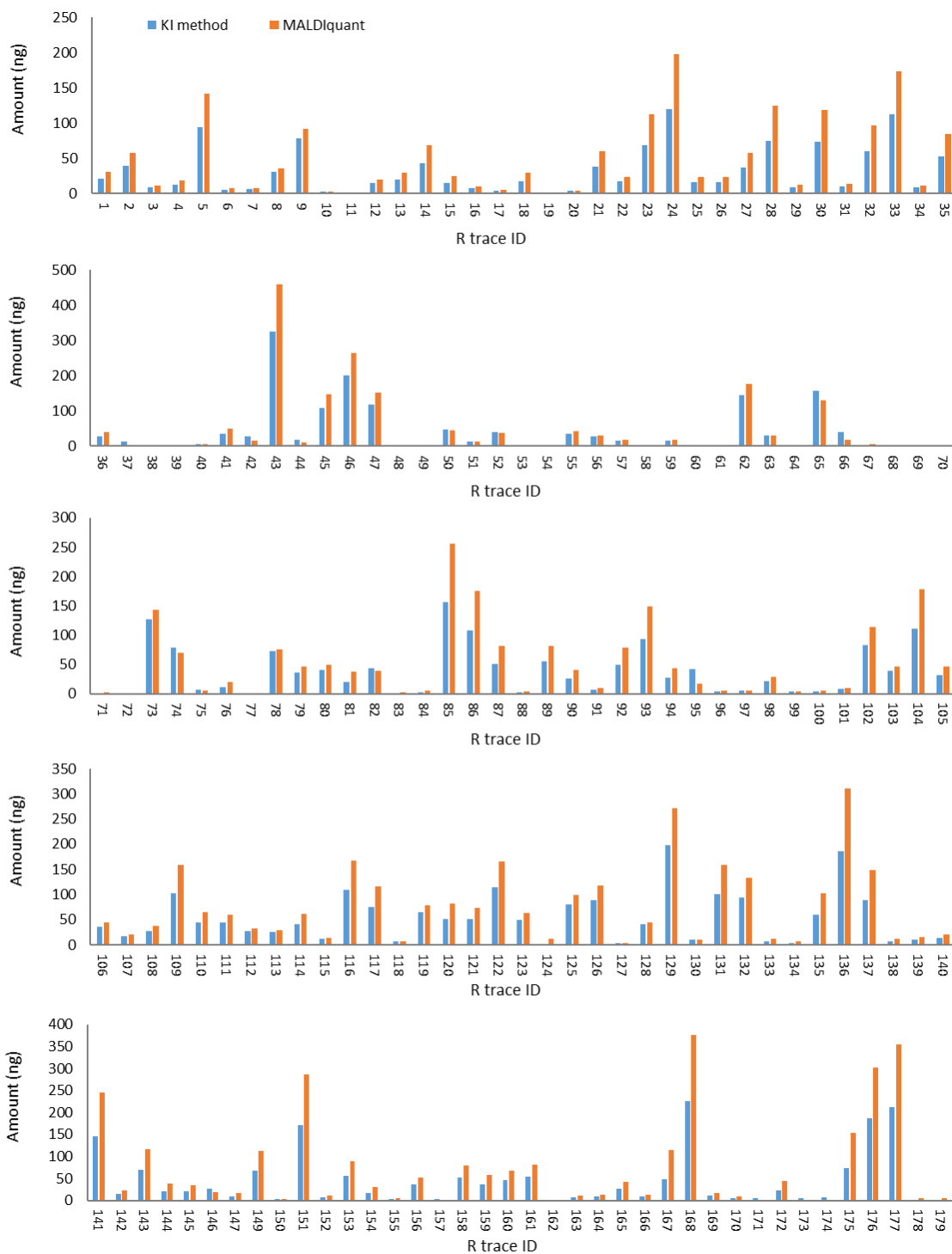


Figure 4-17. Comparing the amount of hexanal per sample, as calculated by either MALDIquant or by the traditional retention index method (tRI). MALDIquant calculates amount based on peak height, and the tRI method based on peak area.

Heptanal (RI 880)

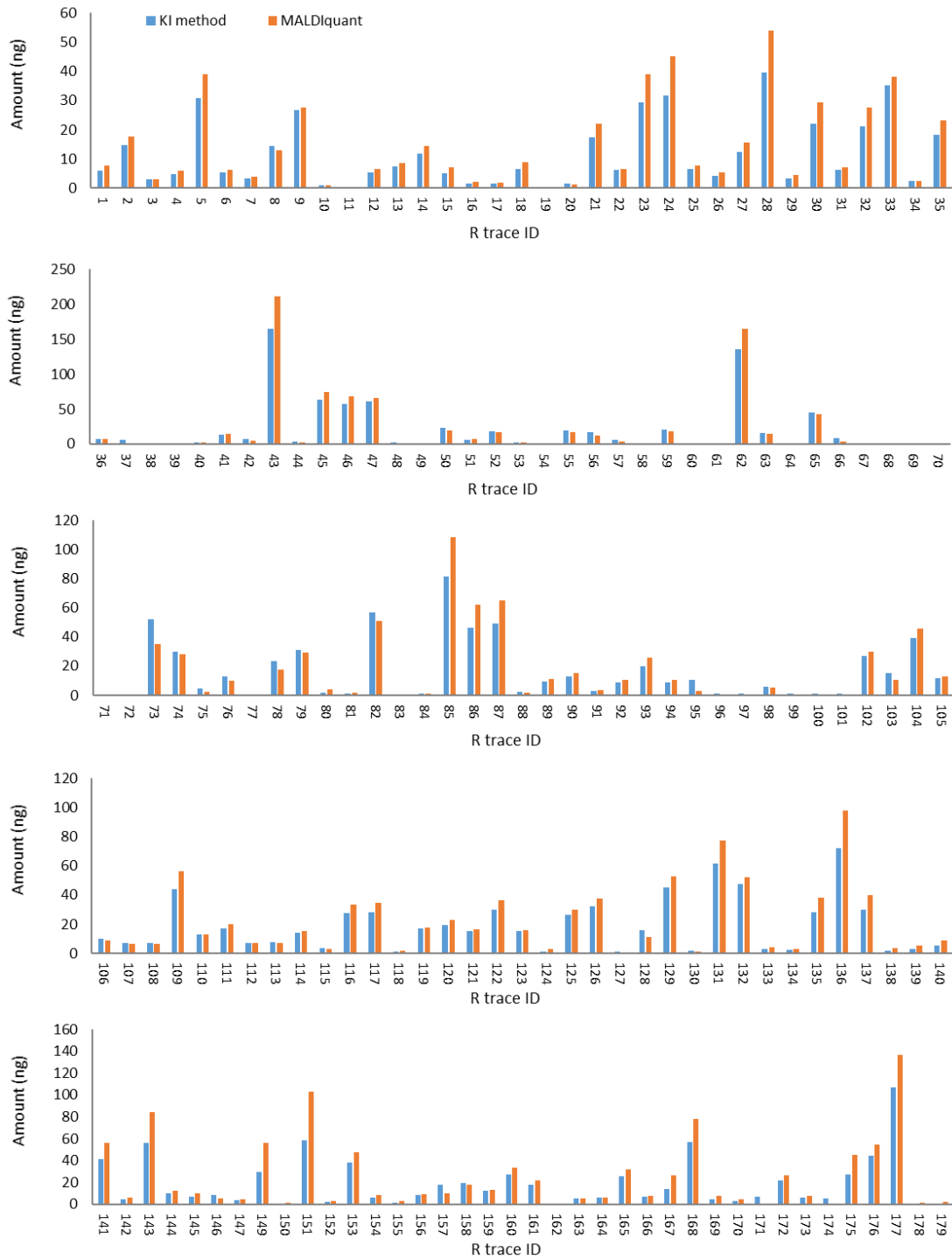


Figure 4-18. Comparing the amount of heptanal per sample, as calculated by either MALDIquant or by the traditional retention index method (tRI). MALDIquant calculates amount based on peak height, and the tRI method based on peak area.

RI 965 (co-eluting 6-methyl-5-hepten-2-one and 1-octen-3-ol)

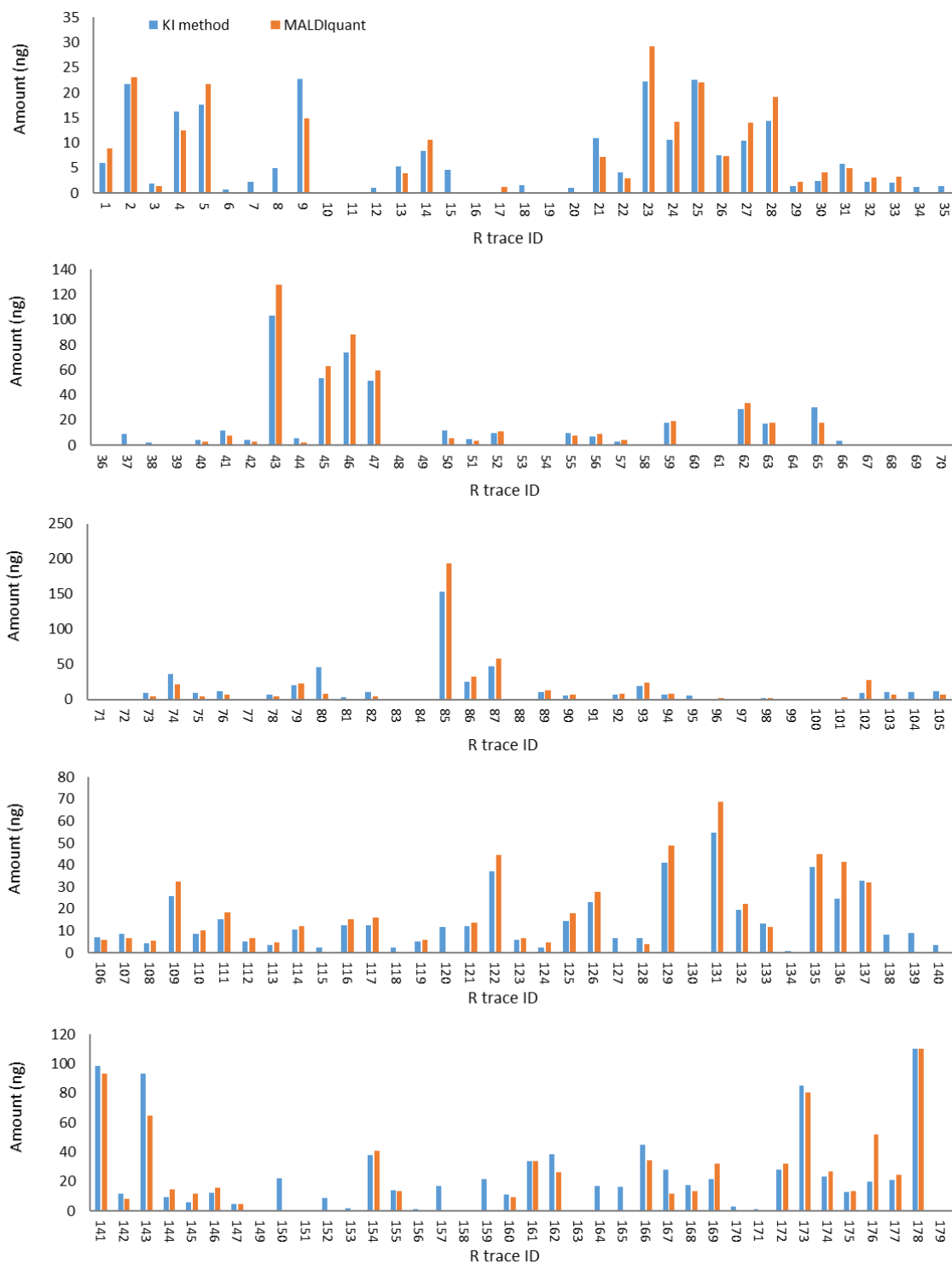


Figure 4-19. Comparing the amount of RI 965 per sample, as calculated by either MALDIquant or by the traditional retention index method (tRI). MALDIquant calculates amount based on peak height, and the tRI method based on peak area.

2-Octanone (RI 971)

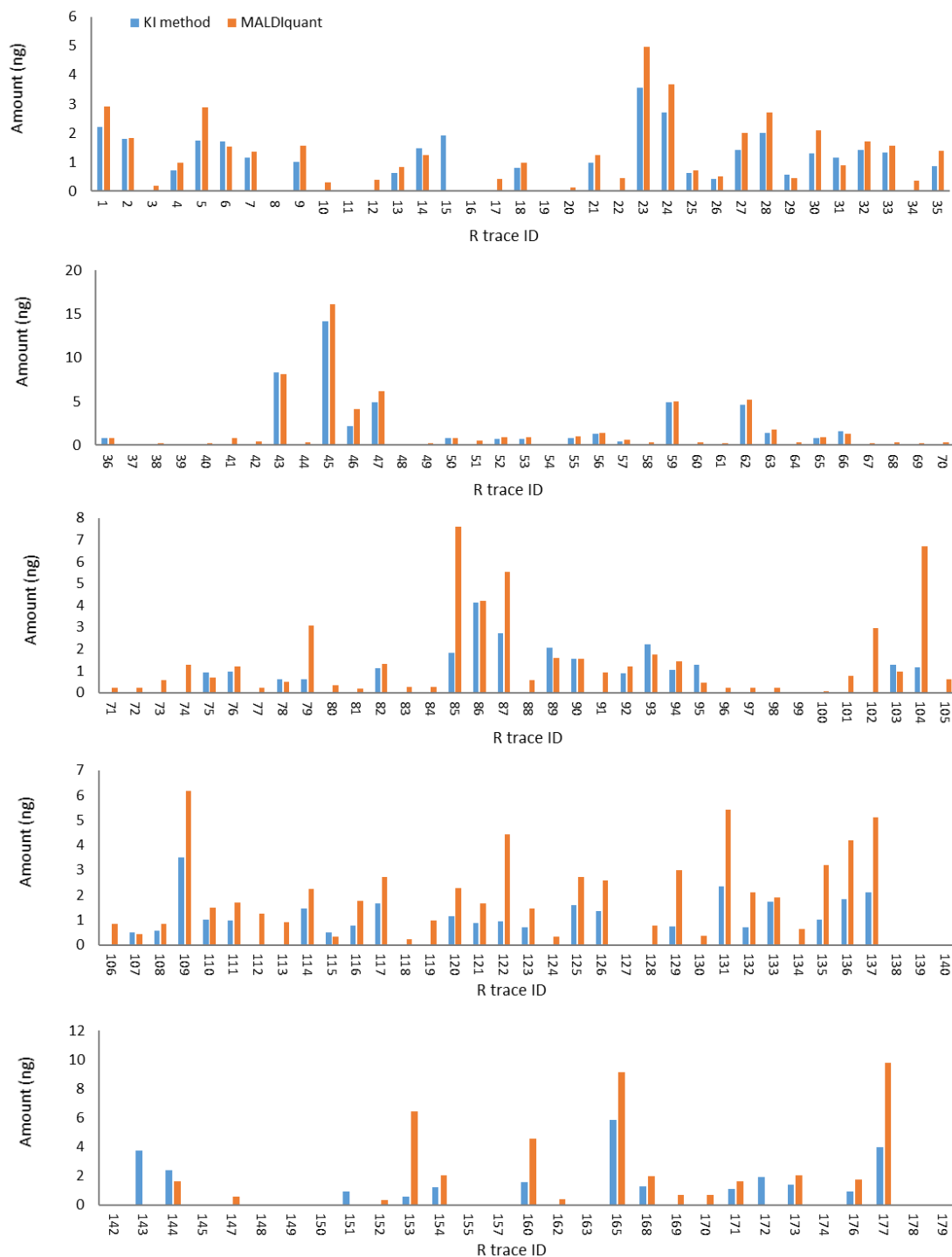


Figure 4-20. Comparing the amount of 2-octanone per sample, as calculated by either MALDIquant or by the traditional retention index method (tRI). MALDIquant calculates amount based on peak height, and the tRI method based on peak area.

Octanal (RI 982)

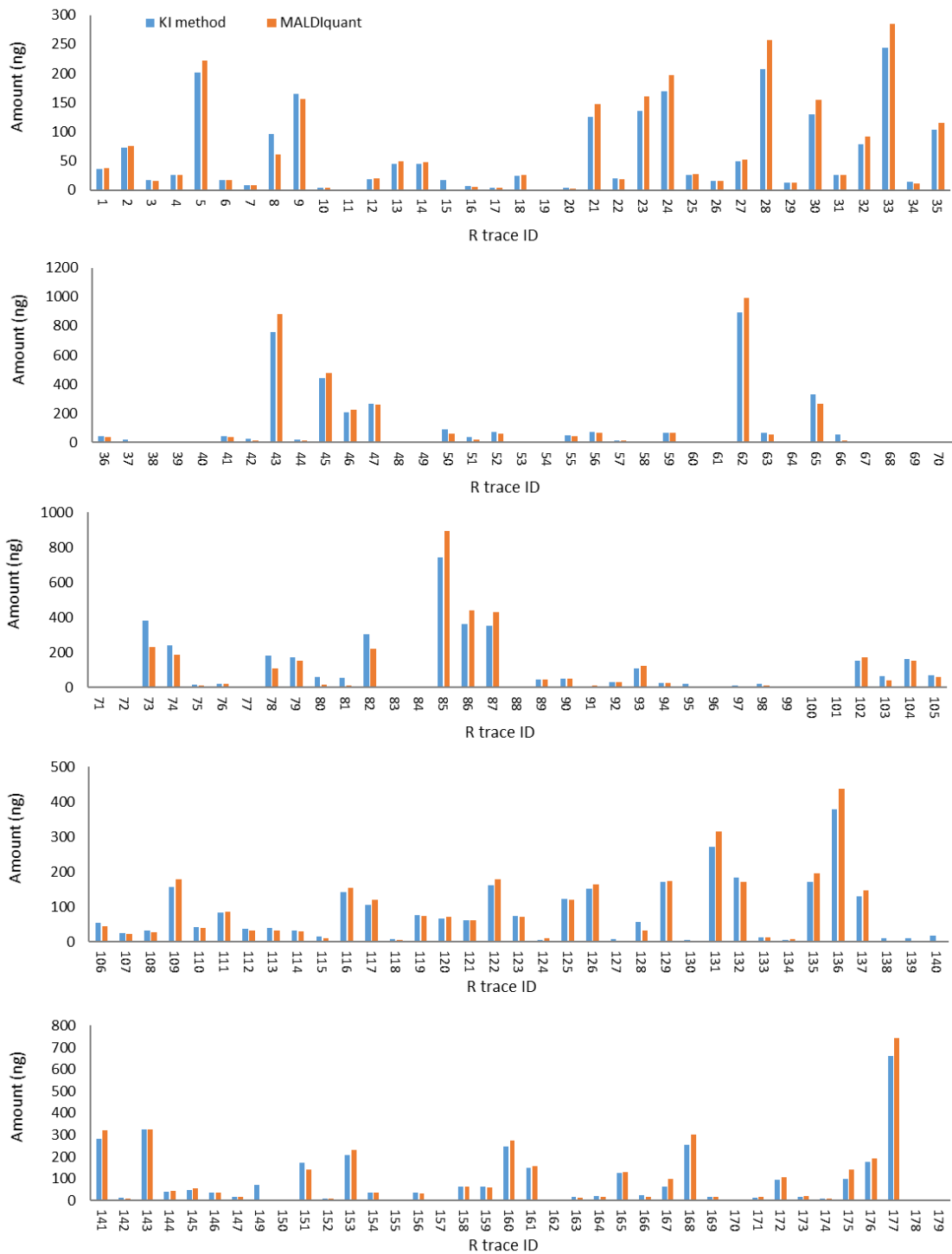


Figure 4-21. Comparing the amount of octanal per sample, as calculated by either MALDIquant or by the traditional retention index method (tRI). MALDIquant calculates amount based on peak height, and the tRI method based on peak area.

(E)-2-Octenal (RI 1035)

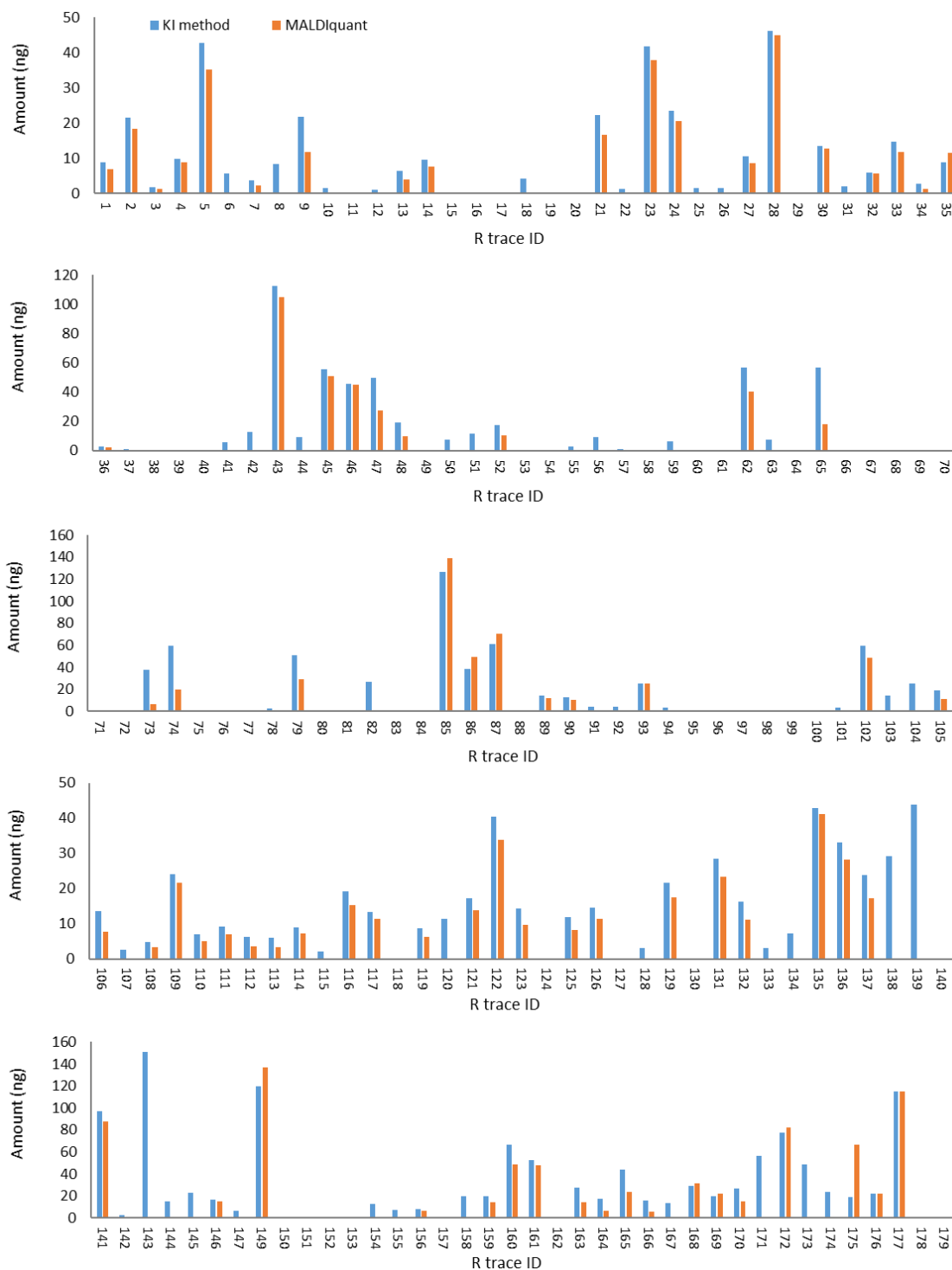


Figure 4-22. Comparing the amount of (E)-2-octenal per sample, as calculated by either MALDIquant or by the traditional retention index method (tRI). MALDIquant calculates amount based on peak height, and the tRI method based on peak area.

Nonanal (RI 1084)

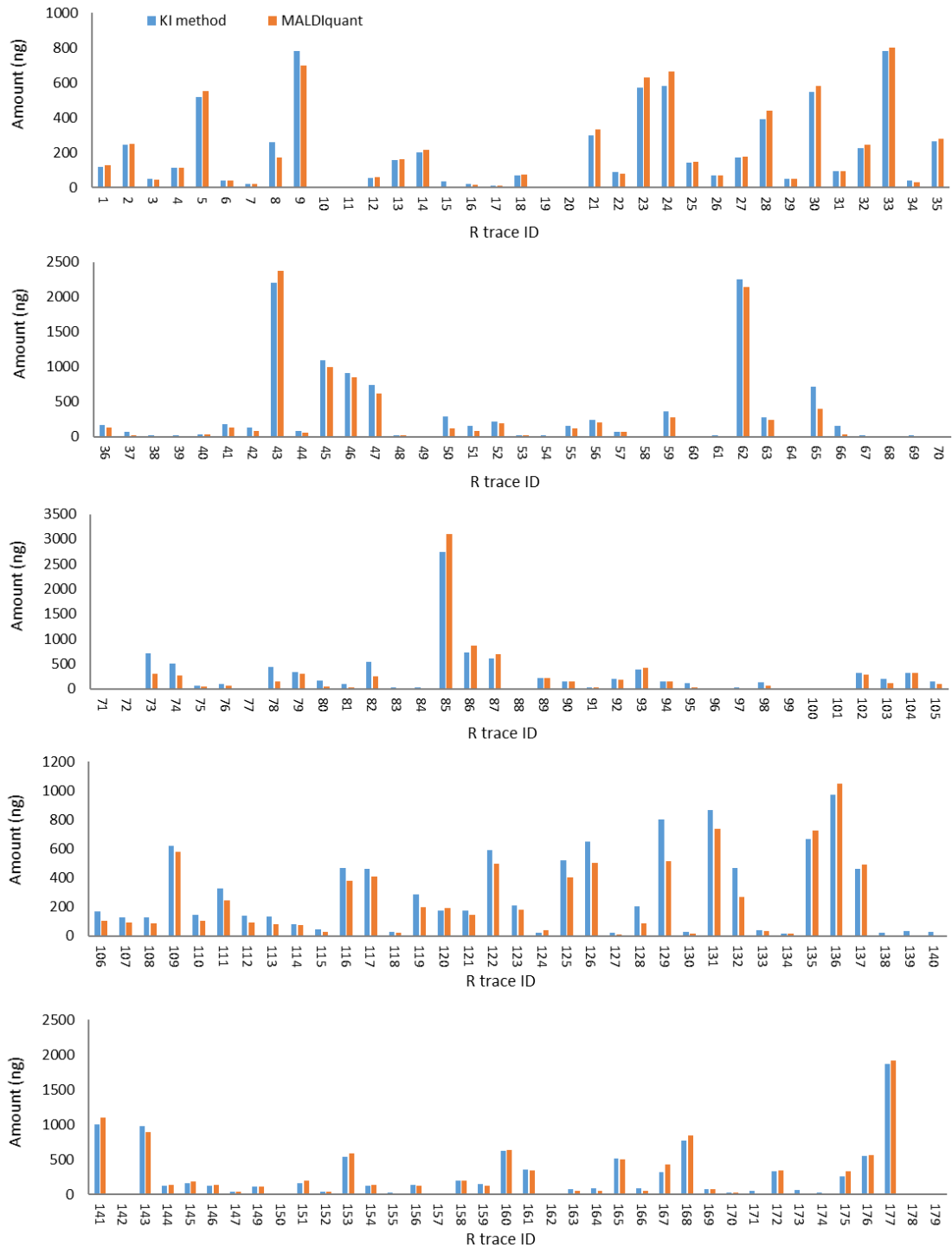


Figure 4-23. Comparing the amount of nonanal per sample, as calculated by either MALDIquant or by the traditional retention index method (tRI). MALDIquant calculates amount based on peak height, and the tRI method based on peak area.

(E)-2-Decenal (RI 1240)

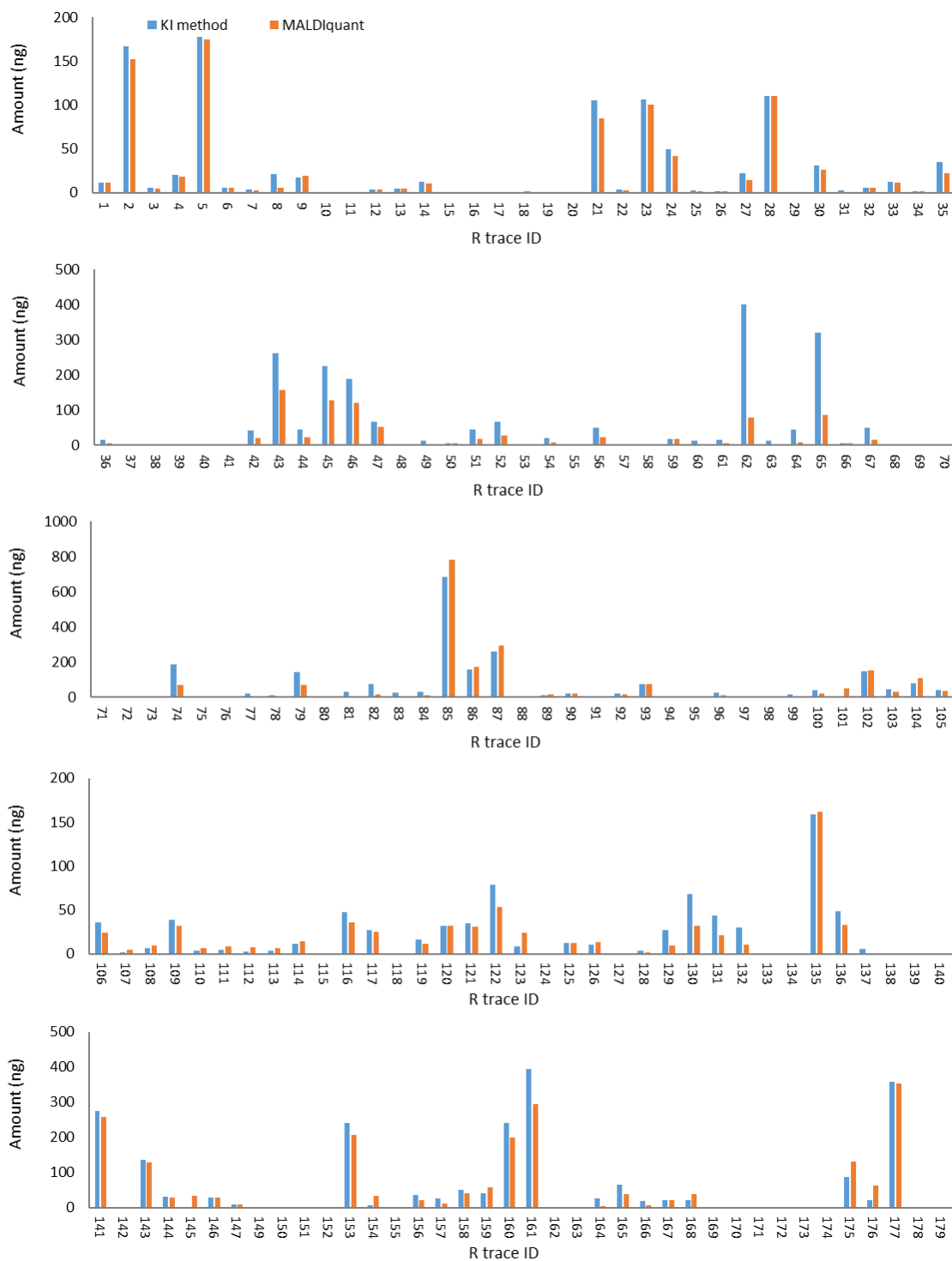


Figure 4-24. Comparing the amount of (E)-2-decenal per sample, as calculated by either MALDIquant or by the traditional retention index method (tRI). MALDIquant calculates amount based on peak height, and the tRI method based on peak area.

5 Odour profile analysis of children naturally infected with *Plasmodium* species

5.1 Introduction

In chapter 2, the odour profile of individuals who had been experimentally-infected (EI) with *Plasmodium falciparum* was compared before, during and after infection. Some of the chemical components of skin odour differed between samples from parasitologically positive and negative people. In the EI work, individuals were sampled for odour shortly after parasites emerged from the liver, in the early stages of infection (acute phase). This chapter describes the analysis of odour samples from asymptomatic malarious children in an endemic region, relative to parasite-free children. In this setting, individuals are more likely to harbour persistent, chronic infections.

It is preferable to investigate any parameters of parasite transmission in the natural setting. This is because laboratory studies do not always fully represent the complexities of the natural environment and, therefore, true biological phenomena may not be described. Field studies (those in the natural setting), however, are more difficult to implement than laboratory-based investigations. This is due to the logistical difficulties of working in the field setting, and because sources of variability are more difficult to control for in that situation. There are often large discrepancies, e.g. infection-exposure, between populations tested in experimental infections (EI) (also known as ‘controlled human malaria infections’ chapter 2) and populations in malaria-endemic regions. Also, and importantly, during experimental infections parasite density is never allowed to increase beyond a certain threshold, for safety reasons. Experimental infection studies therefore by nature investigate early stages of malaria infection, the acute phase. This is particularly pertinent to the current question, where evidence from experimental infections in animal malaria models has suggested that profound changes in attractiveness (that we hypothesise are triggered by changes in odour profile) occur later, during the chronic phase of infection (Cornet et al., 2012; De Moraes et al., 2014). It is often hypothesised that these infection-induced changes are associated with the presence of gametocytes, which in most species, markedly increase during the chronic phase of malaria infection relative to the acute phase. It has also been suggested that the occurrence of such changes during the chronic phase of infection reflects a time lag necessary to assimilate the underlying phenotype, or, that antagonistic effects operating during the acute phase (e.g. repellence induced by low haematocrit bloodmeal) diminish during the chronic phase (Cornet et al., 2012). While we

observed changes in odour profile in the early acute phase in our experimental infections (chapter 2), entirely different changes may be observed in the odour profile of naturally-infected individuals in the endemic setting.

Parasite manipulation (i.e. a parasite-induced alteration of host phenotype that has fitness benefits to the parasite) should be distinguished from differences in pathology between infected and uninfected individuals, which are coincidentally beneficial to the parasite (Poulin, 2010). However, it has been argued that if such 'incidental' changes do influence how efficiently vectors can locate hosts, this would strongly select for parasites that can manipulate these traits (Cornet et al., 2012). Hence, parasite manipulation would rapidly evolve. Early, acute phase, and chronic malaria infections are characterised by distinct immunological responses (Cowman et al., 2016), which will manifest in physiological and pathological changes. Irrespective of changes in attractiveness arising from either parasite manipulation, or from other infection-associated changes, there is good reason to test the odour profile of *Plasmodium*-infected individuals in an endemic setting, where most asymptomatic infections are of a chronic nature.

It is advantageous to test the odour profile of malarious children, rather than adults, which again could not be achieved in EI, for ethical reasons. First, it is thought that in adult females, the monthly fluctuations in hormone balance associated with the menstrual cycle can influence both odour profile (Singh and Bronstad, 2001) and attractiveness to biting insects (Gilbert et al., 1966). For this reason, attractiveness studies generally only recruit either adult males or post-menopausal women. In the EI study (chapter 2), testing was limited to those individuals who were recruited to the vaccination trial, including both men and women. There was a relatively equal sex ratio among those who became parasitologically positive, but it is still possible that the sex of participants influenced the findings. Secondly, in areas of high transmission intensity, children are consistently more likely to be infectious to mosquitoes, because they more often harbour higher gametocyte densities (Bousema and Drakeley, 2011). It is now thought that this does not necessarily equate to a disproportionately greater contribution to malaria transmission, as after adjustment for other factors relevant to transmission including body size and relative exposure, the contribution of the adult population may be greater (Bousema and Drakeley, 2011; Stone et al., 2015). However, *Plasmodium* parasite-induced changes in attractiveness should be tested at the level of the individual, and findings can subsequently be considered in the context of other factors important to transmission. Therefore, those individuals with high transmission potential are of particular interest to this study.

Until recently, only two published studies had tested for changes in attractiveness after *Plasmodium* infection in humans (Batista et al., 2014; Lacroix et al., 2005). While presenting intriguing findings, both studies were hampered by small sample sizes and insensitive parasitological diagnostics. Neither investigated any mechanistic basis for the observed changes in attractiveness. However, data from this project has recently been published by our collaborators confirming previous findings, demonstrating an approximately two-fold increase in attractiveness of gametocytaemic individuals (Busula et al., 2017). We hypothesised that changes in the odour profile of infected individuals underlie changes in attractiveness, as such changes have been documented to govern innate variation in attractiveness (Logan et al. 2008). One study investigated the odour profile following *Plasmodium* infection in a murine model system, and found that significant changes occurred upon infection (De Moraes et al., 2014).

5.2 Aim and objectives

To address this gap, the volatile odour profile of naturally *Plasmodium*-infected children was examined. The aim of this chapter was to compare both quantitatively and qualitatively the volatile compounds emitted from the feet of *Plasmodium*-infected individuals in a malaria-endemic setting, Western Kenya. The analysis of parasitological samples from these children, and details concerning the chemical analysis of odour samples, are described in chapters 2 and 3 respectively.

This aim was achieved through the following objectives:

1. To collect odour samples from the feet of children in Kenya using air entrainment, and analyse these using gas chromatography and GC-mass spectrometry
2. To determine appropriate parasitological categories for the odour profile samples, according to the diagnostic information (as analysed and described in chapter 3) from those individuals from whom the odour samples were taken
3. To test for significant differences in the production of compounds thought to be associated with *Plasmodium* infection, according to the parasitological categories determined in (2)

5.3 Methods

Odour samples were collected using air entrainment techniques from the feet of five- to twelve-year old children, between January and July 2014. The collection protocol intended to sample from all recruited participants three times, once 'during' infection, and twice following treatment with antimalarials. Participants were recruited from four schools (Obambo, Alero, Kamsama and Powo) local to the Thomas Odhiambo Campus of *icipe* in Western Kenya (000251S, 34°131E), all in Suba District, Mbita sub-county, Homabay County.

5.3.1 Study site

The four schools were all were less than 10 km inland from Mbita Point Township, with community livelihoods reliant on fishing, small-scale trading or subsistence farming. The dominant ethnic group is Luo. Access to healthcare facilities is limited and dependent on availability of roads, with one school only being accessible by dirt track. On the local island Rusinga in Lake Victoria, the overall prevalence of malaria was recently estimated to be 10.9 % (Olanga et al., 2015), but other recent studies in the area have found greater parasite prevalence, e.g. 23.7% in a baseline survey also on Rusinga (Homan et al., 2016a), and 40 % *P. falciparum* prevalence predicated in areas around Lake Victoria (Noor et al., 2009). Transmission peaks late in the rainy season, and parasite prevalence in Rusinga at this time was estimated to be 30 % across the whole population (Homan et al., 2016b). *Anopheles funestus* and *An. gambiae* have historically been the primary malaria vectors (Mbogo et al., 2003). However, the use of LLINs and IRS for malaria control in Western Kenya has led to a shift in vector population structure, from endophilic species to the more exophilic and opportunistic *An. arabiensis* (Bayoh et al., 2010; Mutuku et al., 2011).

5.3.2 Study protocol

Schools were recruited and sampling conducted serially, in the following order: Obambo, Alero, Kamsama and Powo. A preliminary visit was made to each school to allow full explanation of the study aims and procedures, discussion with school teachers and/or the school council, and distribution of consent forms in English and Luo. On day zero, twenty children for whom the parent or guardian had given full consent were tested for their malaria status by rapid diagnostic test (RDT), and thick and thin blood films were made. Whole blood samples (50 µL) were stored in RNA protect (250 µL, Qiagen, Cat No: 76526) for future molecular analysis. Auxiliary

(tympanic) temperature, weight and haemoglobin (Hb) levels were also recorded. Any child who met the exclusion criteria of a temperature of greater than 37.5 °C, and was RDT positive, was immediately treated with artemether lumefantrine (AL, weight-dosed artemether-lumefantrine containing 20 mg artemether/120 mg lumefantrine per tablet (Coartem-D™; Novartis, Basel, Switzerland) (WHO 2015)). Overnight, blood films were read and three children were selected for odour profile sampling according to malaria status, with the intention to sample from one child with asexual malaria parasites, one with gametocytes, and one with no parasites. The following day (day one), odour profile sampling was conducted by air entrainment, after which all malaria-positive individuals were treated with AL. Days zero and one constituted round one (R1), and the same procedures were conducted at days seven and eight (R2), and 21 and 22 (R3), with intention to sample from the same children at each visit (Figure 5-1). All sampling was conducted between January and June 2014, encompassing the long rainy season (March to August).

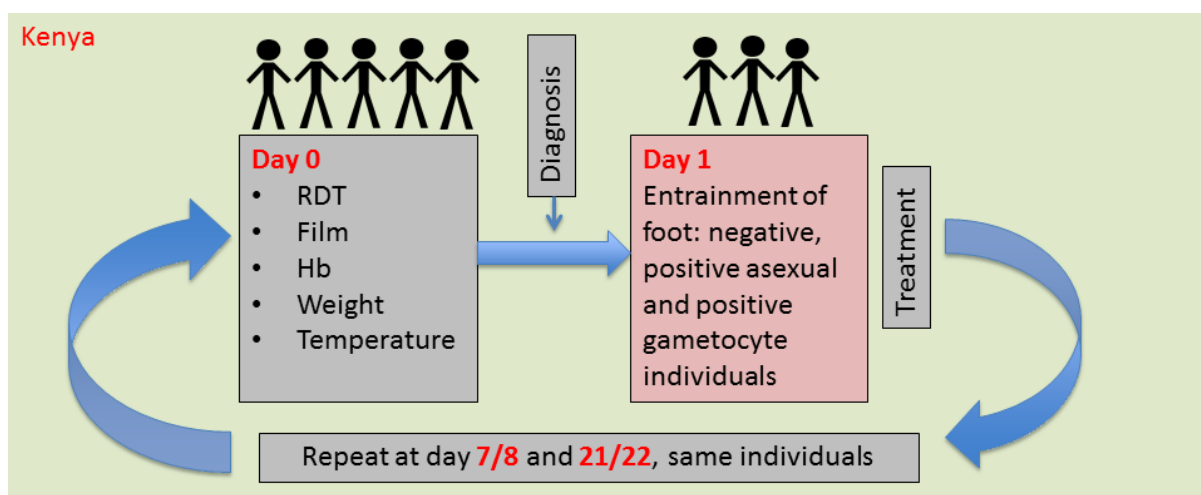


Figure 5-1. Protocol for air entrainment (odour profile sampling) in the Kenya population. Children were recruited for odour sampling in groups of three to represent uninfected, infected with asexual parasites, and gametocyte carriers, if parasite prevalence allowed. Following malaria diagnosis and sampling, individuals with malaria parasites were treated, and the same cohort re-sampled on days 8 and 22.

5.3.3 Ethics

Participants were recruited to the study after obtaining signed consent. The study protocol (NON SSC 389) was approved by the Scientific and Ethical Review Committee of the Kenya Medical Research Institute (KEMRI) (KEMRI/RES/7/3/1). Subsequent chemical analyses of the odour profiles were conducted at the London School of Hygiene & Tropical Medicine (LSHTM) under the ethics reference 8510.

5.3.4 Infection status: parasitology

Participants were tested in the field for their malaria status by point-of-care methods. These measures were used to inform odour profile collection from children of appropriate parasite status. Several molecular-based diagnostic measures were employed retrospectively to fully categorise the infection status of participants. From R3 sampling in the first school, Obambo, and for the remaining sampling period, used RDTs (uRDT) were air dried and stored in sealed plastic bags containing the desiccant silica gel (silicon dioxide). Later, the blood stored on the nitrocellulose strip in the uRDT was used as a DNA template for quantitative polymerase chain reaction (qPCR) to obtain an estimated parasitaemia. As uRDT are not functionally designed for DNA storage, dried blood spots of approximately 5 mm were stored in addition, on Whatman No. 3 filter paper (Whatman, Maidstone, United Kingdom) (wDBS), for the last two schools, for use in the same qPCR for comparative purposes. Both uRDT and wDBS samples were examined for three *Plasmodium* species (*P. falciparum*, *P. malariae* and *P. ovale*) using a nested PCR (Snounou et al., 1993). Finally, the whole blood samples were used as a template for two other qPCR reactions; QT-NASBA qPCR for quantifying *P. falciparum* gametocytes (Schneider et al., 2006), and an 18S-based qPCR for quantifying *P. falciparum* parasitaemia (Hermsen et al., 2001). The parasitological procedures and results are described in detail elsewhere (chapter 3).

5.3.5 Odour profile sampling

Air entrainment procedures were as described for the experimental infection study (chapter 2/2.3.7), with the following modifications: sampling was conducted in a tent, with rugs on the ground to maximise comfort for the participants, Porapak sampling was conducted at approximately 500 mL/min, both filters (Porapak and Tenax) were temporarily stored individually in clean glass storage tubes sealed with a glass stopper and PTFE tape, then placed into a cool box until back at the laboratory, and sealed ampoules containing filters were stored at -20 °C until being shipped to London for chemical analysis. The majority of odour sampling was conducted by collaborators at *icipe*.

5.3.6 Chemical analysis of odour profile: gas chromatography

Chemical analysis of the Porapak filters was conducted at LSHTM and Rothamsted Research, Harpenden (RR). Chemical analysis of the Tenax filters was conducted at RR, and subsequent data analysis performed at the University of Wageningen (The Netherlands) (data not shown).

As for the EI study cohorts (chapter 2), three gas chromatography (GC) machines were used for analysis of the Porapak samples.

5.3.7 Analysis of gas chromatography traces

Due to difficulties in trace alignment between Porapak samples run with large time intervals in between, and on different GC machines, two methods of analysis were used. As described in chapter 2, the traditional method involves calculating a 'retention index' (RI) as a proxy for peak identification, and an estimated peak amount, both by comparison to a reference trace of alkanes. This method requires manual comparison of printed traces to ensure between-sample allocation of the same RI value to the same peaks, as this can vary by several integers according to chromatography conditions and peak shape (discussed in chapter 4). Here, another method of peak analysis was developed, using the R programme MALDIquant to visualize and overlay traces. Like the RI method, steps were undertaken to calibrate peak amount to the reference alkane series.

Traditional retention index (tRI) method

Here, methods were as described in the EI cohort (Integration of GC traces, chapter 2), other than: a lower sensitivity area reject (equivalent to 0.01 ng), and the 'baseline at valleys' setting was used. The difficulties encountered during this process, and the steps taken to circumvent them and subsequently identify the compounds of interest, are described in detail in chapter 4. Ultimately, statistical analysis of compounds of interest (COI) (those thought to have a possible association with *Plasmodium* infection) was performed using the amounts and provisional identifications generated using the tRI method.

MALDIquant method

Traces (samples) were analysed using the R package MALDIquant (R version 3.3.0 "Supposedly Educational"(C) 2016, The R Foundation for Statistical Computing). In brief, raw x,y co-ordinates for traces were exported from the GC software (Agilent ChemStation C.01.04). The y co-ordinates (peak height) were then calibrated to the alkane standards to allow for instrument-specific variation in detector sensitivity, and then adjusted by the precise volume of extract per sample, such that peak height represented the amount of that compound entrained during the

100-minute sampling process. For each trace, a standardised baseline was removed, following an iterative process that determined a cut-off appropriate to all traces. Traces were then visually comparable, allowing inspection for consistent differences between traces from individuals of different parasitological status, with the caveat that samples could only be examined in groups with no major shift in retention time (e.g. following a change in length of column), as x-axis calibration was unfeasible (full details, chapter 4).

5.3.8 Generating compounds of interest and investigating parasitological grouping

Due to peak alignment issues, samples were divided for analysis into several smaller datasets where the peaks were well-aligned (generation of these datasets is described in chapter 4). To determine COI, odour profile datasets (i.e. all odour profile samples including controls) were analysed according to several iterations of parasitological categorisation. Individuals from whom odour samples had been collected were categorised according to their *Plasmodium* infection status. Importantly, each set of parasitological categories was derived from a biological principle, with the following factors taken into consideration: the presence and density of different parasite stages including sexual forms, published behavioural data regarding the attractiveness of *Plasmodium*-infected individuals, behavioural data from collaborators on this project regarding the same and the parasitological status of those participants, and published data concerning the infectivity of individuals to mosquitoes at differing parasitaemias. The presence of *Plasmodium* species other than *falciparum* was ultimately disregarded in this analysis, due to time constraints and small sample sizes. Full details of the categories that were used for exploratory analysis of the COI, and the final parasitological categories used for univariate analysis, are described in appendix 5.8.

Initially, for each version of parasitological categorisation, data were examined using canonical variates analysis (CVA). Good separation of groups was achieved when high parasite density thresholds for parasitological positivity were used (level four categories, appendix 5.8). From these CVA results, compounds with the greatest influence on the separation of groups were determined, and these became COI (appendix 5.9). In an exploratory analysis, these COI were visually examined, per dataset, in MALDIquant. By colouring traces according to parasitological categories (initially, 'level four' categories, see appendix 5.8), candidate compounds could readily be examined for an association with infection (Figure 5-2). This led to further exploration of datasets in MALDIquant: for each dataset, all traces were visually examined for peaks that signified infection (as in Figure 5-2), according to level five to 10 categories (appendix 5.8).

Therefore, two subsets of COI were generated; one derived from the CVA results (level four parasitological categorisation), and the other from peaks that were visually interesting in MALDIquant (parasitological categorisation levels five to 10).

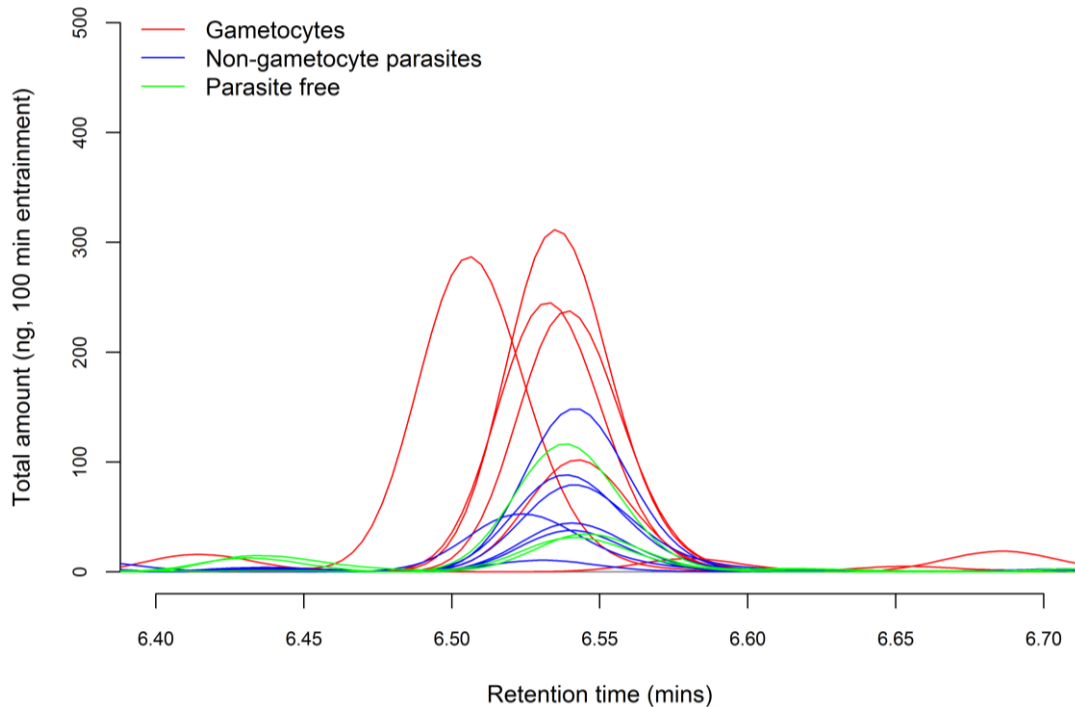


Figure 5-2. Hexanal peak in raw GC output. Individual lines represent odour profile samples, here coloured according to the parasitological status of the individual from whom the odour sample was taken. Note that slight misalignment of peaks does not prevent patterns from being observed, and the true identify of misaligned peaks (e.g. the left-aligned red trace in this image) could be confirmed by the peak retention index.

For both subsets of COI (CVA- and MALDIquant-generated), differences in production according to parasitological category were then examined by comparing group means (and error bars). Peak position for all COI was checked in every sample (visual assessment and comparison of retention indices), collating the entire dataset and allowing robust analysis with maximum sample size. Compound amounts were redefined to be proportional to the total odour sample, thus allowing for temporal variation in sampling efficacy.

Additionally, compounds that had been found to be associated with *Plasmodium* infection in the EI cohorts (chapter 2) were investigated. Of the nine compounds examined (RI 1095, 972, 1193, 1222, 1300, 1362, 1392, 1416, 1509), other than 1509, no possible association with infection was observed. In all, the following COI were shortlisted for robust statistical analysis: RI 774, 797, 958, 1004, 1024, 1400 (CVA-derived); 899, 931, 961, 965, 968, 971, 982, 1009, 1035, 1084, 1175, 1186, 1200, 1236 (MALDIquant-derived); 1509 (EI compound); 880, 1240, 1599 (both CVA-

and MALDIquant-derived). These were chosen on the premise that some differences in compound production were observed according to parasitological category ('level ten', appendix 5.8). From all shortlisted COI, 14 were selected for univariate analyses, as demonstrating evidence of separation according to parasitological categories.

5.3.9 Parasitological categorisation

The parasitological categories used in the final statistical analysis for association between compound production and *Plasmodium* infection are given below, and summarised in Table 5-1. For 'total density', 'quartile' and 'gametocyte' categories, parasite density per odour sample is shown in Figure 5-3, Figure 5-4 and Figure 5-5. For 'total density' categories, the density of gametocytes in those samples is additionally given in Figure 5-3B. For 'gametocyte' categories, total parasite densities are additionally given in Figure 5-5B.

Total density

Any sample that had detectable parasite DNA at an amount greater than a published limit of detection (LOD) for assays, i.e. 0.02 parasites/ μL (p/ μL) for 18S qPCR (Hermsen et al., 2001) and 5 p/ μL for PgMET (Beshir et al., 2010), was taken to be positive. Only samples that were negative by all measures and including at least one molecular diagnostic measure were taken to be negative. For these, RDT positivity was acceptable on an assumption of false positivity by the detection of parasite protein (i.e. histidine-rich protein 2 (HRP-2)) following clearance. All individuals in the gametocyte category were gametocyte positive by microscopy. Parasite positive samples without microscopic gametocytes were further divided into two categories, to reflect higher and lower (total) parasite density (Figure 5-3). The 'higher density' category was primarily informed by 18S qPCR, with samples harbouring more than 50 p/ μL . Where 18S qPCR data were not available PgMET qPCR data were used. Samples with fewer than 50 p/ μL by a molecular test, but microscopic parasites, were retained in the 'higher density' category, as an accepted detection threshold of microscopy is approximately 50 p/ μL , and microscopy is considered to be a 'gold standard' diagnostic tool. For five of six samples that were positive by microscopy but with no other positive diagnostic measure, films were re-read (the film was missing for the sixth). The 'lower density' category was primarily informed by 18S qPCR (0.02–50 p/ μL), but samples were included with fewer than 0.02 p/ μL by 18S qPCR yet detectable parasite DNA (LOD - 50 p/ μL) by another method. Samples with parasite densities beneath test LOD thresholds (i.e. <0.02 p/ μL by 18S qPCR and <5 p/ μL for PgMET) were excluded, as were any

samples that were negative by microscopy but with no verification by a molecular test. Two further samples were excluded: one with an extremely unusual GC trace (indicating a problem during chromatography), and another that was positive by microscopy but negative by 18S and PgMET qPCR, however, the film could not be re-read as it was missing.

Quartiles (extension of 'total density' categories)

Samples in the 'higher density' and 'lower density' categories defined above (n=81) were then subdivided into quartiles according to parasite density (Figure 5-4). As before, samples were allocated to categories according to a hierarchy of diagnostic assays: 18S qPCR > PgMET qPCR > microscopy. Where 18S qPCR result was zero but PgMET qPCR positive, the PgMET value was assumed (any detection of parasite DNA greater than the LOD being considered positive). Where 18S and/or PgMET qPCR were negative or missing, but microscopy was positive, the film was re-read and that value assumed. Two samples with low 18S qPCR parasite density, but high and corresponding PgMET and microscopy density, were allocated according to the two corresponding outcomes. One further sample was excluded as it was positive by nested end-point PCR for *P. falciparum*, but had no quantitative information available.

Gametocytes

Gametocyte carriers were divided into a 'sub-gametocyte' group (gametocytes by QT-NASBA 0.02 - 50 p/μL and no microscopic gametocytes) and 'gametocyte' group (gametocytes by QT-NASBA >50 p/μL, and/or microscopic gametocytes) (Figure 5-5). No samples in the 'asexual' group had detectable gametocytes by QT-NASBA or microscopy, with the caveat that some individuals may have harboured sub-microscopic gametocytes, as 13/48 samples had no QT-NASBA data. These were retained to maximise sample size. Negative individuals were classified as above. Exclusions were as per 'total density' categories.

Positive vs. negative categories

This was a simple comparison of *Plasmodium*-infected vs. uninfected samples. Negative individuals were categorised as above, requiring all test measures to be negative, including at least one molecular test but allowing RDT positivity. Positive samples included those with microscopic parasites or parasite DNA greater than test LOD. Exclusions were as per 'total density' categories.

Chapter 5: Odour profile analysis of children naturally infected with *Plasmodium* species

Table 5-1. Parasitological categories used for statistical analysis of compounds of interest. Asexuals=non-gametocyte stage parasites. RDT=rapid diagnostic test., p/μL=parasites per μL blood. Samples with parasite densities beneath test limit of detection thresholds were excluded from all analyses, as were any samples that were negative by microscopy but which had no verification by a molecular test.

ANALYSIS	CATEGORIES	DESCRIPTION
TOTAL DENSITY (N=117)	Higher density (n=49)	Any asexuals by microscopy, > 50 p/μL by any molecular method
	Lower density (n=32)	Between LOD (by any molecular method) and 50 p/μL, no parasites by microscopy (considered > 50 p/μL due to microscopists' LOD)
	Gametocyte (n=20)	Any gametocytes by microscopy (in reality, <i>P. falciparum</i> only)
	Negative (n=16)	Negative by all measures including at least one molecular test, other than RDT positivity allowed*
GAMETOCYTE (N=116)	Gametocyte (n=28)	Any gametocytes by microscopy (in reality, <i>P. falciparum</i> only), QT-NASBA gametocytes >50/μL
	Sub-gametocyte (n=24)	No gametocytes by microscopy, QT-NASBA gametocytes <50/μL
	Asexual (n=48)	Any asexuals by microscopy, parasites >LOD by any molecular method, no gametocytes by microscopy or QT-NASBA
	Negative (n=16)	Negative by all measures including at least one molecular test, other than RDT positivity allowed*
POSITIVE VS. NEGATIVE (N=117)	Positive (n=101)	Any parasites by microscopy, parasites >LOD by any molecular method, no distinction between different parasite stages.
	Negative (n=16)	Negative by all measures including at least one molecular test, other than RDT positivity allowed*
QUARTILES (N=116)	Low (n=21)	- 0.05-0.98 p/μL by 18S qPCR
		- average p/μL: 0.38
		- median p/μL: 0.30
	Medium-low (n=17)	- 1.61-51.05 p/μL by 18S qPCR
		- average p/μL: 16.77
		- median p/μL: 8.30
	Medium-high (n=19)	- 67.3-567.54 p/μL by 18S qPCR
		- average p/μL: 296.60
- median p/μL: 214.18		
High (n=23)	- 1129.8-946237.16 p/μL by 18S qPCR	
	- average p/μL: 102669.46	
	- median p/μL: 13304.54	
Gametocyte (n=20)	Any gametocytes by microscopy (in reality, <i>P. falciparum</i> only)	
Negative (n=16)	Negative by all measures including at least one molecular test, other than RDT positivity allowed*	

*RDT positivity was allowed on the basis that these tests can remain positive for some time following curative treatment, due to circulating HRP-2 protein.

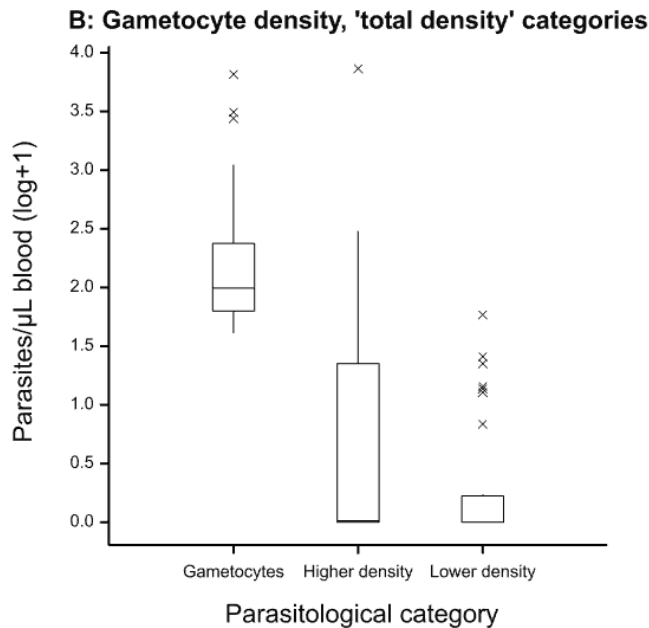
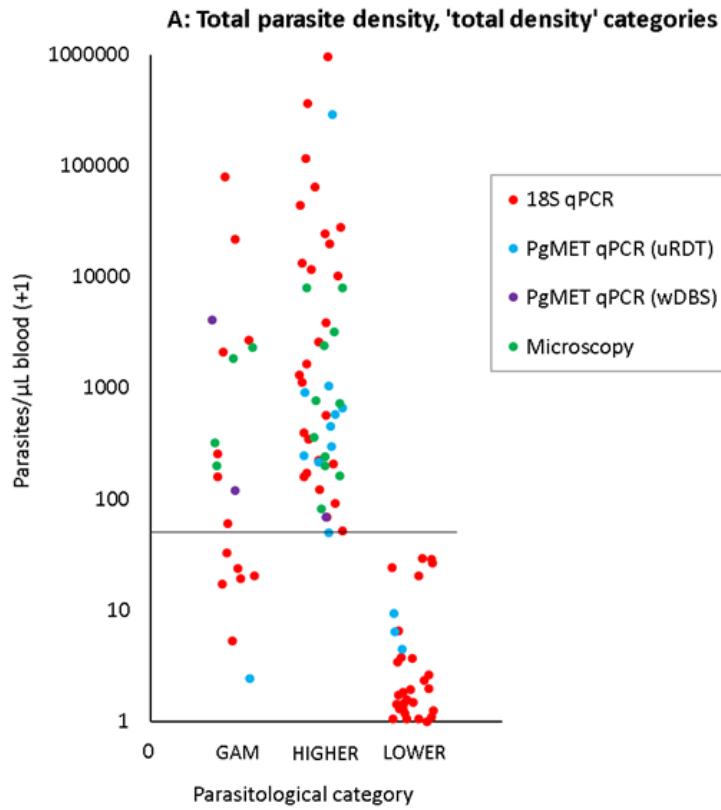


Figure 5-3. 'Total density' parasitological categorisation, showing actual parasite densities p/ μL) per group. **(A)** *Plasmodium* parasite densities: LOWER, total <50 p/ μL blood; HIGHER, total >50 p/ μL blood; GAM, gametocyte carriers by microscopy, here total parasites (all stages) shown. Note, of GAM category samples, 65 % harboured total parasite densities of > 50 p/ μL (HIGHER category). Colours represent the diagnostic technique used to inform categorisation. **(B)** Gametocyte densities per μL blood, in 'total density' categories (measured by QT-NASBA or microscopy).

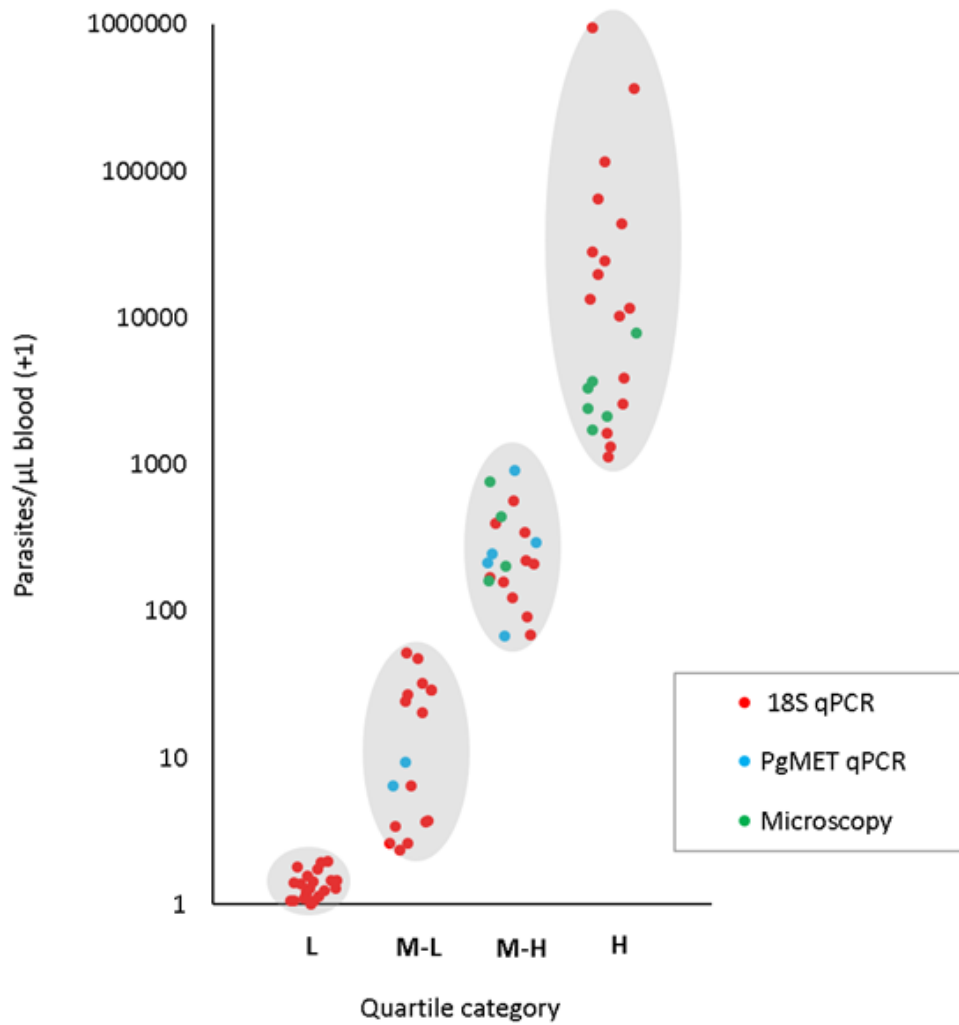


Figure 5-4. 'Quartile' parasitological categorisation, showing actual parasite densities (p/μL) per group. Here all 'higher density' and 'lower density' samples from the 'total density' categories were re-classified: L=low, mean/median parasite density 0.38/0.3, n=21; M-L=medium-low, mean/median parasite density 16.77/8.3, n=17; M-H=medium-high, mean/median parasite density 296.60/214.18, n=19; H=high, mean/median parasite density 102669.46/13304.54, n=23. Colours represent the diagnostic technique used to inform categorisation.

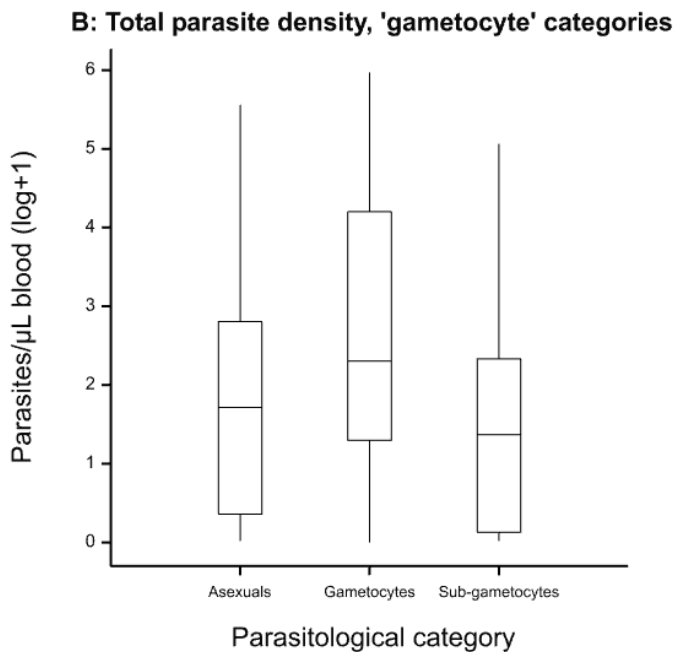
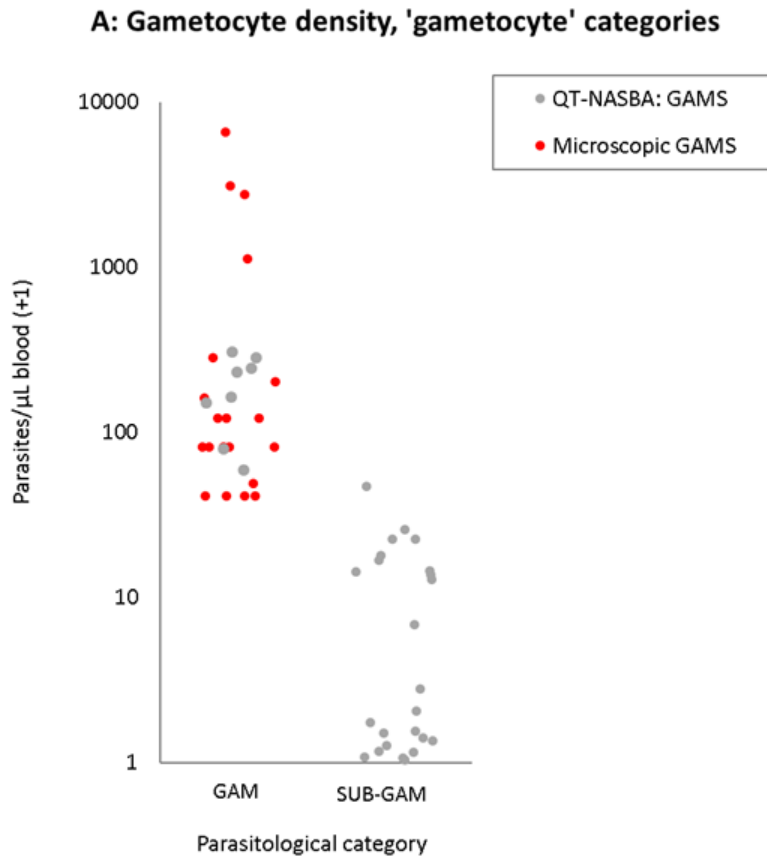


Figure 5-5 'Gametocyte' parasitological categorisation, showing actual parasite densities (μL blood) per group. (A): Gametocyte densities (per μL blood), SUB-GAM, gametocytes $<50/\mu\text{L}$ blood; GAM, gametocytes $>50/\mu\text{L}$ blood or microscopic gametocytes. 'Asexuals' category not shown as there were no gametocytes. Colours represent the diagnostic technique used to inform categorisation. (B) *Plasmodium* densities ($\rho/\mu\text{L}$) in the 'gametocyte' categories.

5.3.10 Statistical analysis of compounds of interest

Compounds of interest, located by either CVA or MALDIquant, were formally tested for an association with parasitological status by linear mixed models (restriction maximum likelihood method, REML). Proportions of the total odour sample (%) were tested, based on amounts generated by the traditional RI method (i.e. by comparing peak area with the alkanes). REML allowed for unequal sample sizes (per parasitological category), and repeated measures on the same individuals, which were unavoidable in this dataset. We tested for the main effects of covariates before the treatment term, and other factors after the treatment term, in a forward selection, parallel-lines, regression analysis approach (Table 5-2, covariates and factors tested). For pairwise comparisons of compound production between treatment groups (e.g. gametocyte vs. negative), the least significant differences (LSDs) at the 5 % level were used to determine significance. Data analysis was conducted using GenStat (16th edition, VSNi).

Table 5-2. Covariates and factors tested with treatment term (parasitology) for significance by forward selection in REML models.

Term	Unit	Description
Covariates		
Age	Years	Age of child from whom odour sample was taken
Haemoglobin	Grams/decilitre	Hb level of child from whom odour sample was taken, as measured by HemoCue
Day of the year	Integer	Number of days since new year
Weight	Kg	Weight of child from whom odour sample was taken
Factors		
Sex	Male, female	Sex of child from whom odour sample was taken
Round	1, 2, 2B, 3, 4	Round of sampling (1-3). 2B represented extra visit made during Obambo sampling, 4 was allocated to all solvent controls as they did not have an associated round.

5.3.11 Ranked production of compounds and intra-individual changes in infection-associated compound production

For infection-associated compounds (IAC) (these found to be statistically associated with infection), production was ranked among all analytes in each sample. To investigate whether within-individual IAC production changed according to parasitological status, average production by individuals whose parasitological status moved between important and significantly different groups was compared (for each IAC, according to the most appropriate parasitological categorisation). As a control, compound production by individuals who remained within those categories over two time points was examined. Peak RI 965 (6-methyl-5-hepten-2-one and 1-octen-3-ol co-eluting) was not investigated over time, as the significant differences in

production lay between negative and lower-density groups with only one individual moving between these, in either direction. Statistical comparisons were made using a two-sample T test, and data analysis was conducted using GenStat (16th edition, VSNi).

5.3.12 Compound identification

IAC were identified by gas chromatography-mass spectrometry (GC-MS) by the same protocols as used in chapter 2, but with the additional use of a quad GC-MS (MSD). The software package used by the MSD was Agilent ChemStation (C.01.04), which again uses the commercial NIST database. Samples for GC-MS were chosen to span all three GC machines used in the original analysis, to further confirm peak alignment between datasets.

Peak enhancement

To confirm the tentative GC-MS identifications, authentic standards were injected onto two GC columns (HP1 and DB wax), simultaneously to samples containing those compounds. With an accurate identification, the resultant peak on the chromatogram should increase in height without an increase in width. Compounds examined, and standards sources, were: hexanal (Sigma-Aldrich), heptanal (Sigma-Aldrich), octanal (Sigma-Aldrich), nonanal (Sigma-Aldrich), (*E*)-2-octenal (Acros Organics), (*E*)-2-decenal (SAFC), 2-octanone (Sigma-Aldrich), 1-octen-3-one (Alfa Aesar), 6-methyl-5-hepten-2-one (Sigma-Aldrich) and 1-octen-3-ol (Alfa Aesar). The latter two compounds were found to co-elute on the standard HP1 column used to run all the samples, while retention times differed on the DB-wax column. The samples used for peak enhancement were: four Kenya GC-EAG blends (negative, no gametocytes, sub-gametocytes, gametocytes; chapter 6), KA078 23MAY14, AL029 13FEB14 and PO014 10JUN14. Authentic standards were diluted to mimic the concentration per sample, and the sample and standard injected simultaneously onto both HP1 and DB wax columns. A standard GC programme was used; 30 °C for 0.1 minutes, increasing by 5 °C/minute to 150 °C, held 0.1 minute then raised by 10 °C/minute to 230 °C, held 25 minutes.

5.4 Results

5.4.1 Summary

One hundred and seventeen odour profile samples were taken from 56 individuals (Table 5-3, appendix 5.10 'odour profile study population'), alongside 59 closed bag controls. Fourteen compounds were formally tested for their association with parasitological status: hexanal, RI 797 (solvent and octane co-eluting), heptanal, nonane, 1-octen-3-one, RI 965 (co-eluting 6-methyl-5-hepten-2-one and 1-octen-3-ol), 2-octanone, octanal, limonene, (*E*)-2-octenal, nonanal, decanal, (*E*)-2-decenal and hexadecane.

Significant differences in compound production, according to 'total density' parasitological categorisation, were observed for the aldehydes heptanal, octanal, nonanal, (*E*)-2-octenal, and (*E*)-2-decenal. Here, increased production was broadly associated with infections of high parasite density (Figure 5-6). In this analysis, the ketone 2-octanone was found to be significantly associated with the presence of microscopic gametocytes. There were interesting trends in the production of peak RI 965, co-eluting 6-methyl-5-hepten-2-one and 1-octen-3-ol, where low parasite densities were associated with reduced production, and higher densities with increased production.

Where significant by 'total density' categorisation, similar patterns in the production of the above compounds according to 'positive vs. negative' categories were observed. However, the production of two further compounds was significantly predicted by 'gametocyte' categories, hexanal and 1-octen-3-one. For both, compound production was increased in samples from individuals harbouring gametocytes, relative to those without parasites or with only asexual stages.

Table 5-3. Characteristics of Kenyan odour profile study population (repeat samples were taken at 1-4 time points on these 56 individuals). Schools constitute the four study sites. N = number of individuals. CNL = controls (odour samples from empty bags).

SCHOOL	N	% MALE	% FEMALE	AGE RANGE (YRS)	ODOUR SAMPLES	CNL SAMPLES
OBAMBO	8	50	50	6 - 11	16	10
ALERO	22	59.09	40.91	6 - 12	44	26
KAMSAMA	10	50	50	5 - 9	19	7
POWO	16	43.75	56.25	5 - 10	38	16
ALL SITES	56	51.79	48.21	5 - 12	117	59

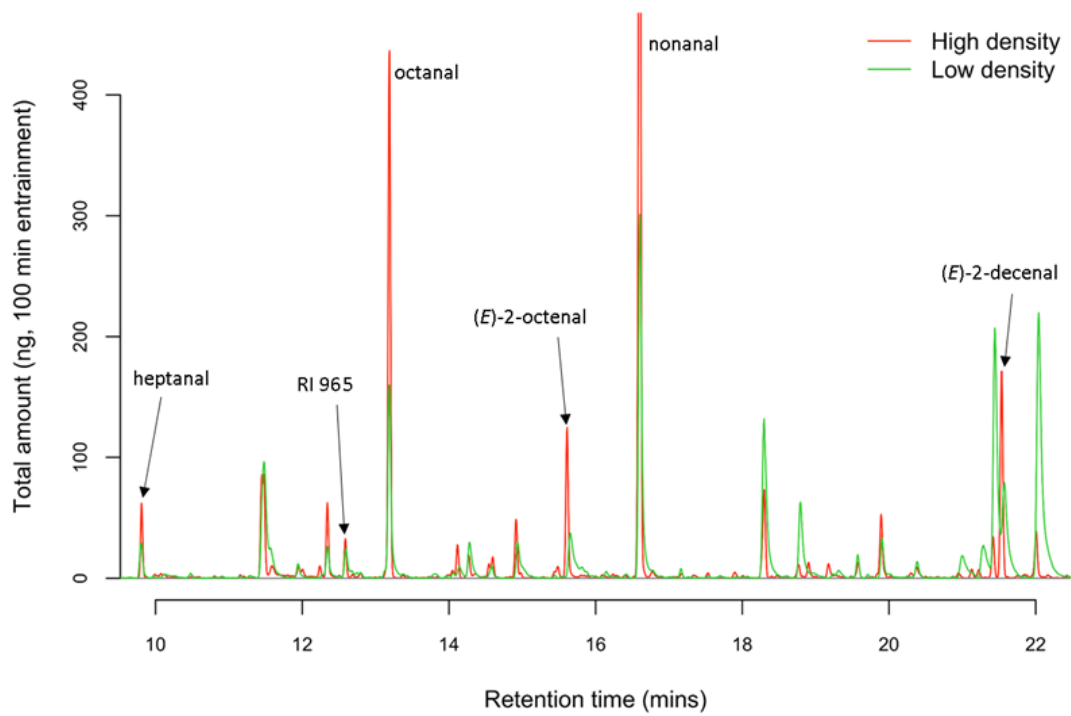


Figure 5-6. The output from gas chromatography is a trace, where compounds are represented by peaks according to the amount present. Here, representative traces from an individual with a 'high density' infection (>50 *Plasmodium* p/ μ L blood) and 'low density' infection (<50 *Plasmodium* p/ μ L blood) are shown. Compounds found to be significant in the 'total density' analysis are annotated.

5.4.2 Compound identification by peak enhancement

Compound identities were confirmed by co-injecting an authentic standard with the sample, and observing an increase in peak height with no increase in peak width. An example is given in Figure 5-7, with all other co-injected compounds in appendix 5.11.

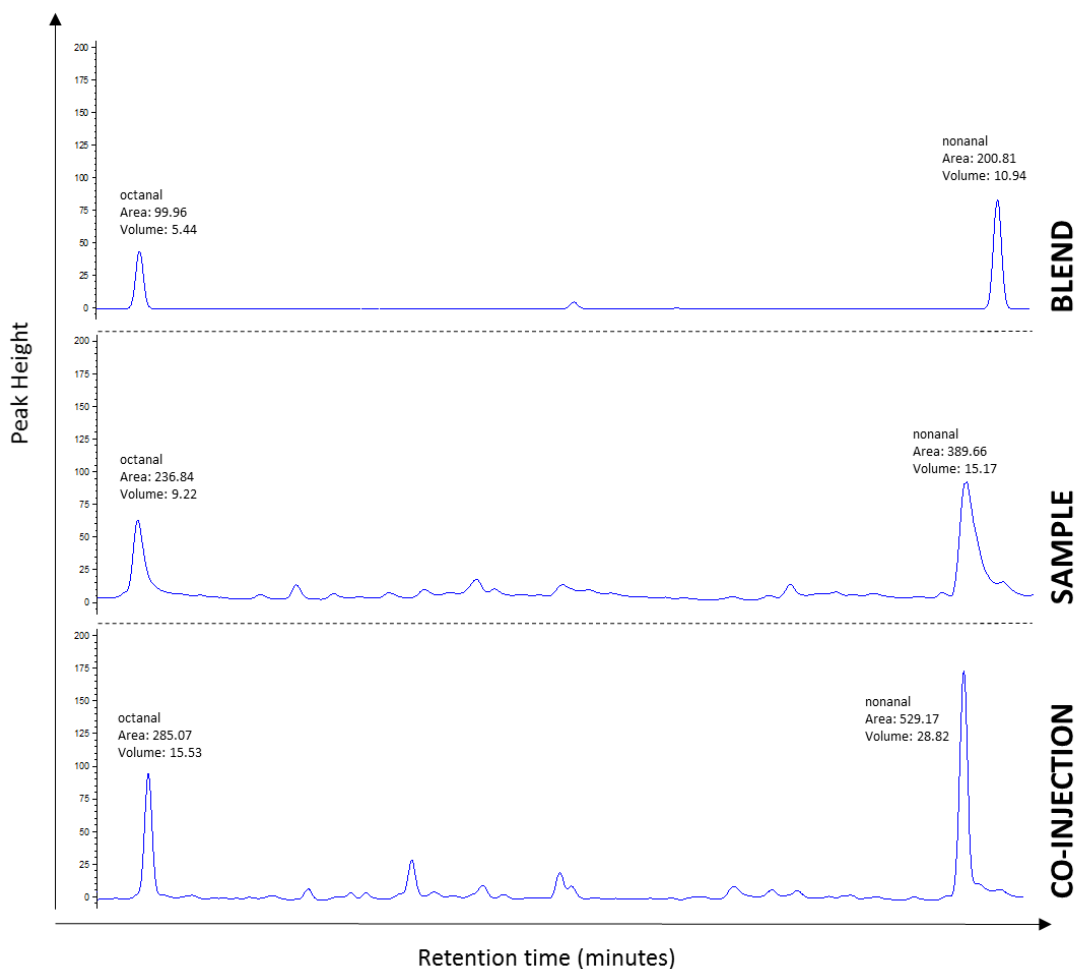


Figure 5-7. Peak enhancement was conducted to formally identify all compounds found to be associated with infection in the statistical analysis (hexanal, heptanal, octanal, nonanal, (*E*)-2-octenal, (*E*)-2-decenal, 2-octanone, 6-methyl-5-hepten-2-one, 1-octen-3-ol and 1-octen-3-one). Here octanal and nonanal are shown, full details for all compounds are given in appendix 5.11.

5.4.3 Infection-associated compounds (IAC)

Each infection-associated compound is addressed individually below. Mean compound production per group is summarised, by parasitological category, at the end of the section in Table 5-4, Table 5-5, Table 5-6 and Table 5-7 (summary tables, 5.4.4). Significant covariates and factors in the REML models, and significant pairwise differences between groups, are given in Table 5-8 ('total density' categories), Table 5-9 ('gametocyte' categories) and Table 5-10 ('positive vs. negative' categories). Standard errors of the difference tables are given in appendix 5.12.

Heptanal (RI 880)

The overall effect of treatment by 'total density' categories on the production of heptanal approached significance ($P=0.085$), and individuals in the 'higher density' category produced significantly more heptanal than those in the 'negative' category (LSD, 5 %) (Figure 5-8A, Figure 5-9). The three parasitologically positive groups ('lower density', 'higher density' and 'gametocytes') produced significantly more heptanal than both control (A) and (B), unlike the 'negative' group which did not produce significantly more heptanal than control (A) (LSD, 5 %). No covariates or factors significantly predicted heptanal production (Table 5-8). Subdividing the 'higher' and 'lower' density groups into four groups, reflecting incremental increases in parasite densities ('quartile' categories), did not give an overall significant treatment effect ($P=0.342$), but there is a progression in heptanal production with increasing parasite density (Figure 5-8B, Table 5-5, Table 5-11). Finally, when all parasitologically positive individuals were grouped and compared to parasite-free individuals, the former produces significantly more heptanal than both control groups, unlike parasite-free individuals (LSD 5 %, Figure 5-8C, Table 5-7). Here, however, the overall treatment effect is not significant ($P=0.253$). Heptanal production was not significantly predicted by the 'gametocyte' categories ($P>0.05$, data not shown).

Chapter 5: Odour profile analysis of children naturally infected with *Plasmodium* species

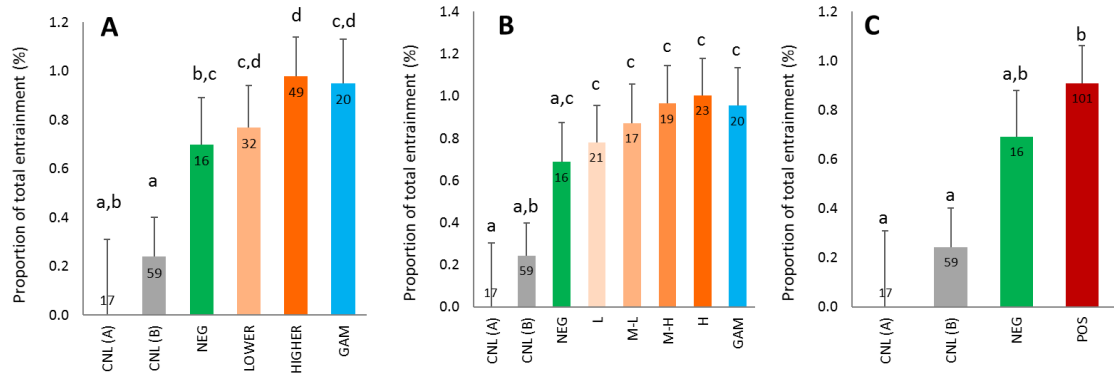


Figure 5-8. Heptanal production (relative to all compounds in odour sample) per group. Predicted means (+SE) given by linear mixed modelling (REML). Sample size in bar ends, significant pairwise differences are indicated by different letters above bars, tested by Least Significant Differences ($P < 0.05$). (A) ‘total density’ categorisation; ‘NEG’=negative, ‘lower’ and ‘higher’ refer approximately to parasite densities of lesser or greater than 50 p/μL, ‘GAM’=microscopic gametocytes (B) ‘quartile’ categorisation; ‘NEG’ and ‘GAM’ as before, L=low, M-L=medium-low, M-H=medium-high and H=high (C) ‘positive vs. negative’ categorisation; ‘positive’=harbouring parasite densities greater than the test lower limit of detection, ‘negative’=parasite free. For all CNL(A)=solvent control, CNL(B)=empty bag control.

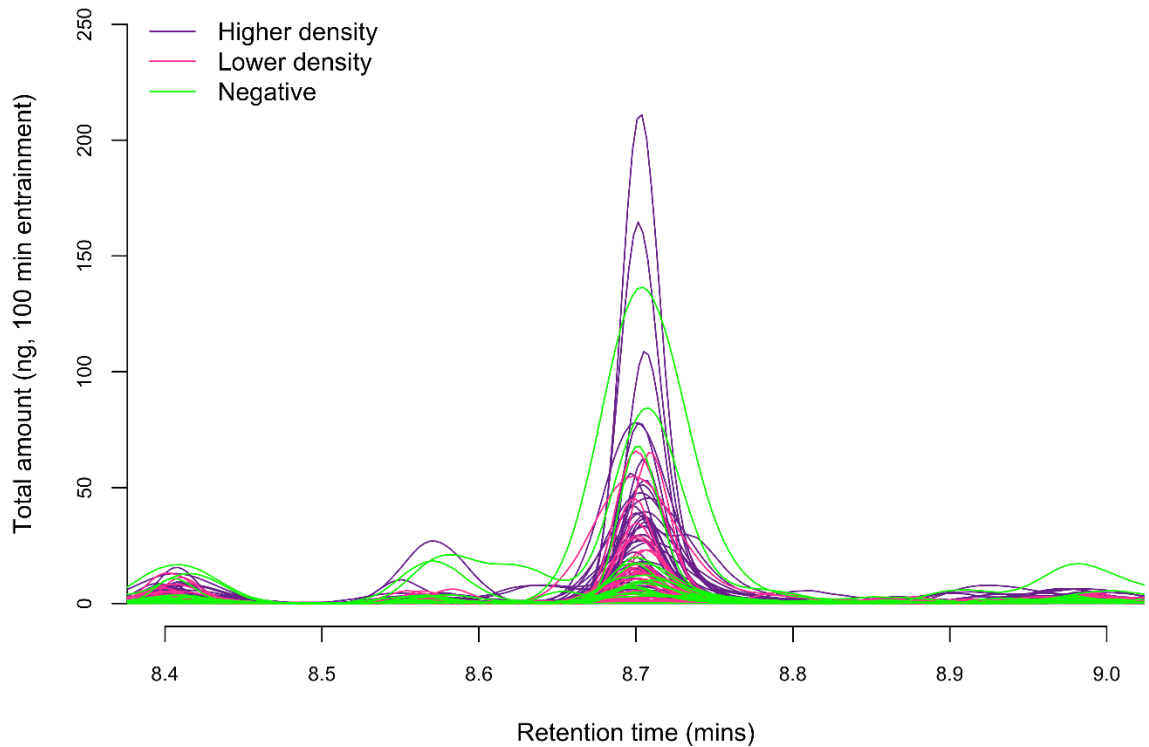


Figure 5-9. Heptanal peak in raw gas chromatography output. Individual lines represent odour profile samples, here coloured according to the parasitological status of the individual from whom the odour sample was taken. ‘Higher density’, samples from individuals with >50 p/μL; ‘lower density’, samples from individuals with <50 p/μL; ‘negative’, samples from parasite-free individuals. Gametocyte carriers are excluded for clarity, as compound production spanned higher and lower parasite density groups.

Octanal (RI 982)

'Total density' categories significantly predicted the production of octanal ($P=0.038$), with those in the 'higher' group producing more than those in the 'lower' group (LSD, 5 %) (Figure 5-10A, Figure 5-11). As with heptanal, all infected groups ('lower density', 'higher density' and 'gametocytes') produced significantly more octanal than CNL(A) and (B), while those in the 'negative' group did not produce more than CNL(A) (LSD, 5 %). Age, age² and sex significantly influenced octanal production. There was an inverse parabolic relationship with age (indicated by a positive age effect, 2.81, and negative age² effect, -0.19) and production peaked at eight years (Figure 5-12). A continuous decrease in octanal production from eight to 12 years was observed. Males produced significantly more octanal than females (5.47 vs. 4.02 % of total sample) (LSD 5 %) (Figure 5-12B). Because there was no interaction between age or sex and parasitological status, factors specific to age and sex and with no relationship to parasitological status (as modelled here) govern octanal production. As with heptanal, further dividing the 'higher' and 'lower' density categories into quartiles revealed a non-significant trend for a progressive increase in octanal production with increasing parasite density (Figure 5-10B, Table 5-5, Table 5-11). When modelled according to gametocyte density, those in the higher density gametocyte category ('GAM') (Figure 5-10C) produced more octanal than 'sub-gametocyte' or 'negative' groups (LSD, 5 %). While the 'GAM' group harboured more parasites overall (Figure 5-5B), this probably indicates some gametocyte-specific effect. Overall, for these categories, the treatment effect was borderline significant ($P=0.061$), while for 'positive vs. negative' categories it was not significant ($P>0.05$) (data not shown).

Chapter 5: Odour profile analysis of children naturally infected with *Plasmodium* species

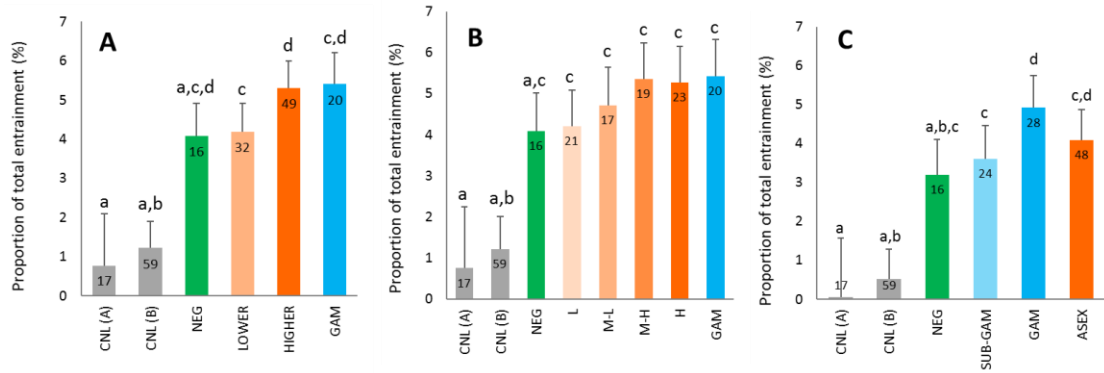


Figure 5-10. Octanal production (relative to all compounds in odour sample) per group. Predicted means (+SE) given by linear mixed modelling (REML). Sample size in bar ends, significant pairwise differences indicated by different letters above bars, tested by Least Significant Differences ($P < 0.05$) (A) 'total density' categorisation; 'NEG'=negative, 'lower' and 'higher' refer approximately to parasite densities of lesser or greater than 50 p/μL, 'GAM'=microscopic gametocytes (B) 'quartile' categorisation; 'NEG' and 'GAM' as before, L=low, M-L=medium-low, M-H=medium-high and H=high (C) 'gametocyte' categorisation; 'NEG' as before, 'SUB-GAM' and 'GAM' refer approximately to gametocyte densities of lesser or greater than 50/μL, 'ASEX'=parasites but no gametocytes. For all CNL(A)=solvent control, CNL(B)=empty bag control.

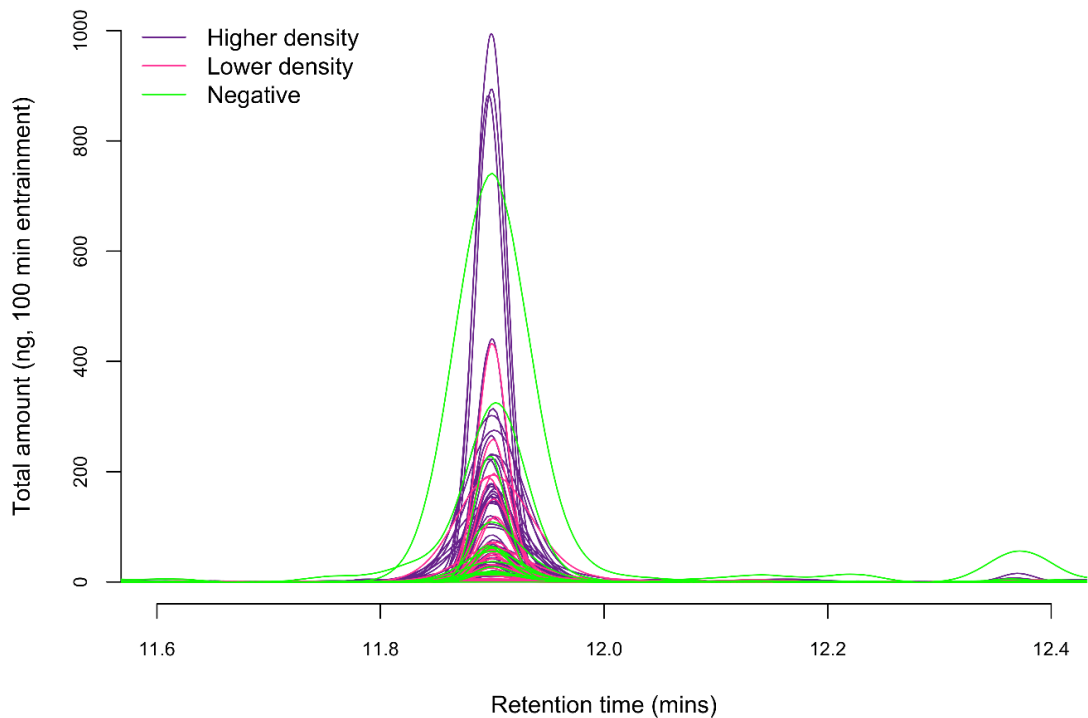


Figure 5-11. Octanal peak in raw gas chromatography output. Individual lines represent odour profile samples, here coloured according to the parasitological status of the individual from whom the odour sample was taken. 'Higher density', samples from individuals with >50 p/μL; 'lower density', samples from individuals with <50 p/μL; 'negative', samples from parasite-free individuals. Gametocyte carriers are excluded for clarity, as compound production spanned higher and lower parasite density groups.

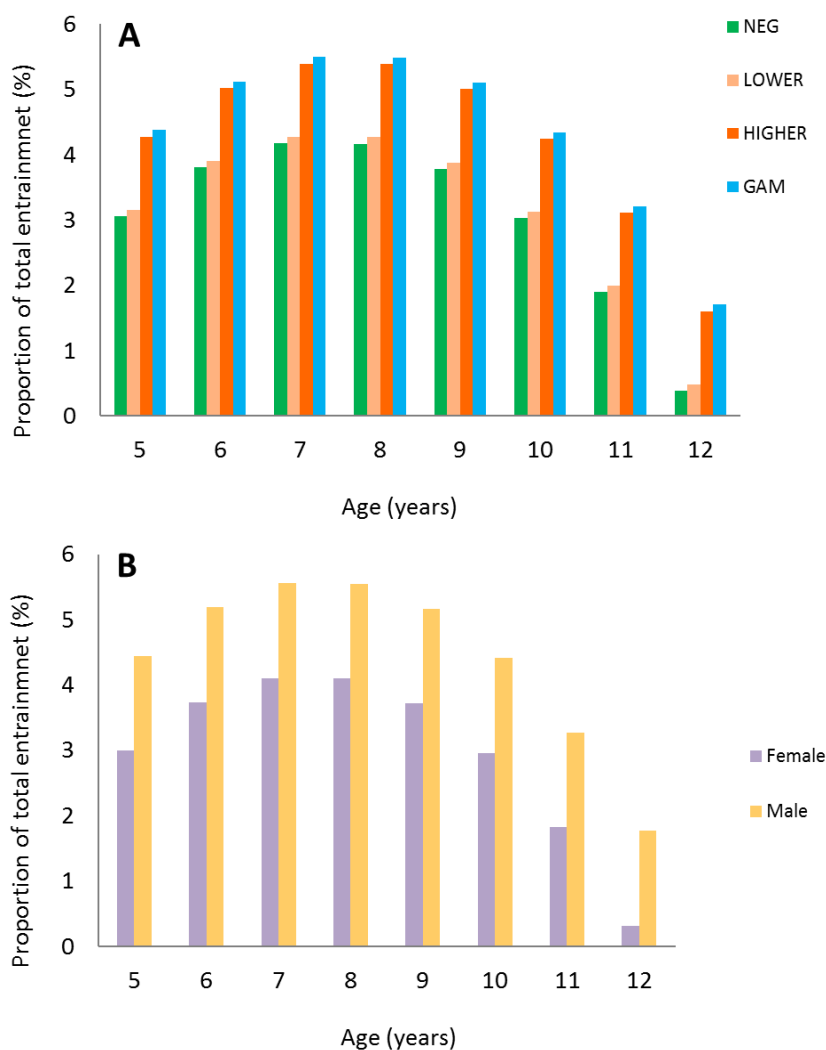


Figure 5-12. There is an inverse parabolic relationship between age and octanal production (REML, predicted means + SE), with a peak at eight years. Octanal production presented as a percentage of all compounds in the odour sample. Samples further split by (A) parasitology ('total density' categories, control groups modelled but omitted as not biologically appropriate), or (B) sex of individual. Predictions for REML covariates have no sample size, population parameters given in Table 5-3 and appendix 5.10.

Nonanal (RI 1084)

The production of nonanal was significantly predicted by 'total density' categories ($P=0.027$) (Figure 5-13A, Figure 5-14). All human odour samples produced significantly more nonanal than controls when pairwise differences were examined (LSD, 5 %), other than the 'lower density' group, whose nonanal production was not significantly greater than CNL(A) (solvent). Individuals in the 'higher density' group produced significantly more nonanal than those in the 'lower density' group (LSD, 5 %), due to both increased production by the former, and a concomitant decrease in production by the latter (Figure 5-13A), relative to parasite-free individuals.

Haemoglobin concentration (Hb) and Hb² were significant covariates ($P=0.034$, $P=0.009$) with a positive effect (16.81) and negative effect (-1.37) respectively. This is indicative of an inverted parabolic relationship between Hb levels and nonanal production, with maximum production at 6.12 g/dL Hb, and from thereon, an increase in Hb levels (i.e. decrease in anaemia) corresponding to a decrease in nonanal production (Figure 5-15). There was no interaction between parasitological status and Hb, indicating an association between nonanal production and Hb levels (or anaemia) that is independent of *Plasmodium* infection. When examining nonanal production by ‘quartile’ categories, the treatment effect approached significance ($P=0.117$) and significant pairwise differences were observed. Individuals with the highest parasite density (H, high), produced significantly more nonanal than individuals with negative and low (L) densities (Figure 5-13B, Table 5-5, Table 5-11). Thus, separating out those individuals with the highest density allowed the difference in nonanal production between these and negative individuals to be observed (not significant in ‘total density’ categories). Neither ‘positive vs. negative’ nor ‘gametocyte’ categories significantly predicted nonanal production ($P>0.05$ for both).

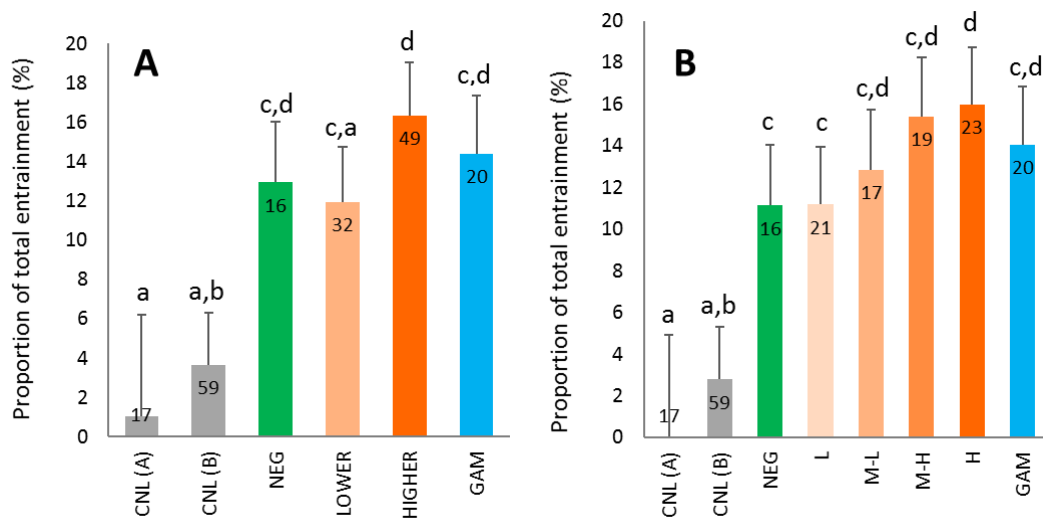


Figure 5-13. Nonanal production (relative to all compounds in odour sample) per group. Predicted means (+SE) given by linear mixed modelling (REML). Sample size in bar ends, significant pairwise differences indicated by different letters above bars, tested by Least Significant Differences ($P<0.05$) (A) ‘total density’ categorisation; ‘NEG’=negative, ‘lower’ and ‘higher’ refer approximately to parasite densities of lesser or greater than 50 p/μL, ‘GAM’=microscopic gametocytes (B) ‘quartile’ categorisation; ‘NEG’ and ‘GAM’ as before, L=low, M-L=medium-low, M-H=medium-high and H=high. For both, CNL(A)=solvent control, CNL(B)=empty bag control.

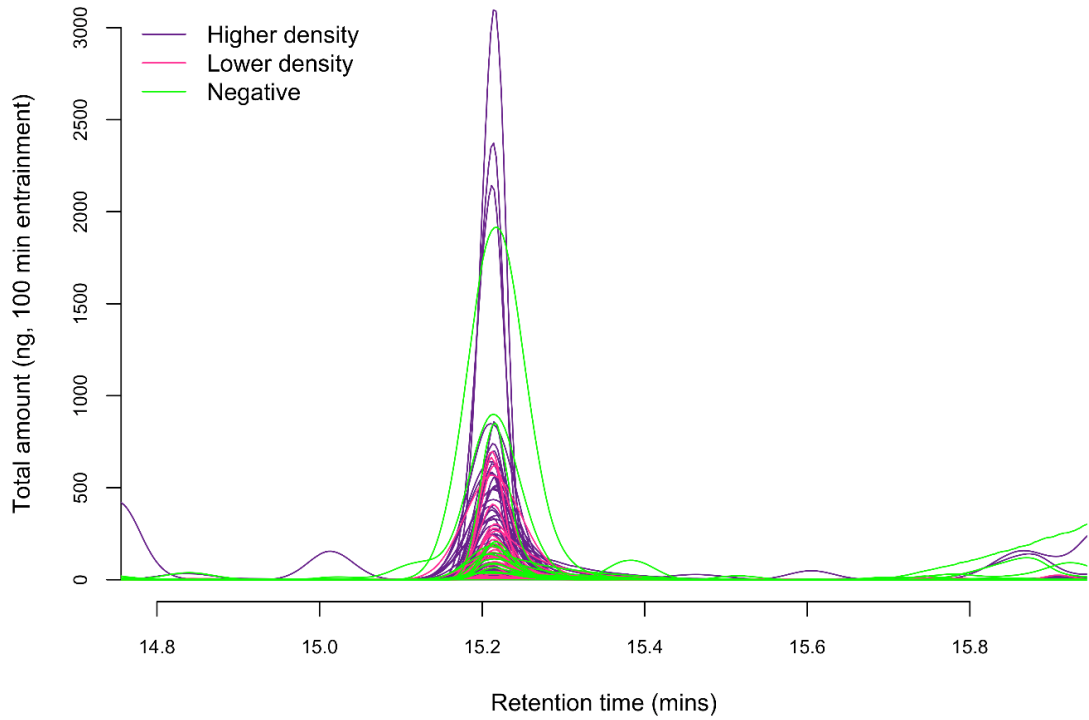


Figure 5-14. Nonanal peak in raw gas chromatography output. Individual lines represent odour profile samples, here coloured according to the parasitological status of the individual from whom the odour sample was taken. 'Higher density', samples from individuals with >50 p/μL; 'lower density', samples from individuals with <50 p/μL; 'negative', samples from parasite-free individuals. Gametocyte carriers are excluded for clarity, as compound production spanned higher and lower parasite density groups.

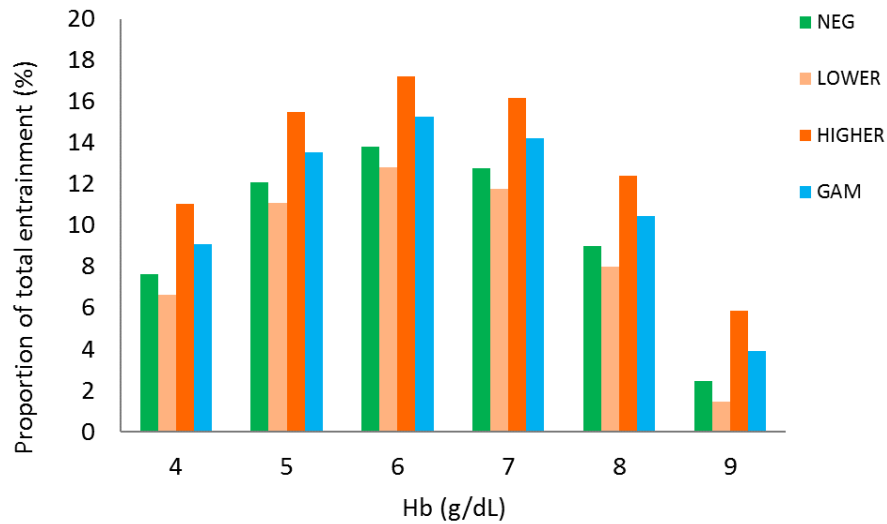


Figure 5-15. There is an inverse parabolic relationship between haemoglobin level and nonanal production (REML, predicted means + SE), with a peak at 6.12 g/dL (averaged across parasitological groups). Nonanal production presented as a percentage of all compounds in the odour sample. Samples split by parasitology ('total density' categories, control groups modelled but omitted as not biologically appropriate). Predictions for REML covariates have no sample size, population parameters given in Table 5-3 and appendix 5.10.

(*E*)-2-Octenal (RI 1035)

By 'total density' categories, all *Plasmodium*-infected groups produced significantly more (*E*)-2-octenal than was found in both controls, while production by the 'negative' group was not significantly different from either control (Figure 5-16A, Figure 5-17). Overall, 'total density' categories approached significance in predicting (*E*)-2-octenal production ($P=0.15$). Here, Round and Hb had significant influence ($P=0.013$ and $P=0.012$ respectively), with a negative effect of Hb indicating decreased (*E*)-2-octenal with increased Hb, or conversely, increased (*E*)-2-octenal being associated with anaemia (Figure 5-18). As with nonanal, there was no interaction between parasitological status and haemoglobin level, indicating a distinct association between (*E*)-2-octenal production and Hb that is independent of the presence of *Plasmodium* parasites. Round was negatively associated with (*E*)-2-octenal production, indicating a decrease over sequential rounds (treatment effects: R1, 0; R2, -0.27; R3, -0.33). Predictions for (*E*)-2-octenal production across all parasitological categories, and at average Hb, are: round one, 0.78; round two, 0.51; round three, 0.46 (proportion of total entrainment, %). Quartile category models were not fitted. 'Gametocyte' categories significantly predicted the production of (*E*)-2-octenal ($P=0.031$) (Figure 5-16B). There was an increase in (*E*)-2-octenal production with increasing density of gametocytes, although the correlation with total parasite density should be considered (Figure 5-5). Here, individuals in both the 'sub-gam' and 'gam' groups (lower and higher density gametocytes) produced significantly more (*E*)-2-octenal than was found in either controls, unlike those with no gametocytes present ('asex' or 'neg' categories). However, differences in production between these groups were not significant (LSD, 5 %). By the binary classification 'positive vs. negative', parasitological status had an overall significant effect on the production of (*E*)-2-octenal ($P=0.04$) (Figure 5-16C). However, there was no significant pairwise difference in (*E*)-2-octenal production between positive and negative groups despite the trend for increased production in the positive group (LSD, 5 %). Overall treatment significance was likely due to the large difference in compound volume between the 'positive' group and ether (CNL (A)).

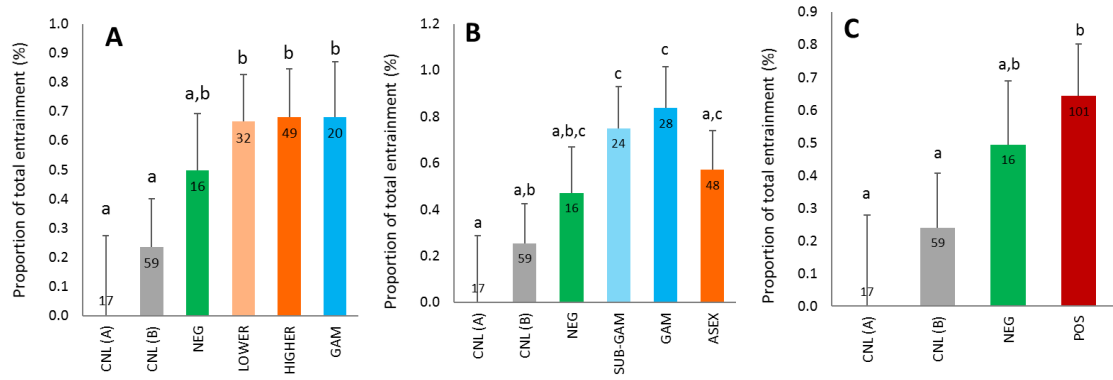


Figure 5-16. (E)-2-Octenal production (relative to all compounds in odour sample) per group. Predicted means (+SE) given by linear mixed modelling (REML). Sample size in bar ends, significant pairwise differences indicated by different letters above bars, tested by Least Significant Differences ($P < 0.05$) (A) 'total density' categorisation; 'NEG'=negative, 'lower' and 'higher' refer approximately to parasite densities of lesser or greater than 50 p/μL, 'GAM'=microscopic gametocytes, (B) 'gametocyte' categorisation; 'NEG' as before, 'SUB-GAM' and 'GAM' refer approximately to gametocyte densities of lesser or greater than 50 p/μL, 'ASEX'=parasites but no gametocytes, (C) 'positive vs. negative' categorisation; 'positive' = harbouring parasite densities greater than the test lower limit of detection, 'negative'=parasite-free. For all CNL(A)=solvent control, CNL(B)=empty bag control.

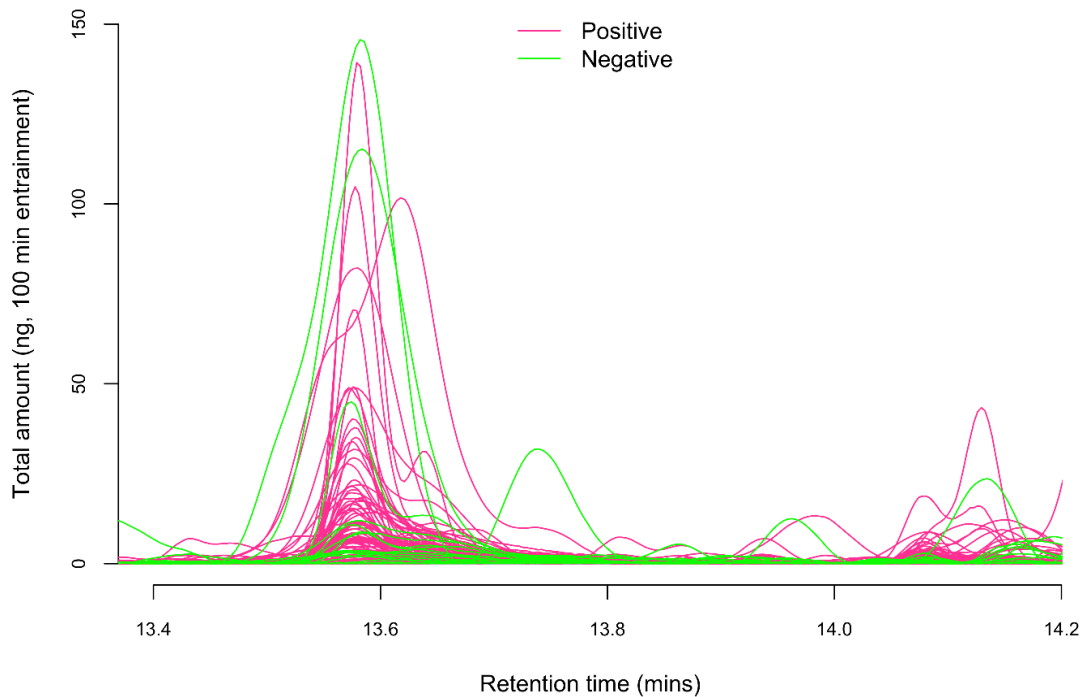


Figure 5-17. (E)-2-Octenal peak in raw gas chromatography output. Individual lines represent odour profile samples, here coloured according to the parasitological status of the individual from whom the odour sample was taken ('positive vs. negative' categories, Table 5-1).

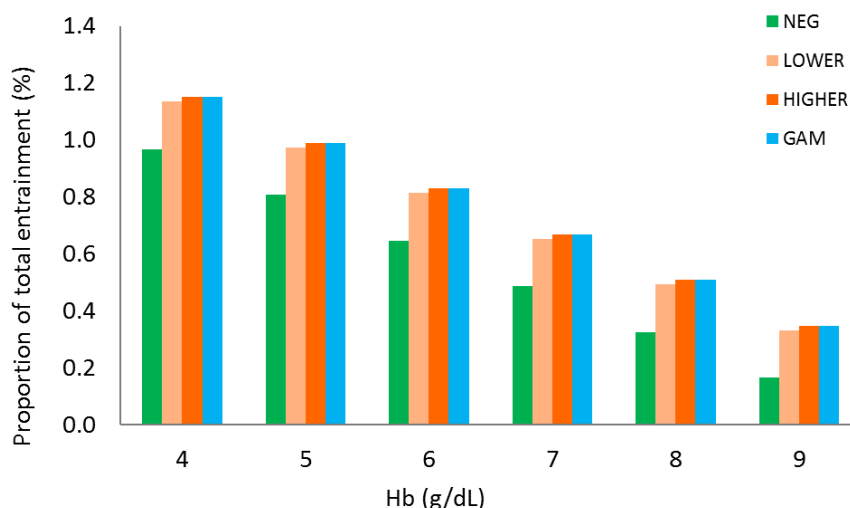


Figure 5-18. (*E*)-2-Octenal production decreased with increasing haemoglobin level (REML, predicted means + SE), shown as a percentage of all compounds in the odour sample. Samples split by parasitology ('total density' categories, control groups modelled but omitted as not biologically appropriate). Predictions for REML covariates have no sample size, population parameters given in Table 5-3 and appendix 5.10.

(*E*)-2-Decenal (RI 1240)

There was a trend for individuals who harboured *Plasmodium* parasites to produce increased (*E*)-2-decenal (Figure 5-19A). As with (*E*)-2-octenal, the 'negative' group did not produce significantly more (*E*)-2-decenal than was detected in the controls, while those carrying any stage or density of parasites produced significantly more than both control (A) and (B) (LSD, 5 %). There was a significant effect of age in the model (treatment effect -0.39) with decreased compound production associated with increased age (Figure 5-21). As there was no interaction with parasitology, this cannot be attributable to changes in malaria prevalence with age. Overall, the effect of 'total density' categorisation on (*E*)-2-decenal production was not significant ($P=0.209$). However, that of 'gametocyte' categories was ($P=0.016$), with individuals in the high density gametocyte group producing significantly more (*E*)-2-decenal than all other groups (LSD, 5 %) (Figure 5-19B). As with octanal, this possibly indicates some gametocyte-specific effect. When categories were merged to the simple 'positive vs. negative' classification, there was an overall significant effect of parasitological status on the production of (*E*)-2-decenal ($P=0.042$) (Figure 5-19C, Figure 5-20). Positive individuals produced significantly more (*E*)-2-decenal than negative individuals (LSD, 5 %).

Chapter 5: Odour profile analysis of children naturally infected with *Plasmodium* species

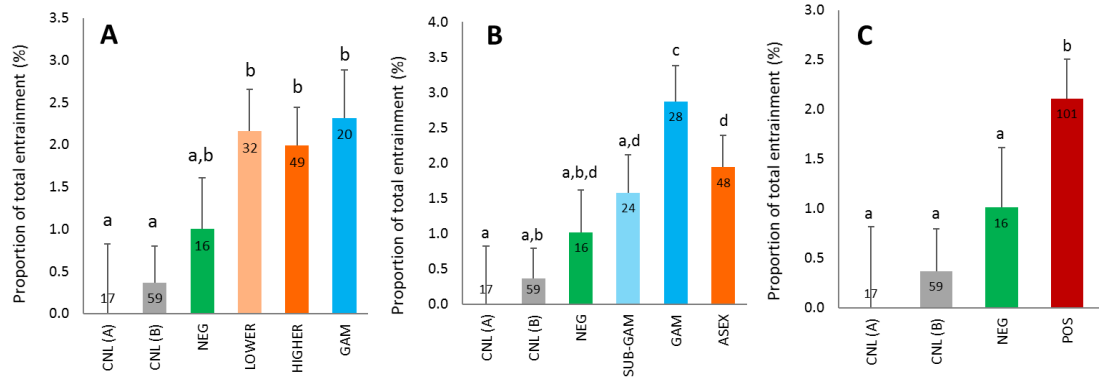


Figure 5-19. (E)-2-Decenal production (relative to all compounds in odour sample) per group. Predicted means (+SE) given by linear mixed modelling (REML). Sample size in bar ends, significant pairwise differences indicated by different letters above bars, tested by Least Significant Differences ($P < 0.05$) (A) 'total density' categorisation; 'NEG' = negative, 'lower' and 'higher' refer approximately to parasite densities of lesser or greater than 50 p/μL, 'GAM' = microscopic gametocytes, (B) 'gametocyte' categorisation; 'NEG' as before, 'SUB-GAM' and 'GAM' refer approximately to gametocyte densities of lesser or greater than 50 p/μL, 'ASEX' = parasites but no gametocytes, (C) 'positive vs. negative' categorisation; 'positive' = harbouring parasite densities greater than the test lower limit of detection, 'negative' = parasite-free. For all CNL(A) = solvent control, CNL(B) = empty bag control.

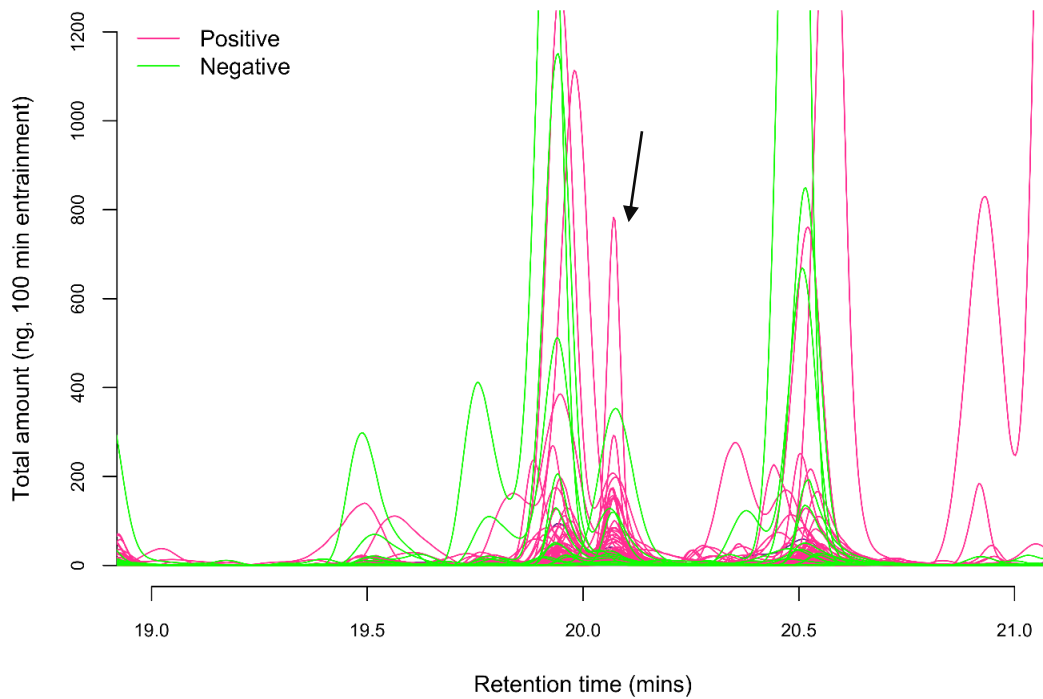


Figure 5-20. (E)-2-Decenal peak (annotated by arrow) in raw gas chromatography output. Individual lines represent odour profile samples, here coloured according to the parasitological status of the individual from whom the odour sample was taken ('positive vs. negative' categories, Table 5-1).

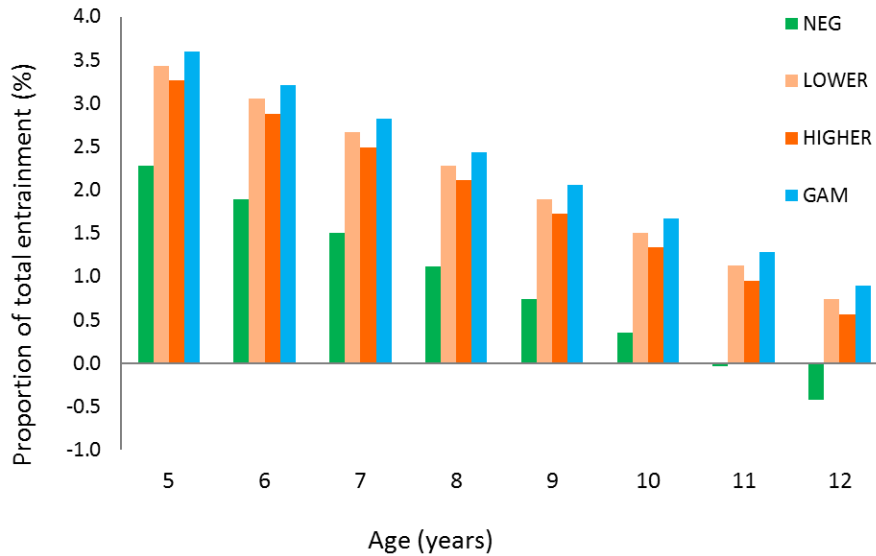


Figure 5-21. (E)-2-Decenal production decreased with increasing age (REML, predicted means + SE), shown as a percentage of all compounds in the odour sample. Samples split by parasitology ('total density' categories, control groups modelled but omitted as not biologically appropriate). Predictions for REML covariates have no sample size, population parameters given in Table 5-3 and appendix 5.10.

6-Methyl-5-hepten-2-one and 1-octen-3-ol (RI 965; co-eluting)

'Total density' categories approached significance in predicting production of RI 965 (co-eluting 6-methyl-5-hepten-2-one and 1-octen-3-ol, $P=0.141$) (Figure 5-22A), although there was no significant difference in production between the human groups. Individuals in the 'lower density' group, however, produced less RI 965 (Table 5-4), with production not greater than CNL(A) or (B), unlike the other (human) groups, which all produced more than CNL(A) (LSD, 5%). There was a significant effect of round ($P=0.003$), with production decreasing from round one to two and increasing again in round three (Proportion of sample [%]: R1, 0.71; R2, 0.36; R3, 0.59, REML). When the 'higher' and 'lower' density samples were further divided into quartiles, the effect of treatment became more significant ($P=0.073$) (Figure 5-22B, Table 5-5, Table 5-11). Individuals in the two highest density groups ('medium high' and 'high') produced significantly more RI 965 than both controls and the 'medium low' group. Production by individuals with 'low' or 'medium low' parasite densities was not significantly different from CNL(A) or (B), while production by 'negative' or 'gametocyte' individuals was intermediate. Therefore, harbouring low densities of parasites correlates with the lowest levels of production of RI 965, high densities with the greatest production, and parasite-free individuals produce intermediate amounts.

Although the effect of treatment by ‘gametocyte’ categories was not significant overall ($P=0.182$), gametocyte carriers (‘sub-gametocyte’ and ‘gametocyte’ groups) produced more than both CNL(A) and (B), unlike the other groups (LSD, 5 %) (Figure 5-22C). This is likely because the gametocyte carriers were largely those individuals in the ‘medium high’ and ‘high’ parasite density quartiles, however, the role of gametocyte stage parasites versus the high density of all stages cannot be disentangled here. That RI 965 production by the ‘asexual’ group was less than that of ‘sub-gametocyte’, with both groups having broadly equivalent total parasite densities, does suggest some gametocyte-specific effect (Figure 5-5B). There was no significant effect of treatment when samples were divided by ‘positive vs. negative’ categories ($P>0.05$).

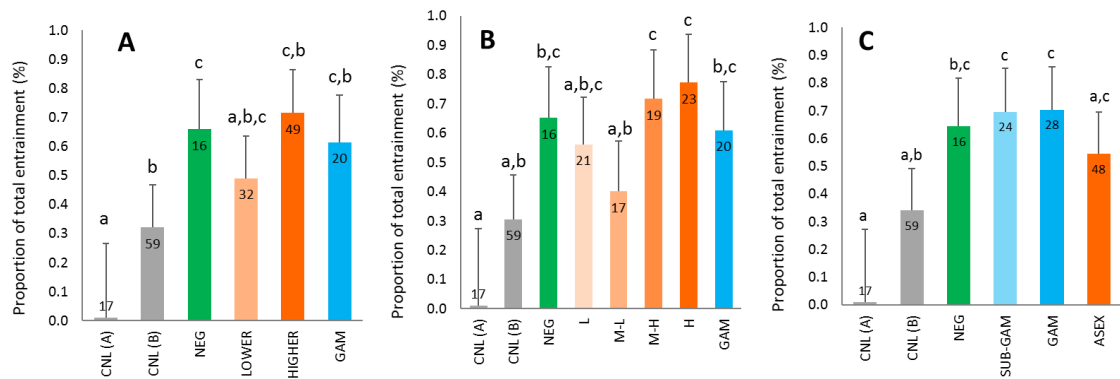


Figure 5-22. RI 965 production (relative to all compounds in odour sample) per group. Predicted means (+SE) given by linear mixed modelling (REML). Sample size in bar ends, significant pairwise differences indicated by different letters above bars, tested by Least Significant Differences ($P<0.05$) (A) ‘total density’ categorisation; ‘NEG’=negative, ‘lower’ and ‘higher’ refer approximately to parasite densities of lesser or greater than 50 p/μL, ‘GAM’=microscopic gametocytes (B) ‘quartile’ categorisation; ‘NEG’ and ‘GAM’ as before, L=low, M-L=medium-low, M-H=medium-high and H=high (C) ‘gametocyte’ categorisation; ‘NEG’ as before, ‘SUB-GAM’ and ‘GAM’ refer approximately to gametocyte densities of lesser or greater than 50 p/μL, ‘ASEX’=parasites but no gametocytes. For all CNL(A)=solvent control, CNL(B)=empty bag control.

2-Octanone (RI 971)

Parasitological status according to ‘total density’ categories was highly predictive for production of the ketone 2-octanone ($P=0.001$) (Figure 5-23A). Individuals in the ‘gametocyte’ group produced significantly more 2-octanone than those in the ‘higher density’, ‘lower density’ or ‘negative’ groups (LSD, 5 %). *Plasmodium*-infected groups produced significantly more 2-octanone than was found in CNL(A) or (B), unlike the ‘negative’ group (LSD, 5 %). When examining compound production as predicted by ‘gametocyte’ categories, 2-octanone was again significantly predicted (overall treatment effect $P=0.002$). Both gametocyte groups (‘gametocyte’ and ‘sub-gametocyte’) produced significantly more 2-octanone than the ‘asexual’ group, infected individuals with no gametocytes (LSD, 5 %) (Figure 5-23B, Figure 5-24). This is supportive of a correlation between gametocyte density and the production of 2-octanone. There was no significant effect of treatment when samples were divided by ‘positive vs. negative’ categories ($P>0.05$).

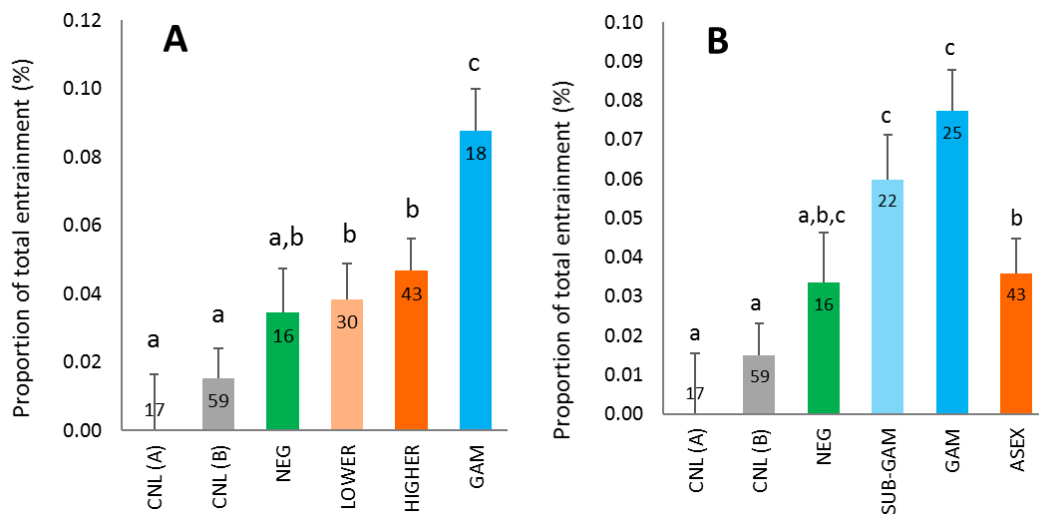


Figure 5-23. 2-Octanone production (relative to all compounds in odour sample) per group. Predicted means (+SE) given by linear mixed modelling (REML). Sample size in bar ends, significant pairwise differences indicated by different letters above bars, tested by Least Significant Differences ($P<0.05$) (A) ‘total density’ categorisation; ‘NEG’=negative, ‘lower’ and ‘higher’ refer approximately to parasite densities of lesser or greater than 50 p/μL, ‘GAM’=microscopic gametocytes, (B) ‘gametocyte’ categorisation; ‘NEG’ as before, ‘SUB-GAM’ and ‘GAM’ refer approximately to gametocyte densities of lesser or greater than 50 p/μL, ‘ASEX’=parasites but no gametocytes. For both CNL(A)=solvent control, CNL(B)=empty bag control.

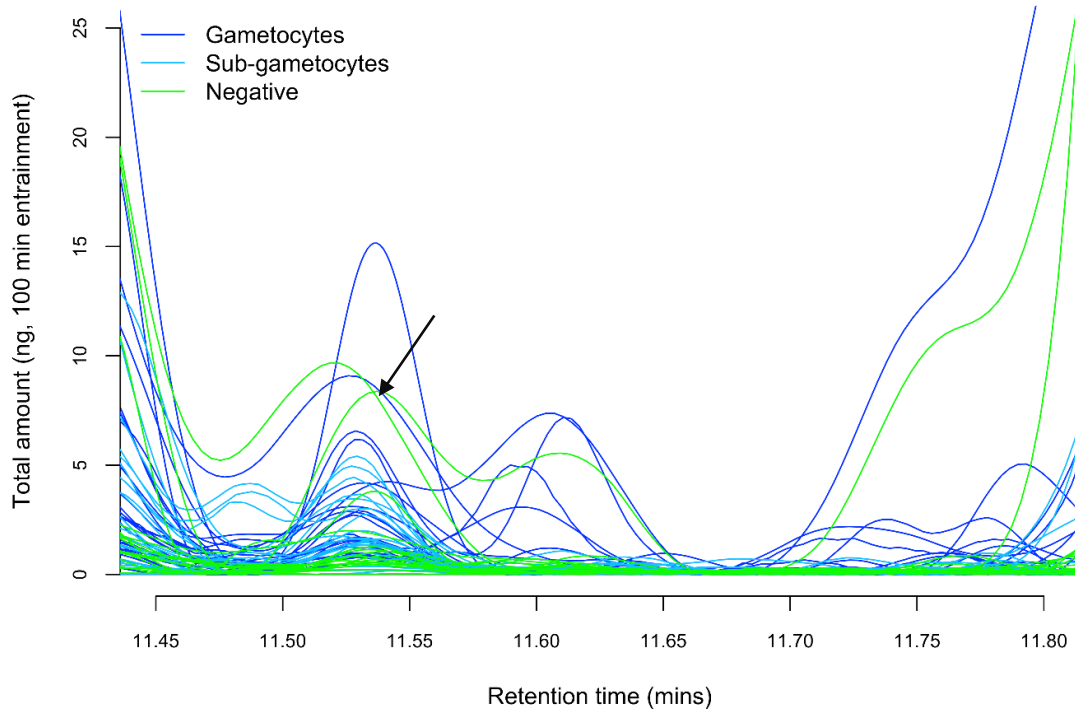


Figure 5-24. 2-Octanone peak (indicated by arrow) in raw gas chromatography output. Individual lines represent odour profile samples, here coloured according to the parasitological status of the individual from whom the odour sample was taken. ‘Gametocytes’, samples from individuals with >50 gametocytes/ μL blood or gametocyte stages by microscopy; ‘sub-gametocyte’, samples from individuals with <50 gametocytes/ μL blood; ‘negative’, samples from parasite-free individuals. Asexual-stage-only carriers are excluded for clarity, as compound production was not significantly increased.

Hexanal (RI 774)

While hexanal production was not significantly predicted by ‘total density’ categories ($P=0.458$), there was a significant treatment effect by ‘gametocyte’ categories ($P=0.036$) (Figure 5-25A, Figure 5-26). Here, individuals in the ‘gametocyte’ group produced more hexanal than those in the ‘negative’ or ‘asexual’ groups, while those with lower density gametocytes (‘sub-gametocyte’ group) had elevated hexanal, but to a lesser extent (only significantly greater than the ‘asexual’ group) (LSD, 5%). That there was no relationship between hexanal production and the total density of parasites, or indeed ‘positive vs. negative’ categorisation ($P>0.05$), indicates this is probably a gametocyte-specific effect. In the ‘gametocyte’ categories model weight and weight² were significant covariates ($P=0.002$ and $P=0.01$ respectively) (Table 5-9), a positive (0.29) and negative (-0.01) effect indicating an inverted parabolic relationship between hexanal production and weight (Figure 5-25B). The predicted peak in hexanal production, averaged over all parasitological categories, was at 21.09 kg.

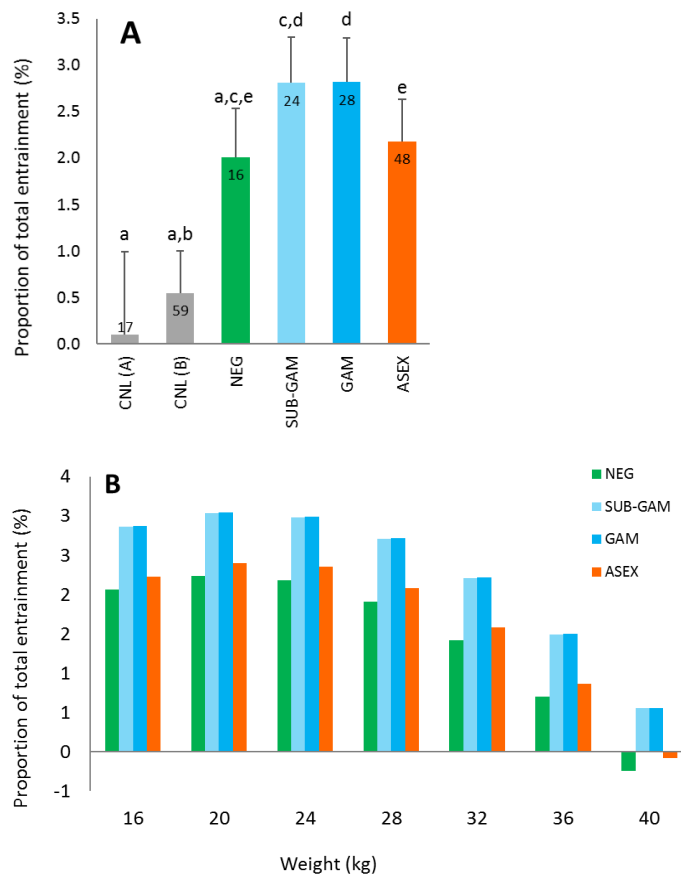


Figure 5-25. Hexanal production (relative to all compounds in odour sample) per group. Predicted means (+SE) given by linear mixed modelling (REML). (A) ‘Gametocyte’ categorisation; ‘NEG’=negative, ‘SUB-GAM’ and ‘GAM’ refer approximately to gametocyte densities of lesser or greater than 50/ μ L, ‘ASEX’=parasites but no gametocytes, CNL(A)=solvent control, CNL(B)=empty bag control. Sample size in bar ends, significant pairwise differences indicated by different letters above bars, tested by Least Significant Differences ($P < 0.05$). (B) Hexanal production increased and then decreased with increasing weight. Samples split by parasitology (‘gametocyte’ categories, control groups modelled but omitted as not biologically appropriate). Predictions for REML covariates have no sample size, population parameters given in Table 5-3 and appendix 5.10.

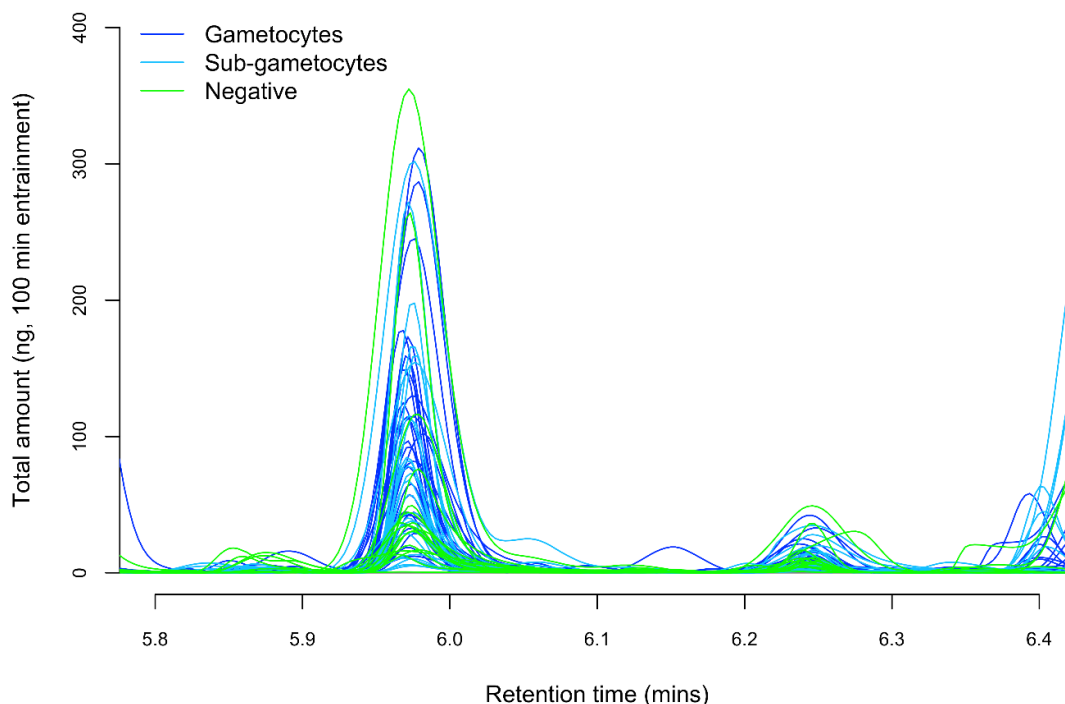


Figure 5-26. Hexanal peak in raw gas chromatography output. Individual lines represent odour profile samples, here coloured according to the parasitological status of the individual from whom the odour sample was taken. 'Gametocytes', samples from individuals with >50 gametocytes/ μL or gametocyte stages by microscopy; 'sub-gametocyte', samples from individuals with <50 gametocytes/ μL ; 'negative', samples from parasite-free individuals. Asexual-stage-only carriers are excluded for clarity, as compound production was not significantly increased.

1-Octen-3-one (RI 958)

As in the case of hexanal, while there was no significant effect of 'total density' categories on the production of 1-octen-3-one ($P > 0.05$), 'gametocyte' categories did significantly predict production ($P = 0.008$) (Figure 5-27, Figure 5-28A). Here, the higher density gametocyte group produced significantly more than the 'asexual' or 'negative' groups (LSD, %), and production was also elevated in the 'sub-gametocyte' group. In this model, the covariates Hb, age and age² were significant, with a negative effect of Hb (-0.08) indicating decreased production with increased Hb (Figure 5-28B). There was a positive effect of age 0.16) and a negative effect of age² (-0.01), indicating a parabolic relationship (Figure 5-28C); however, both age and age² interacted with the treatment term. This meant that for individuals harbouring gametocytes, production of 1-octen-3-one decreased and then increased with age (with troughs at 8.61 years, 'sub-gametocyte', and 9.54 years 'gametocyte'), while for those in the 'negative' or 'asexual' group, production increased and then decreased with age (with peaks at 8.93 years, 'negative', and 7 years 'asexual').

Identification of 1-octen-3-one was complicated by co-elution with phenol in the GC-EAG samples (chapter 6), where the peak was found to be EAG-active. There, co-elution occurred because the GC-EAG programme was shorter to ensure antennal firing for the duration of sample elution, while in this direct analysis of GC traces the peaks were separate. Both compounds were definitively identified by peak enhancement, but due to this complication, only one sample was co-injected with 1-octen-3-one, rather than several as is preferable (Appendix 5.11).

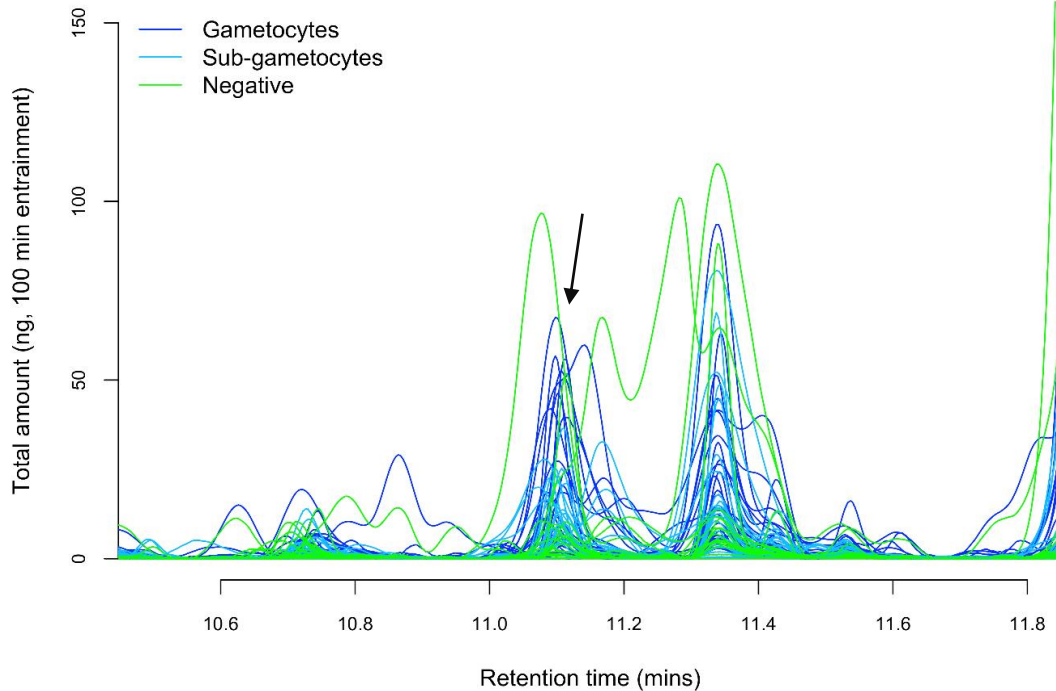


Figure 5-27. 1-Octen-3-one peak in raw gas chromatography output. Individual lines represent odour profile samples, here coloured according to the parasitological status of the individual from whom the odour sample was taken. 'Gametocytes', samples from individuals with >50 gametocytes/ μL blood or gametocyte stages by microscopy; 'sub-gametocyte', samples from individuals with <50 gametocytes/ μL blood; 'negative', samples from parasite-free individuals. Asexual-stage-only carriers are excluded for clarity, as compound production was not significantly increased.

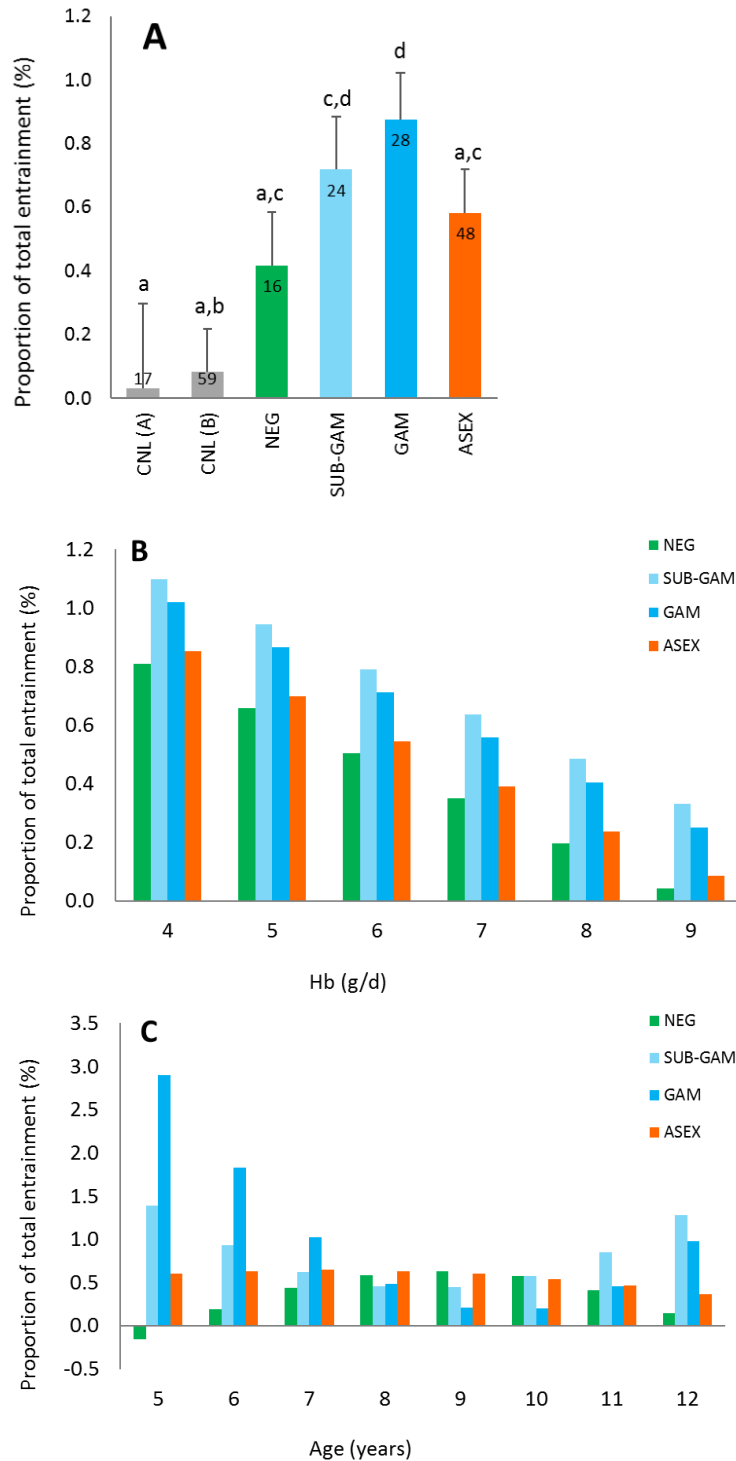


Figure 5-28. 1-Octen-3-one production (relative to all compounds in odour sample) per group. Predicted means (+SE) given by linear mixed modelling (REML). (A) ‘Gametocyte’ categorisation; ‘NEG’=negative, ‘SUB-GAM’ and ‘GAM’ refer approximately to gametocyte densities of lesser or greater than 50/ μ L, ‘ASEX’=parasites but no gametocytes, CNL(A)=solvent control, CNL(B)=empty bag control. Sample size in bar ends, significant pairwise differences indicated by different letters above bars, tested by Least Significant Differences ($P < 0.05$). (B) 1-Octen-3-one production decreased with increasing Hb. Samples split by parasitology (‘gametocyte’ categories, control groups modelled but omitted as not biologically appropriate). Model predictions have no sample size. (C) Age and age² significantly influenced 1-octen-3-one production, however both terms interacted with the main treatment effect (‘gametocyte’ categories). Samples split by parasitology (‘gametocyte’ categories, control groups modelled but omitted as not biologically appropriate). Predictions for REML covariates have no sample size, population parameters given in Table 5-3 and appendix 5.10.

5.4.4 Summary tables: infection-associated compounds

Table 5-4. Mean amount of compound produced per group ('total density' categories), expressed as a percentage of all compounds in odour samples. Predicted means derived from linear mixed modelling (REML). CNL(A) is solvent control, CNL(B) is empty bag control. MHO=6-methyl-5-hepten-2-one, *designates co-elution.

Compound of interest			Mean amount of compound produced per category (%)					
Name	RI	CAS #	Higher	Gametocyte	Lower	Negative	CNL(A)	CNL(B)
Nonanal	1084	124-19-6	16.36	14.41	11.94	12.95	1.04	3.64
Heptanal	880	111-71-7	0.98	0.95	0.77	0.70	0	0.25
Octanal	982	124-13-0	5.30	5.40	4.19	4.09	0.76	1.22
(E)-2-Octenal	1035	2548-87-0	0.68	0.68	0.67	0.50	0	0.24
(E)-2-Decenal	1240	3913-81-3	1.99	2.32	2.16	1.00	0	0.36
MHO & 1-octen-3-ol*	965	110-93-0, 3391-86-4	0.72	0.62	0.49	0.66	0.01	0.32
2-Octanone	971	111-13-7	0.05	0.09	0.04	0.03	0	0.02

Table 5-5. Mean amount of compound produced per group ('quartile' categories), expressed as a percentage of all compounds in odour samples. Predicted means derived from linear mixed modelling (REML). Quartile analysis was conducted for those compounds where production appeared to be correlated with parasite density in the 'total density' categorisation. Densities are (1), low; (2), medium-low; (3), medium-high and (4), high. CNL(A) is solvent control, CNL(B) is empty bag control, Gam=gametocyte category, Neg=negative category, MHO=6-methyl-5-hepten-2-one, *designates co-elution.

Compound of interest			Mean amount of compound produced per category							
Name	RI	CAS #	1	2	3	4	Gam	Neg	CNL(A)	CNL(B)
Heptanal	880	111-71-7	0.78	0.87	0.97	1.00	0.95	0.69	0	0.24
Octanal	982	124-13-0	4.21	4.72	5.35	5.27	5.42	4.09	0.75	1.22
Nonanal	1084	124-19-6	11.19	12.85	15.41	15.99	14.05	11.14	2.79	0.00
MHO & 1-octen-3-ol*	965	110-93-0, 3391-86-4	0.56	0.40	0.72	0.77	0.61	0.65	0.31	0.01

Table 5-6. Mean amount of compound produced per group ('gametocyte' categories), expressed as a percentage of all compounds in odour samples. Predicted means derived from linear mixed modelling (REML). Sub-gam = sub-gametocyte, CNL(A) is solvent control, CNL(B) is empty bag control. MHO=6-methyl-5-hepten-2-one, *designates co-elution.

Compound of interest			Mean amount of compound produced per category					
Name	RI	CAS #	Asexual	Gam	Sub-gam	Neg	CNL(A)	CNL(B)
Hexanal	774	66-25-1	2.18	2.82	2.81	2.01	0.10	0.55
1-Octen-3-one	958	4312-99-6	0.58	0.87	0.72	0.42	0.03	0.08
Octanal	982	124-13-0	4.09	4.92	3.61	3.19	0.05	0.52
(E)-2-Octenal	1035	2548-87-0	0.57	0.84	0.75	0.47	0	0.25
(E)-2-Decenal	1240	3913-81-3	1.94	2.87	1.58	1.02	0	0.36
MHO & 1-octen-3-ol*	965	110-93-0, 3391-86-4	0.54	0.70	0.70	0.64	0.01	0.34

Chapter 5: Odour profile analysis of children naturally infected with *Plasmodium* species

Table 5-7. Mean amount of compound produced per group ('positive vs. negative' categories), expressed as a percentage of all compounds in odour samples. Predicted means derived from linear mixed modelling (REML). CNL(A) is solvent control, CNL(B) is empty bag control.

Compound of interest			Mean amount of compound produced per category			
Name	RI	CAS #	Positive	Negative	CNL(A)	CNL(B)
Heptanal	880	66-25-1	0.910	0.692	0	0.244
(E)-2-Octenal	1035	2548-87-0	0.643	0.495	0	0.240
(E)-2-Decenal	1240	3913-81-3	2.109	1.010	0	0.369

Table 5-8. Significance of covariates and factors from linear mixed modelling (REML) for infection-associated compounds. Here parasitology predicted by 'total density' categories. Sample type refers to human odour profile sample or control (solvent or empty bag). Round is sequential sampling round. P/C=parasitological category. MHO=6-methyl-5-hepten-2-one, *designates co-elution.

Compound	Co-v/Factors	n.d.f.	d.d.f.	F. statistic	P value	Categories with significant pairwise differences
Heptanal	P/C: total density	3	179.6	2.24	0.085	Higher vs. negative
	Sample type	2	8.1	31.21	<0.001	Lower, higher and gametocyte vs. CNL(A)/(B) Negative vs. CNL(B) only
Octanal	P/C: total density	3	174.1	2.88	0.038	Higher vs. lower
	Sample type	2	7.8	47.85	<0.001	Lower, higher and gametocyte vs. CNL(A)/(B)
	Age	1	97.1	10.4	0.002	Negative vs. CNL(B) only
	Age ²	1	94.8	5.59	0.02	
	Sex	1	87.4	9.95	0.002	
Nonanal	P/C: total density	3	176.2	3.13	0.027	Higher vs. lower
	Sample type	2	7.7	44.86	<0.001	Negative, higher and gametocyte vs. CNL(A)/(B)
	Hb	1	181.9	4.54	0.034	Lower vs. CNL(B) only
	Hb ²	1	181.3	6.92	0.009	
(E)-2-Octenal	P/C: total density	3	160.4	1.8	0.15	Lower, higher and gametocyte vs. CNL(A)/(B)
	Sample type	2	8.4	8.53	0.01	
	Hb	1	180.3	6.42	0.012	
	Round	3	125	3.75	0.013	
(E)-2-Decenal	P/C: total density	3	172.7	1.53	0.209	Lower, higher and gametocyte vs. CNL(A)/(B)
	Sample type	2	9.7	11.68	0.003	
	Age	1	78.7	13.29	<0.001	
MHO & 1-octen-3-ol*	P/C: total density	3	174	1.85	0.141	Negative vs. CNL(A)/(B)
	Sample type	2	8.6	9.06	0.008	Higher and gametocyte vs. CNL(A)
	Round	3	149.4	4.93	0.003	
2-Octanone	P/C: total density	3	176.4	5.41	0.001	Gametocyte vs. negative, lower, higher, CNL(A)/(B)
	Sample type	2	10.1	12.04	0.002	Lower and higher vs. CNL(A) and (B)

Chapter 5: Odour profile analysis of children naturally infected with *Plasmodium* species

Table 5-9. Significance of covariates and factors from linear mixed modelling (REML) for infection-associated compounds. Here parasitology predicted by 'gametocyte' categories. Sample type refers to human odour profile sample or control (solvent or empty bag). Round is sequential sampling round, Hb=haemoglobin, P/C=parasitological category. MHO=6-methyl-5-hepten-2-one, *designates co-elution.

Compound	Co-v/Factors	n.d.f.	d.d.f.	F. statistic	P value	Categories with significant pairwise differences
Hexanal	P/C: gametocytes	3	181.6	2.9	0.036	Sub-gametocyte vs. asexual
	Sample type	2	7.9	45.95	<0.001	Gametocyte vs. negative and asexual
	Weight	1	181.3	10.04	0.002	Asexual, sub-gametocyte and gametocyte vs. CNL(A) and (B)
	Weight ²	1	181.2	6.81	0.01	Negative vs. CNL(B) only
1-Octen-3-one	P/C: gametocytes	3	174.9	4.05	0.008	Gametocyte vs. negative and asexual
	Sample type	2	8.2	31.76	<0.001	Gametocyte and sub-gametocyte vs. CNL(A)
	Age	1	174.5	30.05	<0.001	
	Age ²	1	174.5	9.78	0.002	
	Hb	1	176.3	7.07	0.009	
	Age.gam cats	3	174.7	8.51	<0.001	
	Age ² .gam cats	3	174.6	11.37	<0.001	
Octanal	P/C: gametocytes	3	175.9	2.5	0.061	Gametocyte vs. negative and sub-gametocyte
	Sample type	2	7.8	49.13	<0.001	Gametocyte, sub-gametocyte and asexual vs. CNL(A)/(B)
	Age	1	98.9	10.75	0.001	Negative vs. CNL(B)
	Age ²	1	100.3	5.9	0.017	
	Sex	1	89.1	10.93	0.001	
	Age.gam cats	3	176	3.19	0.025	
(E)-2-Octenal	P/C: gametocytes	3	177.9	3.01	0.031	Gametocyte and sub-gametocyte vs. CNL(A)/(B)
	Sample type	2	8.3	8.53	0.01	Asexual vs. CNL(B)
	Hb	1	177.6	6.67	0.011	
	Round	3	128	3.15	0.027	
(E)-2-Decenal	P/C: gametocytes	3	181.9	3.55	0.016	Gametocyte vs. all groups
	Sample type	2	9.6	12.16	0.002	Gametocyte and asexual vs. CNL(A)/(B)
	Age	1	77.7	13.62	<0.001	Sub-gametocyte vs. CNL(B)
MHO & 1-octen-3-ol*	P/C: gametocytes	3	161.6	1.64	0.182	Gametocyte and sub-gametocyte vs. CNL(A)/(B)
	Sample type	2	8.5	8.84	0.008	Asexual vs. CNL(B)
	Round	3	152.6	5.35	0.002	Negative vs. CNL(A)
2-Octanone	P/C: gametocytes	3	174.7	5.24	0.002	Gametocyte vs. all groups
	Sample type	2	11	12.81	0.001	Asexual, sub-gametocyte and gametocyte vs. CNL(A) and (B)

Chapter 5: Odour profile analysis of children naturally infected with *Plasmodium* species

Table 5-10. Significance of covariates and factors from linear mixed modelling (REML) for infection-associated compounds. Here parasitology predicted by 'positive vs. negative' categories. Sample type refers to human odour profile sample or control (solvent or empty bag). Round is sequential sampling round, Hb=haemoglobin, P/C=parasitological category.

Compound	Co-v/Factors	n.d.f.	d.d.f.	F. statistic	P value	Categories with significant pairwise differences
Heptanal	P/C: positive vs. negative	1	184.2	2.72	0.101	Positive vs. CNL(A)/(B)
	Sample type	2	8.1	30.75	<0.001	
(E)-2-Octenal	P/C: positive vs. negative	1	173.1	4.28	0.04	Positive vs. CNL(A)/(B)
	Sample type	2	8.4	8.54	0.01	
	Hb	1	182.1	6.47	0.012	
	Round	3	123.9	4.01	0.009	
(E)-2-Decenal	P/C: positive vs. negative	1	179.9	4.2	0.042	Positive vs. negative, CNL(A)/(B)
	Sample type	2	9.9	11.79	0.002	
	Age	1	79.2	13.37	<0.001	

Table 5-11. Significance of covariates and factors from linear mixed modelling (REML) for infection-associated compounds. Here parasitology predicted by 'quartile' categories. Sample type refers to human odour profile sample or control (solvent or empty bag), round is sequential sampling round, P/C=parasitological category, *designates colution.

Compound	Co-v/Factors	n.d.f.	d.d.f.	F. statistic	P value	Categories with significant pairwise differences
Heptanal	P/C: quartiles	5	178	1.19	0.317	No important pairwise differences
	Sample type	2	8.1	31.65	<0.001	
Octanal	P/C: quartiles	5	171.6	1.26	0.284	No important pairwise differences
	Sample type	2	7.8	47.49	<0.001	
	Age	1	100	8.69	0.004	
	Age ²	1	97.9	4.67	0.033	
	Sex	1	89.5	9.86	0.002	
Nonanal	P/C: quartiles	5	176.4	1.82	0.111	Low and negative vs. high
	Sample type	2	7.8	42.69	<0.001	
MHO & 1-octen-3-ol*	P/C: quartiles	5	172.9	2.01	0.08	Medium-high and high vs. medium-low
	Sample type	2	8.4	9.14	0.008	
	Round	3	144.9	4.8	0.003	

5.4.5 Total amount

While there was a trend for individuals in the ‘higher density’ and ‘gametocyte’ groups to produce a greater total amount of compounds (i.e. all volatiles that eluted between RI 700 and RI 2500, captured by Porapak during the 100-minute entrainment), overall there was no significant effect of treatment by any parasitological grouping (‘total density’, ‘gametocyte’ or ‘positive vs. negative’, all $P>0.05$) (Figure 5-29). In addition to the anticipated significant effect of sample type (i.e. human odour profile vs. controls, $P<0.001$), there was a significant and negative effect of ‘day of the year’ (DofY, $P<0.001$), and positive effect of DofY² ($P=0.036$), indicating a parabolic relationship with a decrease to a minimum (at day 131) and subsequent rise in total amount, over time. However, the squared function (parabolic relationship) interacted with sample type, and examination of the relationship revealed that the subsequent rise in total amount only manifested in the closed bag control. In all human odour samples, the total amount of compounds collected decreased steadily throughout the year (Figure 5-29B).

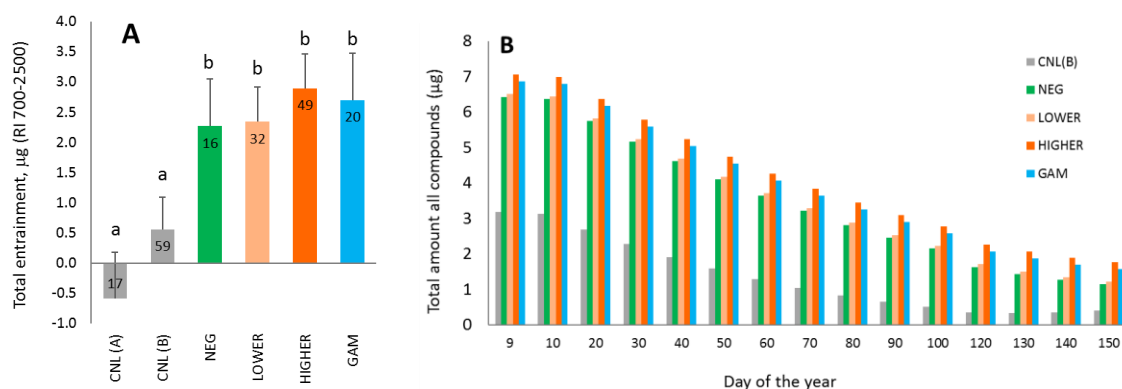


Figure 5-29 (A) Total amount of all compounds collected (100-minute odour profile sampling). Predicted means (+SE) given by linear mixed modelling (REML). Sample size in bar ends, significant pairwise differences indicated by different letters above bars, tested by Least Significant Differences ($P<0.05$). ‘Total density’ categorisation; ‘NEG’=negative, ‘lower’ and ‘higher’ refer approximately to parasite densities of lesser or greater than 50 p/µL, ‘GAM’=microscopic gametocytes, CNL(A) is solvent control, CNL(B) is empty bag control. (B) Total amount of sample decreased over the sampling period, with a subsequent late slight increase in CNL(B) (closed bag control). No values for the analytical control (A; solvent) as not relevant to sampling period.

Table 5-12. Significance of covariates and factors from linear mixed modelling (REML) for total amount of sample. All three parasitological categories were attempted. Sample type refers to human odour profile sample or control (solvent or empty bag). P/C=parasitological category.

Parasitological grouping	Covariates and factors	n.d.f.	d.d.f.	F. statistic	P value
Total density categories	P/C: total density	3	179.8	0.3	0.828
	Sample type	2	161.5	17.72	<0.001
	Day of the year	1	147.1	41.92	<0.001
	Day of the year ²	1	148.8	4.46	0.036
	Day of the year*sample type	1	6.1	136.4	0.015
Gametocyte categories	P/C: gametocytes	3	177	0.31	0.816
	Sample type	2	160.2	17.68	<0.001
	Day of the year	1	144	40.72	<0.001
	Day of the year ²	1	145.8	4.53	0.035
	Day of the year*sample type	1	135.6	6.70	0.011
Positive vs. negative categories	P/C: positive vs. negative	1	185.3	0.02	0.895
	Sample type	2	163.5	17.71	<0.001
	Day of the year	1	146.8	41.63	<0.001
	Day of the year ²	1	148.3	4.51	0.035
	Day of the year*sample type	1	138.7	6.22	0.014

5.4.6 Non-significant: compounds not associated with infection

Peak 797 (octane and solvent co-eluting), nonane, limonene, decanal and hexadecane were tested for association with parasitology by all three predictor variables: 'total density', 'gametocyte' and 'positive vs. negative' categories. None were significantly predicted by parasitological status. Day of the year (DofY), DofY² and Round all significantly affected decanal production (DofY/DofY² $P < 0.001$, round $P < 0.05$), with a general decrease in compound collection according to round. While the production of hexadecane was significantly predicted by 'positive vs. negative' categories, this was probably due to a highly significant pairwise difference between the two controls, as large amounts of hexadecane were found in the bag control. There was no significant difference between positive and negative groups (LSD, 5 %).

5.4.7 Proportion of total odour sample and ranked compound production

Of 117 odour samples included in the above analyses, nonanal was the most highly produced compound in 67 (57 %) samples, with 17 (14 %) and 11 (9 %) samples containing nonanal as the second and third most highly produced, respectively. This means that for 80 % of samples, nonanal was among the top three most highly produced compounds. The average rank for nonanal production among all other compounds (total amount produced during 100-minute entrainment) over the whole dataset was 3.2, while the median rank was 1. For octanal, the average and median ranks were 9 and 4.5 respectively. The average number of non-IAC (here considered to be all compounds entrained other than: nonanal, octanal, heptanal, (*E*)-2-decenal, (*E*)-2-octenal, RI 965, 2-octanone, hexanal and 1-octen-3-one) was 168.27, with IAC making up on average 26.92 % of the total odour profile across all ‘total density’ parasitological categories. In the ‘higher’ category, IAC constituted an average of 30.97 % of the odour profile. The proportion of ‘entire’ odour profile that comprised IAC (compounds determined by all three parasitological categorisations), is given in Figure 5-30.

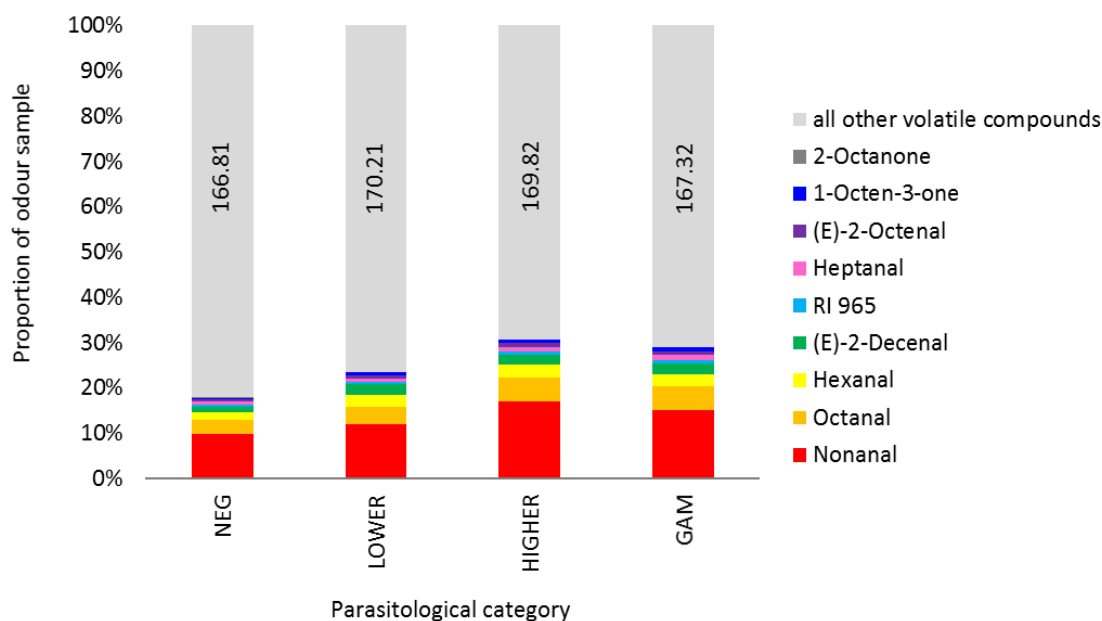


Figure 5-30. The proportion (%) that IAC contributed towards the entire odour profile, grouped by parasitological category (‘total density’ categories used, but compounds from the gametocyte-specific analysis hexanal and 1-octen-3-one are included, to demonstrate their relative contribution to the odour profile). The average number of non-IAC per group (i.e. ‘all other volatile compounds’), annotated in grey bar. RI 965 = co-eluting 6-methyl-5-hepten-2-one and 1-octen-3-ol. Sample sizes are: negative, $n=16$; lower, $n=32$; higher, $n=49$; gametocyte, $n=20$.

5.4.8 Intra-individual changes in IAC production

There was no trend for changed heptanal production by individuals who moved between the 'higher density' and the 'negative' group ($T=0.2$, 14 DF, $P=0.424$), nor by those who remained in either of these categories ($T=0.3$, 20 DF, $P=0.382$) (Figure 5-31). Likewise, for both octanal and nonanal, there was no change in compound production in accordance with parasite density (octanal, decreasing [$T=0.76$, 22 DF, $P=0.229$]; octanal, increasing [$T=0.99$, 18 DF, $P=0.168$]; nonanal, decreasing [$T=1.4$, 22 DF, $P=0.087$]; nonanal, increasing [$T=1.43$, 18 DF, $P=0.085$]), nor was there evidence for changes in production by individuals who remained in either category over two time points (octanal, $T=-1.58$, 24 DF, $P=0.936$; nonanal, $T=-1.56$, 24 DF, $P=0.934$).

Similarly, for both (*E*)-2-octenal and (*E*)-2-decenal, there was no evidence of changes in compound production as parasites were cleared ((*E*)-2-octenal, $T=0.67$, 18 DF, $P=0.256$; (*E*)-2-decenal, $T=0.54$, 18 DF, $P=0.299$) (Figure 5-32) ('positive vs. negative' categorisation). Further evidence for a lack of association between changes in compound production and changes in parasite density were indicated when examining production by individuals who remained positive across two sampling moments. Here, a significant decrease was observed for (*E*)-2-octenal ($T=1.94$, 64 DF, $P=0.029$; (*E*)-2-decenal $T=0.95$, 64 DF, $P=0.173$).

There was, however, a significant decrease in 2-octanone production by individuals who moved from 'gametocyte' to another status (i.e. 'higher density', 'lower density' or 'negative') ($T=2.28$, 8 DF, $P=0.025$), but no difference for those remaining in the same status ($T=1.22$, 46 DF, $P=0.114$) (Figure 5-32).

There was no evidence for changes in the amount of hexanal produced as individuals moved between higher or lower gametocyte density in either direction (increasing gametocyte density, $T=0.67$, 18 DF, $P=0.256$; decreasing gametocyte density, $T=0.55$, 20 DF, $P=0.294$; remaining at same level, $T=-0.92$, 64 DF, $P=0.818$) (Figure 5-33), nor for changes in 1-octen-3-one production as individuals decreased gametocyte density from 'gametocyte' status to 'asexual' or 'negative' ($T=1.27$, 9 DF, $P=0.117$; remaining at same level, $T=0.49$, 36 DF, $P=0.315$).

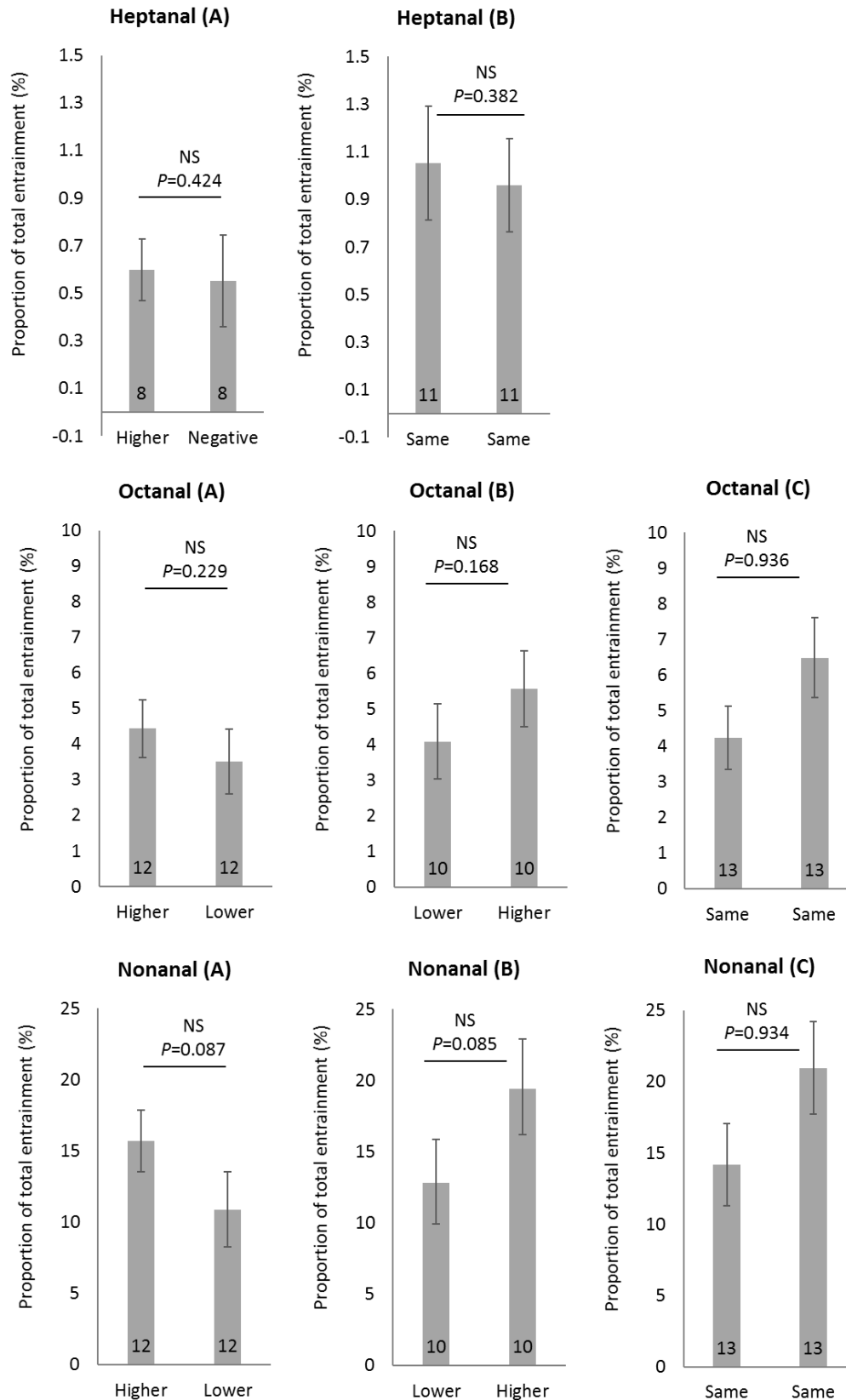


Figure 5-31. Production of IAC within individuals whose parasitological status changed between significant groups (or remained the same) in the 'total density' categorisation. Mean (+/- SEM) compound production (relative to all compounds in odour sample, %) displayed. 'Higher' = 'higher density' category, 'lower' = 'lower density' category. Per compound, 'same' = production by individuals staying within either (A) category. Heptanal, no individuals moved from 'negative' to 'higher'. Significance indicated by P value (T test), sample sizes in bar base.

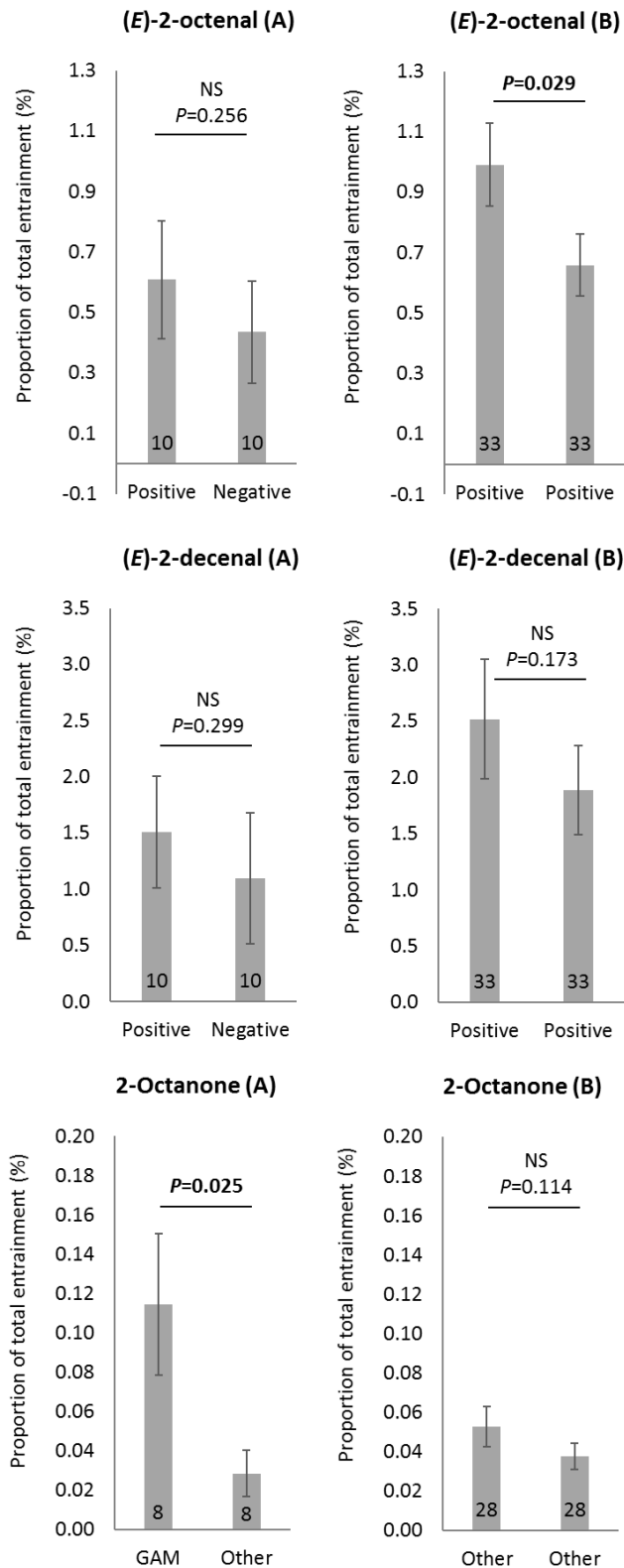


Figure 5-32. Production of IAC within individuals whose parasitological status changed between significant groups (or remained the same). Mean (+/- SEM) compound production (relative to all compounds in odour sample, %) displayed. (E)-2-octenal and (E)-2-decenal, samples presented in 'positive vs. negative' categorisation (Table 5-1), only one individual moved from 'negative' to 'positive' and one from 'negative' to 'negative' (data not shown). 2-Octanone, samples presented in 'total density' categorisation (Table 5-1). 'Gam' = 'gametocyte' category, 'Other' = 'Lower density'/'Higher density'/'Negative'. Only two individuals moved from 'other' to 'gametocyte' (data not shown). Significance indicated by P value (T test), sample sizes in bar base.

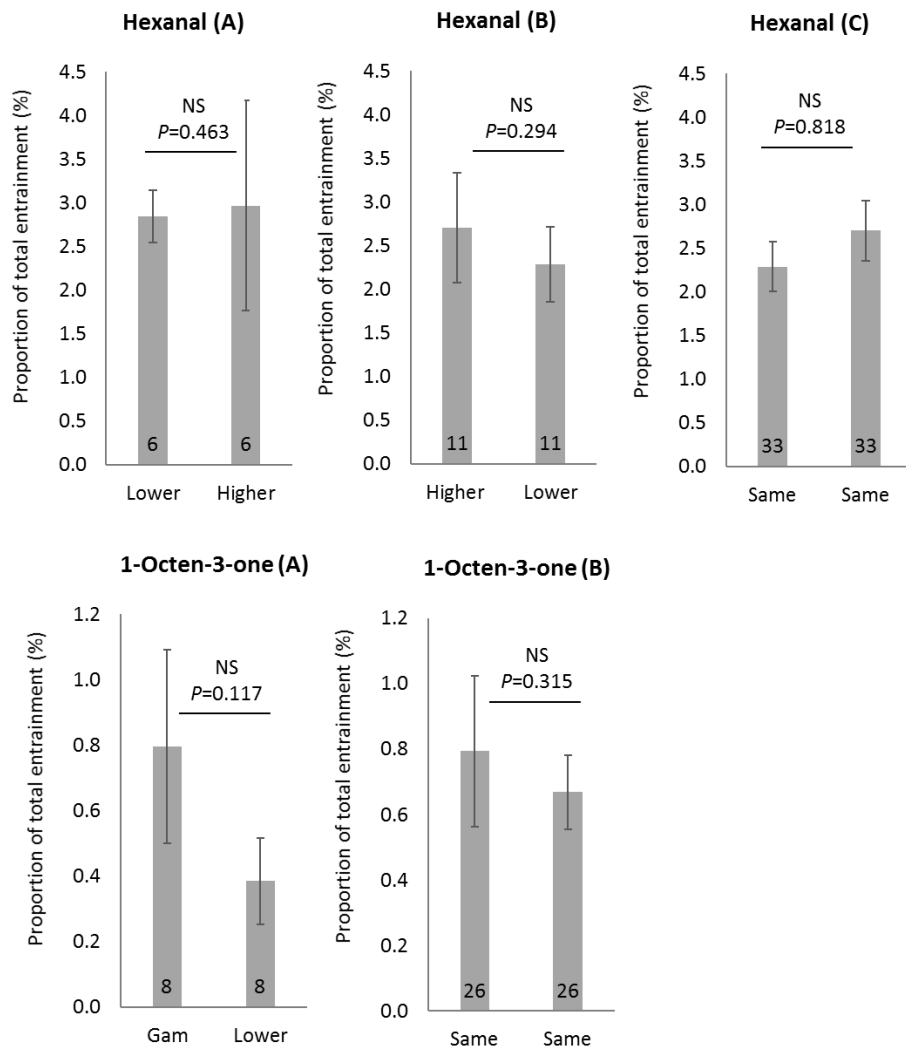


Figure 5-33. Production of IAC within individuals whose parasitological status changed between significant groups (or remained the same) in the 'gametocyte' categorisation. Mean (+/- SEM) compound production (relative to all compounds in odour sample, %) displayed. Hexanal, 'lower' = 'asexual' or 'negative' categories, 'higher' = 'gametocyte' or 'sub-gametocyte'. 1-Octen-3-one, 'Gam' = 'gametocyte' category, 'lower' = 'negative' or 'asexual', only one individual moved from 'lower' to 'gametocyte' (data not shown). Hexanal and 1-octen-3-one, 'same' to 'same' = moving within lower or higher groups. Significance indicated by P value (T test), sample sizes in bar base.

5.5 Discussion

5.5.1 Summary

To test for volatile compounds that were associated with *Plasmodium* infection, the parasitological status of individuals from whom odour samples were taken were categorised in four different ways. Two methods focussed on total parasite density ('total density' and 'quartiles' categories), one on the density of gametocytes present ('gametocyte' categories) and one on the presence of any parasites versus none ('positive vs. negative' categories). These analyses revealed several compounds in the human odour profile that are associated with infection ('infection-associated compounds', IAC). These include the aldehydes hexanal, heptanal, octanal, nonanal, (*E*)-2-octenal, (*E*)-2-decenal, and the ketones 2-octanone and 1-octen-3-one. Production of heptanal, octanal and nonanal (C7-C9) was correlated with the total density of parasites, increasing incrementally with greater densities. Individuals with microscopic gametocytes also produced more aldehydes, yet also often harboured higher total density infections. As modelling C7-C9 production by 'gametocyte' categories was not significant, there was no evidence for a gametocyte-specific effect, with the possible exception of octanal. This, however, was confounded by the association between increased total parasites and increased gametocyte production in this dataset. (*E*)-2-Octenal and (*E*)-2-decenal were found to be produced in greater amounts by all infected persons, and the presence of gametocytes was associated with further increases (a significant effect for (*E*)-2-decenal). The production of hexanal (C6), 1-octen-3-one and 2-octanone was specifically correlated with the presence of gametocytes. The production of peak RI 965 (co-eluting 6-methyl-5-hepten-2-one and 1-octen-3-ol) was decreased at low parasite densities, but with a possible association between increased production and the presence of gametocytes that again was confounded with total parasite density. Overall, these compounds are well-known as components of the human odour profile, and here their association with infection is a quantitative one: that is, all individuals produced these compounds, but the amount emitted changed with *Plasmodium* infection (all increased, other than peak RI 965). The infection-associated aldehydes were among the most highly produced compounds in the odour profile. Changes in the production of IAC, within individuals and over time, did not indicate any shift in production with changing parasitological status, with the exception of 2-octanone. However, low sample sizes may have disallowed such trends to be observed.

5.5.2 *Plasmodium* infection-associated compounds

In a previous study of the attractiveness to mosquitoes of odour cues from *Plasmodium*-infected mice, heightened attractiveness during the 'chronic' phase of infection was accompanied by an overall increase in volatile emissions and the specific increase (or decrease) of certain compounds (De Moraes et al., 2014). To date, that study is the only investigation into the odour profile as a possible basis for differences in attractiveness to mosquitoes between *Plasmodium*-infected and parasite-free individuals. In this thesis, an association between the elevated production of specific volatile compounds in skin odour, and *Plasmodium* infection status, was found. However, an overall increase in volatile emissions from infected persons was not observed. In the murine system, changes in odour profile were restricted to the chronic phase of infection, i.e. the asymptomatic phase after the acute phase in a new infection. Our study included only asymptomatic individuals, as determined by a temperature of less than 37.5 °C, although it is possible that minor symptoms were missed (e.g. a slightly elevated temperature or other malaria-associated symptom). In this malaria-endemic population, in asymptomatic children of 5-12 years, it is probable that the majority were persistent, chronic infections. Although the duration of each infection per individual is unknown in the endemic setting, the 'acute phase' infection profile is generally applicable to the experimental setting, where individuals are exposed to a *Plasmodium* genotype for the first time. De Moraes et al. (2014) describe changes in the (whole body) volatile profile of mice, with a specific focus on the period following subsidence of acute phase symptoms (days 8 to 42 post infection, PI). During this period, they observed an overall elevation of volatile emissions, and changes in the levels of certain compounds, relative to healthy mice. The authors note that mice in the chronic phase (days 13-17 PI) harboured relatively high gametocyte levels, were more attractive to mosquitoes, and had changed volatile emissions. The suggested rationale for odour profile change is that increased mosquito blood-feeding would lead to more *Plasmodium*-infected vectors. However, during these periods, both total parasite densities and gametocyte densities were elevated. In that respect, our study is in agreement with De Moraes et al. (2014), in that changed volatile emissions correlate with higher parasite densities. However, in modelling separately by gametocyte densities, our study found that the production of most infection-associated compounds was increased according to total parasite density, with a gametocyte-specific effect additionally apparent for some compounds but specific only to three (hexanal, 1-octen-3-one and 2-octanone). Further, we did not observe an increase in total emissions. From an evolutionary perspective, we could speculate that a parasite-density dependent transmission signal, generated by all stages, would be functional. This is because in some circumstances,

asexual parasite density indeed correlates with gametocyte density (Koepfli et al., 2015), and greater parasite numbers could provide a stronger signal overall.

Another similarity between these studies is the identification of aldehydes among IAC, with the murine study finding benzaldehyde to be among compounds that statistically predicted infection status. The significance of aldehydes as IAC is discussed below. Finally, it is important to note that the murine study captured all volatiles emitted by entire mice within a sampling chamber. Our study sampled foot volatiles only, and the omission of breath is notable. It is possible that the changes in volatile emissions and attractiveness associated with chronic stage infection in the murine system originated in the breath (De Moraes et al., 2014).

It is interesting to note hexanal has been isolated as a volatile compound from the headspace of the supernatants of *Plasmodium*-infected RBC cultures. Correa et al. (2017) note the presence of this compound above all such cultures, but not above parasite-free cultures, and suggest that the source of hexanal was parasite infection. Another study examined only breath volatiles of individuals who were experimentally-infected with *Plasmodium* parasites, but with no investigation of the entomological relevance (Berna et al., 2015). As for C7-C9 in the current study, the production of specific compounds (thioethers) was correlated tightly with parasite density (all stages, *P. falciparum* parasitaemia). This does not elucidate the origin of such compounds, as both those produced directly by parasites and those produced as a by-product of infection could possibly correlate with parasitaemia levels. It is, however, compelling evidence that the detected signal has been correctly associated with parasite infection. Berna et al. (2015) detected isoprene in the breath of *Plasmodium*-infected individuals, and the likely pathway of production cited was oxidative stress. A similar potential mechanism for production of aldehydes and ketones in the current study is described below.

5.5.3 Aldehydes as a product of oxidative stress

Oxidative stress is a condition characterised by a profusion of chemically reactive oxygen species (ROS), resulting from an imbalance between pro-oxidants and anti-oxidants. ROS are damaging to cells structures, and in malaria, it is thought that oxidative stress has an important role in the development of systemic complications (Percário et al., 2012). Oxidative stress occurs in malaria for several reasons. For growth and replication, malaria parasites in the red blood cells digest haemoglobin (Moore et al., 2006), and during this process they separate haem from globin, releasing toxic free haem (ferri/ferroprotoporphyrin IX (FP)) and ROS (Becker et al., 2004). While

the sequestration of FP into malaria pigment, hemozoin, and possible other FP degradation pathways, captures much of the FP, any that escapes neutralisation will cause redox damage both to host and parasite cells (Becker et al., 2004). In addition to this process, ROS are produced by activated macrophages as the host's immune system attempts to tackle the parasite (Fabbri et al., 2013), although this may be countered, as ingestion of hemozoin by macrophages has been found to reduce their phagocytic function and ROS release (Cunnington et al., 2012; Schwarzer et al., 1992; Schwarzer and Arese, 1996).

One manifestation of oxidative stress is lipid peroxidation, which is recognised to be particularly severe in children with malaria and concomitant riboflavin (vitamin B2) deficiency (Das and Nanda, 1999), known to be highly prevalent in low-income countries (McLean et al., 2007). Lipids, for example those found in membrane structures, are susceptible to oxidation because they have many reactive double bonds (Porter et al., 1995). Downstream products of lipid peroxidation are reactive aldehydes and ketones, and some are used as biomarkers of lipid peroxidation, e.g. malondialdehyde and isoprostanes (Ho et al., 2013). Taken together, it is possible that the increased aldehyde production observed here, and correlated with high parasite density infections, originated via malaria-induced oxidative stress.

5.5.4 Aldehyde production by human skin and the association with disease

It is well established that aldehydes are among the many volatiles emitted by the human skin (Bernier et al. 1999; Curran et al. 2005; Penn et al. 2007; Curran et al. 2010; Harraca et al. 2012; Dormont et al. 2013b), indeed C7-C10 are frequently cited as being among the predominant components of human skin odour (reviewed in Dormont et al. (2013a)). Some studies have demonstrated an association between nonanal or other aldehydes and ageing (Gallagher et al., 2008; Haze et al., 2001; Yamazaki et al., 2010). Both nonanal and 2-nonenal were found to be increased in older individuals, and the likely synthesis pathway was thought to be lipid peroxidation of fatty acids. Haze et al. (2001) noted that (*E*)-2-octenal, another aldehyde IAC in the current study, can be formed by the oxidative degeneration of sebaceous components, specifically, the fatty acids palmitoleic and vaccenic acid. However, both (*E*)-2-octenal and (*E*)-2-decenal would probably be produced by skin bacteria, and production by oxidative stress might be alternatively or in addition to this (Prof. J. Pickett, pers.comm., 02/2017). In examining the headspace composition of fresh and incubated sweat, a study found that of the total amount of compounds sampled, nonanal comprised 2.4 % in fresh sweat and 0.6 % in incubated sweat (Meijerink et al., 2000). Additionally, heptanal, hexanal and octanal were present in the fresh

but not the incubated samples. It seems likely that this decrease is a result of the instability of the aldehydes due to their propensity to oxidise in air (Trombetta et al., 2002). However, the proportions cited by Meijerink et al. (2000) are considerably smaller than those found here, where nonanal contributed on average 9.8 % of the total odour profile in parasite-free individuals and 17.2 % for those with higher parasite density infections. It should also be noted that aldehydes are not specific to human skin, with birds, cow, donkey, goat and sheep all shown to emit these compounds (Jaleta et al., 2016; Syed and Leal, 2009; Tchouassi et al., 2013).

Aldehydes have been found to signify the presence of disease, and this is most often cited as a consequence of oxidative stress. Many studies have investigated volatile organic compounds present in the breath of patients with disorders of the lungs, with the obvious advantage that the pathology of the disease is proximate. Among those, aldehydes have been significantly associated with tuberculosis (Kwiatkowska et al., 1999; Phillips et al., 2007) and lung cancer (Chen et al., 2007; Fuchs et al., 2010). In one study, a pattern recognition algorithm was used to discriminate between volatile compounds from sputum cultures that were positive or negative for *Mycobacterium tuberculosis*. The technique enabled positive cultures to be distinguished with 82.6 % sensitivity and 100 % specificity, with both nonanal and heptanal being among the best discriminative compounds (Phillips et al., 2007). Oxidative stress leading to lipid peroxidation was cited as the mechanism for increased aldehyde production in the affected patients, probably because of the presence of fatty acids in tumour cell membranes (Buljubasic and Buchbauer, 2015). Pentanal, hexanal, octanal and nonanal were found to be exhaled in significantly higher concentration in patients with lung cancer relative to healthy or smoking individuals, although concentrations of exhaled acetaldehyde, propanal, butanal, heptanal and decanal were not significantly different (Fuchs et al., 2010). Elevated concentrations of hexanal and heptanal in the headspace of blood have also been successfully used as biomarkers of lung cancer (Deng et al., 2004; Li et al., 2005), and these and other aldehydes were found to be elevated in patients with childhood cancer (Yazdanpanah et al., 1997). Besides their association with disease, aldehydes have been found to be upregulated in urine following exercise. Hexanal, heptanal, octanal, nonanal and malondialdehyde, again investigated as markers of lipid peroxidation, were examined at time points before and after 60 minutes of cycling exercise. Relative to the day before, they found a significant increase in butanal (in urine) on the day of exercise, and on the following day they found borderline significant increases in octanal and nonanal (Orhan et al., 2004).

5.5.5 Other mechanisms of aldehyde production

Alternatively, or additionally, the aldehydes found here may have been produced directly by *Plasmodium* parasites. In a recent publication, Emami and colleagues (2017) found the aldehydes C8-C10 to be increased in the headspace above red blood cells (RBC) that had been supplemented by (*E*)-4-hydroxy-3-methyl-but-2-enyl pyrophosphate (HMBPP) (hmbRBC). HMBPP is a precursor in the 2-C-methyl-*D*-erythritol 4-phosphate (MEP) pathway, used by *P. falciparum* for isoprenoid production. Headspace extracts from HmbRBC were found to contain C8-C10, monoterpenes and increased CO₂. Both HmbRBC and gametocyte-infected RBC cultures were more attractive to *An. gambiae* s.l. than un-infected RBC, and the authors concluded that HMBPP triggered enhanced release of these compounds in infected red blood cells (iRBC). However, one unresolved issue of this study is the proposed source of terpene compounds from HmbRBC. Red blood cells have no mitochondria, and as such no organelle would be present that synthesises isoprenoids using the MEP route. The study followed another, in which the MEP pathway, not present in animals and fungi, was suggested as the probable source of plant-associated terpene compounds isolated above iRDC cultures (Kelly et al., 2015). Both studies, however, were laboratory-based bioassays, therefore significantly oversimplifying the complex host-parasite relationships that occur in a natural *Plasmodium* infection. Care must be taken in extrapolating such results to a malaria-endemic context. In the current study, the production of aldehydes is increased in individuals with higher-density *Plasmodium* infections. The extent to which the release of volatiles from iRBC would contribute to a profound and systemic increase in aldehyde production, caused by malaria-induced oxidative stress, remains unexplored.

It is important to note that while the lipid peroxidation pathway for aldehyde production is well-established, skin microflora are also known to produce aldehydes. This is particularly relevant to the current study, as odour profiles were sampled from the feet. Anaerobic skin bacteria can be found in hair follicles and sebaceous glands and can produce long chain fatty acids, which are subsequently metabolised into other products, including aldehydes, by aerobic bacteria (Leyden et al. (1991), in Gallagher et al. 2008).

5.5.6 Aldehydes and entomology

The aldehydes heptanal, octanal and nonanal were shown to be electroantennographically active (EAG-active, stimulating an antennal response) to *Anopheles coluzzii* mosquitoes in chapter 6, where their entomological significance is discussed. There is little information regarding an entomological response of any species to the aldehydes (*E*)-2-decenal and (*E*)-2-octenal. These two compounds constitute the alarm pheromone of the brown marmorated stink bug (*Halyomorpha halys*), and have been shown to have antimicrobial properties (Sagun et al., 2016; Trombetta et al., 2002). (*E*)-2-decenal was shown to elicit antennal response in female *Culex quinquefasciatus* (Cooperband et al., 2008), and (*E*)-2-octenal was detected by coupled gas chromatography electroantennography by *An. arabiensis* (Jaleta et al., 2016). Therefore, it is possible that *Anopheles* mosquitoes respond to these two compounds.

Hexanal, found here to be associated with gametocyte carriage, has been previously identified as EAG-active to *Aedes aegypti* (Logan et al., 2008) and *An. gambiae* s.s. (Nyasembe et al., 2012). In the latter study, hexanal was then tested alone against solvent in a dual choice olfactometer, and found to be attractive at all five doses tested. In that study hexanal had been identified by GC-EAG of plant volatiles, leading the authors to conclude that hexanal is used by the malaria vector in plant location. The possibility that hexanal is also used in host location, as is possible due to the increased production of hexanal by gametocyte carriers in the current study, may indicate that this aldehyde has important olfactory roles that transcend different physiological states of the mosquito (a similar suggestion is made for nonanal in chapter 6). In behavioural tests of blends, hexanal has been included and found to be attractive to *An. gambiae* and *An. funestus*, and repellent to *Ae. aegypti* and *Cx. quinquefasciatus*. Nyasembe et al. (2014) tested 'animal' and 'plant' lures in a series of field trials using CDC non-light and MMX traps, hexanal being included in the plant lure. A preliminary field trial did not find hexanal to be attractive alone. The 6-component blend ((*E*)-linalool oxide, β -ocimene, hexanal, β -pinene, limonene and (*E*)- β -farnesene) was more attractive than the control to *An. gambiae* in the CDC non-light trap, when presented together with CO₂. The same blend was significantly attractive to *An. gambiae* and *An. funestus* when presented either with or without CO₂ in MMX traps, but only with borderline or no significance for *An. funestus* in CDC non-light traps (Nyasembe et al., 2014). However, without further experimentation (e.g. blend reductions) it is not possible to determine the contribution of hexanal to this attractiveness.

5.5.7 Non-aldehyde infection-associated compounds

The ketone 2-octanone was found to be produced in low amounts, yet was strongly associated with high density gametocyte carriage. Ketones are known volatiles of human skin, and 2-octanone could again be a product of oxidative stress. 2-Octanone, added to a basic blend of ammonia, lactic acid and tetradecanoic acid, was found to significantly reduce attractiveness to *An. gambiae* s.s. at 0.1 % (Smallegange et al., 2012). 3-Octanone was found to be produced by *Pseudomonas aeruginosa* (Filipiak et al., 2012), a known human skin commensal. Further, an olfactory receptor neuron on the maxillary palps of *An. gambiae* was found to respond weakly to 3-octanone, whereas AgOR8, another maxillary palp receptor, displayed a strong response to 3-octanone (Lu et al., 2007). These limited studies do not provide much indication of the likely entomological significance of 2-octanone, which will need to be investigated by behavioural bioassays.

Similarly, production of the ketone 1-octen-3-one (also known as oct-1-en-3-one) was associated with the presence of gametocytes, being elevated by sub-gametocyte carriers (those individuals with lower-density gametocyte infections) and significantly so in those harbouring higher gametocyte densities. This compound has a characteristic metallic smell, and has been incriminated as the component of skin odour that produces a metallic odour after contact with metal iron, or aqueous ferrous iron (Fe^{2+} , as contained in blood) (Glindemann et al., 2006). It is thought that this, and associated compounds, arise via the reaction of skin peroxides with ferrous iron. While the ferrous iron is formed by sweat-mediated corrosion of iron (Glindemann et al., 2006), the skin lipid peroxides are formed by oxidation of skin lipids (Human Metabolome Database, <http://www.hmdb.ca/metabolites/HMDB31309>, accessed 27/06/17). This is again consistent with its production via a mechanism of oxidative stress. Interestingly, it is thought that the human ability to smell this is an evolutionary adaptation for the ability to smell blood. Further, 1-octen-3-one has been isolated in human urine (Wagenstaller and Buettner, 2013).

Finally, interesting trends were observed here for compound RI 965, which was found to contain co-eluting 6-methyl-5-hepten-2-one and 1-octen-3-ol. The overall pattern of production mimicked that of 6-methyl-5-hepten-2-one in the EI cohort (chapter 2), with production reduced by individuals harbouring lower density infections, relative to parasite-free individuals or those with higher density infections. The terpenoid ketone 6-methyl-5-hepten-2-one is a known human skin volatile (Dormont et al., 2013b; Logan et al., 2008; Meijerink et al., 2000), produced by the terpene pathway (Dormont et al. 2013). The alcohol 1-octen-3-ol is a component of

human sweat (Cork and Park, 1996), formed by oxidative breakdown of linoleic acid, an essential fatty acid which is found in the lipids of cell membranes. Both 6-methyl-5-hepten-2-one and 1-octen-3-ol are frequently cited in the literature as host cues for haematophagous insects, including *Anopheles* species (Logan et al., 2010, 2008; Qiu et al., 2011; Takken et al., 1997). However, due to co-elution, it cannot be stated with certainty that the trends observed represent true biological phenomena, and as such, these compounds are not further discussed here.

5.5.8 Further observations

In this study, nonanal was among the top three most highly produced compounds for more than 80 % of the human odour profile samples, with the other IAC (particularly the aldehydes octanal, hexanal, heptanal and (*E*)-2-decenal) also contributing disproportionately. This is an exciting observation, given that heptanal, octanal and nonanal were found to be entomologically active (chapter 6). Greater amounts of these compounds, relative to all other components of the odour profile, will create a signal that is readily detected. It is tempting to speculate that either the malaria parasite has evolved to manipulate the strongest signals in the odour profile, or that the *Anopheles* mosquito has evolved to detect these. Further, such a robust signal could be beneficial from a disease biomarkers perspective.

Finally, it is necessary to address the possibility that individuals who naturally produce more attractive compounds (e.g. the aldehydes, should they turn out to be attractive to mosquitoes) are bitten more frequently, and thus more often contract malaria. This would result in an association between *Plasmodium* infection and increased amounts of these compounds in skin odour. In the current dataset, the only way to test this empirically was by examining changes in compound production within individuals who moved between parasitological groupings. For all IAC other than 2-octanone, there was no trend for decreased production with decreased parasite burden, or vice versa. Additionally, there was evidence of changes in (*E*)-2-octenal production by individuals who remained positive between two time points. It is possible that sample sizes were too small for this type of post-hoc analysis, a result of high levels of loss-to-follow-up in the Kenyan cohort. Perhaps more convincingly, the correlation between parasite density and amount of heptanal, octanal and nonanal produced in the 'quartiles' analysis is not supportive of this theory. *Plasmodium* parasite density fluctuates in an infection, and this alternative hypothesis would correlate high levels of attractive compounds with all, or variable, levels of parasite density.

5.5.9 Other covariates and factors that were associated with infection

It is likely that many sources of variation affected skin odour in this study, some of which were measured and controlled for in the analysis. However, it is likely that other, un-measured, factors further influenced odour profile. That associations between compound production and parasitology were revealed, despite potentially uncontrolled influences, demonstrates the strength of the described relationships.

There was an association between the production of nonanal, (*E*)-2-octenal and 1-octen-3-one with haemoglobin (Hb) levels. The production of both (*E*)-2-octenal and 1-octen-3-one decreased with increasing Hb, while the production of nonanal was greatest at Hb of approximately 6, and decreased with both more and less anaemia (in a parabolic relationship). In no model was there any interaction with treatment, indicating that factors other than *Plasmodium* infection were associated with the production of these compounds (i.e., decreased compound production with increased haemoglobin was also observed in malaria parasite-free children, therefore the trends cannot be ascribed to malaria-induced anaemia). Anaemia is associated with other infectious diseases, including both hookworm and *Schistosoma mansoni*, both endemic in the region (Black et al., 2010; Butler et al., 2012). The decrease in production of (*E*)-2-octenal, 1-octen-3-one and nonanal (in the upper half of the Hb range), as anaemia decreases, could be expected if these compounds are also increased by other anaemia-inducing infections. This may suggest that these IAC are by-products of an immunological response, rather than being specifically associated with *Plasmodium* infection. Low levels of nonanal production in the very anaemic is harder to resolve, although for the majority of the curve there is a negative association (from Hb 6–9 g/dL). One further factor to consider is the frequent occurrence of malaria and helminthiases co-infections. However, such co-infections are thought to protect against anaemia (Nacher et al., 2012), so this may have presented as confounding with *Plasmodium* infection, i.e. those individuals who had malaria (and helminthiases), producing more IAC, had higher Hb.

There was an inverse parabolic association between age and the production of octanal, indicating increased production with age followed by a decrease (peak at eight years). Curiously, the same relationship was seen only for 1-octen-3-one production by ‘asexual’ and ‘negative’ individuals, while for gametocyte carriers (any density) 1-octen-3-one production decreased and then increased with age (with high production in the youngest age groups). Finally, the

production of (*E*)-2-decenal decreased with increasing age, therefore the (non-*Plasmodium* infection-associated) factors contributing to this are more prevalent among younger children.

Octanal production was associated with sex, with males producing significantly more than females. The normal axillary odour of adult males versus females has been compared, and while approximately the same compounds were observed, there were minor qualitative differences in production (Zeng et al., 1996, 1991). Our observation thus may reflect some inherent, sex-specific, variation in octanal production. An inverted parabolic relationship was found between hexanal production and body weight, with an early peak in production followed by a decrease with increasing weight. It is possible that this confounds with age; however, interactions among covariates were not tested. Previous studies have associated aging with the increased production of a specific aldehyde (2-nonenal) (Haze et al., 2001). There, production was associated with increased oxidative stress in older subjects (>40 years). If age does explain the association in the current study, it seems plausible that increased oxidative stress could occur (or peak) in younger age groups, before decreasing (with increased resilience) with age. Again, it is tempting to associate younger children with an increased prevalence of malaria, but there was no confounding in the model between parasitological status and age, which may have been caused by a lack of compound production in parasite-free individuals.

In terms of study design, round (sampling moment) had a significant effect on the production of (*E*)-2-octenal and RI 965 (6-methyl-5-hepten-2-one and 1-octen-3-ol). (*E*)-2-octenal production decreased with round, while RI 965 production decreased between R1 and R2 but then increased slightly at R3. These decreases possibly indicate intra-individual decrease in stress and sweat production as volunteers became accustomed to the sampling procedures. The total entrained amount of compounds had a parabolic relationship with day of the year, which interacted with sample type. Closer inspection revealed that for all human odour samples and the ether samples, total amount decreased across the whole sampling period. It is possible that, as sampling procedures were practiced, contamination or collection of exogenous compounds was minimised. In the closed bag controls, the same trend is observed until day 131 (sampling period day 9–day 191; 9/01/14 - 10/07/14) where there was a slight rise in total amount. Studying the raw data indicated an increase in the collection of some compounds in the controls, during the last sampling effort (Powo, school). This increase was particularly apparent with decanal. Indeed, a possible association between malaria status and decanal production was

disregarded due to significant contamination in the control. The reasons behind this remain unknown.

5.5.10 Methodological considerations

The natural infections study benefitted from several methodological improvements, relative to the EI study (chapter 2). An obvious advantage here was the number of sampling efforts undertaken in the field over the six-month sampling period. The total amount of compounds collected per sample decreased steadily with time. This could be interpreted in terms of improved sampling technique (i.e. decreased environmental contamination), rather than a true biological phenomenon. By including 'day of the year' as a covariate in our mixed models, and analysing proportions of the odour profile rather than actual amounts, we accounted for this temporal change. A further improvement was the availability of nitrogen gas and charcoal filters at the field research centre, allowing headspace filters to be sealed under purified nitrogen on the same day as collection.

The choice of polymer filter used to capture volatiles may have introduced methodological bias. For example, the production of aldehydes was found to be strongly associated with infection. Aldehydes are highly reactive compounds and can rapidly oxidise in air (Trombetta et al., 2002). That a clear correlation between aldehyde production and infection was observed, specifically a parasite density-dependent relationship, strongly supports these observations as being truly reflective of biological phenomena. In turn, this is indicative of good sampling methods. One issue encountered here that should be considered in similar studies is ambient temperature, as temperatures as high as 45 °C were recorded inside the sampling tent. In addition to the discomfort experienced by volunteers, this occasionally led to the air pumps overheating, and subsequent sampling failure. Further, optimal sampling protocols would have included molecular diagnostic testing to inform choice of individuals for odour profile sampling; however, this was not available at that time. Two other issues are further discussed in the relevant chapters, (1) loss of parasitological data through loss of blood samples (chapter 3), and (2) possible insensitivity in detecting compounds of interest, due to the data analysis methodology (chapter 4).

5.6 Conclusion

In this chapter, quantitative differences in specific compounds of the volatile odour profile of *Plasmodium*-infected individuals, relative to parasite-free individuals, were observed. Increased production of the aldehydes heptanal, octanal, nonanal (C7-C9), (*E*)-2-octenal and (*E*)-2-decenal was shown to be significantly associated with the presence of *Plasmodium* parasites, and further, C7-C9 production was correlated with parasite density. There was a possible association between increased production of octanal, (*E*)-2-octenal, (*E*)-2-decenal and RI 965 (co-eluting 6-methyl-5-hepten-2-one and 1-octen-3-ol) with the presence of gametocytes, however, in this dataset gametocyte density was associated with high total parasite density. The production of 2-octanone, 1-octen-3-one and hexanal was found to be specifically correlated with the presence of gametocytes, and not predicted by the total density of parasites. Oxidative stress, a feature of malaria, is a probable mechanism for the increased production of some of these compounds.

5.7 Chapter references

- Batista, E.P., Costa, E.F., Silva, A. a, 2014. *Anopheles darlingi* (Diptera: Culicidae) displays increased attractiveness to infected individuals with *Plasmodium vivax* gametocytes. *Parasit. Vectors* 7, 251. doi:10.1186/1756-3305-7-251
- Bayoh, M.N., Mathias, D.K., Odiere, M.R., Mutuku, F.M., Kamau, L., Gimnig, J.E., Vulule, J.M., Hawley, W.A., Hamel, M.J., Walker, E.D., Greenwood, B., Enayati, A., Lines, J., Maharaj, R., Hemingway, J., Mendis, K., Rietveld, A., Warsame, M., Bosman, A., Greenwood, B., et al., 2010. *Anopheles gambiae*: historical population decline associated with regional distribution of insecticide-treated bed nets in western Nyanza Province, Kenya. *Malar. J.* 9, 62. doi:10.1186/1475-2875-9-62
- Becker, K., Tilley, L., Vennerstrom, J.L., Roberts, D., Rogerson, S., Ginsburg, H., 2004. Oxidative stress in malaria parasite-infected erythrocytes: Host-parasite interactions. *Int. J. Parasitol.* 34, 163–189. doi:10.1016/j.ijpara.2003.09.011
- Berna, A.Z., McCarthy, J.S., Wang, R.X., Saliba, K.J., Bravo, F.G., Cassells, J., Padovan, B., Trowell, S.C., 2015. Analysis of Breath Specimens for Biomarkers of *Plasmodium falciparum* Infection. *J. Infect. Dis.* 1–9. doi:10.1093/infdis/jiv176
- Bernier, U.R., Booth, M.M., Yost, R.A., 1999. Analysis of human skin emanations by gas chromatography/mass spectrometry. 1. Thermal desorption of attractants for the yellow fever mosquito (*Aedes aegypti*) from handled glass beads. *Anal. Chem.* 3, 1–7.
- Beshir, K.B., Hallett, R.L., Eziefula, A.C., Bailey, R., Watson, J., Wright, S.G., Chiodini, P.L., Polley, S.D., Sutherland, C.J., 2010. Measuring the efficacy of anti-malarial drugs in vivo: quantitative PCR measurement of parasite clearance. *Malar. J.* 9, 312. doi:10.1186/1475-2875-9-312
- Black, C.L., Mwinzi, P.N.M., Muok, E.M.O., Abudho, B., Fitzsimmons, C.M., Dunne, D.W., Karanja, D.M.S., Secor, W.E., Colley, D.G., Mwinzi, P., Muok, E., Abudho, B., Fitzsimmons, C., Dunne, D., Karanja, D., Secor, W., Colley, D., Handzel, T., Karanja, D., Addiss, D., et al., 2010. Influence of Exposure History on the Immunology and Development of Resistance to Human Schistosomiasis *Mansoni*. *PLoS Negl. Trop. Dis.* 4, e637. doi:10.1371/journal.pntd.0000637
- Bousema, T., Drakeley, C., 2011. Epidemiology and infectivity of *Plasmodium falciparum* and *Plasmodium vivax* gametocytes in relation to malaria control and elimination. *Clin. Microbiol. Rev.* 24, 377–410. doi:10.1128/CMR.00051-10
- Buljubasic, F., Buchbauer, G., 2015. The scent of human diseases: a review on specific volatile organic compounds as diagnostic biomarkers. *Flavour Fragr. J.* 30, 5–25. doi:10.1002/ffj.3219
- Busula, A.O., Bousema, T., Mweresa, C.K., Masiga, D., Logan, J.G., Sauerwein, R.W., Verhulst, N.O., Takken, W., de Boer, J.G., 2017. Gametocytaemia increases attractiveness of *Plasmodium falciparum*-infected Kenyan children to *Anopheles gambiae* mosquitoes. *J. Infect. Dis.* 1–5. doi:10.1093/infdis/jix214
- Butler, S.E., Muok, E.M., Montgomery, S.P., Odhiambo, K., Mwinzi, P.M.N., Secor, W.E., Karanja, D.M.S., 2012. Mechanism of anemia in *Schistosoma mansoni*-infected school children in Western Kenya. *Am. J. Trop. Med. Hyg.* 87, 862–7. doi:10.4269/ajtmh.2012.12-0248
- Chen, X., Xu, F., Wang, Y., Pan, Y., Lu, D., Wang, P., Ying, K., Chen, E., Zhang, W., 2007. A study of the volatile organic compounds exhaled by lung cancer cells in vitro for breath diagnosis. *Cancer* 110, 835–844. doi:10.1002/cncr.22844
- Cooperband, M.F., McElfresh, J.S., Millar, J.G., Cardé, R.T., 2008. Attraction of female *Culex quinquefasciatus* Say (Diptera: Culicidae) to odors from chicken feces. *J. Insect Physiol.* 54, 1184–1192. doi:10.1016/j.jinsphys.2008.05.003

- Cork, A., Park, K.C., 1996. Identification of electrophysiologically-active compounds for the malaria mosquito, *Anopheles gambiae*, in human sweat extracts. *Med. Vet. Entomol.* 10, 269–76.
- Cornet, S., Nicot, A., Rivero, A., Gandon, S., 2012. Malaria infection increases bird attractiveness to uninfected mosquitoes. *Ecol. Lett.* 16, 323–9. doi:10.1111/ele.12041
- Correa, R., Coronado, L.M., Garrido, A.C., Durant-Archibold, A.A., Spadafora, C., 2017. Volatile organic compounds associated with *Plasmodium falciparum* infection in vitro. *Parasit. Vectors* 10, 215. doi:10.1186/s13071-017-2157-x
- Cowman, A.F., Healer, J., Marapana, D., Marsh, K., 2016. Malaria: Biology and Disease. *Cell* 167, 610–624. doi:10.1016/j.cell.2016.07.055
- Cunnington, A.J., Njie, M., Correa, S., Takem, E.N., Riley, E.M., Walther, M., 2012. Prolonged Neutrophil Dysfunction after *Plasmodium falciparum* Malaria Is Related to Hemolysis and Heme Oxygenase-1 Induction. *J. Immunol.* 189, 5336–5346. doi:10.4049/jimmunol.1201028
- Curran, A.M., Prada, P.A., Furton, K.G., 2010. The Differentiation of the Volatile Organic Signatures of Individuals Through SPME-GC / MS of Characteristic Human Scent Compounds 55, 50–57. doi:10.1111/j.1556-4029.2009.01236.x
- Curran, A.M., Rabin, S.I., Prada, P.A., Furton, K.G., 2005. Comparison of the volatile organic compounds present in human odor using SPME-GC/MS. *J. Chem. Ecol.* 31, 1607–19.
- Das, B.S., Nanda, N.K., 1999. Evidence for erythrocyte lipid peroxidation in acute *falciparum* malaria. *Trans. R. Soc. Trop. Med. Hyg.* 93, 58–62.
- De Moraes, C.M., Stanczyk, N.M., Betz, H.S., Pulido, H., Sim, D.G., Read, A.F., Mescher, M.C., Science, E.S., Meinwald, J., 2014. Malaria-induced changes in host odors enhance mosquito attraction. *Proc. Natl. Acad. Sci. U. S. A.* doi:10.1073/pnas.1405617111
- Deng, C., Li, N., Zhang, X., 2004. Development of headspace solid-phase microextraction with on-fiber derivatization for determination of hexanal and heptanal in human blood. *J. Chromatogr. B* 813, 47–52. doi:10.1016/j.jchromb.2004.09.007
- Dormont, L., Bessi re, J.-M., Cohuet, A., 2013a. Human skin volatiles: a review. *J. Chem. Ecol.* 39, 569–78. doi:10.1007/s10886-013-0286-z
- Dormont, L., Bessi re, J.-M., McKey, D., Cohuet, A., 2013b. New methods for field collection of human skin volatiles and perspectives for their application in the chemical ecology of human-pathogen-vector interactions. *J. Exp. Biol.* 216, 2783–8. doi:10.1242/jeb.085936
- Emami, S.N., Emami, S.N., Lindberg, B.G., Hua, S., Hill, S., Mozuraitis, R., Birgersson, G., Ignell, R., Faye, I., 2017. A key malaria metabolite modulates vector blood seeking, feeding, and susceptibility to infection. *Science* (80-.). 4563, 1–9.
- Fabbri, C., De, R., Mascarenhas-Netto, C., Lalwani, P., Melo, G.C., Magalh es, B.M., Alexandre, M.A., Lacerda, M.V., Lima, E.S., 2013. Lipid peroxidation and antioxidant enzymes activity in *Plasmodium vivax* malaria patients evolving with cholestatic jaundice. *Malar. J.* 12, 315. doi:10.1186/1475-2875-12-315
- Filipiak, W., Sponring, A., Baur, M., Filipiak, A., Ager, C., Wiesenhofer, H., Nagl, M., Troppmair, J., Amann, A., 2012. Molecular analysis of volatile metabolites released specifically by *staphylococcus aureus* and *pseudomonas aeruginosa*. *BMC Microbiol.* 12, 113. doi:10.1186/1471-2180-12-113
- Fuchs, P., Loeseken, C., Schubert, J.K., Miekisch, W., 2010. Breath gas aldehydes as biomarkers of lung cancer. *Int. J. Cancer* 126, 2663–2670. doi:10.1002/ijc.24970
- Gallagher, M., Wysocki, C.J., Leyden, J.J., Spielman, A.I., Sun, X., Preti, G., 2008. Analyses of volatile organic compounds from human skin. *Br. J. Dermatol.* 159, 780–91. doi:10.1111/j.1365-2133.2008.08748.x
- Gilbert, I.H., Gouck, H.K., Smith, N., 1966. Attractiveness of Men and Women to *Aedes aegypti* and Relative Protection Time Obtained with Deet. *Florida Entomol.* 49, 53. doi:10.2307/3493317

- Glindemann, D., Dietrich, A., Staerk, H.-J., Kusch, P., 2006. The Two Odors of Iron when Touched or Pickled: (Skin) Carbonyl Compounds and Organophosphines. *Angew. Chemie Int. Ed.* 45, 7006–7009. doi:10.1002/anie.200602100
- Harraca, V., Ryne, C., Birgersson, G., Ignell, R., 2012. Smelling your way to food: can bed bugs use our odour? *J Exp Biol* 215, 623–629. doi:10.1242/jeb.065748
- Haze, S., Gozu, Y., Nakamura, S., Kohno, Y., Sawano, K., Ohta, H., Yamazaki, K., 2001. 2-Nonenal newly found in human body odor tends to increase with aging. *J. Invest. Dermatol.* 116, 520–524. doi:10.1046/j.0022-202X.2001.01287.x
- Hermesen, C.C., Telgt, D.S., Linders, E.H., van de Locht, L. a, Eling, W.M., Mensink, E.J., Sauerwein, R.W., 2001. Detection of *Plasmodium falciparum* malaria parasites in vivo by real-time quantitative PCR. *Mol. Biochem. Parasitol.* 118, 247–251. doi:S0166685101003796 [pii]
- Ho, E., Karimi Galougahi, K., Liu, C.-C., Bhindi, R., Figtree, G.A., 2013. Biological markers of oxidative stress: Applications to cardiovascular research and practice. *Redox Biol.* 1, 483–91. doi:10.1016/j.redox.2013.07.006
- Homan, T., Hiscox, A., Mweresa, C.K., Masiga, D., Mukabana, W.R., Oria, P., Maire, N., Pasquale, A. Di, Silkey, M., Alaii, J., Bousema, T., Leeuwis, C., Smith, T.A., Takken, W., Bhatt, S., Weiss, D., et al., 2016a. The effect of mass mosquito trapping on malaria transmission and disease burden (SolarMal): a stepped-wedge cluster-randomised trial. *Lancet* 388, 207–211. doi:10.1016/S0140-6736(16)30445-7
- Homan, T., Maire, N., Hiscox, A., Di Pasquale, A., Kiche, I., Onoka, K., Mweresa, C., Mukabana, W.R., Ross, A., Smith, T.A., Takken, W., Murray, C., Rosenfeld, L., Lim, S., Andrews, K., Foreman, K., Haring, D., Okiro, E., Alegana, V., Noor, A., Snow, R., Tanner, M., Savigny, D., Alonso, P., Brown, G. et al., 2016b. Spatially variable risk factors for malaria in a geographically heterogeneous landscape, western Kenya: an explorative study. *Malar. J.* 15, 1. doi:10.1186/s12936-015-1044-1
- Jaleta, K.T., Hill, S.R., Birgersson, G., Tekie, H., Ignell, R., 2016. Chicken volatiles repel host-seeking malaria mosquitoes. *Malar. J.* 15, 354. doi:10.1186/s12936-016-1386-3
- Kelly, M., Su, C.-Y., Schaber, C., Crowley, J.R., Hsu, F.-F., Carlson, J.R., Odom, A.R., 2015. Malaria parasites produce volatile mosquito attractants. *MBio* 6, e00235-15-. doi:10.1128/mBio.00235-15
- Koepfli, C., Robinson, L.J., Rarau, P., Salib, M., Sambale, N., Wampfler, R., Betuela, I., Nuitragool, W., Barry, A.E., Siba, P., Felger, I., Mueller, I., 2015. Blood-Stage Parasitaemia and Age Determine *Plasmodium falciparum* and *P. vivax* Gametocytaemia in Papua New Guinea. *PLoS One* 10, e0126747. doi:10.1371/journal.pone.0126747
- Kwiatkowska, S., Piasecka, G., Zieba, M., Piotrowski, W., Nowak, D., 1999. Increased serum concentrations of conjugated dienes and malondialdehyde in patients with pulmonary tuberculosis. *Respir. Med.* 93, 272–6.
- Lacroix, R., Mukabana, W.R., Gouagna, L.C., Koella, J.C., 2005. Malaria infection increases attractiveness of humans to mosquitoes. *PLoS Biol.* 3, e298. doi:10.1371/journal.pbio.0030298
- Leyden, J.J., Nordstrom, K.M., McGinley, K.J., 1991. Cutaneous microbiology, in: Goldsmith, L.A. (Ed.), *Physiology, Biochemistry and Molecular Biology of the Skin*. Oxford University Press, New York, pp. 1403–1424.
- Li, N., Deng, C., Yin, X., Yao, N., Shen, X., Zhang, X., 2005. Gas chromatography-mass spectrometric analysis of hexanal and heptanal in human blood by headspace single-drop microextraction with droplet derivatization. *Anal. Biochem.* 342, 318–326. doi:10.1016/j.ab.2005.04.024
- Logan, J.G., Birkett, M.A., Clark, S.J., Powers, S., Seal, N.J., Wadhams, L.J., Mordue Luntz, A.J., Pickett, J.A., 2008. Identification of human-derived volatile chemicals that interfere with attraction of *Aedes aegypti* mosquitoes. *J Chem Ecol* 34, 308–322. doi:10.1007/s10886-008-9436-0

- Logan, J.G., Stanczyk, N.M., Hassanali, A., Kemei, J., Santana, A.E.G., Ribeiro, K. a L., Pickett, J. a, Mordue Luntz, a J., 2010. Arm-in-cage testing of natural human-derived mosquito repellents. *Malar. J.* 9, 239. doi:10.1186/1475-2875-9-239
- Lu, T., Qiu, Y.T., Wang, G., Kwon, J.Y., Rutzler, M., Kwon, H.-W., Pitts, R.J., van Loon, J.J.A., Takken, W., Carlson, J.R., Zwiebel, L.J., 2007. Odor Coding in the Maxillary Palp of the Malaria Vector Mosquito *Anopheles gambiae*. *Curr. Biol.* 17, 1533–1544.
- Mbogo, C.M., Mwangangi, J.M., Nzovu, J., Gu, W., Yan, G., Gunter, J.T., Swalm, C., Keating, J., Regens, J.L., Shililu, J.I., Githure, J.I., Beier, J.C., 2003. Spatial and temporal heterogeneity of *Anopheles* mosquitoes and *Plasmodium falciparum* transmission along the Kenyan coast. *Am. J. Trop. Med. Hyg.* 68, 734–42.
- McLean, E.D., Allen, L.H., Neumann, C.G., Peerson, J.M., Siekmann, J.H., Murphy, S.P., Bwibo, N.O., Demment, M.W., 2007. Low plasma vitamin B-12 in Kenyan school children is highly prevalent and improved by supplemental animal source foods. *J. Nutr.* 137, 676–82.
- Meijerink, J., Braks, M.A.H., Brack, A.A., Adam, W., Dekker, T., Posthumus, M.A., Beek, T.A.V.A.N., Loon, J.J.A. Van, 2000. Identification of Olfactory Stimulants for *Anopheles gambiae* from Human Sweat Samples. *J. Chem. Ecol.* 26, 1367–1382. doi:10.1023/A:1005475422978
- Moore, L.R., Fujioka, H., Williams, P.S., Chalmers, J.J., Grimberg, B., Zimmerman, P.A., Zborowski, M., 2006. Hemoglobin degradation in malaria-infected erythrocytes determined from live cell magnetophoresis. *FASEB J.* 20, 747–9. doi:10.1096/fj.05-5122fje
- Mutuku, F.M., King, C.H., Mungai, P., Mbogo, C., Mwangangi, J., Muchiri, E.M., Walker, E.D., Kitron, U., 2011. Impact of insecticide-treated bed nets on malaria transmission indices on the south coast of Kenya. *Malar. J.* 10, 356. doi:10.1186/1475-2875-10-356
- Nacher, M., Achidi, E.A., Anchang-Kimbi, J.K., Apinjoh, T.O., Mugri, R.N., Chi, H.F., Tata, R.B., Njumkeng, C., Nkock, E.N., Nkuo-Akenji, T., 2012. Helminth-infected patients with malaria: a low profile transmission hub? *Malar. J.* 11, 376. doi:10.1186/1475-2875-11-376
- Noor, A.M., Gething, P.W., Alegana, V.A., Patil, A.P., Hay, S.I., Muchiri, E., Juma, E., Snow, R.W., 2009. The risks of malaria infection in Kenya in 2009. *BMC Infect. Dis.* 9, 180. doi:10.1186/1471-2334-9-180
- Nyaseembe, V.O., Tchouassi, D.P., Kirwa, H.K., Foster, W.A., Teal, P.E.A., Borgemeister, C., Torto, B., 2014. Development and assessment of plant-based synthetic odor baits for surveillance and control of malaria vectors. *PLoS One* 9, e89818. doi:10.1371/journal.pone.0089818
- Nyaseembe, V.O., Teal, P.E.A., Mukabana, W.R., Tumlinson, J.H., Torto, B., 2012. Behavioural response of the malaria vector *Anopheles gambiae* to host plant volatiles and synthetic blends. *Parasit Vectors* 5, 234.
- Olanga, E.A., Okombo, L., Irungu, L.W., Mukabana, W.R., 2015. Parasites and vectors of malaria on Rusinga Island, Western Kenya. *Parasit. Vectors* 8, 250. doi:10.1186/s13071-015-0860-z
- Orhan, H., van Holland, B., Krab, B., Moeken, J., Vermeulen, N.P.E., Hollander, P., Meerman, J.H.N., 2004. Evaluation of a Multi-parameter Biomarker Set for Oxidative Damage in Man: Increased Urinary Excretion of Lipid, Protein and DNA Oxidation Products after One Hour of Exercise. *Free Radic. Res.* 38, 1269–1279. doi:10.1080/10715760400013763
- Penn, D.J., Oberzaucher, E., Grammer, K., Fischer, G., Soini, H.A., Wiesler, D., Novotny, M. V, Dixon, S.J., Xu, Y., Brereton, R.G., 2007. Individual and gender fingerprints in human body odour. *J. R. Soc. Interface* 4, 331–40. doi:10.1098/rsif.2006.0182

- Percário, S., Moreira, D.R., Gomes, B.A.Q., Ferreira, M.E.S., Gonçalves, A.C.M., Laurindo, P.S.O.C., Vilhena, T.C., Dolabela, M.F., Green, M.D., 2012. Oxidative stress in malaria. *Int. J. Mol. Sci.* 13, 16346–72. doi:10.3390/ijms131216346
- Phillips, M., Cataneo, R.N., Condos, R., Ring Erickson, G.A., Greenberg, J., La Bombardi, V., Munawar, M.I., Tietje, O., 2007. Volatile biomarkers of pulmonary tuberculosis in the breath. *Tuberculosis* 87, 44–52. doi:10.1016/j.tube.2006.03.004
- Porter, N.A., Caldwell, S.E., Mills, K.A., 1995. Mechanisms of free radical oxidation of unsaturated lipids. *Lipids* 30, 277–90.
- Poulin, R., 2010. Chapter 5 – Parasite Manipulation of Host Behavior: An Update and Frequently Asked Questions, in: *Advances in the Study of Behavior*. pp. 151–186. doi:10.1016/S0065-3454(10)41005-0
- Qiu, Y.T., Smallegange, R.C., Van Loon, J.J.A., Takken, W., 2011. Behavioural responses of *Anopheles gambiae sensu stricto* to components of human breath, sweat and urine depend on mixture composition and concentration. *Med. Vet. Entomol.* 25, 247–255.
- Sagun, S., Collins, E., Martin, C., Nolan, E.J., Horzempa, J., 2016. Alarm Odor Compounds of the Brown Marmorated Stink Bug Exhibit Antibacterial Activity. *J. Pharmacogn. Nat. Prod.* 2. doi:10.4172/2472-0992.1000119
- Schneider, P., Bousema, T., Omar, S., Gouagna, L., Sawa, P., Schallig, H., Sauerwein, R., 2006. (Sub)microscopic *Plasmodium falciparum* gametocytaemia in Kenyan children after treatment with sulphadoxine-pyrimethamine monotherapy or in combination with artesunate. *Int. J. Parasitol.* 36, 403–8. doi:10.1016/j.ijpara.2006.01.002
- Schwarzer, E., Arese, P., 1996. Phagocytosis of malarial pigment hemozoin inhibits NADPH-oxidase activity in human monocyte-derived macrophages. *Biochim. Biophys. Acta* 1316, 169–75.
- Schwarzer, E., Turrini, F., Ulliers, D., Giribaldi, G., Ginsburg, H., Arese, P., 1992. Impairment of macrophage functions after ingestion of *Plasmodium falciparum*-infected erythrocytes or isolated malarial pigment. *J. Exp. Med.* 176, 1033–41.
- Singh, D., Bronstad, P.M., 2001. Female body odour is a potential cue to ovulation. *Proc. Biol. Sci.* 268, 797–801. doi:10.1098/rspb.2001.1589
- Smallegange, R.C., Bukovinszkiné-Kiss, G., Otieno, B., Mbadi, P. a., Takken, W., Mukabana, W.R., Van Loon, J.J. a., 2012. Identification of candidate volatiles that affect the behavioural response of the malaria mosquito *Anopheles gambiae sensu stricto* to an active kairomone blend: laboratory and semi-field assays. *Physiol. Entomol.* 37, 60–71. doi:10.1111/j.1365-3032.2011.00827.x
- Snounou, G., Viriyakosol, S., Xin Ping Zhu, Jarra, W., Pinheiro, L., do Rosario, V.E., Thaithong, S., Brown, K.N., 1993. High sensitivity of detection of human malaria parasites by the use of nested polymerase chain reaction. *Mol. Biochem. Parasitol.* 61, 315–320. doi:10.1016/0166-6851(93)90077-B
- Stone, W., Gonçalves, B.P., Bousema, T., Drakeley, C., 2015. Assessing the infectious reservoir of *falciparum* malaria: past and future. *Trends Parasitol.* 31, 287–296. doi:10.1016/j.pt.2015.04.004
- Syed, Z., Leal, W.S., 2009. Acute olfactory response of *Culex* mosquitoes to a human- and bird-derived attractant. *Proc. Natl. Acad. Sci. U. S. A.* 106, 18803–8. doi:10.1073/pnas.0906932106
- Takken, W., Dekker, T., Wijnholds, Y.G., 1997. Odor-mediated flight behavior of *Anopheles gambiae giles* *Sensu Stricto* and *An. stephensi liston* in response to CO₂, acetone, and 1-octen-3-ol (Diptera: Culicidae). *J. Insect Behav.* 10, 395–407. doi:10.1007/BF02765606
- Tchouassi, D.P., Sang, R., Sole, C.L., Bastos, A.D.S., Teal, P.E.A., Borgemeister, C., Torto, B., 2013. Common host-derived chemicals increase catches of disease-transmitting mosquitoes and can improve early warning systems for Rift Valley fever virus. *PLoS Negl. Trop. Dis.* 7, e2007. doi:10.1371/journal.pntd.0002007

- Trombetta, D., Saija, A., Bisignano, G., Arena, S., Caruso, S., Mazzanti, G., Uccella, N., Castelli, F., 2002. Study on the mechanisms of the antibacterial action of some plant alpha,beta-unsaturated aldehydes. *Lett. Appl. Microbiol.* 35, 285–90. doi:10.1046/j.1472-765X.2002.01190.x
- Wagenstaller, M., Buettner, A., 2013. Quantitative determination of common urinary odorants and their glucuronide conjugates in human urine. *Metabolites* 3, 637–57. doi:10.3390/metabo3030637
- Yamazaki, S., Hoshino, K., Kusuhara, M., 2010. Odor Associated with Aging. *Anti-Aging Med.* 7, 60–65. doi:10.3793/jaam.7.60
- Yazdanpanah, M., Luo, X., Lau, R., Greenberg, M., Fisher, L.J., Lehotay, D.C., 1997. Cytotoxic aldehydes as possible markers for childhood cancer. *Free Radic. Biol. Med.* 23, 870–8.
- Zeng, X.-N., Leyden, J.J., Spielman, A.I., Preti, G., 1996. Analysis of characteristic human female axillary odors: Qualitative comparison to males. *J. Chem. Ecol.* 22, 237–257. doi:10.1007/BF02055096
- Zeng, X. nong, Leyden, J.J., Lawley, H.J., Sawano, K., Nohara, I., Preti, G., 1991. Analysis of characteristic odors from human male axillae. *J. Chem. Ecol.* 17, 1469–1492. doi:10.1007/BF00983777

5.8 Appendix: Parasitological categorisation for Kenyan odour samples

Analysis was initiated using four datasets: (A) Obambo, all run on GC[1], (B) Alero, run on GC[1]/[2]/[3], (C) Kamsama and Powo samples run on GC [2], (D) Kamsama and Powo samples run on GC[3] (chapter 4/4.3.3). Several different methods of parasitological categorisation were attempted, informed by published studies as well as by behavioural (semi-field) data from the project collaborators (Busula et al., 2017). Categories are given below as levels. Initially, the datasets (above) were examined by canonical variates analysis (CVA) (Table 5-13).

5.8.1 Level one

At this level, categorisation was designed to allocate individuals into the groups that were associated with significant mosquito behavioural responses in the (semi-) field, where high gametocyte densities had been associated with increased attractiveness (Busula et al., 2017). Permutations of this were designed to increase or decrease sample inclusiveness, with separate categories for uncertain diagnoses, e.g. “clearance” (only RDT positivity) (Table 5-13). Each dataset was analysed by CVA for each version of level 1; however, poor separation of groups was achieved.

Chapter 5: Odour profile analysis of children naturally infected with *Plasmodium* species

Table 5-13. Level one parasitological categories attempted in CVA of odour profile datasets. PARA=*Plasmodium* parasites (all stages), gametocytes/GAM= *P. falciparum* gametocyte stages. RDT=rapid diagnostic test. P/ μ L = parasites per microlitre of blood.

Level	Categories	Description
1A	PARA	Presence of any parasites (i.e. any parasite DNA by a molecular test), no gametocytes
	PARA and GAM	Parasites as above, AND gametocytes <500 p/ μ L, or not microscopically detected
	CLEARANCE	Only RDT positive
	GAM	Gametocytes detectable by microscopy or QT-NASBA gametocytes >500 p/ μ L
	NEG	Negative by all diagnostic measures
1B	PARA	1A categories combined: PARA, PARA and GAM, CLEARANCE
	GAM	As 1A
	NEG	As 1A
1C	PARA	1A categories combined: PARA, CLEARANCE
	GAM	1A categories combined: GAM, PARA and GAM
	NEG	As 1A
1D	PARA	1A categories combined: PARA, PARA and GAM
	GAM	As 1A
	NEG	1A categories combined: NEG, CLEARANCE
1E	PARA	As 1A
	GAM	1A categories combined: GAM, PARA and GAM
	NEG	1A categories combined: NEG, CLEARANCE
1A-1E included	all CNL	Closed bag control, CNL(B)
	Ether	Solvent control, CNL(A)

5.8.2 Level two

The published limit of detection (LOD) for molecular diagnostic techniques was used as a threshold for negativity rather than no detectable signal (as per level one), i.e. 0.02 parasites/ μ L (p/ μ L) for QT-NASBA and 18s qPCR (Hermsen et al., 2001), and five p/ μ L for PgMET qPCR (Beshir et al., 2010) (Table 5-14). A threshold of >200 gametocytes/ μ L was used to classify gametocyte carriers, as this has been determined to represent the start of an exponential increase in the proportion of mosquitoes that become infected following a blood-meal (Churcher et al., 2013). Samples that were RDT positive only were considered negative. Here, the Obambo dataset was not analysed due to a lack of gametocyte quantification by QT-NASBA. CVA did not result in separation of groups.

Chapter 5: Odour profile analysis of children naturally infected with *Plasmodium* species

Table 5-14. Level two parasitological categories attempted in CVA of odour profile datasets. PARA=*Plasmodium* parasites (all stages), gametocytes/GAM= *P. falciparum* gametocyte stages. RDT=rapid diagnostic test. P/ μ L = parasites per microlitre of blood.

Level	Categories	Description
2	PARA	Presence of any parasites (i.e. any parasite DNA by a molecular test), no gametocytes, or gametocytes <200 p/ μ L (by QT-NASBA)
	GAM	Gametocytes detectable by microscopy, or QT-NASBA gametocytes >200 p/ μ L
	NEG	Negative by all diagnostic measures but allowing RDT positivity
	CNL	Closed bag control, CNL(B)
	Ether	Solvent control, CNL(A)

5.8.3 Level three

Any samples with a QT-NASBA signal greater than the LOD were included in the gametocyte category (Table 5-15). LOD QT-NASBA values were considered to have no gametocytes. CVA did not result in separation of groups.

Table 5-15. Level three parasitological categories attempted in CVA of odour profile datasets. PARA=*Plasmodium* parasites (all stages), gametocytes/GAM= *P. falciparum* gametocyte stages. RDT=rapid diagnostic test. P/ μ L = parasites per microlitre of blood.

Level	Categories	Description
3	PARA	Presence of any parasites (i.e. any parasite DNA by a molecular test), no gametocytes
	GAM	Gametocytes by QT-NASBA, >0.02 p/ μ L
	NEG	Negative by all diagnostic measures but allowing RDT positivity
	CNL	Closed bag control, CNL(B)
	Ether	Solvent control, CNL(A)

5.8.4 Level four

Categorisation was designed to approximate microscopic levels of detection (Table 5-16), in part due to the mosquito behaviour semi-field data (not shown). This can be taken as a proxy for categorisation with greater parasite density thresholds, due to the reduced sensitivity relative to molecular techniques. In the absence of microscopy data, positives were taken as >80 p/ μ L. The field microscopist's lowest accurately measured parasite density was two parasites/200 white blood cells, equating to 80 p/ μ L. Although this is relatively high for a microscopy LOD (an experienced microscopist may identify as few as 5-20 p/ μ L (Ochola et al., 2006)), the *a priori* field data justified replicating these categories as closely as possible. A high density of gametocytes was retained in the 'GAM' category.

Chapter 5: Odour profile analysis of children naturally infected with *Plasmodium* species

Table 5-16. Level four parasitological categories attempted in CVA of odour profile datasets. PARA=*Plasmodium* parasites (all stages), gametocytes/GAM= *P. falciparum* gametocyte stages. RDT=rapid diagnostic test. P/ μ L = parasites per microlitre of blood.

Level	Categories	Description
4	PARA	Parasites by film, parasites by a molecular test >80 p/ μ L
	GAM	Gametocyte stages by film, and >500 gametocytes/ μ L by QT-NASBA
	NEG	Negative by film, <80 p/ μ L by any molecular measure, allowing RDT positivity
	CNL	Closed bag control, CNL(B)
	Ether	Solvent control, CNL(A)

Level four categorisation allowed reasonable separation of groups by CVA (Figure 5-34). From the CVA, the magnitude of the loadings on each variate (compound) was inspected, to determine which of these contributed most to the differences between group means. Those contributing to separation, by at least 50 % of the influence of the most important compound, were designated 'compounds of interest' (COI).

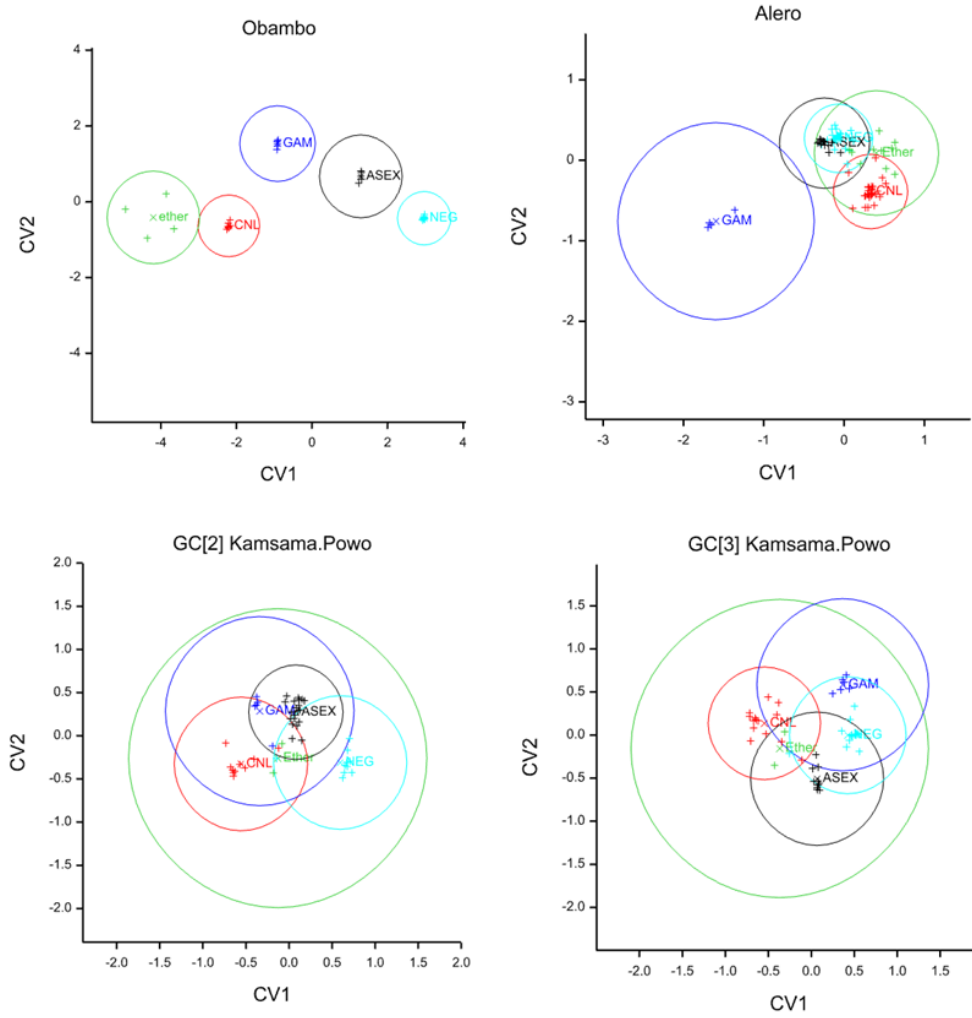


Figure 5-34. The best separation of parasitological groups by CVA was achieved using 'level four' categorisation, designed to mimic microscopic levels of detection.

5.8.5 Level five

An emphasis was placed on the higher parasite densities (Table 5-17). Poor separation of COI (assessed by average production per category) was achieved, nor were further COI identified.

Table 5-17. Level five parasitological categories attempted for separation of group mean COI production. PARA=*Plasmodium* parasites (all stages), gametocytes/GAM= *P. falciparum* gametocyte stages. RDT=rapid diagnostic test. P/ μ L = parasites per microlitre of blood.

Level	Categories	Description
5	PARA	Presence of parasites at >500 p/ μ L by any measure (other than gametocytes)
	Low	Presence of parasites at <500 p/ μ L by any measure
	GAM	Any gametocytes by film, and/or >500 gametocytes/ μ L by QT-NASBA
	NEG	<LOD for any molecular test, allowing RDT positivity
	CNL	Closed bag control, CNL(B)
	Ether	Solvent control, CNL(A)

5.8.6 Levels six - ten

Level six; an extension of level four but with <20 p/ μ L as the positive/negative threshold, as this is an accepted limit of detection for a good slide reader (Ochola et al., 2006). Level seven; samples excluded when parasitological diagnosis relied only upon microscopy (i.e. not corroborated by molecular methods), or where microscopy and another method were not in agreement. Level eight; mimicked actual parasite densities (retrospectively determined) of individuals for whom infection status was seen to influence attraction (semi-field data, not shown), and further sub-division of gametocyte status. Level nine; encompassed positivity in the PARA category with a high degree of sensitivity (i.e. any parasites above test LOD). Level ten; separated low and high parasite density, with low density category approximating a microscopists' limit of detection, and two exclusion categories for individuals with uncertain parasitological status. All shown in Table 5-18. Separation, determined by comparing group means +/- SEM in bar charts, was immediately apparent with level ten categorisation

Chapter 5: Odour profile analysis of children naturally infected with *Plasmodium* species

Table 5-18. Level 6-10 parasitological categories attempted for separation of group mean COI production. PARA=*Plasmodium* parasites (all stages), gametocytes/GAM= *P. falciparum* gametocyte stages. RDT=rapid diagnostic test. P/μL = parasites per microlitre of blood.

Level	Categories	Description
6	PARA	Parasites by microscopy, parasites by a molecular test >20 p/μL
	GAM	Gametocyte stages by microscopy, and >500 gametocytes/μL by QT-NASBA
	NEG	Negative by microscopy, <20 p/μL by any molecular measure, allowing RDT positivity
7	As (6)	As (6), but exclusions: when only microscopy diagnosis available or microscopy and molecular measures disagree
8	PARA microscopy	Parasites (any measure), no gametocytes by microscopy, QT-NASBA data missing
	PARA no-gams	Parasites (any measure), no gametocytes by microscopy or QT-NASBA
	PARA sub-gam	Parasites (any measure), no gametocytes by microscopy, QT-NASBA gametocytes <500 p/μL
	GAM	Gametocytes by microscopy, and/or QT-NASBA gametocytes >500 p/μL
	NEG microscopy	Negative by microscopy, molecular measures missing
	NEG molecular	Negative by molecular measure (/and microscopy)
9	PARA	Any parasites by microscopy, parasites > LOD by any molecular method
	GAM	Any gametocytes by microscopy, and/or >500 gametocytes/μL by QT-NASBA
	NEG	Negative by all diagnostic measures but allowing RDT positivity
	NEG microscopy	Negative by microscopy only
	LOD	'limit of detection' Any sample whose parasite density lay between zero and test LOD, without other diagnostic measures robustly indicating parasites
10	Higher density	Any parasites by microscopy, >50 p/μL by any molecular method
	Lower density	Between LOD (by any molecular method) and 50 p/μL, no parasites by microscopy (considered > 50 p/μL due to microscopists' LOD)
	Gametocyte	Any gametocytes by microscopy
	Negative	Negative by all diagnostic measures but allowing RDT positivity At least one negative molecular measure essential (i.e. confirming 'true' negativity)
	NEG microscopy	Negative by microscopy only - EXCLUDED
	LOD	'limit of detection' Any sample whose parasite density lay between zero and the test LOD, without other diagnostic measures indicating higher parasite density - EXCLUDED
6-10 all included	CNL	Closed bag control, CNL(B)
	Ether	Solvent control, CNL(A)

5.8.7 Appendix references

- Busula, A.O., Bousema, T., Mweresa, C.K., Masiga, D., Logan, J.G., Sauerwein, R.W., Verhulst, N.O., Takken, W., de Boer, J.G., 2017. Gametocytaemia increases attractiveness of *Plasmodium falciparum*-infected Kenyan children to *Anopheles gambiae* mosquitoes. *J. Infect. Dis.* 1–5. doi:10.1093/infdis/jix214
- Churcher, T.S., Bousema, T., Walker, M., Drakeley, C., Schneider, P., Ouédraogo, A.L., Basáñez, M.G., 2013. Predicting mosquito infection from *Plasmodium falciparum* gametocyte density and estimating the reservoir of infection. *Elife* 2013, 1–12. doi:10.7554/eLife.00626
- Ochola, L.B., Vounatsou, P., Smith, T., Mabaso, M.L.H., Newton, C.R.J.C., 2006. The reliability of diagnostic techniques in the diagnosis and management of malaria in the absence of a gold standard. *Lancet Infect. Dis.* 6, 582–8. doi:10.1016/S1473-3099(06)70579-5

5.9 Appendix: Canonical Variates Analysis loadings

Datasets were examined by canonical variates analysis (CVA), using various permutations of parasitological categories. Good separation of groups was achieved when high-density thresholds for parasitological positivity were used (level four categories, appendix 5.8). Those compounds with the greatest influence in separating groups were determined (Table 5-19), which became ‘compounds of interest’ and were subsequently examined by comparing group means (and error bars).

Table 5-19. All compounds contributing to group separation (at least 50% of that of the compound with the greatest loading) for the ‘level four’ parasitological categorisation CVA. Those in bold font did appear infection-associated across all samples and were investigated in final REML analyses. Greatest and smallest loadings are given in shaded boxes.

Dataset	Canonical variate	Proportion of greatest loading	RI
Obambo	CV1 positive	1.00	1746
		0.89	1699
		0.76	1898
		0.75	1489
		0.73	726
		0.70	1453
		0.58	1763
		0.52	1666
	CV1 negative	1.00	1503
		0.88	1304
		0.53	1599 tetradecane?
	CV2 positive	1.00	797 sovent and octane
		0.51	1503
	CV2 negative	1.00	1746
		0.90	1699
		0.61	1489
		0.58	774 hexanal
		0.53	1898
0.51		1453	
0.51		1453	
Alero	CV1 positive	1.00	1346
		0.91	1611
		0.86	1358
		0.85	1520
		0.84	1304
		0.79	1851
		0.79	1306
		0.68	1590
		0.67	1846
		0.51	849
		0.50	1744
	CV1 negative	1.00	1886
	CV2 positive	1.00	1673
		0.73	846
		0.52	1346
	CV2 negative	1.00	1349
		0.78	1368
	GC[2] Kamsama and Powo	CV1 positive	1.00
0.82			849

Chapter 5: Odour profile analysis of children naturally infected with *Plasmodium* species

Dataset	Canonical variate	Proportion of greatest loading	RI	
GC[2] Kamsama and Powo	CV1 positive	0.74	1062	
		0.64	1725	
		0.61	1153	
		0.57	1241	
		0.53	1304	
		0.52	703	
	CV1 negative	1.00	1500	
		0.75	1623	
		0.71	959 RI 958 unknown	
		0.69	1277	
		0.67	861	
		0.65	1626	
		0.64	1301	
		0.61	1100	
		0.59	1000	
		0.51	1025	
		0.51	1609	
		0.51	1606	
		0.50	1644	
		CV2 positive	1.00	700
	0.85		785	
	0.83		1016	
	0.82		723	
	0.79		758	
	0.76		722	
	0.72		1347	
	0.58		1000	
	0.54		1290	
	0.54		1241	
	0.54		1227	
	CV2 negative	1.00	1560	
		0.84	1359	
		0.76	1058	
		0.73	1349	
		0.71	1715	
		0.64	882 heptanal	
		0.63	1400	
		0.57	895	
		0.52	1391	
		GC[3] Kamsama and Powo	CV1 positive	1.00
0.76				1809
0.58				1162
0.57	1798			
0.56	1707			
CV1 negative	1.00		1287	
	0.92		1387	
	0.79		1736	
	0.79		860	
	0.75		1151	
	0.73		876	
	0.67		1495	
	0.66		1189	
	0.66		1006	
	0.58	1738		
	0.58	1599 tetradecane		
	0.57	966 RI 965		
	0.57	1490		
0.55	1418			
0.53	827			

Chapter 5: Odour profile analysis of children naturally infected with *Plasmodium* species

Dataset	Canonical variate	Proportion of greatest loading	RI
GC[3] Kamsama and Powo	CV1 negative	0.52	757
		0.51	1431
		0.51	1481
	CV2 positive	1.00	1554
		0.68	1751
	CV2 negative	1.00	1151
		0.83	1406

5.10 Appendix: 'Natural infections' study population

Table 5-20. Age, sex and number of odour samples taken, per individual in the Kenyan ('natural infections') study. The number of empty bag control samples taken is also shown.

School	Individual	Sex	Age	Odour samples
Obambo	OB001	M	11	1
	OB012	F	8	2
	OB014	F	10	4
	OB018	F	7	1
	OB023	M	11	3
	OB028	F	7	1
	OB032	M	6	2
	OB035	M	6	2
	Empty bag controls			
Alero	AL001	F	6	2
	AL003	M	7	1
	AL005	F	6	1
	AL009	M	6	3
	AL014	M	8	1
	AL015	M	9	2
	AL019	M	6	2
	AL022	F	9	2
	AL024	F	8	3
	AL027	M	9	1
	AL029	M	9	2
	AL037	F	8	2
	AL047	M	9	1
	AL049	F	11	2
	AL054	F	11	1
	AL055	M	12	2
	AL056	M	12	3
	AL059	M	12	3
	AL062	M	8	3
	AL064	M	10	2
AL073	F	10	3	
AL074	F	12	2	
Empty bag controls				26
Kamsama	KA064	M	5	2
	KA065	M	7	2
	KA066	M	7	2
	KA076	F	5	1
	KA078	F	8	3
	KA082	F	6	1
	KA086	F	7	3
	KA088	F	7	1
	KA090	M	9	1
KA094	M	6	3	
Kamsama	Empty bag controls			7
Powo	PO001	M	5	2
	PO011	M	5	2

Chapter 5: Odour profile analysis of children naturally infected with *Plasmodium* species

School	Individual	Sex	Age	Odour samples
Powo	PO001	M	5	2
	PO011	M	5	2
	PO013	F	8	3
	PO014	F	7	2
	PO016	F	7	2
	PO020	F	7	2
	PO022	F	8	1
	PO024	F	10	3
	PO026	M	7	2
	PO032	M	9	2
	PO037	M	10	3
	PO045	F	8	2
	PO046	F	9	3
	PO049	F	8	3
	PO056	M	8	3
	PO059	M	9	3
	Empty bag controls			

5.11 Appendix: compound identification by Peak Enhancement

Peaks were confirmed by co-injecting a blend containing the authentic standard with the sample, and observing an increase in peak height with no increase in peak width. The samples chosen for peak enhancement were the Kenya GC-EAG blends, each comprising samples of similar parasitological status (negative, sub-gametocytes, and gametocytes), and additional samples known to contain the peak under investigation (Table 5-21). By completing co-injections of three samples with authentic standards on two different GC columns, the identity of these compounds was rigorously confirmed. For some co-injections, the amount of standard added was very small, as the added amount was designed to double the amount already present.

Table 5-21. The compounds that were definitively identified by peak enhancement, which samples were used for the process and their location in the appendix. MHO = 6-methyl-5-hepten-2-one, note RI here on HP1 column.

Retention index	GC-MS ID	Sample	Comments	Page number
774	Hexanal	KA078 23MAY14	Successful co-injection	280
		PO014 10JUN14	Successful co-injection	284
880	Heptanal	Negative GC-EAG blend	Successful co-injection	272
		Sub-gam GC-EAG blend	Successful co-injection	276
		Gam GC-EAG blend	Successful co-injection	278
982	Octanal	Negative GC-EAG blend	Successful co-injection	273
		Sub-gam GC-EAG blend	Successful co-injection	276
		Gam GC-EAG blend	Successful co-injection	278
1084	Nonanal	Negative GC-EAG blend	Successful co-injection	273
		Sub-gam GC-EAG blend	Successful co-injection	276
		Gam GC-EAG blend	Successful co-injection	279
1035	(E)-2-Octenal	Negative GC-EAG blend	Successful co-injection	272
		Sub-gam GC-EAG blend	Surprising absence of (E)-2-octenal in the DB wax blend, however, successful co-injection	277
		Gam GC-EAG blend	Successful co-injection	278
1240	(E)-2-Decenal	Negative GC-EAG blend	Successful co-injection, note column cut after sample run allowed proper resolution of peak in HP1	272
		Gam GC-EAG blend	Successful co-injection	279
971	2-Octanaone	Negative GC-EAG blend	Successful co-injection	274
		Gam GC-EAG blend	Successful co-injection	278
965	MHO	Negative GC-EAG blend	Successful co-injection	274
		Sub-gam GC-EAG blend	Successful co-injection	277
		Gam GC-EAG blend	Successful co-injection	278
965	1-Octen-3-ol	Negative GC-EAG blend	Successful co-injection	274
		Sub-gam GC-EAG blend	Successful co-injection	277
		Gam GC-EAG blend	Successful co-injection	278
958	Phenol	KA078 23MAY14	Successful co-injection	281
		AL029 13FEB14	Successful co-injection	282
958	1-Octen-3-one	AL029 13FEB14	Successful co-injection	283

5.11.1 Negative blend

Heptanal, (*E*)-2-octenal and (*E*)-2-decenal

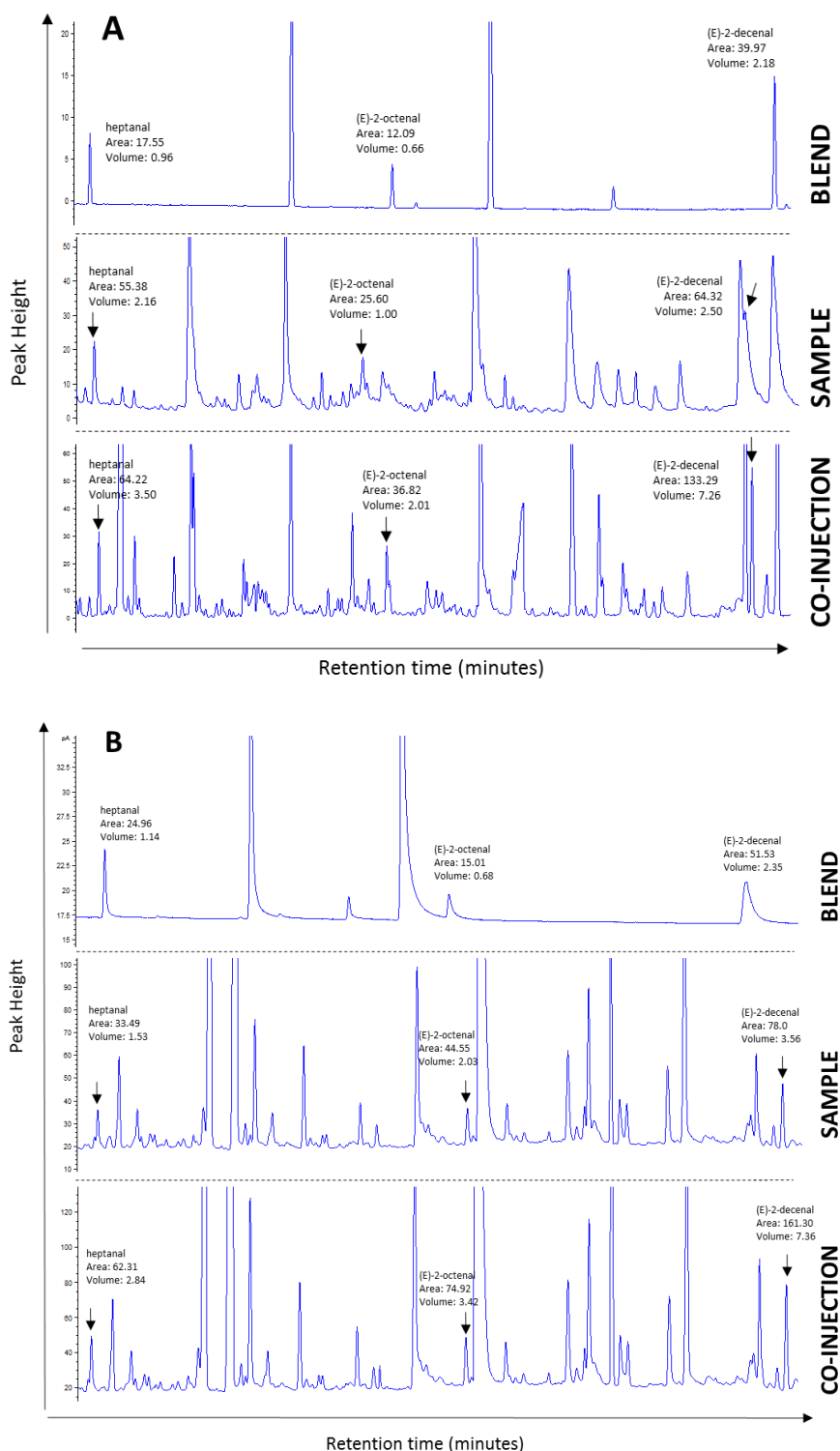


Figure 5-35. Co-injections for standards of heptanal, (*E*)-2-octenal and (*E*)-2-decenal with the 'negative' blend, comprising mixed extracts of 15 parasite-free samples. (A) co-injections on HP1 column, (B) co-injections on DB wax column. Note 'sample' was run on HP1 pre column-cut, hence poor resolution, and could not be repeated due to lack of sample.

Octanal and nonanal

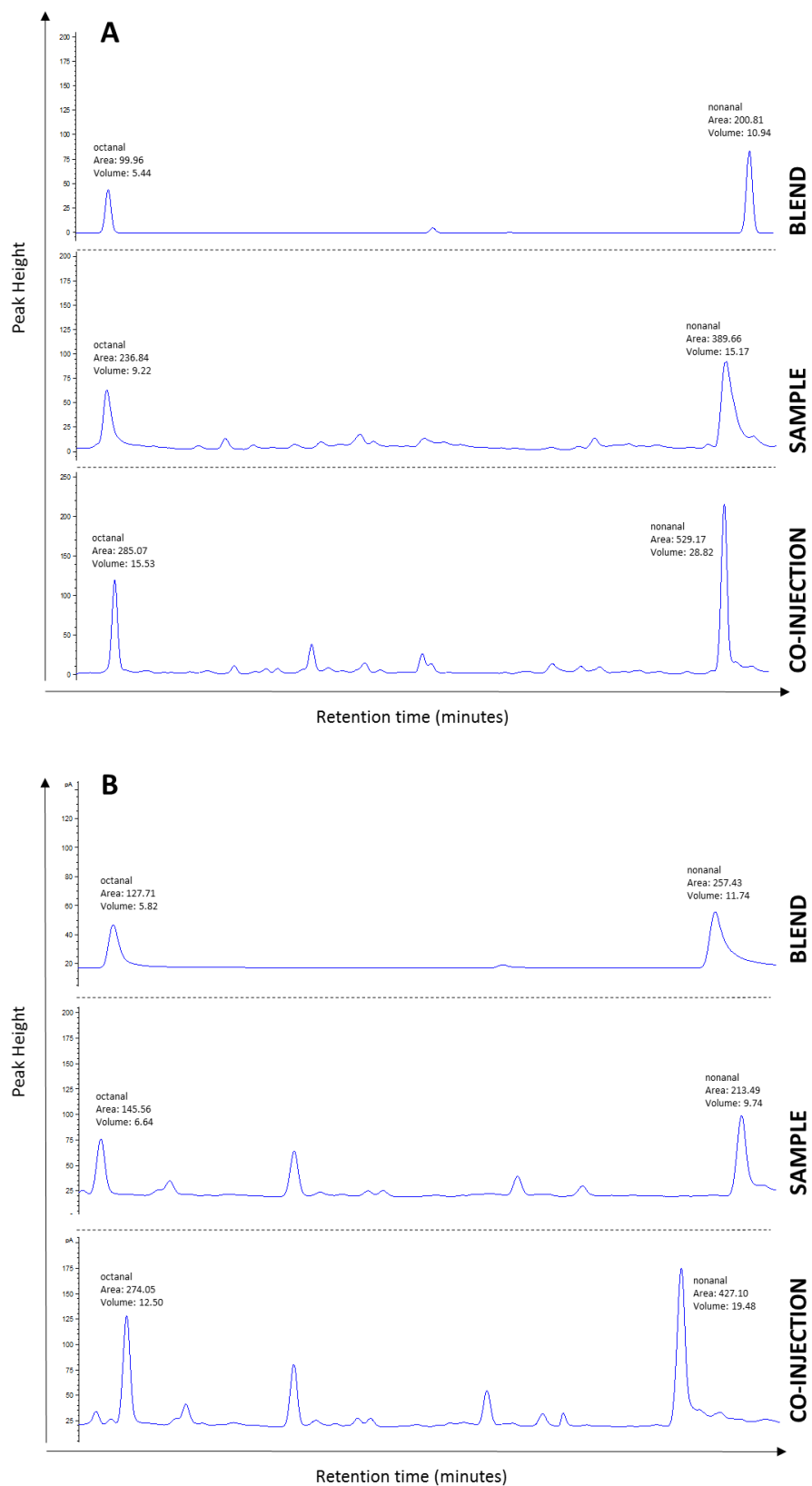


Figure 5-36. Co-injections for standards of octanal and nonanal with the 'negative' blend, comprising mixed extracts of 15 parasite-free samples. (A) co-injections on HP1 column, (B) co-injections on DB wax column. Note 'sample' was run on HP1 pre column-cut, hence poor resolution, and could not be repeated due to lack of sample.

2-Octanone, 6-methyl-5-hepten-2-one and 1-octen-3-ol

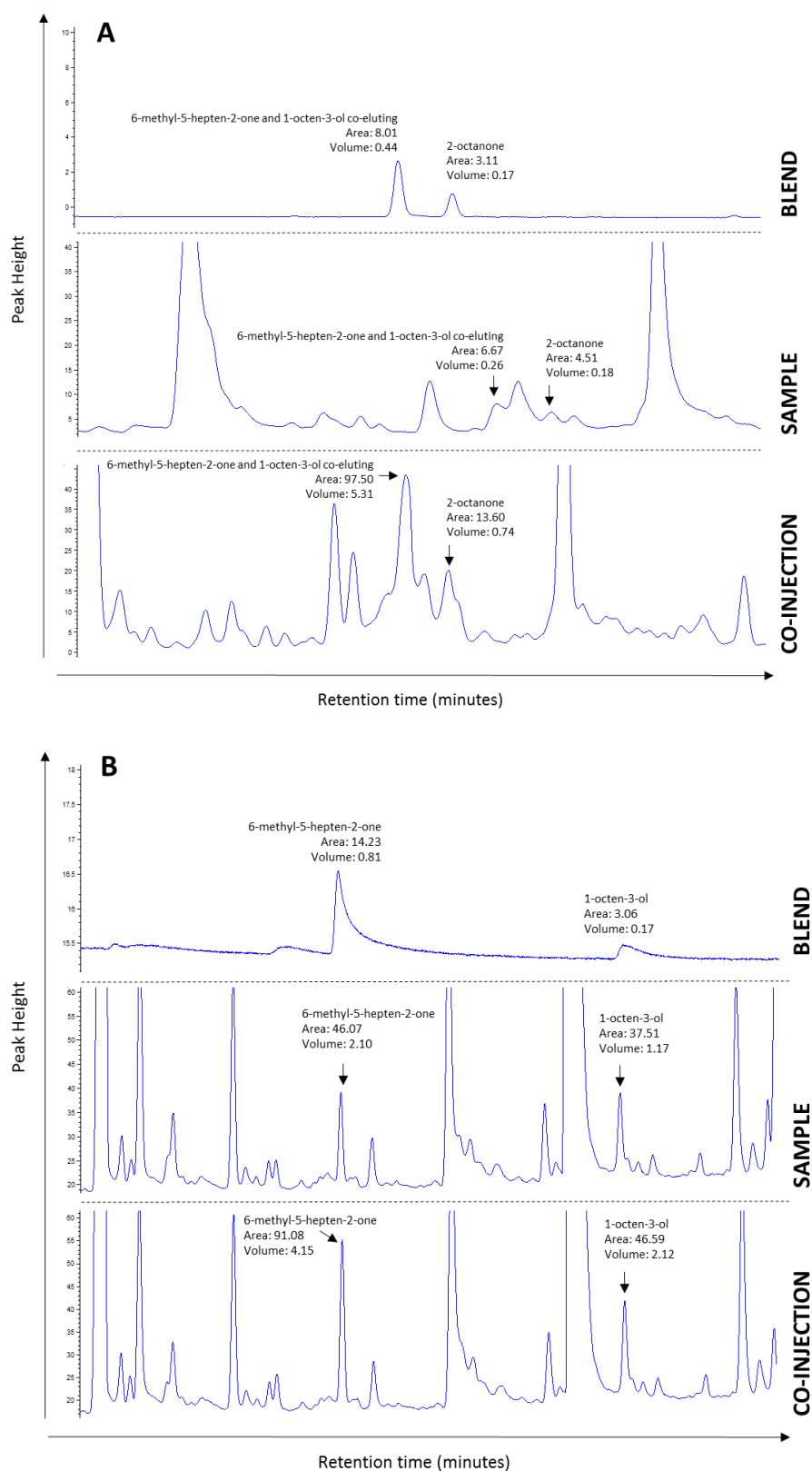


Figure 5-37. Co-injections for standards of 6-methyl-5-hepten-2-one, 1-octen-3-ol and 2-octanone on HP1 column (A). Note, here 6-methyl-5-hepten-2-one and 1-octen-3-ol co-elute. (B) Co-injections of 6-methyl-5-hepten-2-one and 1-octen-3-ol on DB wax column. Note 'sample' was run on HP1 pre column-cut, hence poor resolution, and could not be repeated due to lack of sample.

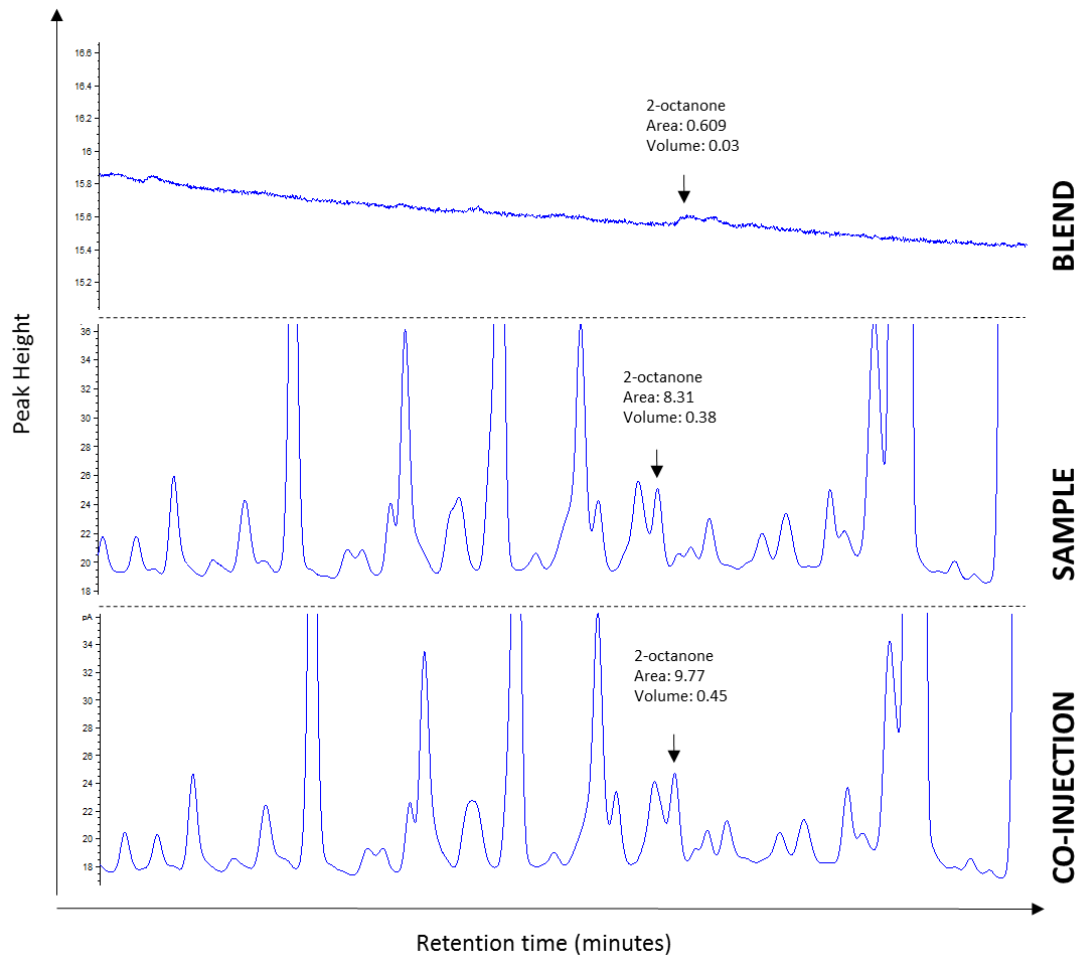


Figure 5-38. Co-injections on a DB wax column for standards of 2-octanone with the 'negative' blend, comprising mixed extracts of 15 parasite-free samples.

5.11.2 Sub-gametocyte blend

Heptanal, octanal and nonanal

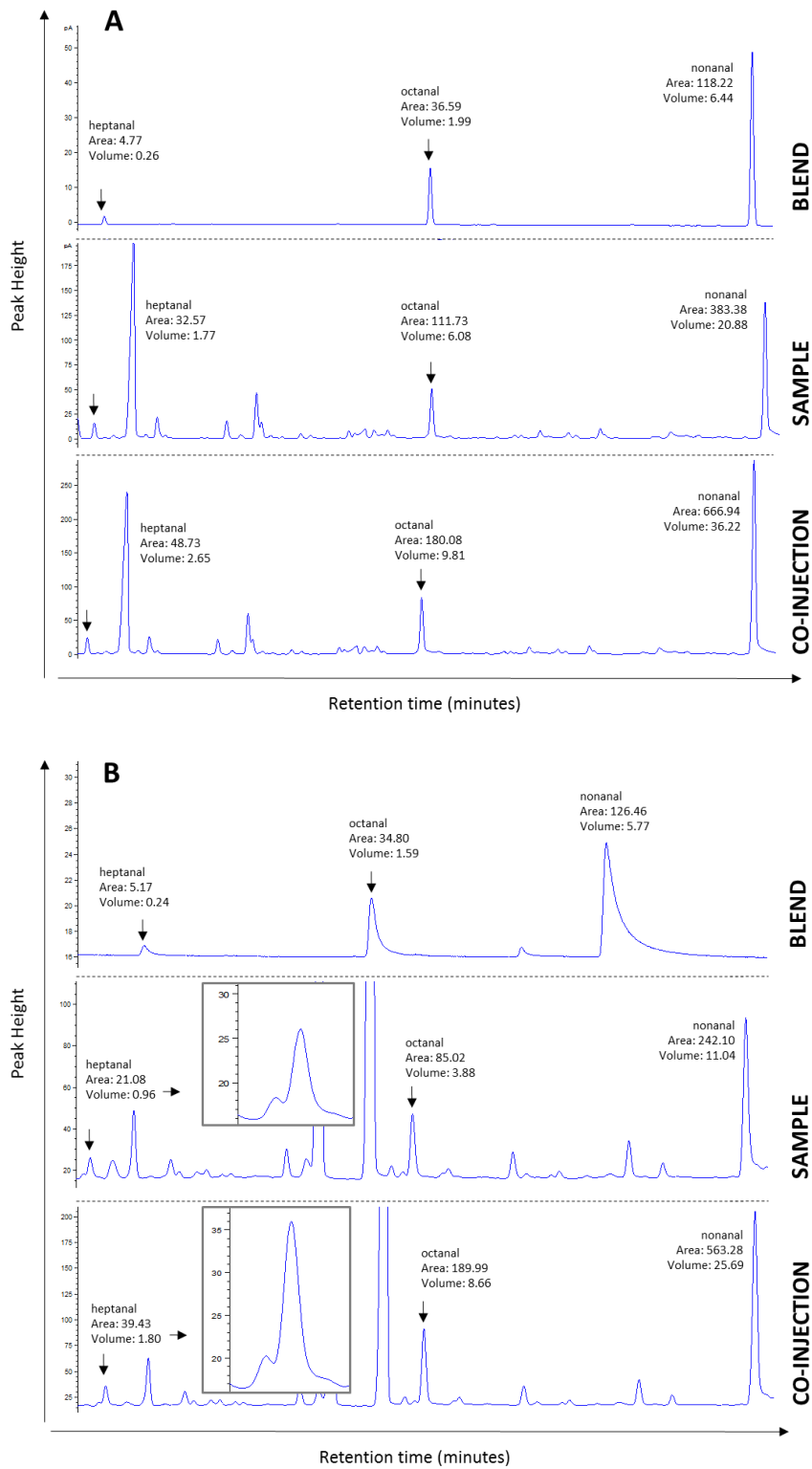


Figure 5-39. Co-injections for standards of heptanal, octanal and nonanal with the 'sub-gametocyte' blend, comprising mixed extracts of 14 samples from lower-density gametocyte infections. (A) co-injections on HP1 column, (B) co-injections on DB wax column.

6-Methyl-5-hepten-2-one, 1-octen-3-ol and (*E*)-2-octenal

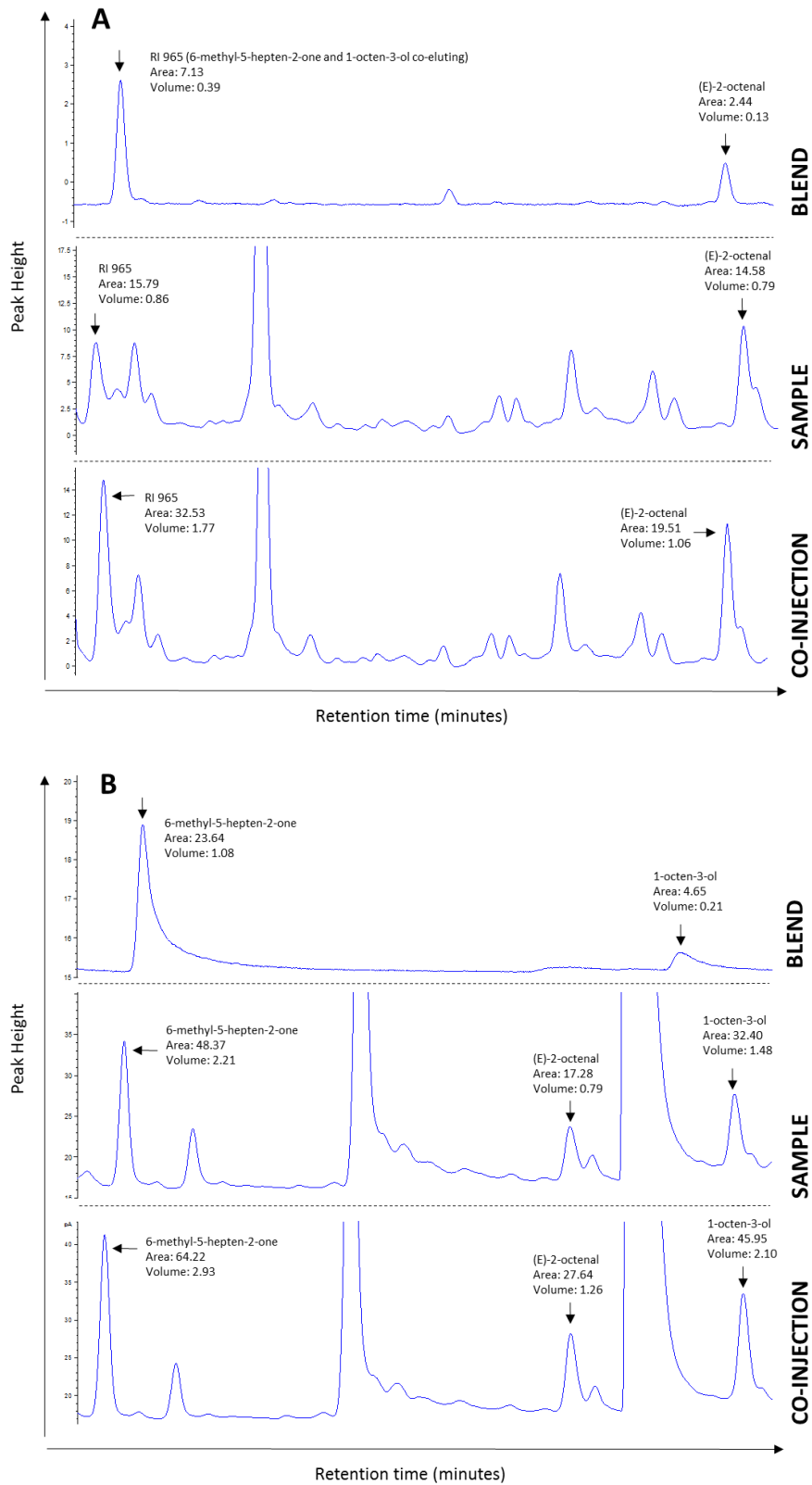


Figure 5-40. Co-injections for standards of 6-methyl-5-hepten-2-one, 1-octen-3-ol and (*E*)-2-octenal with the 'sub-gametocyte' blend, comprising mixed extracts of 14 samples from lower-density gametocyte infections. (A) co-injections on HP1 column, (B) co-injections on DB wax column. Note virtual absence of (*E*)-2-octenal in the DB wax blend.

5.11.3 Gametocyte blend

Heptanal, 6-methyl-5-hepten-2-one, 1-octen-3-ol, 2-octanone, octanal and (*E*)-2-octenal

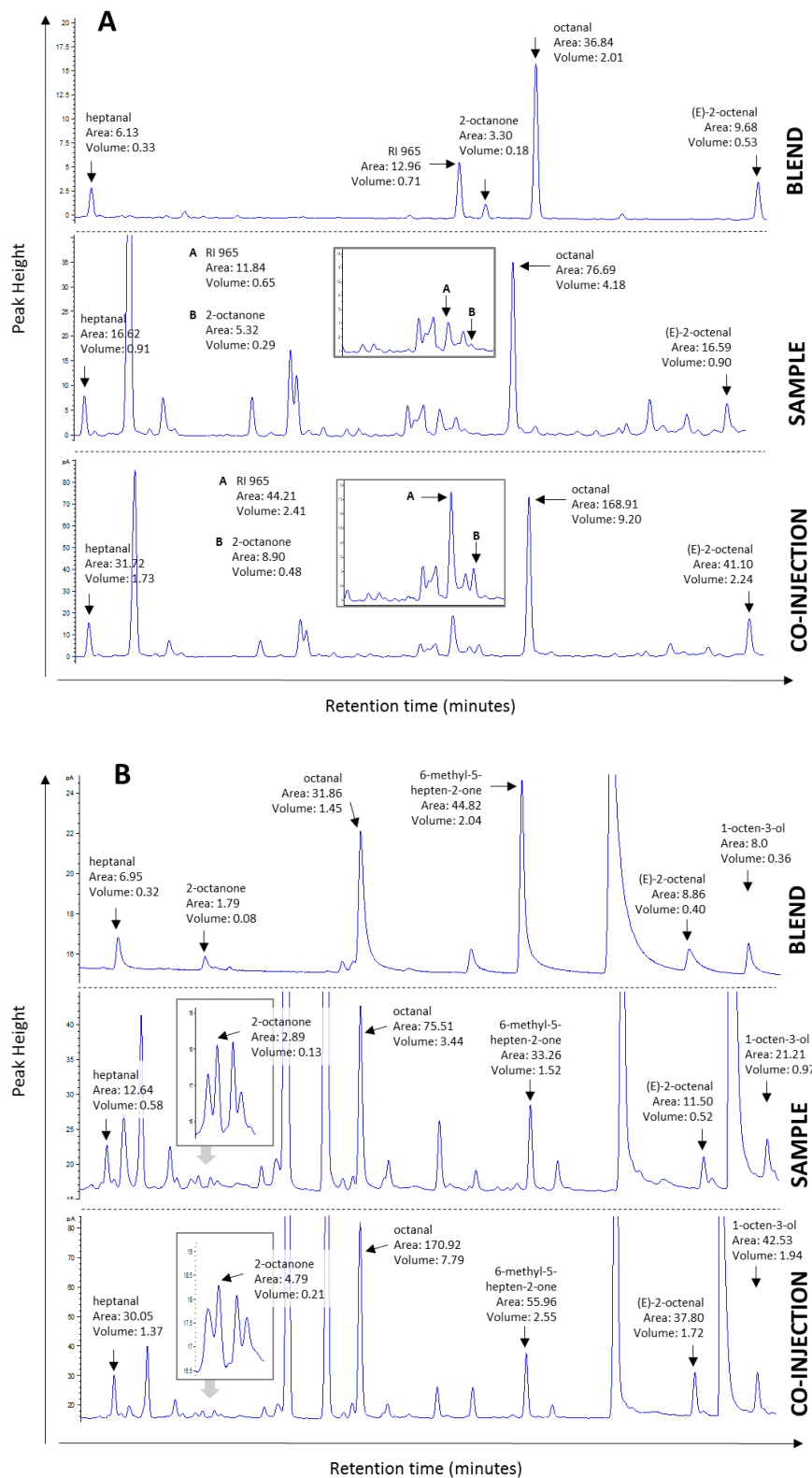


Figure 5-41. Co-injections for standards of heptanal, 6-methyl-5-hepten-2-one, 1-octen-3-ol, 2-octanone, octanal and (*E*)-2-octenal with the 'gametocyte' blend, comprising mixed extracts of 13 samples from high-density gametocyte infections. (A) co-injections on HP1 column, (B) co-injections on DB wax column.

Nonanal and (*E*)-2-decenal

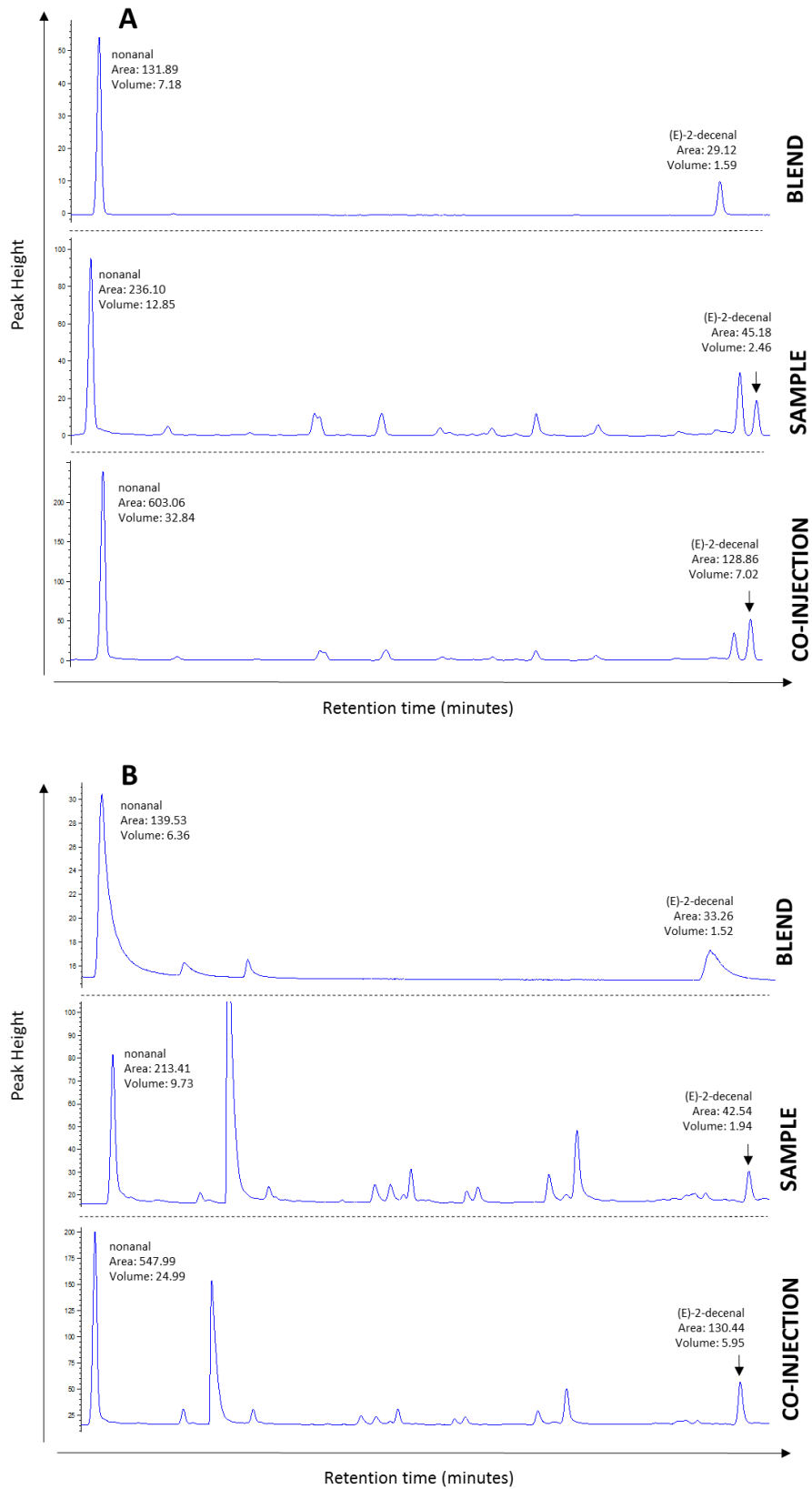


Figure 5-42. Co-injections for standards of nonanal and (*E*)-2-decenal with the 'gametocyte' blend, comprising mixed extracts of 13 samples from high-density gametocyte infections. (A) co-injections on HP1 column, (B) co-injections on DB wax column.

5.11.4 Sample KA078 23MAY14: Hexanal

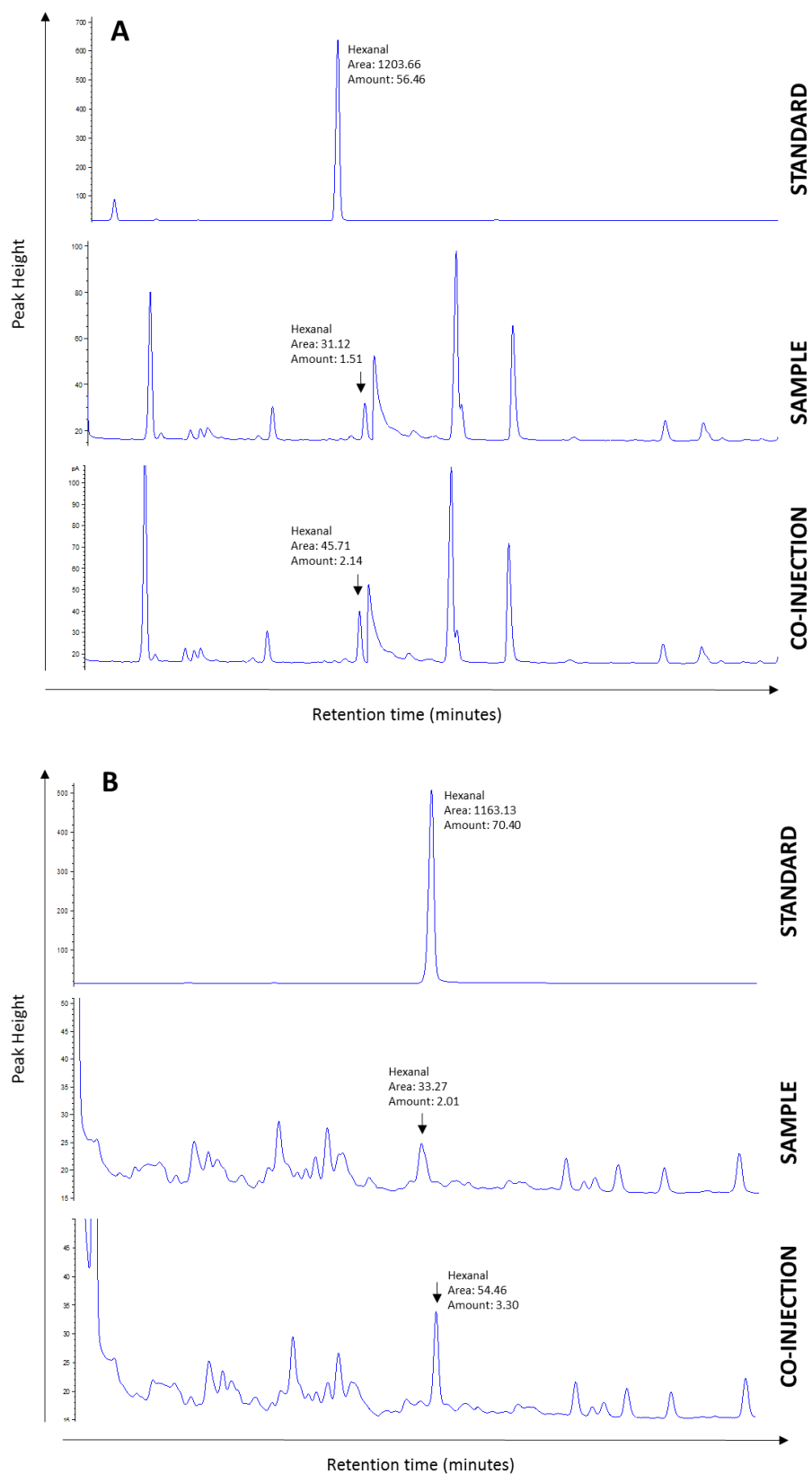


Figure 5-43. Co-injections for hexanal standard with sample KA078 23MAY14 (A) co-injections on HP1 column, (B) co-injections on DB wax column.

5.11.5 Sample KA078 23MAY14: Phenol

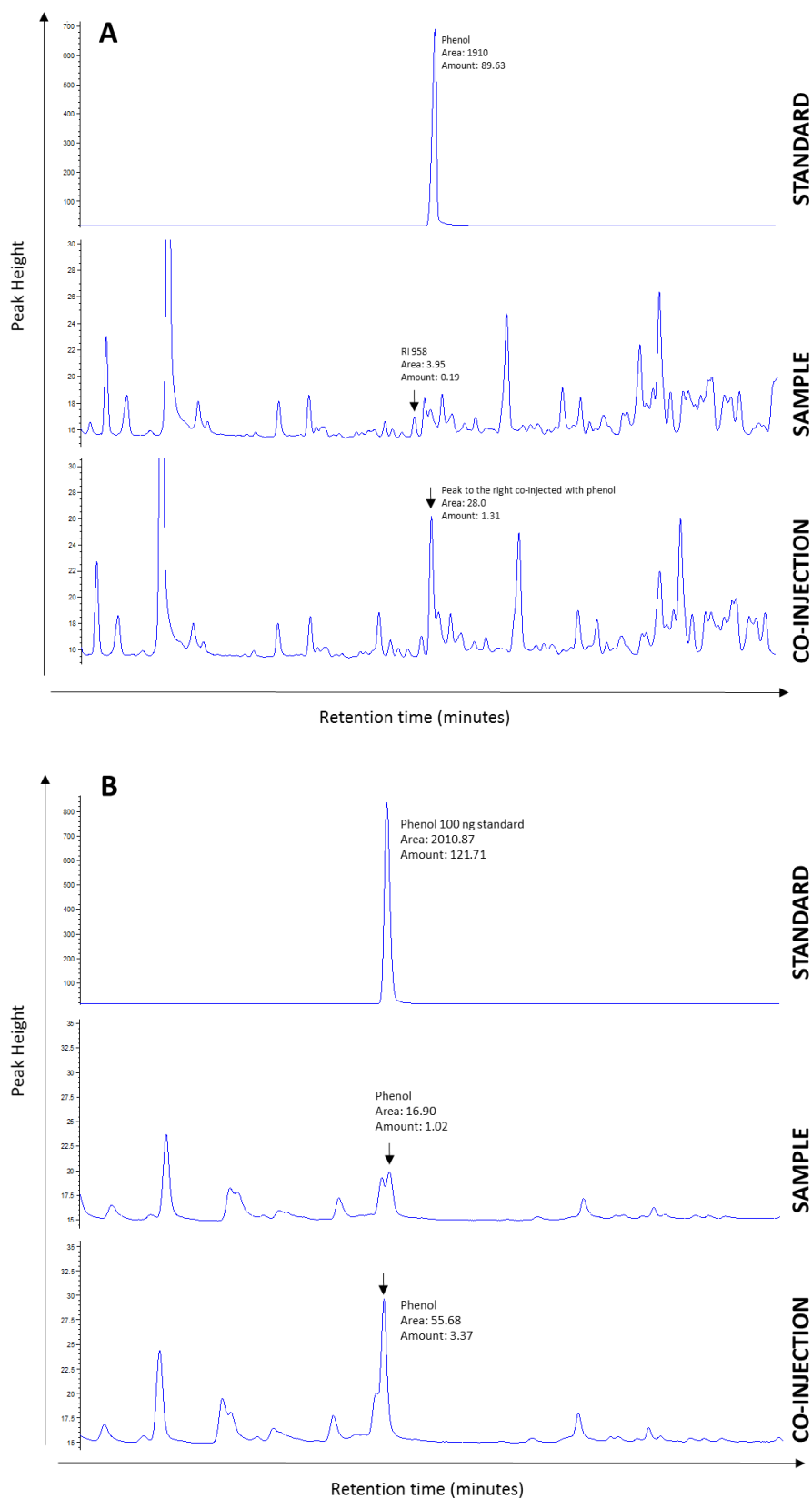


Figure 5-44. Co-injections for phenol standard with sample KA078 23MAY14 (A) co-injections on HP1 column, (B) co-injections on DB wax column. Note this co-injection indicated that the compound of interest, RI 958, was (in the case of the GC analysis) not phenol, as the wrong peak enhanced (A). However, for the GC-EAG analysis, EAG-active RI 958 was co-eluting phenol and 1-octen-3-one, therefore formal identification of phenol was required irrespectively.

5.11.6 Sample AL029 13FEB14: Phenol

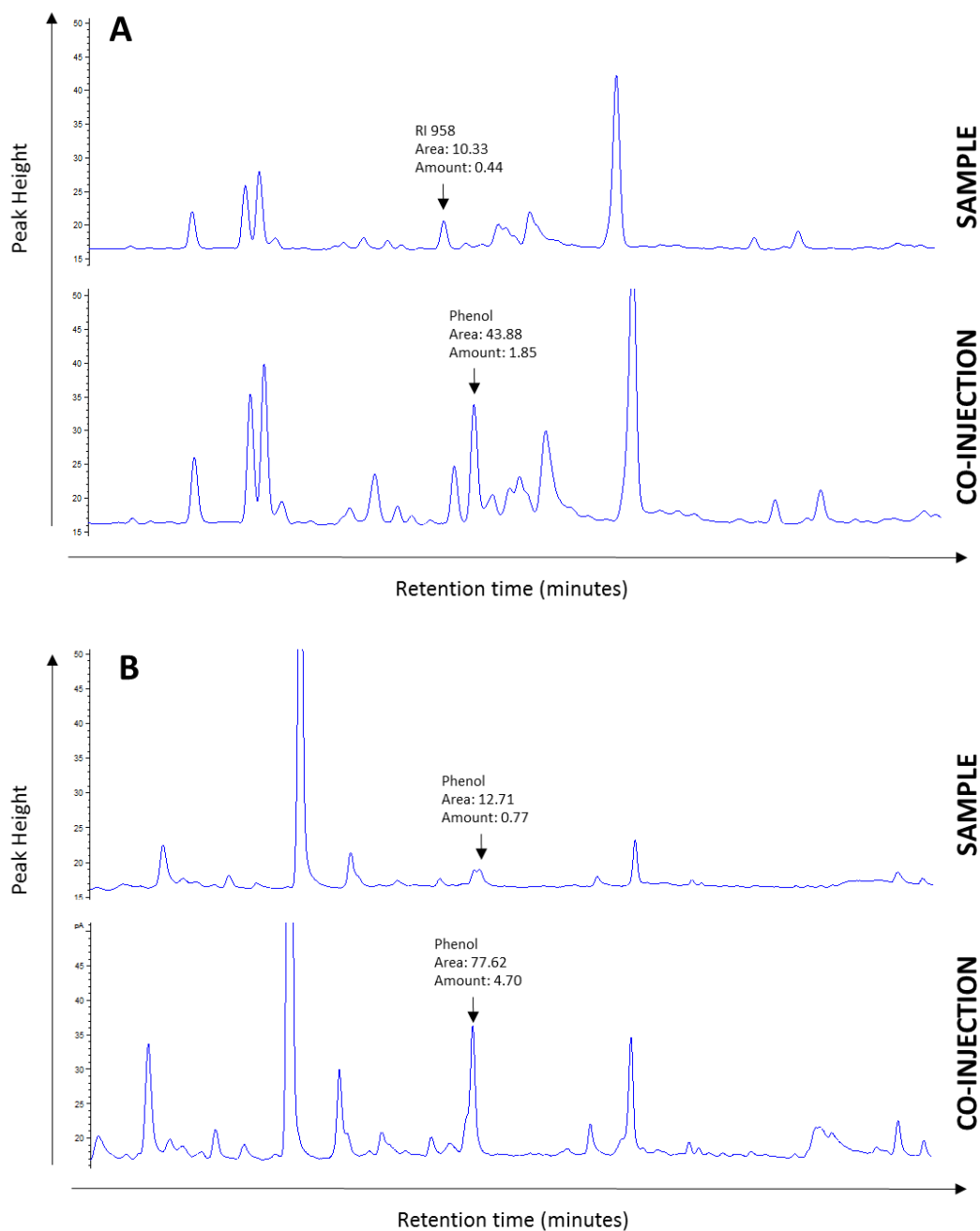


Figure 5-45. Co-injections for phenol standard with sample AL029 13FEB14 (A) co-injections on HP1 column, (B) co-injections on DB wax column. Note this co-injection indicated that the compound of interest, RI 958, was (in the case of the GC analysis) not phenol, as the wrong peak enhanced (A). However, for the GC-EAG analysis, EAG-active RI 958 was co-eluting phenol and 1-octen-3-one, therefore formal identification of phenol was required irrespectively.

5.11.7 Sample AL029 13FEB14: 1-octen-3-one

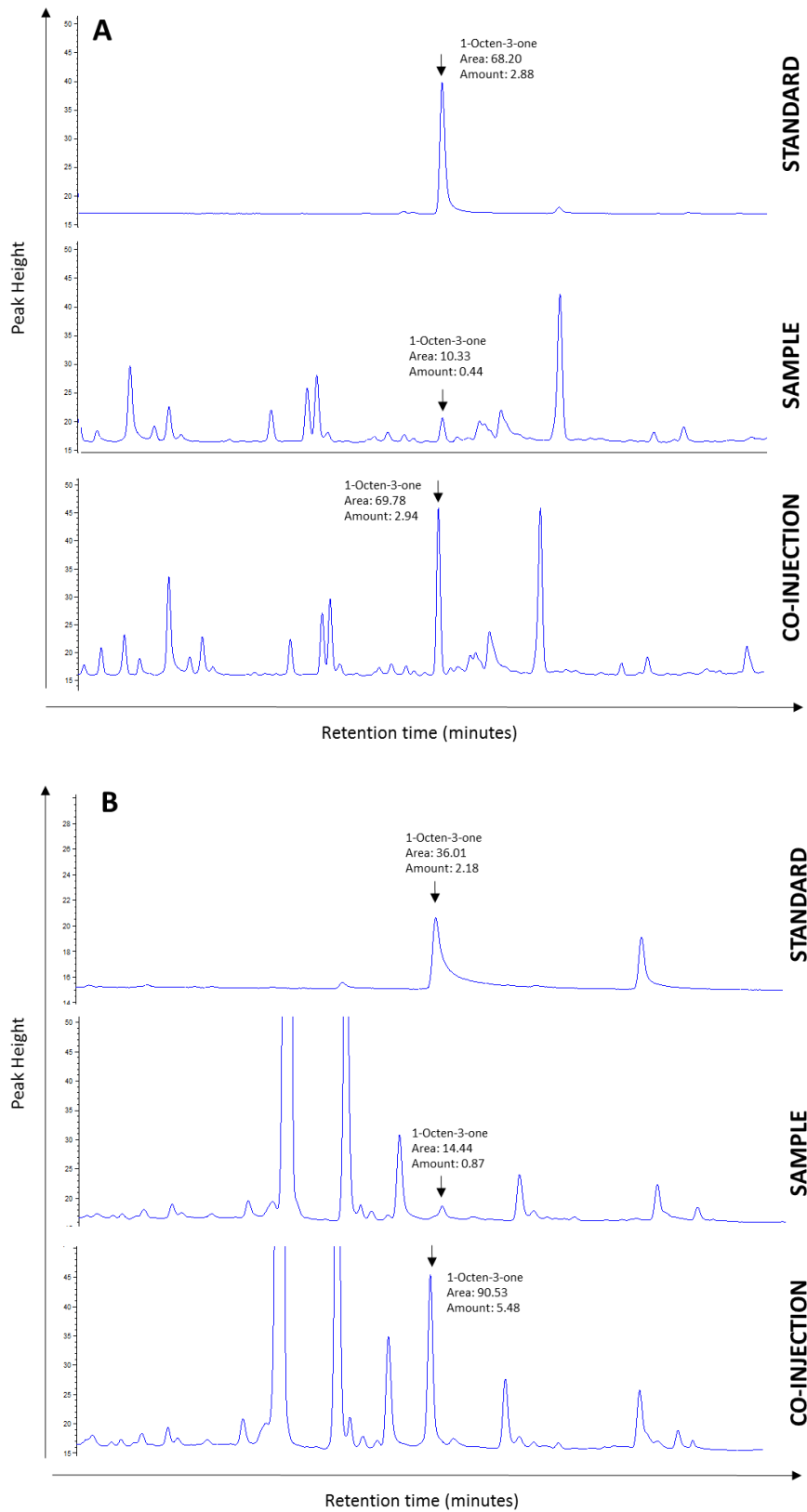


Figure 5-46. Co-injections for 1-octen-3-one standard with sample AL029 13FEB14 (A) co-injections on HP1 column, (B) co-injections on DB wax column. This peak enhancement revealed the correct identity of RI 958 in the GC analysis.

5.11.8 Sample PO014 10JUN14: Hexanal

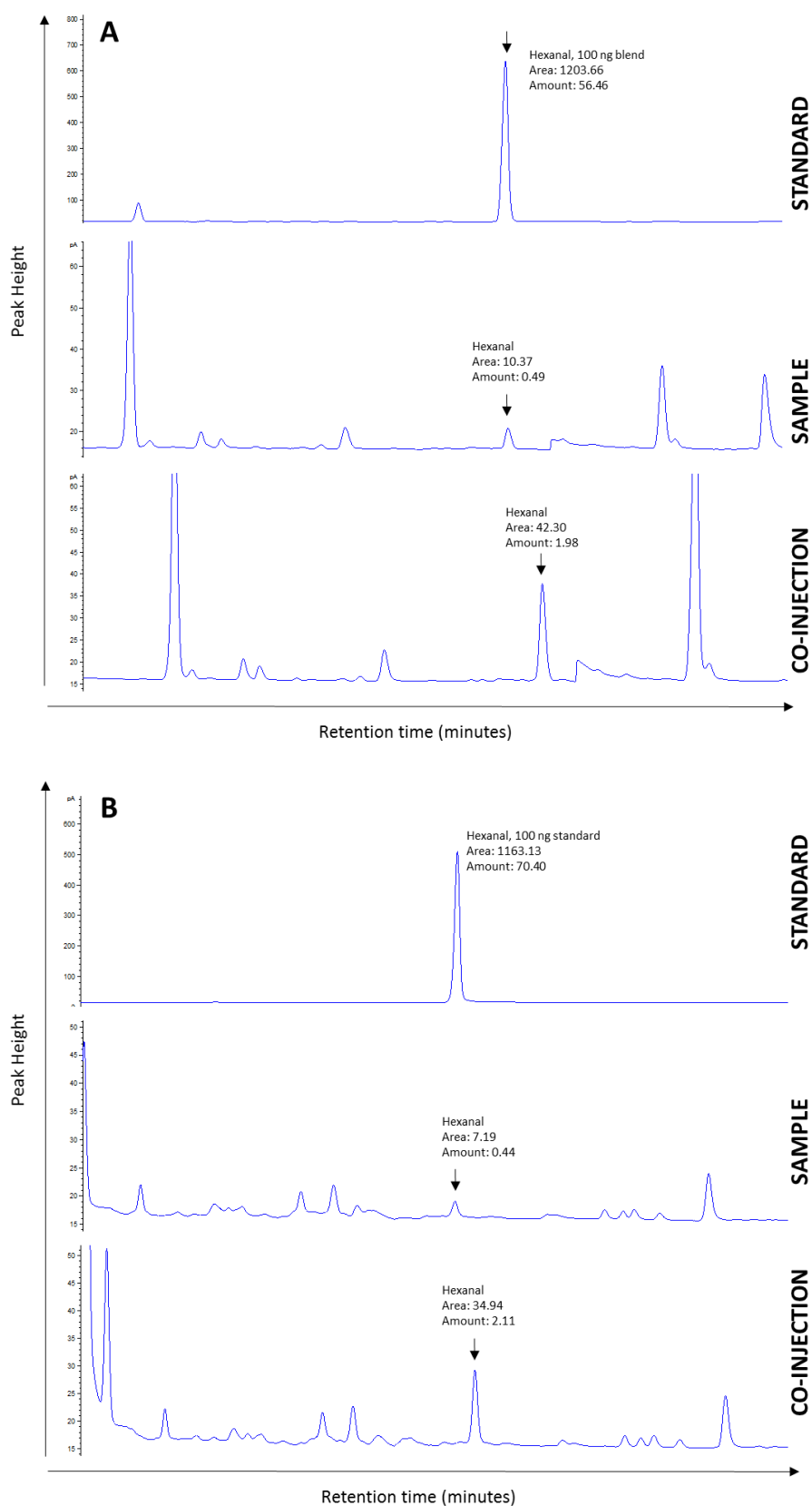


Figure 5-47. Co-injections for hexanal standard with sample PO014 10JUN14 (A) co-injections on HP1 column, (B) co-injections on DB wax column.

5.12 Appendix: SED tables from Kenyan odour profile analysis

Matrices of pairwise comparisons between groups, modelled by parasitological infection status for the compounds of interest identified in all naturally-infected cohorts. Standard errors of differences between groups are shown, as derived from linear mixed models (REML), and compound names or retention indices given. Significance ($P < 0.05$) for comparisons made using the least significant difference (LSD, 5 %) values (= SED multiplied by the 2.5 % t-value) is indicated by a '+' symbol, df = degrees of freedom, av SED = average standard error of the difference.

Heptanal

'Total density'	SED					
Higher density	*					
Gametocytes	0.129	*				
Lower density	0.108	0.139	*			
Negative	0.140 +	0.164	0.151	*		
CNL(A)	0.346 +	0.356 +	0.350 +	0.361	*	
CNL(B)	0.095 +	0.128 +	0.108 +	0.137 +	0.345	*
$df = 179$, $av. SED = 0.2$	Higher density	Gametocytes	Lower density	Negative	CNL(A)	CNL(B)

+ Significance ($P < 0.05$) for comparisons made using the least significant difference (LSD, 5 %) values (= SED multiplied by the 2.5 % t-value).

'Quartiles'	SED						
1	*						
2	0.158	*					
3	0.154	0.160	*				
4	0.145	0.155	0.150	*			
CNL(B)	0.125 +	0.135 +	0.128 +	0.121 +	*		
CNL(A)	0.351 +	0.356 +	0.353 +	0.350 +	0.341	*	
Gametocytes	0.153	0.161	0.157	0.149	0.129 +	0.352 +	*
Negative	0.163	0.171	0.164	0.160	0.138 +	0.357	0.165
$df = 178$, $av. SED = 0.20$	1	2	3	4	CNL(B)	CNL(A)	Gametocytes

'Pos v.s neg'	SED				
Positive	*				
Negative	0.132	*			
CNL(A)	0.344 +	0.362		*	
CNL(B)	0.082 +	0.138 +		0.346	*
$df = 184$, $av. SED = 0.23$	Positive	Negative		CNL(A)	CNL(B)

Octanal

'Total density'	SED				
Higher density	*				
Gametocytes	0.589	*			
Lower density	0.489 +	0.631	*		
Negative	0.634	0.745	0.686	*	
CNL(A)	1.683 +	1.725 +	1.699 +	1.743	*
CNL(B)	0.434 +	0.585 +	0.492 +	0.624 +	1.678
$df = 174$, $av. SED = 0.96$	Higher density	Gametocytes	Lower density	Negative	CNL(A)

Chapter 5: Odour profile analysis of children naturally infected with *Plasmodium* species

'Quartiles'	SED						
1	*						
2	0.732	*					
3	0.705	0.736	*				
4	0.662	0.716	0.686	*			
CNL(B)	0.577 +	0.624 +	0.590 +	0.558 +	*		
CNL(A)	1.708 +	1.731 +	1.717 +	1.703 +	1.664	*	
Gametocytes	0.702	0.737	0.724	0.683	0.592 +	1.714 +	*
Negative	0.749	0.792	0.745	0.734	0.632 +	1.732	0.756
<i>df</i> = 171, <i>av. SED</i> =0.94	1	2	3	4	CNL(B)	CNL(A)	Gametocytes

'Gametocytes'	SED				
Asexual	*				
Gams	0.5246	*			
Sub-gams	0.5733	0.6218 +	*		
Negative	0.6419	0.6978 +	0.7418	*	
CNL(A)	1.7031 +	1.7219 +	1.7355 +	1.7631	*
CNL(B)	0.4341 +	0.5122 +	0.5564 +	0.6276 +	1.6956
<i>df</i> = 175, <i>av. SED</i> =0.97	Asexual	Gams	Sub-gams	Negative	CNL(A)

Nonanal

'Total density'	SED				
Higher density	*				
Gametocytes	1.802	*			
Lower density	1.508 +	1.943	*		
Negative	1.974	2.312	2.097	*	
CNL(A)	5.804 +	5.921 +	5.844	5.972 +	*
CNL(B)	1.321 +	1.783 +	1.499 +	1.924 +	5.789
<i>df</i> = 176, <i>av. SED</i> =3.7	Higher density	Gametocytes	Lower density	Negative	CNL(A)

'Quartiles'	SED						
1	*						
2	2.247	*					
3	2.183	2.258	*				
4	2.057 +	2.198	2.123	*			
CNL(B)	1.778 +	1.912 +	1.823 +	1.720 +	*		
CNL(A)	5.657 +	5.715 +	5.682 +	5.642 +	5.530	*	
Gametocytes	2.169	2.282	2.236	2.115	1.830 +	5.672 +	*
Negative	2.316	2.429	2.323	2.274 +	1.958 +	5.727	2.342
<i>df</i> =176, <i>av. SED</i> =3.01	1	2	3	4	CNL(B)	CNL(A)	Gametocytes

Chapter 5: Odour profile analysis of children naturally infected with *Plasmodium* species

(E)-2-Octenal

'Total density'	SED				
Higher density	*				
Gametocytes	0.177	*			
Lower density	0.153	0.177	*		
Negative	0.189	0.214	0.188	*	
CNL(A)	0.320 +	0.333 +	0.318 +	0.336	*
CNL(B)	0.123 +	0.184 +	0.162 +	0.190	0.320
<i>df</i> = 160, <i>av. SED</i> =0.23	Higher density	Gametocytes	Lower density	Negative	CNL(A)

'Gametocytes'	SED				
Asexual	*				
Gams	0.164	*			
Sub-gams	0.171	0.174	*		
Negative	0.187	0.201	0.206	*	
CNL(A)	0.333	0.337 +	0.338 +	0.348	*
CNL(B)	0.123 +	0.169 +	0.176 +	0.191	0.333
<i>df</i> = 177, <i>av. SED</i> =0.23	Asexual	Gams	Sub-gams	Negative	CNL(A)

'Pos v.s neg'	SED		
Positive	*		
Negative	0.182	*	
CNL(A)	0.320 +	0.340	*
CNL(B)	0.107 +	0.189	0.324
<i>df</i> = 173, <i>av. SED</i> =0.24	Positive	Negative	CNL(A)

(E)-2-Decenal

'Total density'	SED				
Higher density	*				
Gametocytes	0.534	*			
Lower density	0.441	0.570	*		
Negative	0.571	0.673	0.616	*	
CNL(A)	0.940 +	1.002 +	0.962 +	1.025	*
CNL(B)	0.395 +	0.531 +	0.445 +	0.565	0.932
<i>df</i> = 172, <i>av. SED</i> =0.68	Higher density	Gametocytes	Lower density	Negative	CNL(A)

'Gametocytes'	SED				
Asexual	*				
Gams	0.471 +	*			
Sub-gams	0.504	0.553 +	*		
Negative	0.563	0.621 +	0.656	*	
CNL(A)	0.943 +	0.971 +	0.986	1.023	*
CNL(B)	0.392 +	0.463 +	0.495 +	0.558	0.933
<i>df</i> = 181, <i>av. SED</i> =0.39	Asexual	Gams	Sub-gams	Negative	CNL(A)

Chapter 5: Odour profile analysis of children naturally infected with *Plasmodium* species

'Pos v.s neg'	SED		
Positive	*		
Negative	0.549 +	*	
CNL(A)	0.927 +	1.038	*
CNL(B)	0.338 +	0.573	0.940
<i>df</i> = 179, <i>av. SED</i> =0.73	Positive	Negative	CNL(A)

965: 6-Methyl-5-hepten-2-one and 1-octen-3-ol (co-eluting)

'Total density'	SED				
Higher density	*				
Gametocytes	0.147	*			
Lower density	0.133	0.147	*		
Negative	0.160	0.177	0.158	*	
CNL(A)	0.295 +	0.302 +	0.293	0.307 +	*
CNL(B)	0.098	0.151	0.135	0.158 +	0.295
<i>df</i> = 174, <i>av. SED</i> =0.20	Higher density	Gametocytes	Lower density	Negative	CNL(A)

'Quartiles'	SED						
1	*						
2	0.163	*					
3	0.161	0.166	*				
4	0.159	0.168 +	0.162	*			
CNL(B)	0.149	0.158	0.150 +	0.128 +	*		
CNL(A)	0.309	0.315	0.312 +	0.311 +	0.305	*	
Gametocytes	0.160	0.168	0.165	0.159	0.1516 +	0.312	*
Negative	0.170	0.178	0.171	0.175	0.158 +	0.316 +	0.176
<i>df</i> = 172, <i>av. SED</i> =0.20	1	2	3	4	CNL(B)	CNL(A)	Gametocytes

'Gametocytes'	SED				
Asexual	*				
Gams	0.136	*			
Sub-gams	0.143	0.141	*		
Negative	0.158	0.165	0.170	*	
CNL(A)	0.303	0.304 +	0.307 +	0.315 +	*
CNL(B)	0.097 +	0.137 +	0.145 +	0.158	0.303
<i>df</i> = 161, <i>av. SED</i> =0.20	Asexual	Gams	Sub-gams	Negative	CNL(A)

2-Octanone

'Total density'	SED				
Higher density	*				
Gametocytes	0.013 +	*			
Lower density	0.011	0.014 +	*		
Negative	0.014	0.016 +	0.014	*	
CNL(A)	0.019 +	0.021 +	0.019 +	0.021	*
CNL(B)	0.009 +	0.012 +	0.010 +	0.0128	0.019
<i>df</i> = 176, <i>av. SED</i> =0.01	Higher density	Gametocytes	Lower density	Negative	CNL(A)

Chapter 5: Odour profile analysis of children naturally infected with *Plasmodium* species

'Gametocytes'	SED				
Asexual	*				
Gams	0.011 +	*			
Sub-gams	0.012 +	0.013	*		
Negative	0.013	0.015 +	0.015	*	
CNL(A)	0.018 +	0.019 +	0.019 +	0.020	*
CNL(B)	0.009 +	0.011 +	0.012 +	0.013	0.017
<i>df = 174, av. SED=0.01</i>	Asexual	Gams	Sub-gams	Negative	CNL(A)

Hexanal

'Gametocytes'	SED				
Asexual	*				
Gams	0.2874 +	*			
Sub-gams	0.3062 +	0.3343	*		
Negative	0.3547	0.3865 +	0.4044	*	
CNL(A)	1.0019 +	1.0118 +	1.0172 +	1.034	*
CNL(B)	0.2333 +	0.2765 +	0.2966 +	0.3424 +	0.999
<i>df = 181, Av SED=0.55</i>	Asexual	Gams	Sub-gams	Negative	CNL(A)

1-Octen-3-one

'Gametocytes'	SED				
Asexual	*				
Gams	0.1068 +	*			
Sub-gams	0.1293	0.1405	*		
Negative	0.1328	0.1455 +	0.164	*	
CNL(A)	0.2979	0.3026 +	0.3115 +	0.3132	*
CNL(B)	0.0859 +	0.1022 +	0.1264 +	0.1291 +	0.2964
<i>df = 174, Av SED = 0.19</i>	Asexual	Gams	Sub-gams	Negative	CNL(A)

6 Electroantennography of human odour samples

6.1 Introduction

Olfaction is the primary modality by which insects detect their surroundings (Carey et al., 2010; Takken and Knols, 1999). The most important olfactory organs are the antennae, however, the maxillary palps and proboscis are also equipped with mechanical, gustatory and olfactory receptors (Kwon et al., 2006; McInver and Siemicki, 1975). When odour molecules are detected, their quantity and quality is converted into neural code in the olfactory receptor neurons (ORNs) (Qiu and van Loon, 2010). Detection of odour molecules by ORNs triggers cyclic nucleotide-gated ion channels to open, increasing intracellular Ca^{2+} and Na^{+} and causing membrane depolarisation, which at a certain threshold generates an action potential (Ignell et al., 2011). This is conducted to the olfactory lobe of the deutocerebrum (Qiu et al., 2006), the part of the 'arthropod brain' that processes sensory information from the antennae (for more information on olfaction, see chapter 1). By amplifying and detecting the electrical signal generated during this process, electrophysiology can be exploited to reveal responses of the olfactory organ to an odorant. Electrophysiology can be examined at the level of a sensillum (the hair-like sensory structures of the olfactory organs) or of an entire olfactory appendage, e.g. antenna. The latter process is known as electroantennography (EAG), and the response is thought to represent the sum of action potentials generated by all ORNs innervated by that stimulus (Mayer et al., 1984; Syntech, 2004). Because different subsets of ORNs respond to different odours, the extent of EAG depolarisation (i.e. the signal) depends on both the number of ORNs responding, and the maximum value of receptor potentials (Qiu et al., 2013). The signal itself offers no information on the physiology of the insect olfactory receptors, as such EAG is a purely empirical method of practical value (Syntech, 2004), yet this technique has greatly contributed to our understanding of which compounds are important to *Anopheles gambiae*. These are summarised, in addition to compounds demonstrated to influence *An. gambiae* behaviour, in

Table 6-1.

By coupling the study of electrophysiology with gas chromatography (GC), the EAG response can be used to detect which compounds, in a mixture, are of entomological relevance (i.e. are being detected by the arthropod) (GC-EAG). Here, the eluate (the solvent and compounds exiting the column) from the GC machine is split, with a proportion directed to the GC detector (e.g. flame ionisation detector), and the remainder to the electroantennography (EAG) set-up. The dissected olfactory organs (e.g. antennae in EAG) are mounted between two electrodes and

suspended in a purified, humidified airflow to which the GC eluate is added. An olfactory response is stimulated when a compound elutes that is detected by the insect, and this response is amplified, recorded and interpreted with respect to the GC detector output. This technique has been widely used across Insecta for the detection of pheromones and kairomones (Du & Millar 1999; Gikonyo et al. 2003; Qiu et al. 2004; Young et al. 2015).

GC analysis of odour samples (chapters 2 and 5) identified infection-associated compounds (IAC), not those of specific relevance to the mosquito vector. Although entomologically non-active compounds associated with infection are interesting, and of possible relevance as malaria biomarkers, the overarching aim of this thesis was to identify compounds that may constitute semiochemicals that influence *Plasmodium* parasite transmission to the vector. The olfactory organs of insects are highly sensitive, able to detect and respond to tiny amounts of stimulus: for example, the silk moth (*Bombyx mori*) responds behaviourally when only 85 ORNs per antenna each intercept one female-produced sex pheromone molecule per second (Angioy et al., 2003). During analysis of odour samples by GC (chapter 4), peaks may have been missed as they lay beneath detection thresholds, or were hidden by other co-eluting compounds. It is therefore possible that important (i.e. infection-associated and entomologically active) compounds were overlooked, but which could be detected by highly sensitive antennae during GC-EAG. Another justification for the use of GC-EAG in this context was to further investigate any possible association between the specific carriage of the sexual stage *Plasmodium* parasites, gametocytes, and changes in human odour profile. Project collaborators conducted behavioural bioassays with both skin odour alone and 'whole' individuals (all volatiles from human body, notably including breath), designed to test the attractiveness to mosquitoes of individuals harbouring varying *Plasmodium* stages. While the skin odour bioassay indicated an effect of any *Plasmodium* parasite stage on human attractiveness, the 'whole' person bioassay suggested that only those harbouring gametocytes were more attractive (Busula et al., 2017). GC analysis of odour profiles (chapter 5) revealed several compounds whose increased production was associated with a higher total density of parasites. Others, including octanal, (*E*)-2-octenal, (*E*)-2-decenal and RI 965 had a possible additional effect of gametocytes, and three compounds were only produced in association with gametocytes: the ketones 2-octanone, 1-octen-3-one, and the aldehyde hexanal. By GC-EAG testing the odour profiles of individuals specifically harbouring gametocytes, it was possible to further examine for a gametocyte-specific signal, detected by *Anopheles coluzzii*.

Chapter 6: Electroantennography of human odour samples

Table 6-1. Overview of compounds that elicited an electrophysiological (E+) or behavioural (B+, attraction, B-, repellency) response in *Anopheles gambiae*. Concentrations are omitted, as are constituents of complex attractive or repellent blends, as are oviposition behavioural studies. Table adapted from Takken & Knols (2010).

Chemical stimulus	Response	Description	Reference
Ammonia (NH ₃)	E +		Meijerink et al. 2001
	B +/-	Response depends on dose	Braks et al. 2001
	B +/-	Response depends on dose	Smallegange et al. 2005
	B +/-	Response depends on dose	Smallegange et al. 2002
Alcohols			
1-Octen-3-ol	E +		Meijerink & van Loon 1999
3-Methyl-1-butanol	E +		Meijerink et al. 2001
	E +		Qiu et al. 2006
	E +		Suer 2011
	B -	Repellent/inhibitory effect when combined with NH ₃ and lactic acid (LA)	Qiu 2005
	B +	Increased attractiveness of basic blend (NH ₃ and LA and tetradecanoic acid)	Verhulst et al. 2011
	B -	Inhibited attractiveness of NH ₃ and LA	Qiu et al. 2011
	B +	Attractive with CO ₂	van Loon et al. 2015
	B +	Increased attractiveness of blend (NH ₃ , LA, tetradecanoic acid, and CO ₂)	van Loon et al. 2015
4-Ethylphenol	E +		Wang et al. 2010
	E +		Qiu et al. 2006
	B -	Inhibited attractiveness of NH ₃ and LA	Qiu et al. 2011
Aldehydes			
Heptanal	E +		Qiu et al., 2006
	E +		Qiu et al., 2013
	E +		Jaleta et al., 2016
Benzaldehyde	E +		Jaleta et al., 2016
	E +		Wondwosen et al., 2017
	E +		Smallegange et al., 2012
	E +		Tauxe et al., 2013
	B -	Significantly reduced attractiveness of basic blend (NH ₃ and LA and tetradecanoic acid)	Smallegange et al., 2012
Octanal	B -/+	Dose-dependent repellency	Logan et al., 2010
	B +	Significantly enhanced attractiveness of basic blend at lowest concentrations (NH ₃ and LA and tetradecanoic acid)	Smallegange et al., 2012
Nonanal	E +		Rund et al. 2013
	E +		Xu et al., 2010
	E +		Jaleta et al., 2016
	B -/+	Dose-dependent repellency	Logan et al., 2010

Chapter 6: Electroantennography of human odour samples

Chemical stimulus	Response	Description	Reference
Aliphatic carboxylic acids			
Lactic acid	B -	No landing response	Healy & Copland 2000
	B -/+ ?	Not or weakly attractive on its own	Braks et al. 2001
	?	Not or weakly attractive on its own	Smallegange et al. 2002
	B +	Attractive with CO ₂ and human odour	Dekker et al. 2002
	B +	Synergistic with NH ₃ and carboxylic acids	Smallegange et al. 2005
	B +	Synergistic with NH ₃ and carboxylic acids	Smallegange et al. 2009
Acetic acid	E +		Meijerink & van Loon 1999
	E +		Qiu et al., 2006
	E +		Kwon et al., 2006
	B -	No effect in combination with NH ₃ and LA	Smallegange et al. 2009
Propanoic acid (propionic acid)	E +		Meijerink & van Loon 1999
	B +	Synergistic with NH ₃ and LA	Smallegange et al. 2009
2-Methyl propanoic acid (isobutyric acid)	E +		Meijerink & van Loon 1999
	B -	No effect in combination with NH ₃ and LA	Smallegange et al. 2009
Butanoic acid (butyric acid)	E +		Meijerink & van Loon 1999
	B +	Synergistic with NH ₃ and LA	Smallegange et al. 2009
3-Methyl butanoic acid (isovaleric acid)	E +		Meijerink & van Loon 1999
	B +	Synergistic with NH ₃ and LA	Smallegange et al. 2009
	B +	Attractive with CO ₂	van Loon et al. 2015
Pentanoic acid (valeric acid)	E +		Meijerink & van Loon 1999
	B +	Synergistic with NH ₃ and LA	Smallegange et al. 2009
Hexanoic acid (caproic acid)	E +		Meijerink & van Loon 1999
	B -/+	Synergistic with NH ₃ and LA/repellency > dose dependent	Smallegange et al. 2009
Heptanoic acid	B -/+	Synergistic with NH ₃ and LA/repellency > dose dependent	Smallegange et al. 2009
Octanoic acid	B +	Synergistic with NH ₃ and LA	Smallegange et al. 2009
Nonanoic acid	E +		Knols et al., 1997
	E +		Cork and Park, 1996
	E +		Qiu et al., 2006
Tetradecanoic acid	B +	Synergistic with NH ₃ and LA	Smallegange et al. 2009
	B +	Attractive when combined with NH ₃ and LA	Smallegange et al. 2009
Unsaturated carboxylic acids			
7-Octenoic acid	B +	Attractive when combined with dual-port olfactometer NH ₃ and LA	Qiu 2005
Oxocarboxylic acids (oxo acids)			
2-Oxobutanoic acid	B +	Induced landing response	Healy et al. 2002
2-Oxo-3-methylbutanoic acid	B +	Induced landing response	Healy et al. 2002
2-Oxopentanoic acid	B +	Induced landing response	Healy et al. 2002
	B +	Induced landing response	Healy & Copland 2000

Chapter 6: Electroantennography of human odour samples

Chemical stimulus	Response	Description	Reference
2-Oxo-3-methylpentanoic acid	B +	Induced landing response	Healy et al. 2002
2-Oxo-4-methylpentanoic acid	B +	Induced landing response	Healy et al. 2002
2-Oxohexanoic acid	B +	Induced landing response	Healy et al. 2002
2-Oxooctanoic acid	B +	Induced landing response	Healy et al. 2002
Ketones			
Acetone	B -/+	Attractive with NH ₃ and LA; not attractive alone	Qiu et al. 2011
	B +	Activating effect when combined with CO ₂	Takken et al. 1997
	B +	Enhanced the effect of LA, decreased effect of NH ₃	Qiu 2005
	B +	No additional attractiveness when combined with NH ₃ and LA	Qiu 2005
6-Methyl-5-hepten-2-one	E +		McBride et al., 2014
	E +		Lu et al., 2007
	E +		Qiu et al., 2006
	E +		Meijerink et al., 2000
	B -	Repellent	Menger et al., 2014
	B -	Repellent/inhibitory effect when combined with NH ₃ and LA	Qiu 2005
	B -/+	Dose-dependent repellency	Logan et al., 2010
Geranylacetone	E +		Rund et al. 2013
	E +		Meijerink et al., 2001
	E +		Qiu et al., 2006
	E +		Takken et al., 2001
	B -	Repellent/inhibitory effect when combined with NH ₃ and LA	Qiu 2005
	B -	Inhibitory effects at some doses	Qiu et al., 2011
	B -/+	Dose-dependent repellency	Logan et al., 2010
Miscellaneous			
Benzothiazole	B -	Repellent/inhibitory effect	Qiu et al. 2004
Indole	E +		Rund et al. 2013
	B -	Inhibited attractiveness of NH ₃ and LA	Qiu et al. 2011
Butan-1-amine	B +/-	Synergistic with CO ₂	van Loon et al. 2015

6.2 Aim and objectives

The aim of this chapter was to examine the response of *Anopheles coluzzi* to odour sample extract from individuals of differing parasitological status, including *Plasmodium*-infected and *Plasmodium* parasite-free individuals, by coupled GC-EAG.

This aim was achieved through the following objectives:

1. To detect compounds with entomological activity in odour samples from experimentally *Plasmodium*-infected adults, using coupled GC-EAG to measure the antennal response of *Anopheles coluzzii*
 - a. To identify any EAG-active peaks that are only present in the odour of *Plasmodium*-infected individuals, and which might therefore constitute a 'transmission signal'
2. To detect compounds with entomological activity in odour samples from naturally *Plasmodium*-infected children, using coupled GC-EAG to measure the antennal response of *Anopheles coluzzii*
 - a. To identify any EAG-active peaks that are only present in the odour of *Plasmodium*-infected individuals, and which might therefore constitute a 'transmission signal'
3. To further characterise the volatile cues in the human odour profile that are recognised by *Anopheles coluzzii*, and that therefore may be used in mosquito host location

6.3 Methods

Odour samples, previously used in the GC odour profile analysis, were investigated by GC-EAG. The samples were from two studies, one experimentally *Plasmodium*-infected cohort of adults (chapter 2/2.3.6) and one naturally *Plasmodium*-infected cohort of children in Kenya (chapter 5).

6.3.1 Blends of odour sample extract for GC-EAG testing

For each dataset, odour samples from individuals with similar *Plasmodium* infection status were mixed to create odour 'blends' that represented specific parasitological status. For each blend, several samples were combined, to (1) maximise the possibility of including samples with IAC and/or any potential transmission signal, and (2) ensure compounds were present in sufficient quantity. Preparation of the Porapak extracts is described in detail elsewhere (chapters 2 and 5). For the preparation of blends: glassware, charcoal filters and PTFE tubing were cleaned prior to use according to standard protocol (chapter 2/2.3.7). Once created, blends were examined by GC, and approximate amounts per peak calculated using the retention index method (chapter 2).

Experimental infections GC-EAG blends

Blends reflected the odour of individuals before, during and after EI, with a group who were negative during infection (i.e. did not become *Plasmodium* positive) and a group who were positive during infection (i.e. *Plasmodium* parasites were detected). BMGF blends comprised the following: 'Before', nine individuals from day -2 post infection (PI), 'During (-)', nine individuals from days 6 and 8 PI; 'During (+)', nine individuals from days 6 and 8 PI; 'After', 11 parasite-free individuals from day 34 PI; 'Control', six empty bag controls from across all sampling moments. Individuals had been infected by one, two or five bites by mosquitoes infected with either *P. falciparum* NF135 or *P. falciparum* NF166 (chapter 2).

Aliquots from a series of test samples were mixed, concentrated under a stream of charcoal-filtered nitrogen (to 50 μ L) and assayed for antennal response. A proportion equivalent to 1/50th of each odour sample was found to successfully stimulate EAG response, and all further GC-EAG blends were designed to approximate this quantity (1/50th of each of approximately ten samples, per injection).

Natural infections GC–EAG blends

Blends were synthesised by combining odour sample extracts from subsets of individuals representing infection with different *P. falciparum* lifecycle stages. Categorisation (Table 6-2) was designed to strictly separate gametocyte carriers. Samples identified as carrying *P. ovale* or *P. malariae* parasites were not used. However, as this information was not available for all samples, mixed *Plasmodium* species infections cannot be excluded. The GC trace of each sample was examined prior to mixing in case of profound or obvious contamination; on this basis three samples were excluded. Aliquots of all extracts (400 µL) each were mixed and concentrated under a stream of charcoal-filtered nitrogen (to approximately 60 µL).

Table 6-2. Parasitological information GC-EAG blends, Kenya cohort. LOD = test limit of detection. For further information on parasitological diagnosis and interpretation, see chapter 3. P/µL = parasites/µL blood, n = number of odour samples. *When species-specific information available ** Highest value was 304 gametocytes /µL ***RDT positivity was allowed on the basis that these tests can remain positive for some time following curative treatment, due to circulating HRP-2 protein

Categories	Description	Schools	n	Total
<i>P. falciparum</i> no gametocytes	- Parasites by at least one molecular method	Alero	8	10
	- No <i>P. ovale</i> or <i>P. malariae</i> *	Kamsama	1	
	- QT-NASBA negative (no gametocytes)	Powo	1	
<i>P. falciparum</i> sub-gametocyte	- Parasites by at least one molecular method	Obambo	2	14
	- No <i>P. ovale</i> or <i>P. malariae</i> *	Alero	4	
	- QT-NASBA > LOD (gametocytes present)	Kamsama	4	
	- QT-NASBA no higher than 500 p/µL**	Powo	4	
	- No gametocytes by microscopy			
<i>P. falciparum</i> gametocytes	- No <i>P. ovale</i> or <i>P. malariae</i> *	Obambo	2	13
	- Gametocytes by microscopy, or QT-NASBA > 500 p/µL	Alero	2	
	- Asexual parasite counts were disregarded	Kamsama	3	
	- NB// all individuals except one had gametocytes by microscopy	Powo	6	
Negative	Negative by all diagnostic measures but allowing rapid diagnostic test positivity***	Obambo	4	15
		Alero	9	
		Kamsama	1	
		Powo	1	
Control	Closed bag control	Obambo	3	11
		Alero	3	
		Kamsama	2	
		Powo	3	

6.3.2 Mosquitoes

Mosquitoes used for GC-EAG were four- to five-day-old, non-blood-fed female *An. coluzzii* (formerly known as *An. gambiae* M form) N'gouso strain (Habtewold et al., 2016). Larvae were reared from egg papers, and pupae transferred to a climate-controlled incubator for eclosion.

Adults were maintained at 70 % RH, with a 12-hour light dark cycle (scotophase 08:00 – 20:00) and had access to 50 % glucose solution *ad libitum*. During experiments, host-seeking adult females were selected, taken to the experimental room and kept under a light-proof blanket for use within four hours. All experimentation was conducted between the second and the seventh hour of the scotophase.

6.3.3 Study design

The number of responding antennae taken to signify a true response varies by study (Logan et al., 2008; Puri et al., 2006; Qiu et al., 2004). Between three and seven replicates were indicated by sample size calculation (binomial test to detect an outcome with a varying probability [0.2, 0.3, 0.4], two-sided significance level of 0.05, and 90 % power against a null hypothesis of no response). Experiments were designed to generate replicates in this range.

GC-EAG blends (i.e. treatments, representing parasitological categories) were tested in a random order according to a Latin square design, aiming for ten replicates per treatment. This was to decrease the likelihood that short-term, temporal changes in olfactory response (Rund et al., 2013) were not biased to one treatment group.

6.3.4 Gas chromatography-electroantennography

For each mosquito, the head was dissected from the body and the palps and proboscis removed. Half of the 13th (terminal) flagellomere was cut from each antenna to optimise electrical conductivity. The indifferent electrode was then inserted into the back of the head, this prep was mounted onto the EAG apparatus and the antennal tips then guided into the recording electrode to complete the circuit (Figure 6-1). Both electrodes were hand-pulled glass tips inserted over silver wire (diameter 0.37 mm; Harvard Apparatus, Edenbridge, UK) and filled with Ringers' solution (7.55 g NaCl, 0.64 g KCl, 0.22 g CaCl₂, 1.73 g MgCl₂ g, 0.86 g NaHCO₃ and 0.61 g Na₃PO₄ L⁻¹ water). Gas chromatograph [1] (as previously described chapter 2) was used, with the following programme: oven temperature was maintained at 40 °C for 0.5 minute, then increased by 10 °C per minute to 230 °C, where it was held for 20 minutes. The total run time was 39.5 minutes, ensuring that the antennal nerve cells would remain active for the whole duration of sample elution. The eluate was split to the FID detector and EAG interface at a ratio of 1:1. At the EAG interface, the eluate passed from the heated splitter column to a stream of charcoal filtered, humidified air with a flow rate of 400 mL min⁻¹. This airflow was directed over the

Chapter 6: Electroantennography of human odour samples

antenna from 5 mm. The signal was amplified by X 10,000 by the Intelligent Data Acquisition Controller-4 (IDAC-4), and signals were analysed using the computer based software EAD 2000 (Syntech®, The Netherlands). As soon as the sample was injected into GC[1] and recording started, all lights were switched off (including computer monitors), and the room vacated.

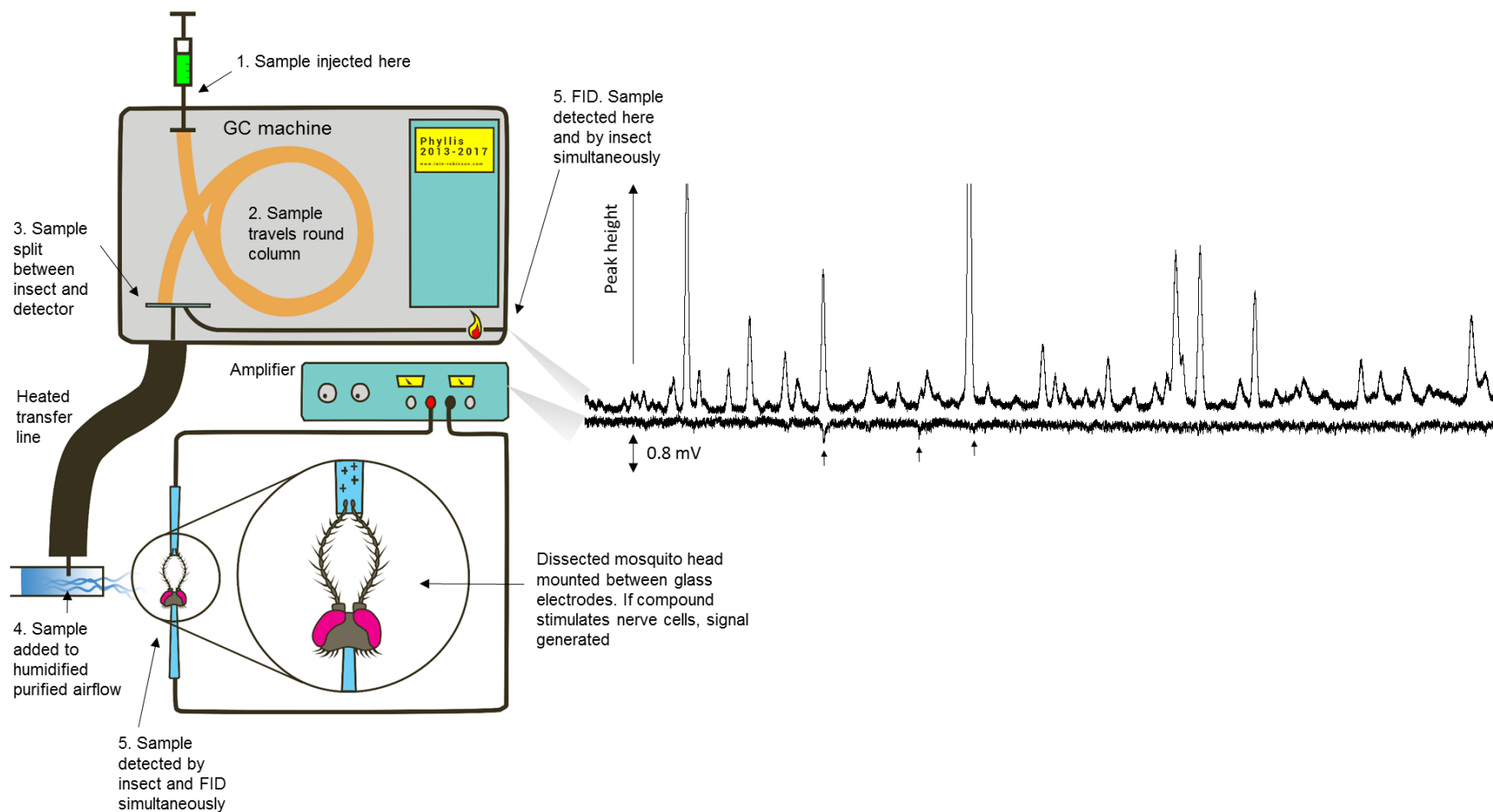


Figure 6-1. GC-EAG circuit. Sample is injected into the gas chromatograph (GC) (1); passes through the column of the GC and separates into its constituent parts (2); at the GC splitter the analytes are split 50:50 to the flame ionisation detector (FID) and the insect (3); the latter proportion passes through a heated transfer line and is added to a stream of filtered, humidified air (4); before this passes over the dissected mosquito head at the same time that the other portion of the sample is detected at the FID (5). Two traces are generated, here the top trace is the GC trace and the bottom the EAD (antennal response). Upwards EAD deflections are noise, while downwards deflections indicate a true response of nerve cell depolarisation. Example responses are marked with arrows. Image courtesy of Iain Robinson, copyright 2017 (www.iain-robinson.com).

6.3.5 Data analysis

For each antennal preparation repetition (rep), the electro-antennographic detection (EAD) trace and relevant GC trace were printed together on lightweight paper (Ryman, 45 GSM). EAD reps with excessive noise, or where the insect died during recording, were disregarded. For each treatment group, the best rep was selected. Antennal responses were annotated (see example response in Figure 6-1), and then the responses in other reps from the same treatment group were added to the first, using a light box to match response position. Here, EAG response was taken as a binary variable (responsive or not), unlike some studies in which amplitude of response is measured (Costantini et al., 2001). Peaks that elicited two or more (BMGF dataset), or three or more (Kenya dataset), antennae responding per treatment group, were considered EAG-active. These were annotated onto the corresponding GC trace for tentative identification by coupled gas chromatography-mass spectrometry (GC-MS). A lower threshold was chosen for the BMGF dataset as fewer antennal repetitions were achieved. For responsive peaks, all responses from all other treatment groups were then added (i.e. less than two or three responses), to give the total number of responses to those peaks across all treatment groups. Latterly, compounds of interest from the odour profile analyses (chapter 2 and 5) were examined in the EAD traces for antennal response, irrespective of a 'response threshold'. Correlations between responding antennae and compound concentration were conducted using GenStat (16th edition, VSNi).

6.3.6 Compound identification by gas chromatography mass spectrometry

Peaks that were found to be EAG-active were identified by GC-MS, by the same protocols as used in chapter 2 (2.3.8). All EAG-active peaks were identified in all blends to maximise certainty of identification. The identity of compounds that were both EAG-active and infection-associated was confirmed by co-injection with authentic standards (Appendix 5.11).

6.4 Results

6.4.1 BMGF dataset (EI cohort)

Across all odour profile treatment groups, 26 peaks were found to be EAG-active by the responses of 22 antennae (Table 6-3). No EAG-active compounds specifically characterised any of the treatment groups (Before, During [-], During [+] and After). EAG-active compounds, considering co-eluting compounds separately, were: two alcohols (2-acetoxyethanol, 2-ethylhexanol), three aromatics (phenol, acetophenone, ethylacetophenone), four aldehydes (heptanal, nonanal, decanal and undecanal), four solvent peaks, one organosulfur (dimethyl sulfone), one carboxylic acid (acetic acid), one ester (triacetin), one fatty acid (nonanoic acid), one long chain alkane (unknown), two terpenoids (geranylacetone, 6-methyl-5-hepten-2-one), one ketone (1-octen-3-one) nine likely artefacts and an unknown compound. Other than 6-methyl-5-hepten-2-one, which co-eluted with acetic acid and a siloxane, none of the EI-IAC were found to be EAG-active. Of all peaks, RI 951 (co-eluting phenol and 1-octen-3-one) and geranylacetone elicited the greatest response (both elicited responses from 73 % of antennae). There was a slight but non-significant correlation between the amount of compound (peak) and percentage response ($r=0.3$, $n=25$ $P=0.17$; RI 791+ excluded as underneath tail of RI 791, cannot measure amount) (Figure 6-2).

6.4.2 Kenyan dataset (NI cohort)

Twenty-two peaks were found to be EAG-active across all treatment groups in the Kenyan dataset by the responses of 34 antennae. Again, no compounds qualitatively characterised one group (Table 6-4). EAG-active compounds, considering co-eluting compounds separately, were: two alkanes (octane and dodecane), four alcohols (1-hexanol, 2-ethylhexanol, 3-octen-2-ol and octen-1-ol), four aldehydes (heptanal, octanal, nonanal, decanal), six aromatics (benzaldehyde, phenol, para cresol, 2-ethyl benzaldehyde, 4-ethyl benzaldehyde, ethylacetophenone), one terpenoid (geranylacetone), one ketone (1-octen-3-one), three solvent peaks, two organosulfurs (dimethyl sulfide and dimethyl sulfone), one possible alkene (2-octene) and three unknowns. Few antennae responded to the NI-IAC (chapter 5) that were retrospectively examined, those that had not been designated EAG-active during the primary analysis (Table 6-5). Of these, peak RI 965 (co-eluting 1-octen-3-ol and 6-methyl-5-hepten-2-one) elicited most responses (12 % antennae responded). Of all EAG-active compounds, nonanal and benzaldehyde elicited the greatest number of responses (68 % and 56 % respectively). Again, there was a slight but non-

significant correlation between the amount of compound (peak) and percentage response ($r=0.187$, $n=22$ $P=0.42$).

6.4.3 Commonality in EAG-activity between both datasets

Neither dataset revealed infection-specific, EAG-active peaks, i.e. EAG-active peaks that were only present in the ‘infected’ groups. Compounds that were EAG-active in both datasets were: dimethyl sulfone, styrene or heptanal (co-eluting), phenol or 1-octen-3-one (co-eluting), 2-ethylhexanol, nonanal, decanal, ethylacetophenone, geranylacetone and the solvent peaks. Of these, heptanal, nonanal and 1-octen-3-one were previously identified as IAC (chapter 5)

Table 6-3. Proportion of all antennae tested that responded to each peak of interest, per treatment group, in the BMGF dataset. Peaks (identified by retention index, RI) were selected as those that elicited >2 responses in one of the treatment groups, and then fewer responses in other groups were added. Table colour scale according to number of responses. Number of antennal preps per treatment group: Before, 5; During [-], 5; During [+], 3; After, 4; Control, 5. Infection-associated compounds from chapter 5 highlighted yellow.

RI	Tentative identification	% responses	BEFORE	D(-)	D(+)	AFTER	CNL
740	Mixed/artefact	27	3	0	3	0	0
791	Solvent*	50	2	2	2	1	4
791+	Unknown	50	2	5	3	1	0
816	Diacetone alcohol	36	1	1	2	2	2
828	Siloxane & 2-acetoxyethanol	27	0	2	2	2	0
854	Dimethyl sulfone*/ethylbenzene	32	1	3	2	1	1
881	Styrene/heptanal*	27	0	1	2	2	1
887	Solvent*	50	3	3	2	2	1
951	Phenol/1-octen-3-one*	73	4	4	3	3	2
965	Acetic acid/siloxane/6-methyl-5-hepten-2-one	41	1	3	1	2	2
1008	Artefact	27	1	0	2	1	2
1014	2-Ethylhexanol*	27	3	2	0	1	0
1045	Acetophenone	36	4	4	0	0	0
1086	Nonanal*	27	2	1	1	2	0
1142	3-Ethyl benzaldehyde	27	2	2	2	0	0
1146	Artefact	41	4	1	3	0	1
1165	Siloxane artefact	27	0	3	3	0	0
	MS						
1181	41/57/68/82/97/109/124/137/165/180	32	0	2	1	2	2
1188	Decanal*	50	3	3	3	2	0
1209	Unknown long chain alkane	27	2	2	0	2	0
1239	Ethylacetophenone*	50	1	3	3	2	2
1245	Nonanoic acid	32	3	3	0	1	0
1289	Undecanal	32	3	2	1	1	0
1296	Triacetin	36	1	3	1	2	1
1342	Artefact	32	3	3	0	0	1
1434	Geranylacetone*	73	4	5	3	4	0

*Identified to be EAG active in both datasets, Mixed = not consistent identification between samples, RI 1181 MS=Ions in mass spec.

Chapter 6: Electroantennography of human odour samples

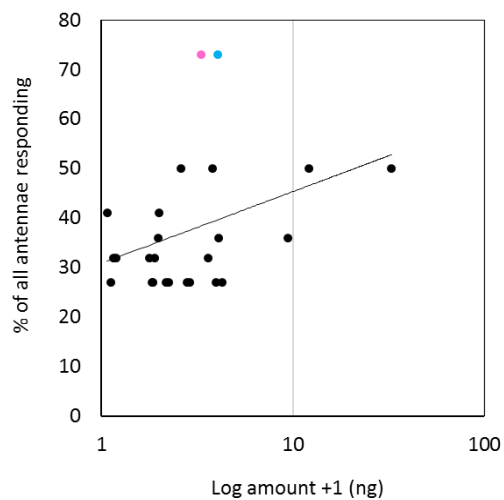


Figure 6-2. The percentage of antennae responding in the BMGF dataset increased with peak amount (ng, log scale, mean of amount in all blends), but was a non-significant correlation ($r=0.3$, $n=25$ $P=0.17$). Dots (one per peak) represent the correlation between the peak amount and proportion of all antennae that responded. Geranylacetone (pink) and RI 951 (blue, co-eluting phenol and 1-octen-3-one) elicited the greatest number of responses. Peak RI 791+ was excluded as the amount was not measurable (immediately adjacent/under another peak).

Chapter 6: Electroantennography of human odour samples

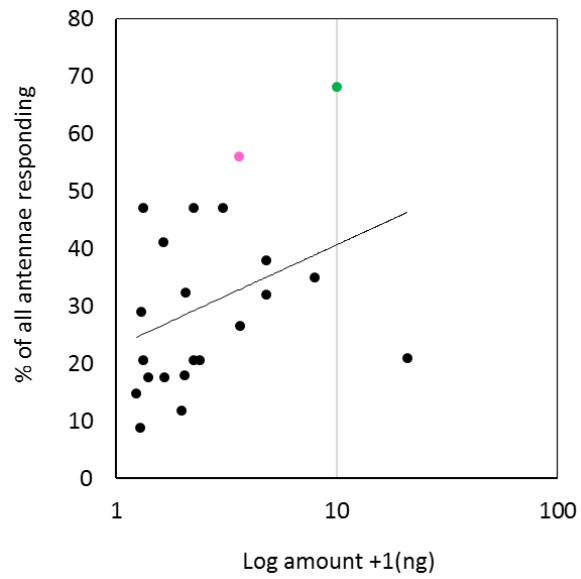
Table 6-4. Proportion of all antennae tested that responded to each peak of interest, per treatment group, in the Kenya dataset. Peaks (identified by retention index, RI) were selected as those that elicited >3 responses in one of the treatment groups, and then fewer responses in other groups were added. Table colour scale according to number of responses. Number of antennal preps per treatment group: Negative (NEG), 7; No gametocyte (NO GAM), 6; Sub-gametocyte (SUB-GAM), 7; Control (CNL), 7. IAC (chapter 5) highlighted yellow.

RI	Tentative identification	% responses	NEG	NO GAM	SUB-GAM	GAM	CNL
716	Methyl Cyclohexane	41	0	4	4	2	4
750	Unknown	18	1	1	4	0	0
781	Dimethyl sulfide	29	5	5	0	0	0
795	Solvent*	12	1	3	0	0	0
801	Octane	47	4	4	5	1	2
853	LHS: 1-Hexanol?, RHS: Dimethyl Sulfone*	21	1	3	1	1	1
880	Heptanal*	18	1	2	1	2	0
889	Solvent*	35	3	4	3	2	2
933	Benzaldehyde	56	7	4	6	1	1
958	Phenol/1-octen-3-one*	47	5	4	4	2	1
982	Octanal	32	5	3	0	3	0
1014	2-Ethylhexanol* or 2-octene	47	5	5	1	4	1
1056	Shoulder (LHS: para cresol, RHS: 3-octen-2-ol), peak octen-1-ol	21	3	3	1	0	N/P
1084	Nonanal*	68	7	5	5	5	1
1118	Unknown	9	N/P	0	3	0	0
1139	2-Ethyl benzaldehyde	26	5	2	2	0	0
1150	4-Ethyl benzaldehyde	18	3	0	1	1	1
1186	Decanal*	32	2	2	4	1	2
1199	Dodecane	15	3	1	0	1	0
1239	Ethylacetophenone*	38	6	3	3	0	1
1389	Unknown	12	0	1	0	0	3
1428	Geranylacetone*	21	3	0	2	0	2

*Identified to be EAG active in both datasets.

Table 6-5. Antennal responses to compounds revealed to be infection-associated by quantitative analysis of (Kenyan) samples by gas chromatography (chapter 5). Table colour scale according to number of responses.

RI	Tentative identification	% responses	NEG	NO GAM	SUB-GAM	GAM	CNL
776	Hexanal	0	0	0	0	0	N/P
965	6-Methyl-5-hepten-2-one/1-octen-3-ol	12	0	1	1	1	1
972	2-Octanone	6	0	0	0	2	0
1035	(E)-2-Octenal	0	0	0	0	0	N/P
1240	(E)-2-Decenal	6	0	1	1	0	0



6.5 Discussion

6.5.1 Summary

Coupled GC-EAG was used to screen for EAG-active compounds in blends of odour samples from both experimentally- and naturally-*Plasmodium*-infected individuals. Across both cohorts, no EAG-active compounds were found only in the parasitologically positive blends. As discussed in the literature review (chapter 1), the evolution of an infected-host avoidance phenotype in mosquitoes might be expected, if the disadvantages (e.g. lower quality bloodmeal) of taking a bloodmeal outweigh any advantages (e.g. reduced host defences, faster engorgement). This forms the basis of the 'deceptive signalling' hypothesis, whereby normal host cues are exaggerated, causing increased attractiveness of that vertebrate to biting insects, but when the blood-meal is in fact detrimental to the insect (Mauck et al., 2010). In these circumstances, as can probably be applied to the human malaria system, it would be expected that any infection-associated 'transmission-signal' is not a distinct and characteristic blend of compounds.

Within both datasets, the same compounds were found to be EAG-active (reviewed in Table 6-6 and Table 6-7) across all treatment groups, irrespective of parasitological status. Importantly however, of the EAG-active peaks, some were analytes that had previously been identified in the GC chemical analysis of odour profiles (chapter 2 and 5) to be significantly associated with *Plasmodium* infection. These included the aldehydes heptanal, octanal and nonanal (C7-C9), and possibly the ketones 6-methyl-5-hepten-2-one and 1-octen-3-one. C7-C9 were found to be produced in significantly greater amounts by individuals harbouring higher densities of parasites (chapter 5), and are therefore promising candidates for a 'transmission' signal. Like in the odour analysis, here 6-methyl-5-hepten-2-one again co-eluted with 1-octen-3-ol, and in this EAG analysis the other ketone 1-octen-3-one co-eluted with phenol, due to the shorter GC run time necessary in GC-EAG. This is a frustrating outcome, given the possible association between the production of these compounds and *Plasmodium* infection.

Infection-associated C7-C9 (chapter 5), 6-methyl-5-hepten-2-one (chapter 2 and 5) and 1-octen-3-one (chapter 5) were definitively identified by peak enhancement in chapter 5, and because of the co-elution with 1-octen-3-one described in this chapter, phenol was also conclusively identified (appendix 5.11). Other than these, the discussion of EAG-active peaks is based solely on their identification by GC-MS and the NIST database (see 2.3.8).

The literature documenting the relevance of aldehydes as host cues for haematophagous insects is extensive, and this significance is logical given the extent to which they contribute to the odour profile of several mammalian species (Jaleta et al., 2016; Tchouassi et al., 2013). C7-C9 are thought to be used by *Anopheles* species as both host cues and oviposition attractants, although compared with *Aedes* and *Culex*, there are fewer studies examining their significance. The EAG response of *An. coluzzii* to these compounds, therefore, is unsurprising.

6.5.2 *Anopheles* response to C7-C9 aldehydes

Nonanal is known to elicit a strong electrophysiological response (i.e. of high amplitude) in *An. gambiae* (Rund et al., 2013), and both octanal and nonanal have been shown to elicit a dose-dependent EAG response in female *An. funestus* (Xu et al., 2010). How this EAG response translates behaviourally, however, is less clear. In some studies, attraction of *Anopheles* species to these aldehydes has been documented. Smallegange et al. (2012) tested octanal, nonanal and decanal, at three concentrations, in an olfactometer against a basic blend of lactic acid, tetradecanoic acid and ammonia. There was an increase in *An. gambiae* s.s. response with 0.1 % octanal, indicating that octanal can function as an attractant, but no other significant responses. Logan et al. (2010) tested the response of *An. gambiae* s.s. by arm-in-cage testing to octanal, nonanal and decanal, alone and in mixtures. All tested compounds and blends were found to elicit repellency. In a recent field trial, a blend of heptanal, octanal, nonanal and decanal was found to be less effective at trapping mosquitoes than one of synthetic plant odours (Nyasembe et al., 2014). However, the aldehyde blend did catch more mosquitoes (*An. gambiae* s.l. and *An. funestus*) than did controls (solvent, or solvent and CO₂), indicating some attractiveness. The circumstances of these two behavioural trials (Logan et al., 2010; Nyasembe et al., 2014) are quite different, and it is possible that compounds are variably active in short-range or long-range circumstances, and/or that different concentrations elicit different responses. Following dose-dependent EAG responses to heptanal and nonanal by *An. arabiensis*, nonanal was tested as a lure in field trials yet was not found to affect the number of *An. arabiensis* trapped (Jaleta et al., 2016). Nonanal was released at a rate of 1 mg/hour, adjacent and below a CDC non-light trap in a house, with a sleeping volunteer. However, the investigators presented the compound alone and without synergistic CO₂, testing against the complete odour profile of an adjacent human. Only a highly attractive compound or blend would attract mosquitoes in such circumstances. In that study, the aldehydes were isolated from the headspace of hair, wool and feathers of non-human hosts (cow, goat and sheep), which

emphasises the non-human-specific nature of these volatiles (Jaleta et al. 2016, and Tchouassi et al. 2013).

In addition to host-seeking cues, a role for nonanal in *Anopheles* oviposition site choice has been documented. Gravid female *An. gambiae* s.s. were found to avoid low doses of nonanal in water for egg laying (Eneh et al., 2016), but a synthetic blend of five active compounds that included nonanal (benzaldehyde, nonanal, p-cymene, limonene and α -pinene) elicited both attraction and oviposition by *An. arabiensis* (Wondwosen et al., 2017). Further, a blend of compounds including nonanal was successful in catching gravid *An. arabiensis* in a semi-field trial (Wondwosen et al., 2016). Although removing nonanal from the blend reduced attraction, nonanal alone was not as attractive as the blend. The significance of nonanal in both host- and oviposition site-location is indicative that the behavioural response to this compound might vary according to the physiological status of the mosquito (Wondwosen et al., 2017). In the current study, the mosquitoes tested were non-bloodfed females that would not have been responsive to oviposition cues. As such, it is probable that the EAG response observed is related to host-seeking.

6.5.3 The response of *Aedes* and *Culex* to C7-C9 aldehydes

A more extensive literature documents the response of *Aedes* and *Culex* species to aldehydes. Heptanal, octanal, nonanal and decanal are known to be EAG-active to *Aedes aegypti* (Ghaninia et al., 2008). The same compounds were identified as being relatively increased in amount in the odour profile of people that were poorly attractive to *Ae. aegypti* (Bernier et al., 2002; Logan et al., 2008). Further testing of topical octanal, nonanal and decanal in arm-in-cage assays found dose-dependent repellency, with nonanal and decanal being the most effective repellents (Logan et al., 2010). A blend including the aldehydes octanal, hexanal, (*Z*)-4-decanal and decanal was found to reduce *Ae. aegypti* landing in a cage assay (Douglas et al., 2005). However, the concentrations of octanal in this blend were very high (40 % of the blend), mimicking levels produced naturally in the seabird odour under investigation. Such concentrations are probably considerably higher than those found naturally in human odour (in this study, octanal contributed on average 0.6 % of the total odour profile of a negative individual). In contrast, one study field-tested aldehyde blends (heptanal, octanal, nonanal and decanal) and also their constituent parts alone. The blends were found to be significantly attractive to *Ae. mcintoshi* and *Ae. ochraceus*, while the aldehydes tested singly (with CO₂) increased captures relative to traps with CO₂ alone but not significantly (Tchouassi et al., 2013).

Aldehydes have been found to be attractive to *Culex* mosquitoes. Nonanal, heptanal and propanal generated a positive behavioural response in host-seeking *Cx. quinquefasciatus* in a wind tunnel bioassay, although this varied according to dose and compound (Puri et al., 2006). Another group compared the odour profiles of humans (from various ethnic backgrounds: Latino, East Indian, White, African, Chinese) and birds, including chickens and pigeons (Syed and Leal, 2009). They observed that, like humans, bird odour samples were dominated by the aldehydes heptanal, octanal, nonanal and decanal, which they found to be EAG-active to *Cx. quinquefasciatus*, and so tested nonanal (with success) in the field as trap bait. This led the authors to suggest that nonanal, as a semiochemical common to the odour of both birds and humans, may be involved in the *Culex* host shifts that lead to West Nile Virus transmission. In other circumstances hexanal, octanal, nonanal and decanal were found not to be attractive to *Cx. quinquefasciatus* (Allan et al., 2006), and variably attractive or repellent at different concentrations (Logan et al., 2010).

The apparent species-specific differences in mosquito response to aldehydes are not surprising, given the well-documented differences in host choice preference and varying ecological niches occupied by *Anopheles*, *Aedes* and *Culex* species. A more general observation can be made that interpretation of a volatile signal depends on context, including the presence or absence of other compounds or possible distance from the source. However, there is an abundance of literature documenting both electrophysiological and behavioural responses of these mosquito species to the C7-C10 aldehydes, and indeed those of other haematophagous arthropods (e.g. Harraca et al. 2012; Gikonyo et al. 2003; Guerenstein & Guerin 2001; Steullet & Guerin 1994). As such, the *An. coluzzii* EAG-activity described here is well supported.

6.5.4 Entomological response to 6-methyl-5-hepten-2-one and 1-octen-3-one

Both 6-methyl-5-hepten-2-one and 1-octen-3-one, found to be IAC in chapters 2 and 5, were present as co-eluting compounds in EAG-active peaks. 6-Methyl-5-hepten-2-one was EAG-active in the EI cohort (co-eluting with acetic acid and a siloxane), while in the NI cohort (where it co-eluted with 1-octen-3-ol) there were several antennal responses (Table 6-5), although not enough to meet the designated 'threshold' of EAG-activity. Given the documented behavioural role and likely repellency of 6-methyl-5-hepten-2-one (Logan et al., 2010, 2008; Menger et al., 2014; Qiu et al., 2011), it seems probable that the EAG responsiveness of these peaks was due, at least in part, to the 6-methyl-5-hepten-2-one.

Given the association between production of 1-octen-3-one by the skin and the presence of gametocytes observed here (chapter 5), the co-elution with phenol, caused by a shorter GC programme in the EAG work, is unfortunate. Phenol is a known component of skin odour (Bernier et al., 2000; Cork and Park, 1996; Curran et al., 2010, 2005; Dormont et al., 2013a; Gallagher et al., 2008; Zeng et al., 1996, 1991). Further, phenol has known entomological significance. The importance of phenolic compounds (including phenol) in host urine for tsetse fly attraction has long been known (Hassanali et al., 1986), and it is thought that these compounds form during breakdown of glucuronates and sulphates by microbial activity (Okech and Hassanali, 1990). Although frequently cited as an electrophysiologically active compound for several species of mosquito (Table 6-6), few studies have specifically tested for a behavioural response to phenol. Kline et al. (1990) tested phenol alone as a mosquito lure in CDC odour baited traps in Florida, against various other compounds and CO₂ alone. While significantly greater catches of *Culex* species (*melanoconium* and *nigripalpus*) were recorded (relative to CO₂ alone), there was no effect on catches of *Anopheles crucians* and significantly less *Aedes taeniorhynchus* were caught. Phenol has also been tested as an oviposition attractant, because of its presence in the headspace of grass-infused water (Du and Millar, 1999; Millar et al., 1992). Together, these studies are indicative that an *An. coluzzii* EAG response to phenol would be unsurprising. In contrast, although 1-octen-3-one is known to be produced by humans (Glindemann et al., 2006; Wagenstaller and Buettner, 2013), no studies documenting entomological relevance of this compound could be found. The significance of 1-octen-3-one production by individuals harbouring gametocytes (chapter 5) merits further investigation of this issue, and an obvious avenue would testing for an EAG response of *An. coluzzii* to phenol and 1-octen-3-one individually.

6.5.5 Other EAG-active compounds

Other than the IAC, many others were found to elicit an EAG response in *An. coluzzii*. Of those expected to be of endogenous origin (Table 6-6, Table 6-7), many have previously been documented as both human volatiles and EAG-active compounds. Several EAG-active compounds were found to be of likely exogenous origin, or possible artefacts of sampling. Indeed, of these, 2-ethylhexanol has been previously cited as an industrial chemical (Dormont et al., 2013b) or possible perfume component (Verhulst et al., 2013), and is commonly accidentally isolated in this type of study (Zhang et al. 2005; Verhulst et al. 2013). It is not uncommon to find that contaminants or solvents elicit EAG activity (Qiu et al., 2004).

6.5.6 Methodological considerations

The frequency of response, i.e. number of antennae responding to a peak, may have been influenced by the amount of compound present. In both datasets, there was a trend towards increased responses (proportion of responding antennae) with larger peaks (greater amounts of compound). In the Kenyan dataset, this could be explained by the entomological response to the large aldehyde peaks. Compound amounts in these blends could not be controlled for, as blends comprised samples from specific individuals, chosen on the basis of parasitological status. This could explain discrepancies in the frequency of antennal response between treatment groups: in some, the concentration may have been beneath the response threshold. While geranylacetone, RI 951 (phenol and 1-octen-3-one), benzaldehyde and nonanal were the four most 'EAG-active' compounds between the two datasets, due to the above reasons, no conclusions should be drawn regarding their relative entomological significance. Measuring the amplitude of EAG depolarisation would have been indicative of the strength of response, but that was considered unnecessary in this context, where the aim was to detect the presence of EAG-active compounds.

While EAG activity signifies that a compound is significant to the insect, both attractants and repellents are known to elicit depolarisation of the ORNs (Blackwell et al., 1997). For this reason, behavioural assays are necessary to understand the role of the compound. For the IAC (chap EI and NI), a useful exercise prior to behavioural testing would be to screen for EAG-activity by conducting 'straight' EAG (i.e. not GC-coupled). For those not found to be EAG-active here, this would determine the entomological significance of the IAC. The rationale in focussing on GC-EAG was to screen for more compounds, rather than to determine the relevance of compounds already identified. Because of the concentration issues discussed above, it is possible that IAC other than C7-C9 and the ketones were EAG-active, yet present here at concentrations beneath the detection threshold, and therefore were not deemed to be so.

6.6 Conclusion

By screening for IAC in odour samples from *Plasmodium*-infected individuals, this chapter identified compounds both already known, and some not yet documented, as EAG-active to *An. coluzzii* (formerly *An. gambiae* s.s. M form). The main finding in the context of the thesis is indication of the entomological significance of some IAC: heptanal, octanal, nonanal, and possibly 6-methyl-5-hepten-2-one and 1-octen-3-one. Taking the findings of this chapter and chapter 5 together, it can be stated that C7-C9 are produced in greater quantities by malaria-infected individuals (specifically those with high parasite density infections), and that these compounds are detected by the malaria vector *An. coluzzii*. Additionally, the production of the ketones 6-methyl-5-hepten-2-one and 1-octen-3-ol is altered in malaria-infected individuals, but their importance to *An. coluzzii* remains unclear. Finally, this chapter adds to the body of literature that describes which compounds elicit EAG-activity in *An. coluzzii*.

Chapter 6: Electroantennography of human odour samples

Table 6-6. Type and likely provenance of compounds eliciting electroantennal response in BMGF dataset. Entomological responses of mosquitoes only. RI = retention index, N/A=not applicable. *Indicates compounds found to be EAG-active in both datasets. Entomological responses in the literature, both electrophysiological (E+) or behavioural (B+, attraction, B-, repellency).

RI	Tentative identification	Compound type	Likely provenance	Human emanation	Entomological response/ref
740	Mixed/artefact	Artefact	Exogenous/system	N/A	N/A
791	Solvent	Solvent	Exogenous/system	N/A	N/A
791+	Unknown	N/A	N/A	N/A	N/A
816	Diacetone alcohol (4-Hydroxy-4-methyl-2-pentanone)	Solvent	Exogenous/system	None found	None found
828	Siloxane	Artefact	Exogenous/system	N/A	N/A
	2-Acetoxyethanol	Alcohol	Exogenous/system	None found	None found
854	Dimethyl sulfone*	Organosulfur	Endogenous/microbial	Engelke et al. 2005; Matsumura et al. 2010	None found
	Ethylbenzene	Solvent	Exogenous/system	N/A	N/A
881	Styrene	Artefact	Exogenous/system	Ellin et al. 1974	N/A
	Heptanal*	Aldehyde	Endogenous	Bernier et al. 2002; Harraca et al. 2012; Meijerink et al. 2000; Ellin et al. 1974; Bernier et al. 1999; Curran et al. 2005	E +/Culex (Puri et al., 2006) E +/Anopheles (Qiu et al., 2006) E +/Aedes (Ghaninia et al., 2008) E +/Aedes, Culex (Tchouassi et al., 2013) E +/Anopheles (Qiu et al., 2013) E +/Anopheles (Jaleta et al., 2016) B +/Anopheles (Nyasembe et al., 2014)
887	Solvent*	Solvent	Exogenous/system	N/A	N/A
951	Phenol*	Aromatic	Endogenous/microbial	Gallagher et al. 2008; Curran et al. 2005; Zeng et al. 1991; Zeng et al. 1996; Wahl et al. 1999; Cork & Park 1996; Bernier et al. 2000	E +/Culex (Du and Millar, 1999) E +/Aedes (Siju et al., 2010) B +/Culex (Kline et al., 1990) B -/Anopheles (Eneh et al., 2016)
	1-Octen-3-one*	Ketone	Endogeneous	Glindemann et al., 2006; Wagenstaller and Buettner, 2013	None found
965	Acetic acid	Carboxylic Acid	Endogenous/microbial	Bernier et al. 2000; Meijerink et al. 2000; Dadamio et al. 2012; Dormont et al. 2013a; Cork & Park 1996; Ara et al. 2006	E +/Culex (Hill et al., 2009) E +/Anopheles (Qiu et al., 2006) E +/Anopheles (Kwon et al., 2006) E +/Aedes (Siju et al., 2010) E +/Anopheles (Meijerink and van Loon, 1999)

Chapter 6: Electroantennography of human odour samples

RI	Tentative identification	Compound type	Likely provenance	Human emanation	Entomological response/ref
	Siloxane	Artefact	Exogenous/system	N/A	N/A
	6-Methyl-5-hepten-2-one	Ketone (terpenoid)	Endogenous	Curran et al. 2005; Bernier et al. 2002; Bernier et al. 2000; Meijerink et al. 2000; Gallagher et al. 2008	E +/-Anopheles (McBride et al., 2014) E +/-Anopheles (Lu et al., 2007) E +/-Culex (Syed and Leal, 2009) E +/-Anopheles (Qiu et al., 2006) E +/-Anopheles (Meijerink et al., 2000) B -/Aedes (Logan et al., 2008) B -/Anopheles (Menger et al., 2014) B -/Culex, Anopheles (Logan et al., 2010)
1008	Artefact	Artefact	Exogenous/system	N/A	N/A
1014	2-Ethylhexanol*	Chiral alcohol	Endogenous	Logan et al. 2008; Yamazaki et al. 2010; Verhulst et al. 2013; Ellin et al. 1974	E +/(related compound 2-ethyl-1-hexanal) / Anopheles (Qiu et al., 2004)
1045	Acetophenone	Aromatic	Endogenous/exogenous	Gallagher et al. 2008; Zhang et al. 2005	E +/-Anopheles (Lu et al., 2007) E +/-Anopheles (Kwon et al., 2006) B +/-Anopheles (Smallegange et al., 2012)
1086	Nonanal*	Aldehyde	Endogenous	Dormont et al. 2013b; Curran et al. 2005; Curran et al. 2010; Gallagher et al. 2008; Haze et al. 2001; Yamazaki et al. 2010; Meijerink et al. 2000; Harraca et al. 2012	E +/-Anopheles (Rund et al., 2013) E +/-Anopheles (Xu et al., 2010) E +/-Aedes (Ghaninia et al., 2008) E +/-Culex (Hill et al., 2009) E +/-B +/-Culex (Puri et al., 2006) E +/-B +/-Culex (Syed and Leal, 2009) E +/-Anopheles (Jaleta et al., 2016) E +/-Culex (Cooperband et al., 2008) E +/-Aedes, Culex, Mansonia (Tchouassi et al., 2013) B + (NS)/Aedes (Tchouassi et al., 2013) B -/Aedes (Logan et al., 2008) B -/Anopheles (Logan et al., 2010) B +/-Culex (Leal et al., 2008)
1142	3-Ethyl Benzaldehyde	Artefact	Porapak contaminant	N/A	N/A
1146	Artefact	Artefact	Exogenous/system	N/A	N/A
1165	Siloxane artefact	Artefact	Exogenous/system	N/A	N/A
1181	Unknown	N/A	N/A	N/A	N/A

Chapter 6: Electroantennography of human odour samples

RI	Tentative identification	Compound type	Likely provenance	Human emanation	Entomological response/ref
1188	Decanal*	Aldehyde	Endogenous	Haze et al. 2001; Curran et al. 2005; Gallagher et al. 2008; Harraca et al. 2012; Cork & Park 1996	E +/Aedes, Culex, Mansoni (Tchouassi et al., 2013) E +/Aedes (Ghaninia et al., 2008) B -/Aedes (Douglas et al., 2005) B -/Aedes (Logan et al., 2008) B -/Aedes (Logan et al., 2010)
1209	Unknown long chain alkane	Long-chain alkane	Endogenous	N/A	N/A
1239	Ethylacetophenone*	Aromatic	Exogenous/system	N/A	N/A
1245	Nonanoic acid	Fatty acid	Endogenous	Zeng et al. 1991; Zeng et al. 1996; Cork & Park 1996; Bernier et al. 2000; Dormont et al. 2013b	E +/Anopheles (Knols et al., 1997) E +/B +/Culex (Puri et al., 2006) E +/Anopheles (Cork and Park, 1996) E +/Anopheles (Qiu et al., 2006) B -/Aedes (Bosch et al., 2000)
1289	Undecanal	Aldehyde	Endogenous	Dormont et al. 2013b; Dormont et al. 2013a; Curran et al. 2005; Curran et al. 2010; Penn et al. 2007; Bernier et al. 1999	E +/Culex (Cooperband et al., 2008)
1296	Triacetin	Ester	Exogenous/system	None found	None found
1342	Artefact	Artefact	N/A	N/A	N/A
1434	Geranylacetone*	Terpenoid	Endogenous	Gallagher et al. 2008; Dormont et al. 2013b; Dormont et al. 2013a; Meijerink et al. 2000; Syed & Leal 2009	E +/Aedes (Ghaninia et al., 2008) E +/Culex (Syed and Leal, 2009) E +/Anopheles (Meijerink et al., 2001) E +/Anopheles (Qiu et al., 2006) E +/Anopheles (Takken et al., 2001) B -/Aedes (Logan et al., 2010) B -/Aedes (Logan et al., 2008) B -/Anopheles (Qiu et al., 2011)

Chapter 6: Electroantennography of human odour samples

Table 6-7. Type and likely provenance of compounds eliciting electroantennal response in Kenyan dataset. Entomological responses of mosquitoes only. RI = retention index, NS=not significant, N/A=not applicable. *Indicates compounds found to be EAG-active in both datasets. Entomological responses in the literature, both electrophysiological (E+) or behavioural (B+, attraction, B-, repellency).

RI	Tentative identification	Compound type	Provenance	Human emanation	Entomological response/ref
716	Methyl cyclohexane	Solvent	Exogenous/system	N/A	N/A
750	Unknown	N/A	N/A	N/A	N/A
781	Dimethyl sulfide	Organosulfur	Endogenous/microbial	Mochalski et al. 2013; Bernier et al. 2000	B +/ <i>Aedes</i> (Bernier et al., 2003) (dimethyl disulphide, with L lactic acid)
795	Solvent	Solvent	Exogenous/system	N/A	N/A
801	Octane	Alkane	Endogenous	None found	None found
853	LHS: 1-Hexanol (unsure identification)	Alcohol	Endogenous	Meijerink et al. 2000; Haze et al. 2001; Ellin et al. 1974	E +/ <i>Anopheles</i> (Suer, 2011)
	RHS: Dimethyl sulfone*	Organosulfur	Endogenous/microbial	See Table 6-6	
880	Heptanal*	Aldehyde	Endogenous	See Table 6-6	
889	Solvent*	Solvent	Exogenous/system	N/A	N/A
933	Benzaldehyde	Aromatic	Endogenous	Curran et al. 2005; Curran et al. 2010; Dormont et al. 2013a; Zhang et al. 2005; Dadamio et al. 2012	E +/ <i>Anopheles</i> (Jaleta et al., 2016) E +/ <i>Anopheles</i> (Wondwosen et al., 2017) E +/ <i>Anopheles</i> (Smallegange et al., 2012) E +/ <i>Anopheles</i> (Tauxe et al., 2013) E +/ <i>Culex</i> (Puri et al., 2006) E +/ <i>Aedes</i> (Logan et al., 2008) E +/ <i>Aedes</i> (Tauxe et al., 2013) B -/ <i>Culex</i> (Allan et al., 2006) B -/ <i>Culex</i> (Puri et al., 2006) B -/ <i>Anopheles</i> (Smallegange et al., 2012) B + (?)/ <i>Anopheles</i> (Wondwosen et al., 2017)
958	Phenol *	Aromatic	Endogenous/microbial	See Table 6-6	
	1-Octen-3-one*	Ketone	Endogenous	See Table 6-6	
982	Octanal	Aldehyde	Endogenous	Gallagher et al. 2008; Logan et al. 2008; Dormont et al. 2013b; Dormont et al. 2013a; Yamazaki et al. 2010; Zhang et al. 2005; Curran et al. 2005; Bernier et al. 1999; Bernier et al. 2000; Meijerink et al. 2000	E +/ <i>Aedes</i> (Ghaninia et al., 2008) E +/ <i>Aedes/Culex/Mansonia</i> (Tchouassi et al., 2013) B + (NS)/ <i>Aedes</i> (Tchouassi et al., 2013) B +/ <i>Culex</i> (Logan et al., 2010) B -/+/ <i>Anopheles</i> (Logan et al., 2010)

Chapter 6: Electroantennography of human odour samples

RI	Tentative identification	Compound type	Provenance	Human emanation	Entomological response/ref
982	Octanal (<i>continued from above</i>)	Aldehyde	Endogenous		B -/ <i>Aedes</i> (Logan et al., 2010) B -/ <i>Aedes</i> (Logan et al., 2008) B +/ <i>Anopheles</i> (Smallegange et al., 2012)
1014	2-Ethylhexanol *	Chiral alcohol	Endogenous	See Table 6-6	
	(or) 2-Octene	Alkene	Endogenous	Bernier et al. 2000; Bernier et al. 2002; Ellin et al. 1974	None found
1056	Shoulder LHS: para cresol (4-methylphenol)	Aromatic	Endogenous/microbial	Cork & Park 1996; Munk et al. 2000; Wahl et al. 1999; Gallagher et al. 2008	E +/ <i>Anopheles</i> (Xu et al., 2010) E +/ <i>Anopheles</i> (Qiu et al., 2013) E +/ <i>Anopheles</i> (Wang et al., 2010) E +/ <i>Anopheles</i> (Hallem et al., 2004) E +/ <i>Anopheles</i> (Costantini et al., 2001) E +/ <i>Anopheles</i> (Cork and Park, 1996) E +/ <i>Culex</i> (Hill et al., 2009) B +/ <i>Aedes</i> (Bentley et al., 1979) B -/ <i>Anopheles</i> (Smallegange et al., 2012)
	Shoulder RHS: 3-octen-2-ol	Alcohol	Endogenous	None found	None found
	Peak: Octen-1-ol	Alcohol	Endogenous	None found	None found
1084	Nonanal*	Aldehyde	Endogenous	See Table 6-6	
1118	Unknown	N/A	N/A	N/A	N/A
1139	2-Ethyl benzaldehyde	Aromatic	Endogenous/exogenous	N/A	N/A
1150	4-Ethyl benzaldehyde	Aromatic	Endogenous/exogenous	N/A	N/A
1186	Decanal*	Aldehyde	Endogenous	See Table 6-6	
1199	Dodecane	Alkane	Endogenous	Zhang et al. 2005; Curran et al. 2005; Curran et al. 2010; Haze et al. 2001; Dormont et al. 2013a	None found
1239	Ethylacetophenone*	Aromatic	Exogenous/system	N/A	N/A
1389	Unknown	N/A	N/A	N/A	N/A
1428	Geranylacetone*	Terpenoid	Endogenous	See Table 6-6	

6.7 Chapter references

- Allan, S. a, Bernier, U.R., Kline, D.L., 2006. Laboratory evaluation of avian odors for mosquito (Diptera: Culicidae) attraction. *J. Med. Entomol.* 43, 225–231. doi:10.1603/0022-2585(2006)043[0225:LEOAOF]2.0.CO;2
- Angioy, A.M., Desogus, A., Barbarossa, I.T., Anderson, P., Hansson, B.S., 2003. Extreme Sensitivity in an Olfactory System. *Chem. Senses* 28, 279–284. doi:10.1093/chemse/28.4.279
- Ara, K., Hama, M., Akiba, S., Koike, K., Okisaka, K., Hagura, T., Kamiya, T., Tomita, F., 2006. Foot odor due to microbial metabolism and its control. *Can. J. Microbiol.* 52, 357–64. doi:10.1139/w05-130
- Bentley, M.D., McDaniel, I.N., Yatagai, M., Lee, H.-P., Maynard, R., 1979. p-Cresol: an Oviposition Attractant of *Aedes triseriatus*. *Environ. Entomol.* 8, 206–209. doi:10.1093/ee/8.2.206
- Bernier, U.R., Booth, M.M., Yost, R.A., 1999. Analysis of human skin emanations by gas chromatography/mass spectrometry. 1. Thermal desorption of attractants for the yellow fever mosquito (*Aedes aegypti*) from handled glass beads. *Anal. Chem.* 3, 1–7.
- Bernier, U.R., Kline, D.L., Barnard, D.R., Schreck, C.E., Yost, R.A., 2000. Analysis of human skin emanations by gas chromatography/mass spectrometry. 2. Identification of volatile compounds that are candidate attractants for the yellow fever mosquito (*Aedes aegypti*). *Anal. Chem.* 72, 747–56.
- Bernier, U.R., Kline, D.L., Posey, K.H., Booth, M.M., Yost, R.A., Barnard, D.R., 2003. Synergistic attraction of *Aedes aegypti* (L.) to binary blends of L-lactic acid and acetone, dichloromethane, or dimethyl disulfide. *J. Med. Entomol.* 40, 653–6.
- Bernier, U.R., Kline, D.L., Schreck, C.E., Yost, R.A., Barnard, D.R., 2002. Chemical analysis of human skin emanations: comparison of volatiles from humans that differ in attraction of *Aedes aegypti* (Diptera: Culicidae). *J. Am. Mosq. Control Assoc.* 18, 186–95.
- Blackwell, A., Wadhams, L.J., Mordue, W., 1997. Electrophysiological and behavioural studies of the biting midge, *Culicoides impunctatus* Goetghebuer (Diptera, Ceratopogonidae): interactions between some plant-derived repellent compounds and a host-odour attractant, 1-octen-3-ol. *Physiol. Entomol.* 22, 102–108. doi:10.1111/j.1365-3032.1997.tb01146.x
- Bosch, O.J., Geier, M., Boeckh, J., 2000. Contribution of Fatty Acids to Olfactory Host Finding of Female *Aedes aegypti*. *Chem. Senses* 25, 323–330. doi:10.1093/oxfordjournals.chemse.a014042
- Braks, M.A.H., Meijerink, J., Takken, W., 2001. The response of the malaria mosquito, *Anopheles gambiae*, to two components of human sweat, ammonia and L-lactic acid, in an olfactometer. *Physiol. Entomol.* 26, 142–148. doi:10.1046/j.1365-3032.2001.00227.x
- Busula, A.O., Bousema, T., Mweresa, C.K., Masiga, D., Logan, J.G., Sauerwein, R.W., Verhulst, N.O., Takken, W., de Boer, J.G., 2017. Gametocytaemia increases attractiveness of *Plasmodium falciparum*-infected Kenyan children to *Anopheles gambiae* mosquitoes. *J. Infect. Dis.* 1–5. doi:10.1093/infdis/jix214
- Carey, A.F., Wang, G., Su, C.-Y., Zwiebel, L.J., Carlson, J.R., 2010. Odorant reception in the malaria mosquito *Anopheles gambiae*. *Nature* 464, 66–71. doi:10.1038/nature08834
- Cooperband, M.F., McElfresh, J.S., Millar, J.G., Cardé, R.T., 2008. Attraction of female *Culex quinquefasciatus* Say (Diptera: Culicidae) to odors from chicken feces. *J. Insect Physiol.* 54, 1184–1192. doi:10.1016/j.jinsphys.2008.05.003

- Cork, A., Park, K.C., 1996. Identification of electrophysiologically-active compounds for the malaria mosquito, *Anopheles gambiae*, in human sweat extracts. *Med. Vet. Entomol.* 10, 269–76.
- Costantini, C., Birkett, M. a, Gibson, G., Ziesmann, J., Sagnon, N.F., Mohammed, H. a, Coluzzi, M., Pickett, J.A., 2001. Electroantennogram and behavioural responses of the malaria vector *Anopheles gambiae* to human-specific sweat components. *Med. Vet. Entomol.* 15, 259–266.
- Curran, A.M., Prada, P.A., Furton, K.G., 2010. The Differentiation of the Volatile Organic Signatures of Individuals Through SPME-GC / MS of Characteristic Human Scent Compounds 55, 50–57. doi:10.1111/j.1556-4029.2009.01236.x
- Curran, A.M., Rabin, S.I., Prada, P.A., Furton, K.G., 2005. Comparison of the volatile organic compounds present in human odor using SPME-GC/MS. *J. Chem. Ecol.* 31, 1607–19.
- Dadamio, J., Van den Velde, S., Laleman, W., Van Hee, P., Coucke, W., Nevens, F., Quiryne, M., 2012. Breath biomarkers of liver cirrhosis. *J. Chromatogr. B Anal. Technol. Biomed. Life Sci.* 905, 17–22. doi:10.1016/j.jchromb.2012.07.025
- Dekker, T., Steib, B., Cardé, R.T., Geier, M., Carde, R.T., Geier, M., 2002. L-lactic acid: a human-signifying host cue for the anthropophilic mosquito *Anopheles gambiae*. *Med. Vet. Entomol.* 16, 91–98. doi:10.1046/j.0269-283x.2002.00345.x
- Dormont, L., Bessière, J.-M., Cohuet, A., 2013a. Human skin volatiles: a review. *J. Chem. Ecol.* 39, 569–78. doi:10.1007/s10886-013-0286-z
- Dormont, L., Bessière, J.-M., McKey, D., Cohuet, A., 2013b. New methods for field collection of human skin volatiles and perspectives for their application in the chemical ecology of human-pathogen-vector interactions. *J. Exp. Biol.* 216, 2783–8. doi:10.1242/jeb.085936
- Douglas, H.D., Co, J.E., Jones, T.H., Conner, W.E., Day, J.F., 2005. Chemical odorant of colonial seabird repels mosquitoes. *J. Med. Entomol.* 42, 647–651. doi:10.1603/0022-2585(2005)042[0647:COOCSR]2.0.CO;2
- Du, Y.J., Millar, J.G., 1999. Electroantennogram and oviposition bioassay responses of *Culex quinquefasciatus* and *Culex tarsalis* (Diptera: Culicidae) to chemicals in odors from Bermuda grass infusions. *J. Med. Entomol.* 36, 158–66.
- Ellin, R.I., Farrand, R.L., Oberst, F.W., Crouse, C.L., Billups, N.B., Koon, W.S., Musselman, N.P., Sidell, F.R., 1974. An apparatus for the detection and quantitation of volatile human effluents. *J. Chromatogr.* 100, 137–52.
- Eneh, L.K., Okal, M.N., Borg-Karlson, A.-K., Fillinger, U., Lindh, J.M., 2016. Gravid *Anopheles gambiae* sensu stricto avoid ovipositing in Bermuda grass hay infusion and its volatiles in two choice egg-count bioassays. *Malar. J.* 15, 276. doi:10.1186/s12936-016-1330-6
- Engelke, U.F.H., Tangerman, A., Willemsen, M.A.A.P., Moskau, D., Loss, S., Mudd, S.H., Wevers, R.A., 2005. Dimethyl sulfone in human cerebrospinal fluid and blood plasma confirmed by one-dimensional ¹H and two-dimensional ¹H-¹³C NMR. *NMR Biomed.* 18, 331–336. doi:10.1002/nbm.966
- Gallagher, M., Wysocki, C.J., Leyden, J.J., Spielman, A.I., Sun, X., Preti, G., 2008. Analyses of volatile organic compounds from human skin. *Br. J. Dermatol.* 159, 780–91. doi:10.1111/j.1365-2133.2008.08748.x
- Ghaninia, M., Larsson, M., Hansson, B.S., Ignell, R., 2008. Natural odor ligands for olfactory receptor neurons of the female mosquito *Aedes aegypti*: use of gas chromatography-linked single sensillum recordings. *J. Exp. Biol.* 211, 3020–3027. doi:10.1242/jeb.016360
- Gikonyo, N.K., Hassanali, A., Njagi, P.G.N., Saini, R.K., 2003. Responses of *Glossina morsitans*

- morsitans to blends of electroantennographically active compounds in the odors of its preferred (buffalo and ox) and nonpreferred (waterbuck) hosts. *J. Chem. Ecol.* 29, 2331–45.
- Glindemann, D., Dietrich, A., Staerk, H.-J., Kusch, P., 2006. The Two Odors of Iron when Touched or Pickled: (Skin) Carbonyl Compounds and Organophosphines. *Angew. Chemie Int. Ed.* 45, 7006–7009. doi:10.1002/anie.200602100
- Guerenstein, P.G., Guerin, P.M., 2001. Olfactory and behavioural responses of the blood-sucking bug *Triatoma infestans* to odours of vertebrate hosts. *J. Exp. Biol.* 204, 585–97.
- Habtewold, T., Duchateau, L., Christophides, G.K., 2016. Flow cytometry analysis of the microbiota associated with the midguts of vector mosquitoes. *Parasit. Vectors* 9, 167. doi:10.1186/s13071-016-1438-0
- Halle, E.A., Nicole Fox, A., Zwiebel, L.J., Carlson, J.R., 2004. Olfaction: mosquito receptor for human-sweat odorant. *Nature* 427, 212–3. doi:10.1038/427212a
- Harraca, V., Ryne, C., Birgersson, G., Ignell, R., 2012. Smelling your way to food: can bed bugs use our odour? *J Exp Biol* 215, 623–629. doi:10.1242/jeb.065748
- Hassanali, A., McDowell, P.G., Owaga, M.L.A., Saini, R.K., 1986. Identification of tsetse attractants from excretory products of a wild host animal, *Syncerus caffer*. *Int. J. Trop. Insect Sci.* 7, 5–9. doi:10.1017/S1742758400003027
- Haze, S., Gozu, Y., Nakamura, S., Kohno, Y., Sawano, K., Ohta, H., Yamazaki, K., 2001. 2-Nonenal newly found in human body odor tends to increase with aging. *J. Invest. Dermatol.* 116, 520–524. doi:10.1046/j.0022-202X.2001.01287.x
- Healy, T.P., Copland, M.J.W., 2000. Human sweat and 2-oxopentanoic acid elicit a landing response from *Anopheles gambiae*. *Med. Vet. Entomol.* 14, 195–200. doi:10.1046/j.1365-2915.2000.00238.x
- Healy, T.P., Copland, M.J.W., Cork, A., Przyborowska, A., Halket, J.M., 2002. Landing responses of *Anopheles gambiae* elicited by oxocarboxylic acids. *Med. Vet. Entomol.* 16, 126–132. doi:10.1046/j.1365-2915.2002.00353.x
- Hill, S.R., Hansson, B.S., Ignell, R., 2009. Characterization of antennal trichoid sensilla from female Southern house mosquito, *Culex quinquefasciatus* say. *Chem. Senses* 34, 231–252. doi:10.1093/chemse/bjn080
- Ignell, R., Sengul, M.S., Hill, S.R., Hansson, B.S., 2011. Odour coding and neural connections, in: Takken, W., Knols, B.G.J. (Eds.), *Olfaction in Vector–Host Interactions, Ecology and Control of Vector-Borne Diseases*. Wageningen Academic Publishers, The Netherlands, pp. 63–90. doi:10.3920/978-90-8686-698-4
- Jaleta, K.T., Hill, S.R., Birgersson, G., Tekie, H., Ignell, R., 2016. Chicken volatiles repel host-seeking malaria mosquitoes. *Malar. J.* 15, 354. doi:10.1186/s12936-016-1386-3
- Kline, D.L., Takken, W., Wood, J.R., Carlson, D.A., 1990. Field studies on the potential of butanone, carbon dioxide, honey extract, 1-octen-3-ol, L-lactic acid and phenols as attractants for mosquitoes. *Med. Vet. Entomol.* 4, 383–91.
- Knols, B.G.J., van Loon, J.J.A., Cork, A., Robinson, R.D., Adam, W., Meijerink, J., Jong, R. De, Takken, W., 1997. Behavioural and electrophysiological responses of the female malaria mosquito *Anopheles gambiae* (Diptera: Culicidae) to Limburger cheese volatiles. *Bull. Entomol. Res.* 87, 151. doi:10.1017/S0007485300027292
- Kwon, H.-W., Lu, T., Rützler, M., Zwiebel, L.J., 2006. Olfactory responses in a gustatory organ of the malaria vector mosquito *Anopheles gambiae*. *Proc. Natl. Acad. Sci. U. S. A.* 103, 13526–31. doi:10.1073/pnas.0601107103

- Leal, W.S., Barbosa, R.M.R., Xu, W., Ishida, Y., Syed, Z., Latte, N., Chen, A.M., Morgan, T.I., Cornel, A.J., Furtado, A., 2008. Reverse and conventional chemical ecology approaches for the development of oviposition attractants for *Culex* mosquitoes. *PLoS One* 3, e3045. doi:10.1371/journal.pone.0003045
- Logan, J.G., Birkett, M.A., Clark, S.J., Powers, S., Seal, N.J., Wadhams, L.J., Mordue Luntz, A.J., Pickett, J.A., 2008. Identification of human-derived volatile chemicals that interfere with attraction of *Aedes aegypti* mosquitoes. *J Chem Ecol* 34, 308–322. doi:10.1007/s10886-008-9436-0
- Logan, J.G., Stanczyk, N.M., Hassanali, A., Kemei, J., Santana, A.E.G., Ribeiro, K. a L., Pickett, J. a, Mordue Luntz, a J., 2010. Arm-in-cage testing of natural human-derived mosquito repellents. *Malar. J.* 9, 239. doi:10.1186/1475-2875-9-239
- Lu, T., Qiu, Y.T., Wang, G., Kwon, J.Y., Rutzler, M., Kwon, H.-W., Pitts, R.J., van Loon, J.J.A., Takken, W., Carlson, J.R., Zwiebel, L.J., 2007. Odor Coding in the Maxillary Palp of the Malaria Vector Mosquito *Anopheles gambiae*. *Curr. Biol.* 17, 1533–1544.
- Matsumura, K., Opiekun, M., Oka, H., Vachani, A., Albelda, S.M., Yamazaki, K., Beauchamp, G.K., 2010. Urinary Volatile Compounds as Biomarkers for Lung Cancer: A Proof of Principle Study Using Odor Signatures in Mouse Models of Lung Cancer. *PLoS One* 5, e8819. doi:10.1371/journal.pone.0008819
- Mauck, K.E., De Moraes, C.M., Mescher, M.C., 2010. Deceptive chemical signals induced by a plant virus attract insect vectors to inferior hosts. *Proc. Natl. Acad. Sci. U. S. A.* 107, 3600–5. doi:10.1073/pnas.0907191107
- Mayer, M.S., Mankin, R.W., Lemire, G.F., 1984. Quantitation of the insect electroantennogram: Measurement of sensillar contributions, elimination of background potentials, and relationship to olfactory sensation. *J. Insect Physiol.* 30, 757–763. doi:10.1016/0022-1910(84)90041-6
- McBride, C.S., Baier, F., Omondi, A.B., Spitzer, S.A., Lutomiah, J., Sang, R., Ignell, R., Vosshall, L.B., 2014. Evolution of mosquito preference for humans linked to an odorant receptor. *Nature* 515, 222–227. doi:10.1038/nature13964
- McInver, S., Siemicki, R., 1975. Palpal sensilla of selected anopheline mosquitoes. *J. Parasitol.* 61, 535–576.
- Meijerink, J., Braks, M.A., Van Loon, J.J., 2001. Olfactory receptors on the antennae of the malaria mosquito *Anopheles gambiae* are sensitive to ammonia and other sweat-borne components. *J. Insect Physiol.* 47, 455–464.
- Meijerink, J., Braks, M.A.H., Brack, A.A., Adam, W., Dekker, T., Posthumus, M.A., Beek, T.A.V.A.N., Loon, J.J.A. Van, 2000. Identification of Olfactory Stimulants for *Anopheles gambiae* from Human Sweat Samples. *J. Chem. Ecol.* 26, 1367–1382. doi:10.1023/A:1005475422978
- Meijerink, J., van Loon, J.J., 1999. Sensitivities of antennal olfactory neurons of the malaria mosquito, *Anopheles gambiae*, to carboxylic acids. *J. Insect Physiol.* 45, 365–373.
- Menger, D.J., Van Loon, J.J.A., Takken, W., 2014. Assessing the efficacy of candidate mosquito repellents against the background of an attractive source that mimics a human host. *Med. Vet. Entomol.* 28, 407–13. doi:10.1111/mve.12061
- Millar, J.G., Chaney, J.D., Mulla, M.S., 1992. Identification of oviposition attractants for *Culex quinquefasciatus* from fermented Bermuda grass infusions. *J. Am. Mosq. Control Assoc.* 8, 11–17.
- Mochalski, P., King, J., Klieber, M., Unterkofler, K., Hinterhuber, H., Baumann, M., Amann, A.,

2013. Blood and breath levels of selected volatile organic compounds in healthy volunteers. *Analyst* 138, 2134–45. doi:10.1039/c3an36756h
- Munk, S., Münch, P., Stahnke, L., Adler-Nissen, J., Schieberle, P., 2000. Primary odorants of laundry soiled with sweat/sebum: Influence of lipase on the odor profile. *J. Surfactants Deterg.* 3, 505–515. doi:10.1007/s11743-000-0150-z
- Nyasembe, V.O., Tchouassi, D.P., Kirwa, H.K., Foster, W.A., Teal, P.E.A., Borgemeister, C., Torto, B., 2014. Development and assessment of plant-based synthetic odor baits for surveillance and control of malaria vectors. *PLoS One* 9, e89818. doi:10.1371/journal.pone.0089818
- Okech, M., Hassanali, A., 1990. The origin of phenolic tsetse attractants from host urine: Studies on the pro-attractants and microbes involved. *Int. J. Trop. Insect Sci.* 11, 363–368. doi:10.1017/S1742758400012789
- Penn, D.J., Oberzaucher, E., Grammer, K., Fischer, G., Soini, H.A., Wiesler, D., Novotny, M. V., Dixon, S.J., Xu, Y., Brereton, R.G., 2007. Individual and gender fingerprints in human body odour. *J. R. Soc. Interface* 4, 331–40. doi:10.1098/rsif.2006.0182
- Puri, S.N., Mendki, M.J., Sukumaran, D., Ganesan, K., Prakash, S., Sekhar, K., 2006. Electroantennogram and Behavioral Responses of *Culex quinquefasciatus* (Diptera: Culicidae) Females to Chemicals Found in Human Skin Emanations. *J. Med. Entomol.* 43, 207–213. doi:10.1603/0022-2585(2006)043[0207:EABROC]2.0.CO;2
- Qiu, Y.-T., Gort, G., Torricelli, R., Takken, W., van Loon, J.J.A., 2013. Effects of blood-feeding on olfactory sensitivity of the malaria mosquito *Anopheles gambiae*: application of mixed linear models to account for repeated measurements. *J. Insect Physiol.* 59, 1111–8. doi:10.1016/j.jinsphys.2013.09.001
- Qiu, Y.-T., van Loon, J.J., 2010. Olfactory physiology of blood-feeding vector mosquitoes., in: Takken, W., Knols, B.G.J. (Eds.), *Olfaction in Vector-Host Interactions*. Wageningen Academic Publishers, Wageningen, pp. 39–61.
- Qiu, Y.-T., van Loon, J.J.A., Takken, W., Meijerink, J., Smid, H.M., 2006. Olfactory Coding in Antennal Neurons of the Malaria Mosquito, *Anopheles gambiae*. *Chem. Senses* 31, 845–63. doi:10.1093/chemse/bjl027
- Qiu, Y.T., 2005. Sensory and behavioural responses of the malaria mosquito *Anopheles gambiae* to human odours. Ph.D. thesis, Wageningen University.
- Qiu, Y.T., Smallegange, R.C., Smid, H., Loon, J.J.A. Van, Galimard, A., Posthumus, M.A., Beek, T. Van, Takken, W., 2004. GC-EAG analysis of human odours that attract the malaria mosquito *Anopheles gambiae* sensu stricto. *Proc. Netherlands Entomol. Soc. Meet.* 15, 59–64.
- Qiu, Y.T., Smallegange, R.C., Van Loon, J.J.A., Takken, W., 2011. Behavioural responses of *Anopheles gambiae* sensu stricto to components of human breath, sweat and urine depend on mixture composition and concentration. *Med. Vet. Entomol.* 25, 247–255.
- Rund, S.S.C., Bonar, N.A., Champion, M.M., Ghazi, J.P., Houk, C.M., Leming, M.T., Syed, Z., Duffield, G.E., 2013. Daily rhythms in antennal protein and olfactory sensitivity in the malaria mosquito *Anopheles gambiae*. *Sci. Rep.* 3, 2494. doi:10.1038/srep02494
- Siju, K.P.P., Hill, S.R., Hansson, B.S., Ignell, R., 2010. Influence of blood meal on the responsiveness of olfactory receptor neurons in antennal sensilla trichodea of the yellow fever mosquito, *Aedes aegypti*. *J. Insect Physiol.* 56, 659–65. doi:10.1016/j.jinsphys.2010.02.002
- Smallegange, R.C., Bukovinszkiné-Kiss, G., Otieno, B., Mbadi, P. a., Takken, W., Mukabana, W.R., Van Loon, J.J. a., 2012. Identification of candidate volatiles that affect the behavioural response of the malaria mosquito *Anopheles gambiae* sensu stricto to an active kairomone

- blend: laboratory and semi-field assays. *Physiol. Entomol.* 37, 60–71. doi:10.1111/j.1365-3032.2011.00827.x
- Smallegange, R.C., Geier, M., Takken, W., 2002. Behavioural responses of *Anopheles gambiae* to ammonia, lactic acid and a fatty acid in a γ -tube olfactometer. *Proc. Exp. Appl. Entomol.* 13, 147–152.
- Smallegange, R.C., Qiu, Y.T., Bukovinszkiné-Kiss, G., Van Loon, J.J.A., Takken, W., 2009. The effect of aliphatic carboxylic acids on olfaction-based host-seeking of the malaria mosquito *Anopheles gambiae sensu stricto*. *J. Chem. Ecol.* 35, 933–43. doi:10.1007/s10886-009-9668-7
- Smallegange, R.C., Qiu, Y.T., van Loon, J.J.A., Takken, W., 2005. Synergism between ammonia, lactic acid and carboxylic acids as kairomones in the host-seeking behaviour of the malaria mosquito *Anopheles gambiae sensu stricto* (Diptera: Culicidae). *Chem. Senses* 30, 145–152.
- Steullet, P., Guerin, P.M., 1994. Identification of vertebrate volatiles stimulating olfactory receptors on tarsus I of the tick *Amblyomma variegatum* Fabricius (Ixodidae). I. Receptors within the Haller's organ capsule. *J. Comp. Physiol. A.* 174, 27–38.
- Suer, R.A., 2011. Unravelling the malaria mosquito's sense of smell: neural and behavioural responses to human-derived compounds. University of Wageningen.
- Syed, Z., Leal, W.S., 2009. Acute olfactory response of *Culex* mosquitoes to a human- and bird-derived attractant. *Proc. Natl. Acad. Sci. U. S. A.* 106, 18803–8. doi:10.1073/pnas.0906932106
- Syntech, 2004. EAG: a Practical Introduction. Syntech 29.
- Takken, W., Dekker, T., Wijnholds, Y.G., 1997. Odor-mediated flight behavior of *Anopheles gambiae sensu stricto* and *An. stephensi liston* in response to CO₂, acetone, and 1-octen-3-ol (Diptera: Culicidae). *J. Insect Behav.* 10, 395–407. doi:10.1007/BF02765606
- Takken, W., Knols, B.G., 1999. Odor-mediated behavior of Afrotropical malaria mosquitoes. *Annu. Rev. Entomol.* 44, 131–57. doi:10.1146/annurev.ento.44.1.131
- Takken, W., Knols, B.G.J. (Eds.), 2010. Olfaction in vector-host interactions. Wageningen Academic Publishers. doi:10.3920/978-90-8686-698-4
- Takken, W., van Loon, J.J., Adam, W., van Loon JJ, Adam, W., 2001. Inhibition of host-seeking response and olfactory responsiveness in *Anopheles gambiae* following blood feeding. *J. Insect Physiol.* 47, 303–310.
- Tauxe, G.M., MacWilliam, D., Boyle, S.M.S.M., Guda, T., Ray, A., Belsito, D., Bickers, D., Bruze, M., Calow, P., Dagli, M.L., Dekant, W., Fryer, A.D., Greim, H., Miyachi, Y., Saurat, J.H., Sipes, I.G., Panel, R.E., Bernier, U.R. et al., 2013. Targeting a dual detector of skin and CO₂ to modify mosquito host seeking. *Cell* 155, 1365–79. doi:10.1016/j.cell.2013.11.013
- Tchouassi, D.P., Sang, R., Sole, C.L., Bastos, A.D.S., Teal, P.E.A., Borgemeister, C., Torto, B., 2013. Common host-derived chemicals increase catches of disease-transmitting mosquitoes and can improve early warning systems for Rift Valley fever virus. *PLoS Negl. Trop. Dis.* 7, e2007. doi:10.1371/journal.pntd.0002007
- van Loon, J.J.A., Smallegange, R.C., Bukovinszkiné-Kiss, G., Jacobs, F., De Rijk, M., Mukabana, W.R., Verhulst, N.O., Menger, D.J., Takken, W., 2015. Mosquito Attraction: Crucial Role of Carbon Dioxide in Formulation of a Five-Component Blend of Human-Derived Volatiles. *J. Chem. Ecol.* doi:10.1007/s10886-015-0587-5
- Verhulst, N.O., Beijleveld, H., Qiu, Y.T., Maliepaard, C., Verduyn, W., Haasnoot, G.W., Claas, F.H.J., Mumm, R., Bouwmeester, H.J., Takken, W., van Loon, J.J. a, Smallegange, R.C., Tong,

- Y., Loon, J.J.A. Van, 2013. Relation between HLA genes, human skin volatiles and attractiveness of humans to malaria mosquitoes. *Infect. Genet. Evol.* 18, 87–93. doi:10.1016/j.meegid.2013.05.009
- Verhulst, N.O., Mbadi, P.A., Kiss, G.B., Mukabana, W.R., van Loon, J.J.A., Takken, W., Smallegange, R.C., 2011. Improvement of a synthetic lure for *Anopheles gambiae* using compounds produced by human skin microbiota. *Malar. J.* 10, 28.
- Wagenstaller, M., Buettner, A., 2013. Quantitative determination of common urinary odorants and their glucuronide conjugates in human urine. *Metabolites* 3, 637–57. doi:10.3390/metabo3030637
- Wahl, H.G., Hoffmann, A., Luft, D., Liebich, H.M., 1999. Analysis of volatile organic compounds in human urine by headspace gas chromatography-mass spectrometry with a multipurpose sampler. *J. Chromatogr. A* 847, 117–25.
- Wang, G., Carey, A.F., Carlson, J.R., Zwiebel, L.J., 2010. Molecular basis of odor coding in the malaria vector mosquito *Anopheles gambiae*. *Proc. Natl. Acad. Sci. U. S. A.* 107, 4418–23. doi:10.1073/pnas.0913392107
- Wondwosen, B., Birgersson, G., Seyoum, E., Tekie, H., Torto, B., Fillinger, U., Hill, S.R., Ignell, R., 2016. Rice volatiles lure gravid malaria mosquitoes, *Anopheles arabiensis*. *Sci. Rep.* 6, 37930. doi:10.1038/srep37930
- Wondwosen, B., Hill, S.R., Birgersson, G., Seyoum, E., Tekie, H., Ignell, R., 2017. A (maize)ing attraction: gravid *Anopheles arabiensis* are attracted and oviposit in response to maize pollen odours. *Malar. J.* 16, 39. doi:10.1186/s12936-016-1656-0
- Xu, W., Cornel, A.J., Leal, W.S., 2010. Odorant-binding proteins of the malaria mosquito *Anopheles funestus* sensu stricto. *PLoS One* 5. doi:10.1371/journal.pone.0015403
- Yamazaki, S., Hoshino, K., Kusuhara, M., 2010. Odor Associated with Aging. *Anti-Aging Med.* 7, 60–65. doi:10.3793/jaam.7.60
- Young, R.M., Burkett-Cadena, N.D., McGaha, T.W., Rodriguez-Perez, M.A., Toé, L.D., Adeleke, M.A., Sanfo, M., Soungalo, T., Katholi, C.R., Noblet, R., Fadamiro, H., Torres-Estrada, J.L., Salinas-Carmona, M.C., Baker, B., Unnasch, T.R., Cupp, E.W., 2015. Identification of Human Semiochemicals Attractive to the Major Vectors of Onchocerciasis. *PLoS Negl. Trop. Dis.* 9, e3450. doi:10.1371/journal.pntd.0003450
- Zeng, X.-N., Leyden, J.J., Spielman, A.I., Preti, G., 1996. Analysis of characteristic human female axillary odors: Qualitative comparison to males. *J. Chem. Ecol.* 22, 237–257. doi:10.1007/BF02055096
- Zeng, X. nong, Leyden, J.J., Lawley, H.J., Sawano, K., Nohara, I., Preti, G., 1991. Analysis of characteristic odors from human male axillae. *J. Chem. Ecol.* 17, 1469–1492. doi:10.1007/BF00983777
- Zhang, Z.M., Cai, J.J., Ruan, G.H., Li, G.K., 2005. The study of fingerprint characteristics of the emanations from human arm skin using the original sampling system by SPME-GC/MS. *J. Chromatogr. B Anal. Technol. Biomed. Life Sci.* 822, 244–252. doi:10.1016/j.jchromb.2005.06.026

7 Discussion and conclusions

The aim of this thesis was to determine whether infection of the human host by *Plasmodium* species alters the skin volatile odour profile in a manner that is detected by *Anopheles* mosquitoes. By examining both experimentally and naturally *Plasmodium*-infected individuals, it was demonstrated that the odour profile is significantly altered by *Plasmodium* infection. This is the first time that the influence of *Plasmodium* infection on human skin odour composition has been investigated. While several studies have found *Plasmodium*-induced changes in human host attractiveness (Batista et al., 2014; Busula et al., 2017; Lacroix et al., 2005), none has examined skin odours, known to be crucially important in mosquito host-seeking, as the possible mechanism.

7.1 Summary of findings

By examining 31 odour samples in the EI BMGF cohort (11 individuals), five compounds were identified that were significantly associated with *Plasmodium falciparum* infection. These 'infection-associated compounds' (IAC) were: 6-methyl-5-hepten-2-one, 1-dodecene, dodecanal, RI 1416 (co-eluting sesquiterpene and phthalate), and methyl dodecanoate. Odour samples from the BMGF cohort were tested for antennal response by *Anopheles coluzzii* (chapter 6). No electroantennographically (EAG)-active compounds were found to be specific to infected odour samples. Additionally, none of the identified IAC elicited antennal response. However, 26 EAG-active peaks were tentatively identified across all antennae tested. These largely confirmed the importance of compounds previously found to be EAG-active or to induce a behavioural response in mosquitoes, with the addition of several putative novel EAG-active compounds.

Next, 117 odour samples were investigated from 56 asymptomatic children of varying *Plasmodium* infection status, from a malaria-endemic region of Western Kenya (chapter 5). In this large field trial, eight compounds were identified whose production was significantly associated with the presence of *Plasmodium* parasites. These were the aldehydes hexanal (C6), heptanal (C7), octanal (C8), nonanal (C9), (*E*)-2-octenal and (*E*)-2-decenal, and the ketones 2-octanone and 1-octen-3-one. Production of the aldehydes C7-C9 was correlated with total density of bloodstream parasites, (*E*)-2-octenal and (*E*)-2-decenal production was associated with any parasitological positivity, and production of hexanal, 2-octanone and 1-octen-3-one

was associated with gametocyte density. The production of the ketones 2-octanone and 1-octen-3-one appeared associated with gametocytes in a density-dependent manner. In addition to association with total parasite density, a possible gametocyte-specific effect on compound production was observed for octanal, (*E*)-2-octenal, (*E*)-2-decenal and peak RI 965 (containing co-eluting 6-methyl-5-hepten-2-one and 1-octen-3-ol). However, in most cases, the effect of gametocytes versus total parasites is not possible to disentangle. When modelled by total parasite density, production of peak RI 965 by individuals with lower density parasites significantly decreased, while that by individuals with higher density parasites was not significantly different to that by parasite-free individuals. Because the peak contained two co-eluting compounds, limited conclusions could be drawn.

Odour samples from the Kenyan cohort were then tested to determine the antennal response of *An. coluzzii* (chapter 6). As with the experimentally-infected cohort, no EAG-active compounds were found to qualitatively distinguish the odour samples of *Plasmodium* parasite-positive individuals. The aldehydes C7-C9, in addition to a peak containing co-eluting 1-octen-3-one and phenol (RI 958), were found to be EAG-active. In the EAG work, 1-octen-3-one co-eluted with phenol because of the shorter GC programme required for EAG experiments. To help determine whether the antennal response was to the infection-associated 1-octen-3-one, or to phenol, further work would be required (i.e. direct EAG testing of those compounds). The possible entomological significance of the gametocyte-associated ketone 1-octen-3-one is disregarded in the following discussion, in the absence of clarification on the mosquito response to this versus phenol. Currently, the mosquito's behavioural response to any of the EAG-active compounds is not known.

7.2 Natural infection IAC in the experimental infection odour profiles

Prior to comparing the infection-associated changes observed in the experimentally- and naturally-infected cohorts, it is important to recognise other, fundamental, differences between these two groups. The experimental infections (EI) cohort comprised healthy, *Plasmodium*-naïve European adults, while the natural infection (NI) cohort involved Kenyan children, 5-12 years old, who may have harboured other (potentially parasitic) infections. Indeed, given the proximity of the study site to Lake Victoria, and the likely occupation of some of the families as fishermen, it seems probable that co-morbidities would include schistosomiasis (Butler et al., 2012). As such, discrepancies between these two cohorts include age, genetic makeup, dietary

factors, general health and exposure to other infections, and previous exposure to malaria. However, for the purposes of speculating that *Plasmodium*-associated changes to odour profile mediate changes in attractiveness to mosquitoes, we can assume that such parasite manipulation might manifest in all individuals in the same way.

In the EI cohort we observed changes in the odour profile of individuals harbouring very low-density *Plasmodium* infections, i.e. positivity as detected by sensitive molecular techniques. Infections were halted by treatment following two positive tests, precluding the development of higher-density infections. In the NI cohort, we observed some changes in odour profile at low parasite density, including increased production of (*E*)-2-octenal and (*E*)-2-decenal, and 2-octanone, hexanal and EAG-active 1-octen-3-one at low gametocyte densities. Production of the EAG-active aldehydes, C7-C9, was not increased in low-density infection. In the NI analysis, parasite densities of less than 50 p/μl were considered 'low', yet densities approaching this threshold (e.g. 40 p/μL) are considerably higher than the densities probably present in the EI cohort. There, the diagnostic technique used had an estimated limit of detection of 0.02 p/μl (Hermsen et al., 2001). Notably, the production of those compounds that may be important to transmission, i.e. the EAG-active C7-C9, was only significantly increased by individuals harbouring the higher density infections (>50 p/μl). In evolutionary terms, it could be hypothesised that odour profile changes occur throughout infection, due to systemic changes instigated by the presence of parasites, but those that influence transmission occur only at higher parasite density. This hypothesis would account for the observed infection-mediated changes to the odour profile in both EI and NI cohorts (even at very low parasite densities, as seen in the EI cohort), and the parasite density-dependent production of EAG-active, entomologically significant C7-C9, a putative 'transmission signal' in the NI cohort. Interestingly, C7 and C9 were both detected as EAG-active compounds in the odour profile of the EI cohort. Their presence in the odour profile is unsurprising, as they are known to be produced by the human skin (as reviewed in chapter 5). This finding neatly reinforces both the entomological importance of these compounds, and the requirement of a high-density parasite infection to stimulate increased production. In mechanistic terms, the production of these EAG-active compounds at higher parasite densities only is predicted by two proposed mechanisms: greater levels of oxidative stress, and greater numbers of parasite-infected RBC, would characterise high-density infections. One compound was significantly associated with infection in both EI and NI cohorts: 6-methyl-5-hepten-2-one, with production decreasing in individuals harbouring low densities of parasites. The probable repellency of 6-methyl-5-hepten-2-one to *Anopheles* (Logan

et al., 2010, 2008; Menger et al., 2014; Qiu et al., 2011), in combination with the rigour of detecting the same compound in two different *Plasmodium*-infected cohorts, should prompt further investigation of this compound, despite co-elution with 1-octen-3-ol.

7.3 Experimental infection IAC in the natural infection odour profiles

While the absence of the NI IAC (EAG-active and otherwise) in the EI cohort might be explained by insufficient parasite densities in the latter, the absence of the EI-IAC (experimental infection-associated compounds) in the NI cohort is more difficult to reconcile. It is possible that these compounds were indeed up-regulated in the NI odour profiles, but the amounts concerned were small, and not detected. As detailed in chapter 4, analytical problems possibly reduced the sensitivity of the NI odour profile analysis. No EAG-response was elicited by the EI-IAC (chapter 6), indicating that a role as putative transmission-signalling compounds is unlikely. It is therefore more probable that the production of these compounds changed because of the altered physiological state of infected persons. In systems involving parasites with multiple developmental states, differential manipulation of the hosts in accordance with the best interests of the current developmental stage has been shown. In the malaria-transmitting anopheline mosquito, it is thought that *Plasmodium* parasites may influence mosquito behaviour to reduce risky bloodmeal seeking while the parasites are present in the (non-transmissible) oocyst stages (Anderson et al., 1999; Koella, 2002), but to increase probing and the likelihood of multiple bloodmeals when the transmissible sporozoites are present in the mosquito's salivary glands (Ponnudurai et al., 1991; Rossignol et al., 1984; Wekesa et al., 1992). In studies of *Plasmodium*-infected vertebrate host attractiveness to mosquitoes, the phenomenon is often associated with the chronic phase, or an increased bloodstream gametocyte density (Batista et al., 2014; Busula et al., 2017; Cornet et al., 2012; Day and Edman, 1983; De Moraes et al., 2014; Lacroix et al., 2005). The initial, acute, phase of clinical malaria constitutes a period of febrile illness, in which the first erythrocytic forms are present and high levels of parasitaemia can be observed. This is followed by the longer chronic phase, where parasite densities are lower, the immune system is controlling infection to a degree, and gametocyte stages are often present at higher density. *P. falciparum* gametocytes require a long maturation process, thus do not appear in the bloodstream until 7-15 days after the first wave of their asexual parasite progenitors (WWARN Gametocyte Study Group, 2016). Specific increases in attractiveness during the chronic phase could be, and often is, interpreted as parasite manipulation favouring the transmissible gametocytes. Not all studies, however,

associate increased attractiveness specifically with gametocytes. In the study by Cornet et al. (2012), while increased attractiveness to mosquitoes was specific to the chronic phase, in this avian malaria system high gametocyte densities are present from the early stages of infection. Indeed, the authors suggested that preference for the chronic phase may be the result of two antagonistic effects: attractiveness mediated by the presence of gametocytes, and repellence induced by a poor quality blood meal in acute stage infection. Asexual parasite density and gametocyte density were found to be positively associated with the propensity of mosquitoes to feed on *P. chabaudi*-infected mice (Ferguson et al., 2003). However, when these factors were combined in a single model, also including red blood cell density (and eliminating non-significant terms), asexual parasite density alone retained the significant association with the proportion of mosquitoes feeding. The relationship between asexual parasite and gametocyte densities remains equivocal (Bousema et al., 2004). While for *P. vivax* gametocyte densities represent a consistent proportion of the total parasite biomass (~10%, Koepfli et al. 2015), the delayed appearance of *P. falciparum* gametocytes from their asexual progenitors makes this association less clear cut (Bousema and Drakeley, 2011; Koepfli et al., 2015). In acute infections, there is a negative association between total parasite density and gametocyte density (WWARN Gametocyte Study Group, 2016) whilst in asymptomatic or chronic infections there is generally a weak positive association between total parasite biomass (or asexual parasite biomass) and gametocyte density (Akim et al., 2000; Bousema and Drakeley, 2011; Koepfli et al., 2015; Slater et al., 2015). Considering this general positive relationship in asymptomatic infections that reflect the bulk of all infections, however, a transmission signal derived from asexuals or all parasite stages (i.e. total density) remains a logical working hypothesis. In the current study, parasitologically positive individuals in the EI cohort were entering the acute phase of infection, with low parasite densities, and were demonstrated to be gametocyte-free by QT-NASBA. A fever of >37.5 °C was a volunteer exclusion criteria in the NI cohort, which should have precluded acute phase individuals. Further, since acute-phase malaria occurs on contracting infection, in an endemic setting it is likely that relatively high infection pressure would result in steady-state, low grade infections in children of this age group.

Thus, one explanation for the observed differences in odour profile is specificity to the different phases of infection, as these are characterised by distinct infection processes. Alternatively, or indeed in addition to this, the NI-IAC may constitute a 'transmission signal', generated by high parasite densities and/or gametocytes. While it has been demonstrated that transmission can occur at very low gametocyte densities (Churcher et al., 2013), transmission at sub-PCR

gametocyte densities is unlikely. Therefore, irrespective of its origin (i.e. induced by gametocytes or high parasite densities), a 'transmission signal' in very early-stage infections with low parasite densities serves little purpose. The absence of the NI-IAC in the EI cohort is consequently supportive of a putative role as a 'transmission signal'.

An interesting finding of the EI study was the possible separation of odour profile based on parasite strain (chapter 2/2.4.5). This finding motivated the species-specific diagnoses conducted on the NI cohort blood samples (chapter 3/3.3.4), and in addition to *P. falciparum*, *P. malariae* and *P. ovale* constituted 5.05 % and 3.96 % respectively of all positive samples (at R1). Time constraints disallowed investigation into species-specific odour profile in the NI samples, and additionally, grouping all *Plasmodium* species maximised power in the NI odour profile analysis. This can be justified on the basis that all *Plasmodium* species are transmitted by the same (human-biting) mosquitoes of the genus *Anopheles*. Therefore, all *Plasmodium* species would benefit equally from maximising human host cues that are attractive to any anopheline mosquito species.

7.4 Do these changes in odour profile constitute parasite manipulation?

An association was observed between the increased production of certain compounds by the skin, and *Plasmodium* infection. Because some of these compounds were shown to elicit an electrophysiological response in *Anopheles*, the changes are consistent with the theory of parasite manipulation, with parasites manipulating host attractiveness in order to maximise their own transmission. Some evidence regarding a possible mechanism for the production pathway of these IAC was revealed according to their identity, as lipid peroxidation of red blood cell and liver cell membranes, caused by malaria-induced oxidative stress, could increase the production of aldehydes and ketones. Oxidative stress is a normal physiological response to factors including infection. However, given the potential fitness benefits of such changes to the odour profile, manifested through the likely influence of aldehydes and ketones on mosquito behaviour, I believe that here we indeed provide empirical evidence of *Plasmodium* parasite manipulation. I propose that *Plasmodium* parasites have hijacked the innate oxidative stress response. Through preferential spread of the parasite genotypes that most elicit this response, and therefore subsequent aldehyde production, the underlying parasite characteristics would be selected for. In this way, *Plasmodium* parasites would evolve to manipulate the human physiological response to infection.

An alternative interpretation of this phenomenon should be discussed, whereby individuals who naturally produce more attractive compounds are more often bitten, with a consequentially increased likelihood of becoming infected. However, under these conditions, changes in an individual's attractiveness after becoming infected, or after clearing an infection, would not occur. In our EI cohort, individuals were odour sampled before, during and after infection, and temporal changes in the odour profile were observed, in keeping with infection status. Here, individuals were randomly selected for infection, and it is unlikely that their innate differences in attractiveness to mosquitoes influenced the infection process. In the NI cohort, study design intended to sample individuals once on recruitment and during infection, and twice following curative treatment at one and three weeks later. However, in the final dataset, there was a shortage of individuals for whom an odour sample was available at both an infected and truly parasite-free time point. This precluded rigorous analysis of intra-individual changes in the production of IAC, according to changing infection status (chapter 5/5.5.8). Greater rigour in antimalarial treatment protocols, potentially with field staff administering the whole course, should be advocated in future studies. This would generate more, paired, 'infected' vs. 'uninfected' samples from the same individual, allowing an investigation of such temporal changes in compound production.

7.5 The behavioural role of infection-associated compounds

Infection with *Plasmodium* parasites was shown here to be correlated with significant changes in human skin odour. In both experimentally- and naturally-infected cohorts, the changes in odour profile were quantitative, not qualitative, in nature. Antennal responsiveness to three (possibly four) of these compounds suggests that it is possible that these, or similar, changes underpin the modifications in attractiveness of *Plasmodium*-infected individuals observed previously (Batista et al., 2014; Busula et al., 2017; Lacroix et al., 2005). As C7-C9 are known components of human skin odour (Bernier et al., 1999; Curran et al., 2010, 2005; Dormont et al., 2013a), and have known entomological significance (Jaleta et al., 2016; Logan et al., 2010; Nyasembe et al., 2014; Smallegange et al., 2012), it is probable that these compounds are used by mosquitoes in the location and selection of a suitable host. If *Plasmodium* infection is detrimental to the fitness of the mosquito (see chapter 1), exaggeration of these cues can be considered to be 'deceptive signalling' (Mauck et al., 2010). The negative consequences of selecting against the recognition of components of host odour, which signal a bloodmeal and

therefore govern reproductive success, would probably be greater than those of imbibing an infected meal. Our findings thus agree with the hypothesised characteristics of a 'supernormal stimuli', being an exaggeration of pre-existing cues (Dawkins and Krebs, 1979; Mauck et al., 2010).

In the absence of behavioural data for *Anopheles* concerning the role of the EAG-active IAC, we cannot yet attribute altered attractiveness to these findings. The lack of behavioural data is complicated by several factors. First, while some compounds are certainly candidates for further investigation (e.g. C7-C9), others require further work (i.e. ascertaining whether 1-octen-3-one or phenol was responsible for the observed EAG activity, chapter 6). 1-Octen-3-one, hexanal and 2-octanone were significantly associated with gametocytes, yet none demonstrated EAG activity, with the possible exception of 1-octen-3-one. No EAG activity was observed for other compounds found to be significantly associated with the presence of parasites, e.g. (*E*)-2-octenal and (*E*)-2-decenal, and only slight EAG activity in response to co-eluting 6-methyl-5-hepten-2-one or 1-octen-3-ol. This is surprising, given the known entomological significance of these co-eluting compounds (Kempe et al., 1993; Logan et al., 2010, 2008; Takken et al., 1997). It is possible that in the blends of odour profile that were EAG tested, these were present at insufficient concentration (i.e. beneath the recognition threshold) to stimulate response. This calls into question the criteria by which IAC should be chosen for behavioural testing.

Further, it is likely that any compound chosen for testing will elicit a spectrum of mosquito behaviours, ranging from repellency to attraction, across a concentration gradient (Dethier, 1954). Therefore, testing the correct concentration of compound is paramount to determining the behavioural response. The odour sampling method used here (air entrainment) is optimal for sampling the emission of volatile compounds (Dormont et al., 2013b). Despite this, the mean amount of compound observed to be produced here, per group, may not exactly represent concentrations emitted in the natural setting. This could be because of sampling bias, including insufficient group sample size, or testing insufficient skin surface area. The foot was chosen for sampling both as it is a preferred biting site of *An. gambiae* (De Jong and Knols, 1995), and to minimise discomfort for volunteers during the sampling process. Although in the natural setting biting insects will experience the odour plume of an entire person, not just the feet, previous studies demonstrate that *Anopheles* respond to foot odour alone (Jawara et al., 2009; Njiru et al., 2006; Olanga et al., 2010; Omolo et al., 2013). If C7-C9 (and/or other IAC) are products of malaria-induced oxidative stress, the compounds will probably be released systemically, and not

via the metabolism of foot bacteria. In this case, it might be expected that the 'infected odour' plume released by a malarious individual in the natural setting would include a greater amount of C7-C9 than was captured from feet alone.

Finally, the speculated 'infected odour' plume would additionally contain other, 'healthy' odour cues, unaffected by the parasitic infection. It might, therefore, be advisable to test IAC against a background of 'healthy' human odour, which would require method optimisation. For these reasons, complicated, and doubtless extensive, laboratory experiments would be necessary to test compounds at appropriate concentrations in order to correctly deduce a behavioural effect. It is interesting, however, to hypothesise about the consequences of IAC as attractive, or as repellent, to mosquitoes.

7.6 Infection-associated compounds are attractive to mosquitoes

If *Plasmodium*-associated changes in the skin odour profile are attractive to the mosquito, it can be hypothesised that infected individuals would be bitten more frequently than parasite-free individuals. This effect may be exaggerated by other aspects of infection: immobility of sick people, reduced defensiveness against biting mosquitoes, and elevated body temperature (febrile episodes) (Schreck et al., 1990; Smart and Brown, 1956). This hypothesis is supported by studies, across different vector-borne disease systems, showing that infected hosts are more attractive than uninfected hosts (Batista et al., 2014; Baylis and Nambiro, 1993; Busula et al., 2017; Cornet et al., 2012; Day and Edman, 1983; De Moraes et al., 2014; Lacroix et al., 2005; Turell et al., 1984). Increased biting of infected individuals, once the transmission signal had been generated, would lead to an increased prevalence of *Plasmodium*-infected mosquitoes. How this would then influence the spread of malaria in a population is probably dependent on other factors governing transmission, including the ecology of local disease vectors, environmental conditions, the extent of interaction between vectors and hosts, human behaviours, or premunition (partial immunity) in the human population. Kingsolver (1987) developed and analysed models that incorporated non-random feeding of mosquitoes on *Plasmodium*-infected individuals according to various scenarios. In one scenario, consistent preference for the infected host at any prevalence of host infection, two outcomes were predicted according to the prevalence of infection in the population. At low host infection prevalence, a stable infected equilibrium was predicted, resulting from continual mosquito

infection due to preference for infected hosts. At higher population levels of host infection however, most mosquito biting was constricted to infected hosts and the spread of infection then limited (Kingsolver, 1987).

An obvious question concerns the possible conflict of interest between *Plasmodium* parasites in the vertebrate host and those in an infected mosquito. The former would benefit from increased attractiveness of the host and increased mosquito biting, whereas it seems probable that the latter would benefit most from the mosquito biting an uninfected host. Multiple infectious bites can lead to 'superinfection', i.e. infection of one host with multiple parasite genotypes. This can lead to within-host competition, either direct competition for host resources (Abkallo et al., 2015), or immune-mediated apparent competition (a parasite lineage encountering a stronger immune response than it would have on its own, due to the presence of other lineages in the mixed infection (Råberg et al., 2017)). For this reason, the parasite in the mosquito vector may 'prefer' the mosquito to bite a naïve host. One study directly tested this phenomenon in an avian malaria system. Cornet et al. (2013) examined the attraction of uninfected, and sporozoite-infected, mosquitoes to chronically *Plasmodium*-infected birds. Here, preference for infected rather than uninfected birds was retained, irrespective of the infection status of the mosquito. The authors concluded that the parasites within the vertebrate host (the bird) were driving host-choice of the infected mosquito. In the *P. chabaudi* rodent malaria model system, *Plasmodium*-infected *An. stephensi* were disproportionately attracted to infected, relative to uninfected, hosts (Ferguson and Read, 2004). Again, it would appear that the parasite in the vertebrate host was favoured. In the human malaria system, this would be an area of outstanding interest for further work.

7.7 Infection-associated compounds are repellent to mosquitoes

If *Plasmodium*-associated changes in the skin odour profile are not attractive to the mosquito, infected people would probably be bitten less frequently than parasite-free individuals. This is in direct opposition to the interests of the parasite in the vertebrate host, as fewer bites would translate into fewer transmission opportunities. This scenario proposes that the fitness of the mosquito would be maximised by evolving to prefer (and take a bloodmeal from) uninfected hosts, thus avoiding some fitness costs of infection. It is likely that adaptations of the parasite and vector (and vertebrate host) constitute an arms race, whereby traits that maximise the fitness of one are countered by the evolution of traits favouring the other. Although the avoidance of

infected persons by mosquitoes would impose severe fitness costs on the *Plasmodium* parasite, it is possible that here we observe a point in such an arms race where the parasite is thus disadvantaged.

7.8 Infection-associated compounds as biomarkers for malaria?

One anticipated outcome of this study was the discovery of volatile compounds that may constitute biomarkers for malaria, which could be exploited for diagnostic purposes. Historically, the equipment required for this type of analytical chemistry was expensive, non-transportable, with low-throughput and requiring expert interpretation. Additionally, the time taken to obtain the results would have hampered use in diagnostics. However, in parallel to increased research into the biomarkers themselves, recent technological developments have resulted in 'sensory arrays', that are capable of detecting profiles of volatile compounds: 'electronic noses'. Although there are now several permutations, all comprise the basic elements of the volatile compounds passing over a sensor array (e.g. conducting polymer array or metal oxide sensor), the sensors conduct according to the degree of binding, and then signal, which is coupled to data-analysis software to give the output (Turner and Magan, 2004). This is a pattern-recognition system, designed for real-time detection and discrimination of analytes (for a review, see Oh et al. (2011)), with the advantages of being relatively simple technology and non-invasive. Electronic noses ('E-noses') have been successfully employed to distinguish some pathological processes. In one study, nine of ten E-nose melanoma diagnoses were confirmed by histological examination (D'Amico et al., 2008); however, the lesion headspace could be compared to adjacent healthy skin of the same individual. E-noses require improvement in terms of sensitivity, selectivity and reproducibility before they can be introduced as routine diagnostic tools (Oh et al., 2011).

Production of the aldehydes C6-C10 has been correlated with many diseases, as oxidative stress is a sequelae of various pathologies including cancer, acute myocardial infarction, neurodegenerative disorders and skin disease (Buljubasic and Buchbauer, 2015). As such, the detection of these compounds as the basis of a diagnostic tool would require further investigation to determine if specific ratios of compounds are sufficiently characteristic. Here, their presence as substantial and significant components of the odour profile is encouraging, in terms of the sensitivity of such a tool. Further, (*E*)-2-octenal, (*E*)-2-decenal, 2-octanone and 1-octen-3-one have had little attention in the literature, and following further investigation, these

may be more specifically associated with *Plasmodium* infection. Taken together, rather than pursuing a 'silver bullet', it may be that a cocktail of compounds, at the relevant ratio, could provide a malaria odour 'signature'. It is also important to note that within our study population, all individuals were asymptomatic. It would be interesting to measure the production of these compounds by symptomatic individuals, and this would possibly lead to a better understanding of their association with *Plasmodium* infection.

7.9 Other significant findings of this thesis

Through investigating the presence of IAC, two significant methodological findings were made. First, the nitrocellulose strip inside used rapid diagnostic tests (RDTs) for malaria can be used as a DNA template for the qPCR PgMET (chapter 3). Secondly, the R package MALDIquant can be successfully applied to GC data, and can greatly assist sample analysis (chapter 4). As reviewed in chapter 3, the possibility of determining precise parasite densities from a point-of-care test, with minimal storage requirements, represents a significant (although not novel (Cnops et al., 2011)) finding. Use of the RDT as a DNA template for PgMET qPCR, however, has not previously been demonstrated, and adds to the recent literature in this field (Nabet et al., 2016; Papa Mze et al., 2016, 2015; Vongsouvath et al., 2016). RDTs are one of the most widely used diagnostic techniques for malaria infection, and the ability to retrospectively gain greater insight into underlying parasite population dynamics is interesting to many researchers. Similarly, the flexibility and precision afforded by MALDIquant in analysing GC data could be of much interest to researchers in analytical chemistry, where such data is still analysed using manual methods which are at times subjective. While MALDIquant can, but does not necessarily, replace these, it can be used in a semi-automated manner whereby automatic but user-defined steps can be easily and quickly visualised and checked. The advantages of MALDIquant to this thesis were profound: here, four of eight IAC were identified via MALDIquant only (including both octanal and nonanal), two were identified by both MALDIquant and the traditional retention index method, and only two by the latter method alone.

7.10 Methodological limitations of the study

Analysis of the odour samples represented a considerable hurdle to the completion of this thesis. As detailed in chapter 4, the issues encountered in GC analysis were not novel, yet were sufficiently extensive to prevent alignment of all traces in one dataset. In future studies involving

GC analysis of many samples, measures should be taken to circumvent these issues as suggested (chapter 4). However, it is important to emphasise that via development of the MALDIquant method, which allowed alignment between subsets of samples to be rigorously validated, it was possible to negotiate these problems and subsequently complete the objectives of the thesis. Another issue that should be avoided in future studies is the use of multiple diagnostic assays for determining parasitological parameters. In this study, extra assays were added (PgMET qPCR and species-specific end-point PCR) to those originally encompassed in the study design (18S qPCR and QT-NASBA to provide molecular measures of parasitaemia). Fortunately, the added methods provided crucial parasite density information for odour samples where the 18S qPCR data was lost. Use of multiple assays, however, added difficulty when allocating odour samples to parasitological categories, requiring the comparability of results to be verified. While these parasitological measures were found to be sufficiently correlated, it was also mostly possible to circumvent the issue by designing parasitological categories in which odour samples were placed by all diagnostic measures. This avoided reliance on one diagnostic assay, apart from the 'quartiles' analysis, for which a specific categorisation protocol was adopted, using a hierarchy of assay importance. In future studies, the consistent use of one diagnostic assay, enabling like-with-like comparison of parasitological data, should be advocated.

7.11 Conclusions

For several decades now, researchers have investigated how infection with malaria parasites, *Plasmodium* species, can change the attractiveness of the vertebrate host to the *Anopheles* mosquito vectors. While evidence for such changes in attractiveness has accumulated, no study has thus far investigated whether these might be manifested by changes in the human skin odour profile. This thesis addressed this question by investigating qualitative and quantitative differences in the odour profile of individuals infected with *Plasmodium* parasites. Samples were compared between individuals harbouring varying parasite densities and stages, within a cohort of experimentally-infected adults and another of naturally-infected children in a malaria-endemic region. The antennal response of *Anopheles coluzzii* mosquitoes was then used to further test for entomologically significant, and infection-associated, compounds in the same odour samples. In both cohorts, constituent compounds of the odour profile were found to vary, in a quantitative manner, with infection status. Individuals in the experimentally-infected cohort were *Plasmodium*-naïve adults in The Netherlands, and infections did not progress past the very early stages of acute-stage blood parasitaemia. Those in the naturally-infected cohort were asymptomatic, school-age children in malaria-endemic Western Kenya, often with relatively low-density and chronic infections. As such, significant differences existed between these two cohorts, and a different subset of infection-associated compounds was identified from each. Three of the infection-associated compounds isolated from the naturally-infected samples, the aldehydes heptanal, octanal and nonanal (C7-C9), were recognised by the antennae of *Anopheles coluzzii*. Further, these aldehydes were very highly-produced constituents of the odour profile, and their increased production was correlated with increased total parasite density. It is hypothesised that *Plasmodium* parasites influence the human odour profile throughout infection, perhaps due to the changed physiology of the host, while those changes that are detected by the *Anopheles* vector only occur at higher parasite densities. While these changes in C7-C9 production may occur indirectly, via malaria-induced oxidative stress, it is possible that such changes impact vertebrate host-mosquito contact, and therefore influence parasite transmission. Further work, however, is necessary to ascertain the role of these compounds in *Anopheles* host-seeking.

7.12 Chapter references

- Abkallo, H.M., Tangena, J.-A., Tang, J., Kobayashi, N., Inoue, M., Zoungrana, A., Colegrave, N., Culleton, R., 2015. Within-host Competition Does Not Select for Virulence in Malaria Parasites; Studies with *Plasmodium yoelii*. *PLOS Pathog.* 11, e1004628. doi:10.1371/journal.ppat.1004628
- Akim, N.I., Drakeley, C., Kingo, T., Simon, B., Senkoro, K., Sauerwein, R.W., 2000. Dynamics of *P. falciparum* gametocytemia in symptomatic patients in an area of intense perennial transmission in Tanzania. *Am. J. Trop. Med. Hyg.* 63, 199–203.
- Anderson, R.A., Koella, J.C., Hurd, H., 1999. The effect of *Plasmodium yoelii nigeriensis* infection on the feeding persistence of *Anopheles stephensi* Liston throughout the sporogonic cycle. *Proc. Biol. Sci.* 266, 1729–33. doi:10.1098/rspb.1999.0839
- Batista, E.P., Costa, E.F., Silva, A. a, 2014. *Anopheles darlingi* (Diptera: Culicidae) displays increased attractiveness to infected individuals with *Plasmodium vivax* gametocytes. *Parasit. Vectors* 7, 251. doi:10.1186/1756-3305-7-251
- Baylis, M., Nambiro, C.O., 1993. The effect of cattle infection by *Trypanosoma congolense* on the attraction, and feeding success, of the tsetse fly *Glossina pallidipes*. *Parasitology* 106 (Pt 4, 357–61.
- Bernier, U.R., Booth, M.M., Yost, R.A., 1999. Analysis of human skin emanations by gas chromatography/mass spectrometry. 1. Thermal desorption of attractants for the yellow fever mosquito (*Aedes aegypti*) from handled glass beads. *Anal. Chem.* 3, 1–7.
- Bousema, J.T., Gouagna, L.C., Drakeley, C.J., Meutstege, A.M., Okech, B.A., Akim, I.N.J., Beier, J.C., Githure, J.I., Sauerwein, R.W., 2004. *Plasmodium falciparum* gametocyte carriage in asymptomatic children in western Kenya. *Malar. J.* 3, 18. doi:10.1186/1475-2875-3-18
- Bousema, T., Drakeley, C., 2011. Epidemiology and infectivity of *Plasmodium falciparum* and *Plasmodium vivax* gametocytes in relation to malaria control and elimination. *Clin. Microbiol. Rev.* 24, 377–410. doi:10.1128/CMR.00051-10
- Buljubasic, F., Buchbauer, G., 2015. The scent of human diseases: a review on specific volatile organic compounds as diagnostic biomarkers. *Flavour Fragr. J.* 30, 5–25. doi:10.1002/ffj.3219
- Busula, A.O., Bousema, T., Mweresa, C.K., Masiga, D., Logan, J.G., Sauerwein, R.W., Verhulst, N.O., Takken, W., de Boer, J.G., 2017. Gametocytaemia increases attractiveness of *Plasmodium falciparum*-infected Kenyan children to *Anopheles gambiae* mosquitoes. *J. Infect. Dis.* 1–5. doi:10.1093/infdis/jix214
- Butler, S.E., Muok, E.M., Montgomery, S.P., Odhiambo, K., Mwinzi, P.M.N., Secor, W.E., Karanja, D.M.S., 2012. Mechanism of anemia in *Schistosoma mansoni*-infected school children in Western Kenya. *Am. J. Trop. Med. Hyg.* 87, 862–7. doi:10.4269/ajtmh.2012.12-0248
- Churcher, T.S., Bousema, T., Walker, M., Drakeley, C., Schneider, P., Ouédraogo, A.L., Basáñez, M.G., 2013. Predicting mosquito infection from *Plasmodium falciparum* gametocyte density and estimating the reservoir of infection. *Elife* 2013, 1–12. doi:10.7554/eLife.00626
- Cnops, L., Boderie, M., Gillet, P., Van Esbroeck, M., Jacobs, J., 2011. Rapid diagnostic tests as a source of DNA for *Plasmodium* species-specific real-time PCR. *Malar. J.* 10, 67. doi:10.1186/1475-2875-10-67
- Cornet, S., Nicot, A., Rivero, A., Gandon, S., 2013. Both infected and uninfected mosquitoes are attracted toward malaria infected birds. *Malar. J.* 12, 179. doi:10.1186/1475-2875-12-179
- Cornet, S., Nicot, A., Rivero, A., Gandon, S., 2012. Malaria infection increases bird attractiveness to uninfected mosquitoes. *Ecol. Lett.* 16, 323–9. doi:10.1111/ele.12041

- Curran, A.M., Prada, P.A., Furton, K.G., 2010. The Differentiation of the Volatile Organic Signatures of Individuals Through SPME-GC / MS of Characteristic Human Scent Compounds 55, 50–57. doi:10.1111/j.1556-4029.2009.01236.x
- Curran, A.M., Rabin, S.I., Prada, P.A., Furton, K.G., 2005. Comparison of the volatile organic compounds present in human odor using SPME-GC/MS. *J. Chem. Ecol.* 31, 1607–19.
- D’Amico, A., Bono, R., Pennazza, G., Santonico, M., Mantini, G., Bernabei, M., Zarlenga, M., Roscioni, C., Martinelli, E., Paolesse, R., Di Natale, C., 2008. Identification of melanoma with a gas sensor array. *Ski. Res. Technol.* 14, 226–236. doi:10.1111/j.1600-0846.2007.00284.x
- Dawkins, R., Krebs, J.R., 1979. Arms Races between and within Species. *Proc. R. Soc. B Biol. Sci.* 205, 489–511.
- Day, J.F., Edman, J.D., 1983. Malaria renders mice susceptible to mosquito feeding when gametocytes are most infective. *J. Parasitol.* 69, 163–70.
- De Jong, R., Knols, B.G.J., 1995. Selection of biting sites on man by two malaria mosquito species. *Experientia* 51, 80–84. doi:10.1007/BF01964925
- De Moraes, C.M., Stanczyk, N.M., Betz, H.S., Pulido, H., Sim, D.G., Read, A.F., Mescher, M.C., 2014. Malaria-induced changes in host odors enhance mosquito attraction. *Proc. Natl. Acad. Sci. U. S. A.* doi:10.1073/pnas.1405617111
- Dethier, V.G., 1954. Olfactory responses of blowflies to aliphatic aldehydes. *J. Gen. Physiol.* 37, 743–51.
- Dormont, L., Bessi ere, J.-M., Cohuet, A., 2013a. Human skin volatiles: a review. *J. Chem. Ecol.* 39, 569–78. doi:10.1007/s10886-013-0286-z
- Dormont, L., Bessi ere, J.-M., McKey, D., Cohuet, A., 2013b. New methods for field collection of human skin volatiles and perspectives for their application in the chemical ecology of human-pathogen-vector interactions. *J. Exp. Biol.* 216, 2783–8. doi:10.1242/jeb.085936
- Ferguson, H.M., Read, A.F., 2004. Mosquito appetite for blood is stimulated by Plasmodium chabaudi infections in themselves and their vertebrate hosts. *Malar. J.* 8, 1–8. doi:10.1186/1475-2875-3-12
- Ferguson, H.M., Rivero, A., Read, A.F., 2003. The influence of malaria parasite genetic diversity and anaemia on mosquito feeding and fecundity. *Parasitology* 127, 9–19.
- Hermesen, C.C., Telgt, D.S., Linders, E.H., van de Locht, L. a, Eling, W.M., Mensink, E.J., Sauerwein, R.W., 2001. Detection of Plasmodium falciparum malaria parasites in vivo by real-time quantitative PCR. *Mol. Biochem. Parasitol.* 118, 247–251. doi:S0166685101003796 [pii]
- Jaleta, K.T., Hill, S.R., Birgersson, G., Tekie, H., Ignell, R., 2016. Chicken volatiles repel host-seeking malaria mosquitoes. *Malar. J.* 15, 354. doi:10.1186/s12936-016-1386-3
- Jawara, M., Smallegange, R.C., Jeffries, D., Nwakanma, D.C., Awolola, T.S., Knols, B.G.J., Takken, W., Conway, D.J., 2009. Optimizing odor-baited trap methods for collecting mosquitoes during the malaria season in The Gambia. *PLoS One* 4, e8167. doi:10.1371/journal.pone.0008167
- Kemme, J.A., Van Essen, P.H., Ritchie, S.A., Kay, B.H., 1993. Response of mosquitoes to carbon dioxide and 1-octen-3-ol in southeast Queensland, Australia. *J. Am. Mosq. Control Assoc.* 9, 431–5.
- Kingsolver, J.G., 1987. Mosquito host choice and the epidemiology of malaria [WWW Document]. URL <http://www.jstor.org/discover/10.2307/2461780?uid=2446975375&uid=3738032&uid=2129&uid=2134&uid=2&uid=70&uid=3&uid=67&uid=62&uid=2446974975&sid=21103231276811>
- Koella, J.C., 2002. Stage-specific manipulation of a mosquito’s host-seeking behavior by the malaria parasite Plasmodium gallinaceum. *Behav. Ecol.* 13, 816–820. doi:10.1093/beheco/13.6.816

- Koepfli, C., Robinson, L.J., Rarau, P., Salib, M., Sambale, N., Wampfler, R., Betuela, I., Nuitragool, W., Barry, A.E., Siba, P., Felger, I., Mueller, I., 2015. Blood-Stage Parasitaemia and Age Determine *Plasmodium falciparum* and *P. vivax* Gametocytaemia in Papua New Guinea. *PLoS One* 10, e0126747. doi:10.1371/journal.pone.0126747
- Lacroix, R., Mukabana, W.R., Gouagna, L.C., Koella, J.C., 2005. Malaria infection increases attractiveness of humans to mosquitoes. *PLoS Biol.* 3, e298. doi:10.1371/journal.pbio.0030298
- Logan, J.G., Birkett, M.A., Clark, S.J., Powers, S., Seal, N.J., Wadhams, L.J., Mordue Luntz, A.J., Pickett, J.A., 2008. Identification of human-derived volatile chemicals that interfere with attraction of *Aedes aegypti* mosquitoes. *J Chem Ecol* 34, 308–322. doi:10.1007/s10886-008-9436-0
- Logan, J.G., Stanczyk, N.M., Hassanali, A., Kemei, J., Santana, A.E.G., Ribeiro, K. a L., Pickett, J. a, Mordue Luntz, a J., 2010. Arm-in-cage testing of natural human-derived mosquito repellents. *Malar. J.* 9, 239. doi:10.1186/1475-2875-9-239
- Mauck, K.E., De Moraes, C.M., Mescher, M.C., 2010. Deceptive chemical signals induced by a plant virus attract insect vectors to inferior hosts. *Proc. Natl. Acad. Sci. U. S. A.* 107, 3600–5. doi:10.1073/pnas.0907191107
- Menger, D.J., Van Loon, J.J.A., Takken, W., 2014. Assessing the efficacy of candidate mosquito repellents against the background of an attractive source that mimics a human host. *Med. Vet. Entomol.* 28, 407–13. doi:10.1111/mve.12061
- Nabet, C., Doumbo, S., Jeddi, F., Sagara, I., Manciuilli, T., Tapily, Amadou, L'Ollivier, C., Djimde, A., Doumbo, O.K., Piarroux, R., 2016. Analyzing Deoxyribose Nucleic Acid from Malaria Rapid Diagnostic Tests to Study *Plasmodium falciparum* Genetic Diversity in Mali. *Am. J. Trop. Med. Hyg.* 94, 1259–1265. doi:10.4269/ajtmh.15-0832
- Njiru, B.N., Mukabana, W.R., Takken, W., Knols, B.G.J., 2006. Trapping of the malaria vector *Anopheles gambiae* with odour-baited MM-X traps in semi-field conditions in western Kenya. *Malar. J.* 5, 39. doi:10.1186/1475-2875-5-39
- Nyasembe, V.O., Tchouassi, D.P., Kirwa, H.K., Foster, W.A., Teal, P.E.A., Borgemeister, C., Torto, B., 2014. Development and assessment of plant-based synthetic odor baits for surveillance and control of malaria vectors. *PLoS One* 9, e89818. doi:10.1371/journal.pone.0089818
- Oh, E.H., Song, H.S., Park, T.H., 2011. Recent advances in electronic and bioelectronic noses and their biomedical applications. *Enzyme Microb. Technol.* 48, 427–437. doi:10.1016/j.enzmictec.2011.04.003
- Olanga, E.A., Okal, M.N., Mbadi, P. a, Kokwaro, E.D., Mukabana, W.R., 2010. Attraction of *Anopheles gambiae* to odour baits augmented with heat and moisture. *Malar. J.* 9, 6. doi:10.1186/1475-2875-9-6
- Omolo, M.O., Njiru, B., Ndiege, I.O., Musau, R.M., Hassanali, A., 2013. Differential attractiveness of human foot odours to *Anopheles gambiae* Giles sensu stricto (Diptera: Culicidae) and variation in their chemical composition. *Acta Trop.* 128, 144–148. doi:10.1016/j.actatropica.2013.07.012
- Ouédraogo, A.L., Bousema, T., Schneider, P., de Vlas, S.J., Ilboudo-Sanogo, E., Cuzin-Ouattara, N., Nébié, I., Roeffen, W., Verhave, J.P., Luty, A.J.F., Sauerwein, R., 2009. Substantial Contribution of Submicroscopical *Plasmodium falciparum* Gametocyte Carriage to the Infectious Reservoir in an Area of Seasonal Transmission. *PLoS One* 4, e8410. doi:10.1371/journal.pone.0008410
- Papa Mze, N., Ahouidi, A.D., Diedhiou, C.K., Silai, R., Diallo, M., Ndiaye, D., Sembene, M., Mboup, S., 2016. Distribution of *Plasmodium* species on the island of Grande Comore on the basis of DNA extracted from rapid diagnostic tests. *Parasite* 23, 34. doi:10.1051/parasite/2016034

- Papa Mze, N., Ndiaye, Y.D., Diedhiou, C.K., Rahamatou, S., Dieye, B., Daniels, R.F., Hamilton, E.J., Diallo, M., Bei, A.K., Wirth, D.F., Mboup, S., Volkman, S.K., Ahoundi, A.D., Ndiaye, D., 2015. RDTs as a source of DNA to study *Plasmodium falciparum* drug resistance in isolates from Senegal and the Comoros Islands. *Malar. J.* 14, 373. doi:10.1186/s12936-015-0861-6
- Ponnudurai, T., Lensen, A.H., van Gemert, G.J., Bolmer, M.G., Meuwissen, J.H., 1991. Feeding behaviour and sporozoite ejection by infected *Anopheles stephensi*. *Trans. R. Soc. Trop. Med. Hyg.* 85, 175–80.
- Qiu, Y.T., Smallegange, R.C., Van Loon, J.J.A., Takken, W., 2011. Behavioural responses of *Anopheles gambiae sensu stricto* to components of human breath, sweat and urine depend on mixture composition and concentration. *Med. Vet. Entomol.* 25, 247–255.
- Råberg, L., Roode, J.C. De, Bell, A.S., Stamou, P., Gray, D., Read, A.F., Ra, L., Roode, J.C. De, Bell, A.S., Stamou, P., Gray, D., Read, A.F., 2017. The Role of Immune-Mediated Apparent Competition in Genetically Diverse Malaria Infections 168, 41–53.
- Rosignol, P.A., Ribeiro, J.M., Spielman, A., 1984. Increased intradermal probing time in sporozoite-infected mosquitoes. *Am. J. Trop. Med. Hyg.* 33, 17–20.
- Schneider, P., Bousema, J.T., Gouagna, L.C., Otieno, S., van de Vegte-Bolmer, M., Omar, S.A., Sauerwein, R.W., 2007. Submicroscopic *Plasmodium falciparum* gametocyte densities frequently result in mosquito infection. *Am. J. Trop. Med. Hyg.* 76, 470–4.
- Schreck, C.E., Kline, D.L., Carlson, D. a, 1990. Mosquito attraction to substances from the skin of different humans. *J. Am. Mosq. Control Assoc.* 6, 406–410.
- Slater, H.C., Ross, A., Ouedraogo, A.L., White, L.J., Nguon, C., Walker, P.G.T., Ngor, P., Aguas, R., Silal, S.P., Dondorp, A.M., La Barre, P., Burton, R., Sauerwein, R.W., Drakeley, C., Smith, T.A., Bousema, T., Ghani, A.C., 2015. Assessing the impact of next-generation rapid diagnostic tests on *Plasmodium falciparum* malaria elimination strategies. *Nature* 528, S94–S101. doi:10.1038/nature16040
- Smallegange, R.C., Bukovinszkiné-Kiss, G., Otieno, B., Mbadi, P. a., Takken, W., Mukabana, W.R., Van Loon, J.J. a., 2012. Identification of candidate volatiles that affect the behavioural response of the malaria mosquito *Anopheles gambiae sensu stricto* to an active kairomone blend: laboratory and semi-field assays. *Physiol. Entomol.* 37, 60–71. doi:10.1111/j.1365-3032.2011.00827.x
- Smart, M.R., Brown, A.W.A., 1956. Studies on the Responses of the female *Aedes* Mosquito. Part VII.—The Effect of Skin Temperature, Hue and Moisture on the Attractiveness of the Human Hand. *Bull. Entomol. Res.* 47, 89. doi:10.1017/S000748530004654X
- Takken, W., Dekker, T., Wijnholds, Y.G., 1997. Odor-mediated flight behavior of *Anopheles gambiae giles* *Sensu Stricto* and *An. stephensi liston* in response to CO₂, acetone, and 1-octen-3-ol (Diptera: Culicidae). *J. Insect Behav.* 10, 395–407. doi:10.1007/BF02765606
- Turell, M.J., Bailey, C.L., Rossi, A.A., 1984. Increased mosquito feeding on rift valley fever virus-infected lambs 33, 1232–1238.
- Turner, A.P.F., Magan, N., 2004. Innovation: Electronic noses and disease diagnostics. *Nat. Rev. Microbiol.* 2, 161–166. doi:10.1038/nrmicro823
- Vongsouvath, M., Phommasone, K., Sengvilaipaseuth, O., Kosoltanapiwat, N., Chantratita, N., Blacksell, S.D., Lee, S.J., de Lamballerie, X., Mayxay, M., Keomany, S., Newton, P.N., Dubot-P?r?s, A., 2016. Using Rapid Diagnostic Tests as a Source of Viral RNA for Dengue Serotyping by RT-PCR - A Novel Epidemiological Tool. *PLoS Negl. Trop. Dis.* 10, e0004704. doi:10.1371/journal.pntd.0004704
- Wekesa, J.W., Copeland, R.S., Mwangi, R.W., 1992. Effect of *Plasmodium falciparum* on blood feeding behavior of naturally infected *Anopheles* mosquitoes in western Kenya. *Am. J. Trop. Med. Hyg.* 47, 484–8.
- WWARN Gametocyte Study Group, 2016. Gametocyte carriage in uncomplicated *Plasmodium falciparum* malaria following treatment with artemisinin combination therapy: a

Chapter 7: Discussion and conclusions

systematic review and meta-analysis of individual patient data. BMC Med. 14, 79.
doi:10.1186/s12916-016-0621-7